Title
Survey and analysis of breast cancer cell line proteomes

Author
Patwardhan, Anil Jayant

Publication Date
2005

Peer reviewed|Thesis/dissertation

Survey and Analysis of Breast Cancer Cell Line Proteomes

by

Anil Jayant Patwardhan

DISSERTATION

Submitted in partial satisfaction of the requirements for the degree of

DOCTOR OF PHILOSOPHY

in

Biological and Medical Informatics

in the

GRADUATE DIVISION

of the

UNIVERSITY OF CALIFORNIA, SAN FRANCISCO

For Dad and Mom

Acknowledgments

Contrary to popular perception, the completion of a dissertation is far from a solitary endeavor. It would not have been possible without the extensive help of many people. I am very grateful to my advisor, Dr. Maria Pallavicini, who gave me the freedom to discover my own paths of interest, while providing the support I needed to follow them to fruition. In addition to introducing me to the world of proteomics, Maria has always prioritized my involvement with the scientific community by fostering my participation in collaborative work and at various scientific meetings. On a more fundamental level, however, Maria has improved the quality of my science- by providing constructive criticisms of my analyses, and by helping me improve as a writer and communicator of complex ideas. I feel fortunate to have worked with her on both a professional and personal level. I would also like to thank members of my oral examination committee, Drs. Joe Gray, Patsy Babbitt, and Mark Segal, who were always willing to take time for advice or consul during their busy schedules for discussion of my analyses. Their continual encouragement and interest in my project is very much appreciated.

This acknowledgement would not be complete without thanking the faculty and staff of the Environmental Molecular Sciences Laboratory at Pacific Northwest National Labs (PNNL). In addition to welcoming me to Washington State, Eric Strittmatter served as my mentor in mass spectrometric data analyses. During my stays at PNNL, Eric introduced me to the sample and data processing pipeline and the in's and out's of protein identification. His guidance and efforts were invaluable throughout our collaboration and contributed greatly to the results discussed in this dissertation. Other members of PNNL, including Dave Camp, Heather Mottaz, and Richard Smith, were helpful in designing the

proteomic studies and conducting the LC-MS/MS analysis. Their expertise and knowledge were a critical component of my own learning and insured a high standard of scientific rigor.

I owe much of my success as a graduate student to my family. My deepest thanks go to my father and mother, Jayant and Madhavi, whose interest in philosophy and religion must have served them well while pondering that Zen-like question, "When will my son ever be done with his PhD?" Although my work continues to be a mystery to them, my parents have continually offered their support and understanding during my graduate career. Their presence as certainly made this journey easier. In addition, a great part of my motivation and focus in my graduate career has come from my wife, Sarita, who quietly reassures me of better things to come after graduate school. Her occasional use of "cool" science words (like "proteome") makes me believe that I can perhaps make an impression almost anywhere. My sister, Reva and my in-laws, Hark and Kusum, also generously lent their moral support and enthusiasm whenever it was needed. Apart from any scientific considerations, this dissertation reflects my family's constant encouragement. It therefore belongs as much to them as it does to me.

Abstract

Molecular profiles of breast cancer are being explored extensively to understand the basis for tumor cell development and behavior. Among the biological molecules involved in breast cancer, proteins are the key effectors of cell properties and behavior. Proteins can be targeted directly by drug-based therapeutics; thus the direct study of the whole range of proteins expressed in a cell at any time (the "proteome") is increasingly becoming an area of great interest.

A combination of high-resolution liquid chromatography, tandem mass spectrometry and various protein identification strategies were used to profile the proteome of various cell lines derived from breast cancer and normal breast epithelium. In an initial study, this data was combined with gene expression information to identify patterns of expression that segregate with breast cancer phenotype. Subsequently, post-translational modifications among these proteins were identified using a protein identification method that incorporates an iterative search strategy. These data were combined with protein-protein interaction data and mRNA abundance information to identify networks of proteins whose regulation segregate according to the cancer phenotype. Finally, the set of peptides identified from previous tandem mass spectrometry experiments were used as a basis for developing a collection of protein markers. These "accurate mass and time tags" were used with peptide labeling techniques to directly measure the relative expression of proteins in various tumor derived cell lines and normal epithelia.

Together, these studies constitute a large-scale qualitative and quantitative proteomic analysis of breast cancer cell lines. The works described herein were used to

identify potential markers and signaling pathways that correlate with cell phenotype and may eventually suggest potential targets for breast cancer therapy. Additional analysis of these proteins and the biochemical pathways in which they are involved may not only further our understanding of breast oncogenesis, but may provide new and valuable targets for further therapeutic research.

Maria D. Paul

Table of Contents

List of Tables

List of Figures

Chapter I

Chapter II

Chapter III

Chapter IV

Chapter V

CHAPTER I

Introduction

Cancer is a group of more than 100 different and distinctive diseases in which cells in the body fail to respond appropriately to environmental and cellular cues that regulate proliferation, differentiation and cell death. World-wide, cancer accounted for over 7 million deaths (13% of total mortality) in 2000 [1]. In women, 14.9% of these cancer-related deaths occur from cancer of the breast tissue [2]. In the United States, breast cancer accounts for 30% of all cancers diagnosed [3] and is the second leading cause of cancer-related death in women, making it a leading subject of medical research.

At the molecular level, cancer is characterized by the accumulation of genetic aberrations. Molecular profiles of breast cancer are being explored extensively to understand the underlying regulation of tumor cell development and behavior. Nucleic acid strategies that survey differences amongst tumors at the DNA and RNA levels have increased understanding of cancer cell heterogeneity and have been used to stratify some tumors into molecular subtypes. However, it is increasingly recognized that only a subset of genes are transcribed and that only a portion of transcripts are translated. Thus, it is not surprising that DNA-based molecular profiles have not fully captured differences in tumor phenotypes, such as response to therapy and metastatic potential. Given that mRNA abundance is not always a reliable indicator of corresponding protein expression [4-6], the study of the whole range of proteins expressed in a cell at any time ("proteomics") offers promise of identifying biomolecules that direct cell function.

Proteins are the key effectors of cell properties and behavior; thus understanding the relationship between protein expression, cellular features and behavior is important to increase understanding of tumor response, develop novel therapies, and identify prognostic markers. Although the global analyses of expressed proteins offer new

opportunities to define molecular signatures of cancer phenotype, global protein surveys are more challenging than DNA based strategies. Protein expression data are more complex and noisy than the underlying genomic sequence information [7]. There are more proteins than genes (~30-50,000) due to multiple alternative splicing, and post-translational modifications (PTMs), generating a highly complex protein mixture. Protein expression may vary by orders of magnitude within a single cell, thus analytical approaches must have both the sensitivity and dynamic range to capture the full extent of the proteome. For example, transcriptional proteins may occur in a few copies per cell, whereas metabolic and structural proteins may have as many as 100,000 copies per cell. Analytical methodologies that are based on direct proteins/peptide measurements do not have the capability to amplify the target, such as occurs with DNA based assays. Thus, it is difficult to detect low abundance proteins.

Fortunately, novel strategies to identify and quantify differentially expressed proteins coupled with the availability of genome and functional databases, are addressing some of these challenges. Considering estimated rates of alternative splicing and PTMs, the number of proteins expressed at any time in a cellular system is typically in the thousands or tens of thousands [8], and may very likely be significantly greater than 90,000 in the human proteome [9]. Consequently, methods to analyze complex protein mixtures must employ technologies that parallel the high-throughput methods developed for gene expression studies, along with high sensitivity and the ability for quantitative analysis. A number of different proteome strategies are in use.

One emerging technology is the protein chip array- the protein equivalent of DNA microarrays. Protein chips attempt to quantitatively analyze the abundance of several

proteins simultaneously using a combination of immobilized protein baits, hybridization techniques, and detection systems. The design of protein chips is a challenge, particularly because specific capture molecules must be designed for all possible proteins encoded by the genome in addition to those that are post-translationally modified. Finding highly specific and high affinity capture molecules is also extremely difficult [10]. The immaturity of this technology is reflected in current commercial offerings- to date, most chips available carry relatively few proteins with no more than a 10 fold increase expected over the next few years [10]. For large-scale proteomics projects where the aim is to determine how complex patterns of protein expression vary with disease, these chips are inadequate.

MS is a powerful analytical technique that can be used to analyze masses of unknown molecules to aid in their subsequent identification and quantification. Recent improvements in the algorithms for comparing spectra against genomic/protein databases and improvements in the protein databases themselves have made mass spectrometry (MS) one of the most effective technologies for the characterization of gene products at the protein level [11]. MS can be used to identify unknown peptides or proteins from even complex biological mixtures. MS-based experiments can also be designed for the elucidation of protein and peptide abundance, PTMs, protein turnover rate, protein location and translocation, protein-protein interactions, and the determination of the structure and chemical properties of various biological molecules. In addition to the study of normal and aberrant pathways within a cell, these attributes have allowed MS to play an increasingly significant role in the diagnosis and treatment of diseases by supplying "fingerprints" and "screens" for various collections of proteins.

A standard technique for proteome analysis has been the combination of MS with 2D gel electrophoresis (2DE), which is theoretically capable of detecting more than 10,000 protein spots [12] simultaneously. In 2DE, proteins are orthogonally separated according to isolectric point and molecular weight, detected by staining, and quantified based on staining intensity. The explosive growth of large-scale genomic databases has enabled the use of MS or tandem mass spectrometry (MS/MS) to identify proteins in excised gel protein spots. Spectral data are compared with information contained in databases of protein sequence, genomic sequence, or expressed sequence tags [13]. In spite of the ability to view a relatively large number of proteins, the separation of integral membrane, membrane associated, hydrophobic, low abundance and strongly acidic/basic proteins, is still a significant problem in 2DE mainly because of inherent solubility and dynamic range problems. Furthermore, the quantification of protein spots is severely hampered by protein co-migration. Multiple proteins in single gel spot make it difficult to determine the constituent protein responsible for measured changes in expression when gels are compared [14]. Finally, the tedious and time-consuming process of extraction, digestion, and analysis of each individual spot is not amenable to high-throughput analysis.

The limits of 2DE have encouraged the development of separation techniques that can be incorporated into a high-throughput system that includes MS analysis. Several recent studies [15-17] have successfully employed multidimensional liquid chromatography coupled with MS/MS (LC-MS/MS) to analyze complex protein mixtures. Unlike 2DE, proteins in LC are digested first and the resulting peptides are then separated for subsequent identification. The precise method varies but usually involves the coupling of

orthogonal liquid separation techniques to produce peptide fractions separated according to charge, size, or hydrophobicity. Peptides are more soluble and easier to separate than parent proteins, thus, this system bypasses many of the limitations of 2DE, including protein insolubility, limited fractionation ranges, and limited recovery of material [16]. In addition to an increased ability to detect proteins from multiple subcellular portions of the cell including those with extremes in pI, MW, abundance, and hydrophobicity [18], LC methods provide a direct interface into mass spectrometers for analysis.

Aside from methodological advances, progress in MS instrumentation has increased throughput relative to conventional technologies. Fourier transform ion cyclotron resonance (FTICR)-MS, in particular, has received considerable attention because of its unsurpassed combination of high resolution, sensitivity and mass measurement accuracy. With a single liquid chromatography separation, FTICR measurements are capable of characterizing peptide mixtures with significantly more than 10^5 components with mass accuracies of <1 ppm [19]. Additionally, the nondestructive nature of FTICR potentially allows multistage MS experiments on the same ion population, facilitating unambiguous identification of proteins easier by generating partial sequence information with greater sensitivity [20]. Coupling this advanced MS instrument with advances in multidimensional separation methods provides the basis for high-throughput studies of proteomes with greater speed, resolution, and sensitivity than is feasible with methods based on alternative technologies. The high mass accuracy of FTICR is also the basis of accurate mass and time tags (AMTs)- a set of highly accurate peptide mass measurements that obviate the need for repeated MS/MS measurements of the same proteome.

Whereas qualitative proteomics plays a critical biological role in identifying proteins in complexes, quantitative proteomics allows the comparison of relative abundances of proteins, which are often modulated in the course of disease. Cells with different phenotypes or grown under different conditions are expected to have different protein expression levels. Although relative mRNA expression profiles have been previously studied in different subsets of breast cancer, the steady-state levels of mature gene products are subject to additional levels of control and quite often, protein levels cannot be accurately inferred from corresponding mRNA expression [4-6]. The power of quantitative proteome analysis is identification of differentially expressed proteins that may contribute to phenotype. In quantitative MS, the relative abundance of two corresponding proteins from each cell line/condition can be determined if the mass of peptides from one of the proteins is modified. Methods of introducing this "heavy" or "light" tag include metabolic labeling [21-23], post-growth amino-acid labeling [24, 25], post-digestion labeling [26], and digestion labeling [27] and are becoming more and more widely used for the relative quantification of protein expression.

This dissertation describes the analysis of several breast cancer cell line proteomes using the strategies and methods described above. The collection of breast cancer cell lines used in this study represent the same spectrum of aberrations found in primary breast tumors, many of which have been well-characterized using mRNA-based arrays. This dissertation encompasses several distinct strategies in analyzing the proteomes of these cell lines.

Chapter II describes the combination of MS/MS data with a meta-analysis of transcriptome data to identify networks of proteins with different transcriptional

regulation in various subsets of breast cancer tissue. Our study augments previous experiments that infer protein expression based solely on gene expression data and is the first study that combines an *in-silico* analysis of SAGE tag expression with proteome data. Chapter III combines proteome data (including PTM analysis) with interactome and mRNA abundance information to identify patterns of protein expression among 4 breast cancer cell lines. An iterative multi-step search strategy was used to identify PTMs. Several proteins that are preferentially modified in cancer cells were identified. Information regarding both unmodified and modified protein forms was combined with publicly available gene expression and protein-protein interaction data to reveal several functionally related proteins that are differentially regulated between non-cancer and cancer cell lines. Finally, Chapters 4 and 5 describe the development and use of AMTs and the ^{18}O-labeling technique to directly measure the relative abundance of proteins in both non-cancer and cancer cell lines. Peptide AMTs obviate the need for the repeated MS/MS measurements while still allowing broad and accurate coverage of a proteome. Together with a reference cell line mixture, trypsin-catalyzed $^{16}O/^{18}O$ peptide labeling, and Fourier transform ion cyclotron resonance mass spectrometry (FTICR-MS), we were able to quantify the relative abundance of 514 proteins in non-cancer and cancer cell lines. A clustering of this dataset allowed us to compare protein expression across cell lines. Protein and mRNA abundances were directly compared using additional gene expression data and revealed several proteins with a 3-fold difference between non-cancer and cancer cell lines at the protein and transcriptional level. Figure 1 summarizes the different stages of analysis described in this dissertation.

These studies constitute a large-scale qualitative and quantitative proteomic analysis of breast cancer cell lines. The work described herein was used to identify potential markers and signaling pathways that correlate with cell phenotype and potential targets for breast cancer therapy. The methods and data described in Chapters 4 and 5 can be used in future studies of additional breast cancer cell lines or tissues to identify molecular determinants of chemotaxic responses, cancer susceptibility, and cellular growth characteristics. Such markers may become increasingly important as novel targeted biological agents are developed for breast cancer.

Sample prep Chromatographic separations Quantitative Labeling ESI-Tandem Mass Spectrometry FTICR-MS	Experimental
Protein identification/Scoring Accurate Mass Tags Protein Abundance Calculation	MS/MS Analysis FTICR Analysis
Functional Annotation Protein expression in breast tissue Protein-protein interactions Post-translational modifications Protein expression across cell lines Proteome expression vs. mRNA expression	Proteome profiling

Figure 1. Summary of proteome analysis of breast cancer cell lines. Experimental methods include preparation of samples for MS-based analysis and acquisition of MS-spectra. MS/MS and FTICR analysis includes techniques used for protein identification and abundance calculations. Finally, cell line proteomes were profiled using a variety of techniques. These include the use of functional, protein-protein interaction, and gene expression information combined with proteome data; the detection of post-translational modifications; and the comparative analysis of protein abundance across cell lines.

References

(1) Shibuya, K.; Mathers, C.; Boschi-Pinto, C.; Lopez, A.; Murray, C. *BMC Cancer* 2002, *2*, 37.

(2) Shibuya, K.; Mathers, C.; Boschi-Pinto, C.; Lopez, A.; Murray, C. *BMC Cancer* 2003, *3*, 20.

(3) Greenlee, R. T.; Murray, T.; Bolden, S.; Wingo, P. A. *CA Cancer J Clin* 2000, *50*, 7-33.

(4) Gygi, S. P.; Rochon, Y.; Franza, B. R.; Aebersold, R. *Mol Cell Biol* 1999, *19*, 1720-1730.

(5) Anderson, L.; Seilhamer, J. *Electrophoresis* 1997, *18*, 533-537.

(6) Futcher, B.; Latter, G. I.; Monardo, P.; McLaughlin, C. S.; Garrels, J. I. *Mol Cell Biol* 1999, *19*, 7357-7368.

(7) Greenbaum, D.; Jansen, R.; Gerstein, M. *Bioinformatics* 2002, *18*, 585-596.

(8) Haynes, P. A.; Yates, J. R., 3rd *Yeast* 2000, *17*, 81-87.

(9) Harrison, P. M.; Kumar, A.; Lang, N.; Snyder, M.; Gerstein, M. *Nucl. Acids. Res.* 2002, *30*, 1083-1090.

(10) Abbott, A. *Nature* 2002, *415*, 112-114.

(11) Pandey, A.; Mann, M. *Nature* 2000, *405*, 837-846.

(12) Klose, J.; Kobalz, U. *Electrophoresis* 1995, *16*, 1034-1059.

(13) Yates, J. R., 3rd; Eng, J. K.; McCormack, A. L.; Schieltz, D. *Anal Chem* 1995, *67*, 1426-1436.

(14) Peng, J.; Gygi, S. P. *J Mass Spectrom* 2001, *36*, 1083-1091.

(15) Lee, S. W.; Berger, S. J.; Martinovic, S.; Pasa-Tolic, L.; Anderson, G. A.; Shen, Y.; Zhao, R.; Smith, R. D. *Proc Natl Acad Sci U S A* 2002, *99*, 5942-5947.

(16) Link, A. J.; Eng, J.; Schieltz, D. M.; Carmack, E.; Mize, G. J.; Morris, D. R.; Garvik, B. M.; Yates, J. R., 3rd *Nat Biotechnol* 1999, *17*, 676-682.

(17) Wolters, D. A.; Washburn, M. P.; Yates, J. R., 3rd *Anal Chem* 2001, *73*, 5683-5690.

(18) Issaq, H. J. *Electrophoresis* 2001, *22*, 3629-3638.

(19) Smith, R. D.; Anderson, G. A.; Lipton, M. S.; Pasa-Tolic, L.; Shen, Y.; Conrads, T. P.; Veenstra, T. D.; Udseth, H. R. *Proteomics* 2002, *2*, 513-523.

(20) Jensen, P. K.; Pasa-Tolic, L.; Anderson, G. A.; Horner, J. A.; Lipton, M. S.; Bruce, J. E.; Smith, R. D. *Anal Chem* 1999, *71*, 2076-2084.

(21) Conrads, T. P.; Alving, K.; Veenstra, T. D.; Belov, M. E.; Anderson, G. A.; Anderson, D. J.; Lipton, M. S.; Pasa-Tolic, L.; Udseth, H. R.; Chrisler, W. B.; Thrall, B. D.; Smith, R. D. *Anal Chem* 2001, *73*, 2132-2139.

(22) Oda, Y.; Huang, K.; Cross, F. R.; Cowburn, D.; Chait, B. T. *Proc Natl Acad Sci U S A* 1999, *96*, 6591-6596.

(23) Veenstra, T. D.; Martinovic, S.; Anderson, G. A.; Pasa-Tolic, L.; Smith, R. D. *J Am Soc Mass Spectrom* 2000, *11*, 78-82.

(24) Gygi, S. P.; Rist, B.; Gerber, S. A.; Turecek, F.; Gelb, M. H.; Aebersold, R. *Nat Biotechnol* 1999, *17*, 994-999.

(25) Griffin, T. J.; Han, D. K.; Gygi, S. P.; Rist, B.; Lee, H.; Aebersold, R.; Parker, K. C. *J Am Soc Mass Spectrom* 2001, *12*, 1238-1246.

(26) Goodlett, D. R.; Keller, A.; Watts, J. D.; Newitt, R.; Yi, E. C.; Purvine, S.; Eng, J. K.; von Haller, P.; Aebersold, R.; Kolker, E. *Rapid Commun Mass Spectrom* 2001, *15*, 1214-1221.

(27) Yao, X.; Freas, A.; Ramirez, J.; Demirev, P. A.; Fenselau, C. *Anal Chem* 2001, *73*, 2836-2842.

Gloss to Chapter II

Chapter II is presented in the form of a journal article submitted to the Journal of Proteome Research and presents results from our first LC-MS/MS analysis. From the initial inception of this thesis, an overarching goal has been the integration of disparate data sources to obtain a comprehensive molecular profile of breast cancer. For the protein analysis component, our study combined a series of sample preparation steps with LC-MS/MS and peptide/protein scoring. This work is a foundation for the analyses described in Chapters 3-5 and encompasses my introduction to sample preparation and protein identification methodologies. It also marks the beginning of our close collaboration with Pacific Northwest National Labs (PNNL), where our samples were subjected to MS/MS analysis.

This study encompasses my first round of wet-lab work, which included a membrane-enrichment procedure developed to mitigate the loss of hydrophobic proteins during LC separations. It also marks my first extended stay at PNNL, where I prepared samples for LC analysis and processed and analyzed MS/MS spectra for protein identification. Our initial approach was to use the PNNL-developed database search algorithm, PARALLAX, for protein identification purposes. However, several limitations of this program- including the lack of parallel processing power and automation- made its use impractical for processing the >700,000 spectra (and growing), which we had acquired. Subsequently, we decided to use the commonly known, SEQUEST algorithm in combination with our own "Discriminant"-based peptide scoring methodology, which is described later in this chapter. Around the same time, the Institute for Systems Biology

(ISB) came out with their own open-source protein scoring algorithm (ProteinProphet), which provided a statistical formalism for identifying proteins from peptides in the presence of sequence homologies (i.e. when a single identified peptide belongs to more than one protein). After false-positive testing using reverse-database searches, we incorporated this program into our analysis pipeline.

Since the results from this round of LC-MS/MS analysis were to be used as potential protein markers in future quantitative FTICR runs (Chapters 4 and 5), we set up a database of potential mass and time (PMT) tags. This database consisted of various parameters associated with each identified peptide and protein: the Discriminant and ProteinProphet score, normalized elution time information, peptide sequence, and various SEQUEST score parameters. The number of peptides/proteins in this database was updated whenever an additional peptide from a cell line was identified within the set of experiments described in Chapters II-V. Ultimately this database served as a "look-up" table in our "AMT" strategy of protein identification (Chapter V).

Discussions with Joe Gray and Maria encouraged me to try to integrate our own protein data with information from gene expression studies and protein-protein interaction databases. This led me to explore the Cancer Genome Anatomy Project (CGAP) as a potential source of information, because 1) it consisted of a large number of Serial Analysis of Gene Expression (SAGE) tags and 2) it is one of the few public repositories of gene expression data from breast tissue. Newly developed CGAP tools, including the "SAGE Digital Gene Expression Displayer" allowed me to compare gene expression across various tissue subsets for just those genes whose proteins we identified. If future quantitative proteomic studies reveal a relatively small set of proteins that are up

or down-regulated in these cell lines (Chapter V), then their gene expression can be evaluated in various subsets of breast cancer using the methods described in this paper.

I elected to use the Ingenuity Pathways Knowledge-Base as a source of protein-protein interaction data for the set of proteins we identified. Several interesting group of proteins were identified using this tool- including interactions with the well-known transcription factor, MYC. However, the bulk of interactions stored in this commercial database was not manually curated and were extracted from literature using a natural language processing algorithm. The algorithm was a bit like a black-box, and included many "inferred" interactions, which I preferred to avoid. In retrospect, the quality of the interaction data presented in this paper is not as strong as the interaction data derived directly from the BIND database, which I describe later in Chapter III. However, the work was valuable, in that it laid the foundation for dataset integration in future studies. Indeed, many of the PERL scripts, SQL queries and database tables, which were written to join the gene expression and proteome data for this paper, were also used for the studies described in Chapters III and V.

CHAPTER II

Integrated Genome and Proteome Analysis of Tissue Heterogeneity In Breast Cancer

Abstract:

The purpose of this study is to investigate whether integration of proteome and genome data is useful to identify networks of proteins with potential relevance in breast cancer. Breast cancer cell-line proteomes were profiled using a combination of subcellular fractionation, multidimensional chromatography, and mass spectrometry. The resulting protein list was combined with a meta-analysis of transcriptome data from primary human tissues. This analysis revealed networks of expressed proteins that are 1) transcriptionally and functionally related and 2) likely to be differentially expressed in various subsets of breast tissues. Clustering and pathway analyses suggest several membrane and ribosomal proteins with differential gene expression patterns in breast cancer subtypes and non-cancer breast tissues. We identified several gene targets that interact with the MYC transcription factor and are likely to be expressed at different levels in these tissue subsets. The combination of proteome and transcriptome data allowed us to focus on proteins expressed in these breast cancer cell lines. This technique augments previous studies that infer protein expression based solely on gene expression data and is the first study that combines an *in-silico* analysis of SAGE tag expression with proteome data.

Introduction

Although gene prediction studies suggest that ~90,000 proteins may be encoded by human genes [1], only a subset of the predicted genes and gene products have been studied in cancer. High throughput nucleic acid-based microarrays have been used to survey DNA copy number alterations [2] and differential gene expression [3] in a number of tumor types. However, it is increasingly recognized that only a subset of genes are transcribed and that only a portion of these transcripts are translated. Thus, it is not surprising that DNA-based molecular profiles do not fully capture differences in tumor phenotypes, such as response to therapy and metastatic potential. Proteome analysis provides opportunities to define the expressed proteins in a sample, thereby facilitating elucidation of relationships between gene expression and phenotype.

Proteins associated with cell membranes participate in multiple cell-environment interactions including cell-cell communications, cell-extracellular interactions, locomotion and migration, and cell signaling. Membrane-associated proteins account for 70% of all known pharmaceutical drug targets [4] and are targets for a number of new drug and antibody-based therapeutics in cancer. Therapies that target estrogen and progesterone receptors and receptor tyrosine kinases are among the most promising in breast cancer [5,6]. Several other membrane-associated proteins such as GTPases, mucins, catenins and kinases also are implicated in carcinogenesis and tumor progression. However, the complexities of the human proteome, and properties of membrane proteins that complicate their isolation, solubilization and retention, have been particularly problematic in membrane proteomics [7]. Fortunately, recent advances in high-performance liquid chromatography and membrane isolation procedures now enable analysis of

hydrophobic proteins, which typically are underrepresented in proteomic datasets. We integrated high throughput proteomic strategies with transcriptional information to identify proteins that are likely to segregate with breast cancer phenotypes. These data may ultimately lead to additional therapeutic targets or prognostic markers for breast cancer, and lend insight into aberrant cell-signaling and cell-environment interactions.

We reduced the complexity of the breast cancer cell line proteome using a combination of subcellular fractionation, separation by strong cation exchange chromatography, and reversed-phase capillary LC followed by MS/MS. The extensive sample fractionation described in this study revealed 2101 distinct gene products, including 964 (46%) that are membrane bound. Additional clustering of these proteins based on corresponding gene expression datasets and pathway analysis was used to identify functionally related groups of proteins with potential relevance to breast cancer.

Materials and Methods

Cells and Sample Preparation

Human breast carcinoma cell lines SKBR-3 (American type culture collection (ATCC):HTB-30), MDA-MB-231 (ATCC:HTB-26), BT-474 (ATCC:HTB-20), and an MCF7 transfectant cell line over-expressing the ERBB2 receptor tyrosine kinase [8] were cultured in ATCC recommended medium containing 2 mM glutamine, 100 μg/mL streptomycin/penicillin, and Genetician (200 μg/mL; Gibco, Carlsbad, CA). Cells were maintained at 37°C in a humidified atmosphere of 95% air and 5% CO_2, washed with phosphate buffered saline (PBS) and harvested at 70% confluency using a cell

disassociation solution per manufacturer's instructions (Cell Dissociation Solution (1×) Non-enzymatic, Sigma, St. Louis, MO).

Sample complexity was reduced using the sucrose-cushion procedure described by Arnott et al. [9]. The resulting membrane fraction was resuspended in a urea solution (7 M urea, 2 M thiourea, 1% CHAPS, 5 mM DTT) and stored at -80° C. Membrane-enriched fractions were prepared separately for all 3 cell lines and then pooled into a single mixture. A fourth membrane enriched fraction was prepared for the SKBR-3 cell line and produced a second aliquot. Both aliquots were enzymatically digested (Sequence Grade Modified, Promega, Madison, WI), reduced with 10 mM DTT, and alkylated with 32 mM iodoacetamide prior to MS/MS analysis.

Peptide Separation

Each aliquot was injected for strong-cation exchange (SCX) chromatography onto a Poly LC (Columbia, MD, USA) Polysulfoethyl A 200 mm x 9.4 mm column preceded by a 10 mm x 10 mm guard column at a flow rate of 4 mL/min. The separations were performed on a Shimadzu LC-10A system using a Unicam 4225 (Thermo Electron, Waltham, MA, USA) UV-Vis detector with mobile phases consisting of Solvent A (10 mM ammonium formate, 25% ACN, pH 3.0), and Solvent B (500 mM ammonium formate, 25% ACN, pH 6.8). Initially, the runs were isocratic at 100% Solvent A for 10 min followed by a linear gradient from solvent A to solvent B over 50 min. The gradient was held at 100% solvent B for 10 min, and then washed with water for 20 min prior to re-equilibrating with 100% Solvent A for 10 min. All SCX fractions (66 in aliquot 1; 68

in aliquot 2; 68 in aliquot 3) were collected, lyophilized to dryness, and stored at –80° C until analyzed. The reversed phase LC method was used as previously reported [10].

MS/MS Analysis, Peptide and Protein Identification

The RPLC column was interfaced with a Finnigan LCQ ion trap mass spectrometer (ThermoFinnigan, San Jose, CA) with an electrospray ionization source. The initial MS survey scan utilized an m/z range of 400-2000 from which the 3 most abundant ions were selected for MS/MS analysis using a collisional energy of 45%. Dynamic exclusion was used to prevent repeated analysis of the same high abundant ion. Peptide identification was performed using SEQUEST v2.7 (ThermoFinnigan, San Jose, CA) [11] and searched with the September 2003 freeze of the human International Protein Index (IPI) database (http://www.ebi.ac.uk/IPI/IPIhelp.html). SEQUEST search was carried out using a +/- 3 Da restriction on parent mass accuracy. Since our samples were alkyated prior to analysis, a dynamic modification was used to identify both unlabeled and iodoacetamide labeled cysteine-containing peptides. Peptides with fewer than 6 amino-acid residues were eliminated to avoid the poor specificity associated with small fragments. The search was unconstrained with respect to enzymatic cleavage, which allows for the detection of peptides not normally associated with trypsin. An independently developed discriminant based program was used to determine peptide confidence probabilities. Our custom discriminant was developed to take advantage of elution time information and tryptic cleavage information, which enhances peptide confidence [12]. The discriminant function is charge state dependent and incorporates tryptic cleavage information (tryptic value); a measure of fit between theoretical and

experimental spectra (score); information about the difference between experimental and theoretical peptide masses (deltaM); and the difference between the top 2 ranking proteins (del_score) added together into a sigmoid function:

$$Sigmoid(a,b,c,x) = \frac{a}{(1+e^{b-x/c})}$$

where the Discriminant (D) =Sigmoid(0.536, 2.355, 0.002, Score) + Sigmoid(-0.428, 0.537, 0.123, deltaM) + Sigmoid(1.10315, 0.124, 0.110, del_score) + Tryptic_value. The larger the value of D, the more confident the match. Our discriminant score cutoff threshold value was set at 0.5, which corresponded to a 5% false positive rate when tested using a tryptically digested mixture of known proteins against a protein sequence database.

The ProteinProphet program [13] was used to identify proteins. In an effort to minimize false positives, protein identification criteria used an 80% protein probability cutoff and a requirement that at least 2 peptides per protein be identified. Using a reverse database methodology, the estimated false positive rate for protein identification was determined to be ~8% [12]. Although ProteinProphet discriminates among degenerate peptide identifications (homologous proteins, splice variants, redundant entries) by taking into account the probabilities that individual protein assignments are correct, we performed additional BLAST searches of our protein list as an added precaution against redundant protein identifications. Six of the 2107 identified proteins had >95% sequence homology to other identified proteins. These were collapsed into single protein entries-reducing the total number of identified proteins from 2107 to 2101.

Identifying Membrane Bound Proteins

Identified proteins were categorized as membrane or non-membrane proteins based on annotation with gene ontology (GO) database terms [14], which classify proteins according to cellular component location. Mappings to GO terms were made using a local installation of the GO database combined with link libraries of IPI protein accession numbers or UniGene identifiers directly to GO Code identification numbers (ftp://ftp.ebi.ac.uk/pub/databases/GO/goa/HUMAN/). Localization information was acquired from the UniProt [15] and InterPro [16] databases for proteins without GO information available. For proteins annotated with multiple locations, organelle assignment was made by selecting the highest assignment score from the PSORTII algorithm [17], which predicts subcellular locations based on amino-acid sequence.

Cluster Analysis of Corresponding Gene Expression Data

We utilized publicly available SAGE-map databases [18] accessed through the Cancer Genome Anatomy Project (CGAP) website (http://cgap.nci.nih.gov) to perform *in-silico* analyses of gene expression in breast tissues. The SAGE Digital Gene Expression Displayer [19] was used to analyze differences in gene expression between various pooled subsets of cancer (estrogen receptor positive (ER+), estrogen receptor negative (ER-), node negative (Node-), node positive (Node+), ductal carcinoma in situ (DCIS), invasive ductal carcinomas (IDC)) and non-cancer breast tissues (Appendix A,

Table S1). Differential gene expression was calculated from the relative frequency of tags occurring in pools of cancer SAGE libraries vs. pools of non-cancer SAGE libraries.

Genes were clustered using the self-organizing map (SOM) module implemented in the GeneCluster 2.0 program [20], which clusters based on a Euclidean distance metric. Genes were grouped (50000 iterations, 42 random seeds) using a 4X4 SOM into 16 non-overlapping clusters. A single cluster represents genes with the most similar expression profiles across all six subsets of cancer tissue relative to non-cancer tissue. Results from the SOM clustering were compared with pair-wise correlations among the 408 genes. A Pearsons correlation matrix was constructed with genes ordered on the x and y axes according to cluster number and then overlaid with clustering information.

Several of these clusters showed differential expression between ER- and ER+ tissues, node- and node+ tissues, or DCIS and IDC tissues and could potentially be used to segregate among these tissue types. These "co-segregating" clusters were investigated further using the GOTree Machine [21], which categorizes input lists of genes into GO categories and examines these lists for enrichment. Co-segregating clusters were examined to determine functional relationships among constituent genes and if any functional groups were overrepresented compared to our reference set of proteins (all the proteins identified with MS/MS). Within each cluster, functional groups with probability scores, $p \leq 0.0001$ were considered to be over-represented in that cluster compared to what would be expected by random sampling from a pool of genes whose products we identified through MS/MS.

Pathway Analysis

Clusters that discriminate among ER- and ER+, Node- and Node+, or DCIS and IDC tissues were analyzed further by examining network gene-protein and protein-protein interactions. UniGene identifiers corresponding to the 106 genes within Clusters 4, 7, 9, and 14 were imported into the Ingenuity Pathway Analysis software (Ingenuity Systems, Mountain View, CA). Genes (61) that had at least a 2-fold difference in expression between cancer tissue subsets and non-cancer tissues were mapped to the pathway networks available in the Ingenuity pathways knowledge base (http://www.ingenuity.com/products/PathwaysKnowledge.pdf) (Table 1).

Results and Discussion

The cell lines used in this study were selected to broadly represent the proteins that are thought to be present in breast cancer tissues. For example, several of the cells lines over-express many members of the receptor tyrosine kinase (RTK) superfamily, including the RTK erbB-2 precursor (NEU/HER2/ERBB2) protein (MCF7-c18, SKBR-3), the Ephrin type-A receptor 2 precursor (ECK/Epithelial cell kinase/EPHA2) RTK protein (MDA-MB-231), and the receptor protein-tyrosine kinase erbB-3 precursor (HER3/ERBB3) (BT-474) protein. Expression of these proteins was confirmed using western-blot analysis (unpublished data) in these cell lines. In addition, two of the cell lines are derived from ER- (MDA-MB-231, SKBR3) breast cancer tissue and two are derived from ER+ (MCF7-c18, BT474) breast cancer tissues. Comparisons of tissue subsets based on expressed proteins from these cell lines allowed us to focus on those functional pathways most likely related to breast cancer.

Combination of all sample aliquots resulted in 724,566 MS/MS spectra corresponding to a total of 42,250 high scoring peptides matching 2,107 proteins listed in the IPI database. Collapsing proteins using a 95% sequence homology cutoff criteria reduced this number to 2101 proteins. Among these proteins, 58% had <20% sequence coverage, 38% had 20-50% sequence coverage, and 2% had sequence coverage >60%. 965 (46%) of the proteins identified were categorized as membrane proteins, 844 (40%) were non-membrane proteins and 292 (14%) had either ambiguous or no localization information available. Membrane bound proteins were further subcategorized into cellular organelles based on the GO, UniProt, and InterPro databases (Figure 1) and ambiguities were resolved using PSORTII. All identified proteins are listed in Table S2 (Appendix A, Table S2) along with the IPI and UniGene accession numbers, protein name, localization information, and the number of peptides used for identification.

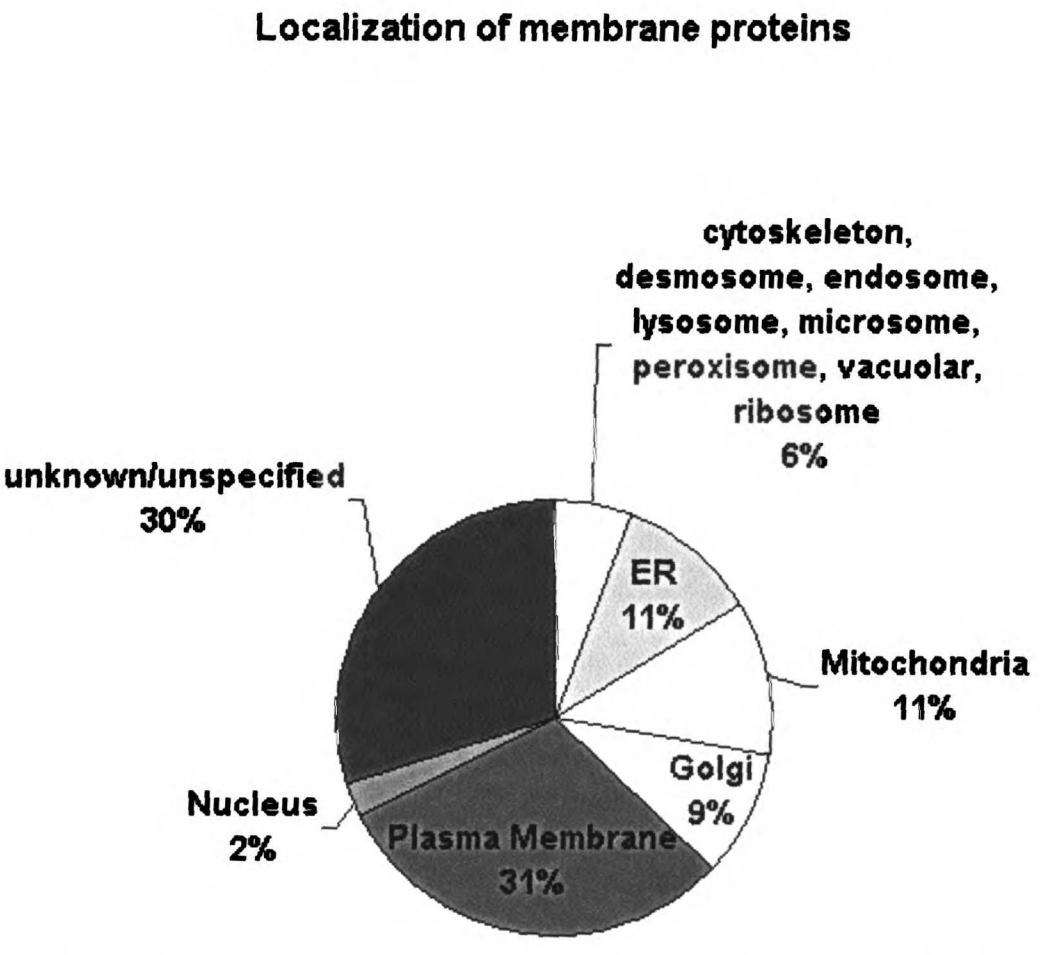

Figure 1. Summary of localization information for 965 membrane proteins identified from MS/MS.

Although 292 proteins lacked localization information, 99 (34%) had at least one transmembrane domain predicted using the TMHMM 2.0 server [22], potentially increasing our fraction of membrane proteins to 51%. However, given the false positive rates associated with many transmembrane prediction algorithms [23] we included only annotated membrane proteins in our sample (46%). Global genome analysis predicts that 20-30% of all open reading frames encode integral membrane proteins [24]; thus our results indicate that our sample is moderately enriched for membrane proteins.

SAGE tag frequencies directly reflect the abundance of mRNAs *in-vivo* and can be used as an indication of global gene expression profiles in breast tissue. The relative frequency of SAGE tags in different tissue libraries has been used to compare transcript populations in both malignant and non-cancer human tissues [18], and to explore differential gene expression in tumor progression [25, 26], metastasis [27], and chemosensitivity [28] of breast tissue. However, this is the first study that combines an *in-silico* meta-analysis of SAGE tag expression with proteome data in an effort to identify differentially expressed networks of proteins (genes) known to be expressed in cancer cell lines.

Data are expressed as sequence odds ratios [19], where the relative presence of a gene between groups of tissues is calculated by determining the proportion of SAGE tags in each pool after normalizing for differences in each pools size. Genes showing at least a 2-fold difference in expression between cancer and non-cancer tissues were identified, evaluated for statistical significance ($p<0.01$) [19 18], and cross-referenced with genes corresponding to proteins identified through MS/MS. For a SAGE tag found either in cancer or non-cancer tissues (not both), a threshold count value of one was inputted so

that an exact odds ratio could be calculated. When multiple SAGE tags occurred for a single gene, only the most frequently occurring tag within the tissue library was included. Genes in which meaningful comparisons could not be made due to missing data (e.g. SAGE tags found in only ER- but not ER+ tissues) were excluded. After applying these criteria, 408 proteins identified with MS/MS had corresponding gene expression data available from CGAP and were displayed in a "psuedo"-gene expression array in which individual rows correspond to genes and columns indicate expression in ER-, ER+, Node-, Node+, DCIS or IDC breast tissue subsets relative to non-cancer tissue. Expression values were row-normalized to a mean of 0 with standard deviation of 1.

Several studies have shown that transcriptionally co-regulated genes are often functionally related [29]. We first identified genes with similar expression profiles amongst various tissue subsets. We then determined whether genes that co-segregate with tissue phenotype are associated with functionally related groups of proteins. Results from the 4X4 SOM clustering produced 16 clusters of genes (Appendix A, Table S3), which are depicted in Figure 2A. These results were then compared with pair-wise correlations among the 408 genes. A Pearsons correlation matrix (Figure 2B) was constructed by ordering genes according to cluster number on the x and y axes and calculating a Pearsons correlation value for all gene pairs. SOM clusters were overlaid on the matrix. Clusters coincided with the highest correlation values (red) among all the pairwise comparisons, indicating that each cluster contained genes with the most similar expression profiles among all tissue subsets.

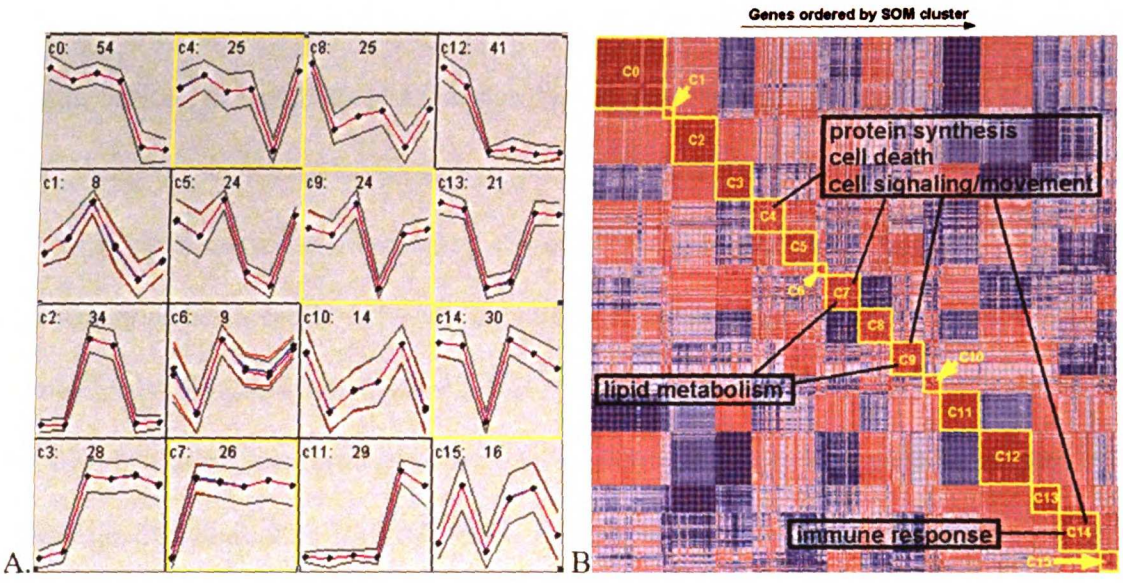

Figure 2. SOM produced clusters and relative gene expression across tissue subsets. Each panel in 2A represents a distinct gene cluster with cluster number and total number of genes denoted at the top. Points within each panel represent the average expression of genes in subsets of cancer tissue relative to non-cancer breast tissue. Tissue subsets (points) are ordered left to right as follows: ER-, ER+, Node-, Node+, DCIS and IDC. SOM defined clusters were compared to results from a Pearsons correlation matrix (2B). Red indicates areas of high correlation and blue indicates areas of low (inverse) correlation. Clusters are indicated with yellow boxes and coincide with the highest correlation values among all pairwise comparisons. Also shown are four clusters that discriminate tissue phenotype and their functional categories.

Cluster numbers 4, 7, 9, and 14 were of interest based on the gene expression profiles shown in Figure 2A. Cluster 4 contained genes whose expression in DCIS and IDC breast tissue relative to non-cancer breast tissue differed. Similarly, Clusters 9 and 14 both discriminated between node – and node + breast tissue, and Cluster 7 discriminated between ER- and ER+ breast tissue. Interactions among the genes within these clusters were identified and overlaid with gene expression data. Networks are based on protein-protein functional or physical interaction data derived from a large curated collection of individually modeled relationships between proteins (genes) in the literature. The networks were ranked by a score, which indicates the probability that a collection of genes equal to or greater than the number in a network could be achieved by chance alone. A score of 30 indicates that there is a 1/10000 chance that these genes are in a network due to random chance. Applying this cutoff resulted in 1-3 networks per cluster. The network which contained the highest number of identified proteins was retained, overlaid with gene expression data (Appendix A, Table S3), and compared across tissue types (Figure 3). The overlaid gene data was un-normalized for genes across tissue subsets in order to preserve true differences in expression. This approach allowed us to view tissue-specific expression information in a context of biological networks. Each cluster also was examined using enrichment analysis and pathway information to determine if they contained groups of functionally related genes (Figure 2B; Figure 4). All clusters are described in Table 1 and include genes mapped to the pathway database, the percentage of genes that encode membrane proteins, the tissues in which the genes are differentially expressed, and functional groups.

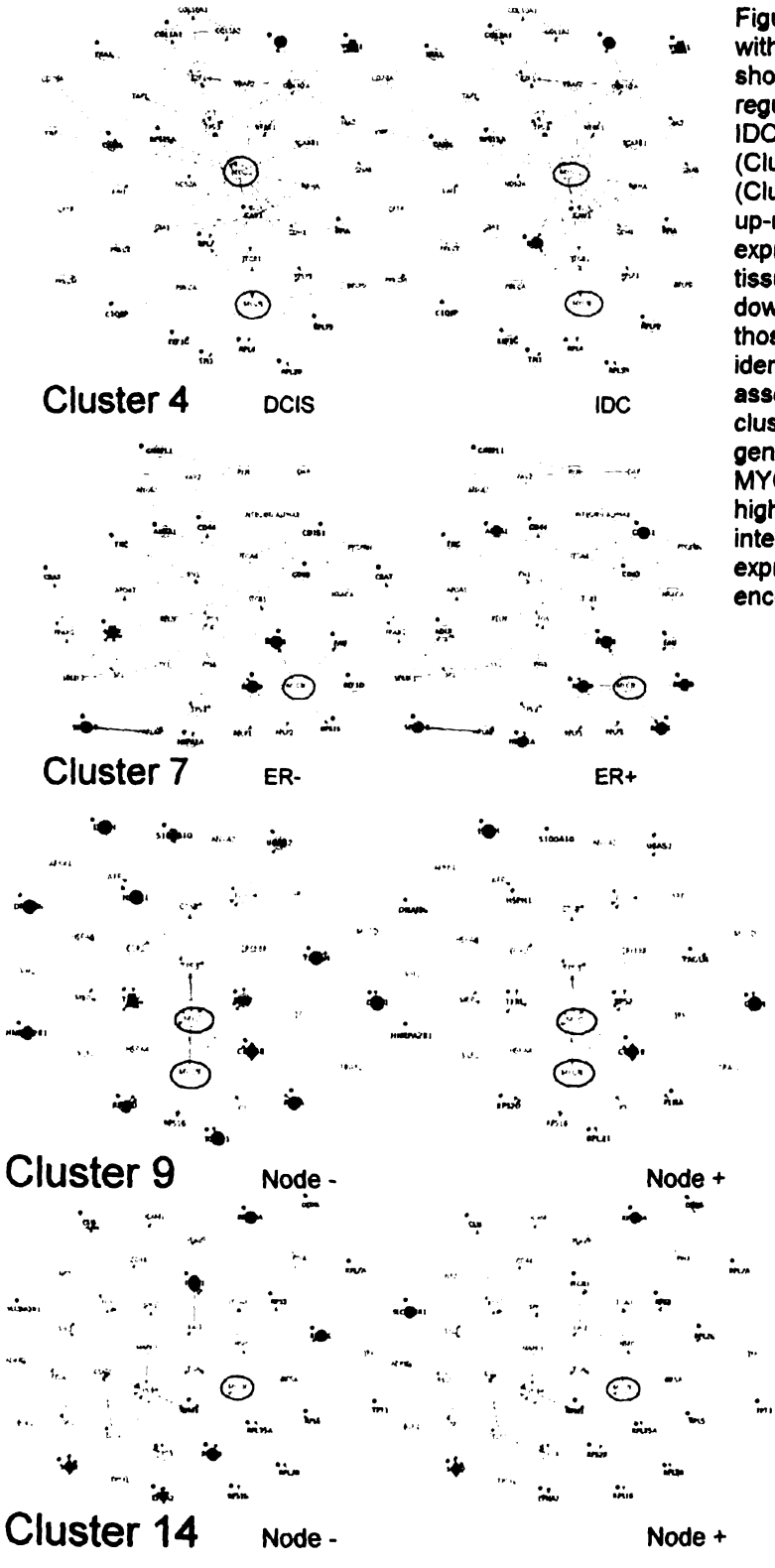

Figure 3. Pathways for proteins within Clusters 4, 7, 9 and 14 showing differential transcriptional regulation of proteins in DCIS and IDC tissues (Cluster 4), ER status (Cluster 7) and node status (Clusters 9,14). Red indicates up-regulation compared to expression in non-cancer breast tissue, and green indicates down-regulation. An * indicates those colored proteins that were identified by MS/MS, had associated genes within the cluster, and had corresponding gene expression information. The MYC and NMYC proteins are highlighted with blue circles and interact with differentially expressed genes and/or proteins encoded by those genes.

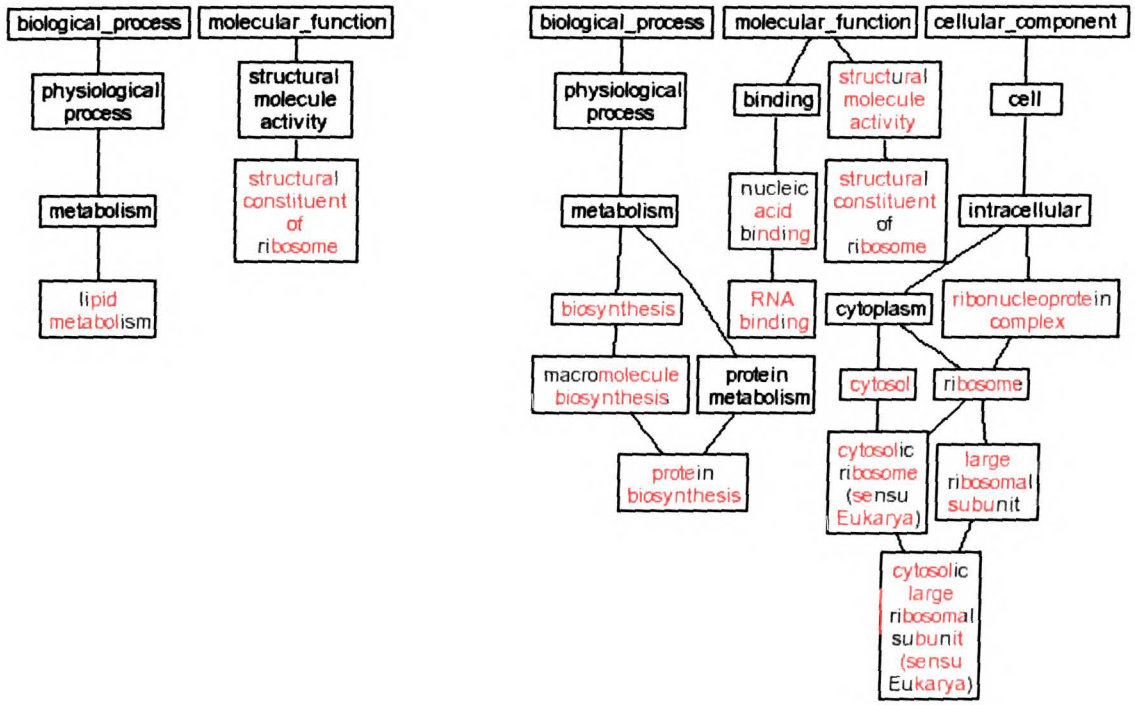

Figure 4. Acyclic graph of over-represented GO categories in clusters 7 (left) and cluster 4 (right). Groups in red are over-represented when compared to a random sampling from MS identified proteins ($p \leq 0.0001$)

Notably, all the clusters contained groups of genes that encode proteins involved in cell death and protein synthesis/RNA binding. For example, Cluster 4 contained several mitochondrial, peroxisomal, and endoplasmic reticulum genes encoding proteins involved in cell death (PPIA, CAV1, TRA1); cell signaling/immune response (TRA1, CAV1, C1QBP, COL1A1); and protein synthesis (RPL4, RPL7, RPLP2, RPL39, RPS15A). In Cluster 7, proteins involved in lipid metabolism (LDLR, CRAT), cell-cell signaling and movement (CD44, CD151, TNC, ANX1, GNB2L1), cell death (HSPA1A) and protein synthesis (FAU, RPLPO, RPS15, RPS24, EEF1D) were differentially regulated between ER- and ER+ tissues. Cluster 9 contained genes associated with cell signaling/interaction (HNRPA2B1, CNN1); cell movement (S100A10, ENAH, FLNA, CNN1); cell death (FLNA, TFRC, DNAJB6); protein synthesis (RPL31, RPS20, RPS7) and lipid metabolism (S100A10). Cluster14 contained several genes associated with cell movement (EPHA2, ITGB1, NPM1, TPT1), cell adhesion (ITGB1, EPHA2), cell death (ITGB1, SOD2, CLU, NPM1, EPHA2, TPT1), immune response (ITGB1, SOD2, TPT1), and protein synthesis (RPL26, RPS3, RPL10A, RPL35A, RPL38, RPL5, RPL7A, RPS16, RPS23).

Figure 3 displays interactions among differentially regulated proteins within these four clusters. The networks are based only on proteins that are expressed in breast cancer cell lines for which transcript data is available. Each network incorporates a heatmap representation of gene expression in various subsets of cancer tissues relative to non-cancer tissue. The tissue comparisons used in the network analysis were picked based on biological relevancy and whether or not the average expression of genes within a cluster differed between tissue types (Figure 2A). Each network also includes several non-

colored proteins that are components of the networks but were either not identified or did not have gene expression information available.

Our pathway analysis revealed that proteins encoded by similarly expressed genes often interact directly with one another. These "sub-networks" often contain genes that are differentially expressed between different tissue phenotypes. In all four clusters many of the genes differentially expressed between tissue subsets interact with the protein, MYC (c-myc, Myc proto-oncogene protein) and/or the related neuroblastoma derived homologue, MYCN (n-myc, N-myc proto-oncogene protein) (Figure 3) or encode proteins that interact with MYC.

For example, in Cluster 4, the ribosomal (RPL7, EEF1G) genes and the gene (TPL1) that encodes for a multifunctional glycolytic pathway protein are under-expressed in DCIS and over-expressed in IDC relative to non-cancer tissues. All of these genes/proteins interact with MYC/MYCN. Similarly, in Cluster 7, genes encoding ribosomal proteins (EEF1D, RPS15, RPS24), which are under-expressed in ER- and over-expressed in ER+ relative to non-cancer tissues, interact with MYCN. In Cluster 9, the ribosomal (RPS7, RPS20, RPL31) genes and genes encoding plasma membrane (TFRC), and cytoskeletal (FLNA) proteins all interact with MYC/MYCN and are differentially expressed according to node status. The ribosomal genes in Cluster 14 (RPS3, RPS23, RPL38, RPS26) show contrasting expression profiles to that in Cluster 9. They are under-expressed in node- tissues relative to non-cancer tissues and have increased expression or over-expression in node+ tissues. Examination of the MYC-target gene database [30], which curates information regarding putative MYC targets,

revealed that several of these genes are associated with MYC expression based on DNA microarray, SAGE, and differential hybridization studies.

MYC is a nuclear protein that functions as a sequence-specific DNA-binding transcription factor and controls many genes encoding products that regulate ribosome biogenesis, protein translation, apoptosis, cell mass and proliferation [31-33]. In contrast to the tightly regulated MYC gene in normal cells, which only express the gene when cells actively divide, cancer cells may express the gene in an uncontrolled fashion as the result of genetic aberrations. Nearly all types of human cancer over-express MYC, although the frequency of this alteration varies greatly[34]. Immunohistochemical studies have shown that about 50-100% of all breast cancer cases have increased levels of MYC proteins [35-37] and studies of mRNA and gene amplification are even more variable [38]. However, a recent in-situ study examining the correlation of MYC gene amplification with mRNA and protein expression indicates that gene amplification appears to be a key regulator of MYC mRNA and protein [39]. Notably, the MYC protein itself was not identified in our dataset, pointing to the limitations of proteome coverage associated with our technique. However, its presence can be inferred from the large number of proteins identified in these cell lines that are encoded by MYC interacting genes or that interact directly with MYC/NMYC. Amplification of the NMYC gene, which also encodes a transcription factor, is associated with a variety of human tumors, although it is most frequently associated with neuroblastoma, where the levels of amplification appear to increase as the tumor progresses [40]. Many of the NMYC interactions in Figure 3, however, may also occur with MYC, given the high degree of sequence homology between the two proteins. Since many of these MYC/MYCN interacting genes/proteins are differentially regulated

in pathways associated with tissue phenotype, it is reasonable to assume that MYC plays an important role in determining tumor heterogeneity in breast cancer.

Several recent studies have shown that MYC directly or indirectly binds thousands of potential target genes [41-43]. However, only 7-10% of these genes show a transcriptional response to MYC activation or repression [30], indicating that not all MYC associated genes may be effectors of MYC function [44]. The clustering of putative MYC targets based on expression profiles and the identification of their corresponding protein products allowed us to focus on those MYC targets most likely regulated in various breast tissue subsets. Since many of these genes are similarly expressed and are involved in functions normally associated with MYC (ribosome biogenesis and protein translation), it is likely that their transcription is tightly regulated by MYC in breast cancer tissue.

Several genes that were differentially expressed among tissue subsets encode membrane bound protein products. Many of these have been associated with tumor metastasis (TRA1 [45,46], CD44 [47], CD151 [48], ITGB1 [49], EPHA2 [50], COL1A1 [51], TFRC [52], LDLR [53]). However, we identified one protein, C1QBP, whose role in cancer is not well-defined. The protein encoded by the C1QBP (complement component 1, Q subcomponent binding protein) gene lies in the mitochondrial matrix, interacts with 3 protein kinases (Figure 3, Cluster 4) and is differentially regulated in DCIS and IDC tissues. Its exact function is unknown, but it is believed to be involved in immune response. Although studies have not implicated this protein in cancer invasion, it is noteworthy that, like CD44 (a known marker of tumor metastasis), this protein has been shown to bind hyaluronic acid. Recent studies have suggested that some of the steps in

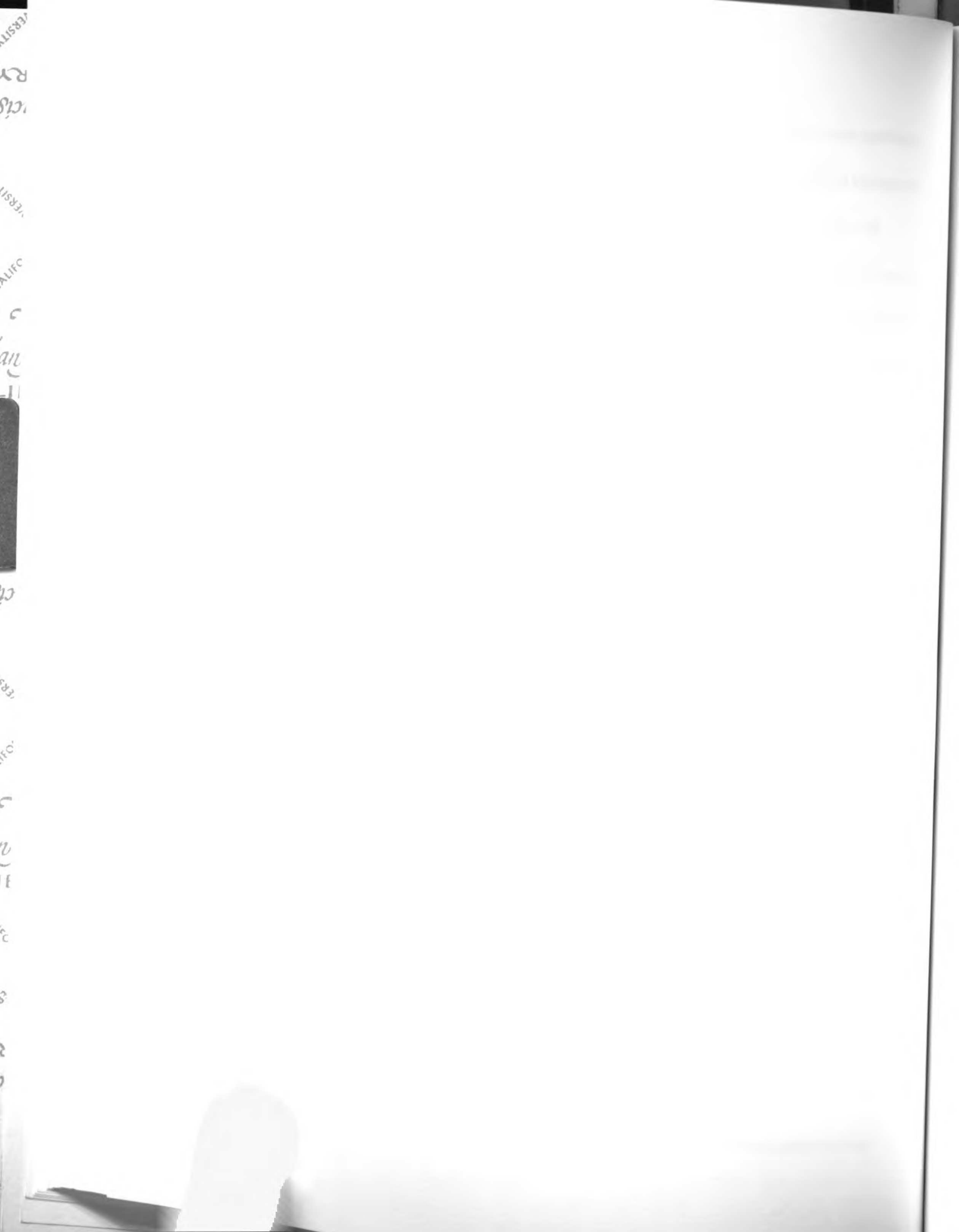

the catabolism of hyalyronic acid can be commandeered by cancer cells in the process of growth, invasion, and metastatic spread [54-57].

Concluding Remarks

In summary, our study identified a large collection of proteins from a breast cancer cell-line panel using high-throughput tandem MS techniques. By combining transcriptome data with proteome data we were able to show that several networks of proteins present in breast cancer cell lines appear to be differentially regulated among various subsets of breast tissue. The putative functions of some of these genes may suggest potential roles in the initiation and/or progression of breast carcinomas. Additional experiments using high-throughput techniques, such as mRNA *in situ* hybridization or immunohistochemical analysis on tissue-microarrays, are required to validate differential gene expression in tissue. We also hope to use the information presented here to direct future quantitative proteomics studies. Additional analysis of these genes and the biochemical pathways in which they are involved will not only further our understanding of breast oncogenesis, but may also provide new and valuable targets for translational research.

Table 1. Four gene clusters with segregating expression profiles revealed by SOM clustering, and the membrane percentages and GO categories represented by their protein products.

Cluster	Genes	Percent membrane proteins	Tissue comparison	Functional groups
4	CAV1, RPL4, RPL39, RPLP2, **TPI1**, RPL36, **RPS15A**, PPIA, **CANX**, **COL1A1**, **TRA1**, EPHX1, PSAP, PEX19, VPS41, MLPH, RPS14, **EEF1G**, **RPL7**, SF1, TRIM25, MFGE8, RPS29, DDX3X, **C1QBP**, **PXF**	41%	DCIS and IDC	protein synthesis, cell signaling/proliferation, cell death
7	RPLP0, WDR1, SLC39A14, CAT, **HSPA1A**, ANXA1, **TNC**, CD44, ACADVL, GNB2L1, FAU, NT5C2, **RPS24**, **CD151**, CRIP2, PKD1like, MYADM, UGCG, CRAT, **RPS15**, SEC61B, RPL36A, **LDLR**, ELOVL5, CD63, **EEF1D**	46%	ER- and ER+	lipid metabolism, cell-cell signaling and movement, cell death, protein synthesis
9	DST, CNN1, KIAA1007, NOTCH2, **HSPH1**, **DNAJB6**, **RPS20**, **S100A10**, **RPL31**, **TAGLN**, COX5B, ENAH, SQLE, MAP1LC3B, OCIA, PDLIM1, B3GALT4, ATP5A1, **UBA52**, **RPS7**, **HNRPA2B1**, **FLNA**, HMGCS1, **TFRC**	29%	Node – and Node +	cell signaling/interaction, cell movement, cell death, protein synthesis, lipid metabolism
14	GEM, **SOD2**, ACO2, **RPL10A**, LDHB, GBF1, LITAF, NAGLU, RPL7A, PPP2CB, RPS16, **RPL38**, RPL35A, NPM1, TPT1, **RPL26**, RPL5, **RPS23**, MGST1, **DDX5**, **SLC9A3R1**, CTNNAL1, CLCN3, **CLU**, **ITGB1**, IGHG1, **EPHA2**, HLA-A, F11R, **RPS3**	33%	Node – and Node +	cell movement, cell adhesion, cell death, immune response, protein synthesis

*Genes shown in bold had at least a 2-fold difference in expression between listed tissue types and were mapped to the pathway database.

Appendix A

Table S1. 31 tissue-specific SAGE libraries taken from the Cancer Genome Anatomy Project (CGAP) site and used for comparative gene expression.

Table S2. 2101 proteins identified with MS/MS, the corresponding IPI identifiers, gene symbol, membrane localization information, # unique peptides, and protein name.

Table S3. Expression for 408 genes whose protein products were identified with MS/MS.

Acknowledgements

This work was supported by the NIH CA86135 (MP), the NIH National Center for Research Resources (RR18522) and the Environmental Molecular Sciences Laboratory (a national scientific user facility sponsored by the Department of Energy's Office of Biological and Environmental Research and located at Pacific Northwest National Laboratory). Pacific Northwest National Laboratory is operated by Battelle Memorial Institute for the U.S. Department of Energy under contract DE-AC06-76RLO-1830. The authors would like to thank Scott Dixon and Katy Williams for advice and help in sample preparation and Heather Mottaz for help in chromatography and preparing samples for mass spectrometry.

References

(1) Harrison, P. M.; Kumar, A.; Lang, N.; Snyder, M.; Gerstein, M. *Nucl. Acids. Res.* 2002, *30*, 1083-1090.

(2) Albertson, D. G. *Breast Cancer Res Treat* 2003, *78*, 289-298.

(3) Pusztai, L.; Ayers, M.; Stec, J.; Clark, E.; Hess, K.; Stivers, D.; Damokosh, A.; Sneige, N.; Buchholz, T. A.; Esteva, F. J.; Arun, B.; Cristofanilli, M.; Booser, D.; Rosales, M.; Valero, V.; Adams, C.; Hortobagyi, G. N.; Symmans, W. F. *Clin Cancer Res* 2003, *9*, 2406-2415.

(4) Hopkins, A. L.; Groom, C. R. *Nat Rev Drug Discov* 2002, *1*, 727-730.

(5) Slamon, D. J.; Leyland-Jones, B.; Shak, S.; Fuchs, H.; Paton, V.; Bajamonde, A.; Fleming, T.; Eiermann, W.; Wolter, J.; Pegram, M.; Baselga, J.; Norton, L. *N Engl J Med* 2001, *344*, 783-792.

(6) Cohen, M. H.; Williams, G. A.; Sridhara, R.; Chen, G.; Pazdur, R. *Oncologist* 2003, *8*, 303-306.

(7) Santoni, V.; Molloy, M.; Rabilloud, T. *Electrophoresis* 2000, *21*, 1054-1070.

(8) Benz, C. C.; Scott, G. K.; Sarup, J. C.; Johnson, R. M.; Tripathy, D.; Coronado, E.; Shepard, H. M.; Osborne, C. K. *Breast Cancer Res Treat* 1993, *24*, 85-95.

(9) Arnott, D.; Kishiyama, A.; Luis, E. A.; Ludlum, S. G.; Marsters, J. C., Jr.; Stults, J. T. *Mol Cell Proteomics* 2002, *1*, 148-156.

(10) Shen, Y.; Zhao, R.; Belov, M. E.; Conrads, T. P.; Anderson, G. A.; Tang, K.; Pasa-Tolic, L.; Veenstra, T. D.; Lipton, M. S.; Udseth, H. R.; Smith, R. D. *Anal Chem* 2001, *73*, 1766-1775.

(11) Yates, J. R., 3rd; Eng, J. K.; McCormack, A. L.; Schieltz, D. *Anal Chem* 1995, *67*, 1426-1436.

(12) Strittmatter EF, K. L., Petritis K, Mottaz HM, Anderson GA, Shen Y, Jacobs JM, Camp DG, Smith RD *Journal of Proteome Research* 2004, *3*, 760-769.

(13) Nesvizhskii, A. I.; Keller, A.; Kolker, E.; Aebersold, R. *Anal Chem* 2003, *75*, 4646-4658.

(14) Ashburner, M.; Ball, C. A.; Blake, J. A.; Botstein, D.; Butler, H.; Cherry, J. M.; Davis, A. P.; Dolinski, K.; Dwight, S. S.; Eppig, J. T.; Harris, M. A.; Hill, D. P.; Issel-Tarver, L.; Kasarskis, A.; Lewis, S.; Matese, J. C.; Richardson, J. E.; Ringwald, M.; Rubin, G. M.; Sherlock, G. *Nat Genet* 2000, *25*, 25-29.

(15) Apweiler, R.; Bairoch, A.; Wu, C. H.; Barker, W. C.; Boeckmann, B.; Ferro, S.; Gasteiger, E.; Huang, H.; Lopez, R.; Magrane, M.; Martin, M. J.; Natale, D. A.; O'Donovan, C.; Redaschi, N.; Yeh, L. S. *Nucleic Acids Res* 2004, *32 Database issue*, D115-119.

(16) Mulder, N. J.; Apweiler, R.; Attwood, T. K.; Bairoch, A.; Barrell, D.; Bateman, A.; Binns, D.; Biswas, M.; Bradley, P.; Bork, P.; Bucher, P.; Copley, R. R.; Courcelle, E.; Das, U.; Durbin, R.; Falquet, L.; Fleischmann, W.; Griffiths-Jones, S.; Haft, D.; Harte, N.; Hulo, N.; Kahn, D.; Kanapin, A.; Krestyaninova, M.; Lopez, R.; Letunic, I.; Lonsdale, D.; Silventoinen, V.; Orchard, S. E.; Pagni, M.; Peyruc, D.; Ponting, C. P.; Selengut, J. D.; Servant, F.; Sigrist, C. J.; Vaughan, R.; Zdobnov, E. M. *Nucleic Acids Res* 2003, *31*, 315-318.

(17) Nakai, K.; Horton, P. *Trends Biochem Sci* 1999, *24*, 34-36.

(18) Lal, A.; Lash, A. E.; Altschul, S. F.; Velculescu, V.; Zhang, L.; McLendon, R. E.; Marra, M. A.; Prange, C.; Morin, P. J.; Polyak, K.; Papadopoulos, N.; Vogelstein, B.; Kinzler, K. W.; Strausberg, R. L.; Riggins, G. J. *Cancer Res* 1999, *59*, 5403-5407.

(19) Strausberg, R. L.; Camargo, A. A.; Riggins, G. J.; Schaefer, C. F.; de Souza, S. J.; Grouse, L. H.; Lal, A.; Buetow, K. H.; Boon, K.; Greenhut, S. F.; Simpson, A. J. *Pharmacogenomics J* 2002, *2*, 156-164.

(20) Reich, M.; Ohm, K.; Angelo, M.; Tamayo, P.; Mesirov, J. P. *Bioinformatics* 2004, *20*, 1797-1798.

(21) Zhang, B.; Schmoyer, D.; Kirov, S.; Snoddy, J. *BMC Bioinformatics* 2004, *5*, 16.

(22) Krogh, A.; Larsson, B.; von Heijne, G.; Sonnhammer, E. L. *J Mol Biol* 2001, *305*, 567-580.

(23) Moller, S.; Croning, M. D.; Apweiler, R. *Bioinformatics* 2001, *17*, 646-653.

(24) Wallin, E.; von Heijne, G. *Protein Sci* 1998, *7*, 1029-1038.

(25) Porter, D. A.; Krop, I. E.; Nasser, S.; Sgroi, D.; Kaelin, C. M.; Marks, J. R.; Riggins, G.; Polyak, K. *Cancer Res* 2001, *61*, 5697-5702.

(26) Yousef, G. M.; Yacoub, G. M.; Polymeris, M. E.; Popalis, C.; Soosaipillai, A.; Diamandis, E. P. *Br J Cancer* 2004, *90*, 167-172.

(27) Porter, D.; Lahti-Domenici, J.; Keshaviah, A.; Bae, Y. K.; Argani, P.; Marks, J.; Richardson, A.; Cooper, A.; Strausberg, R.; Riggins, G. J.; Schnitt, S.; Gabrielson, E.; Gelman, R.; Polyak, K. *Mol Cancer Res* 2003, *1*, 362-375.

(28) Seth, P.; Krop, I.; Porter, D.; Polyak, K. *Oncogene* 2002, *21*, 836-843.

(29) DeRisi, J. L.; Iyer, V. R.; Brown, P. O. *Science* 1997, *278*, 680-686.

(30) Zeller, K. I.; Jegga, A. G.; Aronow, B. J.; O'Donnell, K. A.; Dang, C. V. *Genome Biol* 2003, *4*, R69.

(31) Boon, K.; Caron, H. N.; van Asperen, R.; Valentijn, L.; Hermus, M. C.; van Sluis, P.; Roobeek, I.; Weis, I.; Voute, P. A.; Schwab, M.; Versteeg, R. *Embo J* 2001, *20*, 1383-1393.

(32) Iritani, B. M.; Eisenman, R. N. *Proc Natl Acad Sci U S A* 1999, *96*, 13180-13185.

(33) Johnston, L. A.; Prober, D. A.; Edgar, B. A.; Eisenman, R. N.; Gallant, P. *Cell* 1999, *98*, 779-790.

(34) Nesbit, C. E.; Tersak, J. M.; Prochownik, E. V. *Oncogene* 1999, *18*, 3004-3016.

(35) Agnantis, N. J.; Mahera, H.; Maounis, N.; Spandidos, D. A. *Eur J Gynaecol Oncol* 1992, *13*, 309-315.

(36) Pietilainen, T.; Lipponen, P.; Aaltomaa, S.; Eskelinen, M.; Kosma, V. M.; Syrjanen, K. *Anticancer Res* 1995, *15*, 959-964.

(37) Spaventi, R.; Pavelic, K.; Pavelic, Z. P.; Gluckman, J. L. *Eur J Cancer* 1994, *30A*, 723-724.

(38) Liao, D. J.; Dickson, R. B. *Endocr Relat Cancer* 2000, *7*, 143-164.

(39) Blancato, J.; Singh, B.; Liu, A.; Liao, D. J.; Dickson, R. B. *Br J Cancer* 2004, *90*, 1612-1619.

(40) Ibson, J. M.; Rabbitts, P. H. *Oncogene* 1988, *2*, 399-402.

(41) Fernandez, P. C.; Frank, S. R.; Wang, L.; Schroeder, M.; Liu, S.; Greene, J.; Cocito, A.; Amati, B. *Genes Dev* 2003, *17*, 1115-1129.

(42) Li, Z.; Van Calcar, S.; Qu, C.; Cavenee, W. K.; Zhang, M. Q.; Ren, B. *Proc Natl Acad Sci U S A* 2003, *100*, 8164-8169.

(43) Orian, A.; van Steensel, B.; Delrow, J.; Bussemaker, H. J.; Li, L.; Sawado, T.; Williams, E.; Loo, L. W.; Cowley, S. M.; Yost, C.; Pierce, S.; Edgar, B. A.; Parkhurst, S. M.; Eisenman, R. N. *Genes Dev* 2003, *17*, 1101-1114.

(44) Patel, J. H.; Loboda, A. P.; Showe, M. K.; Showe, L. C.; McMahon, S. B. *Nat Rev Cancer* 2004, *4*, 562-568.

(45) FXie, D.; Jauch, A.; Miller, C. W.; Bartram, C. R.; Koeffler, H. P. *Int J Oncol* 2002, *21*, 499-507.

(46) Kasukabe, T.; Okabe-Kado, J.; Honma, Y. *Blood* 1997, *89*, 2975-2985.

(47) Marhaba, R.; Zoller, M. *J Mol Histol* 2004, *35*, 211-231.

(48) Kohno, M.; Hasegawa, H.; Miyake, M.; Yamamoto, T.; Fujita, S. *Int J Cancer* 2002, *97*, 336-343.

(49) Wang, H. Y.; Liu, S. X.; Zhang, M. *Acta Pharmacol Sin* 2003, *24*, 646-650.

(50) Fox, B. P.; Kandpal, R. P. *Biochem Biophys Res Commun* 2004, *318*, 882-892.

(51) Oue, N.; Hamai, Y.; Mitani, Y.; Matsumura, S.; Oshimo, Y.; Aung, P. P.; Kuraoka, K.; Nakayama, H.; Yasui, W. *Cancer Res* 2004, *64*, 2397-2405.

(52) Ryschich, E.; Huszty, G.; Knaebel, H. P.; Hartel, M.; Buchler, M. W.; Schmidt, J. *Eur J Cancer* 2004, *40*, 1418-1422.

(53) Li, Y.; Wood, N.; Grimsley, P.; Yellowlees, D.; Donnelly, P. K. *Invasion Metastasis* 1998, *18*, 240-251.

(54) Murray, D.; Morrin, M.; McDonnell, S. *Anticancer Res* 2004, *24*, 489-494.

(55) Kim, H. R.; Wheeler, M. A.; Wilson, C. M.; Iida, J.; Eng, D.; Simpson, M. A.; McCarthy, J. B.; Bullard, K. M. *Cancer Res* 2004, *64*, 4569-4576.

(56) Avigdor, A.; Goichberg, P.; Shivtiel, S.; Dar, A.; Peled, A.; Samira, S.; Kollet, O.; Hershkoviz, R.; Alon, R.; Hardan, I.; Ben-Hur, H.; Naor, D.; Nagler, A.; Lapidot, T. *Blood* 2004, *103*, 2981-2989.

(57) Shuster, S.; Frost, G. I.; Csoka, A. B.; Formby, B.; Stern, R. *Int J Cancer* 2002, *102*, 192-197.

Gloss to Chapter III

Portions of Chapter III are presented in the form of an article submitted to the Journal of Proteome Research for publication. As in the previous study, we wanted the integrate genome and proteome data to provide a more in depth understanding of the molecular profile of breast cancer cells. Since combining information from breast tissues (gene expression) with cell lines (proteome) is potentially problematic, we wished to use mRNA and protein data derived from the same cell populations. A search for alternative gene expression data sources quickly pointed me to the Stanford Microarray Database (SMD), which supplies a wealth of publicly available gene expression studies on a variety of organisms and diseases, including cancer. Fortunately, I was able to find studies that explored mRNA expression patterns in the same cell lines for which we had proteome data.

A major difference between this study and the previous work is the use of the X!Tandem algorithm for protein identification. While the majority of proteomic researchers currently use commercially packaged programs, many proteomic journals have been pushing to use open-source instrument-independent algorithms for peptide and protein identifications. Although we were currently using the open source ProteinProphet program for protein identification, we were still using the proprietary SEQUEST algorithm for peptides. Late 2003 and early 2004 produced a cluster of papers describing a variety of open-source algorithms for peptide identification- each with its own purported advantages. Although most of the programs work essentially the same way (comparing a list of experimental fragment ion masses to theoretical ones), the peptide

scoring systems, associated false positive rates, and output data formats made some programs more attractive than others. I first tested X!Tandem because we required a locally installed protein identification program among several computers in our laboratory. The X!Tandem/GPM program was compiled and installed on our own computers using a simple Apache Web Server interface, making it an ideal solution for distributed computing environments. In addition, most parameters in the search algorithm were user-definable, which would become increasingly important as our lab produced more and more MS/MS spectra from various types of samples. The program was very well documented and had recently been favorably compared to other commercially developed programs like Mascot and SEQUEST. In addition, input instructions and output formats for X!Tandem are specified in a standardized XML format, which is quickly becoming a preferred mode of data exchange in the proteomics community. A distinct advantage of XML formatted output, is that all the database search results could be contained in a single well-specified document and viewed by anybody who has the ability to view XML. In my case, I could run the database searches myself, store the results in XML format and send (ftp) the output to PNNL, which they could view through their own web-server interface.

My biggest reason to use X!Tandem, however, came from our interest in identifying post-translational modifications (PTMs) in our samples. Searching for multiple PTMs types in a set of tryptically digested peptides can produce high false positive rates, simply because of the high number of possible PTM combinations that can add up to identical peptide masses. Although most algorithms could be tailored to some of our search strategies (described in the chapter), X!Tandem was the only algorithm that could readily incorporate our process of "refinement"- a 2-step process that searches for

PTMs among a restricted set of proteins identified from an initial unmodified search. In addition, mass modifications in X!Tandem can be manually specified by the user, allowing for an infinite number of potential mass searches on any amino-acid residue.

I also had the opportunity to travel to the International Society of Analytical Cytology (ISAC) Conference held in Montpelier, France, where Maria and I gave a short tutorial on comparative proteomics. At one of the meetings, I talked to Trey Ideker, an accomplished researcher in systems biology and a lead developer of the visualization tool, Cytoscape. After reading about some of the comparative network analysis work he did with yeast, I realized that Cytoscape would be a perfect tool for visualizing our own proteome data. Combined with protein-protein interaction data extracted from BIND, Cytoscape has proven to be a powerful tool in summarizing biological pathways within our samples.

CHAPTER III

Comparison of Normal and Breast Cancer Cell Lines using Proteome, Genome and Interactome Data

Anil J. Patwardhan, Eric F. Strittmatter, David G. Camp II, Richard D. Smith, Maria G. Pallavicini

Portions submitted for publication in the Journal of Proteome Research

Abstract

Normal and cancer cell line proteomes were profiled using high throughput mass spectrometry techniques. Application of protein-level and peptide-level sample fractionation combined with LC-MS/MS analysis enabled identification of 2,235 unmodified proteins representing a broad range of functional and compartmental classes. An iterative multi-step search strategy was used to identify post-translational modifications, revealing several proteins that are preferentially modified in cancer cells. Information regarding both unmodified and modified protein forms was combined with publicly available gene expression and protein-protein interaction data. The resulting integrated dataset revealed several functionally related proteins that are differentially regulated between normal and cancer cell lines.

Introduction

In eukaryotic cells, expression of biologically active proteins is regulated at multiple levels. At the transcriptional level, chromosomal structure as well as the processing and stability of mRNA transcripts influence gene expression. Direct measurement of mRNA transcript abundance using high throughput nucleic acid-based microarrays has been used to quantify gene expression both in whole genomes and in perturbed conditions, such as cancer. In such studies, the abundance of the corresponding proteins and their biological activity are inferred from these intermediary steps of protein production. However, while gene prediction studies suggest that ~90,000 proteins may be encoded by human genes, it is increasingly recognized that only a subset of mRNA transcripts are translated into mature protein products [1] and several labs have shown that mRNA measurements do not always correlate strongly with protein expression [2-4]. In addition, downstream regulatory events are not fully predicted from a static genome or assessed through RNA or DNA analyses. Thus, gene regulation and expression is increasingly being investigated at the translational level using protein-based assays.

Proteomic based measurements are now widespread and have been performed on a multitude of organisms using 2D PAGE or mass spectrometry based techniques. Tandem mass spectrometry (MS/MS) is a powerful technique to identify the primary structure of a protein and can be used to directly determine the complement of proteins associated with various biological processes. Mass spectrometry based proteomic methods can potentially inform on regulatory aspects of protein expression, such as rates of protein turnover, protein translocation and protein interactions. MS/MS protein identification may also be used to reveal global patterns of post-translational modifications (PTMs), which help

confer or modify protein function and allow several gene products with different functions to be produced from a single coding sequence. They influence the activity, localization, turnover, and interactions of proteins [5] and are one of the main mechanisms by which higher order diversity is generated in eukaryotes. More than 340 types of PTMs have been identified in proteins (http://www.abrf.org/index.cfm/dm.home), with many assigned functional roles in mammalian systems. Many PTMs change the molecular weight of a native protein, thereby allowing detection using sensitive mass spectrometry based techniques. Recent advances in protein/peptide level separation strategies and multi-step analyses now enable the identification of both modified and unmodified proteins even in complex biological mixtures.

However, while MS/MS proteome analysis is often considered a high throughput technique, the challenges of extracting meaningful data from lists of proteins present in different cell states are increasingly recognized. Several recent studies have integrated proteome data with transcriptome data to examine the relationship between RNA and protein abundance within various biological [6,7] and disease [8] processes. Our study adds a third source of high throughput data, protein-protein interactions, to reveal networks of functionally related proteins that may be differentially regulated in breast cancer cell lines. The integration of these large genome and proteome-wide datasets potentially reveals protein networks with distinguishing patterns of transcriptional and post-translational regulation in normal vs. aberrant phenotypes, thus providing information that extends beyond the identification of proteins.

The purpose of our study is to identify groups of functionally related proteins that show qualitative differences in expression between normal and cancer cell lines. Three

cancer cell lines were selected to represent different features of breast cancer phenotypes, including variations in estrogen receptor status and receptor tyrosine kinase (RTK) expression. One of the cell lines (MDA-MB-231) is derived from ER negative (ER-) breast cancer tissue and two (MCF7-c18, BT474) are derived from ER positive (ER+) breast cancer tissues. In addition, some of the cancer cells lines over-express several members of the RTK superfamily, including the RTK erbB-2 precursor (NEU/HER2/ERBB2) protein (MCF7-c18), the Ephrin type-A receptor 2 precursor (ECK/Epithelial cell kinase/EPHA2) RTK protein (MDA-MB-231), the epidermal growth factor receptor precursor (ERBB1/EGFR) RTK protein (BT474) and the receptor protein-tyrosine kinase erbB-3 precursor (HER3/ERBB3) (BT-474) protein. A non-cancerous human mammary epithelial cell line (HMEC) was used for comparison.

The complexity of the cell line proteomes was reduced using a combination of subcellular fractionation, peptide separation by strong cation exchange chromatography, and high resolution reversed-phase capillary LC combined with MS/MS. The resulting spectra were iteratively searched for eight forms of PTMs using a multi-step search strategy. We integrated our combined dataset of modified and unmodified proteins with publicly available genome and interactome datasets in order to achieve a broad view of how protein expression is modulated in cancer cell lines. Among the proteins detected, several "novel" modifications and expression profiles appear to differentially segregate in normal and breast cancer cells.

Materials and Methods

Cells and Sample Preparation

The human mammary epithelial cell line HMEC (American type culture collection (ATCC):HTB-30) and human breast carcinoma cell lines MDA-MB-231 (ATCC:HTB-26), BT-474 (ATCC:HTB-20), and an MCF7 transfectant cell line [9] were cultured in ATCC recommended medium containing 2 mM glutamine, 100 μg/mL streptomycin/penicillin, and Genetician (200 μg/mL; Gibco, Carlsbad, CA). Approval for the conduct of this research was obtained from the Institutional Review Boards of the University of California and the Pacific Northwest National Laboratory in accordance with federal regulations. Cells were maintained at 37°C in a humidified atmosphere of 95% air and 5% CO_2, washed with phosphate buffered saline (PBS) and harvested at 70% confluency using a cell disassociation solution per manufacturer's instructions (Cell Dissociation Solution (1×) Non-enzymatic, Sigma, St. Louis, MO).

Membrane-enriched fractions were prepared separately for the 4 cell lines using the sucrose-cushion procedure described by Arnott et al. [10]. An aliquot from the membrane enriched fraction was prepared from the HMEC cell line and run through chromatography columns prior to MS/MS analysis. Membrane enriched fractions from the three carcinoma cell lines were pooled into a single mixture and separated into two aliquots, which were separately run through chromatography columns for duplicate analysis. All three aliquots were enzymatically digested (Sequence Grade Modified, Promega, Madison, WI), reduced with 10 mM DTT, and alkylated with 32 mM iodoacetamide prior to MS/MS analysis.

Peptide separation

Each aliquot was injected for strong-cation exchange (SCX) chromatography onto a Poly LC (Columbia, MD, USA) Polysulfoethyl A 200 mm x 9.4 mm column preceded by a 10 mm x 10 mm guard column at a flow rate of 4 mL/min. The separations were performed on a Shimadzu LC-10A system using a Unicam 4225 (Thermo Electron, Waltham, MA, USA) UV-Vis detector with mobile phases consisting of Solvent A (10 mM ammonium formate, 25% ACN, pH 3.0), and Solvent B (500 mM ammonium formate, 25% ACN, pH 6.8). Initially, the runs were isocratic at 100% Solvent A for 10 min followed by a linear gradient from solvent A to solvent B over 50 min. The gradient was held at 100% solvent B for 10 min, and then washed with water for 20 min prior to re-equilibrating with 100% Solvent A for 10 min. All SCX fractions (64 in aliquot 1; 68 in aliquot 2; 68 in aliquot 3) were collected, lyophilized to dryness, and stored at –80° C until analyzed. Reversed phase capillary LC separations were performed as previously reported [11].

Peptide, Protein and PTM identification

The capillary LC column was interfaced with a Finnigan LCQ ion trap mass spectrometer (ThermoFinnigan, San Jose, CA) with an electrospray ionization source. The initial MS survey scan utilized an m/z range of 400-2000 from which the 3 most abundant ions were selected for MS/MS analysis using collision energy of 45%. Dynamic exclusion was used to prevent repeated analysis of the same high abundance ions.

Unmodified peptide identification was performed using the open source identification algorithm, X!Tandem [12] implemented in a locally installed version of the Global Proteome Machine (GPM) [13]. The single spectra set from the HMEC cell line and two spectra sets from the duplicate cancer mixture analyses were individually searched against the December 2004 freeze of the human IPI database (http://www.ebi.ac.uk/IPI/IPIhelp.html) using a +/- 3 Da restriction on parent mass error, a 0.8 fragment mass error, and a contrast angle of 40° (default spectra filter). The search was enzymatically constrained for trypsin and allowed for 1 missed cleavage site. An expectation value (e-value)<.001 was used as a threshold for determining correct protein hits in addition to the requirement of two peptides/protein. In order to estimate the false positive rate associated with this threshold criteria, the three spectra sets were rerun against a set of nonsense peptides generated from a reverse ordered IPI database using the same search parameters. This methodology resulted in the identification of 2,235 unmodified proteins with an estimated false positive rate of <1% as estimated by both the reverse database and stochastic methods employed by X!Tandem.

A "database" of these unmodified proteins was constructed and interrogated further with three spectra sets allowing for eight forms of PTMs. Spectra were iteratively searched against this restricted set of proteins for dynamic modifications associated with phosphorylation, acetylation, O-GlcNAc, palmitoylation, C-mannosylation, hydroxylation, glucosylation, and S-nitrosylation using rules previously defined by the FindMod software tool [14]. Protein identifications and estimated false positive rates were calculated for each of the 24 runs (3 spectra sets X 8 PTM types) as described above. Receiver-operator curve (ROC) characteristics on all PTM searches done against a reverse

database indicated that the optimum false positive rate for protein identification was 5%. E-value thresholds were picked so estimated false positive rates were standardized at 5% across all PTM searches. In addition, spectra filter (contrast angle) values were selected so a standard number of spectra were used for protein identifications among all 3 sample runs. Since modified proteins are unlikely to be present in a sample unless the unmodified form is also present, we chose to focus only on those proteins identified in all 3 spectra sets during the unmodified search. PTMs associated with these 234 "core" proteins were the focus of all subsequent analysis for determining differential modifications in the normal and cancer cell lines.

Protein-Protein Interactions, Gene Expression Profiling, and Visualization

The entire set of protein-protein interaction data derived from high throughput two hybrid, mass spectrometry, and antibody-based experiments was downloaded from the BIND database. Interactions that have been shown experimentally and published in at least one peer-reviewed journal were retained, while those based on computational simulations were excluded from our analysis. The "core" protein set was cross-referenced with the pair-wise interaction data and was expanded to include proteins identified in at least one of our LC-MS/MS experiments that interacted directly with any of the "core" proteins. Conversely, some "core" proteins where eliminated from further analysis due to the lack of interaction data associated with them. The resulting "modified core dataset" (MCD) served as the basis for the visualization of interaction and gene expression data in future analyses.

A gene expression dataset representing 8102 human genes was obtained for the HMEC, MCF7, MDA-MD-231, and BT474 cell lines, as provided by Perou et. al. [15] through the Stanford Microarray Database [16]. In each cell line, the ratio of the abundance of transcripts of each gene to the median abundance of the gene's transcripts among a panel of 11 reference cell lines [15] is represented by a graduated red-green color scheme in the original gene expression array. Red indicates transcript levels above the median, green indicates transcript levels below the median, and color saturation reflects the magnitude of the ratio relative to the median for each gene. Normalized gene expression data was obtained for several proteins in the MCD protein dataset using default values for spot quality and expression differences (unflagged spots, regression coefficient >0.6). Using the open-source GeneCluster 2.0 program, a self-organizing map (SOM) clustering method was used to group these proteins into 12 non-overlapping clusters on the basis of similarity in the pattern with which their expression varied over the 4 cell lines (50000 iterations, 42 random seeds, 3 X 4 SOM, default parameters) [17].

Text files incorporating both the interaction and gene expression data were created and uploaded into the open-source program, Cytoscape [18] for visualization. Cytoscape is a network graphing program that represents proteins as nodes and interactions as edges/links between nodes. Networks of these interconnected nodes were picked for further discussion by 1) focusing on proteins thought to be associated with cancer, 2) focusing on proteins that were differentially modified in HMEC and Cancer and 3) by employing a modular complex detection (MCODE) Cytoscape plug-in that automatically detects high interconnected (dense) regions of networks [19]. Highly connected proteins (paxillin, PXN; vinculin, VCN) that showed a disproportionate number of interactions

catalogued in the BIND database, often served as delimiters when deciding on the size and extent of clusters picked for further investigation.

Results and Discussion

Application of the protein-level and peptide-level sample fractionations, combined with LC-MS/MS analysis, enabled confident identification of 2,235 unmodified proteins, representing a broad range of functional and compartmental classes. Figure 1A displays the number of detected proteins and the amount of overlap among the three sample runs. We identified a subset of 234 "core" proteins whose unmodified forms were detected in all samples (Appendix B, Table S1), comprising ~10% of the total proteins identified in our study. The majority of proteins detected were encoded by distinct genes. However, our dataset included several isoforms/alternative splice forms of the same gene product, which is a consequence of the sequence redundancy inherent in the IPI database used for protein identifications. Figure 1B shows the number of 'redundant' proteins detected using different sequence homology percentages for both the entire protein dataset (black) and the subset of "core" proteins (gray). As expected, the redundancy increased at lower threshold values. However, all of the proteins we identified were non-redundant at 95% sequence homology, a value commonly used in constructing 'stringent' non-redundant databases that are publicly available. Since the redundancy in our dataset was low, and considering that multiple isoforms of the same protein often have distinct biological roles within a cell, we elected to use the entire complement of 2,235 proteins and the 234 "core" proteins for subsequent functional analyses (Figure 1C).

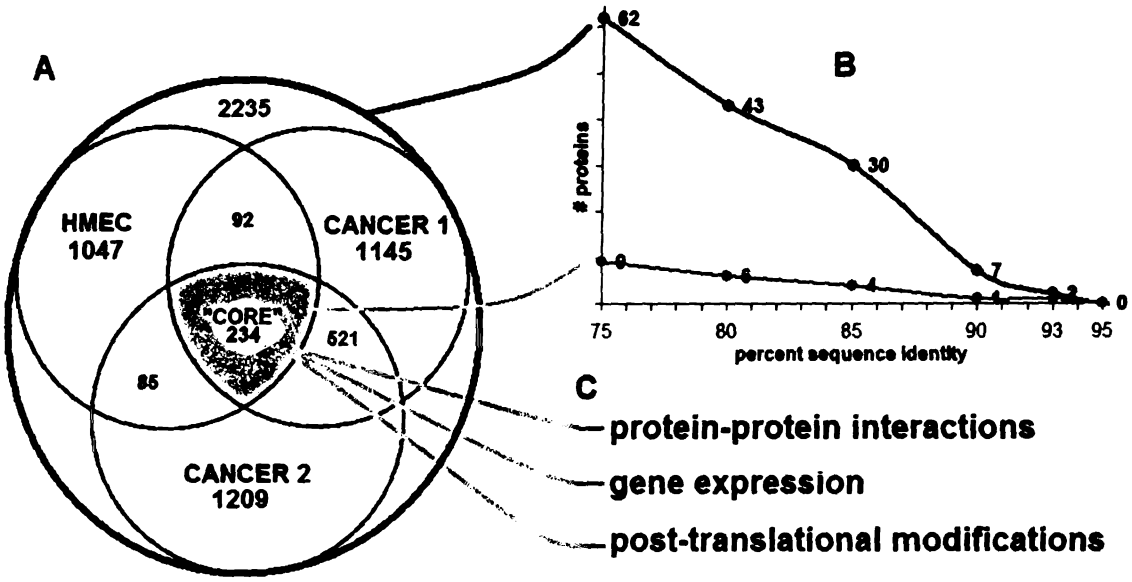

Figure 1. (A) displays the number of unmodified proteins detected in the HMEC cell line and in replicate runs of cancer samples. The redundancy within our list of detected proteins as determined by different sequence homology criteria is shown in (B). A common set of 234 "core" proteins were grouped using interactome and gene expression data and were further investigated for the occurrence of PTMs (C)

The classification of proteins using gene ontology (GO) terms has proven to be an effective method of grouping proteins into functional classes. Figure 2 displays the distribution (using the GO controlled vocabulary) of proteins across various biological processes, cellular organelles, and cellular membranes for the 3 samples and the common "core" protein set. Localization information was available for approximately 50% of the proteins; 45% of these were associated with the plasma membrane or organelle membranes (Appendix B, Table S1). The compositions of proteins in the replicate cancer analyses were similar with respect to both function and cellular location. The total number of HMEC proteins associated with the nucleus (30%) and plasma membrane (10%) differs slightly from values obtained in similar organelles in the cancer cell lines (12%/24% respectively) (Figure 2). A significant element of the variability of proteins identified in each analysis is attributable to membrane enrichment procedures, which are susceptible to sample loss. Selective protein losses resulting from sample processing procedures can be likened to loss of information in gene expression studies, where data for gene expression may be missing due to poor hybridization conditions or spot detection. Like comparative gene expression studies, the functional analysis we present below focuses only on those data points present across all experimental conditions (cell lines). This "core" protein-set insures that any differences seen among proteins in our samples are most likely attributable to true biological variation rather than sample processing or analysis biases.

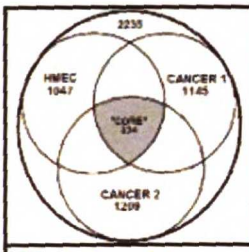

	HMEC	CANCER 1	CANCER 2	CORE	
					21-30%
					11-20%
					6-10%
					0-5%
Nucleic acid metabolism	153	68	66	24	Functional Categories
Signal transduction	98	147	153	29	
Carbohydrate metabolism	42	37	43	14	
Lipid metabolism	41	63	57	12	
Energy pathways	36	34	35	16	
Cell adhesion	34	46	58	16	
Cell motility	26	40	27	11	
Cell death	20	17	18	0	
Immune response	18	23	30	3	
Cell-cell signaling	14	14	16	4	
Regulation of cell proliferation	14	14	17	4	
Nucleus	163	79	80	28	Localization (n=510)
Cytoskeleton	86	78	76	38	
Mitochondrion	58	79	84	24	
ER	46	80	88	9	
Ribosome	29	18	25	11	
Golgi	28	46	51	6	
Plasma membrane	53	148	165	31	
Unknown	44	43	50	7	
Plasma membrane	53	148	165	31	Membrane Compartment (n=510)
Endomembrane system	17	32	30	0	
Nuclear membrane	14	8	8	0	
Mitochondrial membrane	11	26	27	9	
ER membrane	0	19	17	0	
Golgi membrane	0	7	7	0	

Figure 2. Distribution of detected proteins categorized according to biological functions, cellular locations, and membrane compartments for the HMEC, duplicate cancer samples, and "core" protein set. For cellular compartment categories, values are color coded

according to the percentage of total cellular proteins annotated by GO (510) that are represented.

Despite the popularity of GO based functional descriptions, limited gene coverage and the lack of experimental evidence associated with many GO annotations suggests that complimentary methods may be useful for comparative analysis of cell lines. In order to place the identified proteins in an interpretable biological context, we combined the results of our LC-MS/MS analyses with both protein-protein interaction data and mRNA gene expression studies. Unlike GO, which infers many functional assignments based on sequence homology to known proteins, the interaction (interactome) and expression datasets we used rely solely on primary experimental evidence.

Although several interaction databases currently exist, the Biomolecular Interaction Database (BIND) [20] was chosen as our interactome source because it is easily accessible, high quality, and frequently updated. We modified the "core" protein dataset to include and exclude identified proteins according to the availability of corresponding protein interaction data from the BIND database. Thirty additional proteins identified by LC-MS/MS in only 1-2 of the samples were added to the "core" dataset based on protein-protein interaction evidence available in BIND. Since multiple sources of experimental evidence in BIND indicated that these 30 proteins physically interacted with "core" proteins, we felt their inclusion was reasonable, even though they were not themselves "core" proteins. Conversely, twenty proteins with no interaction data available were eliminated. The resulting 244 interacting proteins constituted the "modified core dataset" (MCD). Considering that transcriptionally co-regulated genes are often functionally related [21], we also sought to identify clusters of these 244 interacting proteins that had

similar transcript expression profiles and that showed differential transcript abundances between the HMEC and cancer cell lines. Gene expression data for 85 of the proteins in the MCD dataset was obtained from a high-throughput microarray study investigating transcript abundance in a variety of cell lines and tumor tissue [15] (Figure 3).

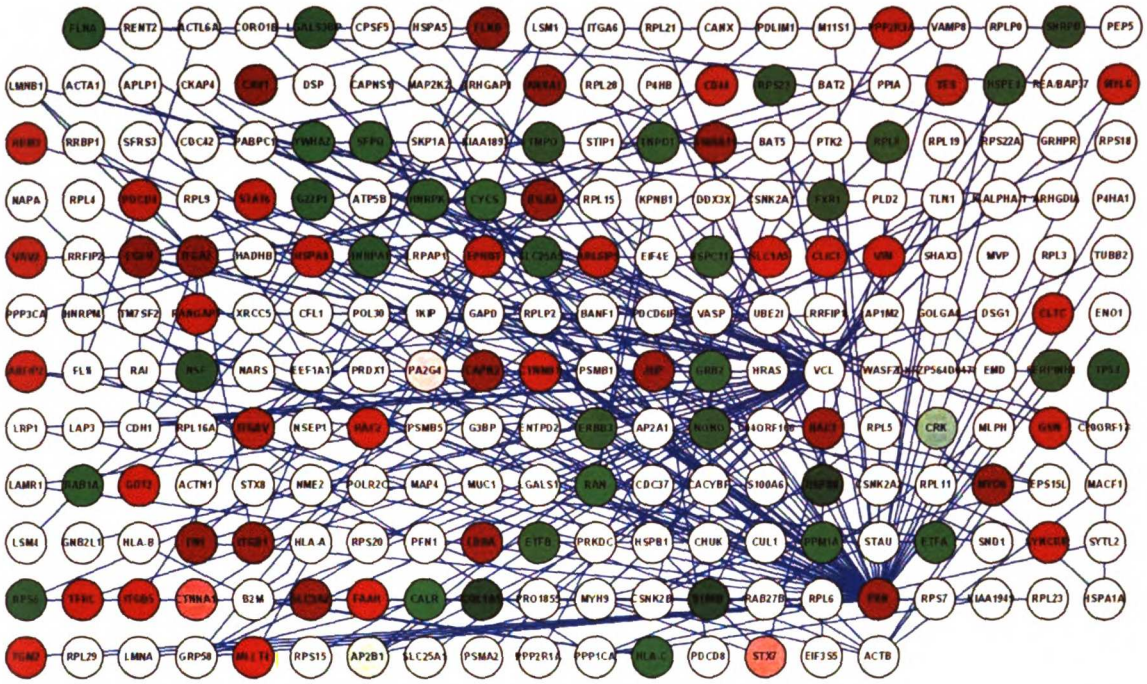

Figure 3. Interactions derived from the BIND database for the MCD protein set overlaid with corresponding gene expression data from the HMEC cell line (when available), where red indicates increased mRNA abundance and green indicated reduced mRNA abundance relative to a reference panel of cell lines. Individual gene names correspond to the identified proteins represented by a node.

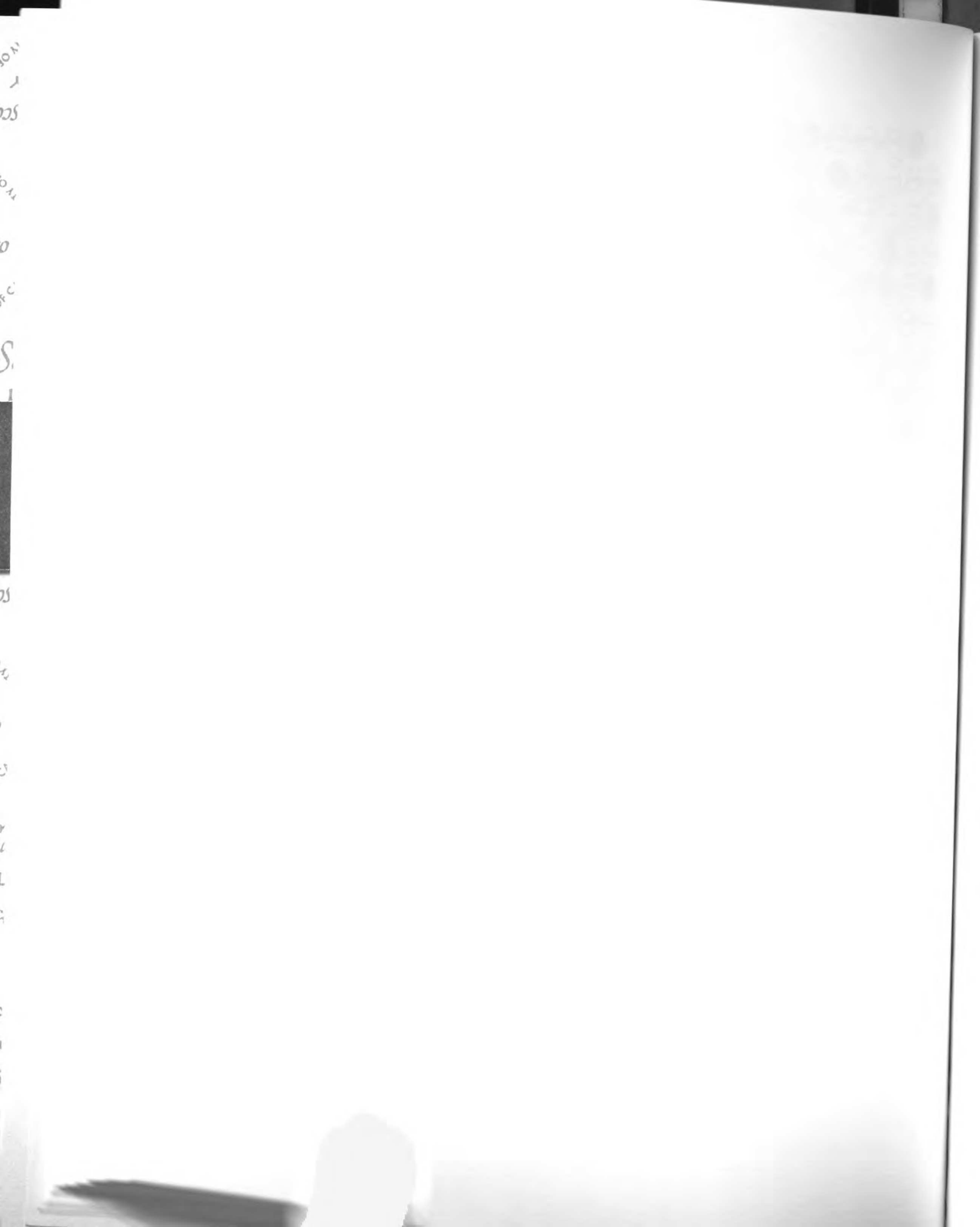

Figure 4 displays a single MCD-derived protein network that incorporates gene expression data in addition to the results from our clustering method. Nine interacting proteins (SLC3A2, PXN, ITGB1, ITGA2, FLNB, ITGB4, ITGAV, ITGA3, EGFR-yellow borders) were clustered together according to their gene expression profiles across the 4 cell lines. These proteins showed decreased transcript abundance in the cancer cell lines compared to HMEC cells. Notably, this cluster contains several integrin subunit (ITGB1, ITGB2, ITGB3, ITGAV, ITGB4) proteins that play a role in cellular adhesion and bind components of the extracellular matrix. There is evidence that the upregulation and downregulation of integrin receptors may play a role in cancer invasion and metastasis by altering the ability of cells to adhere to surrounding cells and the extracellular matrix [22]. The epidermal growth factor receptor (EGFR) protein shared a similar transcript profile with several of the integrin subunits across all 4 cell lines. Although no direct interaction data regarding EGFR and integrins were available in the BIND database, several reports suggest that EGFR receptor activation is governed by integrin mediated phosphorylation during cell adhesion [23-25]. More recently, the negative regulation of EGFR through integrin mediated activation of protein tyrosine phosphatase has also been described [26].

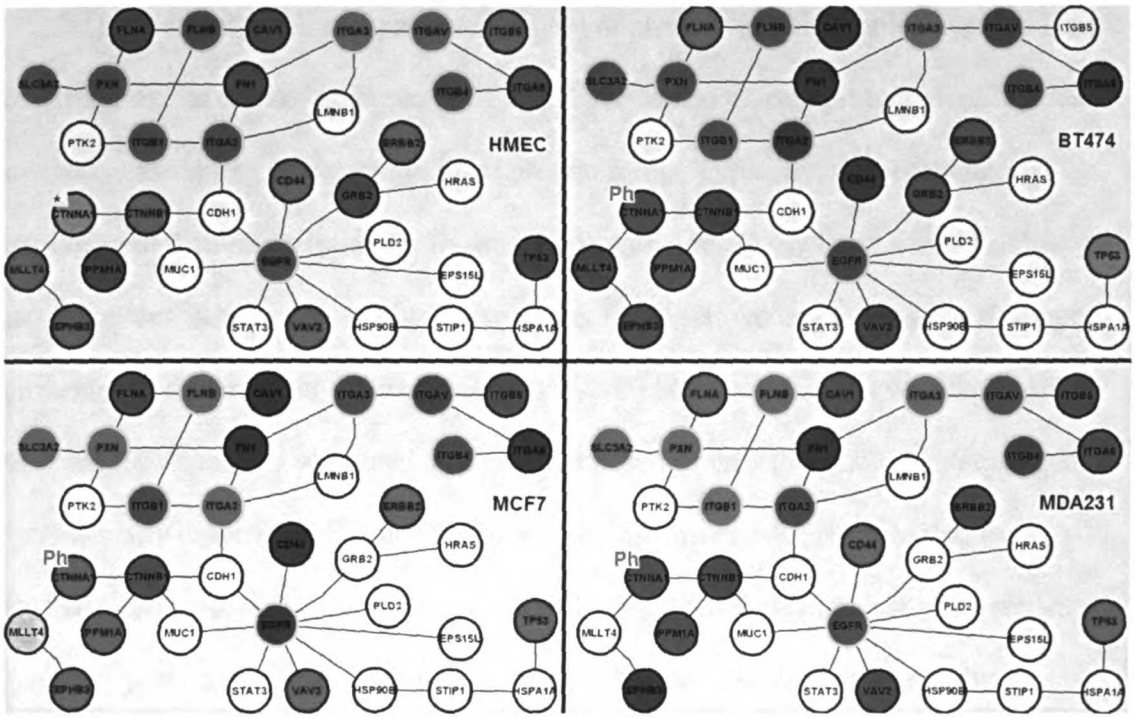

Figure 4. A single MCD derived network showing a highly interconnected group of proteins. Gene symbols correspond to the proteins identified in our sample. Hierarchical clustering of gene expression data revealed 9 proteins (yellow borders) in this network with similar transcript expression patterns across cell lines. Transcript expression data is overlaid for the HMEC, BT474, MCF7, and MDA-MB-231 cell line as indicated. Red indicates increased mRNA abundance and green indicats reduced mRNA abundance relative to a Reference panel of cell lines [15]. The "Ph" superscript indicates that phosphorylation was detected preferentially in the cancer cell lines and was absent in HMEC (*).

In addition to the comparative analysis of proteins in our samples, we also sought to exploit one of the key advantages of mass spectrometry based protein identification methods - the ability to detect modified protein forms. Typically, the combinatorial explosion of different peptide forms associated with a relatively large number of allowed modifications incurs a large false positive rate. However, we employed several search strategies to constrain the errors associated with PTM detection. First we searched for selected PTMs using a restricted database composed of only those 2,235 proteins that were initially detected in a non-PTM search. An estimated false positive rate was standardized across all PTM searches by replicating each search against a reversed-sequence protein database. The results of the PTM search were then filtered by sub-selecting the group of 234 "core" proteins whose unmodified forms were detected in all 3 sample runs (Appendix B, Table S1). This subset of proteins served as the focus of our PTM analysis with the rationale that the observation of a modified protein is more likely correct if its unmodified counterpart is also present. Finally, we required that the presence of a modification must be detected in both (replicate) cancer analyses. Although this constraint greatly reduced the number of modifications we considered as biologically relevant, we believe it was necessary to obtain a high confidence dataset and decrease the likelihood of false positives. The modified peptides can be found in this restricted set of proteins with high confidence despite the limited sensitivity of our approach. A summary of our PTM search strategy is summarized in Figure 5. We constrained our analysis to 8 types of PTMs: acetylation, glucosylation, C-mannosylation, S-nitrosylation, hydroxylation, phosphorylation, palmitoylation, and the monosaccharide O-linked beta-N-acetylglucosamine (O-GlcNAc). We were able to confidently detect more than 400

protein modifications for the "core" protein set (Appendix B, Table S1). However, only a small fraction of these modifications were detected in both cancer runs and even fewer had modifications occurring at the same peptide residue. Figure 6 displays the number of modified proteins detected across 8 PTMs in the duplicate cancer runs for 2,235 detected proteins and in the subset of 234 "core" proteins using these stringent criteria. Hydroxylation was the most frequent PTM identified in our samples. Approximately 30% of the hydroxylated proteins in our sample were associated with the extracellular matrix or cytoskeletal proteins, a finding consistent with the role of hydroxylation in collagen formation, actin binding, and crosslinking. The high number of hydroxylated proteins reflects the large proportion of cytoskeletal proteins in our dataset. In contrast, C-Mannosylation was detected in only a few proteins within our sample.

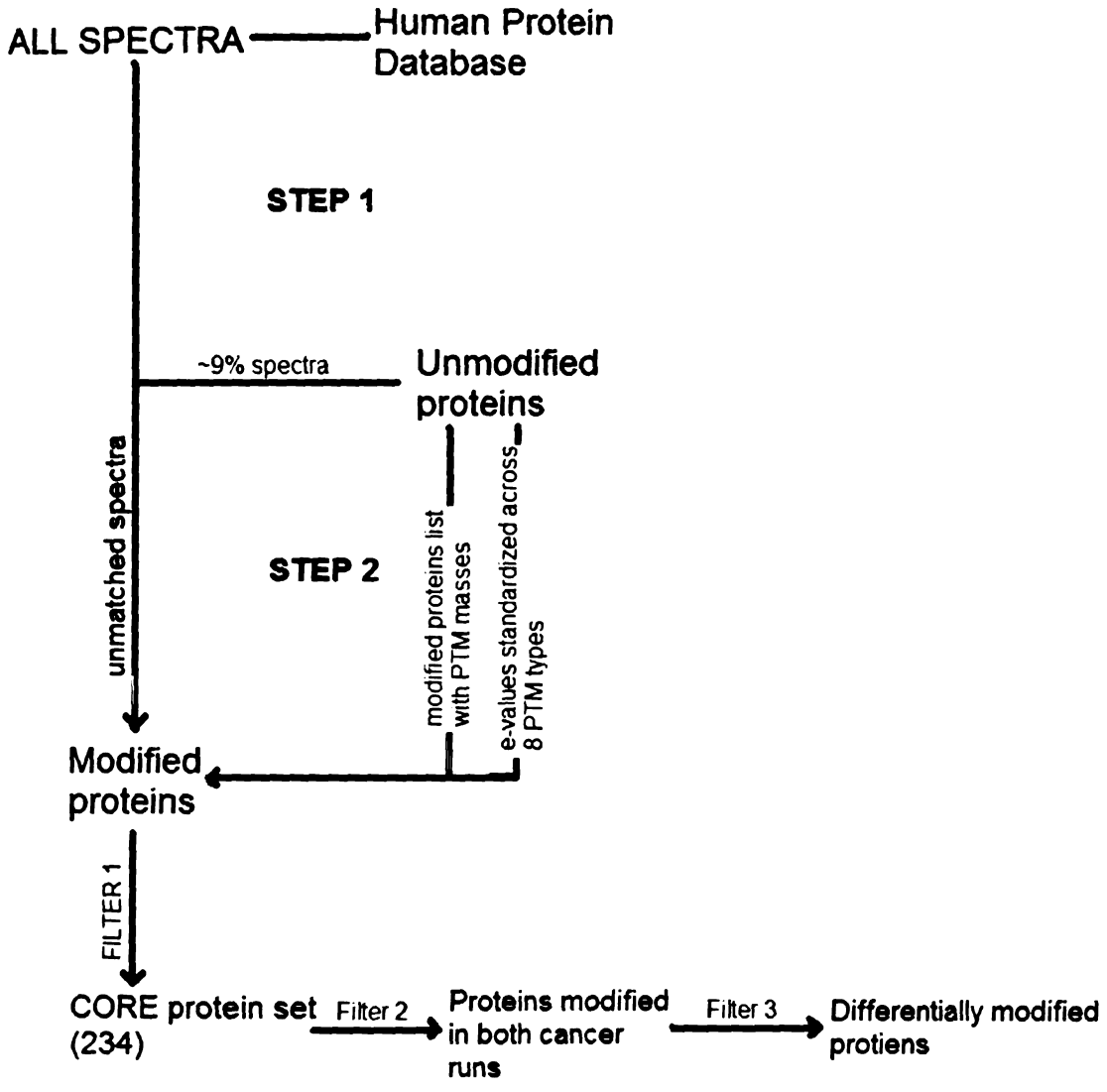

Figure 5. Diagram summarizing PTM search strategy. A 2-step process was used to identify modified proteins from a collection of unmodified proteins detected during a non-PTM search using standardized e-value thresholds calculated from reverse-sequence database searches. The collection of modified proteins were then filtered to include only those proteins with unmodified proteins identified in all 3 samples (Filter 1). This core protein set was further filtered to include only those proteins with modified forms detected in both cancer runs (Filter 2) and lacked modification in the HMEC cell line (Filter 3).

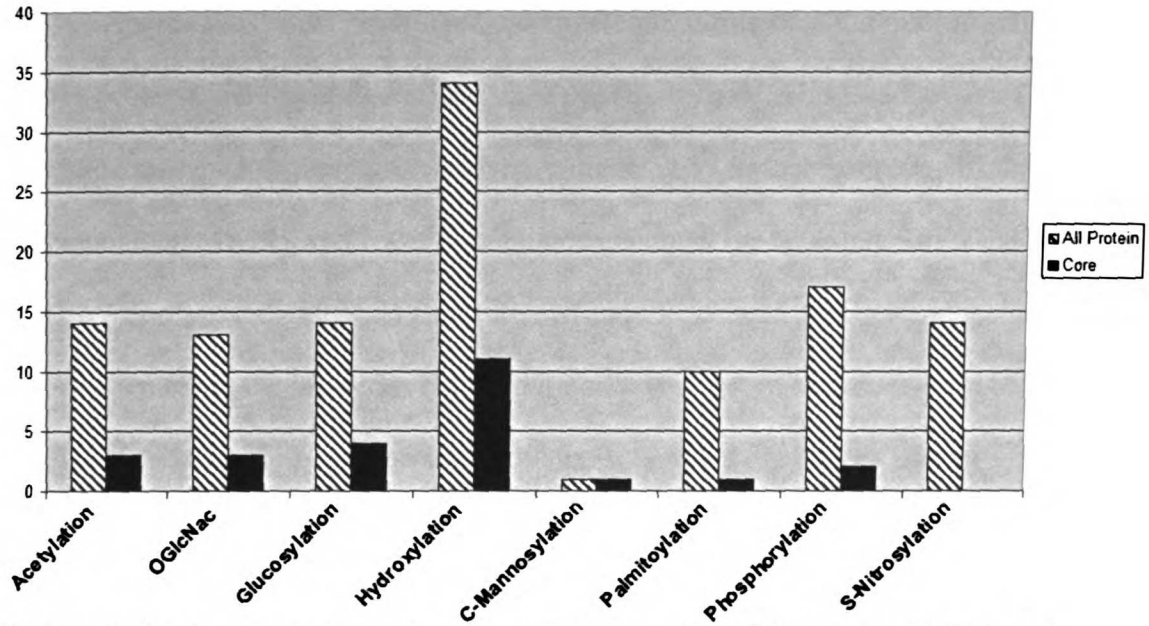

Figure 6. Number of modified proteins detected across 8 PTM categories for 2,235 proteins and the subset of 234 "core" proteins. Only those proteins modified in both cancer runs are included in this figure.

Among the "core" protein set, a comparison of fragment ion masses indicated that eleven proteins were modified on the same peptide residue in both cancer runs (Table 1). Modifications on 5 of these proteins were confirmed by further inspection of the corresponding MS/MS spectra after taking into account the occurrence of b and y-ions. Figure 7 displays individual fragmentation spectra for these 5 proteins and includes information about the ion-series detected for each peptide. In each case the modified residue was detected as a y type-ion, providing additional confidence that the modification was identified correctly. Additional confirmation of the phosphorylated protein was done by manually searching MS/MS spectra and confirming the loss of phosphoric acid (H_3PO_4), which is phosphopeptide-specific and generally represents a phosphopeptide's major fragmentation pathway. Four of these proteins (Coronin-1 Beta (CORO1B), Citrate Synthase (CS), eukaryotic translation elongation factor 1 alpha 1 (EEF1A1), and catenin, alpha 1 (CTNNA1)) were observed in both cancer runs, but were absent in the HMEC sample. These "differential" modifications are not definitive, since the absence of the corresponding modification in HMEC could theoretically be attributable to our sub-selection procedures or to the under-sampling inherent in MS based identification techniques. However, given that the modified proteins were sufficiently abundant to be detected in both duplicate cancer analyses, it is unlikely that the absence of a modification in HMEC would be a result of undersampling, particularly for a "core" protein. Thus, these data suggest that further studies exploring the functional significance of PTMs present in the cancer cell lines and absent in HMEC may be warranted. These data augment previous studies suggesting that selected PTMs play important roles in tumor progression, such as cell cycle check point, differentiation, and apoptosis [27-29].

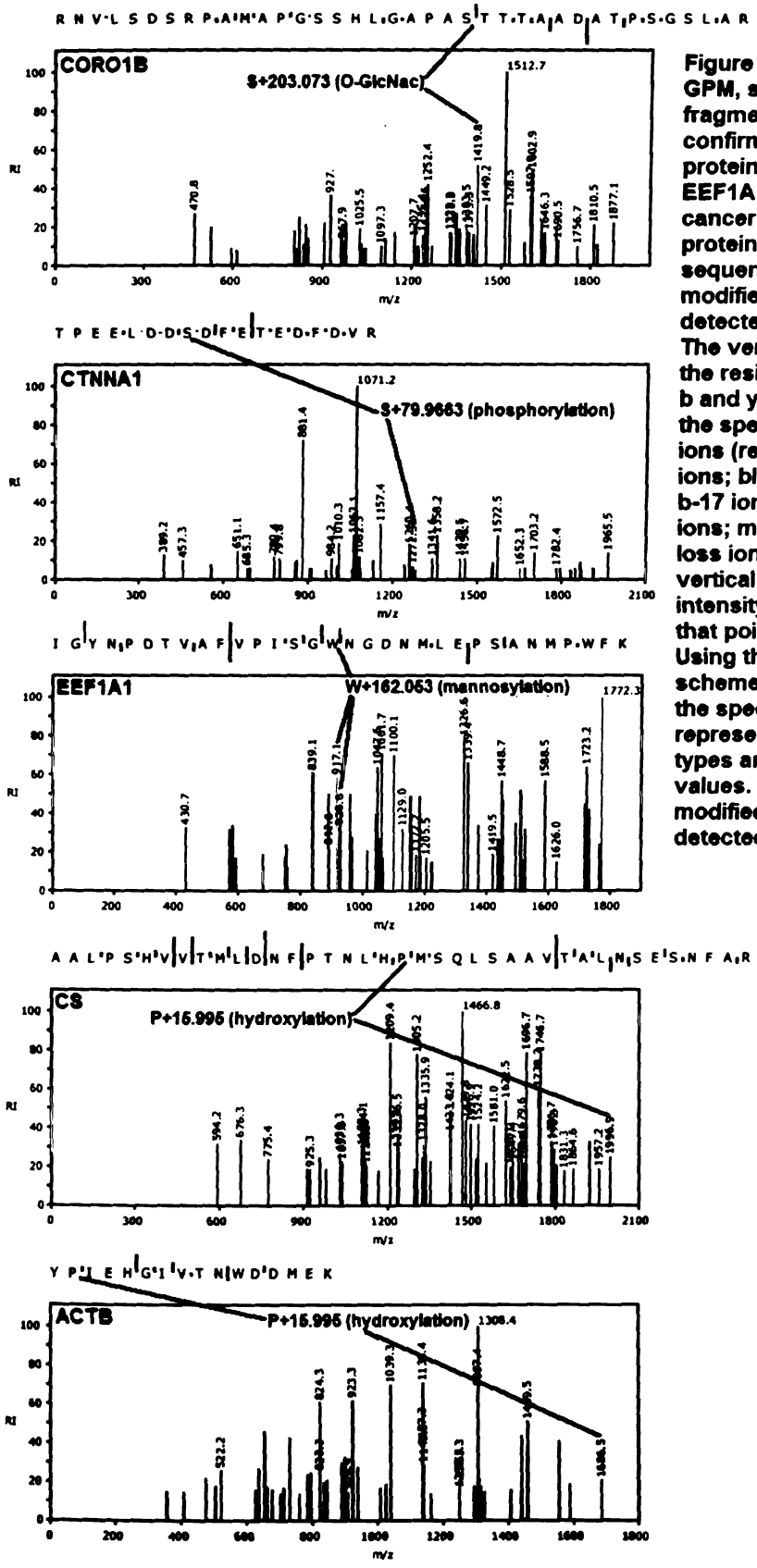

Figure 7. Output from the GPM, showing MS/MS fragmentation spectra that confirm modifications for 5 proteins (CORO1B, CTNNA1, EEF1A1, CS, ACTB) in the cancer cell lines. For each protein the peptide sequence from which the modified residue was detected is listed at the top. The vertical lines between the residues represents the b and y ion break down from the spectrum for assigned ions (red: y ions; yellow: y-17 ions; blue: b ions; green: b-17 ions; black: unassigned ions; mauve: trivial neutral loss ions). The length of the vertical lines represents the intensity of the ion peak at that point in the sequence. Using the same color scheme, vertical lines within the spectrum diagram represents different ion types and peaks at m/z values. For all 5 proteins, modified residues were detected as y-type ions.

UPI00000707D2:
log(e) = -83.4

(validate

```
  1 MTAVHAGNINFKWDPKSLEIRTLAVERLLEPLVTQVTTLVNTNSKGPSNKKRGRSKKAHV  60
 61 LAASVEQATENFLEKGDKIAKESQFLKEELVVAVEDVRKQGDLMKAAAGEFADDPCSSVK 120
121 RGNMVRAAPALLSAVTRLLILADMADVYKLLVQLKVVEDGILKLRNAGNEQDLGNQYKAL 180
181 KPEVDKLNIMAAKRQQELKDVGHRDQMAAAARGILQSNVPILYTASQACLQHPDVAAYKAN 240
241 RDLIYKQLQQAVTGISNAAQATASDDASQHQGGGGGELAYALNNFDKQIIVDPLSFSEER 300
301 FRPSLEERLESIISGAALMADSSCTRDDRRERIVAECNAVRQACRTCVSEYMGNAGRKER 360
361 SDALNSAIDKMTKKTRDLRRQLRKAVMDHVSDSFLETNVPLLVLIEAAKNGNEKEVKEYA 420
421 QVFREHANKLIEVANLACSISNNEEGVKLVRMSASQLEAGCPQVINAATWALAPKPQSKL 480
481 AQENMDLFKEQWEKQVRVLTDAVDDITSIDDFLAVSENHILEDVNKCVIALQEKDVDGLD 540
541 RTAGAIRGRAARVIHVVTSEMDNYEPGVYTEKVLEATKLLSNTVMPRFTEQVEAAVEALS 600
601 SDPAQPMDENEFIDASRLVYDGIRDIRKAVLMIRTPEELDDSDFETEDFDVRSETSVQTE 660
661 DDQLIAGQSARAIMAQLPQEQFAKIREQVASFQEEKSKLDAEVSKWDDSGNDIIVLAKQM 720
721 CMIMMEMTDFTRGKGPLKNTSDVISAAKKIAEAGSRMDKLGRTIRDHCPDSACKQDLLAY 780
781 LQRIALYCHQLNICSKVKAEVQNLGGELVVSGNCDTCGALQGLKGWPPPLCLATHWVDSA 840
841 MSLIQAAKNLMNAVVQTVKASYVASTKYQKSQGMASLNLPAVSMKMKAPEKKPLVKREKQ 900
901 DETQTKIKRASQKKHVNPVQALSEFKAMDSI                              931
```

spectrum	log (e)	log (I)	m+h	delta	z	sequence
85183.1	-1.8	7.37	1970.118	0.632	1	aver[28]LLEPLVTQVTTLVNTNSK[45]gpsn
232738.1	-5.8	5.57	2085.099	-0.069	2	grsk[57]KAHVLAASVEQATENFLEK[75]gdki
182302.1	-3.4	7.30	2257.147	1.143	3	rskk[58]AHVLAASVEQATENFLEKGDK[78]iake
153047.1	-11.2	7.90	1957.004	0.586	2	rskk[58]AHVLAASVEQATENFLEK[75]gdki
192976.1	-2.2	7.08	1640.942	1.778	1	nqyk[179]ALKPEVDKLNIMAAK[193]rqqe
96096.1	-5.4	6.04	4103.930	1.010	3	liyk[247]QLQQAVTGISNAAQATASDDASQHQGGGGGELAYALNNFDK[287]qiiv
90571.1	-3.0	7.80	1532.797	0.774	2	nfdk[288]QIIVDPLSFSEER[300]frps
100741.1	-2.1	7.11	1033.517	1.953	1	rker[361]SDALNSAIDK[370]mtkk
159582.1	-4.6	6.11	2839.528	0.722	3	rqlr[384]KAVMDHVSDSFLETNVPLLVLIEAAK[409]ngne
134865.1	-1.8	6.77	1908.917	0.823	2	pqsk[480]LAQENMDLFKEQWEK[494]qvrv
91538.1	-3.0	7.62	3200.585	1.145	3	kqvr[498]VLTDAVDDITSIDDFLAVSENHILEDVNK[526]cvia
128698.1	-9.5	7.92	2310.097	0.173	2	raar[553]VIHVVTSEMDNYEPGVYTEK[572]vlea
44112.1	-4.0	6.33	2238.861	-0.011	2	lmir[635]TPEELDDSDFETEDFDVR[652]sets
106490.1	-3.7	5.82	2188.115	0.835	2	eksk[699]DAEVSKWDDSGNDIIVLAK[718]qmcm
84687.1	-3.2	7.38	1445.728	0.218	1	evsk[706]WDDSGNDIIVLAK[718]qmcm
105929.1	-1.4	6.99	1805.522	-0.132	1	gplk[739]NTSDVISAAK[748]kiae
111501.1	-1.8	7.77	1216.673	1.897	1	qaak[849]NLMNAVVQTVK[859]asyv
193193.1	-4.3	6.60	1368.728	0.632	2	sqkk[915]HVNPVQALSEFK[926]amds

bond	^{+1}y	$^{+1}y^{*}$	^{+1}b	$^{+1}b^{*}$
T_1	2137.812	2120.796	102.051	85.035
P_2	2040.759	2023.743	199.104	182.088
E_3	1911.717	1894.701	328.146	311.130
E_4	1782.674	1765.658	457.189	440.173
L_5	1669.590	1652.574	570.273	553.257
D_6	1554.563	1537.547	685.300	668.284
D_7	1439.536	1422.520	800.327	783.311
S_8	1272.538	1255.522	967.325	950.309
D_9	1157.511	1140.495	1082.352	1065.336
F_{10}	1010.443	993.427	1229.420	1212.404
E_{11}	881.400	864.384	1358.463	1341.447
T_{12}	780.352	763.336	1459.511	1442.495
E_{13}	651.310	634.294	1588.553	1571.537
D_{14}	536.283	519.267	1703.580	1686.564
F_{15}	389.214	372.198	1850.649	1833.633
D_{16}	274.187	257.171	1965.676	1948.660
V_{17}	175.119	158.103	2064.744	2047.728

Figure 8. Expanded peptide coverage and fragmentation information for CTNNA1, which was phosphorylated. Identified peptides are highlighted in red in the protein sequence and listed with corresponding scoring information. The ion-series for the phosphorylated peptide is shown at the bottom

Recently several projects aimed at elucidating unknown gene products using predictive approaches have shown that PTMs are important features for determining protein function [30, 31]. In particular, several programs that include PTMs as predictive input have successfully classified so called 'orphan proteins'- proteins with no homology to protein of known function [32]. Since the absence or presence of modifications can influence or determine the functional activity of a protein, we incorporated PTM information for the five confirmed modifications listed in Table 1 in the MCD-derived networks.

The phosphorylated form of the alpha-1 catenin (CTNNA1/Cadherin-associated protein/Alpha E-catenin) protein was preferentially expressed in the cancer cell lines (Figure 4). CTNNA1 is associated with the cytoplasmic domain of a variety of cadherins, producing a complex that is linked to the actin filament network. The CTNNA1-cadherin complex has a key role in cell adhesion [33]. Downregulation of the expression of cadherin or catenin family members or activation of signaling pathways that prevent the assembly of the adhesion complex [34] have been implicated in altered cell adhesion properties. Mutations in the alpha-catenin gene, CTNNA1, have been shown to lead to the loss of cell-cell adhesion in different types of cancer [35, 36] and several studies have shown that phosphorylation of tyrosine residues on beta-catenin regulates cell-cell adhesion [37-39]. While similar phosphorylative regulation of the alpha-catenin protein is not yet well established in cancer, our results suggest that further investigation may be warranted.

Figure 9 displays two MCD-derived networks that contain three modified proteins. Of particular interest is the O-GlcNAc modification of the Coronin-1B (CORO1B) protein, which was also preferentially detected in the cancer cell line mixture . CORO1B

is a cytoskeletal protein postulated to be involved in cytokinesis, motility, and signal transduction [40]. Most O-GlcNAc-modified proteins are preferentially restricted to the cytoplasm and nucleus. Previous studies regarding the O-GlcNAc modification in cytoskeletal proteins have shown that proteins such as vinculin, talin, synapsin, clathrin carry O-GlcNAc moieties [41], implicating the role of O-GlcNAc in mediating protein-protein interactions involved in a wide variety of cellular functions, including the organization of the cytoskeleton. To our knowledge, our data are the first to indicate an O-GlcNAc modification of Coronin-1B. Interestingly, CORO1B also binds directly with actin (ACTB), which we detected as hydroxylated in both the HMEC and cancer cell lines.

A mannosylated form of the EEF1A1 protein was also preferentially detected in the cancer cell lines. This cytoplasmic protein promotes the binding of tRNA to ribosomes during protein biosynthesis and is involved in cytoskeletal remodeling [42] and is ubiquitously expressed. Overexpression of EEF1A has frequently been implicated in tumor development [43-45] and EEF1A is a putative oncogene in ovarian cancer [46]. EEF1A1 has been shown previously to be post-translationally modified, most notably by methylation of lysine residues [47] and the addition of ethanolamine-phosphoglycerol to glutamine residues [48]. C-mannosylation, however, has not been reported previously for EEF1A1. C-mannosylation has previously been described in several proteins, including RNase2, interleukin-12, complements (C6, C7, C8a, C8b, and C9), properdin, thrombospondin, F-spondin, the erythropoietin receptor, and mucins (MUC5AC and MUC5B) [49-54]. The recognition sequence for C-mannosylation in most of these proteins is Trp-X-X-Trp, where the first tryptophan residue is modified [55]. However, modification of

EEF1A1 in our study revealed C-mannosylation of tryptophan residues outside the Trp-X-X-Trp motif- a result similar to studies of the human complement system [56]. Although the biological significance of C-mannosylation has not been fully established, recent studies have implicated this modification in hyperglycemic conditions [57] and as part of the normal intracellular biosynthetic route of secreted proteins [58]. Given the putative role of EEF1A in tumor development, further investigation and validation should explore the role of C-mannosylated EEF1A1 in the cancer phenotype.

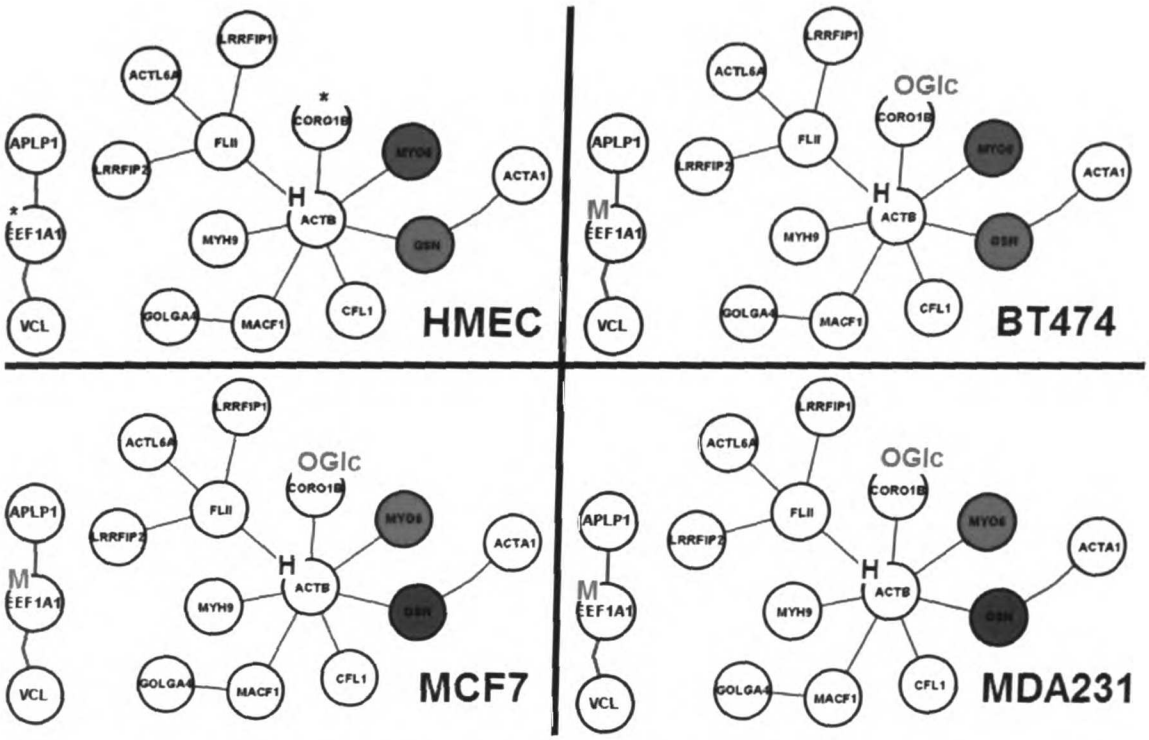

Figure 9. Two MCD derived networks. Superscripts indicate PTMs (OGlc- O-GlcNAc; H-hydroxylation; M-mannosylation) detected only in the cancer sample and absent in HMEC (*). Gene expression data is overlaid for the HMEC, BT474, MCF7, and MDA-MB-231 cell line as indicated.

Conclusion

Using high-throughput LC-MS/MS techniques, we confidently identified a collection of unmodified and post-translationally modified proteins. By combining this dataset with other high-throughput protein-protein interaction and gene expression datasets, we isolated functionally related proteins whose regulation appears to segregate with the cancer phenotype. By focusing only on those proteins commonly expressed in all our samples we were able to 1) subselect only those transcripts that are actually translated into mature protein products and 2) compare expression data between cancer and non-cancer cell lines. The additional protein-protein interaction data added a functional component, which allowed us to identify groups of binding proteins whose transcriptional profile differed across these cell lines, thus facilitating the study of biologically relevant metabolic pathways in cancer. Our proteome data allowed us to examine the post-translational regulation of protein expression, which is not predicted from RNA or DNA analyses. Many of the proteins we identified had previously undocumented modifications that were preferentially expressed in the cancer cell lines. The native and modified forms of these proteins may serve as targets in future quantitative proteomics studies in order to determine the significance of these modifications in cancer.

Table 1. Peptide e-values, peptide mass, experimental/theoretical mass difference, charge state, and modified sequences are shown for eleven proteins with PTMs detected in both cancer runs, as indicated by fragment ion masses. Proteins in red indicate those modifications that were further confirmed by inspection of MS/MS spectra. Modified residues are also shown in red.

Modification	Symbol	Run	log(e)	mass	delta	z	modified sequence
Acetylation	S100A11	1	-1	4024	0.673	3	[67]LDTNSDGQLDFSEFLNLIGGLAMA CHDSFLKAVPSQK[103]
		2	-2.5	3542	2.511	3	[65]KLDTNSDGQLDFSEFLNLIGGLAM ACHDSFLK[97]
	HSP90B	1	-1.3	2772	0.974	3	[286]TKPIWTRNPDDITQEEYGEFYK[306]
		2	-2.1	2772	-0.3	3	[286]TKPIWTRNPDDITQEEYGEFYK[306]
OGlcNac	CORO1B	1	-1.2	3726	-0.19	3	[410]NVLSDSRPAMAPGSSHLGAPAS TTTAADATPSGSLAR[446]
		2	-1.2	3726	-0.19	3	[410]NVLSDSRPAMAPGSSHLGAPAS TTTAADATPSGSLAR[446]
Hydroxylation	CS	1	-3.5	4168	2.55	3	[79]AALPSHVVTMLDNFPTNLHPMSQ LSAAVTALNSESNFAR[117]
		2	-4.1	4168	1	3	[79]AALPSHVVTMLDNFPTNLHPMSQ LSAAVTALNSESNFAR[117]
	ITGB4	1	-2.1	3617	0.506	3	[792]WKVTNNMQRPGFATHAASINPT ELVPYGLSLR[823]
		2	-2	3617	0.716	3	[792]WKVTNNMQRPGFATHAASINPT ELVPYGLSLR[823]
	ACTB	1	-1.9	1963	2.359	2	[69]YPIEHGIVTNWDDMEK[84]
		2	-1.1	1963	2.919	2	[69]YPIEHGIVTNWDDMEK[84]
	VIL2	1	-1.1	1489	0.745	2	[295]RKPDTIEVQQMK[306]
		2	-2.5	1489	0.475	2	[295]RKPDTIEVQQMK[306]
Mannosylation	EEF1A1	1	-1.2	3730	-1.22	3	[181]IGYNPDTVAFVPISGWNGDNMLE PSANMPWFK[212]
		2	-1.2	3858	-2.97	3	[180]KIGYNPDTVAFVPISGWNGDNML EPSANMPWFK[212]
Palmitoylation	ARL6IP5	1	-2.4	3172	-1.21	3	[160]TPMGMLDALEQQEEGINRLTDYI SK[185]
		2	-1.9	3172	0.737	3	[160]TPMGMLDALEQQEEGINRLTDYI SK[185]
Phosphorylation	CTNNA1	1	-4	2239	-0.01	2	[635]TPEELDDSDFETEDFDVR[652]
		2	-4.1	2239	0.659	2	[635]TPEELDDSDFETEDFDVR[652]

Appendix B

Table S1. Table listing IPI identifiers and corresponding PTMs for the 2,235 proteins identified with MS/MS in the normal cell line run and the duplicate cancer mixture runs using filtering and scoring criteria as shown. 234 "core" proteins (yellow) had their unmodified protein forms identified in all 3 spectra sets.

Acknowledgements

This work was supported by the NIH CA86135 (MP), the NIH National Center for Research Resources (RR18522), and the Environmental Molecular Science Laboratory (a national scientific user facility sponsored by the Department of Energy's Office of Biological and Environmental Research and located at Pacific Northwest National Laboratory). Pacific Northwest National Laboratory is a multi-program national laboratory operated by Battelle Memorial Institute for the U.S. Department of Energy under contract DE-AC05-76RLO-1830. The authors would like to thank Scott Dixon and Katy Williams for advice and help in sample preparation and Heather Mottaz for help in chromatography and preparing samples for proteome analysis.

Reference

(1) Harrison, P. M.; Kumar, A.; Lang, N.; Snyder, M.; Gerstein, M. *Nucl. Acids. Res.* **2002**, *30*, 1083-1090.

(2) Anderson, L.; Seilhamer, J. *Electrophoresis* **1997**, *18*, 533-537.

(3) Futcher, B.; Latter, G. I.; Monardo, P.; McLaughlin, C. S.; Garrels, J. I. *Mol Cell Biol* **1999**, *19*, 7357-7368.

(4) Gygi, S. P.; Rochon, Y.; Franza, B. R.; Aebersold, R. *Mol Cell Biol* **1999**, *19*, 1720-1730.

(5) Mann, M.; Jensen, O. N. *Nat Biotechnol* **2003**, *21*, 255-261.

(6) McRedmond, J. P.; Park, S. D.; Reilly, D. F.; Coppinger, J. A.; Maguire, P. B.; Shields, D. C.; Fitzgerald, D. J. *Mol Cell Proteomics* **2004**, *3*, 133-144.

(7) Kleffmann, T.; Russenberger, D.; von Zychlinski, A.; Christopher, W.; Sjolander, K.; Gruissem, W.; Baginsky, S. *Curr Biol* **2004**, *14*, 354-362.

(8) Mootha, V. K.; Lepage, P.; Miller, K.; Bunkenborg, J.; Reich, M.; Hjerrild, M.; Delmonte, T.; Villeneuve, A.; Sladek, R.; Xu, F.; Mitchell, G. A.; Morin, C.; Mann, M.; Hudson, T. J.; Robinson, B.; Rioux, J. D.; Lander, E. S. *Proc Natl Acad Sci U S A* **2003**, *100*, 605-610.

(9) Benz, C. C.; Scott, G. K.; Sarup, J. C.; Johnson, R. M.; Tripathy, D.; Coronado, E.; Shepard, H. M.; Osborne, C. K. *Breast Cancer Res Treat* **1993**, *24*, 85-95.

(10) Arnott, D.; Kishiyama, A.; Luis, E. A.; Ludlum, S. G.; Marsters, J. C., Jr.; Stults, J. T. *Mol Cell Proteomics* **2002**, *1*, 148-156.

(11) Shen, Y.; Zhao, R.; Belov, M. E.; Conrads, T. P.; Anderson, G. A.; Tang, K.; Pasa-Tolic, L.; Veenstra, T. D.; Lipton, M. S.; Udseth, H. R.; Smith, R. D. *Anal Chem* **2001**, *73*, 1766-1775.

(12) Craig, R.; Beavis, R. C. *Bioinformatics* **2004**, *20*, 1466-1467.

(13) Craig, R.; Cortens, J. P.; Beavis, R. C. *J Proteome Res* **2004**, *3*, 1234-1242.

(14) Wilkins, M. R.; Gasteiger, E.; Gooley, A. A.; Herbert, B. R.; Molloy, M. P.; Binz, P. A.; Ou, K.; Sanchez, J. C.; Bairoch, A.; Williams, K. L.; Hochstrasser, D. F. *J Mol Biol* **1999**, *289*, 645-657.

(15) Perou, C. M.; Sorlie, T.; Eisen, M. B.; van de Rijn, M.; Jeffrey, S. S.; Rees, C. A.; Pollack, J. R.; Ross, D. T.; Johnsen, H.; Akslen, L. A.; Fluge, O.; Pergamenschikov, A.; Williams, C.; Zhu, S. X.; Lonning, P. E.; Borresen-Dale, A. L.; Brown, P. O.; Botstein, D. *Nature* **2000**, *406*, 747-752.

(16) Ball, C. A.; Awad, I. A.; Demeter, J.; Gollub, J.; Hebert, J. M.; Hernandez-Boussard, T.; Jin, H.; Matese, J. C.; Nitzberg, M.; Wymore, F.; Zachariah, Z. K.; Brown, P. O.; Sherlock, G. *Nucleic Acids Res* **2005**, *33 Database Issue*, D580-582.

(17) Reich, M.; Ohm, K.; Angelo, M.; Tamayo, P.; Mesirov, J. P. *Bioinformatics* **2004**, *20*, 1797-1798.

(18) Shannon, P.; Markiel, A.; Ozier, O.; Baliga, N. S.; Wang, J. T.; Ramage, D.; Amin, N.; Schwikowski, B.; Ideker, T. *Genome Res* **2003**, *13*, 2498-2504.

(19) Bader, G. D.; Hogue, C. W. *BMC Bioinformatics* **2003**, *4*, 2.

(20) Bader, G. D.; Betel, D.; Hogue, C. W. *Nucleic Acids Res* **2003**, *31*, 248-250.

(21) DeRisi, J. L.; Iyer, V. R.; Brown, P. O. *Science* **1997**, *278*, 680-686.

(22) Shimizu, H.; Koyama, N.; Asada, M.; Yoshimatsu, K. *Int J Oncol* **2002**, *21*, 1073-1079.

(23) Miyamoto, S.; Teramoto, H.; Gutkind, J. S.; Yamada, K. M. *J. Cell Biol.* **1996**, *135*, 1633-1642.

(24) Moro, L.; Dolce, L.; Cabodi, S.; Bergatto, E.; Erba, E. B.; Smeriglio, M.; Turco, E.; Retta, S. F.; Giuffrida, M. G.; Venturino, M.; Godovac-Zimmermann, J.; Conti, A.; Schaefer, E.; Beguinot, L.; Tacchetti, C.; Gaggini, P.; Silengo, L.; Tarone, G.; Defilippi, P. *J Biol Chem* **2002**, *277*, 9405-9414.

(25) Moro, L.; Venturino, M.; Bozzo, C.; Silengo, L.; Altruda, F.; Beguinot, L.; Tarone, G.; Defilippi, P. *Embo J* **1998**, *17*, 6622-6632.

(26) Mattila, E.; Pellinen, T.; Nevo, J.; Vuoriluoto, K.; Arjonen, A.; Ivaska, J. *Nat Cell Biol* **2005**, *7*, 78-85.

(27) Vaghefi, H.; Neet, K. E. *Oncogene* **2004**, *23*, 8078-8087.

(28) Tomonaga, T.; Matsushita, K.; Yamaguchi, S.; Oh-Ishi, M.; Kodera, Y.; Maeda, T.; Shimada, H.; Ochiai, T.; Nomura, F. *Clin Cancer Res* **2004**, *10*, 2007-2014.

(29) Thompson, H. G.; Harris, J. W.; Brody, J. P. *Int J Cancer* **2004**, *111*, 338-347.

(30) Jensen, L. J.; Gupta, R.; Staerfeldt, H. H.; Brunak, S. *Bioinformatics* **2003**, *19*, 635-642.

(31) Jensen, L. J.; Ussery, D. W.; Brunak, S. *Genome Res* **2003**, *13*, 2444-2449.

(32) de Lichtenberg, U.; Jensen, T. S.; Jensen, L. J.; Brunak, S. *J Mol Biol* **2003**, *329*, 663-674.

(33) Ben-Ze'ev, A.; Geiger, B. *Curr Opin Cell Biol* **1998**, *10*, 629-639.

(34) Vanpoucke, G.; Nollet, F.; Tejpar, S.; Cassiman, J. J.; van Roy, F. *Biochim Biophys Acta* **2002**, *1574*, 262-268.

(35) Hirano, S.; Kimoto, N.; Shimoyama, Y.; Hirohashi, S.; Takeichi, M. *Cell* **1992**, *70*, 293-301.

(36) Bullions, L. C.; Notterman, D. A.; Chung, L. S.; Levine, A. J. *Mol Cell Biol* **1997**, *17*, 4501-4508.

(37) Roura, S.; Miravet, S.; Piedra, J.; de Herreros, A. G.; Dunach, M. *J. Biol. Chem.* **1999**, *274*, 36734-36740.

(38) Piedra, J.; Martinez, D.; Castano, J.; Miravet, S.; Dunach, M.; de Herreros, A. G. *J. Biol. Chem.* **2001**, *276*, 20436-20443.

(39) Kinch, M. S.; Clark, G. J.; Der, C. J.; Burridge, K. *J. Cell Biol.* **1995**, *130*, 461-471.

(40) Okumura, M.; Kung, C.; Wong, S.; Rodgers, M.; Thomas, M. L. *DNA Cell Biol* **1998**, *17*, 779-787.

(41) Hart, G. W. *Annu Rev Biochem* **1997**, *66*, 315-335.

(42) Yang, F.; Demma, M.; Warren, V.; Dharmawardhane, S.; Condeelis, J. *Nature* **1990**, *347*, 494-496.

(43) Thornton, S.; Anand, N.; Purcell, D.; Lee, J. *J Mol Med* **2003**, *81*, 536-548.

(44) Tatsuka, M.; Mitsui, H.; Wada, M.; Nagata, A.; Nojima, H.; Okayama, H. *Nature* **1992**, *359*, 333-336.

(45) Shen, R.; Su, Z. Z.; Olsson, C. A.; Fisher, P. B. *Proc Natl Acad Sci U S A* **1995**, *92*, 6778-6782.

(46) Anand, N.; Murthy, S.; Amann, G.; Wernick, M.; Porter, L. A.; Cukier, I. H.; Collins, C.; Gray, J. W.; Diebold, J.; Demetrick, D. J.; Lee, J. M. *Nat Genet* **2002**, *31*, 301-305.

(47) Hiatt, W. R.; Garcia, R.; Merrick, W. C.; Sypherd, P. S. *Proc Natl Acad Sci U S A* **1982**, *79*, 3433-3437.

(48) Whiteheart, S. W.; Shenbagamurthi, P.; Chen, L.; Cotter, R. J.; Hart, G. W. *J. Biol. Chem.* **1989**, *264*, 14334-14341.

(49) Gonzalez de Peredo, A.; Klein, D.; Macek, B.; Hess, D.; Peter-Katalinic, J.; Hofsteenge, J. *Mol Cell Proteomics* **2002**, *1*, 11-18.

(50) Furmanek, A.; Hofsteenge, J. *Acta Biochim Pol* **2000**, *47*, 781-789.

(51) Furmanek, A.; Hess, D.; Rogniaux, H.; Hofsteenge, J. *Biochemistry* **2003**, *42*, 8452-8458.

(52) Hartmann, S.; Hofsteenge, J. *J. Biol. Chem.* **2000**, *275*, 28569-28574.

(53) Hofsteenge, J.; Huwiler, K. G.; Macek, B.; Hess, D.; Lawler, J.; Mosher, D. F.; Peter-Katalinic, J. *J. Biol. Chem.* **2001**, *276*, 6485-6498.

(54) Perez-Vilar, J.; Randell, S. H.; Boucher, R. C. *Glycobiology* **2004**, *14*, 325-337.

(55) Krieg, J.; Hartmann, S.; Vicentini, A.; Glasner, W.; Hess, D.; Hofsteenge, J. *Mol. Biol. Cell* **1998**, *9*, 301-309.

(56) Hofsteenge, J.; Blommers, M.; Hess, D.; Furmanek, A.; Miroshnichenko, O. *J. Biol. Chem.* **1999**, *274*, 32786-32794.

(57) Ihara, Y.; Manabe, S.; Kanda, M.; Kawano, H.; Nakayama, T.; Sekine, I.; Kondo, T.; Ito, Y. *Glycobiology* **2005**, *15*, 383-392.

(58) Krieg, J.; Glasner, W.; Vicentini, A.; Doucey, M.-A.; Loffler, A.; Hess, D.; Hofsteenge, J. *J. Biol. Chem.* **1997**, *272*, 26687-26692.

Gloss to Chapter IV

Much of the work described in Chapter II involved the identification of potential peptide markers, which could later be used to identify proteins based solely on accurate mass and elution time measurements. This accurate mass and time (AMT) tag strategy has been used by various groups to identify proteins in bacterial organisms, with >99% proteome coverage. Several characteristics of mammalian proteomes (complexity, sequence homologies), however, complicate the identification of proteins based on AMTs. This chapter describes the method of validating AMTs from FTICR data and several issues that should be considered when trying to create a database of potential peptide markers in mammalian proteomes.

CHAPTER IV

Accurate Mass and Time Tags

Introduction

Tandem mass spectrometry (MS/MS) has become a widely used method to identify proteins in complex mixtures. A typical MS/MS analysis compares experimental peptide fragmentation spectra to theoretical spectra from a translated genomic database for identification of the peptide and its parent protein [1]. This strategy, coupled with extensive liquid chromatography (LC) separations has demonstrated the potential for broad proteome coverage based upon the analysis of complex polypeptide mixtures [2]. However, in LC-MS/MS experiments, the number of peptide identifications is severely restricted because of the time required to disassociate the peptides individually and the limited number of peptides that can be selected for a fragmentation at a single elution time (Figure 1). In addition, this strategy is not cumulative; subsequent analyses of the same proteome do not benefit from information obtained in previous analyses. The presence of a protein must be confirmed by MS/MS and database search methods each time, regardless of whether or not the protein has been detected previously. These constraints make the comprehensive characterization of entire proteomes impractical for complex organisms.

Accurate mass measurements of peptides captured as accurate mass and elution time (AMT) tags can obviate the need for the repeated MS/MS measurements of the same proteome and serve as a basis for a larger number of identifications in a single experiment. The utility of AMTs for protein identification derives from the specificity of mass measurements for peptides, and the relatively small number of possible peptide sequences for a specific organism compared to the number of theoretically possible peptides. The AMT strategy involves the combined use of these accurate mass

measurements with LC elution time information for the detection of marker peptides at high-throughput, while still retaining the specificity associated with MS/MS protein identifications. Combined with quantitative labeling methods, an AMT database allows a much broader coverage of protein expression than is available with other competing technologies (i.e. protein arrays).

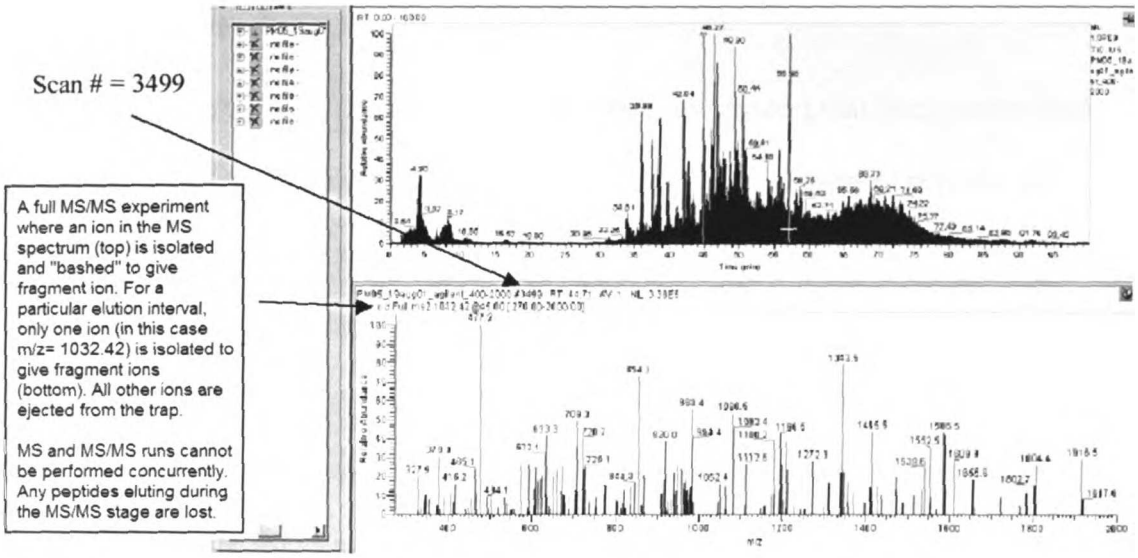

Figure 1. Display of MS and MS/MS experiment. Peptide identification is limited by the cycle time of the MS instrument. Any peptides eluting during MS/MS are lost.

The AMT Strategy

The generation of AMTs is based on a two stage process that uses conventional MS and FTICR-MS instrumentation. In the first stage, trypsin digested peptides are analyzed by LC-MS/MS using a conventional ion mass spectrometer. High scoring identifications, termed putative mass and time (PMT) tags are identified from the MS/MS analysis of various cell lines using a database search program as described previously in Chapter II. These peptides are then validated by the detection of the predicted peptides accurate masses (within 5 ppm) using FTICR MS in a corresponding sample at an equivalent elution time. The matching involves finding groups of ions in the data, computing their median monoisotopic mass, and comparing the mass and elution time of the group with the mass and normalized elution time (NET) of each peptide in the PMT tag database. This process is summarized in Figure 2.

A validated peptide is then termed an accurate mass and time tag (AMT). The collection of AMTs may be visualized in 2 dimensions as shown in Figure 3. The molecular weight of a PMT identified with conventional MS/MS is plotted against its NET. Overlaid on top of the figure are blue boxes, which indicate species detected during FTICR MS. The placement of the box on the y-axis indicates the species mass (range of +/-5 ppm) as measured on the FTICR and the horizontal width of the boxes represents the expected elution range for a particular peptide (allowing for some known error rate that occurs- +/- 5% normalized elution time). A peptide is converted to an AMT if it is detected on the FTICR within these tolerances.

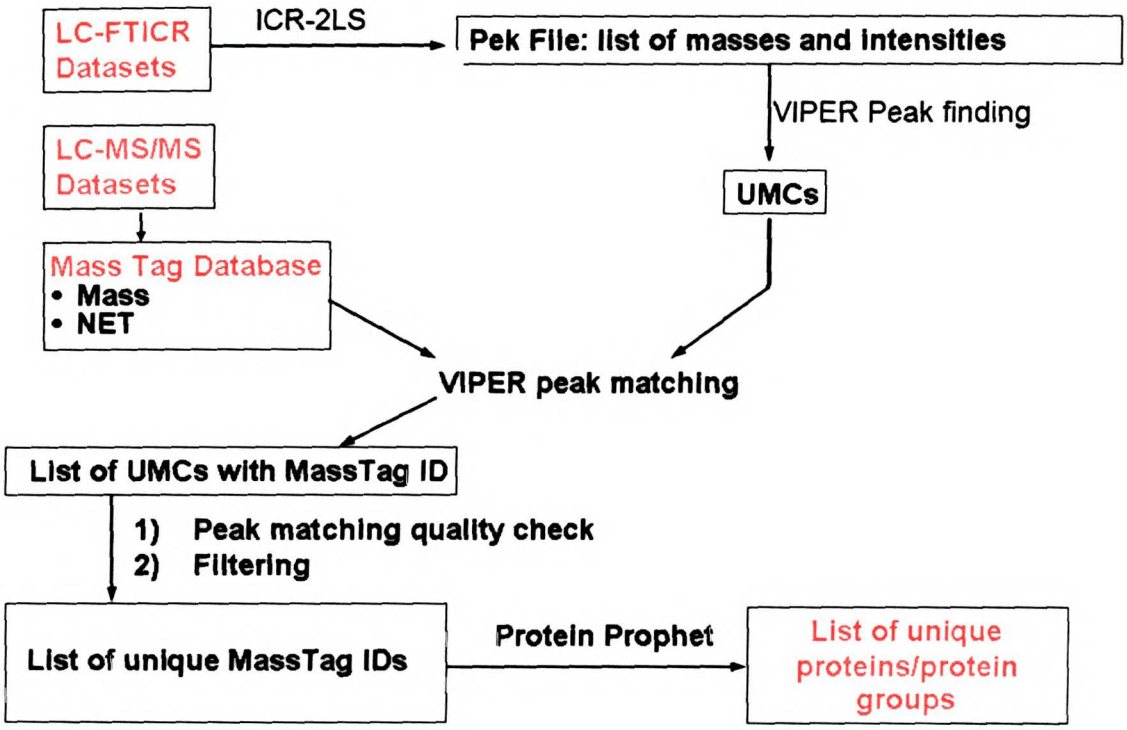

Figure 2. Overview of AMT matching process. The matching involved finding groups of ions in the FTICR data and clustering them according to their median monoisotopic masses and elution times. The resulting unique mass classes (UMCs) are compared with the mass and normalized elution time of each peptide in the PMT tag database. Those that match within certain tolerances are termed AMTs.

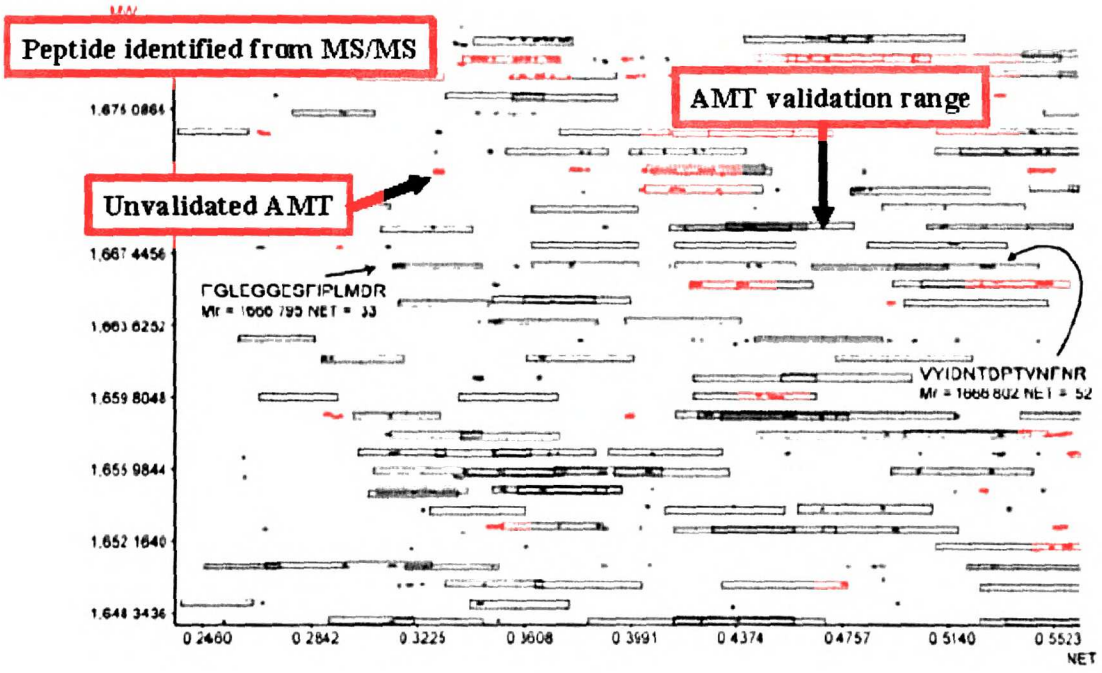

Figure 3. 2D visual display of PMTs with NET (x-axis) plotted against molecular weight (y-axis). A peptide is converted to an AMT if it is detected in the FTICR within the tolerances represented by blue boxes.

Theoretical Considerations

In principle, AMT-based protein identification allows high-throughput proteome measurements because only distinctive masses and LC elution times are needed to identify a protein[3] (no sequence information or peptide fragmentation spectra is needed). In the proteome of the bacterial organism *D. Radiodurans*, for instance, ~50% of the peptides predicted from an in-silico tryptic digestion have unique masses at mass measurement accuracies (MMA) $\leq$ 1 ppm and can be used to identify 99.5% of the predicted proteins potentially expressed by the organism [4]. In these studies, AMTs were successfully used for protein identification by combining initial identifications using MS/MS-database searching strategies with validation using high MMA and elution time criteria [3,5]. This strategy successfully identified 61% of the predicted open reading frames (ORFs) for *D. Radiodurans*, the broadest proteome coverage for any organism to date [4]. While these initial studies focused on bacterial genomes, the strategy can be extended to any organism whose genome has been sequenced, including Homo Sapiens.

Only a small fraction of the theoretically possible peptide sequences are actually present in the proteome of a living organism. The number of theoretically possible sequences of length, N can be simply calculated as 20^N (assuming N distinct amino acids) while the actual number of sequences present in a genome spans a single order of magnitude for typical peptide lengths. Although the number of proteins in the human proteome has not yet been defined, recent findings of human genome projects have estimated that each of our ORFs produces 2 to 3 different gene products for a total of ~85,000 proteins (not including PTMs). In addition, the average human gene contains 4 exons totaling 1,350 base pairs and thus encodes an average protein of ~450 amino acids.

Considering that trypsin cleaves every ~9 residues, we can expect an ideal tryptic digest of the human proteome to yield ~4,250,000 peptide sequences. This number represents only 8.3 X 10^{-4}% of the total number of possible nine-mer peptides ($4X10^6/20^9*100$)- illustrating that only a fraction of possible proteins will be expressed in any given cell type [6] (this assumes that a particular sequence is unique in the proteome).

Given sufficient MMA and the relatively small fraction of expressed peptides compared to theoretical peptides, many unique peptide masses can be confidently attributed to proteins of the human proteome. The number of distinguishable peptides in actual measurements, however depends on the MMA [6]. It is worthwhile knowing, therefore, what percentage of peptides from a perfect *in-silico* tryptic digest of the human proteome have unique masses at 1 ppm- the mass accuracy of the FTICR instrument used in our analysis. *In-silico* digestion of the human protein sequence database (SwissProt, 01/05/04) revealed that ~30% of peptides are distinguishable by mass alone. It should be noted, however, that this number represents the lower bound of our peptide coverage, since our AMT strategy also uses predicted elution time information in distinguishing peptides.

The complexity of the mammalian proteome and increased sequence homologies among proteins poses additional challenges. In mammalian systems, sequence motifs are shared among proteins that are functionally similar or share a common evolutionary ancestor. Protein sequence homologies may complicate the unambiguous identification of a protein from a single peptide sequence, because many peptide fragments identified using MS/MS can be found in multiple proteins and represent commonly found functional domains. These peptides would normally not be candidates as AMTs in our

dataset, unless they (1) occur in combination with other peptides that can uniquely identify a protein or (2) are still able to distinguish multiple isoforms/alternative splice forms of the same gene product.

A ideal *in-silico* tryptic digest of the 2,299 proteins stored in our PMT database results in 71,422 peptides. Of these, 1,468 (2%) peptides occur in more than one protein stored in the PMT database (Appendix C, Table S1). Further investigation of these results, however, shows that 1,409 (96%) of these peptides merely occur in alternative splice forms/isomers of the same gene product. Since the sequence database used for protein identification (IPI) assigns distinct identifiers to alternative forms of the same protein, the peptides in Table S1 merely reflects the amount of protein variants that exist in our PMT database. All the peptides in Table S1, however, uniquely identify a protein in our PMT database when used in combination with other peptides. This is because the ProteinProphet program, which we used for protein identification in MS/MS analysis (Chapter I), discriminates among degenerate identifications (homologous proteins, splice variants, isoforms, redundant entries) when assigning probabilities that individual protein assignments are correct. Considering that multiple isoforms of the same protein often have distinct biological roles within a cell, we elected to retain the entire complement of protein isoforms and alternative splice forms in our AMT dataset.

The actual set of peptides in our experimental (PMT) dataset did not completely reflect the number of peptides expected from an ideal *in-silico* digest. This is attributable to 1) the undersampling inherent in MS/MS methodology, 2) the presence of low-quality uninterpretable spectra and 3) instances of missed tryptic cleavages. Our PMT database consisted of 33,631 confidently identified (Discriminant > 0.5) peptides representing the

2,299 proteins, each with recorded mass and elution time information. The high peptide/protein ratio (14.6) is due to the identification of multiple peptides belonging to the same protein and the positional overlap of many of the peptides within the protein sequence (i.e. AAFDDAIAELDTLSEESYK and AAFDDAIAELDTLSEESYKDSTLIMQLLR are produced by different cleavage patterns yet represent the same protein). A Mass Tag Identification (ID) number was assigned to each peptide. For AMT validation, this PMT database was compared to elution time and accurate mass measurements of peptides detected in our FTICR analysis. Matching Mass Tag IDs were assigned to those peptides meeting the matching criteria described above. Figure 4 displays the database tables holding both the PMT data from LC-MS/MS analysis and subset of peptides identified using an AMT strategy described in the following chapter.

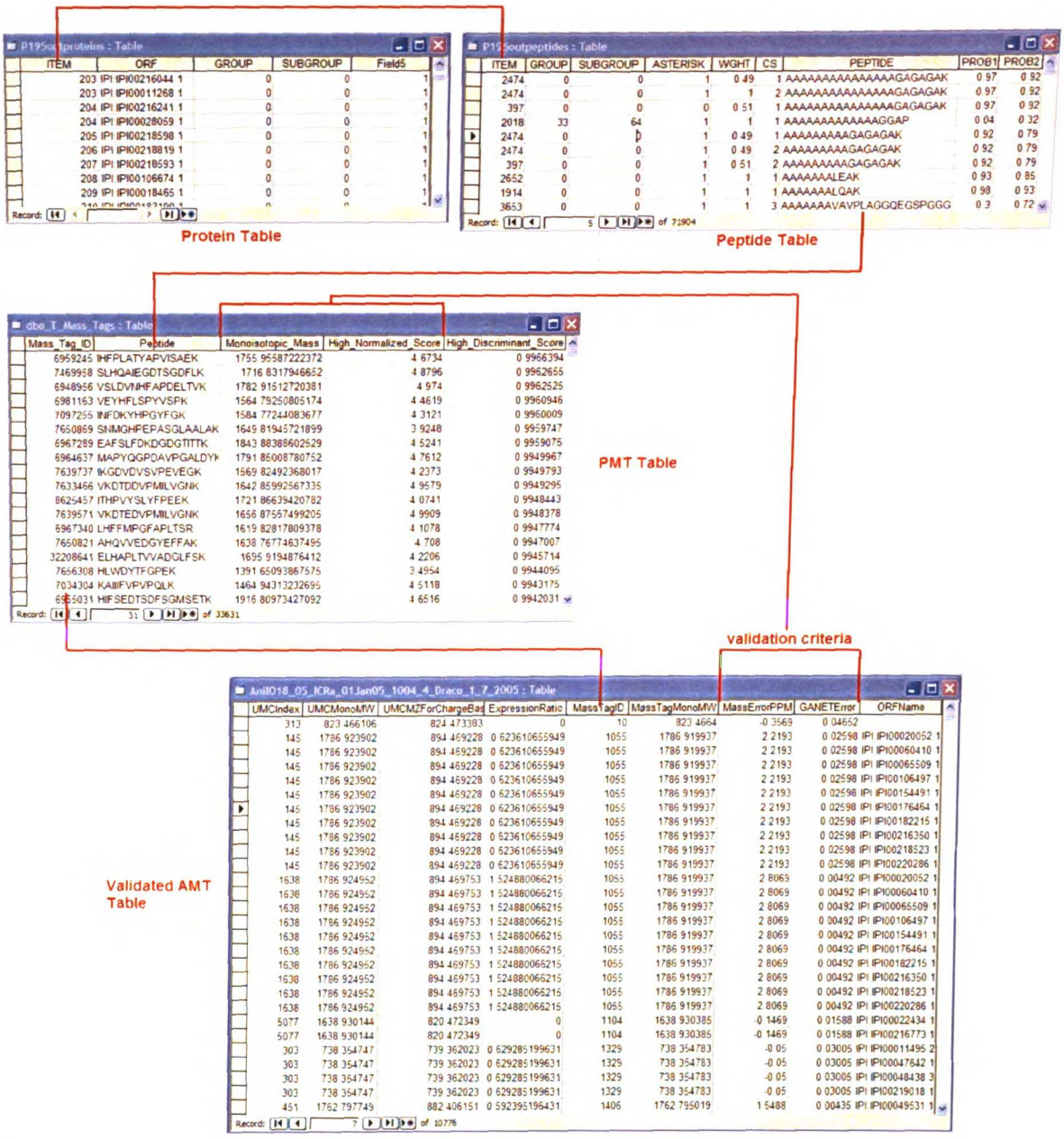

Figure 4. Tables storing information for potential mass and time (PMT) tags identified from LC-MS/MS and validated accurate mass and time (AMT) tags using FTICR measurements. Mass Tag IDs were assigned for peptides with distinctive masses and elution times and recorded in the PMT table. The observation of these peptides within certain mass and elution time tolerances with the FTICR results in a validated marker peptide for a protein. For brevity, not all fields or peptides are shown. Primary keys that join tables are indicated by red lines. The validation criteria are also indicated in the PMT and AMT tables.

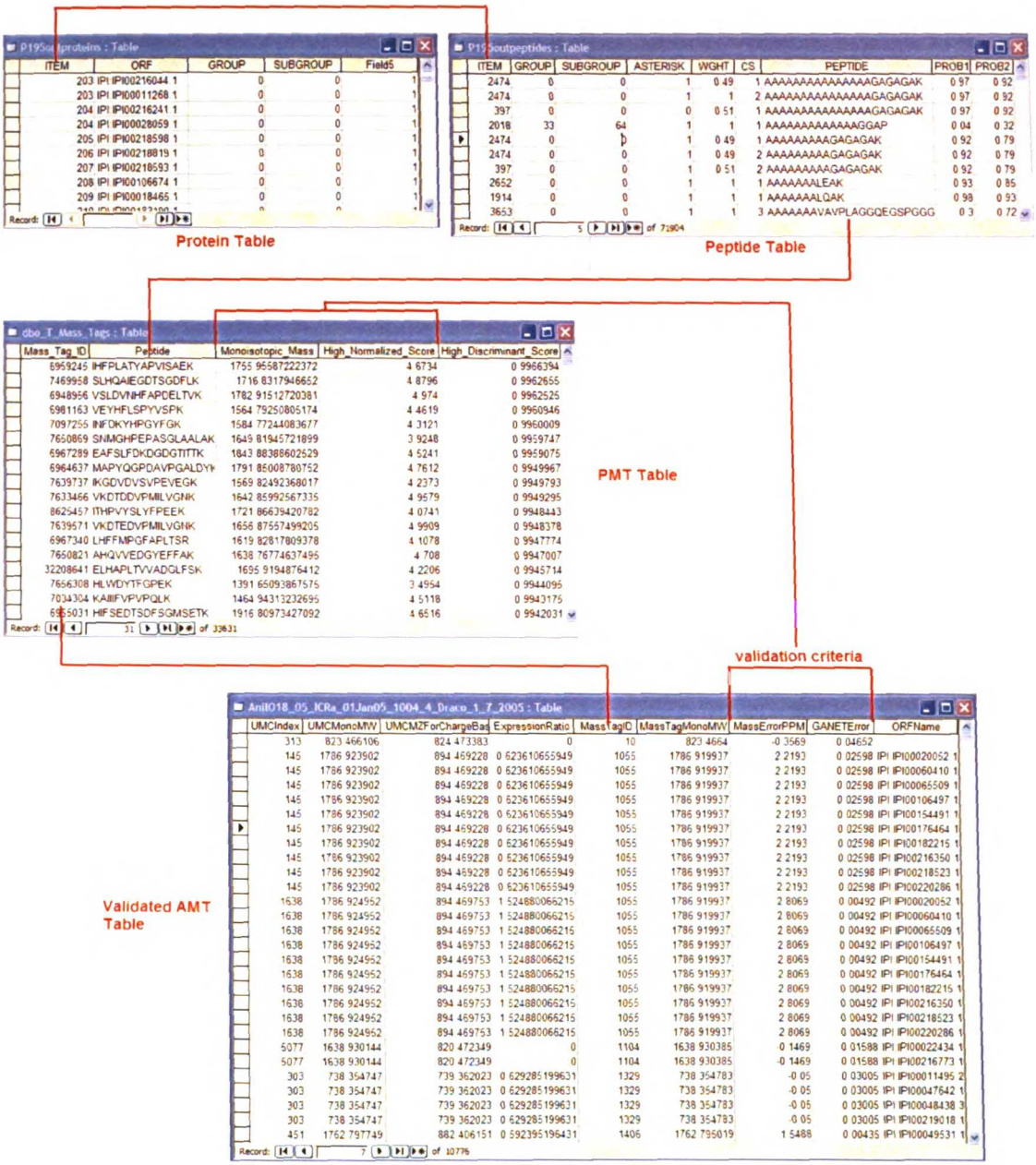

Figure 4. Tables storing information for potential mass and time (PMT) tags identified from LC-MS/MS and validated accurate mass and time (AMT) tags using FTICR measurements. Mass Tag IDs were assigned for peptides with distinctive masses and elution times and recorded in the PMT table. The observation of these peptides within certain mass and elution time tolerances with the FTICR results in a validated marker peptide for a protein. For brevity, not all fields or peptides are shown. Primary keys that join tables are indicated by red lines. The validation criteria are also indicated in the PMT and AMT tables.

References

(1) Yates, J. R., 3rd; Eng, J. K.; McCormack, A. L.; Schieltz, D. *Anal Chem* **1995**, *67*, 1426-1436.

(2) Washburn, M. P.; Wolters, D.; Yates, J. R., 3rd *Nat Biotechnol* **2001**, *19*, 242-247.

(3) Smith, R. D.; Anderson, G. A.; Lipton, M. S.; Pasa-Tolic, L.; Shen, Y.; Conrads, T. P.; Veenstra, T. D.; Udseth, H. R. *Proteomics* **2002**, *2*, 513-523.

(4) Lipton, M. S.; Pasa-Tolic, L.; Anderson, G. A.; Anderson, D. J.; Auberry, D. L.; Battista, J. R.; Daly, M. J.; Fredrickson, J.; Hixson, K. K.; Kostandarithes, H.; Masselon, C.; Markillie, L. M.; Moore, R. J.; Romine, M. F.; Shen, Y.; Strittmatter, E.; Tolic, N.; Udseth, H. R.; Venkateswaran, A.; Wong, K. K.; Zhao, R.; Smith, R. D. *Proc Natl Acad Sci U S A* **2002**, *99*, 11049-11054.

(5) Petritis, K.; Kangas, L. J.; Ferguson, P. L.; Anderson, G. A.; Pasa-Tolic, L.; Lipton, M. S.; Auberry, K. J.; Strittmatter, E. F.; Shen, Y.; Zhao, R.; Smith, R. D. *Anal Chem* **2003**, *75*, 1039-1048.

(6) Clauser, K. R.; Baker, P.; Burlingame, A. L. *Anal Chem* **1999**, *71*, 2871-2882.

Gloss to Chapter V

Portions of Chapter V are presented in the form of an article submitted to Proteomics for publication. A long-term objective of my thesis has been to work toward a high-throughput strategy for measuring protein expression among cell lines. Other investigators in the UCSF Cancer Center used comparative genomic hybridization (CGH) techniques to investigate genomic alterations in the NCI60 panel of cell lines, which have been characterized pharmacologically and are used to screen potential anticancer drugs. Similar efforts using cDNA microarrays have been carried out by researchers at Stanford University as part of the "NCI60 Cancer Microarray Project". A proteomic profile of these cell lines would provide valuable information that could not otherwise be obtained using these nucleic-acid based techniques. Although the results presented in this chapter focus on only 5 cell lines, the potential mass and time (PMT) tag database can be used to quantify proteins in potentially all NCI60 cell lines using FTICR-MS. Moreover, several of the techniques used in nucleic-acid based analyses (clustering, normalization, functional annotation) were readily adapted for use with our protein expression dataset.

Compared to gene expression studies, few quantitative proteomic studies have been performed in cancer. Fortunately, the recent commercial availability of various peptide labeling reagents promises to make this an area of rapid research. PNNL is one of the labs at the forefront of MS-based quantitative proteomics. Discussions with Maria and the PNNL faculty were invaluable in helping me decide how to design our experiments. Several months at PNNL also allowed me to use the tools necessary to identify and validate AMT marker peptides. In some respects, this chapter represents the culmination of previous work– drawing on an ever expanding peptide mass database

(based on previous LC-MS/MS analysis, chapters II and III) to quantitatively evaluate cell line proteomes.

CHAPTER V

Quantitative Proteome Analysis of Breast Cancer Cell Lines using ^{18}O-Labeling and the Accurate Mass and Time Tag Strategy

Anil J. Patwardhan, Eric F. Strittmatter, David G. Camp II, Richard D. Smith, Maria G. Pallavicini

Portions submitted for publication in Proteomics

Abstract

Proteome comparison of cell lines derived from breast cancer and normal breast epithelium provide opportunities to identify differentially expressed proteins and pathways associated with specific phenotypes. We employed trypsin-catalyzed $^{16}O/^{18}O$ peptide labeling, FT-ICR mass spectrometry, and an accurate mass and time (AMT) tag strategy to simultaneously compare the relative abundance of hundreds of proteins in non-cancer and cancer cell lines derived from breast tissue. Development of a reference panel of cell lines provided a novel approach to facilitate comparisons of relative protein abundance amongst multiple cell lines and across multiple experiments. A peptide database generated from multidimensional LC separations and MS/MS analysis was used for subsequent AMT tag-based peptide identifications. This peptide database represented a total of 2,299 proteins, including 514 that were quantified in 5 cell lines using the AMT tag and $^{16}O/^{18}O$ strategies. Eighty-six proteins showed at least a 3-fold protein abundance change between cancer and non-cancer cell lines. A comparison of protein expression profiles with previously published gene expression data revealed that 21 of these proteins also had $\geq$3-fold differences at the transcriptional level between the non-cancer and cancer cell lines. Clustering of protein abundance ratios revealed that several groups of proteins were differentially expressed between the cancer cell lines.

Introduction

Breast cancer is the most frequently diagnosed cancer in women and accounts for 30% of all cancers diagnosed in the United States [1]. While remarkable progress has been made in treatment of this disease, its' heterogeneous response to therapy and unknown etiology indicate that considerable progress has yet to be made. Molecular profiling of breast tumors using high throughput nucleic acid-based microarrays has been used to stratify some tumors into molecular subtypes [2-7]. However, it is increasingly recognized that transcriptional mechanisms do not always mirror translation [8] and several studies have shown that mRNA abundance measurements do not always correlate with protein expression [9-11]. Thus, efforts to directly identify expressed proteins and assess differential protein expression are key to elucidating molecular signatures associated with cell phenotype.

The use of chromatographic or electrophoretic separations combined with mass spectrometry (MS) for large-scale proteome analysis has played a critical role in the rapid identification of new protein targets, and the underlying molecular events associated with cancer development, progression and severity [12, 13]. The majority of MS-based surveys of breast cancer proteomes have relied on qualitative analysis of primary peptide sequence to identify proteins within the cell/tissue [14, 15]. MS has also been used to assess potential translocation of proteins [16], characterize post-translational modifications [17] and protein complexes, and to elaborate signaling pathways [18] in breast cancer proteomes. However, while protein abundances and activities are often modulated in the course of various cancers, qualitative MS analyses cannot definitively measure differences in protein expression. In qualitative MS, the absence of a detected

protein may reflect undersampling inherent in tandem MS-based protein identification techniques (i.e. false negatives), rather than a true lack of expression. Thus, increasing effort has been placed on development and application of more quantitative strategies. Although quantitative MS methods are also susceptible to false negatives in the identification process, they provide direct comparisons of proteins/peptide abundances. Variations in protein abundances across comparative samples can then be used to make biological inferences. A number of peptide/protein labeling and 2-DE methods have been combined with MS to measure differential protein expression [19-21], including several that have been used to detect differences in tumor phenotype or drug effects [22-27]. These techniques include pre and post-digestion labeling strategies, such as the isotope coded affinity tag (ICAT) reagent [19], 2-D DIGE [23], and activity-based protein profiling (APBB) [27].

Several laboratories have reported the applicability of post-digestion tryptic peptide $^{16}O/^{18}O$ labeling for quantitative comparison of protein abundances in complex samples [28-31]. In a typical peptide labeling procedure, peptides in one sample are isotopically labeled with ^{18}O and compared to a second sample prepared with unlabeled water (^{16}O). MS measurements of these labeled peptides distinguish the two samples by comparison of these isotopically "light" and "heavy" peptide forms. The ratio of intensities of the peptide peaks in a given mass spectrum provides a relative ratio of abundance of the two species. ^{18}O-labeling incorporates two atoms of ^{18}O in essentially all tryptic peptides, potentially providing greater proteome coverage than other residue-specific labeling methods (e.g. ICAT) [30]. However, even with unbiased peptide

labeling methods, the undersampling inherent in MS-based identification techniques limits the number of proteins quantified in complex samples.

Recently, an accurate mass and time (AMT) tag strategy has been used for global proteome analysis of complex samples [32]. AMT tags utilize information combined from multiple MS/MS measurements to identify peptides, thereby minimizing the constraints of undersampling. AMT tag-based protein identification allows high-throughput proteome measurements because only distinctive masses and LC elution times are needed to identify a protein [33]. The generation of AMT tags is based on a two stage process that uses conventional MS/MS followed by FTICR-MS. With mass measurement accuracies of <1ppm [33], the FTICR instrument detects peptide masses that can be confidently attributed to distinctive proteins of the human proteome, while retaining the specificity associated with MS/MS protein identification. Recent studies indicate that the relative abundance of hundreds of proteins can be assessed by combining the AMT tag strategy with ^{18}O-labeling [34, 35]. Peptide labeling strategies in combination with the AMT tag strategy provides broader coverage of quantitative protein expression than other MS-based approaches and eliminates the need for repeated LC-MS/MS measurements of the same proteome [32, 33].

We extended and modified quantitative AMT-based approaches to estimate relative protein abundances in tumor derived cell lines and normal breast epithelia. The complexity of the cellular proteomes was reduced using extensive peptide and protein level fractionation. Each fraction was subjected to MS/MS to generate peptide mass measurements that served as potential peptide markers for breast derived cells. When combined with FTICR-MS and $^{16}O/^{18}O$ peptide labeling, these peptide markers enabled

quantification of a wide functional range of proteins. We developed a novel approach to facilitate comparison of multiple proteomes. A single reference mixture composed of several cell-lines was used as a common baseline for relative protein abundances across individual cell line proteomes. This common reference mixture, combined with cluster-based discrimination methods, revealed several groups of functionally related and differentially expressed proteins. In addition, relative protein abundances were compared with publicly available gene expression datasets to assess differences between protein and mRNA expression profiles. Together these strategies provide a way to quantitatively evaluate protein expression in multiple cancer phenotypes while providing broad coverage of breast cancer cell line proteomes.

Materials and Methods

Sample Preparation

The breast cancer cell lines used in this study were selected to represent characteristic features of breast cancer phenotypes, including variations in estrogen receptor status and receptor tyrosine kinase (RTK) expression, which previously have been used to stratify tumors into clinical and molecular subtypes [2, 5, 36]. In this study, two cell lines (MDA-231, SKBR-3) are derived from ER negative (ER-) breast cancer tissue and two cell lines (MCF7-c18, BT-474) are derived from ER positive (ER+) breast cancer tissues. The human mammary epithelial cell line (HMEC), which is derived from non-cancerous breast tissue, was used for comparison.

HMEC (Cambrex: CC-2551) and human breast carcinoma cell lines SKBR-3 (American type culture collection (ATCC):HTB-30), MDA-MB-231 (ATCC:HTB-26),

BT-474 (ATCC:HTB-20), and an MCF7 transfectant cell line over-expressing the ERBB2 receptor tyrosine kinase [37] were cultured in Cambrex/ATCC recommended medium containing 2 mM glutamine, 100 µg/mL streptomycin/penicillin, and Genetician (200 µg/mL; Gibco, Carlsbad, CA). Cells were maintained at 37°C in a humidified atmosphere of 95% air and 5% CO2, washed with phosphate buffered saline (PBS) and harvested at 70% confluency using a cell disassociation solution per manufacturer's instructions (Cell Dissociation Solution (1×) Non-enzymatic, Sigma, St. Louis, MO).

For each cell line, sample complexity was reduced using the sucrose-cushion procedure described by Arnott et al. [16]. Membrane-enriched fractions were prepared separately for each cell line, were resuspended in a urea solution (7 M urea, 2 M thiourea, 1% CHAPS, 5 mM DTT) and stored at -80° C. Fractions were enzymatically digested (Sequence Grade Modified, Promega, Madison, WI), reduced with 10 mM DTT, and alkylated with 32 mM iodoacetamide prior to LC-MS/MS analysis or LC-FTICR mass spectrometry.

Identification of Potential Mass and Time Tags by LC-MS/MS

A combined mixture of MDA-MB-231, MCF7-c18, and BT-474 cell lines, along with single cell line samples of HMEC and SKBR-3, were analyzed by LC-MS/MS for protein detection. Each sample was processed for strong-cation exchange (SCX) chromatography by directly injecting the lysate onto a Poly LC (Columbia, MD, USA) Polysulfoethyl A 200 mm x 9.4 mm column preceded by a 10 mm x 10 mm guard column at a flow rate of 4 mL/min. The separations were performed on a Shimadzu LC-10A system using a Unicam 4225 (Thermo Electron, Waltham, MA, USA) UV-Vis

detector with mobile phases consisting of Solvent A (10 mM ammonium formate, 25% ACN, pH 3.0), and Solvent B (500 mM ammonium formate, 25% ACN, pH 6.8). Initially, the runs were isocratic at 100% Solvent A for 10 min followed by a linear gradient from solvent A to solvent B over 50 min. The gradient was held at 100% solvent B for 10 min, and then washed with water for 20 min prior to re-equilibrating with 100% Solvent A for 10 min. All SCX fractions (~65 fractions each for the combined mixture and single cell lines) were collected, lyophilized to dryness, and stored at –80° C until analyzed by LC-MS/MS.

The reversed phase capillary LC method was used as reported previously [38]. The RPLC column was interfaced with a Finnigan LCQ ion trap mass spectrometer (ThermoFinnigan, San Jose, CA) with an ESI source. The initial MS survey scan utilized an m/z range of 400-2000 from which the 3 most abundant ions were selected for MS/MS analysis using a collisional energy of 45%. Dynamic exclusion was used to prevent repeated analysis of the same high abundant ion. Peptide identification was performed using SEQUEST v2.7 (ThermoFinnigan, San Jose, CA) [39] and searched with the September 2003 freeze of the human International Protein Index (IPI) database (http://www.ebi.ac.uk/IPI/IPIhelp.html). SEQUEST search was carried out using a +/- 3 Da restriction on parent mass accuracy. Since our samples were alkyated prior to analysis, a dynamic modification was used to identify both unlabeled and iodoacetamide labeled cysteine-containing peptides. Peptides with fewer than 6 amino-acid residues were eliminated to avoid low specificity associated with small peptide fragments. The search was unconstrained with respect to enzymatic cleavage to allow detection of peptides not normally associated with trypsin. An independently developed discriminant

based program was used to determine peptide confidence probabilities. The discriminant score takes advantage of elution time information and tryptic cleavage information, which enhances peptide confidence [40].

All peptides that passed the filtering criteria were input into the ProteinProphet program [41], which generated a final non-redundant list of proteins. In an effort to minimize false positives, an 80% probability cutoff and at least 2 peptides per protein were required for protein identification. Peptides for each protein were then entered into a potential mass and time (PMT) tag database, which stored peptide mass and elution time information for multiple LC-MS/MS runs.

$^{16}O/^{18}O$ Labeling of Peptide Mixtures

Trypsin-catalyzed $^{16}O/^{18}O$ labeling was performed as described previously [34, 35]. A single equimolar mixture composed of six cell lines (BT-474, HMEC, SKBR-3, MDA-231, MCF7-c18, MCF7) was created using the sample preparation procedures described above. This mixture served as a common "reference" against which all single cell lines were compared and served to normalized relative abundance values. Peptides from this reference sample were labeled with ^{16}O and peptides from the single cell line samples were labeled with ^{18}O. ^{16}O and ^{18}O-labeled samples were pooled so that the reference panel was compared to each cell line individually: Reference (^{16}O) vs. HMEC (^{18}O); Reference (^{16}O) vs. BT-474 (^{18}O); Reference (^{16}O) vs. SKBR-3 (^{18}O); Reference (^{16}O) vs. MCF7-c18 (^{18}O); Reference (^{16}O) vs. MDA-231 (^{18}O). To determine the inherent variability of our labeling strategy, a control comparison was also performed: Reference (^{16}O) vs. Reference (^{18}O). Samples were lyophilized prior to LC/FTICR.

Detection of Accurate Mass and Time Tags and Abundance Ratios by LC/FTICR

Each $^{16}O/^{18}O$ pooled sample was analyzed twice by LC/FTICR resulting in a total of 12 experimental runs (5 cell line comparisons X 2 replicates+ 2 control runs). Peptides were analyzed using an electrospray ionization interface coupled to an 11.5 Tesla FTICR mass spectrometer (Smith et al. 2002). The acquired FTICR spectra (10^5 resolution) were processed and deconvoluted using ICR-2LS [33]. These data were filtered to include only "paired" peptide peaks ($^{16}O/^{18}O$ labeled) with unique masses and normalized elution times. The peak lists for each analysis were then matched against the PMT tags defined previously using software developed in-house at Pacific Northwest National Laboratory. An AMT tag was designated if the masses and elution times matched within a certain tolerance (+/-5 ppm and +/- 0.05 normalized elution time (NET)). The LC-FTICR analysis only assigns AMT tags which correspond to previously identified PMT tags from the LC-MS/MS runs. Figure 1 summarizes the overall strategy for the quantitative analysis of cell lines using the AMT process.

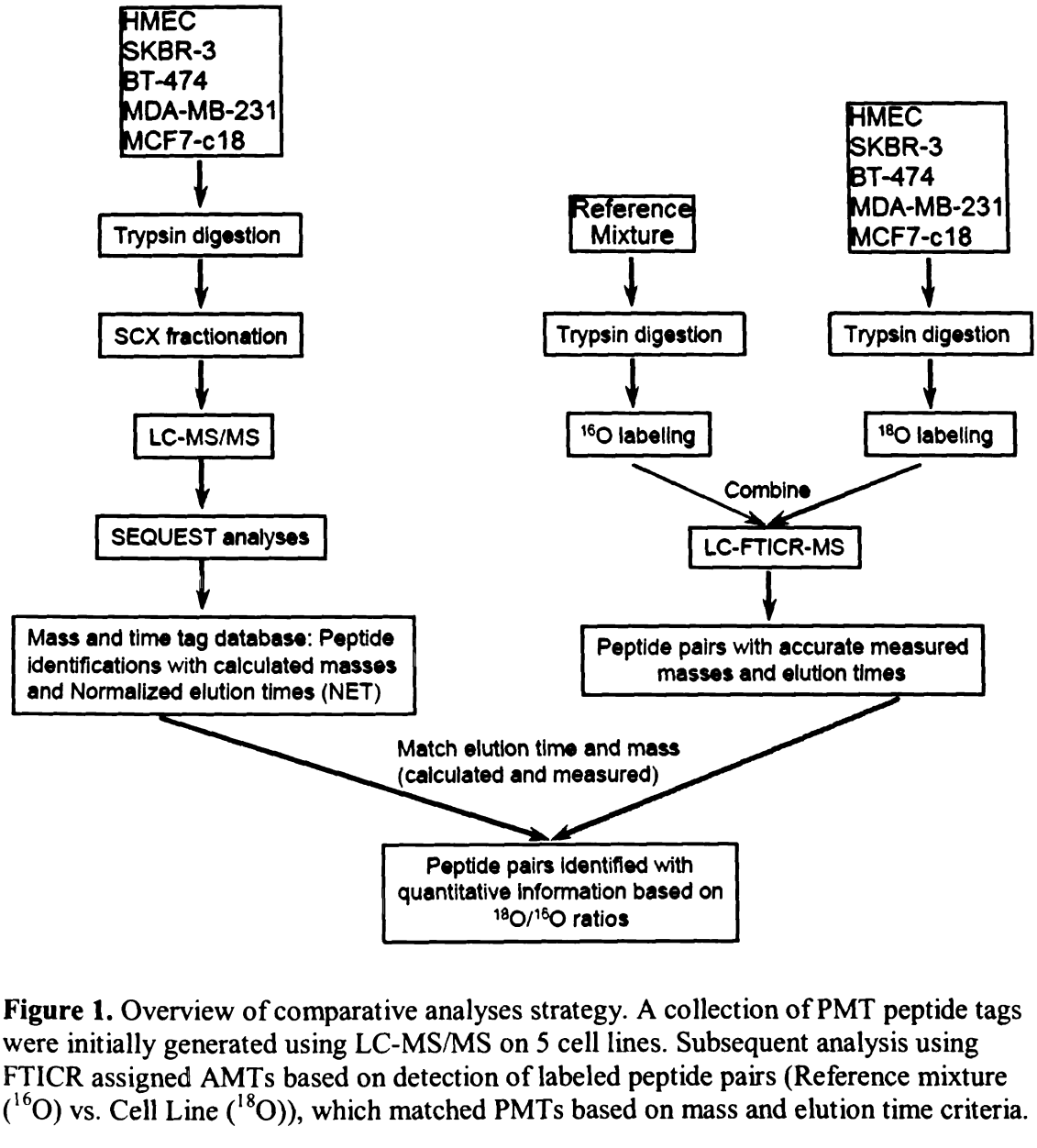

Figure 1. Overview of comparative analyses strategy. A collection of PMT peptide tags were initially generated using LC-MS/MS on 5 cell lines. Subsequent analysis using FTICR assigned AMTs based on detection of labeled peptide pairs (Reference mixture (^{16}O) vs. Cell Line (^{18}O)), which matched PMTs based on mass and elution time criteria.

Abundance ratios for labeled peptide pairs were calculated as previously reported [42, 43]. Ratios from multiple observations of the same peptide across different analyses were averaged to give one ratio per peptide. The abundance ratio for each protein was calculated by averaging the ratio of multiple unique peptides stemming from the same protein. In replicate runs, where two different abundances may be calculated for the same protein, we retained the abundance ratio with the lowest percent deviation across constituent peptides. The resulting protein abundance ratios were inverted so that the intensity of the ^{16}O labeled peptide (the reference panel) would be the denominator for all cell line comparisons ($^{18}O/^{16}O$).

Every comparison was filtered to include only "paired" ($^{16}O/^{18}O$ labeled) peptide peaks with unique masses and normalized elution times. This filtered dataset included several gene products with identical abundance ratios, a consequence of the redundancy inherent in the IPI database and the sequence homology of proteins within the database. Although ProteinProphet discriminates among degenerate identifications (homologous proteins, splice variants, isoforms) by assigning probabilities that individual peptide assignments are correct, we performed additional filtering of our dataset so that only a single set of abundance ratios were present for a collection of protein isoforms/alternative splice forms. To obtain a dataset in which proteins were compared across different cell lines, we eliminated proteins that were only quantified in the two control experiments (Reference vs. Reference).

Cluster Analysis

A hierarchical clustering (HCL) algorithm [44] implemented in the TIGR MultiExperiment Viewer 3.0 software program [45] was used to group 93 proteins based on their calculated relative protein abundances (average linkage, 8 terminal nodes, distance metric= Pearson's correlation). Proteins were selected based on the presence of abundance ratios for at least 4 of the 5 cell lines studied (HMEC, BT-474, SKBR-3, MDA-MB-231, MCF7-c18). Cell line experiments were scale-normalized to reduce the effects of biases that may be introduced during the labeling procedure. Values for individual proteins were mean normalized and log-transformed prior to clustering.

Comparison of Protein Abundances and Published mRNA Expression Data

A gene expression dataset [46] representing 8102 human genes was obtained for HMEC, SKBR-3, MDA-MD-231, and BT-474 through the Stanford Microarray Database [47]. In each cell line, the ratio of the abundance of transcripts of each gene to the median abundance of the gene's transcripts among a panel of 11 reference cell lines [46] was retrieved. Normalized (mean) raw data were obtained for genes using default values for spot quality and expression differences (unflagged spots, regression coefficient >0.6). This dataset was cross referenced with our set of protein expression values. Since mRNA expression and protein abundance ratios were not directly comparable due to differences in the composition of the reference cell line panels within each experiment the mRNA and protein abundance data were re-normalized so that intensities in HMEC served as the common reference through which the two datasets could be compared. For example, in the BT-474 cell line relative abundance measurements were re-normalized:

For mRNA: (Gene $X_{BT\text{-}474}$/Gene $X_{mRNA\ reference}$)/(Gene X_{HMEC}/Gene $X_{mRNA\ reference}$)

= Gene $X_{BT\text{-}474}$/Gene X_{HMEC}

where "Gene $X_{BT\text{-}474}$/Gene $X_{mRNA\ reference}$" indicates the mRNA abundance of a gene "X" in the BT-474 cell line relative to the reference panel of cells.

For proteins: (Protein $X_{BT\text{-}474}$/Protein $X_{protein\ reference}$)/Protein X_{HMEC}/Protein $X_{protein\ reference}$)

= Protein $X_{BT\text{-}474}$/Protein X_{HMEC}

where "Protein $X_{BT\text{-}474}$/Protein $X_{protein\ reference}$" indicates the protein abundance derived for protein "X" from ^{18}O labeled peptides in the BT-474 cell line and ^{16}O labeled peptides in the protein reference panel.

The resulting expression ratios were scale-normalized so that the dynamic ranges of gene and protein expression levels were comparable. Corresponding log values were calculated for display purposes.

Results/Discussion

Detection of Accurate Mass and Time (AMT) Tags and $^{16}O/^{18}O$ Labeled Proteins

The components of our quantitative proteomics strategy included generation of a reference cell line mixture, trypsin-catalyzed ^{18}O labeling, FTICR, and the AMT tag approach, to quantify relative protein expression in non-cancer and breast cancer cell lines. The false positive rate for MS/MS based protein identification was estimated to be ~8% as determined by reverse-database searches [40]. We obtained a collection of 33,631 identified peptides representing a non-redundant list of 2,299 confident protein

identifications. Each of the 2,299 proteins had at least two different peptides that could potentially serve as AMT tags for relative abundance measurements using LC-FTICR. The calculated masses and normalized LC elution times (NET) for PMT tags were used to created a peptide database that served as a "look-up table" to identify peptides from LC-FTICR analysis. LC-FTICR analysis of the reference panel and the four individual cell lines was used to validate AMT tags. The highly sensitive FTICR measurements provided both (1) AMT tag-derived peptide identifications without the need for repeated LC-MS/MS analyses and (2) sufficient resolution of the 4 Da mass difference of $^{16}O/^{18}O$ labeled pairs, allowing precise abundance ratio measurements. Figure 2 is a 2-D representation of labeled peptide pairs from the HMEC vs. Reference mixture comparison.

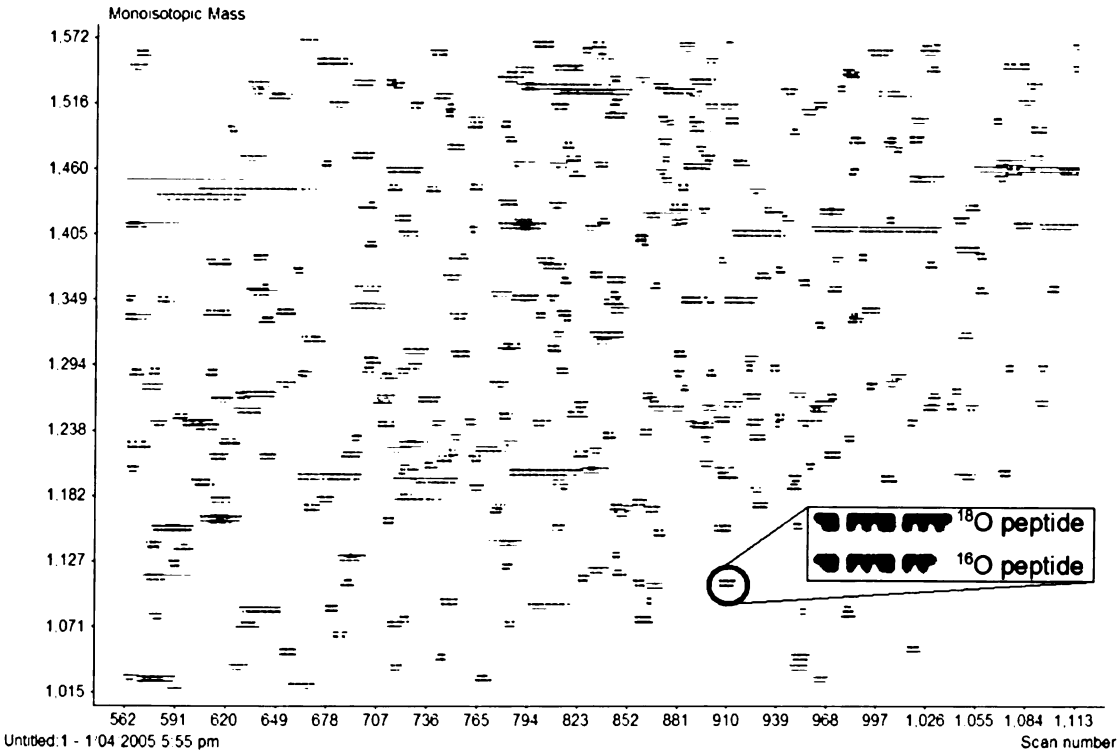

Figure 2. Two-dimensional representation of labeled peptide pairs from the Reference mixture (16O) vs. HMEC (18O) comparison, with peptide mass (x-axis) and normalized elution time represented by scan number (y-axis). Inset shows a single labeled peptide pair differentiated by 4 Da.

The protein quantification and filtering approaches used in our study are summarized in Figure 3. Spectra from the 12 LC-FTICR experiments were matched with peptides in the PMT tag database and filtered for "paired" ($^{16}O/^{18}O$ labeled) peptide peaks, to yield a total of 870 proteins. Additional filtering of our dataset collapsed 327 degenerate quantifications (homologous proteins, splice variants, isoforms) into a set of minimally redundant proteins and eliminated 26 proteins that were quantified in only two control experiments (Reference vs. Reference). After filtering, 517 quantified proteins remained, representing the union (U) of quantified proteins in each of the 5 cell line comparisons. The Reference (^{16}O) vs. HMEC (^{18}O) and Reference (^{16}O) vs. BT-474 (^{18}O) comparisons yielded the greatest number of quantified proteins (304 and 371 respectively). The Reference (^{16}O) vs. MCF7c18 (^{18}O) produced the fewest (115) number of quantified proteins.

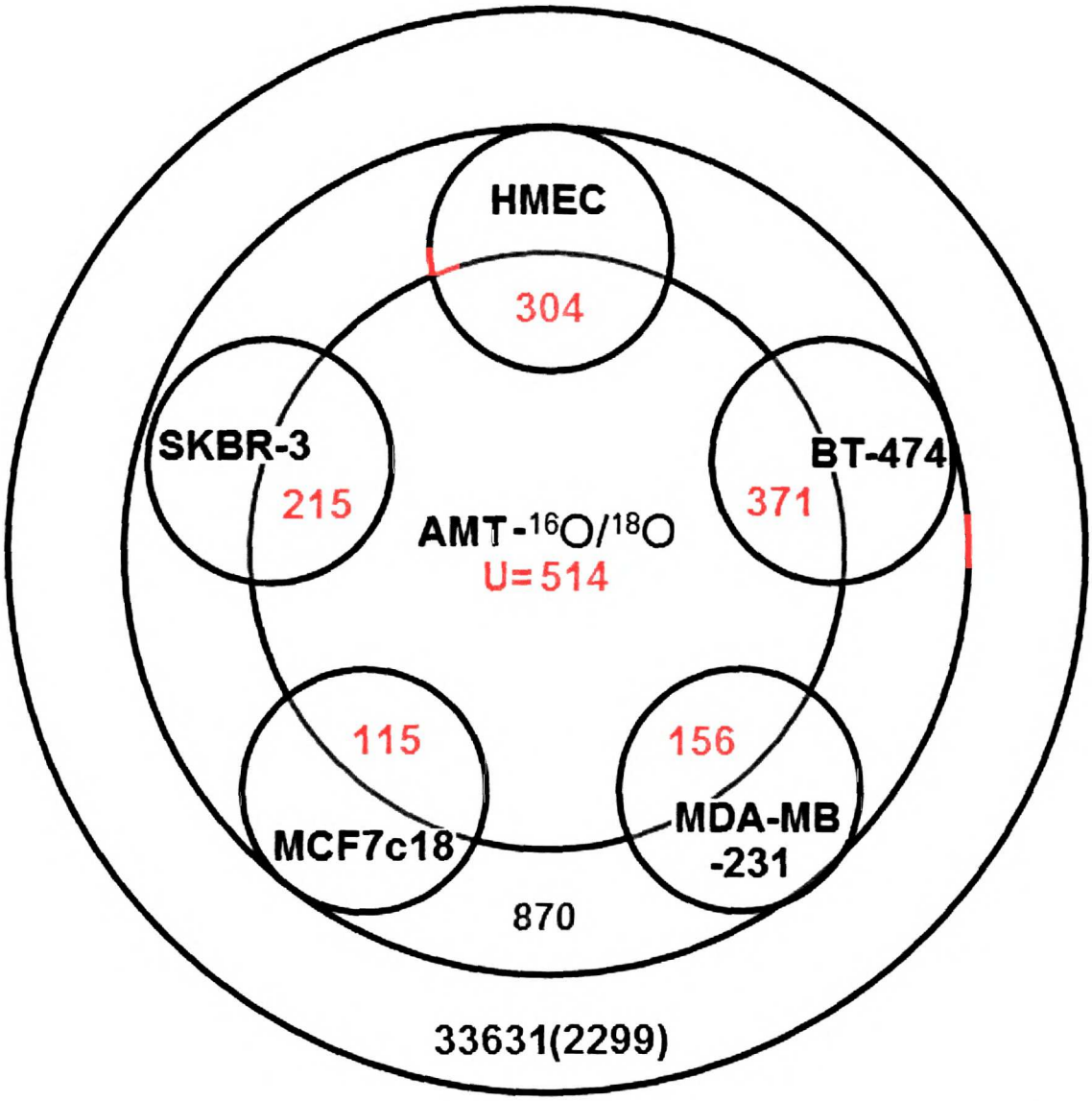

Figure 3. Summary of the number of proteins detected and quantified. 33631 peptides representing 2,299 proteins were stored in the PMT tag database (outer circle-blue). The AMT tag and $^{16}O/^{18}O$ strategies quantified 870 of these proteins among the 12 experiments (middle circle-green). After filtering to include only those proteins quantified in the 5 cell lines comparisons and to exclude redundant abundance ratios, 514 proteins remained (red). The numbers of proteins quantified within each individual cell line are also shown.

Proteins were classified according to various gene ontology (GO) [48] categories to determine the cellular compartments represented among our quantified proteins. The distribution of organelle assignments is displayed in Figure 4 (top) for proteins in the PMT tag database and the subset of quantified proteins. The classification of annotated proteins in the human proteome is shown for comparison. Since not all proteins have GO annotations available, the percentage of only those "cellular" proteins (annotated by GO as being a cell component) present in each organelle are also noted. This facilitates comparison of the various GO categories across each protein dataset, while accounting for any differences that might be due to annotation coverage. 68% (1563/2,299) of all the proteins represented in the PMT tag database and 88% (452/514) of the quantified proteins were classified as "cellular" by GO. For the PMT tag and $^{16}O/^{18}O$ labeling strategies, the overall distribution of proteins in various organelles generally parallels the distribution of proteins in the entire human proteome. However, some differences were observed. Notably, the proportion of nuclear proteins was greatly reduced in our group of identified proteins (18.0% PMT; 16.2% $^{16}O/^{18}O$) compared to the entire set of annotated proteins in the human proteome (31.8%). In contrast, mitochondrial (12.9% PMT; 10.8% $^{16}O/^{18}O$), cytoskeletal (11.4% PMT; 16.8% $^{16}O/^{18}O$), ER (10.8% PMT; 11.1% $^{16}O/^{18}O$), and ribosomal (8.1% PMT; 10.4% $^{16}O/^{18}O$) compartments were slightly enriched. In all three groups, the greatest proportion of membrane proteins occurred in the plasma membrane (Figure 4; bottom). Other organelle membranes were slightly enriched in our set of proteins compared to their distribution in the entire human proteome.

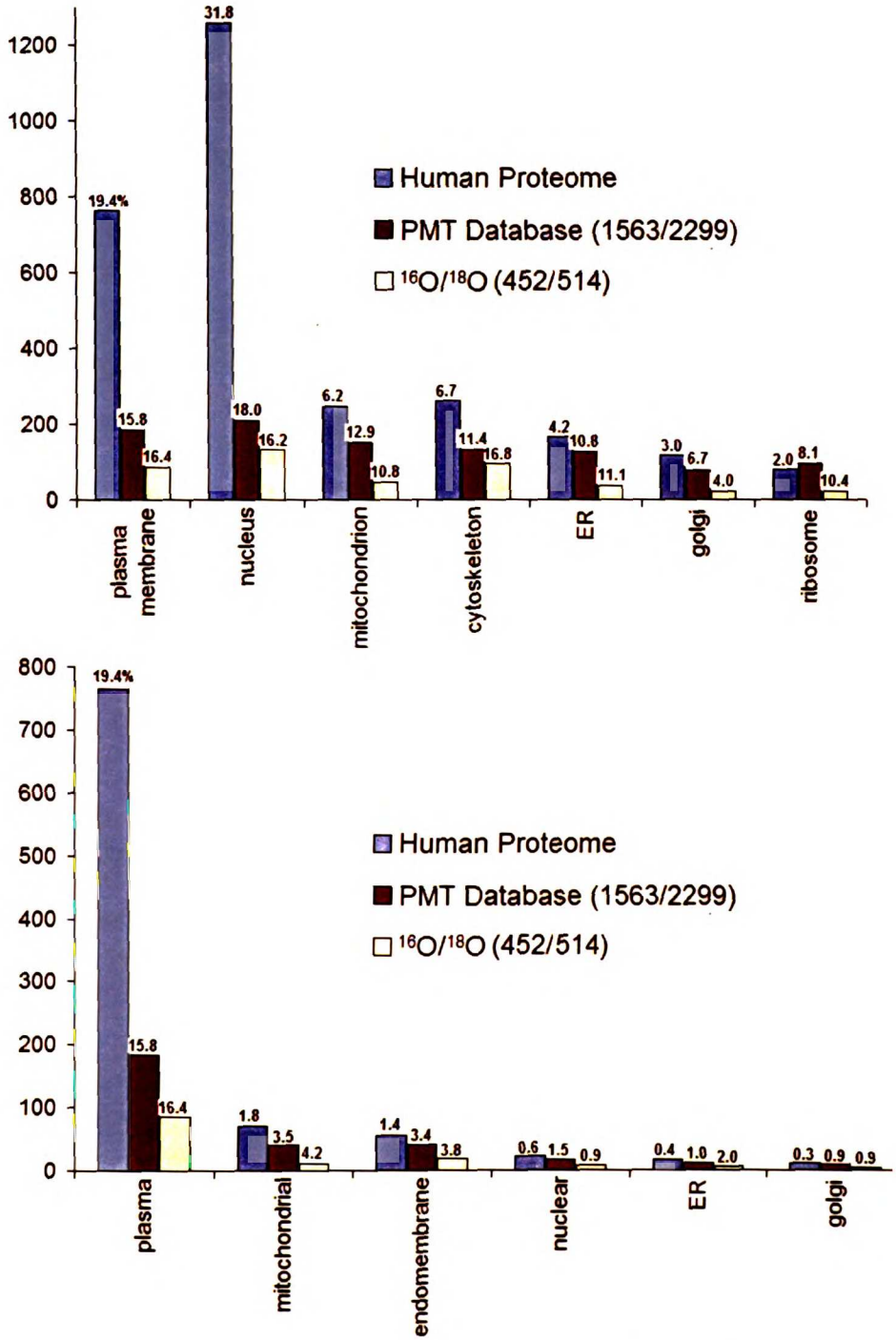

Figure 4. The distribution of proteins detected using the AMT and $^{16}O/^{18}O$ labeling strategies. Organelle assignments were made using GO categories. The distribution of proteins predicted from the entire human genome is shown for comparative purposes. Numbers above bars indicate proteins in that organelle expressed as a percentage of the total number of "cellular" proteins annotated in GO (1162 annotated/2,299 PMT database and 452 annotated/514 $^{16}O/^{18}O$ quantified proteins). The distribution of detected proteins across various membrane compartments within the cell is shown in the bottom graph.

Protein Abundance Accuracy and Precision

In order to determine the experimental bias associated with peptide labeling and detection, we assessed the accuracy of relative protein abundance measurements. Two identical aliquots of the Reference sample were separately digested into peptides, labeled with either ^{16}O or ^{18}O and then combined for LC-FTICR analysis. Figure 5 displays the distribution of abundance ratios for 334 peptide pairs detected in two separate control experiments. As expected, the distribution for detected peptide pairs displayed a Gaussian-like distribution centered at 1.0, demonstrating the accuracy of relative abundance measurements even in complex samples. These results are consistent with previous evaluations of peptide abundance accuracy using the ^{18}O labeling procedure [20, 30, 34, 35]. Figure 6 shows the normalized fold changes of 304 proteins in HMEC. The majority of proteins (95%) showed less than a 3-fold change relative to the Reference sample. The standard deviations for abundance ratios are shown as error bars and represent the variability among peptide abundance ratios (precision) for the same protein. Among those proteins with multiple labeled peptides detected in HMEC, the majority (52%) showed <30% deviation in abundance among their constituent peptides. Sources of abundance variation among peptides from the same protein have been discussed previously [20, 30, 34, 35] and include 1) a low level of spontaneous exchange of ^{18}O-labeled peptides back to ^{16}O; (2) an error in assignment due to the small percentage of false peptide identifications; (3) the presence of multiple isoforms of the same protein; and 4) the effects of posttranslational modifications, which may lead to different abundance ratios for different detected peptides from the same protein. In this study, we minimized the effects of errors in peptide assignment by using a discriminant based

scoring method that incorporates both elution time and tryptic cleavage information [40]. In addition, spontaneous $^{18}O/^{16}O$ exchange was minimized in our samples by "quenching" residual trypsin activity as previously described [35].

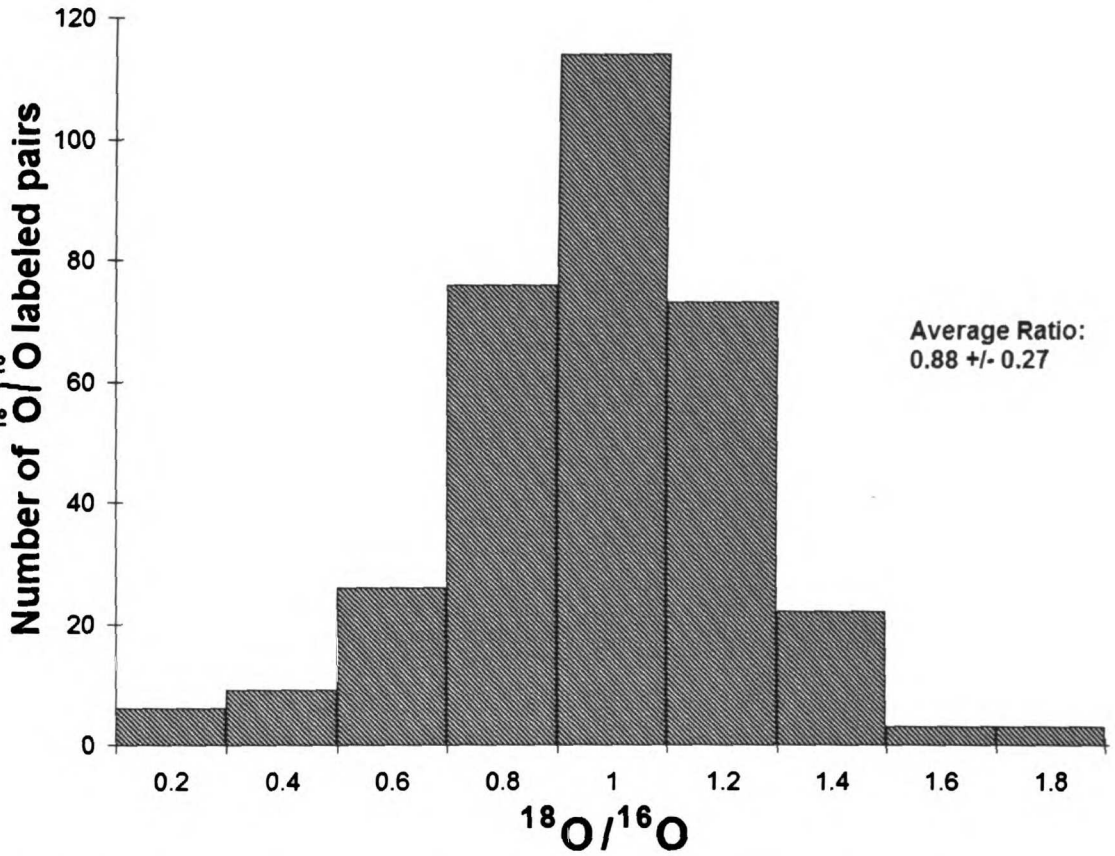

Figure 5. Ratio distribution of 334 detected peptide pairs in LC-FTICR analysis of the 1:1 labeled control reference samples.

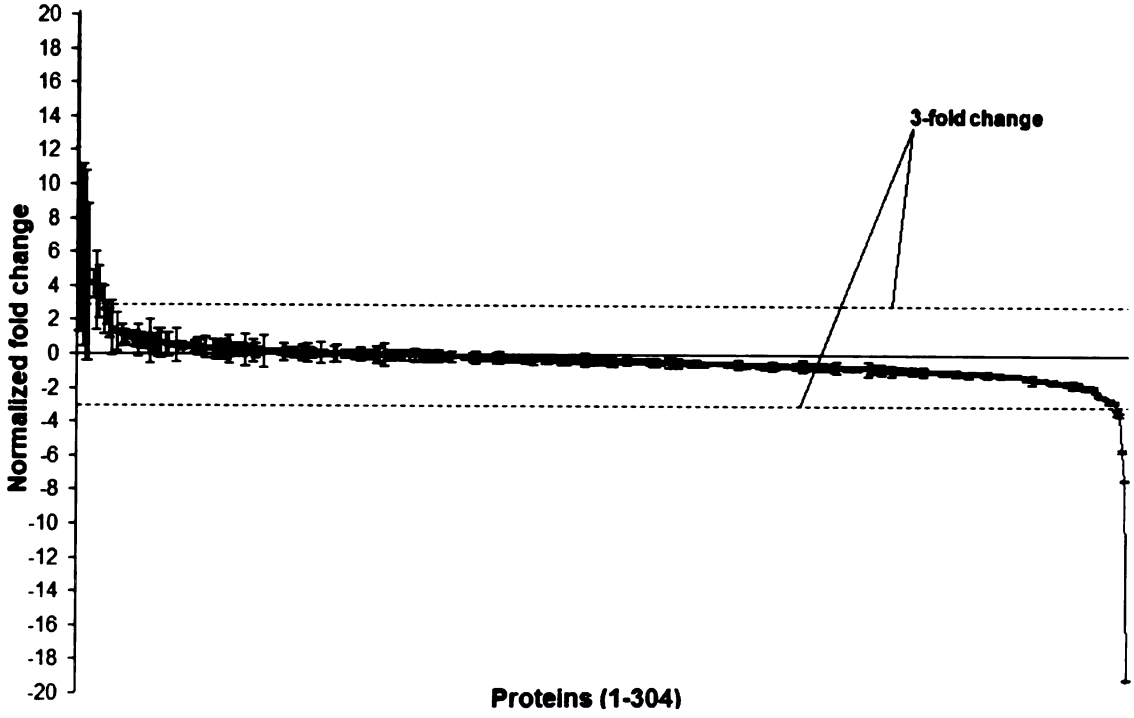

Figure 6. Normalized fold changes for quantified proteins in the HMEC cell line. For ratios smaller than one, inverted ratios were calculated as [-1/R] and then normalized to zero. Error bar for each protein indicates the standard deviation for abundance ratios from multiple peptides. Proteins without error bars were identified with single peptides.

Comparative Analyses of Cell Line Proteomes

Cell phenotype or environmental manipulations are associated with differences in protein expression. In nucleic-acid based expression arrays, pair-wise comparisons are made simultaneously through the use of a common "reference" set of cell lines or tissues. However, in quantitative proteome studies using stable isotope labeling, each experimental condition is compared individually with other conditions (i.e., normal vs. diseased tissue or untreated vs. treated cell line). Thus, a comparative proteomic study of 5 cell lines would normally require 10 pair-wise labeling experiments. By providing a common reference against which all cell lines can be compared, our study enabled the pooling of different 16O/18O experiments into a single dataset and minimized the number of experiments (5) required for comparison of protein abundance among multiple conditions.

This pooled dataset consisted of 514 proteins quantified across ten experiments (5 cell line comparisons X 2 replicates). Figure 7 (left) displays the number of peptide tags identified for each protein in each of the experiments. Proteins (rows) are displayed across all ten experiments (columns), with deeper shades of yellow indicating increasing numbers of tryptic peptides identified for particular proteins (range 2-65). Log-transformed abundance ratios for all quantified proteins in the 10 experiments are displayed in Figure 7 (right). In all cases the Reference mixture was labeled with 16O and the "paired" 18O labeled peptide was in the comparative cell line. The calculated abundance ratios, standard deviations, and number of peptides used for identification are available in supplemental materials (Table S1). No correlations between the number of peptide tags identified and the calculated 16O/18O abundance ratios were found (Figure

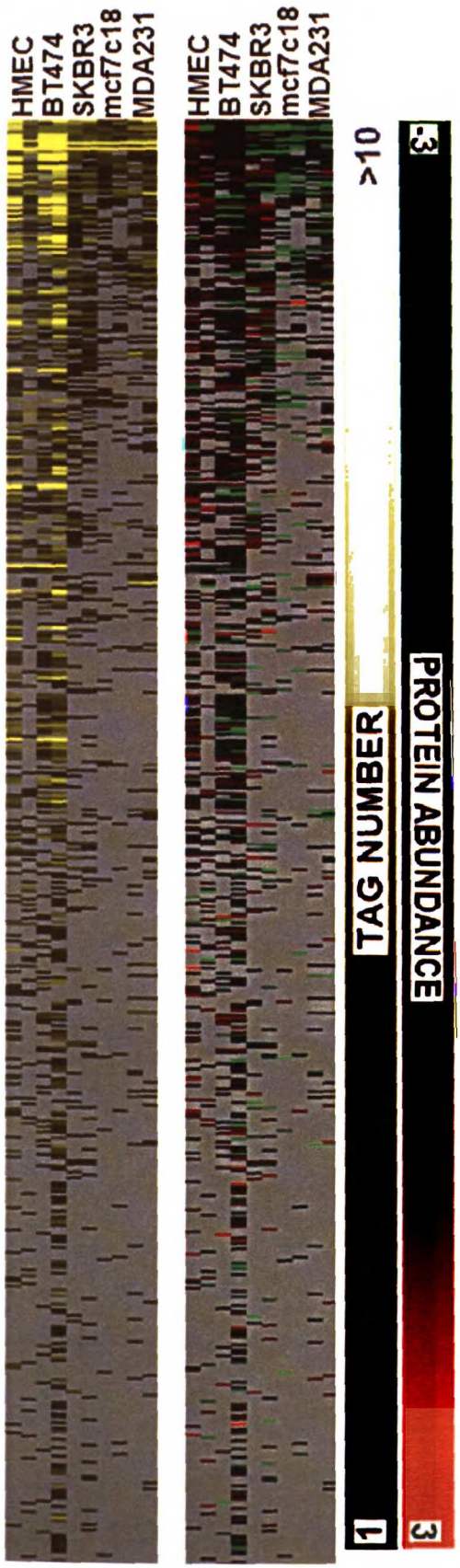

Figure 7.

Pooled dataset with the 514 quantified proteins (in rows) identified from 5 cell lines done in replicate (10 columns). The proteins are sorted in decreasing order down rows by the number of experiments in which a labeled (18O/16O) peptide pair was detected with the reference panel. Left matrix shows number of peptide tags that were detected for proteins across cell lines. Areas in gray indicate that no peptide pairs were found. Right matix shows calculated abundance ratios represented by a red-green color scheme. Red indicates increased protein abundance in a particular cell line relative to the reference mixture, green indicates protein levels below the reference mixture, and color saturation reflects the magnitude of the ratio relative to the reference mixture.

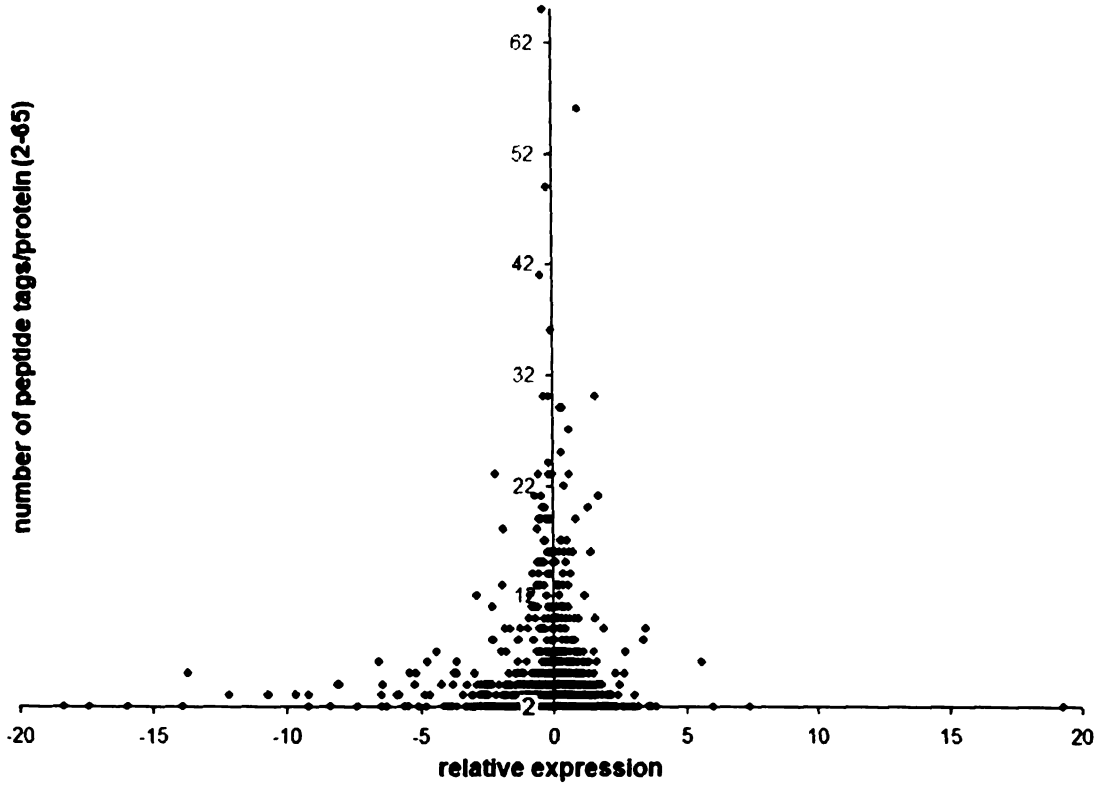

Figure 8. Comparison of relative protein abundance (x-axis) vs. number of peptide tags/proteins identified by FTICR in Reference mixture (^{16}O) vs. HMEC (^{18}O) comparison. No correlation between tag number and relative abundance was evident.

The entire set of quantified proteins (Figure 7) was examined for differences in protein abundance between HMEC and the cancer cell lines. Eighty-six proteins showed at least a 3-fold difference in abundance ratios between HMEC and at least one of the cancer cell lines (Table S2). These proteins were located in various organelles throughout the cell, including the cytoplasm (16 proteins), cytoskeleton (23), endoplasmic reticulum (4), mitochondria (5), nucleus (8), plasma membrane (11), and ribosome (6). A selected list of 36 proteins arranged by cellular location (via GO) is displayed in Table 1 along with the corresponding peptide tag information. In general our confidence in the abundance ratio of a protein is inversely related to the percent deviation across its constitutive peptide abundances. Seventeen proteins had a <40% deviation in abundance for constituent peptides detected in both HMEC and cancer cell lines for which a 3-fold difference was shown.

The cytoskeletal protein, cytokeratin 18 (CK18), is among the proteins displaying >3-fold increase in expression in the cancer cell lines compared to HMEC, with high relative expression in both BT-474 and MDA-231. Figure 9 displays a collection of spectra for CK18 peptides and their relative abundance in various cell lines compared to the Reference mixture. CK18 expression has been correlated with tumor metastasis and may function as a prognostic indicator in breast cancer [49-52]. Our results are consistent with other proteome analysis of breast tissue using two-dimensional difference gel electrophoresis (2-D DIGE) technology, which revealed increased CK18 protein expression in infiltrating ductal carcinoma of the breast compared to normal tissue [23]. However, previous studies using monoclonal antibodies to CK18 in breast cancer cell lines [49] and tumor tissue [53] have shown reduced expression in highly metastatic cell

lines/invasive carcinomas and increased expression in weakly metastatic cell lines or benign tissue. The lack of consensus among these studies may be due to the different types tissue/cell lines/sample preparations used for analysis in each study or experimental variation between antibody-based and high-throughput quantification techniques.

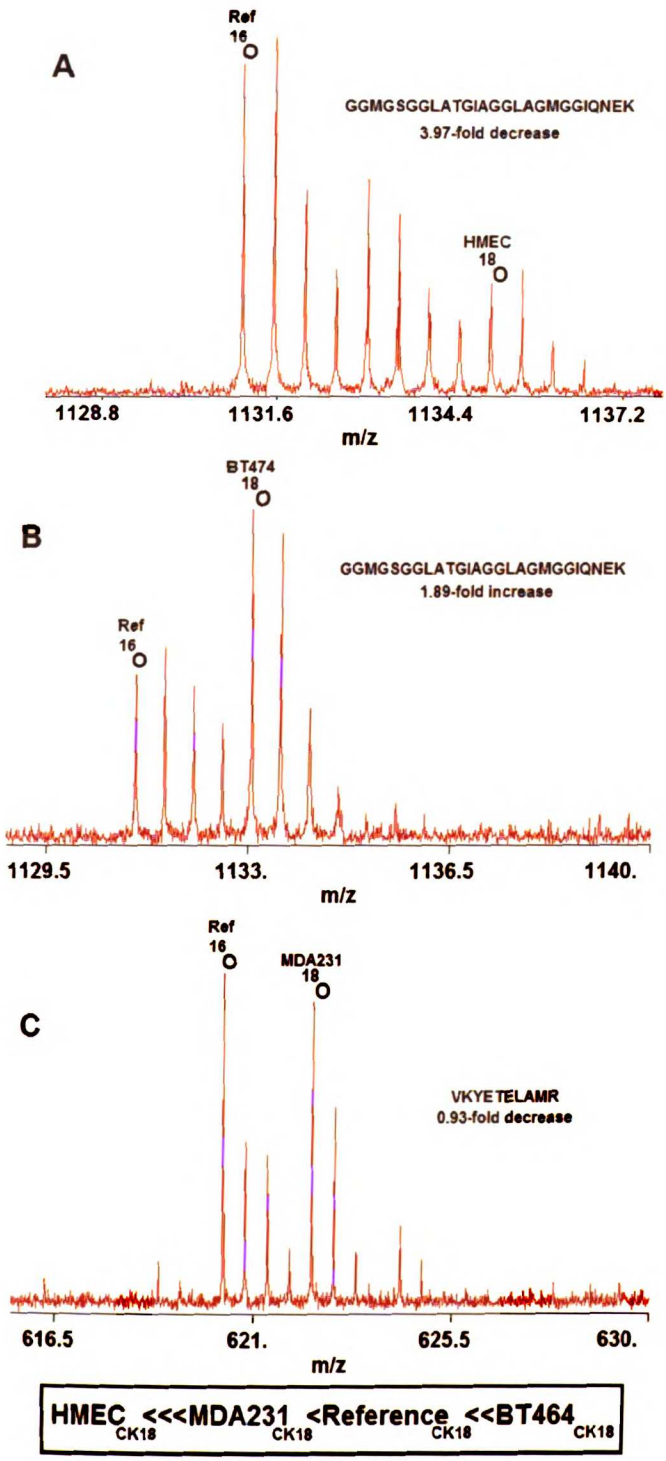

Figure 9. Mass spectra for 3 peptide pairs in the Keratin 18 protein showing relative peptide abundance between the (A) HMEC (^{18}O) and Reference (^{16}O); (B) BT-474 (^{18}O) and Reference (^{16}O); and (C) MDA-231 (^{18}O) and Reference (^{16}O) comparisons.

Several proteins displayed >3-fold decrease in abundance in cancer cells compared to HMEC. The 90kDa heat shock beta 1 protein (HSP90B/HSPCB), which showed >3-fold decrease in expression in SKBR-3 cell lines relative to HMEC, is a molecular chaperone protein that plays a key role in the stability and function of a diverse set of 'client' proteins, many of which are implicated in breast cancer progression and resistance to therapy (estrogen receptor, receptor tyrosine kinases, p53) [54, 55]. Previous studies of HSP90 expression with cancer progression have produced varied results, particularly among the HSP90B subunit, which is constitutively and highly expressed among most tissues [56]. A recent MS-based study revealed increased expression of HSP90B in metastatic cell lines compared to non-metastatic cells [57], while other studies have shown no association of HSP90B with cell proliferation [58]. The S100 calcium binding protein A2 (S100A2) showed relatively high expression in HMEC, but low expression in the SKBR-3, which is consistent with previous studies that implicate S100A2 as a tumor suppressor gene; expressed in normal breast tissue but downregulated during breast cancer progression [59]. Our study also showed reduced expression of the calreticulin protein in the MDA-231 and MCF7c18 cell lines relative to HMEC. This finding contrasts with previous studies showing increased expression of calreticulin in malignant breast tissue compared to normal/benign tissue using 2-D PAGE techniques [60, 61]. This discrepancy could be due to differences between breast tissue and cultured cells with regard to heterogeneity or may reflect differing stages of protein processing/translocation during analysis.

The use of a reference mixture enabled application of cluster-based discrimination methods to group proteins according to protein abundance. Ninety-three proteins

displaying relative abundance ratios in at least 4 of the 5 cell lines studied were clustered (Figure 10). Five of these clusters were selected for display (Figure 11) based on their expression profiles along with the biological or cellular locations associated with the constituent proteins in each cluster. Several proteins associated with protein metabolism (nucleotide binding, protein binding, protein biosynthesis, protein folding) were represented in these clusters, as well as several plasma membrane, cytoskeletal, ribosomal, endoplasmic reticulum, and nuclear proteins. Six proteins in cluster 1 (C1) had increased expression in the BT-474 cell line compared to the other cell lines.

Given that the BT-474 is derived from ER^+ breast cancer tissue and that estrogen receptors (ER) indicate a favorable prognosis in breast carcinoma [62, 63], we were particularly interested in the set of proteins upregulated in this cell line. Calreticulin protein, known to modulate gene expression by interacting with the consensus motif KxFF[K/R]R present in the DNA binding domain of all nuclear receptors, including ERs [64, 65] was in the C1 cluster. Previous studies using transfected cells lines have implicated the ER pathway in the negative modulation of cancer invasion by calreticulin [66]. In our study, the upregulation of calreticulin in the BT-474 cell line is consistent with ER-calreticulin mediated cancer repression. In cluster 2 (C2) 8 proteins were decreased in BT-474 and increased in SKBR-3 compared to their abundances in HMEC, MCF7c18, and MDA-231. Among these proteins are lactate dehydrogenase and moesin, both investigated previously with regard to ER status. Studies of lactate dehydrogenase in breast cancer have shown contradictory results regarding its association with estrogen receptor status [67, 68]. Our study indicates overexpression of this protein in SKBR3 relative to its expression in BT-474, and may suggest an inverse correlation with ER

status. Additional validation using other approaches will be needed to confirm this relationship. Previous PCR-based hybridization techniques show overexpression of moesin in ER^- breast carcinoma cell lines compared to ER^+ breast carcinomas [69], a result consistent with the moesin expression profile in our study. Other group of proteins in clusters 4 and 5 (C4, C5) were similar for the BT-474, SKBR-3, and MCF8c18 cell lines, but showed opposite patterns of expression in HMEC and MDA-231. In contrast, the set of 12 proteins in cluster 7 (C7) showed decreased expression in both HMEC and MDA-231 compared to their expression in the other cell lines.

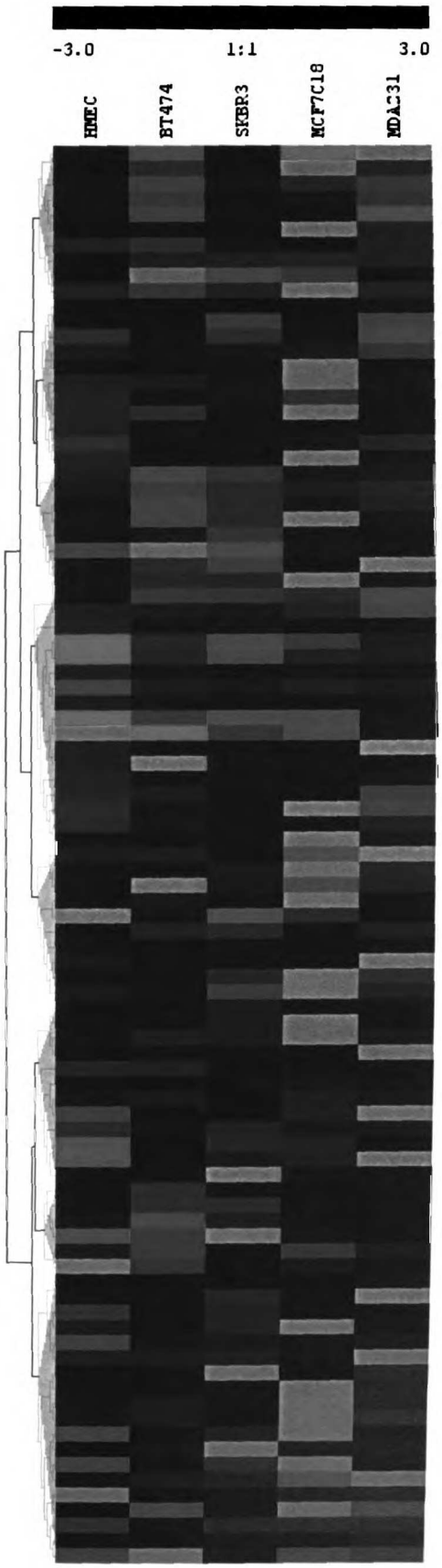

Figure 10

Results of hierarchical clustering of 93 proteins across 5 cell lines. Clusters are indicated by dendogram on left

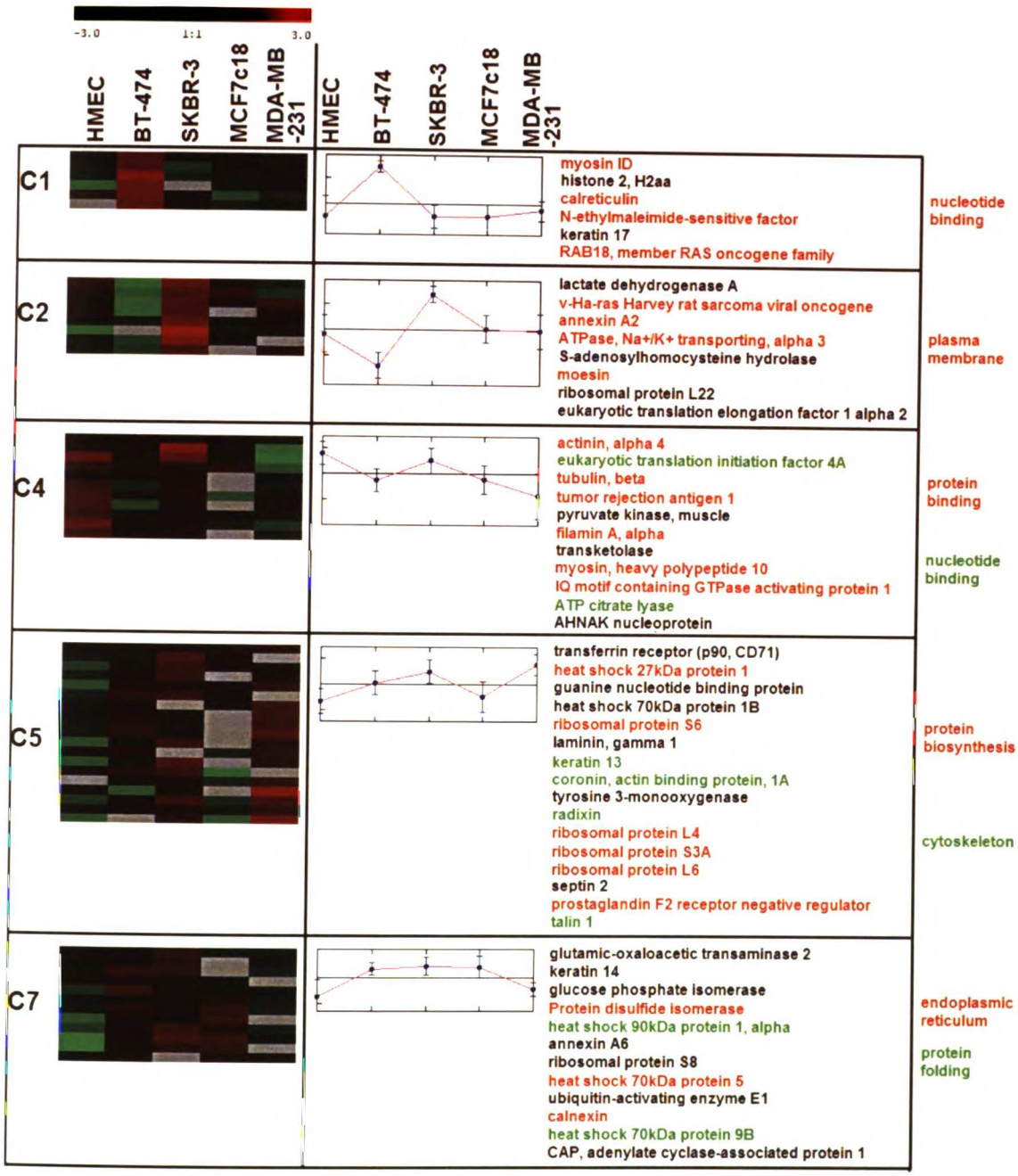

Figure 11. Five selected groups of proteins based on results of hierarchical clustering. Expression matrices on left indicate expression of proteins relative to the reference mixture. Centroid graphs in center of figure indicate average expression of clustered proteins across cell lines. Individual proteins belonging to each cluster are shown to the right. Protein highlighted in red and green indicate those that belong to GO-derived categories denoted in the rightmost column.

Comparison of Protein Abundance and mRNA Expression Ratios

A comparison of protein and transcript abundances in these cell lines provides information regarding the variability of protein abundances between cell lines relative to gene expression. These comparisons potentially reveal the extent to which transcripts are translated into mature protein products. 156 proteins in our protein abundance dataset (Figure 7) had corresponding gene expression data available [46] for at least one of the cell lines (HMEC, BT-474, SKBR-3, MDA-231; No gene expression data was available for the MCF7c18 cell line). Our renormalization strategy enabled comparisons between mRNA expression and protein abundance ratios and restricted our dataset to 184 measurements of 70 genes/proteins. Figure 12 displays the comparison of protein and mRNA expression for this restricted dataset after re-scaling. Correlations (Pearson's correlation) among transcript and protein expression in the combined (r^2=0.10) or individual cell line comparisons (BT-474: r^2=0.20; MDA-231: r^2=0.10; SKBR-3: r^2=-0.05) were not detected. We also investigated correlations among gene and proteins in various GO-defined functional groups. Previous studies show moderate correlations among various subsets of genes [70-72]. Our data indicated low correlations among these subsets, with only 9 transcriptional proteins showing moderate correlation (r^2=0.54, 23 measurements) between their mRNA and protein abundances (Figure 13).

Although the overall correlation between protein and mRNA abundance measurements was poor, a >3-fold difference at both the protein and transcript level was seen for a few genes/proteins. Table 2 displays mRNA and protein abundance ratios for 21 proteins in various cancer cells relative to HMEC. Eighteen proteins showed "congruent" expression profiles, with both mRNA and protein measurements similarly

under or over-expressed, thereby providing complimentary evidence of differential regulation between HMEC and cancer cell lines. Several of these proteins, including the CK18, tumor rejection antigen 1 (P14625); leukotriene A4 hydrolase (P09960), and beta actin (P02570) proteins also had relatively confident quantifications (Table 1, *) and would therefore be top candidates for future investigations of cancer markers in these cell lines.

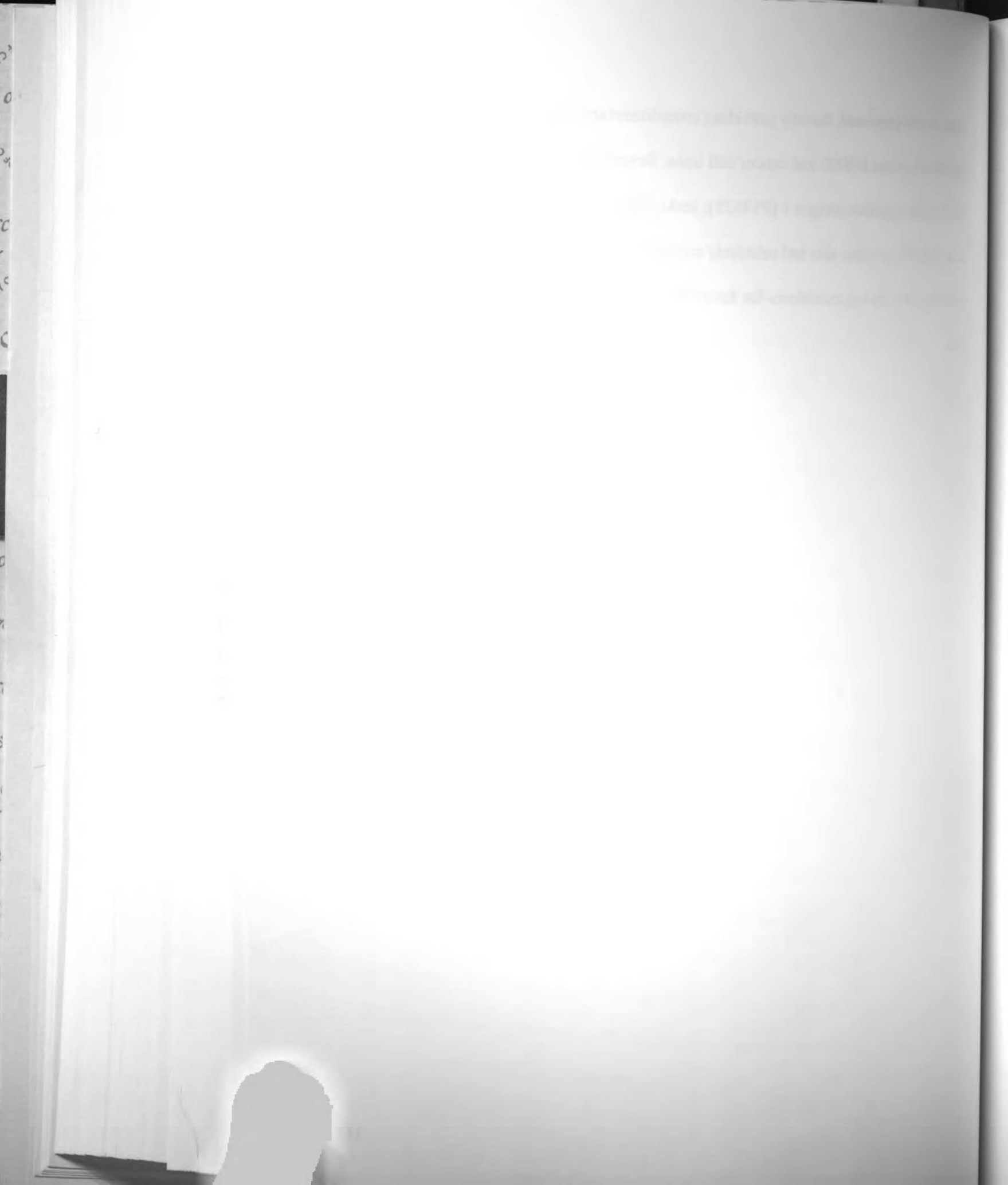

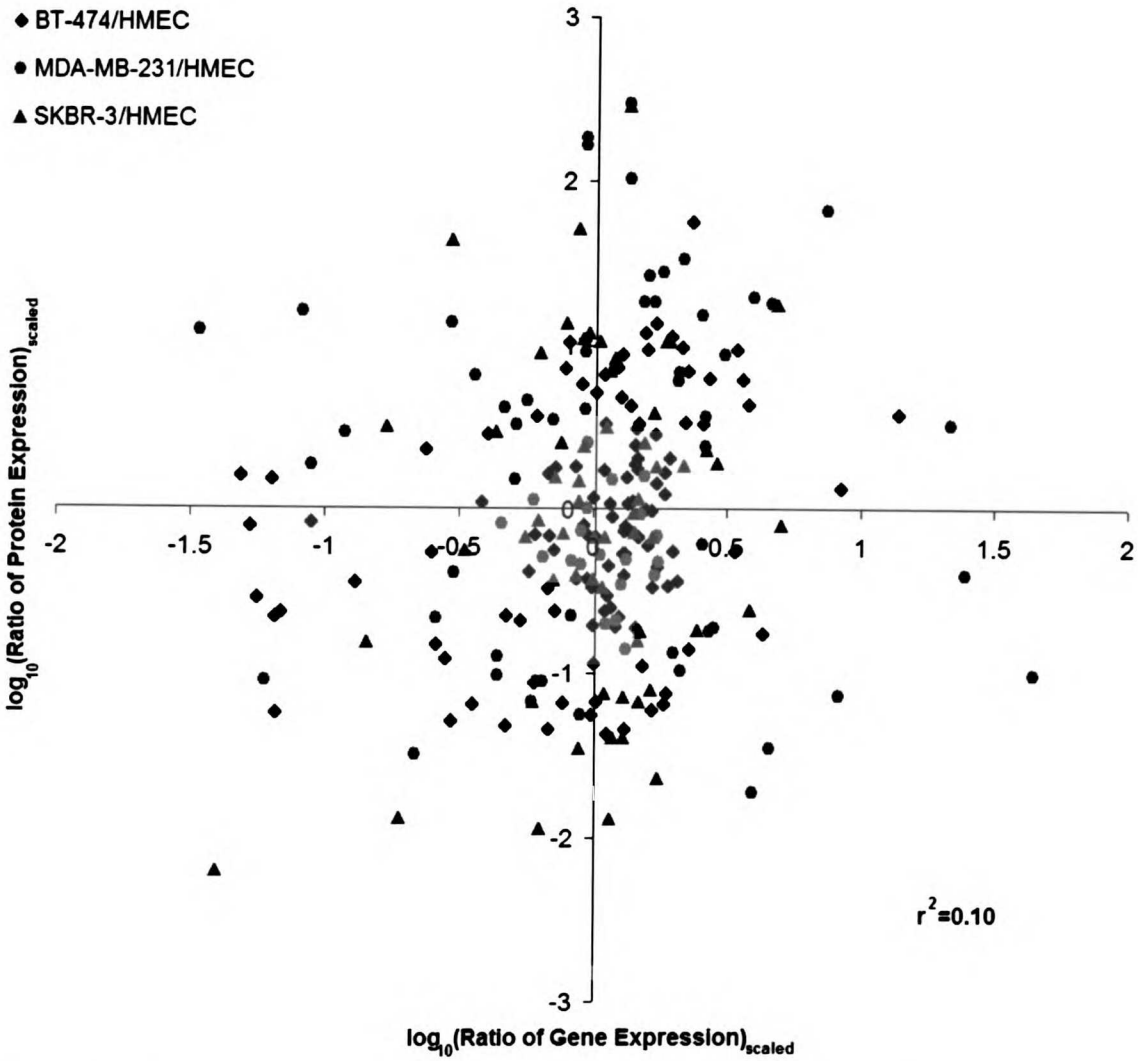

Figure 12. Comparison of mRNA (x-axis) and protein (y-axis) expression for 184 measurements (70 genes) across 3 cancer cell lines relative to the HMEC cell line (correlation, r^2=.10). Values were scale-normalized so that the dynamic ranges of gene and protein expression levels were comparable and the corresponding log values were calculated.

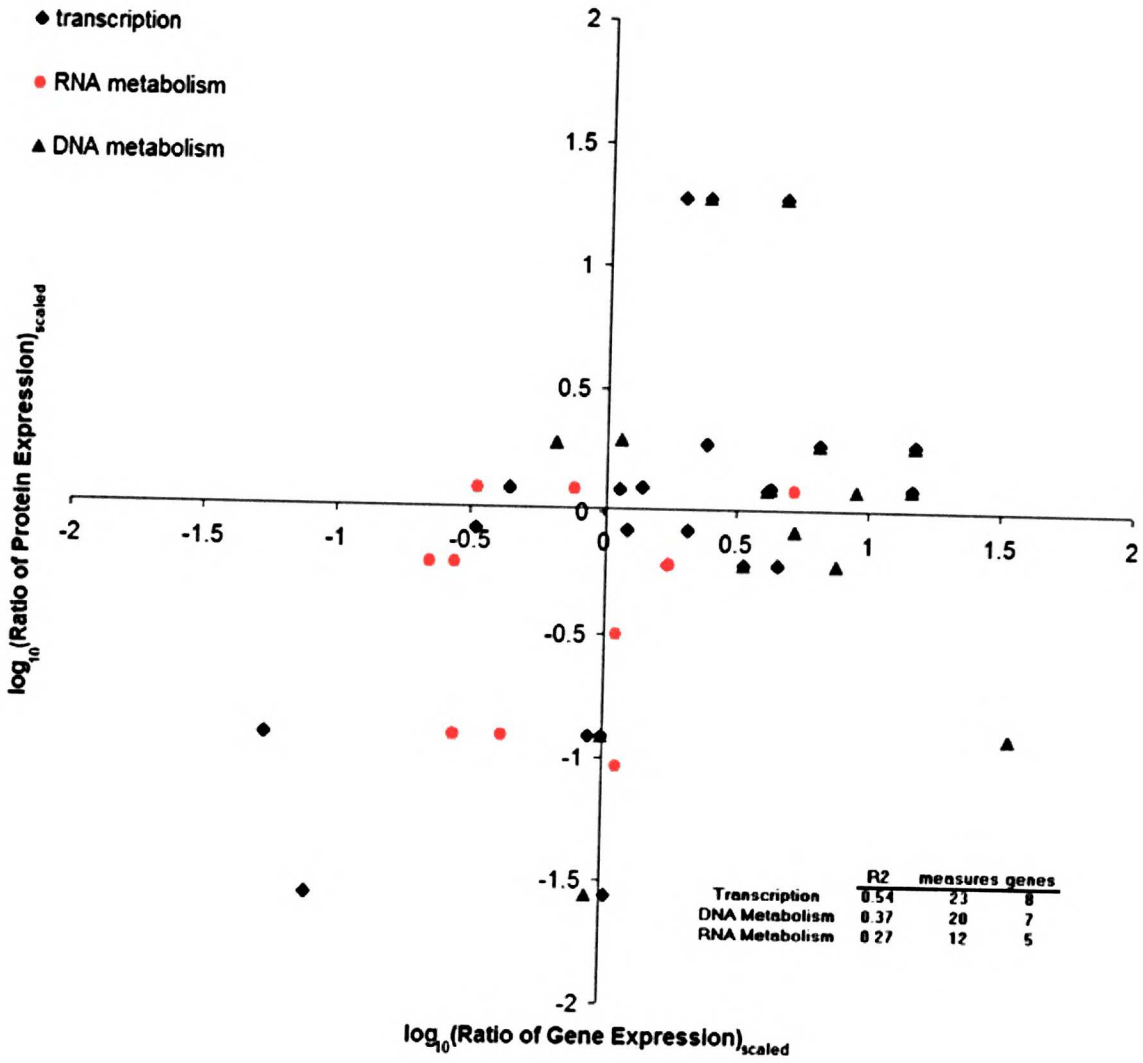

Figure 13. Correlations of mRNA and proteins abundances for proteins associated with transcription, DNA and RNA metabolism.

Concluding Remarks

This study constitutes a large quantitative analysis of breast cancer cell line proteomes. Using a Reference mixture of cell lines, ^{18}O peptide labeling, FTICR mass spectrometry, and the AMT tag strategy we were able to identify multiple proteins that were differentially expressed among non-cancer and cancer cell lines. The significance of differing patterns of protein expression among cell lines requires further validation using tissue samples. Information accumulated in the PMT tag database can be used repeatedly to support direct quantitative measurements of proteins in future experiments of breast cancer tissue or additional cell lines. Additional analysis of these proteins and the biochemical pathways in which they are involved will not only further our understanding of breast oncogenesis, but will also provide new and valuable targets for translational research.

Table 1. Selected list of 36 proteins with at least a 3-fold difference in protein abundance between cancer cell lines (BT-474, MDA-231, SKBR-3, MCF7c18) and the HMEC cell line. Average protein abundances ratios (avg) <1 indicate a decrease in protein expression relative to the Reference mixture. Values highlighted in green indicate >3.0-fold decrease and those highlighted in red indicate >3.0-fold increase in expression relative to HMEC. For each cell line the number of peptides used to calculate average abundance ratios for each protein are shown (c). Gray shading indicates the percent deviation among constituent peptides. Proteins with <40% deviation among multiple labeled peptides were considered more confident quantifications and are indicated with an (*). Proteins are listed according to subcellular location as determined by GO annotations (CS, cytoskeleton; ER, endoplasmic reticulum; L, lysosomal; PM, plasma membrane).

	>3X HMEC	<20% dev		<30% dev		<40% dev				>40% dev		
	<3X HMEC	HMEC		BT-474		SKBR-3		Mcf7c18		MDA-231		
SPN	DESCRIPTION	avg	c	avg	c	avg	c	avg	c	avg	c	
P00338	lactate dehydrogenase A	1.14	2	0.13	6	1.96	2	0.72	4	1.19	2	Cytoplasm
*P08238	heat shock 90kDa 1, Beta	1.75	2	1.11	16	0.53	2	0.98	4	0.29	2	
*P09960	leukotriene A4 hydrolase	1.72	2			0.38	2	2.11	2	1	2	
P13693	tumor protein, translationally-controlled 1	2.07	2	0.27	3	1.29	2	7.02	2			
*P18669	phosphoglycerate mutase 1	1.89	6	0.59	2							
*P42655	tyrosine 3-monooxygenase activation protein, epsilon	3.35	5	0.89	4					2.32	2	
*P15311	villin 2	2.88	3	1.17	7	0.56	2	0.3	2	0.47	4	
*P07737	profilin 1	1.27	3	0.42	2							CS
*Q14204	dynein	3.16	3	0.86	2							
*P16475	myosin, light peptide 6	2.52	5	0.74	3							
*P02570	actin, beta	2.61	2	0.65	19	0.81	3	0.8	2	1.62	3	
*P05783	keratin 18	0.22	2	1.69	3					1.04	2	
P35579	myosin, heavy polypeptide 9	2.65	30	0.86	30	0.73	20	0.61	11	0.75	13	
P46940	Ras GTPase-activating-like protein IQGAP1	2.13	7	0.97	4	1.86	4	0.37	3	0.13	3	
P11021	78 kDa glucose-regulated	1.25	13	0.96	11	1.27	2	0.41	2	0.56	3	ER
*P27797	calreticulin	2.12	3	2.33	4	1.16	2	0.36	2	0.62	2	
*P14625	tumor rejection antigen 1	1.92	7	0.6	4	1.23	3			0.56	2	
P07339	cathepsin D	1.51	3	1.25	3	0.34	2					L
O95573	acyl-CoA synthetase LC 3	2.02	3	0.51	2							Mitochondria
P06576	ATP synthase, beta	0.57	8	1.94	10							

*P25705	ATP synthase, alpha subunit,1	0.8	4	2.65	6							
P40926	malate dehydrogenase 2, NAD	0.36	4	1.35	6							
P49748	Acyl Coenzyme A dehydrogen	0.57	2	2.08	2							
O43707	actinin, alpha 4	2.19	1 2	0.91	7	2.01	7	1.18	3	0.5	6	nucleus
*P02304	histone H4	0.29	4	4.08	3							
*P16106	histone 1	0.2	2	2.6	2	2.83	2					
O75531	barrier autointegration factor 1	0.08	3	1.18	2							
P01112	Transforming p21/H-Ras-1	0.56	3			2.73	4	0.31	1	0.54	1	PM
P01118	Transforming p21; v-Ki-ras2	0.44	2			4.89	2					
P07355	annexin A2	1.74	4	0.3	1 1	2.3	2	0.72	2	0.46	4	
P51153	RAB13, member RAS	2.06	2	1.2	2	0.8	2	0.46	2	0.33	2	
O88386	RAB10, member RAS	2.3	2	1.73	2	0.8	2			0.36	2	
P00938	triosephosphate isomerase 1	1.32	7	0.43	8							
*P29034	S100 calcium binding protein A2	20.3	2			2.18	2					
Q9Y3F4	serine/threonine kinase receptor associated protein	1.65	3	0.71	3	0.36	2			1.27	4	
*P29401	Transketolase	2.52	7	0.61	7	1.4	4			0.96	2	

Table 2. List of 21 proteins showing at least a 3-fold difference in both protein and mRNA expression between cancer and HMEC cells. Values highlighted in red indicate >3-fold increase and those in green indicate >3-fold decrease relative to HMEC. Three proteins with >3-fold increase in mRNA expression showed >3-fold decrease in protein expression (incongruent expression).

	cancer/HMEC				
	mRNA	protein	SPN	Description	cell line
congruent expression			O95573	acyl-CoA synthetase long-chain family member 3	BT-474
			P00338	lactate dehydrogenase A	
			P02570	actin, beta	
	3.420	7.824	P05783	keratin 18	
			P14625	tumor rejection antigen 1	
			P23526	S-adenosylhomocysteine hydrolase	
			P26640	valyl-tRNA synthetase 2	
			Q01813	phosphofructokinase, platelet	
			P14786	pyruvate kinase	MDA-231
			P35214	tyrosine 3-monooxygenase activation protein, gamma	
			P46940	Ras GTPase-activating-like protein IQGAP1	
			P53396	ATP citrate lyase	
			Q00765	Polyposis locus protein 1	
			P01118	v-Ki-ras2 Kirsten rat sarcoma viral oncogene homolog; Transforming protein p21b	SKBR-3
	4.592	11.170	P02570	actin, beta	
			P09960	leukotriene A4 hydrolase	
			P28288	ATP-binding cassette, sub-family D (ALD), member 3	
			P35579	myosin, heavy polypeptide 9	
incongruent expression	41.687		O00159	myosin IC	SKBR-3
	12.445		P07339	cathepsin D	
	9.226		P15311	villin 2	

Appendix D

Table S1. Abundance ratios for 514 proteins quantified across cell lines

Table S2. List of 86 proteins with at least a 3-fold difference in protein abundance between cancer cell lines (BT-474, MDA-231, SKBR-3, MCF7c18) and the HMEC cell line.

Acknowledgements

This work was supported by the NIH CA86135 (MP), the NIH National Center for Research Resources (RR18522), and the Environmental Molecular Science Laboratory (a national scientific user facility sponsored by the Department of Energy's Office of Biological and Environmental Research and located at Pacific Northwest National Laboratory). Pacific Northwest National Laboratory is a multi-program national laboratory operated by Battelle Memorial Institute for the U.S. Department of Energy under contract DE-AC05-76RLO-1830. The authors would like to thank Scott Dixon and Katy Williams for advice and help in sample preparation and Heather Mottaz for help in chromatography and preparing samples for proteome analysis.

References

1. Greenlee, R. T., Murray, T., Bolden, S. and Wingo, P. A., *CA Cancer J Clin* 2000, 50, 7-33.

2. Pusztai, L., Ayers, M., Stec, J., Clark, E., *et al.*, *Clin Cancer Res* 2003, 9, 2406-2415.

3. Zajchowski, D. A., Bartholdi, M. F., Gong, Y., Webster, L., *et al.*, *Cancer Res* 2001, 61, 5168-5178.

4. Ross, D. T. and Perou, C. M., *Dis Markers* 2001, 17, 99-109.

5. Weisz, A., Basile, W., Scafoglio, C., Altucci, L., *et al.*, *J Cell Physiol* 2004, 200, 440-450.

6. Wilson, K. S., Roberts, H., Leek, R., Harris, A. L. and Geradts, J., *Am J Pathol* 2002, 161, 1171-1185.

7. Pollack, J. R., Sorlie, T., Perou, C. M., Rees, C. A., *et al.*, *Proc Natl Acad Sci U S A* 2002, 99, 12963-12968.

8. Harrison, P. M., Kumar, A., Lang, N., Snyder, M. and Gerstein, M., *Nucl. Acids. Res.* 2002, 30, 1083-1090.

9. Anderson, L. and Seilhamer, J., *Electrophoresis* 1997, 18, 533-537.

10. Futcher, B., Latter, G. I., Monardo, P., McLaughlin, C. S. and Garrels, J. I., *Mol Cell Biol* 1999, 19, 7357-7368.

11. Gygi, S. P., Rochon, Y., Franza, B. R. and Aebersold, R., *Mol Cell Biol* 1999, 19, 1720-1730.

12. Rodland, K. D., *Clinical Biochemistry* 2004, 37, 579.

13. Domon, B. and Broder, S., *J Proteome Res* 2004, 3, 253-260.

14. Adam, P. J., Boyd, R., Tyson, K. L., Fletcher, G. C., *et al.*, *J Biol Chem* 2003, 278, 6482-6489.

15. Wu, S. L., Hancock, W. S., Goodrich, G. G. and Kunitake, S. T., *Proteomics* 2003, 3, 1037-1046.

16. Arnott, D., Kishiyama, A., Luis, E. A., Ludlum, S. G., *et al.*, *Mol Cell Proteomics* 2002, 1, 148-156.

17. Edberg, D. D., Bruce, J. E., Siems, W. F. and Reeves, R., *Biochemistry* 2004, 43, 11500-11515.

18. Zhang, H., Wu, W., Du, Y., Santos, S. J., *et al.*, *J Biol Chem* 2004, 279, 19457-19463.

19. Gygi, S. P., Rist, B., Gerber, S. A., Turecek, F., *et al.*, *Nat Biotechnol* 1999, 17, 994-999.

20. Stewart, II, Thomson, T. and Figeys, D., *Rapid Commun Mass Spectrom* 2001, 15, 2456-2465.

21. Oda, Y., Huang, K., Cross, F. R., Cowburn, D. and Chait, B. T., *Proc Natl Acad Sci U S A* 1999, 96, 6591-6596.

22. Gehrmann, M. L., Fenselau, C. and Hathout, Y., *J Proteome Res* 2004, 3, 403-409.

23. Somiari, R. I., Sullivan, A., Russell, S., Somiari, S., *et al.*, *Proteomics* 2003, 3, 1863-1873.

24. Hathout, Y., Riordan, K., Gehrmann, M. and Fenselau, C., *J Proteome Res* 2002, 1, 435-442.

25. Li, J., Zhang, Z., Rosenzweig, J., Wang, Y. Y. and Chan, D. W., *Clin Chem* 2002, 48, 1296-1304.

26. Haab, B. B., *Mol Cell Proteomics* 2005, 4, 377-383.

27. Jessani, N., Humphrey, M., McDonald, W. H., Niessen, S., *et al.*, *PNAS* 2004, 101, 13756-13761.

28. Zang, L., Palmer Toy, D., Hancock, W. S., Sgroi, D. C. and Karger, B. L., *J Proteome Res* 2004, 3, 604-612.

29. Staes, A., Demol, H., Van Damme, J., Martens, L., *et al.*, *J Proteome Res* 2004, 3, 786-791.

30. Heller, M., Mattou, H., Menzel, C. and Yao, X., *J Am Soc Mass Spectrom* 2003, 14, 704-718.

31. Brown, K. J. and Fenselau, C., *J Proteome Res* 2004, 3, 455-462.

32. Lipton, M. S., Pasa-Tolic, L., Anderson, G. A., Anderson, D. J., *et al.*, *Proc Natl Acad Sci U S A* 2002, 99, 11049-11054.

33. Smith, R. D., Anderson, G. A., Lipton, M. S., Pasa-Tolic, L., *et al.*, *Proteomics* 2002, 2, 513-523.

34. Liu, T., Qian, W. J., Strittmatter, E. F., Camp, D. G., 2nd, *et al.*, *Anal Chem* 2004, 76, 5345-5353.

35. Qian, W. J., Monroe, M. E., Liu, T., Jacobs, J. M., *et al.*, *Mol Cell Proteomics* 2005.

36. Borg, A., Tandon, A. K., Sigurdsson, H., Clark, G. M., *et al.*, *Cancer Res* 1990, 50, 4332-4337.

37. Benz, C. C., Scott, G. K., Sarup, J. C., Johnson, R. M., *et al.*, *Breast Cancer Res Treat* 1993, 24, 85-95.

38. Shen, Y., Zhao, R., Belov, M. E., Conrads, T. P., *et al.*, *Anal Chem* 2001, 73, 1766-1775.

39. Yates, J. R., 3rd, Eng, J. K., McCormack, A. L. and Schieltz, D., *Anal Chem* 1995, 67, 1426-1436.

40. Strittmatter EF, K. L., Petritis K, Mottaz HM, Anderson GA, Shen Y, Jacobs JM, Camp DG, Smith RD, *Journal of Proteome Research* 2004, 3, 760-769.

41. Nesvizhskii, A. I., Keller, A., Kolker, E. and Aebersold, R., *Anal Chem* 2003, 75, 4646-4658.

42. Johnson, K. L. and Muddiman, D. C., *J Am Soc Mass Spectrom* 2004, 15, 437-445.

43. Yao, X., Freas, A., Ramirez, J., Demirev, P. A. and Fenselau, C., *Anal Chem* 2001, 73, 2836-2842.

44. Eisen, M. B., Spellman, P. T., Brown, P. O. and Botstein, D., *Proc Natl Acad Sci U S A* 1998, 95, 14863-14868.

45. Saeed, A. I., Sharov, V., White, J., Li, J., *et al.*, *Biotechniques* 2003, 34, 374-378.

46. Perou, C. M., Sorlie, T., Eisen, M. B., van de Rijn, M., *et al.*, *Nature* 2000, 406, 747-752.

47. Ball, C. A., Awad, I. A., Demeter, J., Gollub, J., *et al.*, *Nucleic Acids Res* 2005, 33 Database Issue, D580-582.

48. Ashburner, M., Ball, C. A., Blake, J. A., Botstein, D., *et al.*, *Nat Genet* 2000, 25, 25-29.

49. Schaller, G., Fuchs, I., Pritze, W., Ebert, A., *et al.*, *Clin Cancer Res* 1996, 2, 1879-1885.

50. Pantel, K., Schlimok, G., Braun, S., Kutter, D., *et al.*, *J Natl Cancer Inst* 1993, 85, 1419-1424.

51. Linder, S., Havelka, A. M., Ueno, T. and Shoshan, M. C., *Cancer Lett* 2004, 214, 1-9.

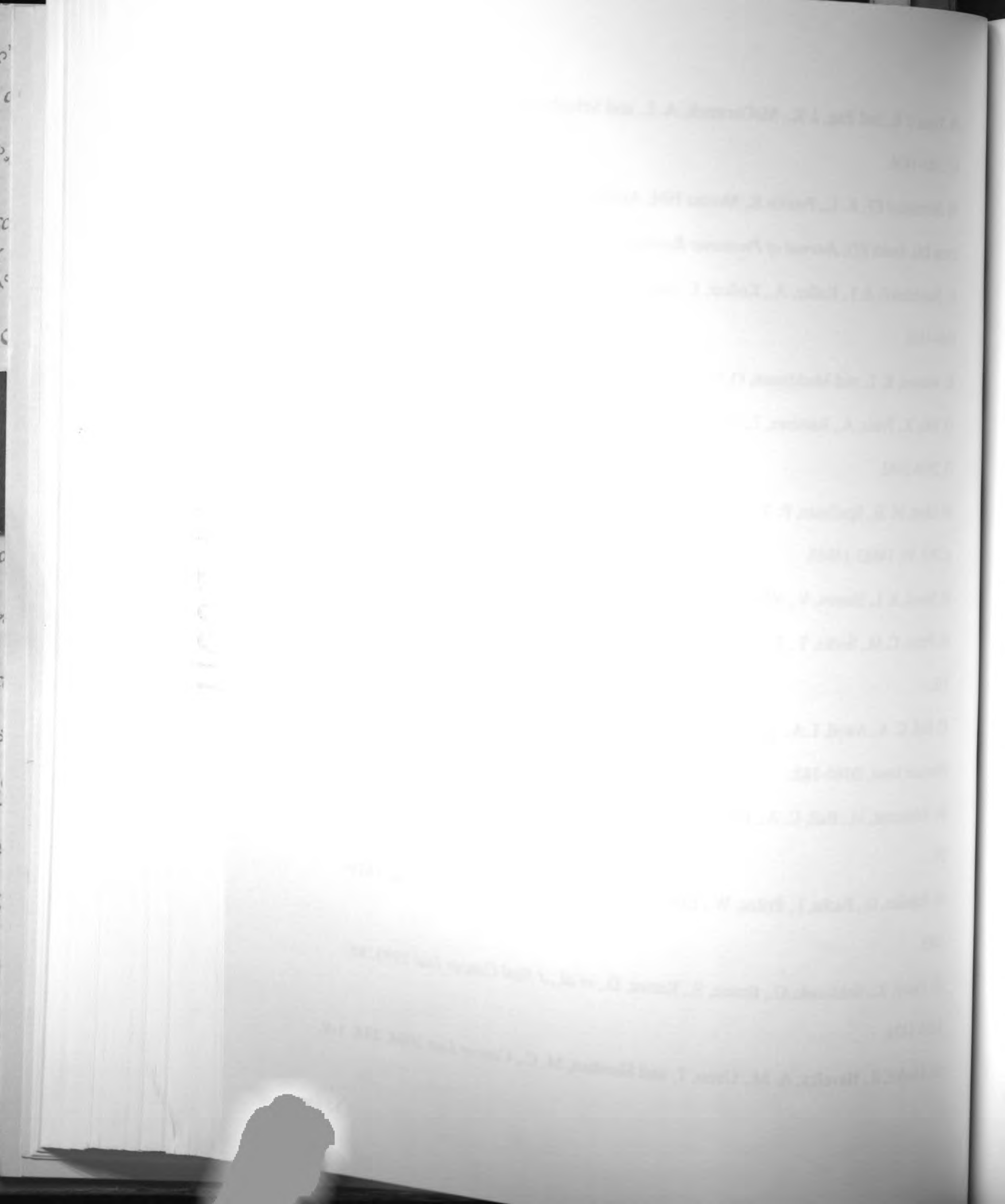

52. Woelfle, U., Sauter, G., Santjer, S., Brakenhoff, R. and Pantel, K., *Clin Cancer Res* 2004, 10, 2670-2674.

53. Rudland, P. S., Leinster, S. J., Winstanley, J., Green, B., *et al.*, *J Histochem Cytochem* 1993, 41, 543-553.

54. Pratt, W. B. and Toft, D. O., *Endocr Rev* 1997, 18, 306-360.

55. Pratt, W. B., *Annu Rev Pharmacol Toxicol* 1997, 37, 297-326.

56. Csermely, P., Schnaider, T., So, Prime, *et al.*, *Pharmacology & Therapeutics* 1998, 79, 129.

57. Hayashi, E., Kuramitsu, Y., Okada, F., Fujimoto, M., *et al.*, *Proteomics* 2005.

58. Yano, M., Naito, Z., Yokoyama, M., Shiraki, Y., *et al.*, *Cancer Letters* 1999, 137, 45.

59. Lee, S. W., Tomasetto, C., Swisshelm, K., Keyomarsi, K. and Sager, R., *Proc Natl Acad Sci U S A* 1992, 89, 2504-2508.

60. Bini, L., Magi, B., Marzocchi, B., Arcuri, F., *et al.*, *Electrophoresis* 1997, 18, 2832-2841.

61. Franzen, B., Linder, S., Alaiya, A. A., Eriksson, E., *et al.*, *Electrophoresis* 1997, 18, 582-587.

62. Thompson, E. W., Paik, S., Brunner, N., Sommers, C. L., *et al.*, *J Cell Physiol* 1992, 150, 534-544.

63. Rochefort, H., Platet, N., Hayashido, Y., Derocq, D., *et al.*, *J Steroid Biochem Mol Biol* 1998, 65, 163-168.

64. Dedhar, S., *Trends Biochem Sci* 1994, 19, 269-271.

65. Dedhar, S., Rennie, P. S., Shago, M., Hagesteijn, C. Y., *et al.*, *Nature* 1994, 367, 480-483.

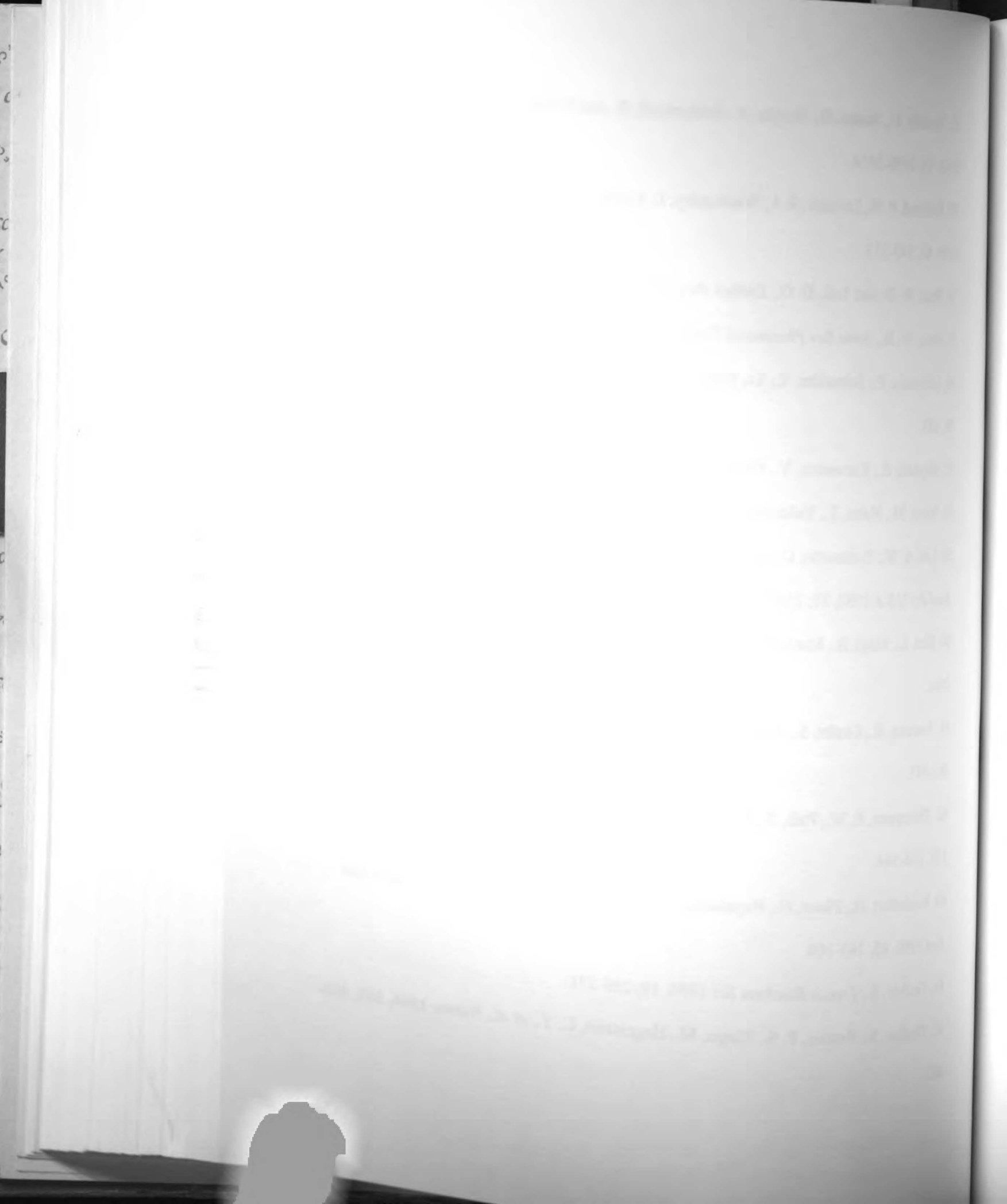

66. Platet, N., Cunat, S., Chalbos, D., Rochefort, H. and Garcia, M., *Mol Endocrinol* 2000, 14, 999-1009.

67. Brentani, M. M. and Nagai, M. A., *Cancer Detect Prev* 1983, 6, 241-247.

68. Keshgegian, A. A., *Clin Chim Acta* 1980, 108, 399-402.

69. Carmeci, C., Thompson, D. A., Kuang, W. W., Lightdale, N., *et al.*, *Surgery* 1998, 124, 211-217.

70. Griffin, T. J., Gygi, S. P., Ideker, T., Rist, B., *et al.*, *Mol Cell Proteomics* 2002, 1, 323-333.

71. Tian, Q., Stepaniants, S. B., Mao, M., Weng, L., *et al.*, *Mol Cell Proteomics* 2004, 3, 960-969.

72. Greenbaum, D., Jansen, R. and Gerstein, M., *Bioinformatics* 2002, 18, 585-596.

CHAPTER VI

Conclusion

The term "proteome", first suggested in 1994 by Marc Wilkins, refers to proteins that are encoded and expressed by a genome. Wilkins defines "proteomics" as "the study of proteins, how they're modified, when and where they're expressed, how they're involved in the metabolic pathways and how they interact with each other." This dissertation attempts to describe the proteome of breast cancer cell lines according to these definitions, using a variety of MS-based strategies and bioinformatics techniques.

In Chapter II, we integrated proteome data from breast cancer cell lines with an in-silico analysis of SAGE tag expression derived from primary human breast tissues. This study allowed us to reveal networks of expressed proteins that are transcriptionally and functionally related and are likely to be differentially expressed in clinical subsets of breast tissues. The putative functions and locations of some of these proteins suggest potential roles in the initiation and/or progression of breast carcinomas. Chapter III describes an extension of our protein identification methodology, which uses an iterative multi-step search to incorporate PTM information. This dataset was then combined with mRNA abundance information and functional information to identify similar/differing patterns of transcriptional and post-translational regulation that appear to segregate with the cancer phenotype. Additional protein-protein interaction data allowed us to identify groups of binding proteins whose transcriptional profile differed across these cell lines, thus facilitating the study of biologically relevant metabolic pathways in cancer. Finally, Chapters 4 and 5 describe the development and use of a "Reference" cell mixture, FTICR, AMTs and the ^{18}O-labeling technique to directly measure the relative expression of proteins in both non-cancer and cancer cell lines. These strategies allowed us to

compare hundreds of proteins among several cell lines simultaneously, and facilitated one of the largest quantitative proteomic studies of breast cancer to date.

Together, these studies constitute a large-scale qualitative and quantitative proteomic analysis of breast cancer cell lines. In future studies of chemotaxic responses, cancer susceptibility, and cellular growth characteristics, the set of proteins described in Chapters 3 and 5 can be used as a baseline in evaluating potential peptide markers associated with an even larger panel of cancer cell lines. Since the cell lines we used in these studies carry some of the same pathway aberrations as found in primary tumors, they also provide an opportunity to increase our understanding of the signaling proteins and pathways associated with tumorogenisis. However, further validation using tissue samples is required to evaluate which proteins may play important roles in the initiation, progression, and response of breast carcinomas to therapy. Additional analysis of these proteins and the biochemical pathways in which they are involved will not only further our understanding of breast oncogenesis, but may provide new and valuable targets for further therapeutic research.

Appendix A

Table S1. 31 tissue-specific SAGE libraries taken from the Cancer Genome Anatomy Project (CGAP) site and used for comparative gene expression. Libraries are described as estrogen receptor (ER) positive and negative, node positive and negative, ductal carcinomas in situ (DCIS), invasive ductal carcinomas (IDC) and normal (Norm) breast tissues. Also shown are the number of SAGE tags in each library.

Tissue Library	Tags	Norm	DCIS	IDC	Node+	Node-	ER+	ER-
SAGE_Breast_carcinoma_AP_DCIS-2	28719		x					
SAGE_Breast_carcinoma_myoepithelium__AP_DCIS6	81452		x					
SAGE_Breast_carcinoma_stroma_B_DCIS6	57049		x					
SAGE_Breast_carcinoma_epithelium_AP_DCIS6	72857		x					
SAGE_Breast_carcinoma_B_DCIS-5	43098		x					
SAGE_Breast_carcinoma_AP_DCIS-3	57402		x					
SAGE_Breast_carcinoma_B_DCIS-4	60605		x					
SAGE_Vascular_Endothelium_Breast_carcinoma_AP_DCIS	63314		x					
SAGE_Breast_carcinoma_MD_DCIS	40783		x				x	
SAGE_Breast_carcinoma_B_BWHT18	50777		x			x	x	
SAGE_Breast_carcinoma_epithelium_AP_DCIS7	89184		x		x			
SAGE_Breast_carcinoma_myoepithelium_AP_DCIS7	37435		x		x			
SAGE_Breast_carcinoma_B_95-347	67070			x	x		x	
SAGE_Breast_metastatic_carcinoma_B_95-348	60343			x	x		x	
SAGE_Breast_metastatic_carcinoma_B_95-260	45087			x	x			x
SAGE_Breast_carcinoma_B_95-259	39364			x	x			x
SAGE_Breast_carcinoma_B_IDC-4	64095			x		x		x
SAGE_Breast_carcinoma_B_IDC-3	68891			x		x	x	
SAGE_Breast_carcinoma_B_IDC-5	60451			x		x	x	
SAGE_Breast_carcinoma_stroma_B_IDC7	68024			x			x	
SAGE_Breast_carcinoma_epithelium_AP_IDC7	73410			x			x	
SAGE_Breast_carcinoma_B_CT15	21889			x				
SAGE_Breast_normal_endothelium_AP_1	33115	x						
SAGE_Breast_normal_AP_myoepithelial1	57222	x						
SAGE_Breast_normal_organoid_B	58181	x						
SAGE_Breast_normal_FS_NER	34565	x						
SAGE_Breast_normal_organoid_B_2	59327	x						
SAGE_Breast_normal_B_hyperplasia1	61704	x						
SAGE_Breast_normal_myoepithelium_AP_IDC7	69006	x						
SAGE_Breast_normal_epithelium_AP_1	48729	x						
SAGE_Breast_normal_AP_Br_N	37121	x						

Table S2: 2101 proteins identified with MS/MS, the corresponding IPI identifiers, gene symbol, membrane localization information, # unique peptides, and protein name. Specific localization information is listed only for membrane proteins.

IPI	Gene	Membrane protein?	Location	# peps	Protein Name
IPI00218170	STOML2	membrane	cytoskeleton	31	stomatin (EPB72)-like 2
IPI00174107	CDC42EP4	membrane	cytoskeleton	2	CDC42 effector protein (Rho GTPase binding) 4
IPI00024067	JUP	membrane	cytoskeleton	65	junction plakoglobin
IPI00107774	SPTAN1	membrane	cytoskeleton	102	spectrin, alpha, non-erythrocytic 1 (alpha-fodrin)
IPI00042916	SYNE2	membrane	cytoskeleton	13	spectrin repeat containing, nuclear envelope 2
IPI00012831	CDC42BPA	membrane	cytoskeleton	2	CDC42 binding protein kinase alpha (DMPK-like)
IPI00098902	ANK2	membrane	cytoskeleton	11	ankyrin 2, neuronal
IPI00015346	HIP1	membrane	cytoskeleton	39	huntingtin interacting protein 1
IPI00216486	DSG2	membrane	desmosome	12	desmoglein 2
IPI00221232	RHBDF1	membrane	endoplasmic reticulum	7	rhomboid family 1 (Drosophila)
IPI00166742	PPIB	membrane	endoplasmic reticulum	14	peptidylprolyl isomerase B (cyclophilin B)
IPI00032409	SDCBP	membrane	endoplasmic reticulum	11	syndecan binding protein (syntenin)
IPI00100981	CGI-100	membrane	endoplasmic reticulum	8	CGI-100 protein
IPI00016670	SDF2L1	membrane	endoplasmic reticulum	7	stromal cell-derived factor 2-like 1
IPI00220416	LMAN1	membrane	endoplasmic reticulum	36	lectin, mannose-binding, 1
IPI00219156	PIGS	membrane	endoplasmic reticulum	16	phosphatidylinositol glycan, class S
IPI00215611	GRP58	membrane	endoplasmic reticulum	54	glucose regulated protein, 58kDa
IPI00180385	ITPR2	membrane	endoplasmic reticulum	11	inositol 1,4,5-triphosphate receptor, type 2
IPI00008529	SSR1	membrane	endoplasmic reticulum	6	signal sequence receptor, alpha (translocon-associated protein alpha)
IPI00005687	SCD	membrane	endoplasmic reticulum	11	stearoyl-CoA desaturase (delta-9-desaturase)
IPI00217260	HSGP25L2G	membrane	endoplasmic reticulum	17	gp25L2 protein
IPI00007756	CALR	membrane	endoplasmic reticulum	18	calreticulin
IPI00026119	SRPRB	membrane	endoplasmic reticulum	11	signal recognition particle receptor, B subunit
IPI00171696	LMAN2L	membrane	endoplasmic reticulum	3	lectin, mannose-binding 2-like
IPI00218733	SYBL1	membrane	endoplasmic reticulum	4	synaptobrevin-like 1
IPI00013895	ATP2A2	membrane	endoplasmic	38	ATPase, Ca++ transporting,

			reticulum		cardiac muscle, slow twitch 2
IPI00023412	HYOU1	membrane	endoplasmic reticulum	12	hypoxia up-regulated 1
IPI00021805	STX17	membrane	endoplasmic reticulum	10	syntaxin 17
IPI00024973	DHCR24	membrane	endoplasmic reticulum	37	24-dehydrocholesterol reductase
IPI00011253	HSPA5	membrane	endoplasmic reticulum	75	heat shock 70kDa protein 5 (glucose-regulated protein, 78kDa)
IPI00217391	P4HB	membrane	endoplasmic reticulum	32	procollagen-proline, 2-oxoglutarate 4-dioxygenase (proline 4-hydroxylase), beta polypeptide (protein disulfide isomerase; thyroid hormone binding protein p55)
IPI00028987	SSR4	membrane	endoplasmic reticulum	9	signal sequence receptor, delta (translocon-associated protein delta)
IPI00009156	AGPAT1	membrane	endoplasmic reticulum	2	1-acylglycerol-3-phosphate O-acyltransferase 1 (lysophosphatidic acid acyltransferase, alpha)
IPI00000041	HM13	membrane	endoplasmic reticulum	8	histocompatibility (minor) 13
IPI00017508	GCS1	membrane	endoplasmic reticulum	30	glucosidase I
IPI00025974	SPTLC1	membrane	endoplasmic reticulum	7	serine palmitoyltransferase, long chain base subunit 1
IPI00003949	C12orf8	membrane	endoplasmic reticulum	5	chromosome 12 open reading frame 8
IPI00218924	CANX	membrane	endoplasmic reticulum	37	calnexin
IPI00063408	BCAP31	membrane	endoplasmic reticulum	27	B-cell receptor-associated protein 31
IPI00032903	SSR2	membrane	endoplasmic reticulum	6	signal sequence receptor, beta (translocon-associated protein beta)
IPI00022164	PTGFRN	membrane	endoplasmic reticulum	14	prostaglandin F2 receptor negative regulator
IPI00182599	SPC12	membrane	endoplasmic reticulum	4	signal peptidase 12kDa
IPI00152002	ZMPSTE24	membrane	endoplasmic reticulum	31	zinc metalloproteinase (STE24 homolog, yeast)
IPI00027284	BCAP29	membrane	endoplasmic reticulum	2	B-cell receptor-associated protein 29
IPI00007427	JPH1	membrane	endoplasmic reticulum	2	junctophilin 1
IPI00154491	TRA1	membrane	endoplasmic reticulum	23	tumor rejection antigen (gp96) 1
IPI00032003	FLJ22649	membrane	endoplasmic reticulum	3	hypothetical protein FLJ22649 similar to signal peptidase SPC22/23
IPI00219674	SPTLC2	membrane	endoplasmic reticulum	13	serine palmitoyltransferase, long chain base subunit 2

IPI00215790	POR	membrane	endoplasmic reticulum	48	P450 (cytochrome) oxidoreductase
IPI00160622	TAP2	membrane	endoplasmic reticulum	8	transporter 2, ATP-binding cassette, sub-family B (MDR/TAP)
IPI00006617	SOAT1	membrane	endoplasmic reticulum	4	sterol O-acyltransferase (acyl-Coenzyme A: cholesterol acyltransferase) 1
IPI00216170	DIA1	membrane	endoplasmic reticulum	27	diaphorase (NADH) (cytochrome b-5 reductase)
IPI00216318	MAN1B1	membrane	endoplasmic reticulum	16	mannosidase, alpha, class 1B, member 1
IPI00179357	SEC61B	membrane	endoplasmic reticulum	3	Sec61 beta subunit
IPI00215916	CDS1	membrane	endoplasmic reticulum	2	CDP-diacylglycerol synthase (phosphatidate cytidylyltransferase) 1
IPI00219909	KTN1	membrane	endoplasmic reticulum	59	kinectin 1 (kinesin receptor)
IPI00016372	PIGO	membrane	endoplasmic reticulum	7	phosphatidylinositol glycan, class O
IPI00217579	CDC91L1	membrane	endoplasmic reticulum	7	CDC91 cell division cycle 91-like 1 (S. cerevisiae)
IPI00008530	LRPAP1	membrane	endoplasmic reticulum	4	low density lipoprotein receptor-related protein associated protein 1
IPI00107117	UGCG	membrane	endoplasmic reticulum	3	UDP-glucose ceramide glucosyltransferase
IPI00030439	RHBDL6	membrane	endoplasmic reticulum	2	rhomboid-like protein 6
IPI00008200	CYP1B1	membrane	endoplasmic reticulum	2	cytochrome P450, family 1, subfamily B, polypeptide 1
IPI00002521	TAP1	membrane	endoplasmic reticulum	7	transporter 1, ATP-binding cassette, sub-family B (MDR/TAP)
IPI00217519	DGAT1	membrane	endoplasmic reticulum	7	diacylglycerol O-acyltransferase homolog 1 (mouse)
IPI00105799	RDH11	membrane	endoplasmic reticulum	14	retinol dehydrogenase 11 (all-trans and 9-cis)
IPI00027350	TRAM1	membrane	endoplasmic reticulum	8	translocation associated membrane protein 1
IPI00164305	DHCR7	membrane	endoplasmic reticulum	6	7-dehydrocholesterol reductase
IPI00005969	EBP	membrane	endoplasmic reticulum	6	emopamil binding protein (sterol isomerase)
IPI00019345	ALDH3A2	membrane	endoplasmic reticulum	22	aldehyde dehydrogenase 3 family, member A2
IPI00005162	IGSF8	membrane	endoplasmic reticulum	4	immunoglobulin superfamily, member 8
IPI00024779	RPN2	membrane	endoplasmic reticulum	64	ribophorin II
IPI00013296	RPN1	membrane	endoplasmic reticulum	70	ribophorin I
IPI00007755	TLOC1	membrane	endoplasmic	3	translocation protein 1

			reticulum		
IPI00171445	FLJ32096	membrane	endoplasmic reticulum	2	hypothetical protein FLJ32096
IPI00012005	RTN3	membrane	endoplasmic reticulum	7	reticulon 3
IPI00027235	TOR1B	membrane	endoplasmic reticulum	3	torsin family 1, member B (torsin B)
IPI00216691	FKBP2	membrane	endoplasmic reticulum	2	FK506 binding protein 2, 13kDa
IPI00026087	PIGK	membrane	endoplasmic reticulum	14	phosphatidylinositol glycan, class K
IPI00220739	ALG6	membrane	endoplasmic reticulum	3	asparagine-linked glycosylation 6 homolog (yeast, alpha-1,3-glucosyltransferase)
IPI00217664	POMT2	membrane	endoplasmic reticulum	2	protein-O-mannosyltransferase 2
IPI00019906	PLOD	membrane	endoplasmic reticulum	2	procollagen-lysine, 2-oxoglutarate 5-dioxygenase (lysine hydroxylase, Ehlers-Danlos syndrome type VI)
IPI00024920	ELOVL1	membrane	endoplasmic reticulum	2	elongation of very long chain fatty acids (FEN1/Elo2, SUR4/Elo3, yeast)-like 1
IPI00014376	TXNDC4	membrane	endoplasmic reticulum	8	thioredoxin domain containing 4 (endoplasmic reticulum)
IPI00220803	PLOD3	membrane	endoplasmic reticulum	3	procollagen-lysine, 2-oxoglutarate 5-dioxygenase 3
IPI00028814	POMT1	membrane	endoplasmic reticulum	2	protein-O-mannosyltransferase 1
IPI00013930	SEC63	membrane	endoplasmic reticulum	16	SEC63-like (S. cerevisiae)
IPI00183114	ASPH	membrane	endoplasmic reticulum	16	aspartate beta-hydroxylase
IPI00005160	SRPR	membrane	endoplasmic reticulum	15	signal recognition particle receptor ('docking protein')
IPI00024742	ERN1	membrane	endoplasmic reticulum	3	ER to nucleus signalling 1
IPI00027270	ATP2A3	membrane	endoplasmic reticulum	4	ATPase, Ca++ transporting, ubiquitous
IPI00017726	CALU	membrane	endoplasmic reticulum	24	calumenin
IPI00012512	CDIPT	membrane	endoplasmic reticulum	35	CDP-diacylglycerol--inositol 3-phosphatidyltransferase (phosphatidylinositol synthase)
IPI00001568	CYB5	membrane	endoplasmic reticulum	15	cytochrome b-5
IPI00000874	DDOST	membrane	endoplasmic reticulum	18	dolichyl-diphosphooligosaccharide-protein glycosyltransferase
IPI00024551	DYSF	membrane	endoplasmic reticulum	23	dysferlin, limb girdle muscular dystrophy 2B (autosomal recessive)

IPI00032831	ERO1L	membrane	endoplasmic reticulum	18	ERO1-like (S. cerevisiae)
IPI00221225	ERP70	membrane	endoplasmic reticulum	38	protein disulfide isomerase related protein (calcium-binding protein, intestinal-related)
IPI00010214	FDFT1	membrane	endoplasmic reticulum	25	farnesyl-diphosphate farnesyltransferase 1
IPI00017728	H6PD	membrane	endoplasmic reticulum	4	hexose-6-phosphate dehydrogenase (glucose 1-dehydrogenase)
IPI00023711	HMGCR	membrane	endoplasmic reticulum	10	3-hydroxy-3-methylglutaryl-Coenzyme A reductase
IPI00017334	ITPR3	membrane	endoplasmic reticulum	8	inositol 1,4,5-triphosphate receptor, type 3
IPI00216295	RCN1	membrane	endoplasmic reticulum	2	reticulocalbin 1, EF-hand calcium binding domain
IPI00220642	RRBP1	membrane	endoplasmic reticulum	6	ribosome binding protein 1 homolog 180kDa (dog)
IPI00166785	RTN4	membrane	endoplasmic reticulum	11	reticulon 4
IPI00026824	SCAP	membrane	endoplasmic reticulum	19	SREBP CLEAVAGE-ACTIVATING PROTEIN
IPI00000692	SPC18	membrane	endoplasmic reticulum	29	signal peptidase complex (18kD)
IPI00185684	SREBF2	membrane	endoplasmic reticulum	11	sterol regulatory element binding transcription factor 2
IPI00032801	SSR3	membrane	endoplasmic reticulum	4	signal sequence receptor, gamma (translocon-associated protein gamma)
IPI00053607	STX18	membrane	endoplasmic reticulum	39	syntaxin 18
IPI00028091	SURF4	membrane	endoplasmic reticulum	31	surfeit 4
IPI00015756	TAPBP	membrane	endoplasmic reticulum	3	TAP binding protein (tapasin)
IPI00018871	TM7SF2	membrane	endoplasmic reticulum	34	transmembrane 7 superfamily member 2
IPI00012011	WFS1	membrane	endoplasmic reticulum	26	Wolfram syndrome 1 (wolframin)
IPI00029730	STX7	membrane	endosomes	10	syntaxin 7
IPI00024705	ATP6V1B2	membrane	endosomes	14	ATPase, H+ transporting, lysosomal 56/58kDa, V1 subunit B, isoform 2
IPI00006211	EEA1	membrane	endosomes	2	early endosome antigen 1, 162kD
IPI00031045	NPC1	membrane	endosomes	9	Niemann-Pick disease, type C1
IPI00030919	STARD3	membrane	endosomes	22	START domain containing 3
IPI00059472	TM9SF2	membrane	endosomes	27	transmembrane 9 superfamily member 2
IPI00166315	SNX17	membrane	endosomes	11	sorting nexin 17
IPI00006865	STARD3NL	membrane	endosomes	28	STARD3 N-terminal like
IPI00001960	VAMP5	membrane	endosomes	4	vesicle-associated membrane protein 5 (myobrevin)

IPI00010491	MAPBPIP	membrane	golgi	5	mitogen-activated protein-binding protein-interacting protein
IPI00033494	RAB9A	membrane	golgi	12	RAB9A, member RAS oncogene family
IPI00022018	STX5A	membrane	golgi	10	syntaxin 5A
IPI00025311	ARL10C	membrane	golgi	22	ADP-ribosylation factor-like 10C
IPI00179843	SEC22L1	membrane	golgi	38	SEC22 vesicle trafficking protein-like 1 (S. cerevisiae)
IPI00220245	CLIC4	membrane	golgi	14	chloride intracellular channel 4
IPI00007280	MRLC2	membrane	golgi	9	myosin regulatory light chain MRLC2
IPI00218848	RAB11B	membrane	golgi	18	RAB11B, member RAS oncogene family
IPI00007074	LMAN2	membrane	golgi	25	lectin, mannose-binding 2
IPI00015980	RAB35	membrane	golgi	19	RAB35, member RAS oncogene family
IPI00025091	RNP24	membrane	golgi	15	coated vesicle membrane protein
IPI00183161	RAB8A	membrane	golgi	17	RAB8A, member RAS oncogene family
IPI00020436	C15orf22	membrane	golgi	9	chromosome 15 open reading frame 22
IPI00024915	ATP7B	membrane	golgi	9	ATPase, Cu++ transporting, beta polypeptide (Wilson disease)
IPI00002894	GDI2	membrane	golgi	12	GDP dissociation inhibitor 2
IPI00170959	GOSR1	membrane	golgi	10	golgi SNAP receptor complex member 1
IPI00006664	RAB2	membrane	golgi	25	RAB2, member RAS oncogene family
IPI00183695	RAB18	membrane	golgi	11	RAB18, member RAS oncogene family
IPI00219469	B4GALT1	membrane	golgi	8	UDP-Gal:betaGlcNAc beta 1,4- galactosyltransferase, polypeptide 1
IPI00010414	MAN2A1	membrane	golgi	9	mannosidase, alpha, class 2A, member 1
IPI00216153	SGPL1	membrane	golgi	20	sphingosine-1-phosphate lyase 1
IPI00220906	ARFGEF2	membrane	golgi	3	ADP-ribosylation factor guanine nucleotide-exchange factor 2 (brefeldin A-inhibited)
IPI00016373	RAB33B	membrane	golgi	5	RAB33B, member RAS oncogene family
IPI00020164	GALNT3	membrane	golgi	19	UDP-N-acetyl-alpha-D-galactosamine:polypeptide N-acetylgalactosaminyltransferase 3 (GalNAc-T3)
IPI00009950	VDP	membrane	golgi	3	vesicle docking protein p115
IPI00218675		membrane	golgi	6	Transcribed sequence with

					weak similarity to protein sp:P39194 (H.sapiens) ALU7_HUMAN Alu subfamily SQ sequence contamination warning entry
IPI00060031	GLG1	membrane	golgi	17	golgi apparatus protein 1
IPI00081025	STIP1	membrane	golgi	9	stress-induced-phosphoprotein 1 (Hsp70/Hsp90-organizing protein)
IPI00220362	RINT-1	membrane	golgi	6	Rad50-interacting protein 1
IPI00013122	POFUT1	membrane	golgi	4	protein O-fucosyltransferase 1
IPI00007697	MAN1A1	membrane	golgi	5	mannosidase, alpha, class 1A, member 1
IPI00007682	SIAT4A	membrane	golgi	6	sialyltransferase 4A (beta-galactoside alpha-2,3-sialyltransferase)
IPI00026247	GBF1	membrane	golgi	3	golgi-specific brefeldin A resistance factor 1
IPI00221089	GABARAPL2	membrane	golgi	2	GABA(A) receptor-associated protein-like 2
IPI00019359	VPS45A	membrane	golgi	28	vacuolar protein sorting 45A (yeast)
IPI00027402	SNX8	membrane	golgi	2	sorting nexin 8
IPI00219034	B4GALT4	membrane	golgi	2	UDP-Gal:betaGlcNAc beta 1,4- galactosyltransferase, polypeptide 4
IPI00106642	B3GNT6	membrane	golgi	2	UDP-GlcNAc:betaGal beta-1,3-N-acetylglucosaminyltransferase 6
IPI00013950	STX10	membrane	golgi	5	syntaxin 10
IPI00026530	OSBP	membrane	golgi	9	oxysterol binding protein
IPI00161630	FUT8	membrane	golgi	10	fucosyltransferase 8 (alpha (1,6) fucosyltransferase)
IPI00070849	KIAA1598	membrane	golgi	2	KIAA1598
IPI00008411	MGAT1	membrane	golgi	3	mannosyl (alpha-1,3-)-glycoprotein beta-1,2-N-acetylglucosaminyltransferase
IPI00023780	ARL1	membrane	golgi	2	ADP-ribosylation factor-like 1
IPI00013847	PAK4	membrane	golgi	5	p21(CDKN1A)-activated kinase 4
IPI00032561	ZDHHC3	membrane	golgi	2	zinc finger, DHHC domain containing 3
IPI00007309	KIAA0830	membrane	golgi	4	KIAA0830 protein
IPI00007676	HERC2	membrane	golgi	10	hect domain and RLD 2
IPI00165280	MAN1A2	membrane	golgi	3	mannosidase, alpha, class 1A, member 2
IPI00034241	UNC13B	membrane	golgi	2	unc-13 homolog B (C. elegans)
IPI00014053	GNAL	membrane	golgi	4	guanine nucleotide binding protein (G protein), alpha

					activating activity polypeptide, olfactory type
IPI00219804	GALNT2	membrane	golgi	5	UDP-N-acetyl-alpha-D-galactosamine:polypeptide N-acetylgalactosaminyltransferase 2 (GalNAc-T2)
IPI00217966	EBAG9	membrane	golgi	2	estrogen receptor binding site associated, antigen, 9
IPI00170532	ENTPD7	membrane	golgi	2	ectonucleoside triphosphate diphosphohydrolase 7
IPI00006675	SLC9A7	membrane	golgi	5	solute carrier family 9 (sodium/hydrogen exchanger), isoform 7
IPI00045502	ADAM10	membrane	golgi	12	a disintegrin and metalloproteinase domain 10
IPI00097511	TUWD12	membrane	golgi	5	TUWD12
IPI00181700	GALNT1	membrane	golgi	5	UDP-N-acetyl-alpha-D-galactosamine:polypeptide N-acetylgalactosaminyltransferase 1 (GalNAc-T1)
IPI00009147	ANK3	membrane	golgi	15	ankyrin 3, node of Ranvier (ankyrin G)
IPI00186821	GOLGB1	membrane	golgi	27	golgi autoantigen, golgin subfamily b, macrogolgin (with transmembrane signal), 1
IPI00015834	PIK4CA	membrane	golgi	12	phosphatidylinositol 4-kinase, catalytic, alpha polypeptide
IPI00046057	GOLPH4	membrane	golgi	4	golgi phosphoprotein 4
IPI00010232	GOLGA2	membrane	golgi	2	golgi autoantigen, golgin subfamily a, 2
IPI00220469	MGAT5	membrane	golgi	2	mannosyl (alpha-1,6-)-glycoprotein beta-1,6-N-acetyl-glucosaminyltransferase
IPI00012772	ARF4	membrane	golgi	9	ADP-ribosylation factor 4
IPI00220345	GOLGA1	membrane	golgi	2	golgi autoantigen, golgin subfamily a, 1
IPI00178772	SPTBN2	membrane	golgi	21	spectrin, beta, non-erythrocytic 2
IPI00025049		membrane	golgi	3	Transcribed sequence with moderate similarity to protein sp:P39193 (H.sapiens) ALU6_HUMAN Alu subfamily SP sequence contamination warning entry
IPI00219178	ARF5	membrane	golgi	10	ADP-ribosylation factor 5
IPI00009225	TOM1L1	membrane	golgi	2	target of myb1-like 1 (chicken)
IPI00152686	TRIP11	membrane	golgi	3	thyroid hormone receptor interactor 11
IPI00028086	SPTBN5	membrane	golgi	4	spectrin, beta, non-

					erythrocytic 5
IPI00027505	AP1M1	membrane	golgi	28	adaptor-related protein complex 1, mu 1 subunit
IPI00218921	B3GAT3	membrane	golgi	19	beta-1,3-glucuronyltransferase 3 (glucuronosyltransferase I)
IPI00007611	B4GALT3	membrane	golgi	10	UDP-Gal:betaGlcNAc beta 1,4- galactosyltransferase, polypeptide 3
IPI00220985	BET1	membrane	golgi	12	BET1 homolog (S. cerevisiae)
IPI00016608	COPE	membrane	golgi	3	coatomer protein complex, subunit epsilon
IPI00030236	GORASP2	membrane	golgi	28	golgi reassembly stacking protein 2, 55kDa
IPI00026182	GOSR2	membrane	golgi	37	golgi SNAP receptor complex member 2
IPI00153017	PKN2	membrane	golgi	38	protein kinase N2
IPI00028481	PSEN1	membrane	golgi	29	presenilin 1 (Alzheimer disease 3)
IPI00025803	RAB1A	membrane	golgi	28	RAB1A, member RAS oncogene family
IPI00031131	RAB25	membrane	golgi	33	RAB25, member RAS oncogene family
IPI00045486	RAB4A	membrane	golgi	13	RAB4A, member RAS oncogene family
IPI00022187	RAB4B	membrane	golgi	18	RAB4B, member RAS oncogene family
IPI00021785	RAB6A	membrane	golgi	4	RAB6A, member RAS oncogene family
IPI00021086	RER1	membrane	golgi	33	RER1 homolog (S. cerevisiae)
IPI00008433	SNX3	membrane	golgi	36	sorting nexin 3
IPI00015972	STX16	membrane	golgi	19	syntaxin 16
IPI00025482	TGOLN2	membrane	golgi	34	trans-golgi network protein 2
IPI00008527	VAMP4	membrane	golgi	27	vesicle-associated membrane protein 4
IPI00003856	M6PR	membrane	lysosomes	9	mannose-6-phosphate receptor (cation dependent)
IPI00220327	TMEM9	membrane	lysosomes	2	transmembrane protein 9
IPI00028508	GBA	membrane	lysosomes	10	glucosidase, beta; acid (includes glucosylceramidase)
IPI00022256	LAMP2	membrane	lysosomes	8	lysosomal-associated membrane protein 2
IPI00025252	ACP2	membrane	lysosomes	3	acid phosphatase 2, lysosomal
IPI00020058	IGF2R	membrane	lysosomes	39	insulin-like growth factor 2 receptor
IPI00007752	LRP2	membrane	lysosomes	7	low density lipoprotein-related protein 2
IPI00000816	LAMP1	membrane	lysosomes	8	lysosomal-associated membrane protein 1
IPI00008274	CD63	membrane	lysosomes	2	CD63 antigen (melanoma 1 antigen)

IPI00030157	VPS11	membrane	lysosomes	5	vacuolar protein sorting 11 (yeast)
IPI00005204	CLN3	membrane	lysosomes	10	ceroid-lipofuscinosis, neuronal 3, juvenile (Batten, Spielmeyer-Vogt disease)
IPI00043085	GBA	membrane	lysosomes	3	glucosidase, beta; acid (includes glucosylceramidase)
IPI00031461	PSAP	membrane	lysosomes	29	prosaposin (variant Gaucher disease and variant metachromatic leukodystrophy)
IPI00166746	SCARB2	membrane	lysosomes	26	scavenger receptor class B, member 2
IPI00024773	VPS18	membrane	lysosomes	19	vacuolar protein sorting protein 18
IPI00005030	HMOX2	membrane	microsomes	18	heme oxygenase (decycling) 2
IPI00023550	EPHX1	membrane	microsomes	31	epoxide hydrolase 1, microsomal (xenobiotic)
IPI00013933	CYP51A1	membrane	microsomes	10	cytochrome P450, family 51, subfamily A, polypeptide 1
IPI00014808	SQLE	membrane	microsomes	10	squalene epoxidase
IPI00181137	MGST3	membrane	microsomes	29	microsomal glutathione S-transferase 3
IPI00013976	PGRMC2	membrane	microsomes	19	progesterone receptor membrane component 2
IPI00218187	UQCRB	membrane	mitochondria	8	ubiquinol-cytochrome c reductase binding protein
IPI00216298	MGST1	membrane	mitochondria	6	microsomal glutathione S-transferase 1
IPI00218683	Bit1	membrane	mitochondria	16	Bcl-2 inhibitor of transcription
IPI00217121	UQCRC2	membrane	mitochondria	41	ubiquinol-cytochrome c reductase core protein II
IPI00027240	CYCS	membrane	mitochondria	3	cytochrome c, somatic
IPI00220301	ATP5J	membrane	mitochondria	6	ATP synthase, H+ transporting, mitochondrial F0 complex, subunit F6
IPI00011126	ATP5D	membrane	mitochondria	4	ATP synthase, H+ transporting, mitochondrial F1 complex, delta subunit
IPI00012066	COX6A1	membrane	mitochondria	5	cytochrome c oxidase subunit VIa polypeptide 1
IPI00012442	QP-C	membrane	mitochondria	4	low molecular mass ubiquinone-binding protein (9.5kD)
IPI00031545	HADH2	membrane	mitochondria	6	hydroxyacyl-Coenzyme A dehydrogenase, type II
IPI00032140	NDUFA8	membrane	mitochondria	9	NADH dehydrogenase (ubiquinone) 1 alpha subcomplex, 8, 19kDa
IPI00027009	UQCRH	membrane	mitochondria	3	ubiquinol-cytochrome c reductase hinge protein
IPI00216237	UQCRC1	membrane	mitochondria	22	ubiquinol-cytochrome c

					reductase core protein I
IPI00103175	TIMM23	membrane	mitochondria	3	translocase of inner mitochondrial membrane 23 homolog (yeast)
IPI00024378	TOMM40	membrane	mitochondria	19	translocase of outer mitochondrial membrane 40 homolog (yeast)
IPI00155635	MLSTD2	membrane	mitochondria	5	male sterility domain containing 2
IPI00010896	ATP5O	membrane	mitochondria	8	ATP synthase, H+ transporting, mitochondrial F1 complex, O subunit (oligomycin sensitivity conferring protein)
IPI00010438	COX5B	membrane	mitochondria	5	cytochrome c oxidase subunit Vb
IPI00017897	COX6C	membrane	mitochondria	7	cytochrome c oxidase subunit VIc
IPI00029744	SPAG1	membrane	mitochondria	4	sperm associated antigen 1
IPI00011247	ATP5L	membrane	mitochondria	3	ATP synthase, H+ transporting, mitochondrial F0 complex, subunit g
IPI00009976	COX4I1	membrane	mitochondria	12	cytochrome c oxidase subunit IV isoform 1
IPI00013007	SLC25A11	membrane	mitochondria	11	solute carrier family 25 (mitochondrial carrier; oxoglutarate carrier), member 11
IPI00100796	NDUFA5	membrane	mitochondria	3	NADH dehydrogenase (ubiquinone) 1 alpha subcomplex, 5, 13kDa
IPI00013306	GBAS	membrane	mitochondria	6	glioblastoma amplified sequence
IPI00152409	COX5A	membrane	mitochondria	13	cytochrome c oxidase subunit Va
IPI00216730	SLC25A3	membrane	mitochondria	11	solute carrier family 25 (mitochondrial carrier; phosphate carrier), member 3
IPI00177964	CKMT1	membrane	mitochondria	3	creatine kinase, mitochondrial 1 (ubiquitous)
IPI00029046	CYC1	membrane	mitochondria	13	cytochrome c-1
IPI00073172	SLC25A1	membrane	mitochondria	11	solute carrier family 25 (mitochondrial carrier; citrate transporter), member 1
IPI00005161	NDUFS1	membrane	mitochondria	9	NADH dehydrogenase (ubiquinone) Fe-S protein 1, 75kDa (NADH-coenzyme Q reductase)
IPI00014424	IMMT	membrane	mitochondria	28	inner membrane protein, mitochondrial (mitofilin)
IPI00059185	ADK	membrane	mitochondria	5	adenosine kinase
IPI00027448	ATP5B	membrane	mitochondria	48	ATP synthase, H+ transporting, mitochondrial F1 complex, beta polypeptide
IPI00009634	SLC25A5	membrane	mitochondria	29	solute carrier family 25

					(mitochondrial carrier; adenine nucleotide translocator), member 5
IPI00009943	HADHB	membrane	mitochondria	24	hydroxyacyl-Coenzyme A dehydrogenase/3-ketoacyl-Coenzyme A thiolase/enoyl-Coenzyme A hydratase (trifunctional protein), beta subunit
IPI00006579	SDHB	membrane	mitochondria	2	succinate dehydrogenase complex, subunit B, iron sulfur (Ip)
IPI00221101	CDS2	membrane	mitochondria	7	CDP-diacylglycerol synthase (phosphatidate cytidylyltransferase) 2
IPI00020191	NDUFS4	membrane	mitochondria	2	NADH dehydrogenase (ubiquinone) Fe-S protein 4, 18kDa (NADH-coenzyme Q reductase)
IPI00026268	ATP5A1	membrane	mitochondria	46	ATP synthase, H+ transporting, mitochondrial F1 complex, alpha subunit, isoform 1, cardiac muscle
IPI00216319	P17.3	membrane	mitochondria	3	neuronal protein 17.3
IPI00215815	TOMM70A	membrane	mitochondria	7	translocase of outer mitochondrial membrane 70 homolog A (yeast)
IPI00030888	CPT1A	membrane	mitochondria	39	carnitine palmitoyltransferase 1A (liver)
IPI00024933	NDUFB8	membrane	mitochondria	2	NADH dehydrogenase (ubiquinone) 1 beta subcomplex, 8, 19kDa
IPI00179569	PTGES2	membrane	mitochondria	4	prostaglandin E synthase 2
IPI00020599	GRIM19	membrane	mitochondria	4	cell death-regulatory protein GRIM19
IPI00219729	ABCB6	membrane	mitochondria	18	ATP-binding cassette, sub-family B (MDR/TAP), member 6
IPI00216308	SFXN1	membrane	mitochondria	12	sideroflexin 1
IPI00218236	GOT2	membrane	mitochondria	7	glutamic-oxaloacetic transaminase 2, mitochondrial (aspartate aminotransferase 2)
IPI00023510	VDAC3	membrane	mitochondria	6	voltage-dependent anion channel 3
IPI00219682	LOC114971	membrane	mitochondria	2	hypothetical protein LOC114971
IPI00029447	PYCS	membrane	mitochondria	9	pyrroline-5-carboxylate synthetase (glutamate gamma-semialdehyde synthetase)
IPI00217169	AFG3L2	membrane	mitochondria	21	AFG3 ATPase family gene 3-like 2 (yeast)
IPI00007812	AMID	membrane	mitochondria	3	apoptosis-inducing factor (AIF)-like mitochondrion-

					associated inducer of death
IPI00001620	NDUFB6	membrane	mitochondria	2	NADH dehydrogenase (ubiquinone) 1 beta subcomplex, 6, 17kDa
IPI00171834	FLJ10375	membrane	mitochondria	8	hypothetical protein FLJ10375
IPI00217617	MTX2	membrane	mitochondria	3	metaxin 2
IPI00220719	SYNJ2BP	membrane	mitochondria	4	synaptojanin 2 binding protein
IPI00025346	SLC25A24	membrane	mitochondria	14	solute carrier family 25 (mitochondrial carrier; phosphate carrier), member 24
IPI00020600	SLC9A6	membrane	mitochondria	2	solute carrier family 9 (sodium/hydrogen exchanger), isoform 6
IPI00025329	MTX1	membrane	mitochondria	4	metaxin 1
IPI00027107	NDUFA6	membrane	mitochondria	3	NADH dehydrogenase (ubiquinone) 1 alpha subcomplex, 6, 14kDa
IPI00029155	SLC25A16	membrane	mitochondria	4	solute carrier family 25 (mitochondrial carrier; Graves disease autoantigen), member 16
IPI00215914	BDH	membrane	mitochondria	2	3-hydroxybutyrate dehydrogenase (heart, mitochondrial)
IPI00017344	OXA1L	membrane	mitochondria	4	oxidase (cytochrome c) assembly 1-like
IPI00012048	BCS1L	membrane	mitochondria	3	BCS1-like (yeast)
IPI00156269	NDUFV3	membrane	mitochondria	2	NADH dehydrogenase (ubiquinone) flavoprotein 3, 10kDa
IPI00218337	COX11	membrane	mitochondria	2	COX11 homolog, cytochrome c oxidase assembly protein (yeast)
IPI00219910	NNT	membrane	mitochondria	18	nicotinamide nucleotide transhydrogenase
IPI00012613	ABCF2	membrane	mitochondria	2	ATP-binding cassette, sub-family F (GCN20), member 2
IPI00020887	SDHA	membrane	mitochondria	16	succinate dehydrogenase complex, subunit A, flavoprotein (Fp)
IPI00157442	NDUFS5	membrane	mitochondria	2	NADH dehydrogenase (ubiquinone) Fe-S protein 5, 15kDa (NADH-coenzyme Q reductase)
IPI00018280	SPG7	membrane	mitochondria	2	spastic paraplegia 7, paraplegin (pure and complicated autosomal recessive)
IPI00185451	PPIF	membrane	mitochondria	2	peptidylprolyl isomerase F (cyclophilin F)
IPI00006372	ABCE1	membrane	mitochondria	2	ATP-binding cassette, sub-

					family E (OABP), member 1
IPI00220222	ABCB7	membrane	mitochondria	3	ATP-binding cassette, sub-family B (MDR/TAP), member 7
IPI00215987	MCCC2	membrane	mitochondria	3	methylcrotonoyl-Coenzyme A carboxylase 2 (beta)
IPI00021840	CPT2	membrane	mitochondria	3	carnitine palmitoyltransferase II
IPI00022649	CGI-51	membrane	mitochondria	2	CGI-51 protein
IPI00177817	PPP2R1A	membrane	mitochondria	13	protein phosphatase 2 (formerly 2A), regulatory subunit A (PR 65), alpha isoform
IPI00010720	GAF1	membrane	mitochondria	4	gamma-SNAP-associated factor 1
IPI00034159	MTB	membrane	mitochondria	2	more than blood homolog
IPI00020124	MTCH1	membrane	mitochondria	7	mitochondrial carrier homolog 1 (C. elegans)
IPI00031169	SLC25A25	membrane	mitochondria	2	solute carrier family 25 (mitochondrial carrier; phosphate carrier), member 25
IPI00215780	BCL2L13	membrane	mitochondria	2	BCL2-like 13 (apoptosis facilitator)
IPI00017072	CNKSR2	membrane	mitochondria	2	connector enhancer of kinase suppressor of Ras 2
IPI00014577	ACADVL	membrane	mitochondria	5	acyl-Coenzyme A dehydrogenase, very long chain
IPI00024660	ATP5C1	membrane	mitochondria	11	ATP synthase, H+ transporting, mitochondrial F1 complex, gamma polypeptide 1
IPI00220377	ATP5F1	membrane	mitochondria	36	ATP synthase, H+ transporting, mitochondrial F0 complex, subunit b, isoform 1
IPI00004488	BZRP	membrane	mitochondria	24	benzodiazapine receptor (peripheral)
IPI00022275	C1QBP	membrane	mitochondria	16	complement component 1, q subcomponent binding protein
IPI00152412	COX7A2	membrane	mitochondria	33	cytochrome c oxidase subunit VIIa polypeptide 2 (liver)
IPI00060414	CRAT	membrane	mitochondria	39	carnitine acetyltransferase
IPI00020472	CYB5-M	membrane	mitochondria	5	cytochrome b5 outer mitochondrial membrane precursor
IPI00177968	EFA6R	membrane	mitochondria	24	ADP-ribosylation factor guanine nucleotide factor 6
IPI00170976	HTATIP2	membrane	mitochondria	20	HIV-1 Tat interactive protein 2, 30kDa
IPI00064193	NDUFA10	membrane	mitochondria	34	NADH dehydrogenase (ubiquinone) 1 alpha subcomplex, 10, 42kDa

IPI00018855	NDUFA4	membrane	mitochondria	13	NADH dehydrogenase (ubiquinone) 1 alpha subcomplex, 4, 9kDa
IPI00016858	NDUFAB1	membrane	mitochondria	4	NADH dehydrogenase (ubiquinone) 1, alpha/beta subcomplex, 1, 8kDa
IPI00180413	NDUFB10	membrane	mitochondria	24	NADH dehydrogenase (ubiquinone) 1 beta subcomplex, 10, 22kDa
IPI00215719	NDUFS2	membrane	mitochondria	21	NADH dehydrogenase (ubiquinone) Fe-S protein 2, 49kDa (NADH-coenzyme Q reductase)
IPI00221091	NDUFV1	membrane	mitochondria	32	NADH dehydrogenase (ubiquinone) flavoprotein 1, 51kDa
IPI00000001	PDCD8	membrane	mitochondria	27	programmed cell death 8 (apoptosis-inducing factor)
IPI00016077	SLC25A10	membrane	mitochondria	33	solute carrier family 25 (mitochondrial carrier; dicarboxylate transporter), member 10
IPI00003018	SLC25A12	membrane	mitochondria	37	solute carrier family 25 (mitochondrial carrier, Aralar), member 12
IPI00215761	SMAP-1	membrane	mitochondria	34	smooth muscle cell associated protein-1
IPI00000877	UQCRFS1	membrane	mitochondria	31	ubiquinol-cytochrome c reductase, Rieske iron-sulfur polypeptide 1
IPI00152540	VDAC2	membrane	mitochondria	20	voltage-dependent anion channel 2
IPI00025086	YME1L1	membrane	mitochondria	8	YME1-like 1 (S. cerevisiae)
IPI00005980	NUP210	membrane	nucleus	19	nucleoporin 210
IPI00219217	EMD	membrane	nucleus	9	emerin (Emery-Dreifuss muscular dystrophy)
IPI00026271	FLJ10201	membrane	nucleus	3	hypothetical protein FLJ10201
IPI00010105	CLIC1	membrane	nucleus	9	chloride intracellular channel 1
IPI00220125	MTAC2D1	membrane	nucleus	9	membrane targeting (tandem) C2 domain containing 1
IPI00021923	VAT1	membrane	nucleus	9	vesicle amine transport protein 1 homolog (T californica)
IPI00027214	NPM1	membrane	nucleus	15	nucleophosmin (nucleolar phosphoprotein B23, numatrin)
IPI00215777	PHLDA1	membrane	nucleus	5	pleckstrin homology-like domain, family A, member 1
IPI00215767	LBR	membrane	nucleus	6	lamin B receptor
IPI00013890	RUVBL1	membrane	nucleus	2	RuvB-like 1 (E. coli)
IPI00003968	USF1	membrane	nucleus	16	upstream transcription factor 1
IPI00007084	LMNB1	membrane	nucleus	7	lamin B1

IPI00012028	LASS4	membrane	nucleus	7	LAG1 longevity assurance homolog 4 (S. cerevisiae)
IPI00003406	ROD1	membrane	nucleus	2	ROD1 regulator of differentiation 1 (S. pombe)
IPI00026111	XPO1	membrane	nucleus	4	exportin 1 (CRM1 homolog, yeast)
IPI00216307	UBE2J1	membrane	nucleus	3	ubiquitin-conjugating enzyme E2, J1 (UBC6 homolog, yeast)
IPI00166066	ZDHHC7	membrane	nucleus	2	zinc finger, DHHC domain containing 7
IPI00027773	ZC3HAV1	membrane	nucleus	3	zinc finger CCCH type, antiviral 1
IPI00009896	ATP11B	membrane	nucleus	2	ATPase, Class VI, type 11B
IPI00220401	APLP2	membrane	nucleus	7	amyloid beta (A4) precursor-like protein 2
IPI00174976	COLEC12	membrane	nucleus	3	collectin sub-family member 12
IPI00006482	PPP1R9B	membrane	nucleus	36	protein phosphatase 1, regulatory subunit 9B, spinophilin
IPI00015102	TREX1	membrane	nucleus	8	three prime repair exonuclease 1
IPI00018465	UNC84A	membrane	nucleus	13	unc-84 homolog A (C. elegans)
IPI00216465	PEX3	membrane	peroxisome	5	peroxisomal biogenesis factor 3
IPI00026689	PEX14	membrane	peroxisome	8	peroxisomal biogenesis factor 14
IPI00180671	SLC27A2	membrane	peroxisome	18	solute carrier family 27 (fatty acid transporter), member 2
IPI00055628	PEX13	membrane	peroxisome	2	peroxisome biogenesis factor 13
IPI00007814	MPV17	membrane	peroxisome	2	MpV17 transgene, murine homolog, glomerulosclerosis
IPI00023647	ABCD3	membrane	peroxisome	20	ATP-binding cassette, sub-family D (ALD), member 3
IPI00017596	PEX11B	membrane	peroxisome	3	peroxisomal biogenesis factor 11B
IPI00017381	PXMP2	membrane	peroxisome	2	peroxisomal membrane protein 2, 22kDa
IPI00221092	AGPS	membrane	peroxisome	4	alkylglycerone phosphate synthase
IPI00024638	SLC25A17	membrane	peroxisome	2	solute carrier family 25 (mitochondrial carrier; peroxisomal membrane protein, 34kDa), member 17
IPI00016703	PEX1	membrane	peroxisome	2	peroxisome biogenesis factor 1
IPI00031397	ACSL1	membrane	peroxisome	11	acyl-CoA synthetase long-chain family member 1
IPI00003833	PEX16	membrane	peroxisome	37	peroxisomal biogenesis factor 16
IPI00003802	PEX19	membrane	peroxisome	38	peroxisomal biogenesis factor 19

IPI00215736	MUC1	membrane	plasma membrane	2	mucin 1, transmembrane
IPI00061796	CLTC	membrane	plasma membrane	130	clathrin, heavy polypeptide (Hc)
IPI00029264	IGSF3	membrane	plasma membrane	19	immunoglobulin superfamily, member 3
IPI00003362	CELSR2	membrane	plasma membrane	16	cadherin, EGF LAG seven-pass G-type receptor 2 (flamingo homolog, Drosophila)
IPI00010796	GNG12	membrane	plasma membrane	7	guanine nucleotide binding protein (G protein), gamma 12
IPI00028369	SPEC2	membrane	plasma membrane	2	non-kinase Cdc42 effector protein SPEC2
IPI00019385	SVIL	membrane	plasma membrane	3	supervillin
IPI00016707	PICALM	membrane	plasma membrane	13	phosphatidylinositol binding clathrin assembly protein
IPI00016621	RALA	membrane	plasma membrane	24	v-ral simian leukemia viral oncogene homolog A (ras related)
IPI00002406	ATRN	membrane	plasma membrane	8	attractin
IPI00167811	PGRMC1	membrane	plasma membrane	24	progesterone receptor membrane component 1
IPI00178877	AMOTL1	membrane	plasma membrane	4	angiomotin like 1
IPI00218990	STX6	membrane	plasma membrane	8	syntaxin 6
IPI00031691	RRAS2	membrane	plasma membrane	6	related RAS viral (r-ras) oncogene homolog 2
IPI00102884	SNAP29	membrane	plasma membrane	8	synaptosomal-associated protein, 29kDa
IPI00219834	COL12A1	membrane	plasma membrane	4	collagen, type XII, alpha 1
IPI00219482	EVPL	membrane	plasma membrane	4	envoplakin
IPI00009333	PPL	membrane	plasma membrane	9	periplakin
IPI00099463	PTPRK	membrane	plasma membrane	15	protein tyrosine phosphatase, receptor type, K
IPI00015894	VAPB	membrane	plasma membrane	36	VAMP (vesicle-associated membrane protein)-associated protein B and C
IPI00218918	MGC5395	membrane	plasma membrane	6	hypothetical protein MGC5395
IPI00025277	RAB13	membrane	plasma membrane	14	RAB13, member RAS oncogene family
IPI00011167	ATP6V1A	membrane	plasma membrane	30	ATPase, H+ transporting, lysosomal 70kDa, V1 subunit A
IPI00020495	SCRIB	membrane	plasma membrane	52	scribbled homolog (Drosophila)
IPI00171438	BASP1	membrane	plasma	48	brain abundant, membrane

			membrane		attached signal protein 1
IPI00180211	STX8	membrane	plasma membrane	6	syntaxin 8
IPI00003348	INSR	membrane	plasma membrane	6	insulin receptor
IPI00034205	ERBB2IP	membrane	plasma membrane	11	erbb2 interacting protein
IPI00099654	TNS	membrane	plasma membrane	4	tensin
IPI00019025	ATP6V1E1	membrane	plasma membrane	9	ATPase, H+ transporting, lysosomal 31kDa, V1 subunit E isoform 1
IPI00156689	AP2M1	membrane	plasma membrane	22	adaptor-related protein complex 2, mu 1 subunit
IPI00027442	NRCAM	membrane	plasma membrane	5	neuronal cell adhesion molecule
IPI00008388	DSP	membrane	plasma membrane	44	desmoplakin
IPI00003527	PLSCR3	membrane	plasma membrane	3	phospholipid scramblase 3
IPI00170981	GNG5	membrane	plasma membrane	6	guanine nucleotide binding protein (G protein), gamma 5
IPI00024619		membrane	plasma membrane	7	Data not found
IPI00009880	SNAP23	membrane	plasma membrane	19	synaptosomal-associated protein, 23kDa
IPI00012493	IL1RL1LG	membrane	plasma membrane	7	interleukin 1 receptor-like 1 ligand
IPI00220664	GNB1	membrane	plasma membrane	21	guanine nucleotide binding protein (G protein), beta polypeptide 1
IPI00154565	VDAC1	membrane	plasma membrane	25	voltage-dependent anion channel 1
IPI00219220	RAB5A	membrane	plasma membrane	10	RAB5A, member RAS oncogene family
IPI00152441	STOM	membrane	plasma membrane	17	stomatin
IPI00217725	ATP2B4	membrane	plasma membrane	31	ATPase, Ca++ transporting, plasma membrane 4
IPI00002186	DST	membrane	plasma membrane	4	dystonin
IPI00216309	ARF1	membrane	plasma membrane	15	ADP-ribosylation factor 1
IPI00005745	RAB5B	membrane	plasma membrane	10	RAB5B, member RAS oncogene family
IPI00215636	SLC12A2	membrane	plasma membrane	63	solute carrier family 12 (sodium/potassium/chloride transporters), member 2
IPI00011662	PI4KII	membrane	plasma membrane	7	phosphatidylinositol 4-kinase type II
IPI00216619	TACSTD2	membrane	plasma membrane	13	tumor-associated calcium signal transducer 2
IPI00217030	SLC25A13	membrane	plasma membrane	16	solute carrier family 25, member 13 (citrin)
IPI00173359	ALCAM	membrane	plasma	27	activated leukocyte cell

			membrane		adhesion molecule
IPI00008167	ATP6V1C1	membrane	plasma membrane	6	ATPase, H+ transporting, lysosomal 42kDa, V1 subunit C, isoform 1
IPI00017592	AP2A2	membrane	plasma membrane	17	adaptor-related protein complex 2, alpha 2 subunit
IPI00011633	LU	membrane	plasma membrane	10	Lutheran blood group (Auberger b antigen included)
IPI00007426	PRSS8	membrane	plasma membrane	6	protease, serine, 8 (prostasin)
IPI00020719	AP1B1	membrane	plasma membrane	17	adaptor-related protein complex 1, beta 1 subunit
IPI00021807	GNB2	membrane	plasma membrane	23	guanine nucleotide binding protein (G protein), beta polypeptide 2
IPI00020647	PARD6B	membrane	plasma membrane	7	par-6 partitioning defective 6 homolog beta (C. elegans)
IPI00033469	LGALS3	membrane	plasma membrane	19	lectin, galactoside-binding, soluble, 3 (galectin 3)
IPI00084495	LETM1	membrane	plasma membrane	14	leucine zipper-EF-hand containing transmembrane protein 1
IPI00003062	DEGS	membrane	plasma membrane	2	degenerative spermatocyte homolog, lipid desaturase (Drosophila)
IPI00178677	NT5E	membrane	plasma membrane	22	5'-nucleotidase, ecto (CD73)
IPI00219150	PIP5K1B	membrane	plasma membrane	2	phosphatidylinositol-4-phosphate 5-kinase, type I, beta
IPI00045511	GENX-3414	membrane	plasma membrane	6	genethonin 1
IPI00100773	STIM1	membrane	plasma membrane	4	stromal interaction molecule 1
IPI00171410	RALB	membrane	plasma membrane	25	v-ral simian leukemia viral oncogene homolog B (ras related; GTP binding protein)
IPI00183119	CD9	membrane	plasma membrane	9	CD9 antigen (p24)
IPI00221226	CD99	membrane	plasma membrane	3	CD99 antigen
IPI00010153	SLC9A3R2	membrane	plasma membrane	14	solute carrier family 9 (sodium/hydrogen exchanger), isoform 3 regulator 2
IPI00000296	ITM2B	membrane	plasma membrane	6	integral membrane protein 2B
IPI00024911	CEACAM6	membrane	plasma membrane	8	carcinoembryonic antigen-related cell adhesion molecule 6 (non-specific cross reacting antigen)
IPI00026830	SLC16A3	membrane	plasma membrane	6	solute carrier family 16 (monocarboxylic acid transporters), member 3

IPI00008454	GNB2L1	membrane	plasma membrane	6	guanine nucleotide binding protein (G protein), beta polypeptide 2-like 1
IPI00013271	LRRC1	membrane	plasma membrane	14	leucine rich repeat containing 1
IPI00021147	SLMAP	membrane	plasma membrane	6	sarcolemma associated protein
IPI00009960	LRP1	membrane	plasma membrane	14	low density lipoprotein-related protein 1 (alpha-2-macroglobulin receptor)
IPI00168878	TPBG	membrane	plasma membrane	14	trophoblast glycoprotein
IPI00007034	EPHB4	membrane	plasma membrane	17	EphB4
IPI00027499	YKT6	membrane	plasma membrane	3	SNARE protein Ykt6
IPI00023979	CNNM3	membrane	plasma membrane	12	cyclin M3
IPI00018237	FXYD3	membrane	plasma membrane	2	FXYD domain containing ion transport regulator 3
IPI00024936	LIN7C	membrane	plasma membrane	5	lin-7 homolog C (C. elegans)
IPI00016613	MSN	membrane	plasma membrane	59	moesin
IPI00017292	PIP5K1A	membrane	plasma membrane	8	phosphatidylinositol-4-phosphate 5-kinase, type I, alpha
IPI00009456	TGFBR1	membrane	plasma membrane	2	transforming growth factor, beta receptor I (activin A receptor type II-like kinase, 53kDa)
IPI00032242	PVRL2	membrane	plasma membrane	6	poliovirus receptor-related 2 (herpesvirus entry mediator B)
IPI00186614	VIL2	membrane	plasma membrane	24	villin 2 (ezrin)
IPI00218200	GIT1	membrane	plasma membrane	3	G protein-coupled receptor kinase interactor 1
IPI00215933	ADAM9	membrane	plasma membrane	3	a disintegrin and metalloproteinase domain 9 (meltrin gamma)
IPI00025845	EPB41L2	membrane	plasma membrane	9	erythrocyte membrane protein band 4.1-like 2
IPI00045249	PODXL	membrane	plasma membrane	7	podocalyxin-like
IPI00061087	SLC19A1	membrane	plasma membrane	4	solute carrier family 19 (folate transporter), member 1
IPI00021475	NAPA	membrane	plasma membrane	11	N-ethylmaleimide-sensitive factor attachment protein, alpha
IPI00217529	TRIP6	membrane	plasma membrane	6	thyroid hormone receptor interactor 6
IPI00017899	OCLN	membrane	plasma membrane	6	occludin

IPI00026302	ARHGEF1	membrane	plasma membrane	12	Rho guanine nucleotide exchange factor (GEF) 1
IPI00029750	ST14	membrane	plasma membrane	11	suppression of tumorigenicity 14 (colon carcinoma, matriptase, epithin)
IPI00007058	ADCY9	membrane	plasma membrane	4	adenylate cyclase 9
IPI00014457	CD97	membrane	plasma membrane	7	CD97 antigen
IPI00164311	ENTH	membrane	plasma membrane	5	enthoprotin
IPI00020468	EEF1G	membrane	plasma membrane	4	eukaryotic translation elongation factor 1 gamma
IPI00022538	LAMR1	membrane	plasma membrane	4	laminin receptor 1 (ribosomal protein SA, 67kDa)
IPI00022048	RRAS	membrane	plasma membrane	6	related RAS viral (r-ras) oncogene homolog
IPI00166512	DLG1	membrane	plasma membrane	26	discs, large homolog 1 (Drosophila)
IPI00004416	DAG1	membrane	plasma membrane	8	dystroglycan 1 (dystrophin-associated glycoprotein 1)
IPI00004397	NCAM2	membrane	plasma membrane	11	neural cell adhesion molecule 2
IPI00007188	RAI3	membrane	plasma membrane	13	retinoic acid induced 3
IPI00010418	ANXA2	membrane	plasma membrane	103	annexin A2
IPI00001028	KDELR2	membrane	plasma membrane	4	KDEL (Lys-Asp-Glu-Leu) endoplasmic reticulum protein retention receptor 2
IPI00152996	PAK2	membrane	plasma membrane	2	p21 (CDKN1A)-activated kinase 2
IPI00215997	CLDN3	membrane	plasma membrane	4	claudin 3
IPI00030154	SLC7A5	membrane	plasma membrane	10	solute carrier family 7 (cationic amino acid transporter, y+ system), member 5
IPI00219263	AP2S1	membrane	plasma membrane	3	adaptor-related protein complex 2, sigma 1 subunit
IPI00147227	SLC33A1	membrane	plasma membrane	3	solute carrier family 33 (acetyl-CoA transporter), member 1
IPI00174757	GNAI3	membrane	plasma membrane	26	guanine nucleotide binding protein (G protein), alpha inhibiting activity polypeptide 3
IPI00031821	APOM	membrane	plasma membrane	4	apolipoprotein M
IPI00000705	FLOT1	membrane	plasma membrane	24	flotillin 1
IPI00027412	GNB4	membrane	plasma membrane	8	guanine nucleotide binding protein (G protein), beta polypeptide 4
IPI00006666	CDC42	membrane	plasma	16	cell division cycle 42 (GTP

			membrane		binding protein, 25kDa)
IPI00025491	SMPD2	membrane	plasma membrane	3	sphingomyelin phosphodiesterase 2, neutral membrane (neutral sphingomyelinase)
IPI00032304	TCIRG1	membrane	plasma membrane	8	T-cell, immune regulator 1, ATPase, H+ transporting, lysosomal V0 protein a isoform 3
IPI00219675	MARCKS	membrane	plasma membrane	13	myristoylated alanine-rich protein kinase C substrate
IPI00032515	NOTCH3	membrane	plasma membrane	8	Notch homolog 3 (Drosophila)
IPI00013896	NUMB	membrane	plasma membrane	3	numb homolog (Drosophila)
IPI00074327	SORT1	membrane	plasma membrane	10	sortilin 1
IPI00010133	AP2A1	membrane	plasma membrane	32	adaptor-related protein complex 2, alpha 1 subunit
IPI00220766	PAG	membrane	plasma membrane	2	phosphoprotein associated with glycosphingolipid-enriched microdomains
IPI00028582	SLC7A2	membrane	plasma membrane	9	solute carrier family 7 (cationic amino acid transporter, y+ system), member 2
IPI00174808	LDLR	membrane	plasma membrane	8	low density lipoprotein receptor (familial hypercholesterolemia)
IPI00013981	SLC31A1	membrane	plasma membrane	4	solute carrier family 31 (copper transporters), member 1
IPI00149950	CAPN1	membrane	plasma membrane	4	calpain 1, (mu/I) large subunit
IPI00030531	MC1R	membrane	plasma membrane	25	melanocortin 1 receptor (alpha melanocyte stimulating hormone receptor)
IPI00022058	SLC2A1	membrane	plasma membrane	9	solute carrier family 2 (facilitated glucose transporter), member 1
IPI00021167	SYPL	membrane	plasma membrane	4	synaptophysin-like protein
IPI00022793	CD151	membrane	plasma membrane	3	CD151 antigen
IPI00033025	EPHA2	membrane	plasma membrane	12	EphA2
IPI00165529	KCNH4	membrane	plasma membrane	3	potassium voltage-gated channel, subfamily H (eag-related), member 4
IPI00018931	GRK6	membrane	plasma membrane	4	G protein-coupled receptor kinase 6
IPI00021560	SLC7A6	membrane	plasma membrane	5	solute carrier family 7 (cationic amino acid transporter, y+ system),

					member 6
IPI00020557	ENG	membrane	plasma membrane	2	endoglin (Osler-Rendu-Weber syndrome 1)
IPI00004670	MYO1A	membrane	plasma membrane	8	myosin IA
IPI00010841	SLC1A5	membrane	plasma membrane	18	solute carrier family 1 (neutral amino acid transporter), member 5
IPI00024670	CELSR3	membrane	plasma membrane	2	cadherin, EGF LAG seven-pass G-type receptor 3 (flamingo homolog, Drosophila)
IPI00009111	TLN1	membrane	plasma membrane	30	talin 1
IPI00014377	FGFR4	membrane	plasma membrane	5	fibroblast growth factor receptor 4
IPI00022832	LANCL2	membrane	plasma membrane	2	LanC lantibiotic synthetase component C-like 2 (bacterial)
IPI00061987	MCOLN1	membrane	plasma membrane	2	mucolipin 1
IPI00011216	SLC30A1	membrane	plasma membrane	7	solute carrier family 30 (zinc transporter), member 1
IPI00006547	PALM	membrane	plasma membrane	3	paralemmin
IPI00011229	CEACAM5	membrane	plasma membrane	12	carcinoembryonic antigen-related cell adhesion molecule 5
IPI00174860	C4.4A	membrane	plasma membrane	4	GPI-anchored metastasis-associated protein homolog
IPI00008310	EPN3	membrane	plasma membrane	6	epsin 3
IPI00031583	CLCN5	membrane	plasma membrane	3	chloride channel 5 (nephrolithiasis 2, X-linked, Dent disease)
IPI00219755	ITM1	membrane	plasma membrane	18	integral membrane protein 1
IPI00178408	FRS2	membrane	plasma membrane	2	fibroblast growth factor receptor substrate 2
IPI00032150	FZD6	membrane	plasma membrane	3	frizzled homolog 6 (Drosophila)
IPI00011217	LPP	membrane	plasma membrane	5	LIM domain containing preferred translocation partner in lipoma
IPI00006970	EGFR	membrane	plasma membrane	18	epidermal growth factor receptor (erythroblastic leukemia viral (v-erb-b) oncogene homolog, avian)
IPI00016638	PRKCA	membrane	plasma membrane	3	protein kinase C, alpha
IPI00166128	SLC6A6	membrane	plasma membrane	2	solute carrier family 6 (neurotransmitter transporter, taurine), member 6
IPI00027986	TDE1	membrane	plasma membrane	3	tumor differentially expressed 1

IPI00216158	ATP8B1	membrane	plasma membrane	25	ATPase, Class I, type 8B, member 1
IPI00217702	BMPR1A	membrane	plasma membrane	2	bone morphogenetic protein receptor, type IA
IPI00218850	EPHB2	membrane	plasma membrane	4	EphB2
IPI00027180	CNNM2	membrane	plasma membrane	3	cyclin M2
IPI00102070	SLC5A6	membrane	plasma membrane	6	solute carrier family 5 (sodium-dependent vitamin transporter), member 6
IPI00220834	ADAM15	membrane	plasma membrane	4	a disintegrin and metalloproteinase domain 15 (metargidin)
IPI00030960	CXADR	membrane	plasma membrane	5	coxsackie virus and adenovirus receptor
IPI00043598	GALNT7	membrane	plasma membrane	16	UDP-N-acetyl-alpha-D-galactosamine:polypeptide N-acetylgalactosaminyltransferase 7 (GalNAc-T7)
IPI00025728	NRP1	membrane	plasma membrane	5	neuropilin 1
IPI00169373	SLC12A7	membrane	plasma membrane	21	solute carrier family 12 (potassium/chloride transporters), member 7
IPI00219770	ITGA2	membrane	plasma membrane	24	integrin, alpha 2 (CD49B, alpha 2 subunit of VLA-2 receptor)
IPI00021302	CELSR1	membrane	plasma membrane	6	cadherin, EGF LAG seven-pass G-type receptor 1 (flamingo homolog, Drosophila)
IPI00010340	GFRA1	membrane	plasma membrane	3	GDNF family receptor alpha 1
IPI00168884	PTPRG	membrane	plasma membrane	5	protein tyrosine phosphatase, receptor type, G
IPI00020567	LOC144363	membrane	plasma membrane	15	hypothetical protein LOC144363
IPI00021782	AMFR	membrane	plasma membrane	8	autocrine motility factor receptor
IPI00010810	CD58	membrane	plasma membrane	2	CD58 antigen, (lymphocyte function-associated antigen 3)
IPI00184959	GPAA1	membrane	plasma membrane	8	GPAA1P anchor attachment protein 1 homolog (yeast)
IPI00030934	PLXNA1	membrane	plasma membrane	4	plexin A1
IPI00024919	PTK7	membrane	plasma membrane	9	PTK7 protein tyrosine kinase 7
IPI00008569	SLC20A1	membrane	plasma membrane	2	solute carrier family 20 (phosphate transporter), member 1
IPI00221233	LOC92799	membrane	plasma membrane	3	hypothetical protein BC007653

IPI00014149	SLC7A1	membrane	plasma membrane	3	solute carrier family 7 (cationic amino acid transporter, y+ system), member 1
IPI00005585	SLC6A14	membrane	plasma membrane	10	solute carrier family 6 (neurotransmitter transporter), member 14
IPI00023919	NAPG	membrane	plasma membrane	7	N-ethylmaleimide-sensitive factor attachment protein, gamma
IPI00000948	EPHA1	membrane	plasma membrane	12	EphA1
IPI00032342	PKP4	membrane	plasma membrane	4	plakophilin 4
IPI00178885	PTPRE	membrane	plasma membrane	4	protein tyrosine phosphatase, receptor type, E
IPI00059279	SLC16A1	membrane	plasma membrane	2	solute carrier family 16 (monocarboxylic acid transporters), member 1
IPI00102213	ABCC5	membrane	plasma membrane	9	ATP-binding cassette, sub-family C (CFTR/MRP), member 5
IPI00182679	EFNB2	membrane	plasma membrane	2	ephrin-B2
IPI00106296	CLPTM1	membrane	plasma membrane	22	cleft lip and palate associated transmembrane protein 1
IPI00152303	GPR39	membrane	plasma membrane	3	G protein-coupled receptor 39
IPI00168565	KIAA0310	membrane	plasma membrane	9	KIAA0310
IPI00219525	ALOX12B	membrane	plasma membrane	2	arachidonate 12-lipoxygenase, 12R type
IPI00022462	AFAP	membrane	plasma membrane	3	actin filament associated protein
IPI00107324	CPNE2	membrane	plasma membrane	4	copine II
IPI00015602	ZYX	membrane	plasma membrane	5	zyxin
IPI00026991	BTN2A1	membrane	plasma membrane	3	butyrophilin, subfamily 2, member A1
IPI00178107	ITGA5	membrane	plasma membrane	4	integrin, alpha 5 (fibronectin receptor, alpha polypeptide)
IPI00027032	GNAI2	membrane	plasma membrane	31	guanine nucleotide binding protein (G protein), alpha inhibiting activity polypeptide 2
IPI00004022	AP2B1	membrane	plasma membrane	38	adaptor-related protein complex 2, beta 1 subunit
IPI00009922	CDCP1	membrane	plasma membrane	5	CUB domain-containing protein 1
IPI00005200	EPHB3	membrane	plasma membrane	9	EphB3
IPI00101335	SORL1	membrane	plasma membrane	3	sortilin-related receptor, L(DLR class) A repeats-containing

IPI00032038	ABCC3	membrane	plasma membrane	18	ATP-binding cassette, sub-family C (CFTR/MRP), member 3
IPI00028883	TRIO	membrane	plasma membrane	4	triple functional domain (PTPRF interacting)
IPI00163699	GEM	membrane	plasma membrane	2	GTP binding protein overexpressed in skeletal muscle
IPI00219149	BAIAP2	membrane	plasma membrane	21	BAI1-associated protein 2
IPI00000765	GNAS	membrane	plasma membrane	42	GNAS complex locus
IPI00019997	PODLX2	membrane	plasma membrane	3	endoglycan
IPI00219365	SLC20A2	membrane	plasma membrane	2	solute carrier family 20 (phosphate transporter), member 2
IPI00030959	DLG5	membrane	plasma membrane	2	discs, large homolog 5 (Drosophila)
IPI00014232	M11S1	membrane	plasma membrane	4	membrane component, chromosome 11, surface marker 1
IPI00163602	ABCC1	membrane	plasma membrane	13	ATP-binding cassette, sub-family C (CFTR/MRP), member 1
IPI00016720	ANTXR1	membrane	plasma membrane	32	anthrax toxin receptor 1
IPI00028062	AP1G1	membrane	plasma membrane	31	adaptor-related protein complex 1, gamma 1 subunit
IPI00165052	AP1M2	membrane	plasma membrane	10	adaptor-related protein complex 1, mu 2 subunit
IPI00005733	APP	membrane	plasma membrane	2	amyloid beta (A4) precursor protein (protease nexin-II, Alzheimer disease)
IPI00025463	ARF6	membrane	plasma membrane	38	ADP-ribosylation factor 6
IPI00040309	ATP2B1	membrane	plasma membrane	17	ATPase, Ca++ transporting, plasma membrane 1
IPI00013894	ATP7A	membrane	plasma membrane	25	ATPase, Cu++ transporting, alpha polypeptide (Menkes syndrome)
IPI00021828	BMPR2	membrane	plasma membrane	19	bone morphogenetic protein receptor, type II (serine/threonine kinase)
IPI00005740	CAV1	membrane	plasma membrane	11	caveolin 1, caveolae protein, 22kDa
IPI00102427	CD44	membrane	plasma membrane	15	CD44 antigen (homing function and Indian blood group system)
IPI00215980	CD47	membrane	plasma membrane	20	CD47 antigen (Rh-related antigen, integrin-associated signal transducer)
IPI00216311	CD59	membrane	plasma membrane	3	CD59 antigen p18-20 (antigen identified by monoclonal antibodies

					16.3A5, EJ16, EJ30, EL32 and G344)
IPI00002821	CDH1	membrane	plasma membrane	12	cadherin 1, type 1, E-cadherin (epithelial)
IPI00002520	CLCN7	membrane	plasma membrane	22	chloride channel 7
IPI00180986	CLTA	membrane	plasma membrane	2	clathrin, light polypeptide (Lca)
IPI00022291	CNNM4	membrane	plasma membrane	33	cyclin M4
IPI00153006	COL1A1	membrane	plasma membrane	7	collagen, type I, alpha 1
IPI00021905	CYB561	membrane	plasma membrane	12	cytochrome b-561
IPI00219685	DAF	membrane	plasma membrane	7	decay accelerating factor for complement (CD55, Cromer blood group system)
IPI00072224	DDR1	membrane	plasma membrane	10	discoidin domain receptor family, member 1
IPI00217381	DLG3	membrane	plasma membrane	6	discs, large homolog 3 (neuroendocrine-dlg, Drosophila)
IPI00001159	DNAJC11	membrane	plasma membrane	3	DnaJ (Hsp40) homolog, subfamily C, member 11
IPI00030389	EEF1B2	membrane	plasma membrane	10	eukaryotic translation elongation factor 1 beta 2
IPI00022937	EPB41	membrane	plasma membrane	10	erythrocyte membrane protein band 4.1 (elliptocytosis 1, RH-linked)
IPI00016461	EPHB1	membrane	plasma membrane	35	EphB1
IPI00027830	EPN1	membrane	plasma membrane	11	epsin 1
IPI00015973	ERBB3	membrane	plasma membrane	7	v-erb-b2 erythroblastic leukemia viral oncogene homolog 3 (avian)
IPI00183736	FADS2	membrane	plasma membrane	23	fatty acid desaturase 2
IPI00005107	FLJ22222	membrane	plasma membrane	12	hypothetical protein FLJ22222
IPI00006663	FLNB	membrane	plasma membrane	30	filamin B, beta (actin binding protein 278)
IPI00027789	FLOT2	membrane	plasma membrane	39	flotillin 2
IPI00179326	GIT2	membrane	plasma membrane	10	G protein-coupled receptor kinase interactor 2
IPI00031438	GOLPH2	membrane	plasma membrane	25	golgi phosphoprotein 2
IPI00058192	GPRC5C	membrane	plasma membrane	12	G protein-coupled receptor, family C, group 5, member C
IPI00173461	HDLBP	membrane	plasma membrane	17	high density lipoprotein binding protein (vigilin)
IPI00167492	HLA-A	membrane	plasma membrane	25	major histocompatibility complex, class I, A
IPI00218796	HRAS	membrane	plasma	9	v-Ha-ras Harvey rat sarcoma

			membrane		viral oncogene homolog
IPI00018120	HYAL2	membrane	plasma membrane	31	hyaluronoglucosaminidase 2
IPI00000105	IGSF1	membrane	plasma membrane	32	immunoglobulin superfamily, member 1
IPI00008964	ITGA3	membrane	plasma membrane	11	integrin, alpha 3 (antigen CD49C, alpha 3 subunit of VLA-3 receptor)
IPI00157215	ITGA6	membrane	plasma membrane	11	integrin, alpha 6
IPI00028108	ITGB1	membrane	plasma membrane	8	integrin, beta 1 (fibronectin receptor, beta polypeptide, antigen CD29 includes MDF2, MSK12)
IPI00009253	JAG2	membrane	plasma membrane	20	jagged 2
IPI00000032	KAI1	membrane	plasma membrane	30	kangai 1 (suppression of tumorigenicity 6, prostate; CD82 antigen (R2 leukocyte antigen, antigen detected by monoclonal and antibody IA4))
IPI00178376	KIAA0664	membrane	plasma membrane	37	KIAA0664 protein
IPI00024998	KIAA1181	membrane	plasma membrane	2	KIAA1181 protein
IPI00021187	MAGED1	membrane	plasma membrane	11	melanoma antigen, family D, 1
IPI00026154	MLLT4	membrane	plasma membrane	25	myeloid/lymphoid or mixed-lineage leukemia (trithorax homolog, Drosophila); translocated to, 4
IPI00003373	MPZL1	membrane	plasma membrane	30	myelin protein zero-like 1
IPI00166711	NET-7	membrane	plasma membrane	39	transmembrane 4 superfamily member tetraspan NET-7
IPI00065466	NF2	membrane	plasma membrane	14	neurofibromin 2 (bilateral acoustic neuroma)
IPI00218788	NOTCH2	membrane	plasma membrane	39	Notch homolog 2 (Drosophila)
IPI00013912	NUCB2	membrane	plasma membrane	38	nucleobindin 2
IPI00025729	PARD3	membrane	plasma membrane	35	par-3 partitioning defective 3 homolog (C. elegans)
IPI00027230	PFKP	membrane	plasma membrane	27	phosphofructokinase, platelet
IPI00218235	PITRM1	membrane	plasma membrane	36	pitrilysin metalloproteinase 1
IPI00219419	PLD2	membrane	plasma membrane	32	phospholipase D2
IPI00183807	PLEC1	membrane	plasma membrane	39	plectin 1, intermediate filament binding protein 500kDa
IPI00031091	PPFIBP1	membrane	plasma membrane	38	PTPRF interacting protein, binding protein 1 (liprin beta

					1)
IPI00024787	PTPRA	membrane	plasma membrane	31	protein tyrosine phosphatase, receptor type, A
IPI00011454	PTPRF	membrane	plasma membrane	6	protein tyrosine phosphatase, receptor type, F
IPI00217479	PTX1	membrane	plasma membrane	5	PTX1 protein
IPI00013495	RAB5C	membrane	plasma membrane	19	RAB5C, member RAS oncogene family
IPI00001922	RDX	membrane	plasma membrane	26	radixin
IPI00014555	SDBCAG84	membrane	plasma membrane	31	serologically defined breast cancer antigen 84
IPI00016610	SDFR1	membrane	plasma membrane	14	stromal cell derived factor receptor 1
IPI00008034	SEC31L1	membrane	plasma membrane	13	SEC31-like 1 (S. cerevisiae)
IPI00026627	SLC11A2	membrane	plasma membrane	37	solute carrier family 11 (proton-coupled divalent metal ion transporters), member 2
IPI00028264	SLC1A4	membrane	plasma membrane	25	solute carrier family 1 (glutamate/neutral amino acid transporter), member 4
IPI00026812	SLC25A4	membrane	plasma membrane	5	solute carrier family 25 (mitochondrial carrier; adenine nucleotide translocator), member 4
IPI00186798	SLC29A1	membrane	plasma membrane	22	solute carrier family 29 (nucleoside transporters), member 1
IPI00002790	TJP2	membrane	plasma membrane	11	tight junction protein 2 (zona occludens 2)
IPI00023860	TMP21	membrane	plasma membrane	25	transmembrane trafficking protein
IPI00006451	VAMP2	membrane	plasma membrane	34	vesicle-associated membrane protein 2 (synaptobrevin 2)
IPI00005864	VAPA	membrane	plasma membrane	30	VAMP (vesicle-associated membrane protein)-associated protein A, 33kDa
IPI00021073		membrane	plasma membrane	10	Data not found
IPI00005129	SLC39A10	membrane	ribosome	2	solute carrier family 39 (zinc transporter), member 10
IPI00152237	TJP1	membrane	unknown/unspecified	21	tight junction protein 1 (zona occludens 1)
IPI00018145	CYP20A1	membrane	unknown/unspecified	5	cytochrome P450, family 20, subfamily A, polypeptide 1
IPI00009629	LAMA5	membrane	unknown/unspecified	6	laminin, alpha 5
IPI00031522	PLXND1	membrane	unknown/unspecified	5	plexin D1
IPI00012353	LMTK2	membrane	unknown/unspecified	6	lemur tyrosine kinase 2
IPI00185832	RHOB	membrane	unknown/uns	15	ras homolog gene family,

			pecified		member B
IPI00100030	TTN	membrane	unknown/uns pecified	26	titin
IPI00024403	RAP1A	membrane	unknown/uns pecified	18	RAP1A, member of RAS oncogene family
IPI00216587	KIAA1033	membrane	unknown/uns pecified	3	KIAA1033 protein
IPI00029017	BSG	membrane	unknown/uns pecified	8	basigin (OK blood group)
IPI00181874	MLP	membrane	unknown/uns pecified	22	MARCKS-like protein
IPI00009368	STX4A	membrane	unknown/uns pecified	20	syntaxin 4A (placental)
IPI00030262	RGS19IP1	membrane	unknown/uns pecified	8	regulator of G-protein signalling 19 interacting protein 1
IPI00004403	RAB27B	membrane	unknown/uns pecified	10	RAB27B, member RAS oncogene family
IPI00007061	HIG1	membrane	unknown/uns pecified	5	likely ortholog of mouse hypoxia induced gene 1
IPI00018206	DNAJC5	membrane	unknown/uns pecified	16	DnaJ (Hsp40) homolog, subfamily C, member 5
IPI00021954	FADS1	membrane	unknown/uns pecified	10	fatty acid desaturase 1
IPI00019912	ABCC4	membrane	unknown/uns pecified	2	ATP-binding cassette, sub-family C (CFTR/MRP), member 4
IPI00001580	LAD1	membrane	unknown/uns pecified	2	ladinin 1
IPI00181965	FLJ20421	membrane	unknown/uns pecified	14	hypothetical protein FLJ20421
IPI00016513	STXBP1	membrane	unknown/uns pecified	4	syntaxin binding protein 1
IPI00020060	ITGAV	membrane	unknown/uns pecified	21	integrin, alpha V (vitronectin receptor, alpha polypeptide, antigen CD51)
IPI00000875	AKAP13	membrane	unknown/uns pecified	4	A kinase (PRKA) anchor protein 13
IPI00218996	LOC56926	membrane	unknown/uns pecified	32	hypothetical protein from EUROIMAGE 2021883
IPI00218719	C20orf3	membrane	unknown/uns pecified	17	chromosome 20 open reading frame 3
IPI00017184	CAP1	membrane	unknown/uns pecified	10	CAP, adenylate cyclase-associated protein 1 (yeast)
IPI00031595	GNA13	membrane	unknown/uns pecified	43	guanine nucleotide binding protein (G protein), alpha 13
IPI00181283	ORMDL2	membrane	unknown/uns pecified	4	ORM1-like 2 (S. cerevisiae)
IPI00216620	NINJ1	membrane	unknown/uns pecified	6	ninjurin 1
IPI00031804	BCMP11	membrane	unknown/uns pecified	4	breast cancer membrane protein 11
IPI00024095	KIAA0152	membrane	unknown/uns pecified	10	KIAA0152 gene product
IPI00040687	SI	membrane	unknown/uns	3	sucrase-isomaltase (alpha-

			pecified		glucosidase)
IPI00020470	AUP1	membrane	unknown/uns pecified	5	ancient ubiquitous protein 1
IPI00100674	SIGIRR	membrane	unknown/uns pecified	10	single Ig IL-1R-related molecule
IPI00102743	STX12	membrane	unknown/uns pecified	7	syntaxin 12
IPI00007249	ATP11A	membrane	unknown/uns pecified	3	ATPase, Class VI, type 11A
IPI00029992	ATP6V1F	membrane	unknown/uns pecified	10	ATPase, H+ transporting, lysosomal 14kDa, V1 subunit F
IPI00020418	SACM1L	membrane	unknown/uns pecified	20	SAC1 suppressor of actin mutations 1-like (yeast)
IPI00019376	LOC55831	membrane	unknown/uns pecified	7	30 kDa protein
IPI00024247	SCARB1	membrane	unknown/uns pecified	12	scavenger receptor class B, member 1
IPI00008847	KIAA0102	membrane	unknown/uns pecified	15	KIAA0102 gene product
IPI00218729	C7orf21	membrane	unknown/uns pecified	3	chromosome 7 open reading frame 21
IPI00006566	MPP5	membrane	unknown/uns pecified	11	membrane protein, palmitoylated 5 (MAGUK p55 subfamily member 5)
IPI00028911	ATP1A1	membrane	unknown/uns pecified	95	ATPase, Na+/K+ transporting, alpha 1 polypeptide
IPI00024348	MTCH2	membrane	unknown/uns pecified	12	mitochondrial carrier homolog 2 (C. elegans)
IPI00005159	KIAA1715	membrane	unknown/uns pecified	12	KIAA1715
IPI00217898	C11orf15	membrane	unknown/uns pecified	3	chromosome 11 open reading frame 15
IPI00005208	SYTL1	membrane	unknown/uns pecified	7	synaptotagmin-like 1
IPI00017030	SPINT2	membrane	unknown/uns pecified	7	serine protease inhibitor, Kunitz type, 2
IPI00008365	ATP1B3	membrane	unknown/uns pecified	18	ATPase, Na+/K+ transporting, beta 3 polypeptide
IPI00022334	GNG10	membrane	unknown/uns pecified	2	guanine nucleotide binding protein (G protein), gamma 10
IPI00009843	DER1	membrane	unknown/uns pecified	6	derlin-1
IPI00033058	PRKCD	membrane	unknown/uns pecified	5	protein kinase C, delta
IPI00006214	SELS	membrane	unknown/uns pecified	2	selenoprotein S
IPI00005751	TXNDC	membrane	unknown/uns pecified	14	thioredoxin domain containing
IPI00216976	SIPA1L3	membrane	unknown/uns pecified	3	signal-induced proliferation-associated 1 like 3
IPI00176010	DP1	membrane	unknown/uns	13	polyposis locus protein 1

			pecified		
IPI00171152	SCAMP2	membrane	unknown/uns pecified	9	secretory carrier membrane protein 2
IPI00102952	FLJ10525	membrane	unknown/uns pecified	6	hypothetical protein FLJ10525
IPI00154690	DDX1	membrane	unknown/uns pecified	3	DEAD (Asp-Glu-Ala-Asp) box polypeptide 1
IPI00026125	SUSD2	membrane	unknown/uns pecified	8	sushi domain containing 2
IPI00026358	ATP6AP2	membrane	unknown/uns pecified	9	ATPase, H+ transporting, lysosomal accessory protein 2
IPI00219146	TPARL	membrane	unknown/uns pecified	11	TPA regulated locus
IPI00026260	TRPM4	membrane	unknown/uns pecified	25	transient receptor potential cation channel, subfamily M, member 4
IPI00026034	TFRC	membrane	unknown/uns pecified	79	transferrin receptor (p90, CD71)
IPI00157734	ATP6V0A1	membrane	unknown/uns pecified	18	ATPase, H+ transporting, lysosomal V0 subunit a isoform 1
IPI00011899	SLC27A4	membrane	unknown/uns pecified	13	solute carrier family 27 (fatty acid transporter), member 4
IPI00012102	ARL6IP	membrane	unknown/uns pecified	4	ADP-ribosylation factor-like 6 interacting protein
IPI00016558	ALG12	membrane	unknown/uns pecified	4	asparagine-linked glycosylation 12 homolog (yeast, alpha-1,6-mannosyltransferase)
IPI00002214	SLC4A2	membrane	unknown/uns pecified	26	solute carrier family 4, anion exchanger, member 2 (erythrocyte membrane protein band 3-like 1)
IPI00219157	MRVLDC1	membrane	unknown/uns pecified	3	MARVEL (membrane-associating) domain containing 1
IPI00140420	RGS19	membrane	unknown/uns pecified	4	regulator of G-protein signalling 19
IPI00152701	KIAA0776	membrane	unknown/uns pecified	31	KIAA0776
IPI00010644	CAMLG	membrane	unknown/uns pecified	2	calcium modulating ligand
IPI00022624	CCM1	membrane	unknown/uns pecified	4	cerebral cavernous malformations 1
IPI00023958	ABCF1	membrane	unknown/uns pecified	3	ATP-binding cassette, sub-family F (GCN20), member 1
IPI00218827	CACNA2D 2	membrane	unknown/uns pecified	2	calcium channel, voltage-dependent, alpha 2/delta subunit 2
IPI00004839	SEL1L	membrane	unknown/uns pecified	21	sel-1 suppressor of lin-12-like (C. elegans)
IPI00177680	SCAMP1	membrane	unknown/uns pecified	8	secretory carrier membrane protein 1

IPI00025796	CPNE3	membrane	unknown/unspecified	20	copine III
IPI00029016	KIAA0143	membrane	unknown/unspecified	10	KIAA0143 protein
IPI00009342	CGI-141	membrane	unknown/unspecified	2	CGI-141 protein
IPI00024368	SLC9A1	membrane	unknown/unspecified	12	solute carrier family 9 (sodium/hydrogen exchanger), isoform 1 (antiporter, Na+/H+, amiloride sensitive)
IPI00015833	PLCB3	membrane	unknown/unspecified	22	phospholipase C, beta 3 (phosphatidylinositol-specific)
IPI00018213	PPAP2C	membrane	unknown/unspecified	2	phosphatidic acid phosphatase type 2C
IPI00166225	AD-017	membrane	unknown/unspecified	4	glycosyltransferase AD-017
IPI00180597	C8orf20	membrane	unknown/unspecified	2	chromosome 8 open reading frame 20
IPI00216240	CLN6	membrane	unknown/unspecified	10	ceroid-lipofuscinosis, neuronal 6, late infantile, variant
IPI00090327	ENPP4	membrane	unknown/unspecified	6	ectonucleotide pyrophosphatase/phosphodiesterase 4 (putative function)
IPI00219446	ATP1A3	membrane	unknown/unspecified	35	ATPase, Na+/K+ transporting, alpha 3 polypeptide
IPI00185135	C1orf8	membrane	unknown/unspecified	2	chromosome 1 open reading frame 8
IPI00002372	DNASE1L1	membrane	unknown/unspecified	2	deoxyribonuclease I-like 1
IPI00029735	LOC58489	membrane	unknown/unspecified	4	hypothetical protein from EUROIMAGE 588495
IPI00030530	BAMBI	membrane	unknown/unspecified	2	BMP and activin membrane-bound inhibitor homolog (Xenopus laevis)
IPI00018248	BSPRY	membrane	unknown/unspecified	5	B-box and SPRY domain containing
IPI00219447	ATP9A	membrane	unknown/unspecified	20	ATPase, Class II, type 9A
IPI00021978	SLC4A7	membrane	unknown/unspecified	9	solute carrier family 4, sodium bicarbonate cotransporter, member 7
IPI00008982	C14orf9	membrane	unknown/unspecified	4	chromosome 14 open reading frame 9
IPI00026994	DNAJA1	membrane	unknown/unspecified	11	DnaJ (Hsp40) homolog, subfamily A, member 1
IPI00044683	SEMA4C	membrane	unknown/unspecified	16	sema domain, immunoglobulin domain (Ig), transmembrane domain (TM) and short cytoplasmic domain, (semaphorin) 4C
IPI00000181	ULBP3	membrane	unknown/uns	2	UL16 binding protein 3

			pecified		
IPI00012535	FLJ10579	membrane	unknown/uns pecified	3	hypothetical protein FLJ10579
IPI00001091	PLA2G4C	membrane	unknown/uns pecified	2	phospholipase A2, group IVC (cytosolic, calcium-independent)
IPI00005190	FLJ21749	membrane	unknown/uns pecified	2	hypothetical protein FLJ21749
IPI00218336	CEPT1	membrane	unknown/uns pecified	3	choline/ethanolaminephosph otransferase
IPI00064209	VPS13C	membrane	unknown/uns pecified	6	vacuolar protein sorting 13C (yeast)
IPI00101486	ERBB2	membrane	unknown/uns pecified	129	v-erb-b2 erythroblastic leukemia viral oncogene homolog 2, neuro/glioblastoma derived oncogene homolog (avian)
IPI00063220	VAMP3	membrane	unknown/uns pecified	5	vesicle-associated membrane protein 3 (cellubrevin)
IPI00151462	KIAA0195	membrane	unknown/uns pecified	4	KIAA0195 gene product
IPI00073763	KIAA0953	membrane	unknown/uns pecified	5	KIAA0953
IPI00001602	DKFZp434 H2226	membrane	unknown/uns pecified	4	hypothetical protein DKFZp434H2226
IPI00178165	SLC35E1	membrane	unknown/uns pecified	4	solute carrier family 35, member E1
IPI00178892	PPP1R16A	membrane	unknown/uns pecified	3	protein phosphatase 1, regulatory (inhibitor) subunit 16A
IPI00053486	STXBP3	membrane	unknown/uns pecified	23	syntaxin binding protein 3
IPI00019898	ARHGAP17	membrane	unknown/uns pecified	3	Rho GTPase activating protein 17
IPI00024642	ENTPD2	membrane	unknown/uns pecified	5	ectonucleoside triphosphate diphosphohydrolase 2
IPI00007254	STRN	membrane	unknown/uns pecified	5	striatin, calmodulin binding protein
IPI00018730	VRK2	membrane	unknown/uns pecified	3	vaccinia related kinase 2
IPI00215637	C22orf5	membrane	unknown/uns pecified	2	chromosome 22 open reading frame 5
IPI00177423	FCGRT	membrane	unknown/uns pecified	3	Fc fragment of IgG, receptor, transporter, alpha
IPI00176602	MAL2	membrane	unknown/uns pecified	9	mal, T-cell differentiation protein 2
IPI00003166	SYTL4	membrane	unknown/uns pecified	6	synaptotagmin-like 4 (granuphilin-a)
IPI00023728	AFURS1	membrane	unknown/uns pecified	9	ATPase family homolog up-regulated in senescence cells
IPI00018576	ITGB6	membrane	unknown/uns pecified	5	integrin, beta 6
IPI00007364	KIAA0033	membrane	unknown/uns pecified	3	KIAA0033 protein
IPI00008986	SLC38A2	membrane	unknown/uns	4	solute carrier family 38,

			pecified		member 2
IPI00013909	ABHD2	membrane	unknown/uns pecified	2	abhydrolase domain containing 2
IPI00219385	MGC39558	membrane	unknown/uns pecified	2	beta 1,3-N-acetylgalactosaminyltransfera se-II
IPI00027851	C20orf108	membrane	unknown/uns pecified	3	chromosome 20 open reading frame 108
IPI00219840	CLSTN2	membrane	unknown/uns pecified	2	calsyntenin 2
IPI00220039	COMMD5	membrane	unknown/uns pecified	2	COMM domain containing 5
IPI00025717	PDGFRB	membrane	unknown/uns pecified	3	platelet-derived growth factor receptor, beta polypeptide
IPI00218647	C10orf69	membrane	unknown/uns pecified	13	chromosome 10 open reading frame 69
IPI00021996	GPR56	membrane	unknown/uns pecified	8	G protein-coupled receptor 56
IPI00216293	ADCY6	membrane	unknown/uns pecified	11	adenylate cyclase 6
IPI00063217	MBC2	membrane	unknown/uns pecified	57	likely ortholog of mouse membrane bound C2 domain containing protein
IPI00103876	C9orf5	membrane	unknown/uns pecified	10	chromosome 9 open reading frame 5
IPI00007411	CKLFSF6	membrane	unknown/uns pecified	3	chemokine-like factor super family 6
IPI00013860	IFITM3	membrane	unknown/uns pecified	7	interferon induced transmembrane protein 3 (1-8U)
IPI00012837	KIAA1228	membrane	unknown/uns pecified	22	KIAA1228 protein
IPI00153014	C15orf2	membrane	unknown/uns pecified	2	chromosome 15 open reading frame 2
IPI00061531	ADIPOR1	membrane	unknown/uns pecified	2	adiponectin receptor 1
IPI00065500	CDKAL1	membrane	unknown/uns pecified	3	CDK5 regulatory subunit associated protein 1-like 1
IPI00167111	ELOVL5	membrane	unknown/uns pecified	4	ELOVL family member 5, elongation of long chain fatty acids (FEN1/Elo2, SUR4/Elo3-like, yeast)
IPI00005775	LNPEP	membrane	unknown/uns pecified	34	leucyl/cystinyl aminopeptidase
IPI00002107	SLC38A1	membrane	unknown/uns pecified	11	solute carrier family 38, member 1
IPI00025072	XYLT2	membrane	unknown/uns pecified	2	xylosyltransferase II
IPI00019982	NCKAP1	membrane	unknown/uns pecified	17	NCK-associated protein 1
IPI00221002	ATP6V0A4	membrane	unknown/uns pecified	4	ATPase, H+ transporting, lysosomal V0 subunit a isoform 4
IPI00025971	BFSP1	membrane	unknown/uns pecified	3	beaded filament structural protein 1, filensin

IPI00217962	C14orf171	membrane	unknown/unspecified	2	chromosome 14 open reading frame 171
IPI00005689	CLCN3	membrane	unknown/unspecified	7	chloride channel 3
IPI00097790	VTI1B	membrane	unknown/unspecified	5	vesicle transport through interaction with t-SNAREs homolog 1B (yeast)
IPI00164434	BAT5	membrane	unknown/unspecified	6	HLA-B associated transcript 5
IPI00215805	KIAA1409	membrane	unknown/unspecified	3	KIAA1409
IPI00029173	TSAP6	membrane	unknown/unspecified	4	dudulin 2
IPI00032128	VPS26	membrane	unknown/unspecified	3	vacuolar protein sorting 26 (yeast)
IPI00006205	ARHGAP12	membrane	unknown/unspecified	5	Rho GTPase activating protein 12
IPI00217975	TM9SF4	membrane	unknown/unspecified	12	transmembrane 9 superfamily protein member 4
IPI00000945	CNP	membrane	unknown/unspecified	19	2',3'-cyclic nucleotide 3' phosphodiesterase
IPI00008207	LPAAT-e	membrane	unknown/unspecified	3	acid acyltransferase-epsilon
IPI00006176	RALBP1	membrane	unknown/unspecified	4	ralA binding protein 1
IPI00171422	C6orf96	membrane	unknown/unspecified	2	chromosome 6 open reading frame 96
IPI00101408	MFGE8	membrane	unknown/unspecified	2	milk fat globule-EGF factor 8 protein
IPI00220835	KIAA0792	membrane	unknown/unspecified	5	KIAA0792 gene product
IPI00023983	CPD	membrane	unknown/unspecified	23	carboxypeptidase D
IPI00011937	GPR48	membrane	unknown/unspecified	2	G protein-coupled receptor 48
IPI00177386	MGC3262	membrane	unknown/unspecified	4	hypothetical protein MGC3262
IPI00220578	NQO3A2	membrane	unknown/unspecified	14	NAD(P)H:quinone oxidoreductase type 3, polypeptide A2
IPI00002225	SLC39A14	membrane	unknown/unspecified	2	solute carrier family 39 (zinc transporter), member 14
IPI00103736	MRVLDC2	membrane	unknown/unspecified	5	MARVEL (membrane-associating) domain containing 2
IPI00001885	ABCA3	membrane	unknown/unspecified	2	ATP-binding cassette, sub-family A (ABC1), member 3
IPI00014434	SLC9A8	membrane	unknown/unspecified	2	solute carrier family 9 (sodium/hydrogen exchanger), isoform 8
IPI00023161	GPR107	membrane	unknown/unspecified	13	G protein-coupled receptor 107
IPI00011736	CKAP4	membrane	unknown/unspecified	43	cytoskeleton-associated protein 4
IPI00004977	SPTBN1	membrane	unknown/uns	77	spectrin, beta, non-

			pecified		erythrocytic 1
IPI00017940	C20orf140	membrane	unknown/uns pecified	2	chromosome 20 open reading frame 140
IPI00030128	SLC2A10	membrane	unknown/uns pecified	4	solute carrier family 2 (facilitated glucose transporter), member 10
IPI00024234	JAG1	membrane	unknown/uns pecified	2	jagged 1 (Alagille syndrome)
IPI00030320	MYADM	membrane	unknown/uns pecified	2	myeloid-associated differentiation marker
IPI00006182	SLC27A3	membrane	unknown/uns pecified	12	solute carrier family 27 (fatty acid transporter), member 3
IPI00007210	TM7SF3	membrane	unknown/uns pecified	2	transmembrane 7 superfamily member 3
IPI00009609	USP30	membrane	unknown/uns pecified	2	ubiquitin specific protease 30
IPI00032968	FAM18B	membrane	unknown/uns pecified	5	family with sequence similarity 18, member B
IPI00217421	KIAA1724	membrane	unknown/uns pecified	5	selenoprotein I, 1
IPI00103093	PIGN	membrane	unknown/uns pecified	3	phosphatidylinositol glycan, class N
IPI00062151	C6orf110	membrane	unknown/uns pecified	2	chromosome 6 open reading frame 110
IPI00027438	NCSTN	membrane	unknown/uns pecified	9	nicastrin
IPI00073772	SLC39A3	membrane	unknown/uns pecified	2	solute carrier family 39 (zinc transporter), member 3
IPI00011307	PVRL1	membrane	unknown/uns pecified	2	poliovirus receptor-related 1 (herpesvirus entry mediator C; nectin)
IPI00029105	ALG2	membrane	unknown/uns pecified	3	asparagine-linked glycosylation 2 homolog (yeast, alpha-1,3-mannosyltransferase)
IPI00060114	PLXDC2	membrane	unknown/uns pecified	3	plexin domain containing 2
IPI00013678	SLC39A9	membrane	unknown/uns pecified	2	solute carrier family 39 (zinc transporter), member 9
IPI00216172	HS2ST1	membrane	unknown/uns pecified	5	heparan sulfate 2-O-sulfotransferase 1
IPI00152880	XTP3TPA	membrane	unknown/uns pecified	2	XTP3-transactivated protein A
IPI00217643	FLJ10305	membrane	unknown/uns pecified	2	hypothetical protein FLJ10305
IPI00101952	ECE1	membrane	unknown/uns pecified	27	endothelin converting enzyme 1
IPI00012451	FLJ10407	membrane	unknown/uns pecified	4	hypothetical protein FLJ10407
IPI00159072	ABCC10	membrane	unknown/uns pecified	5	ATP-binding cassette, sub-family C (CFTR/MRP), member 10
IPI00015911	C11orf2	membrane	unknown/uns pecified	2	chromosome 11 open reading frame2
IPI00029712	KIAA0368	membrane	unknown/uns	5	KIAA0368

			pecified		
IPI00173946	KIAA0934	membrane	unknown/uns pecified	3	KIAA0934
IPI00009997	CAS1	membrane	unknown/uns pecified	2	O-acetyltransferase
IPI00220718	LRP10	membrane	unknown/uns pecified	4	low density lipoprotein receptor-related protein 10
IPI00026044	KIAA1706	membrane	unknown/uns pecified	2	KIAA1706 protein
IPI00030363	PLXNA3	membrane	unknown/uns pecified	4	plexin A3
IPI00182728	RICS	membrane	unknown/uns pecified	2	Rho GTPase-activating protein
IPI00063273	SLC12A6	membrane	unknown/uns pecified	5	solute carrier family 12 (potassium/chloride transporters), member 6
IPI00219382	SLC15A4	membrane	unknown/uns pecified	2	solute carrier family 15, member 4
IPI00218926	SLC26A6	membrane	unknown/uns pecified	10	solute carrier family 26, member 6
IPI00012585	PLD3	membrane	unknown/uns pecified	2	phospholipase D3
IPI00009339	PTDSS1	membrane	unknown/uns pecified	3	phosphatidylserine synthase 1
IPI00216939	SPTA1	membrane	unknown/uns pecified	3	spectrin, alpha, erythrocytic 1 (elliptocytosis 2)
IPI00016786	SNTB2	membrane	unknown/uns pecified	4	syntrophin, beta 2 (dystrophin-associated protein A1, 59kDa, basic component 2)
IPI00017670	UNC93B1	membrane	unknown/uns pecified	2	unc-93 homolog B1 (C. elegans)
IPI00013408	ADCY5	membrane	unknown/uns pecified	29	adenylate cyclase 5
IPI00024971	AGPAT3	membrane	unknown/uns pecified	8	1-acylglycerol-3-phosphate O-acyltransferase 3
IPI00066608	ATP13A	membrane	unknown/uns pecified	20	ATPase type 13A
IPI00216370	ATP1B1	membrane	unknown/uns pecified	21	ATPase, Na+/K+ transporting, beta 1 polypeptide
IPI00005966	ATP2C1	membrane	unknown/uns pecified	19	ATPase, Ca++ transporting, type 2C, member 1
IPI00024821	ATP6AP1	membrane	unknown/uns pecified	32	ATPase, H+ transporting, lysosomal accessory protein 1
IPI00025156	ATP6V0A2	membrane	unknown/uns pecified	22	ATPase, H+ transporting, lysosomal V0 subunit a isoform 2
IPI00100060	B7H3	membrane	unknown/uns pecified	20	B7 homolog 3
IPI00059683	C13orf11	membrane	unknown/uns pecified	39	chromosome 13 open reading frame 11
IPI00002070	C14orf1	membrane	unknown/uns pecified	17	chromosome 14 open reading frame 1

IPI00014456	C14orf114	membrane	unknown/unspecified	33	chromosome 14 open reading frame 114
IPI00219301	C14orf160	membrane	unknown/unspecified	12	chromosome 14 open reading frame 160
IPI00029819	C20orf142	membrane	unknown/unspecified	4	chromosome 20 open reading frame 142
IPI00216241	C8orf2	membrane	unknown/unspecified	27	chromosome 8 open reading frame 2
IPI00010353	CD99L2	membrane	unknown/unspecified	31	CD99 antigen-like 2
IPI00021926	CDW92	membrane	unknown/unspecified	18	CDW92 antigen
IPI00061403	CLMN	membrane	unknown/unspecified	32	calmin (calponin-like, transmembrane)
IPI00216205	COMT	membrane	unknown/unspecified	36	catechol-O-methyltransferase
IPI00006756	DIBD1	membrane	unknown/unspecified	12	disrupted in bipolar affective disorder 1
IPI00183232	DNAJA2	membrane	unknown/unspecified	26	DnaJ (Hsp40) homolog, subfamily A, member 2
IPI00006779	DSC2	membrane	unknown/unspecified	2	desmocollin 2
IPI00183540	ENPP1	membrane	unknown/unspecified	38	ectonucleotide pyrophosphatase/phosphodiesterase 1
IPI00021347	F11R	membrane	unknown/unspecified	38	F11 receptor
IPI00022774	FAAH	membrane	unknown/unspecified	37	fatty acid amide hydrolase
IPI00101524	FLNA	membrane	unknown/unspecified	15	filamin A, alpha (actin binding protein 280)
IPI00016022	GABARAP	membrane	unknown/unspecified	22	GABA(A) receptor-associated protein
IPI00026848	GGT1	membrane	unknown/unspecified	2	gamma-glutamyltransferase 1
IPI00023048	GNA12	membrane	unknown/unspecified	33	guanine nucleotide binding protein (G protein) alpha 12
IPI00015018	GPSN2	membrane	unknown/unspecified	32	glycoprotein, synaptic 2
IPI00171573	GRB2	membrane	unknown/unspecified	3	growth factor receptor-bound protein 2
IPI00016853	HLA-C	membrane	unknown/unspecified	12	major histocompatibility complex, class I, C
IPI00026646	IGF1R	membrane	unknown/unspecified	19	insulin-like growth factor 1 receptor
IPI00056414	IGHG1	membrane	unknown/unspecified	21	immunoglobulin heavy constant gamma 1 (G1m marker)
IPI00060201	INPP5A	membrane	unknown/unspecified	36	inositol polyphosphate-5-phosphatase, 40kDa
IPI00166484	ITGB4	membrane	unknown/unspecified	23	integrin, beta 4
IPI00178014	ITGB5	membrane	unknown/unspecified	11	integrin, beta 5
IPI00003861	ITSN1	membrane	unknown/uns	6	intersectin 1 (SH3 domain

			pecified		protein)
IPI00021264	KIAA0767	membrane	unknown/uns pecified	39	KIAA0767 protein
IPI00216577	KIAA0779	membrane	unknown/uns pecified	22	KIAA0779 protein
IPI00180140	LTBR	membrane	unknown/uns pecified	29	lymphotoxin beta receptor (TNFR superfamily, member 3)
IPI00107738	MFN2	membrane	unknown/uns pecified	30	mitofusin 2
IPI00020464	MGC4170	membrane	unknown/uns pecified	19	MGC4170 protein
IPI00186344	MPDU1	membrane	unknown/uns pecified	31	mannose-P-dolichol utilization defect 1
IPI00025341	MRVLDC3	membrane	unknown/uns pecified	9	MARVEL (membrane-associating) domain containing 3
IPI00178125	NUDC	membrane	unknown/uns pecified	17	nuclear distribution gene C homolog (A. nidulans)
IPI00151672	PIGQ	membrane	unknown/uns pecified	14	phosphatidylinositol glycan, class Q
IPI00219205	PLXNB2	membrane	unknown/uns pecified	6	plexin B2
IPI00031480	PON2	membrane	unknown/uns pecified	28	paraoxonase 2
IPI00017602	PSK-1	membrane	unknown/uns pecified	36	type I transmembrane receptor (seizure-related protein)
IPI00000138	PVR	membrane	unknown/uns pecified	18	poliovirus receptor
IPI00180183	RAP1B	membrane	unknown/uns pecified	8	RAP1B, member of RAS oncogene family
IPI00216951	RAP2C	membrane	unknown/uns pecified	27	RAP2C, member of RAS oncogene family
IPI00023474	RBM3	membrane	unknown/uns pecified	37	RNA binding motif (RNP1, RRM) protein 3
IPI00000137	SCAMP3	membrane	unknown/uns pecified	37	secretory carrier membrane protein 3
IPI00007772	SLC35A2	membrane	unknown/uns pecified	11	solute carrier family 35 (UDP-galactose transporter), member A2
IPI00163984	SLC39A6	membrane	unknown/uns pecified	22	solute carrier family 39 (zinc transporter), member 6
IPI00026665	SLC39A7	membrane	unknown/uns pecified	35	solute carrier family 39 (zinc transporter), member 7
IPI00177661	SLC3A2	membrane	unknown/uns pecified	31	solute carrier family 3 (activators of dibasic and neutral amino acid transport), member 2
IPI00000070	SPAG9	membrane	unknown/uns pecified	36	sperm associated antigen 9
IPI00219518	SPINL	membrane	unknown/uns pecified	3	spinster-like
IPI00003451	ST7	membrane	unknown/uns pecified	5	suppression of tumorigenicity 7

IPI00221070	STX3A	membrane	unknown/unspecified	13	syntaxin 3A
IPI00217467	TACSTD1	membrane	unknown/unspecified	34	tumor-associated calcium signal transducer 1
IPI00000151	TETRAN	membrane	unknown/unspecified	36	tetracycline transporter-like protein
IPI00014262	TJP3	membrane	unknown/unspecified	35	tight junction protein 3 (zona occludens 3)
IPI00006672	TM9SF1	membrane	unknown/unspecified	35	transmembrane 9 superfamily member 1
IPI00002949	TMEM15	membrane	unknown/unspecified	36	transmembrane protein 15
IPI00166860	TMEM30A	membrane	unknown/unspecified	15	transmembrane protein 30A
IPI00175029	TMEPAI	membrane	unknown/unspecified	14	transmembrane, prostate androgen induced RNA
IPI00184275	UTP14C	membrane	unknown/unspecified	15	UTP14, U3 small nucleolar ribonucleoprotein, homolog C (yeast)
IPI00028914	VPS41	membrane	unknown/unspecified	21	vacuolar protein sorting 41 (yeast)
IPI00011285	SMBP	membrane	unknown/unspecified	6	SM-11044 binding protein
IPI00152453	VEZATIN	membrane	unknown/unspecified	5	transmembrane protein vezatin
IPI00101026	ATP6V0D1	membrane	vacuolar	12	ATPase, H+ transporting, lysosomal 38kDa, V0 subunit d isoform 1
IPI00220194	ATP6V0C	membrane	vacuolar	3	ATPase, H+ transporting, lysosomal 16kDa, V0 subunit c
IPI00009507	FLJ20625	n/a		15	hypothetical protein FLJ20625
IPI00014301	RAB14	n/a		33	RAB14, member RAS oncogene family
IPI00014068	C20orf178	n/a		12	chromosome 20 open reading frame 178
IPI00015799	UBE2N	n/a		3	ubiquitin-conjugating enzyme E2N (UBC13 homolog, yeast)
IPI00011996	DHTKD1	n/a		4	dehydrogenase E1 and transketolase domain containing 1
IPI00005087	ARHGEF12	n/a		14	Rho guanine nucleotide exchange factor (GEF) 12
IPI00031707	MGC12981	n/a		7	hypothetical protein MGC12981
IPI00010092	ATAD1	n/a		11	ATPase family, AAA domain containing 1
IPI00004536	UNQ6077	n/a		14	AAAP6077
IPI00000788	YWHAG	n/a		24	tyrosine 3-monooxygenase/tryptophan 5-monooxygenase activation protein, gamma polypeptide
IPI00215888	LOC93380	n/a		9	hypothetical protein

					LOC93380
IPI00037383	MAP2K1IP 1	n/a		14	mitogen-activated protein kinase kinase 1 interacting protein 1
IPI00021267	VTI1A	n/a		5	vesicle transport through interaction with t-SNAREs homolog 1A (yeast)
IPI00017522		n/a		9	Similar to 40S ribosomal protein S10 (LOC158104), mRNA
IPI00025054	FLJ36812	n/a		3	hypothetical protein FLJ36812
IPI00020004	ARL10B	n/a		14	ADP-ribosylation factor-like 10B
IPI00017330	CALM3	n/a		20	calmodulin 3 (phosphorylase kinase, delta)
IPI00022631	TAO1	n/a		13	thousand and one amino acid protein kinase
IPI00003807	CPAMD8	n/a		2	C3 and PZP-like, alpha-2-macroglobulin domain containing 8
IPI00008453	MO25	n/a		6	MO25 protein
IPI00220487	FLJ11200	n/a		12	hypothetical protein FLJ11200
IPI00007799	KIAA1040	n/a		3	KIAA1040 protein
IPI00021709	NTE	n/a		7	neuropathy target esterase
IPI00013415	DKFZP564 D0478	n/a		2	hypothetical protein DKFZp564D0478
IPI00159899	RAB11A	n/a		21	RAB11A, member RAS oncogene family
IPI00017567	YWHAE	n/a		34	tyrosine 3-monooxygenase/tryptophan 5-monooxygenase activation protein, epsilon polypeptide
IPI00003985	MGC45714	n/a		7	hypothetical protein MGC45714
IPI00154648	ENTPD8	n/a		6	ectonucleoside triphosphate diphosphohydrolase 8
IPI00015786	ZFPL1	n/a		6	zinc finger protein-like 1
IPI00017895	RDH14	n/a		9	retinol dehydrogenase 14 (all-trans and 9-cis)
IPI00219111	C9orf83	n/a		4	chromosome 9 open reading frame 83
IPI00141564	MGC14839	n/a		6	similar to RIKEN cDNA 2310030G06 gene
IPI00216069	HAK	n/a		2	heart alpha-kinase
IPI00007461	PPP1CB	n/a		17	protein phosphatase 1, catalytic subunit, beta isoform
IPI00151334	MPP7	n/a		25	membrane protein, palmitoylated 7 (MAGUK p55 subfamily member 7)
IPI00149964	AIP1	n/a		3	atrophin-1 interacting protein 1
IPI00171501	ZSIG11	n/a		9	putative secreted protein

					ZSIG11
IPI00220422	Shax3	n/a		4	Snf7 homologue associated with Alix 3
IPI00001952	FLJ20296	n/a		7	hypothetical protein FLJ20296
IPI00015246	FLJ20793	n/a		12	FLJ20793 protein
IPI00218893	CD109	n/a		2	CD109 antigen (Gov platelet alloantigens)
IPI00011416		n/a		2	Data not found
IPI00029831	E2IG4	n/a		4	hypothetical protein, estradiol-induced
IPI00220373	C10orf58	n/a		4	chromosome 10 open reading frame 58
IPI00001404	CTL2	n/a		10	CTL2 gene
IPI00161430	C1orf31	n/a		2	chromosome 1 open reading frame 31
IPI00103162	MCLC	n/a		8	Mid-1-related chloride channel 1
IPI00005491	FLJ35155	n/a		5	hypothetical protein FLJ35155
IPI00101106	C3orf10	n/a		3	chromosome 3 open reading frame 10
IPI00015902	PHGDHL1	n/a		3	phosphoglycerate dehydrogenase like 1
IPI00028931	RHOT2	n/a		12	ras homolog gene family, member T2
IPI00008787	CORO1B	n/a		14	coronin, actin binding protein, 1B
IPI00007940	SDK1	n/a		2	sidekick homolog 1 (chicken)
IPI00019472	FBXL20	n/a		5	F-box and leucine-rich repeat protein 20
IPI00000865	DAAM1	n/a		13	dishevelled associated activator of morphogenesis 1
IPI00027233	GL009	n/a		2	hypothetical protein GL009
IPI00014976	DKFZP564 B167	n/a		4	DKFZP564B167 protein
IPI00024264	LOC113230	n/a		3	hypothetical protein LOC113230
IPI00011916	KIAA1324	n/a		13	mabal
IPI00026089	FLJ38482	n/a		5	hypothetical protein FLJ38482
IPI00220444	CYFIP1	n/a		29	cytoplasmic FMR1 interacting protein 1
IPI00022143	IKIP	n/a		6	IKK interacting protein
IPI00015345	GALGT2	n/a		11	UDP-GalNAc:Neu5Acalpha2-3Galbeta-R beta1,4-N-acetylgalactosaminyltransferase
IPI00181853	ENAH	n/a		4	enabled homolog (Drosophila)
IPI00220965	SEC8L1	n/a		17	SEC8-like 1 (S. cerevisiae)
IPI00168451	PIP5K2C	n/a		5	phosphatidylinositol-4-phosphate 5-kinase, type II, gamma

IPI00009145	C13orf1	n/a		5	chromosome 13 open reading frame 1
IPI00008599		n/a		18	Similar to ribosomal protein L4; 60S ribosomal protein L4; homologue of Xenopus ribosomal protein L1 (LOC158345), mRNA
IPI00002134	GCN1L1	n/a		19	GCN1 general control of amino-acid synthesis 1-like 1 (yeast)
IPI00060569	LOC55971	n/a		24	insulin receptor tyrosine kinase substrate
IPI00183627	FLJ39370	n/a		2	hypothetical protein FLJ39370
IPI00001639	RAB1B	n/a		43	RAB1B, member RAS oncogene family
IPI00024816	LOC90580	n/a		2	hypothetical protein BC011833
IPI00012429	FLJ14525	n/a		2	hypothetical protein FLJ14525
IPI00015801	EFHD1	n/a		3	EF hand domain containing 1
IPI00008919	EXOC8	n/a		5	exocyst complex component 8
IPI00159900	GOLGA7	n/a		3	golgi autoantigen, golgin subfamily a, 7
IPI00027785	PIGT	n/a		14	phosphatidylinositol glycan, class T
IPI00003783	ARHGEF16	n/a		3	Rho guanine exchange factor (GEF) 16
IPI00006421	RAB10	n/a		25	RAB10, member RAS oncogene family
IPI00059604	EHD1	n/a		42	EH-domain containing 1
IPI00166571		n/a		3	Similar to Zinc finger protein 20 (Zinc finger protein KOX13) (DKFZp572P0920) (LOC342970), mRNA
IPI00004425	C14orf66	n/a		2	chromosome 14 open reading frame 66
IPI00183768	C9orf77	n/a		3	chromosome 9 open reading frame 77
IPI00220255	PDCD6IP	n/a		11	programmed cell death 6 interacting protein
IPI00024993	PI4K2B	n/a		5	phosphatidylinositol 4-kinase type-II beta
IPI00165596	SEC6L1	n/a		13	SEC6-like 1 (S. cerevisiae)
IPI00026618	PLCD3	n/a		7	phospholipase C, delta 3
IPI00163089		n/a		2	Data not found
IPI00056478	DIRC2	n/a		2	disrupted in renal carcinoma 2
IPI00018398	ALS2CR4	n/a		5	amyotrophic lateral sclerosis 2 (juvenile) chromosome region, candidate 4
IPI00011026	MRPS24	n/a		2	mitochondrial ribosomal protein S24
IPI00023205	DOLPP1	n/a		4	dolichyl pyrophosphate

					phosphatase 1
IPI00032995	DP1L1	n/a		3	polyposis locus protein 1-like 1
IPI00102844	MAP1LC3B	n/a		2	microtubule-associated protein 1 light chain 3 beta
IPI00024292	DDX3X	n/a		7	DEAD (Asp-Glu-Ala-Asp) box polypeptide 3, X-linked
IPI00106966		n/a		6	Similar to Reticulon protein 3 (Neuroendocrine-specific protein-like 2) (NSP-like protein II) (NSPLII) (LOC152905), mRNA
IPI00059263		n/a		14	Transcribed sequence with strong similarity to protein pir:EFHU1 (H.sapiens) EFHU1 translation elongation factor eEF-1 alpha-1 chain - human
IPI00215948	LOC93343	n/a		2	hypothetical protein BC011840
IPI00029236		n/a		17	Data not found
IPI00220952	FLJ14397	n/a		2	hypothetical protein FLJ14397
IPI00006669	FLJ32421	n/a		4	hypothetical protein FLJ32421
IPI00154760	KIAA0090	n/a		40	KIAA0090 protein
IPI00008395	C10orf74	n/a		2	chromosome 10 open reading frame 74
IPI00002483	SEC5L1	n/a		7	SEC5-like 1 (S. cerevisiae)
IPI00004669	DKFZP564 G2022	n/a		13	DKFZP564G2022 protein
IPI00004503	FLJ23375	n/a		3	hypothetical protein FLJ23375
IPI00220785	OCIA	n/a		2	ovarian carcinoma immunoreactive antigen
IPI00006476	FLJ22955	n/a		3	hypothetical protein FLJ22955
IPI00022810		n/a		8	Similar to 60S ribosomal protein L15 (LOC402694), mRNA
IPI00152729	FLJ14466	n/a		4	hypothetical protein FLJ14466
IPI00103059	C10orf9	n/a		5	chromosome 10 open reading frame 9
IPI00045841	SLC35F2	n/a		4	solute carrier family 35, member F2
IPI00002497	FLJ13868	n/a		10	hypothetical protein FLJ13868
IPI00219159	FLJ12875	n/a		2	hypothetical protein FLJ12875
IPI00015713	LOC120224	n/a		2	hypothetical protein BC016153
IPI00026907	LRRC8	n/a		15	leucine rich repeat containing 8
IPI00030907	MGC21416	n/a		4	hypothetical protein

					MGC21416
IPI00215638	TMEM24	n/a		2	transmembrane protein 24
IPI00181841	EAP30	n/a		3	EAP30 subunit of ELL complex
IPI00179597	C10orf42	n/a		4	chromosome 10 open reading frame 42
IPI00012726	USP19	n/a		2	ubiquitin specific protease 19
IPI00016449	DHRSX	n/a		3	dehydrogenase/reductase (SDR family) X-linked
IPI00023557	DKFZp762O076	n/a		3	hypothetical protein DKFZp762O076
IPI00023699	UXS1	n/a		3	UDP-glucuronate decarboxylase 1
IPI00027486	CGI-49	n/a		15	CGI-49 protein
IPI00009941	ANKFY1	n/a		8	ankyrin repeat and FYVE domain containing 1
IPI00013233	SCFD2	n/a		6	sec1 family domain containing 2
IPI00045928	C18orf8	n/a		5	chromosome 18 open reading frame 8
IPI00020455	C6orf143	n/a		6	chromosome 6 open reading frame 143
IPI00044765	FLJ20160	n/a		2	FLJ20160 protein
IPI00000194	C20orf22	n/a		16	chromosome 20 open reading frame 22
IPI00180917	LOC92305	n/a		2	hypothetical protein BC009331
IPI00160428	C2orf33	n/a		5	chromosome 2 open reading frame 33
IPI00009906	ESAM	n/a		2	endothelial cell adhesion molecule
IPI00016801	MYPN	n/a		4	myopalladin
IPI00012268	LOC129642	n/a		3	hypothetical protein BC016005
IPI00007866	KIAA1049	n/a		2	KIAA1049 protein
IPI00064382	FLJ20533	n/a		2	hypothetical protein FLJ20533
IPI00016739	KIAA0599	n/a		2	KIAA0599
IPI00219642	KLP1	n/a		2	K562 cell-derived leucine-zipper-like protein 1
IPI00005264	LRP11	n/a		2	low density lipoprotein receptor-related protein 11
IPI00004310	C1orf27	n/a		7	chromosome 1 open reading frame 27
IPI00006668	C21orf5	n/a		2	chromosome 21 open reading frame 5
IPI00012347	FLJ14681	n/a		4	hypothetical protein FLJ14681
IPI00008726	PEX26	n/a		3	peroxisome biogenesis factor 26
IPI00215898	GTPBP5	n/a		3	GTP binding protein 5 (putative)
IPI00102113	SNX27	n/a		9	sorting nexin family member 27

IPI00178748	TMEM16A	n/a		9	transmembrane protein 16A
IPI00031982	C2orf30	n/a		2	chromosome 2 open reading frame 30
IPI00100282	MGC15397	n/a		3	similar to RIKEN cDNA 5730578N08 gene
IPI00009852	LOC116238	n/a		4	hypothetical protein BC014072
IPI00010349	TMEM16F	n/a		9	transmembrane protein 16F
IPI00003482	FBXL16	n/a		3	F-box and leucine-rich repeat protein 16
IPI00218448	OBSCN	n/a		7	obscurin, cytoskeletal calmodulin and titin-interacting RhoGEF
IPI00061281	FLJ12716	n/a		2	FLJ12716 protein
IPI00030282	C9orf114	n/a		4	chromosome 9 open reading frame 114
IPI00067744	MGC5508	n/a		3	hypothetical protein MGC5508
IPI00216072	MOSPD2	n/a		6	motile sperm domain containing 2
IPI00068506	FLJ20174	n/a		3	hypothetical protein FLJ20174
IPI00009693	LONP	n/a		3	peroxisomal lon protease
IPI00063784	MUC5B	n/a		10	mucin 5, subtype B, tracheobronchial
IPI00219916	DHRS7	n/a		9	dehydrogenase/reductase (SDR family) member 7
IPI00032959	SEC15L2	n/a		6	SEC15-like 2 (S. cerevisiae)
IPI00220472	FLJ14803	n/a		2	hypothetical protein FLJ14803
IPI00032187	ARHGEF17	n/a		4	Rho guanine nucleotide exchange factor (GEF) 17
IPI00025726	FLJ20674	n/a		3	hypothetical protein FLJ20674
IPI00063334	C14orf24	n/a		2	chromosome 14 open reading frame 24
IPI00033075	CHCHD1	n/a		3	coiled-coil-helix-coiled-coil-helix domain containing 1
IPI00025874		n/a		3	Similar to alpha2-glucosyltransferase (LOC144245), mRNA
IPI00005537	C10orf70	n/a		3	chromosome 10 open reading frame 70
IPI00184972		n/a		9	Similar to ribosomal protein S3a; 40S ribosomal protein S3a; v-fos transformation effector protein 1 (LOC146053), mRNA
IPI00060523	DHRS8	n/a		2	dehydrogenase/reductase (SDR family) member 8
IPI00151710	MGC31963	n/a		3	kidney predominant protein NCU-G1
IPI00002128	USP35	n/a		2	ubiquitin specific protease 35
IPI00216123		n/a		4	Data not found
IPI00008861	FLJ90724	n/a		2	hypothetical protein

					FLJ90724
IPI00005921	STK11IP	n/a		8	serine/threonine kinase 11 interacting protein
IPI00007118	UGDH	n/a		2	UDP-glucose dehydrogenase
IPI00066382	FLJ12436	n/a		2	hypothetical protein FLJ12436
IPI00019004	TEBP	n/a		2	unactive progesterone receptor, 23 kD
IPI00102885	FLJ32867	n/a		3	FLJ32867 protein
IPI00031458	KIAA1919	n/a		2	KIAA1919
IPI00023703	OTUB1	n/a		4	OTU domain, ubiquitin aldehyde binding 1
IPI00008475	BRI3BP	n/a		4	BRI3 binding protein
IPI00218342	CGI-07	n/a		3	CGI-07 protein
IPI00181734	hIAN6	n/a		3	human immune associated nucleotide 6
IPI00100715	SYTL2	n/a		14	synaptotagmin-like 2
IPI00019350	POF1B	n/a		3	premature ovarian failure, 1B
IPI00220055	COMTD1	n/a		2	catechol-O-methyltransferase domain containing 1
IPI00107698	SMAP-5	n/a		6	golgi membrane protein SB140
IPI00020228	IGSF4C	n/a		2	immunoglobulin superfamily, member 4C
IPI00023704	PERLD1	n/a		3	perl-like domain containing 1
IPI00015952		n/a		3	Data not found
IPI00178018	MGC10084	n/a		3	hypothetical protein MGC10084
IPI00217418	VRK1	n/a		2	vaccinia related kinase 1
IPI00028946	ATAD3A	n/a		9	ATPase family, AAA domain containing 3A
IPI00185465		n/a		5	Data not found
IPI00021985		n/a		7	Data not found
IPI00220251	CASKIN2	n/a		10	CASK interacting protein 2
IPI00067804	DOCK9	n/a		9	dedicator of cytokinesis 9
IPI00099055	ShrmL	n/a		2	Shroom-related protein
IPI00031697	FLJ40432	n/a		3	hypothetical protein FLJ40432
IPI00169283		n/a		15	Transcribed sequence with strong similarity to protein pdb:1I4D (H.sapiens) D Chain D, Crystal Structure Analysis Of Rac1-Gdp Complexed With Arfaptin
IPI00220071	FZR1	n/a		3	fizzy/cell division cycle 20 related 1 (Drosophila)
IPI00016007	OSBPL10	n/a		3	oxysterol binding protein-like 10
IPI00218014	TIMM50	n/a		6	translocase of inner mitochondrial membrane 50 homolog (yeast)
IPI00184824	ATP6V0D2	n/a		2	ATPase, H+ transporting, lysosomal 38kDa, V0 subunit

					d isoform 2
IPI00009329	ILVBL	n/a		31	ilvB (bacterial acetolactate synthase)-like
IPI00011631	UBXD2	n/a		7	UBX domain containing 2
IPI00018274	MLPH	n/a		10	melanophilin
IPI00181130	DKFZp564 K142	n/a		6	implantation-associated protein
IPI00015608	DOCK6	n/a		5	dedicator of cytokinesis 6
IPI00220063	LOC83693	n/a		2	steroid dehydrogenase-like
IPI00219575	MGC11102	n/a		2	hypothetical protein MGC11102
IPI00011592	TA-LRRP	n/a		3	T-cell activation leucine repeat-rich protein
IPI00024478	PYCR2	n/a		2	pyrroline-5-carboxylate reductase family, member 2
IPI00004968	SVH	n/a		3	SVH protein
IPI00160775	FLJ10587	n/a		3	hypothetical protein FLJ10587
IPI00168379	GA17	n/a		4	dendritic cell protein
IPI00221368	CDK5RAP3	n/a		8	CDK5 regulatory subunit associated protein 3
IPI00009633	KIAA0825	n/a		2	KIAA0825 protein
IPI00004451	MFN1	n/a		3	mitofusin 1
IPI00022002	AAAS	n/a		6	achalasia, adrenocortical insufficiency, alacrimia (Allgrove, triple-A)
IPI00163897	SHANK2	n/a		4	SH3 and multiple ankyrin repeat domains 2
IPI00010483	RUNDC1	n/a		5	RUN domain containing 1
IPI00021440	ACBD5	n/a		34	acyl-Coenzyme A binding domain containing 5
IPI00163509	ACTN4	n/a		5	actinin, alpha 4
IPI00216470	C17orf28	n/a		37	chromosome 17 open reading frame 28
IPI00009439	C19orf27	n/a		4	chromosome 19 open reading frame 27
IPI00022353	C20orf24	n/a		2	chromosome 20 open reading frame 24
IPI00103397	C22orf2	n/a		7	chromosome 22 open reading frame 2
IPI00106550	C2orf4	n/a		7	chromosome 2 open reading frame 4
IPI00024305	C6orf89	n/a		20	chromosome 6 open reading frame 89
IPI00011238	C9orf75	n/a		17	chromosome 9 open reading frame 75
IPI00023137	CA12	n/a		22	carbonic anhydrase XII
IPI00218782	CRR9	n/a		9	cisplatin resistance related protein CRR9p
IPI00006957	DNAJA3	n/a		35	DnaJ (Hsp40) homolog, subfamily A, member 3
IPI00220571	DNAJC10	n/a		12	DnaJ (Hsp40) homolog, subfamily C, member 10
IPI00028491	DOCK7	n/a		26	dedicator of cytokinesis 7

IPI00013393	E2IG5	n/a		35	growth and transformation-dependent protein
IPI00216143	FLJ11029	n/a		7	hypothetical protein FLJ11029
IPI00045764	FLJ11273	n/a		23	hypothetical protein FLJ11273
IPI00009544	FLJ11336	n/a		24	hypothetical protein FLJ11336
IPI00180765	FLJ12443	n/a		31	hypothetical protein FLJ12443
IPI00026519	FLJ12806	n/a		7	hypothetical protein FLJ12806
IPI00171003	FLJ14957	n/a		13	hypothetical protein FLJ14957
IPI00006093	FLJ20297	n/a		4	hypothetical protein FLJ20297
IPI00219204	FLJ22390	n/a		31	hypothetical protein FLJ22390
IPI00021750	FLJ23091	n/a		15	putative NFkB activating protein 373
IPI00028005	FLJ25351	n/a		25	hypothetical protein FLJ25351
IPI00152007	FLJ25477	n/a		4	hypothetical protein FLJ25477
IPI00005155	HSPC121	n/a		22	butyrate-induced transcript 1
IPI00012851	KIAA1463	n/a		36	KIAA1463 protein
IPI00013897	LENG4	n/a		4	leukocyte receptor cluster (LRC) member 4
IPI00024157	LISCH7	n/a		23	liver-specific bHLH-Zip transcription factor
IPI00166051	LOC134147	n/a		2	hypothetical protein BC001573
IPI00060107	LOC159090	n/a		32	similar to hypothetical protein MGC17347
IPI00105827	LOC221955	n/a		24	KCCR13L
IPI00184161	LOC283820	n/a		27	hypothetical protein LOC283820
IPI00002236	LOC375759	n/a		25	hypothetical protein LOC375759
IPI00005731	LOC400451	n/a		13	hypothetical gene supported by AK075564; BC060873
IPI00180102	LZTS2	n/a		22	leucine zipper, putative tumor suppressor 2
IPI00020491	MAP4K4	n/a		38	mitogen-activated protein kinase kinase kinase kinase 4
IPI00021532	MARK3	n/a		39	MAP/microtubule affinity-regulating kinase 3
IPI00002535	MGC3222	n/a		5	hypothetical protein MGC3222
IPI00019746	MGC33867	n/a		22	hypothetical protein MGC33867
IPI00006084	MGC4368	n/a		33	hypothetical protein MGC4368
IPI00022543	MGC5352	n/a		23	hypothetical protein MGC5352

IPI00005578	NICE-3	n/a		31	NICE-3 protein
IPI00011445	NSE2	n/a		6	breast cancer membrane protein 101
IPI00160421	NT5C3	n/a		30	5'-nucleotidase, cytosolic III
IPI00020510	PALM2	n/a		33	paralemmin 2
IPI00026138	PCNXL3	n/a		18	pecanex-like 3 (Drosophila)
IPI00006006	PDCD10	n/a		10	programmed cell death 10
IPI00031822	PDE8A	n/a		4	phosphodiesterase 8A
IPI00149529	PEX11G	n/a		2	peroxisomal biogenesis factor 11 gamma
IPI00002507	PKD1-like	n/a		7	polycystic kidney disease 1-like
IPI00022778	PPP1CA	n/a		14	protein phosphatase 1, catalytic subunit, alpha isoform
IPI00019230	PPP2CB	n/a		15	protein phosphatase 2 (formerly 2A), catalytic subunit, beta isoform
IPI00008918	PQLC1	n/a		39	PQ loop repeat containing 1
IPI00022542	QSCN6	n/a		8	quiescin Q6
IPI00031008	RBAF600	n/a		16	retinoblastoma-associated factor 600
IPI00027078	REPS1	n/a		17	RALBP1 associated Eps domain containing 1
IPI00217954	RPL36A	n/a		9	ribosomal protein L36a
IPI00031493	S100A16	n/a		11	S100 calcium binding protein A16
IPI00008258	SELT	n/a		33	selenoprotein T
IPI00013302	SKD3	n/a		3	suppressor of potassium transport defect 3
IPI00019146	TOR2A	n/a		8	torsin family 2, member A
IPI00010104	TRIM25	n/a		29	tripartite motif-containing 25
IPI00023730	UNQ1912	n/a		39	HGS_RE408
IPI00008616	UNQ501	n/a		15	MBC3205
IPI00025818	USP32	n/a		13	ubiquitin specific protease 32
IPI00017617	VMP1	n/a		26	likely ortholog of rat vacuole membrane protein 1
IPI00179103	VPS29	n/a		7	vacuolar protein sorting 29 (yeast)
IPI00030116	VPS4A	n/a		37	vacuolar protein sorting 4A (yeast)
IPI00219826		n/a		22	MRNA; cDNA DKFZp686G03142 (from clone DKFZp686G03142)
IPI00014236		n/a		9	Data not found
IPI00023879		n/a		20	Data not found
IPI00002961	FASN	non-mem		68	fatty acid synthase
IPI00008260	HBXIP	non-mem		6	hepatitis B virus x interacting protein
IPI00061779	OGDH	non-mem		14	oxoglutarate (alpha-ketoglutarate) dehydrogenase (lipoamide)
IPI00001726	RPL30	non-mem		7	ribosomal protein L30
IPI00152785	CRIP2	non-mem		12	cysteine-rich protein 2

IPI00107555	ECT2	non-mem		5	epithelial cell transforming sequence 2 oncogene
IPI00010037	RPLP2	non-mem		15	ribosomal protein, large P2
IPI00181890	KIAA1007	non-mem		5	KIAA1007 protein
IPI00015180	RAB22A	non-mem		17	RAB22A, member RAS oncogene family
IPI00013234	UBE1	non-mem		5	ubiquitin-activating enzyme E1 (A1S9T and BN75 temperature sensitivity complementing)
IPI00027860	UREB1	non-mem		5	upstream regulatory element binding protein 1
IPI00170934	SOD1	non-mem		3	superoxide dismutase 1, soluble (amyotrophic lateral sclerosis 1 (adult))
IPI00017800	S100A11	non-mem		13	S100 calcium binding protein A11 (calgizzarin)
IPI00183933	RPS3	non-mem		19	ribosomal protein S3
IPI00013744	ARPC5L	non-mem		3	actin related protein 2/3 complex, subunit 5-like
IPI00217466	CHP	non-mem		18	calcium binding protein P22
IPI00092641	ATM	non-mem		3	ataxia telangiectasia mutated (includes complementation groups A, C and D)
IPI00031420	AGR2	non-mem		21	anterior gradient 2 homolog (Xenopus laevis)
IPI00003765	UBA52	non-mem		30	ubiquitin A-52 residue ribosomal protein fusion product 1
IPI00153023	CSRP1	non-mem		7	cysteine and glycine-rich protein 1
IPI00179487	RPL38	non-mem		6	ribosomal protein L38
IPI00221244	CEP2	non-mem		4	centrosomal protein 2
IPI00027192	EIF5A	non-mem		9	eukaryotic translation initiation factor 5A
IPI00016910	YWHAB	non-mem		34	tyrosine 3-monooxygenase/tryptophan 5-monooxygenase activation protein, beta polypeptide
IPI00031410	PRSS15	non-mem		3	protease, serine, 15
IPI00016197	RPLP0	non-mem		13	ribosomal protein, large, P0
IPI00013146	ANXA5	non-mem		18	annexin A5
IPI00014361	PRDX2	non-mem		6	peroxiredoxin 2
IPI00179453	CAPZA1	non-mem		6	capping protein (actin filament) muscle Z-line, alpha 1
IPI00015029	ARPC3	non-mem		4	actin related protein 2/3 complex, subunit 3, 21kDa
IPI00141318	B3GALT4	non-mem		12	UDP-Gal:betaGlcNAc beta 1,3-galactosyltransferase, polypeptide 4
IPI00005614	RAB21	non-mem		16	RAB21, member RAS oncogene family
IPI00003384	PFN1	non-mem		10	profilin 1
IPI00220291	BANF1	non-mem		8	barrier to autointegration

					factor 1
IPI00011651	RAB31	non-mem		6	RAB31, member RAS oncogene family
IPI00025770	ARPC1B	non-mem		5	actin related protein 2/3 complex, subunit 1B, 41kDa
IPI00004671	RPL26	non-mem		13	ribosomal protein L26
IPI00010187	ATP6V1D	non-mem		5	ATPase, H+ transporting, lysosomal 34kDa, V1 subunit D
IPI00103541	PRDX1	non-mem		11	peroxiredoxin 1
IPI00030702	C15orf24	non-mem		9	chromosome 15 open reading frame 24
IPI00022953	ANXA4	non-mem		13	annexin A4
IPI00151170	S100A14	non-mem		15	S100 calcium binding protein A14
IPI00187043	PHB	non-mem		16	prohibitin
IPI00060314	CLIC3	non-mem		3	chloride intracellular channel 3
IPI00000010	LITAF	non-mem		4	lipopolysaccharide-induced TNF factor
IPI00020226	RPL34	non-mem		2	ribosomal protein L34
IPI00220219	ACTR3	non-mem		15	ARP3 actin-related protein 3 homolog (yeast)
IPI00019209	CFL1	non-mem		30	cofilin 1 (non-muscle)
IPI00216292	DSTN	non-mem		8	destrin (actin depolymerizing factor)
IPI00070943	DPM1	non-mem		19	dolichyl-phosphate mannosyltransferase polypeptide 1, catalytic subunit
IPI00025100	BCAS1	non-mem		12	breast carcinoma amplified sequence 1
IPI00182304	TXNDC7	non-mem		18	thioredoxin domain containing 7 (protein disulfide isomerase)
IPI00219424	ARPC5	non-mem		2	actin related protein 2/3 complex, subunit 5, 16kDa
IPI00221223	ATP5I	non-mem		5	ATP synthase, H+ transporting, mitochondrial F0 complex, subunit e
IPI00017529	YARS	non-mem		26	tyrosyl-tRNA synthetase
IPI00018415	MPDZ	non-mem		3	multiple PDZ domain protein
IPI00010237	RPS11	non-mem		12	ribosomal protein S11
IPI00171819	PRDX5	non-mem		5	peroxiredoxin 5
IPI00219524	POLD1	non-mem		3	polymerase (DNA directed), delta 1, catalytic subunit 125kDa
IPI00021831	PPIA	non-mem		21	peptidylprolyl isomerase A (cyclophilin A)
IPI00218606	S100A10	non-mem		13	S100 calcium binding protein A10 (annexin II ligand, calpactin I, light polypeptide (p11))
IPI00217751	VASP	non-mem		10	vasodilator-stimulated phosphoprotein

IPI00099650	PDLIM1	non-mem		3	PDZ and LIM domain 1 (elfin)
IPI00102685	RPS15	non-mem		7	ribosomal protein S15
IPI00013623	ZAP128	non-mem		4	peroxisomal long-chain acyl-coA thioesterase
IPI00021594	PTP4A1	non-mem		9	protein tyrosine phosphatase type IVA, member 1
IPI00164586	HSPE1	non-mem		9	heat shock 10kDa protein 1 (chaperonin 10)
IPI00170814	CDC37	non-mem		6	CDC37 cell division cycle 37 homolog (S. cerevisiae)
IPI00023035	NEB	non-mem		3	nebulin
IPI00012912	RPS13	non-mem		11	ribosomal protein S13
IPI00215921	KRT9	non-mem		11	keratin 9 (epidermolytic palmoplantar keratoderma)
IPI00006713	RPS17	non-mem		8	ribosomal protein S17
IPI00179586	HIP-55	non-mem		4	src homology 3 domain-containing protein HIP-55
IPI00107347	RPL28	non-mem		12	ribosomal protein L28
IPI00000581	HSD17B12	non-mem		28	hydroxysteroid (17-beta) dehydrogenase 12
IPI00163403	RPL10A	non-mem		15	ribosomal protein L10a
IPI00004962	LDHA	non-mem		12	lactate dehydrogenase A
IPI00100460	GNAQ	non-mem		21	guanine nucleotide binding protein (G protein), q polypeptide
IPI00103599	RPL8	non-mem		9	ribosomal protein L8
IPI00101049	CCT4	non-mem		5	chaperonin containing TCP1, subunit 4 (delta)
IPI00168482	RAI14	non-mem		6	retinoic acid induced 14
IPI00027728	RPL13	non-mem		9	ribosomal protein L13
IPI00101135	HINT1	non-mem		3	histidine triad nucleotide binding protein 1
IPI00024726	KRT18	non-mem		34	keratin 18
IPI00009829	CAPZA2	non-mem		3	capping protein (actin filament) muscle Z-line, alpha 2
IPI00011090	NIPSNAP1	non-mem		6	nipsnap homolog 1 (C. elegans)
IPI00178352	RPS5	non-mem		11	ribosomal protein S5
IPI00030536	RPLP1	non-mem		6	ribosomal protein, large, P1
IPI00022033	KRT1	non-mem		18	keratin 1 (epidermolytic hyperkeratosis)
IPI00026314	TUBB2	non-mem		46	tubulin, beta, 2
IPI00103242	FARP1	non-mem		32	FERM, RhoGEF (ARHGEF) and pleckstrin domain protein 1 (chondrocyte-derived)
IPI00182852	SH3BP4	non-mem		13	SH3-domain binding protein 4
IPI00163849	PAFAH1B3	non-mem		4	platelet-activating factor acetylhydrolase, isoform Ib, gamma subunit 29kDa
IPI00216654	LAMB1	non-mem		2	laminin, beta 1
IPI00077853	PPP1CC	non-mem		18	protein phosphatase 1,

					catalytic subunit, gamma isoform
IPI00033349	TXN	non-mem		3	thioredoxin
IPI00152662	RPL35	non-mem		10	ribosomal protein L35
IPI00100024	C19orf21	non-mem		25	chromosome 19 open reading frame 21
IPI00009797	PRDX6	non-mem		3	peroxiredoxin 6
IPI00013369	PSMC1	non-mem		4	proteasome (prosome, macropain) 26S subunit, ATPase, 1
IPI00027011	PCBP2	non-mem		7	poly(rC) binding protein 2
IPI00028387	SERPINH1	non-mem		21	serine (or cysteine) proteinase inhibitor, clade H (heat shock protein 47), member 1, (collagen binding protein 1)
IPI00169324	PACSIN2	non-mem		8	protein kinase C and casein kinase substrate in neurons 2
IPI00176427	RPL36	non-mem		4	ribosomal protein L36
IPI00218891	SSBP1	non-mem		4	single-stranded DNA binding protein 1
IPI00028275	MGC4171	non-mem		4	hypothetical protein MGC4171
IPI00161009	HIST2H2AB	non-mem		7	histone 2, H2ab
IPI00010235	LRRC16	non-mem		2	leucine rich repeat containing 16
IPI00185643	C6orf49	non-mem		3	chromosome 6 open reading frame 49
IPI00150757	ARPC2	non-mem		21	actin related protein 2/3 complex, subunit 2, 34kDa
IPI00028338	EEF1A2	non-mem		22	eukaryotic translation elongation factor 1 alpha 2
IPI00017598	SQRDL	non-mem		7	sulfide quinone reductase-like (yeast)
IPI00217234	TPT1	non-mem		3	tumor protein, translationally-controlled 1
IPI00031030	PTP4A2	non-mem		5	protein tyrosine phosphatase type IVA, member 2
IPI00004278	YWHAH	non-mem		15	tyrosine 3-monooxygenase/tryptophan 5-monooxygenase activation protein, eta polypeptide
IPI00007144	RPL12	non-mem		8	ribosomal protein L12
IPI00052815	KRT19	non-mem		35	keratin 19
IPI00166833	TPI1	non-mem		6	triosephosphate isomerase 1
IPI00217918	RPL19	non-mem		9	ribosomal protein L19
IPI00019640	TUFM	non-mem		11	Tu translation elongation factor, mitochondrial
IPI00182027	NME1	non-mem		6	non-metastatic cells 1, protein (NM23A) expressed in
IPI00013712	PHPT1	non-mem		3	phosphohistidine phosphatase 1
IPI00004533	BLVRB	non-mem		6	biliverdin reductase B (flavin

					reductase (NADPH))
IPI00183643	SDF2	non-mem		6	stromal cell-derived factor 2
IPI00013010	ARHGEF11	non-mem		2	Rho guanine nucleotide exchange factor (GEF) 11
IPI00166317	RAB3-GAP150	non-mem		2	rab3 GTPase-activating protein, non-catalytic subunit (150kD)
IPI00151594	CCT2	non-mem		7	chaperonin containing TCP1, subunit 2 (beta)
IPI00028472	RPS6	non-mem		7	ribosomal protein S6
IPI00029012	CCT5	non-mem		7	chaperonin containing TCP1, subunit 5 (epsilon)
IPI00003927	RPS19	non-mem		11	ribosomal protein S19
IPI00103516	KIAA0174	non-mem		6	KIAA0174 gene product
IPI00216408	PAI-RBP1	non-mem		14	PAI-1 mRNA-binding protein
IPI00152881	CD2AP	non-mem		6	CD2-associated protein
IPI00021983	RPL18	non-mem		16	ribosomal protein L18
IPI00021076	RPS15A	non-mem		9	ribosomal protein S15a
IPI00011644	STAU	non-mem		11	staufen, RNA binding protein (Drosophila)
IPI00156651	CCT8	non-mem		5	chaperonin containing TCP1, subunit 8 (theta)
IPI00020407	G22P1	non-mem		8	thyroid autoantigen 70kDa (Ku antigen)
IPI00182938	ATP6V1H	non-mem		6	ATPase, H+ transporting, lysosomal 50/57kDa, V1 subunit H
IPI00002965	LDHB	non-mem		2	lactate dehydrogenase B
IPI00007634	RPS14	non-mem		7	ribosomal protein S14
IPI00008708	ITGB4BP	non-mem		5	integrin beta 4 binding protein
IPI00029337	FAM3C	non-mem		6	family with sequence similarity 3, member C
IPI00185371	PKM2	non-mem		40	pyruvate kinase, muscle
IPI00156774	SFN	non-mem		10	stratifin
IPI00009542	NDUFA9	non-mem		9	NADH dehydrogenase (ubiquinone) 1 alpha subcomplex, 9, 39kDa
IPI00162109	DBN1	non-mem		15	drebrin 1
IPI00176903	LOC54499	non-mem		4	putative membrane protein
IPI00024650	VBP1	non-mem		2	von Hippel-Lindau binding protein 1
IPI00215918	GSDML	non-mem		7	gasdermin-like
IPI00179059	FKBP8	non-mem		7	FK506 binding protein 8, 38kDa
IPI00219526	CCT7	non-mem		7	chaperonin containing TCP1, subunit 7 (eta)
IPI00166640	PTPN1	non-mem		28	protein tyrosine phosphatase, non-receptor type 1
IPI00032971	CDC2	non-mem		4	cell division cycle 2, G1 to S and G2 to M
IPI00217941	DKFZP564O123	non-mem		5	DKFZP564O123 protein

IPI00180783	FLJ10808	non-mem		3	hypothetical protein FLJ10808
IPI00023174	MAPRE1	non-mem		5	microtubule-associated protein, RP/EB family, member 1
IPI00003648	RFC4	non-mem		3	replication factor C (activator 1) 4, 37kDa
IPI00220645	RPS16	non-mem		12	ribosomal protein S16
IPI00005126	ACSL3	non-mem		30	acyl-CoA synthetase long-chain family member 3
IPI00073111	ENO1	non-mem		20	enolase 1, (alpha)
IPI00171163	FLJ20084	non-mem		7	hypothetical protein FLJ20084
IPI00029737	SF3B3	non-mem		2	splicing factor 3b, subunit 3, 130kDa
IPI00171455	KIF14	non-mem		3	kinesin family member 14
IPI00001780	RPL9	non-mem		6	ribosomal protein L9
IPI00107357	ANXA1	non-mem		8	annexin A1
IPI00181175	PDCD6	non-mem		4	programmed cell death 6
IPI00218343	TBC1D10	non-mem		6	TBC1 domain family, member 10
IPI00218673	MRPS36	non-mem		2	mitochondrial ribosomal protein S36
IPI00167639	TXNDC5	non-mem		4	thioredoxin domain containing 5
IPI00011241	C9orf58	non-mem		3	chromosome 9 open reading frame 58
IPI00219314	PARK7	non-mem		5	Parkinson disease (autosomal recessive, early onset) 7
IPI00218207	AARS	non-mem		2	alanyl-tRNA synthetase
IPI00025278	DCXR	non-mem		5	dicarbonyl/L-xylulose reductase
IPI00215998	SLC9A3R1	non-mem		32	solute carrier family 9 (sodium/hydrogen exchanger), isoform 3 regulator 1
IPI00009963	DC13	non-mem		2	DC13 protein
IPI00185567	RPS20	non-mem		5	ribosomal protein S20
IPI00044369	SNRPD1	non-mem		2	small nuclear ribonucleoprotein D1 polypeptide 16kDa
IPI00020030	SRC	non-mem		10	v-src sarcoma (Schmidt-Ruppin A-2) viral oncogene homolog (avian)
IPI00016849	DDT	non-mem		2	D-dopachrome tautomerase
IPI00012201	RPS4X	non-mem		20	ribosomal protein S4, X-linked
IPI00012197	UACA	non-mem		3	uveal autoantigen with coiled-coil domains and ankyrin repeats
IPI00217822	JAK1	non-mem		8	Janus kinase 1 (a protein tyrosine kinase)
IPI00023122	JWA	non-mem		5	cytoskeleton related vitamin A responsive protein
IPI00011603		non-mem		8	Hypothetical protein

					MGC3260, mRNA (cDNA clone IMAGE:6269444), partial cds
IPI00220366	CTNND2	non-mem		7	catenin (cadherin-associated protein), delta 2 (neural plakophilin-related arm-repeat protein)
IPI00012475	SMCR7	non-mem		4	Smith-Magenis syndrome chromosome region, candidate 7
IPI00151743	RPL11	non-mem		5	ribosomal protein L11
IPI00008524	PBXIP1	non-mem		7	pre-B-cell leukemia transcription factor interacting protein 1
IPI00025160	ANXA6	non-mem		57	annexin A6
IPI00220526	RPL23	non-mem		10	ribosomal protein L23
IPI00020513	CCT3	non-mem		9	chaperonin containing TCP1, subunit 3 (gamma)
IPI00181783	DNAJB11	non-mem		5	DnaJ (Hsp40) homolog, subfamily B, member 11
IPI00029054	IFRG15	non-mem		14	IFRG15 protein
IPI00008085	C9orf87	non-mem		5	chromosome 9 open reading frame 87
IPI00019862	CENPE	non-mem		2	centromere protein E, 312kDa
IPI00029787	CSNK2A1	non-mem		6	casein kinase 2, alpha 1 polypeptide
IPI00216793	CTNNB1	non-mem		63	catenin (cadherin-associated protein), beta 1, 88kDa
IPI00106674	ACTN1	non-mem		65	actinin, alpha 1
IPI00183400	MARK2	non-mem		17	MAP/microtubule affinity-regulating kinase 2
IPI00220540	RPL31	non-mem		9	ribosomal protein L31
IPI00023531	RPS24	non-mem		6	ribosomal protein S24
IPI00029813	BC-2	non-mem		4	putative breast adenocarcinoma marker (32kD)
IPI00044299	MYO1C	non-mem		99	myosin IC
IPI00171459	DKFZP434 P1750	non-mem		5	DKFZP434P1750 protein
IPI00031571	PSME1	non-mem		2	proteasome (prosome, macropain) activator subunit 1 (PA28 alpha)
IPI00030255	EIF4A1	non-mem		11	eukaryotic translation initiation factor 4A, isoform 1
IPI00023530	PLS1	non-mem		10	plastin 1 (I isoform)
IPI00001933	RAC1	non-mem		19	ras-related C3 botulinum toxin substrate 1 (rho family, small GTP binding protein Rac1)
IPI00219591	CORO1A	non-mem		9	coronin, actin binding protein, 1A
IPI00216760	GLO1	non-mem		3	glyoxalase I
IPI00074330	MGRN1	non-mem		5	mahogunin, ring finger 1

IPI00180475	MSF	non-mem		16	MLL septin-like fusion
IPI00007133	YES1	non-mem		24	v-yes-1 Yamaguchi sarcoma viral oncogene homolog 1
IPI00219335	DDEF2	non-mem		6	development and differentiation enhancing factor 2
IPI00166036	PRKRA	non-mem		3	protein kinase, interferon-inducible double stranded RNA dependent activator
IPI00168635	CDC10	non-mem		5	CDC10 cell division cycle 10 homolog (S. cerevisiae)
IPI00220991	MRPS23	non-mem		5	mitochondrial ribosomal protein S23
IPI00215919	VPS35	non-mem		12	vacuolar protein sorting 35 (yeast)
IPI00012093	SMPDL3B	non-mem		12	sphingomyelin phosphodiesterase, acid-like 3B
IPI00100920	RHOD	non-mem		4	ras homolog gene family, member D
IPI00001710	RAB32	non-mem		6	RAB32, member RAS oncogene family
IPI00071696	CDA08	non-mem		11	T-cell immunomodulatory protein
IPI00101062	CTSD	non-mem		19	cathepsin D (lysosomal aspartyl protease)
IPI00220115	ASPM	non-mem		5	asp (abnormal spindle)-like, microcephaly associated (Drosophila)
IPI00102244	MRPS2	non-mem		2	mitochondrial ribosomal protein S2
IPI00152101	PYCR1	non-mem		5	pyrroline-5-carboxylate reductase 1
IPI00166467	RPL37A	non-mem		4	ribosomal protein L37a
IPI00217967	NDP52	non-mem		8	nuclear domain 10 protein
IPI00152332	XRCC5	non-mem		18	X-ray repair complementing defective repair in Chinese hamster cells 5 (double-strand-break rejoining; Ku autoantigen, 80kDa)
IPI00217537	SHOC2	non-mem		7	soc-2 suppressor of clear homolog (C. elegans)
IPI00101923	ARHGAP1	non-mem		5	Rho GTPase activating protein 1
IPI00010212	CAT	non-mem		6	catalase
IPI00157790	ETFA	non-mem		5	electron-transfer-flavoprotein, alpha polypeptide (glutaric aciduria II)
IPI00032087	COBL	non-mem		11	cordon-bleu homolog (mouse)
IPI00010251	GRB7	non-mem		4	growth factor receptor-bound protein 7
IPI00008288	PRDX3	non-mem		6	peroxiredoxin 3
IPI00022608	KIAA0103	non-mem		10	KIAA0103

IPI00072232	TAX1BP3	non-mem		2	Tax1 (human T-cell leukemia virus type I) binding protein 3
IPI00022434	PSMC5	non-mem		3	proteasome (prosome, macropain) 26S subunit, ATPase, 5
IPI00017976	TBL2	non-mem		18	transducin (beta)-like 2
IPI00176629	TRIP12	non-mem		2	thyroid hormone receptor interactor 12
IPI00103873	FLJ11301	non-mem		10	hypothetical protein FLJ11301
IPI00023186	PGD	non-mem		4	phosphogluconate dehydrogenase
IPI00217622	CS	non-mem		12	citrate synthase
IPI00011953	LYPLA2	non-mem		2	lysophospholipase II
IPI00030179	C14orf156	non-mem		3	chromosome 14 open reading frame 156
IPI00216933	HBA2	non-mem		2	hemoglobin, alpha 2
IPI00219283	PRO1855	non-mem		12	hypothetical protein PRO1855
IPI00168502	RPL7A	non-mem		18	ribosomal protein L7a
IPI00006674	MRPL50	non-mem		2	mitochondrial ribosomal protein L50
IPI00027447	CSTB	non-mem		2	cystatin B (stefin B)
IPI00216312	NOC4	non-mem		6	neighbor of COX4
IPI00022710	RPL14	non-mem		13	ribosomal protein L14
IPI00175227	SHMT2	non-mem		9	serine hydroxymethyltransferase 2 (mitochondrial)
IPI00220502	C6orf109	non-mem		3	chromosome 6 open reading frame 109
IPI00219835	Septin8	non-mem		7	septin 8
IPI00218922	ABR	non-mem		8	active BCR-related gene
IPI00029015	F5	non-mem		3	coagulation factor V (proaccelerin, labile factor)
IPI00010469	PLCD1	non-mem		4	phospholipase C, delta 1
IPI00028400	ALDH2	non-mem		8	aldehyde dehydrogenase 2 family (mitochondrial)
IPI00186569	CCM2	non-mem		7	cerebral cavernous malformation 2
IPI00027762	DAP3	non-mem		5	death associated protein 3
IPI00025190	MVP	non-mem		5	major vault protein
IPI00000897	PRKCSH	non-mem		10	protein kinase C substrate 80K-H
IPI00218476	DKFZP761 D0211	non-mem		19	hypothetical protein DKFZp761D0211
IPI00074683	PTPN2	non-mem		5	protein tyrosine phosphatase, non-receptor type 2
IPI00169434	DHRS2	non-mem		3	dehydrogenase/reductase (SDR family) member 2
IPI00024466	PACSIN3	non-mem		14	protein kinase C and casein kinase substrate in neurons 3
IPI00152967	GANAB	non-mem		34	glucosidase, alpha; neutral AB

IPI00102069	HSPCA	non-mem		56	heat shock 90kDa protein 1, alpha
IPI00020884	PCBP1	non-mem		3	poly(rC) binding protein 1
IPI00180124	RAB23	non-mem		2	RAB23, member RAS oncogene family
IPI00220151	RP2	non-mem		3	retinitis pigmentosa 2 (X-linked recessive)
IPI00003515	NAP1L1	non-mem		5	nucleosome assembly protein 1-like 1
IPI00064039	NSF	non-mem		30	N-ethylmaleimide-sensitive factor
IPI00166971	PCYOX1	non-mem		7	prenylcysteine oxidase 1
IPI00101766	PPFIA2	non-mem		5	protein tyrosine phosphatase, receptor type, f polypeptide (PTPRF), interacting protein (liprin), alpha 2
IPI00163644	HADHA	non-mem		15	hydroxyacyl-Coenzyme A dehydrogenase/3-ketoacyl-Coenzyme A thiolase/enoyl-Coenzyme A hydratase (trifunctional protein), alpha subunit
IPI00163749	MRPL3	non-mem		4	mitochondrial ribosomal protein L3
IPI00218564	RPS8	non-mem		6	ribosomal protein S8
IPI00013452	HSD17B4	non-mem		8	hydroxysteroid (17-beta) dehydrogenase 4
IPI00179581	FYCO1	non-mem		3	FYVE and coiled-coil domain containing 1
IPI00015974	STXBP2	non-mem		7	syntaxin binding protein 2
IPI00165254	ATIC	non-mem		7	5-aminoimidazole-4-carboxamide ribonucleotide formyltransferase/IMP cyclohydrolase
IPI00164688	PRKDC	non-mem		12	protein kinase, DNA-activated, catalytic polypeptide
IPI00217242	ANXA3	non-mem		5	annexin A3
IPI00024585	Septin11	non-mem		6	septin 11
IPI00044762	BCKDK	non-mem		2	branched chain alpha-ketoacid dehydrogenase kinase
IPI00180643	SH120	non-mem		5	putative G-protein coupled receptor
IPI00220603	ACTR2	non-mem		11	ARP2 actin-related protein 2 homolog (yeast)
IPI00217715	LAP1B	non-mem		5	lamina-associated polypeptide 1B
IPI00007765	LLGL2	non-mem		43	lethal giant larvae homolog 2 (Drosophila)
IPI00043307	MYO18A	non-mem		14	myosin XVIIIA
IPI00217347	NF1	non-mem		5	neurofibromin 1 (neurofibromatosis, von Recklinghausen disease, Watson disease)

IPI00163951	OAT	non-mem		3	ornithine aminotransferase (gyrate atrophy)
IPI00010746	ALDOC	non-mem		5	aldolase C, fructose-bisphosphate
IPI00220741	ITCH	non-mem		12	itchy homolog E3 ubiquitin protein ligase (mouse)
IPI00019427	WBSCR21	non-mem		5	Williams Beuren syndrome chromosome region 21
IPI00005089	NME2	non-mem		9	non-metastatic cells 2, protein (NM23B) expressed in
IPI00032495	GNS	non-mem		6	glucosamine (N-acetyl)-6-sulfatase (Sanfilippo disease IIID)
IPI00009505	HSPA5BP1	non-mem		3	heat shock 70kDa protein 5 (glucose-regulated protein, 78kDa) binding protein 1
IPI00011635	KPNA2	non-mem		2	karyopherin alpha 2 (RAG cohort 1, importin alpha 1)
IPI00010740	RPL27A	non-mem		4	ribosomal protein L27a
IPI00180003	SND1	non-mem		16	staphylococcal nuclease domain containing 1
IPI00024143	CRKL	non-mem		4	v-crk sarcoma virus CT10 oncogene homolog (avian)-like
IPI00032137	HSPC117	non-mem		3	hypothetical protein HSPC117
IPI00017480	ARHGEF7	non-mem		8	Rho guanine nucleotide exchange factor (GEF) 7
IPI00220566	IQGAP1	non-mem		120	IQ motif containing GTPase activating protein 1
IPI00009504	CHCHD3	non-mem		4	coiled-coil-helix-coiled-coil-helix domain containing 3
IPI00152562	LRRC5	non-mem		6	leucine rich repeat containing 5
IPI00006117	PBP	non-mem		8	prostatic binding protein
IPI00220490	JM4	non-mem		3	JM4 protein
IPI00008490	ALG1	non-mem		3	asparagine-linked glycosylation 1 homolog (yeast, beta-1,4-mannosyltransferase)
IPI00180806	MDH1	non-mem		3	malate dehydrogenase 1, NAD (soluble)
IPI00166264	ZNF333	non-mem		3	zinc finger protein 333
IPI00181732	GPI	non-mem		16	glucose phosphate isomerase
IPI00177534	SCFD1	non-mem		19	sec1 family domain containing 1
IPI00217307	SOD2	non-mem		4	superoxide dismutase 2, mitochondrial
IPI00165027	GK001	non-mem		35	GK001 protein
IPI00031225	HSRG1	non-mem		9	HSV-1 stimulation-related gene 1
IPI00179418	GGH	non-mem		3	gamma-glutamyl hydrolase (conjugase, folylpolygammaglutamyl

					hydrolase)
IPI00017855	HEXA	non-mem		3	hexosaminidase A (alpha polypeptide)
IPI00011099	SUCLA2	non-mem		3	succinate-CoA ligase, ADP-forming, beta subunit
IPI00023006	TST	non-mem		2	thiosulfate sulfurtransferase (rhodanese)
IPI00100410	AKAP11	non-mem		2	A kinase (PRKA) anchor protein 11
IPI00217871	HIBADH	non-mem		2	3-hydroxyisobutyrate dehydrogenase
IPI00021820	KIF5B	non-mem		7	kinesin family member 5B
IPI00185600	TNKS1BP1	non-mem		3	tankyrase 1 binding protein 1, 182kDa
IPI00003815	KRT7	non-mem		21	keratin 7
IPI00169267	CDC42BPB	non-mem		14	CDC42 binding protein kinase beta (DMPK-like)
IPI00023244	WASF2	non-mem		3	WAS protein family, member 2
IPI00019989	HGS	non-mem		6	hepatocyte growth factor-regulated tyrosine kinase substrate
IPI00220492	PIP5K2A	non-mem		5	phosphatidylinositol-4-phosphate 5-kinase, type II, alpha
IPI00183097	PRDX4	non-mem		5	peroxiredoxin 4
IPI00220300	LACTB	non-mem		2	lactamase, beta
IPI00030397	MRPL46	non-mem		2	mitochondrial ribosomal protein L46
IPI00218598	PIK3R2	non-mem		3	phosphoinositide-3-kinase, regulatory subunit, polypeptide 2 (p85 beta)
IPI00029137	VAV2	non-mem		6	vav 2 oncogene
IPI00002505	DDX6	non-mem		4	DEAD (Asp-Glu-Ala-Asp) box polypeptide 6
IPI00027626	EIF3S3	non-mem		2	eukaryotic translation initiation factor 3, subunit 3 gamma, 40kDa
IPI00220289	FNDC3	non-mem		3	fibronectin type III domain containing 3
IPI00178042	FBP1	non-mem		3	fructose-1,6-bisphosphatase 1
IPI00219994	MTHFD2	non-mem		3	methylene tetrahydrofolate dehydrogenase (NAD+ dependent), methenyltetrahydrofolate cyclohydrolase
IPI00219823	SIM2	non-mem		3	single-minded homolog 2 (Drosophila)
IPI00010865	DLD	non-mem		7	dihydrolipoamide dehydrogenase (E3 component of pyruvate dehydrogenase complex, 2-oxo-glutarate complex, branched chain keto acid dehydrogenase complex)

IPI00182327	IGFBP2	non-mem		2	insulin-like growth factor binding protein 2, 36kDa
IPI00013478	KIAA1728	non-mem		3	KIAA1728 protein
IPI00029601	ACAT1	non-mem		6	acetyl-Coenzyme A acetyltransferase 1 (acetoacetyl Coenzyme A thiolase)
IPI00165594	VPS4B	non-mem		3	vacuolar protein sorting 4B (yeast)
IPI00061926	ACOX1	non-mem		5	acyl-Coenzyme A oxidase 1, palmitoyl
IPI00030876	HEXB	non-mem		4	hexosaminidase B (beta polypeptide)
IPI00004806	DAP13	non-mem		2	13kDa differentiation-associated protein
IPI00015947	PSMD14	non-mem		3	proteasome (prosome, macropain) 26S subunit, non-ATPase, 14
IPI00024523	STUB1	non-mem		2	STIP1 homology and U-Box containing protein 1
IPI00216349	D8S2298E	non-mem		2	reproduction 8
IPI00033022	PSMC6	non-mem		2	proteasome (prosome, macropain) 26S subunit, ATPase, 6
IPI00218651	EIF4EL3	non-mem		2	eukaryotic translation initiation factor 4E-like 3
IPI00025447	IPO4	non-mem		5	importin 4
IPI00009846	UBE2L3	non-mem		2	ubiquitin-conjugating enzyme E2L 3
IPI00179667	VCP	non-mem		53	valosin-containing protein
IPI00021458	EEF1D	non-mem		5	eukaryotic translation elongation factor 1 delta (guanine nucleotide exchange protein)
IPI00032331	PP	non-mem		2	pyrophosphatase (inorganic)
IPI00152953	CNN1	non-mem		2	calponin 1, basic, smooth muscle
IPI00217841	STK16	non-mem		3	serine/threonine kinase 16
IPI00171433	SEC10L1	non-mem		5	SEC10-like 1 (S. cerevisiae)
IPI00172656	ACAA1	non-mem		4	acetyl-Coenzyme A acyltransferase 1 (peroxisomal 3-oxoacyl-Coenzyme A thiolase)
IPI00031820	FLJ10074	non-mem		5	hypothetical protein FLJ10074
IPI00017251	KRT8	non-mem		34	keratin 8
IPI00019770	MDH2	non-mem		13	malate dehydrogenase 2, NAD (mitochondrial)
IPI00166704	DARS	non-mem		3	aspartyl-tRNA synthetase
IPI00029717	DKFZp566O084	non-mem		14	DKFZP566O084 protein
IPI00219005	GNPTAG	non-mem		2	N-acetylglucosamine-1-phosphotransferase, gamma subunit
IPI00031023	GSTM3	non-mem		2	glutathione S-transferase M3

					(brain)
IPI00017283	HNRPA2B1	non-mem		4	heterogeneous nuclear ribonucleoprotein A2/B1
IPI00183177	QARS	non-mem		2	glutaminyl-tRNA synthetase
IPI00171013	FH	non-mem		4	fumarate hydratase
IPI00182213	HIST1H1E	non-mem		5	histone 1, H1e
IPI00009057	RBBP7	non-mem		2	retinoblastoma binding protein 7
IPI00216008	FLJ13855	non-mem		2	hypothetical protein FLJ13855
IPI00219018	TMOD3	non-mem		3	tropomodulin 3 (ubiquitous)
IPI00013230	MCF2L	non-mem		3	MCF.2 cell line derived transforming sequence-like
IPI00025869	PSMA5	non-mem		2	proteasome (prosome, macropain) subunit, alpha type, 5
IPI00024707	SRP72	non-mem		3	signal recognition particle 72kDa
IPI00029738	HNRPU	non-mem		5	heterogeneous nuclear ribonucleoprotein U (scaffold attachment factor A)
IPI00217449	MAC30	non-mem		4	hypothetical protein MAC30
IPI00180386	CORO1C	non-mem		10	coronin, actin binding protein, 1C
IPI00157144	ATP5H	non-mem		18	ATP synthase, H+ transporting, mitochondrial F0 complex, subunit d
IPI00059366	PSME2	non-mem		4	proteasome (prosome, macropain) activator subunit 2 (PA28 beta)
IPI00219038	DNAJC13	non-mem		21	DnaJ (Hsp40) homolog, subfamily C, member 13
IPI00164486	RPS7	non-mem		14	ribosomal protein S7
IPI00106495	GPD2	non-mem		12	glycerol-3-phosphate dehydrogenase 2 (mitochondrial)
IPI00102860	KIAA0877	non-mem		4	KIAA0877 protein
IPI00217468	MR-1	non-mem		3	myofibrillogenesis regulator 1
IPI00217465	DDB1	non-mem		2	damage-specific DNA binding protein 1, 127kDa
IPI00004074	ECH1	non-mem		4	enoyl Coenzyme A hydratase 1, peroxisomal
IPI00027367	EPPK1	non-mem		22	epiplakin 1
IPI00216403	IDE	non-mem		3	insulin-degrading enzyme
IPI00170645	LRPPRC	non-mem		19	leucine-rich PPR-motif containing
IPI00216746	NAGLU	non-mem		4	N-acetylglucosaminidase, alpha- (Sanfilippo disease IIIB)
IPI00171903	SCO1	non-mem		3	SCO cytochrome oxidase deficient homolog 1 (yeast)
IPI00027392	JTV1	non-mem		3	JTV1 gene
IPI00012473	SF3B1	non-mem		3	splicing factor 3b, subunit 1, 155kDa

IPI00003865	PSMD5	non-mem		3	proteasome (prosome, macropain) 26S subunit, non-ATPase, 5
IPI00025512	KPNB1	non-mem		8	karyopherin (importin) beta 1
IPI00185652	GLB1	non-mem		2	galactosidase, beta 1
IPI00220705	MAP2K2	non-mem		3	mitogen-activated protein kinase kinase 2
IPI00024284	TMX2	non-mem		6	thioredoxin-related transmembrane protein 2
IPI00218993	ECHS1	non-mem		3	enoyl Coenzyme A hydratase, short chain, 1, mitochondrial
IPI00011107	PSMC3	non-mem		3	proteasome (prosome, macropain) 26S subunit, ATPase, 3
IPI00219330	WNT3A	non-mem		2	wingless-type MMTV integration site family, member 3A
IPI00025644	CTNNA1	non-mem		99	catenin (cadherin-associated protein), alpha 1, 102kDa
IPI00181639	IGFBP5	non-mem		4	insulin-like growth factor binding protein 5
IPI00106502	IQGAP2	non-mem		8	IQ motif containing GTPase activating protein 2
IPI00186217	KIAA0763	non-mem		2	KIAA0763 gene product
IPI00167860	MYH14	non-mem		10	myosin, heavy polypeptide 14
IPI00165976	CTSC	non-mem		3	cathepsin C
IPI00033429	RPL32	non-mem		9	ribosomal protein L32
IPI00009865	CTNNA2	non-mem		18	catenin (cadherin-associated protein), alpha 2
IPI00081551	DHX9	non-mem		2	DEAH (Asp-Glu-Ala-His) box polypeptide 9
IPI00215642	FLJ39582	non-mem		2	hypothetical protein FLJ39582
IPI00010292	GEMIN5	non-mem		4	gem (nuclear organelle) associated protein 5
IPI00000173	PABPC4	non-mem		5	poly(A) binding protein, cytoplasmic 4 (inducible form)
IPI00219752	CAD	non-mem		2	carbamoyl-phosphate synthetase 2, aspartate transcarbamylase, and dihydroorotase
IPI00012989	KIAA1893	non-mem		2	G protein-regulated inducer of neurite outgrowth 1
IPI00218193	ARMCX3	non-mem		2	armadillo repeat containing, X-linked 3
IPI00003479	GLUD2	non-mem		13	glutamate dehydrogenase 2
IPI00184873	PSMD2	non-mem		5	proteasome (prosome, macropain) 26S subunit, non-ATPase, 2
IPI00218139	RAB17	non-mem		4	RAB17, member RAS oncogene family
IPI00166518	CLU	non-mem		6	clusterin (complement lysis

					inhibitor, SP-40,40, sulfated glycoprotein 2, testosterone-repressed prostate message 2, apolipoprotein J)
IPI00172591	PKP2	non-mem		15	plakophilin 2
IPI00162330	CNAP1	non-mem		2	chromosome condensation-related SMC-associated protein 1
IPI00186997	DKFZp564I1922	non-mem		3	adlican
IPI00182383	IREB2	non-mem		4	iron-responsive element binding protein 2
IPI00030287	DECR1	non-mem		2	2,4-dienoyl CoA reductase 1, mitochondrial
IPI00019502	H2AFZ	non-mem		8	H2A histone family, member Z
IPI00029208	KIAA0089	non-mem		2	KIAA0089 protein
IPI00220610	MYO1E	non-mem		2	myosin IE
IPI00016760	NISCH	non-mem		2	nischarin
IPI00221369	PMPCB	non-mem		2	peptidase (mitochondrial processing) beta
IPI00100956	MRPL12	non-mem		10	mitochondrial ribosomal protein L12
IPI00216121	NACA	non-mem		2	nascent-polypeptide-associated complex alpha polypeptide
IPI00008455	DPP7	non-mem		2	dipeptidylpeptidase 7
IPI00215758	SERPINE1	non-mem		2	serine (or cysteine) proteinase inhibitor, clade E (nexin, plasminogen activator inhibitor type 1), member 1
IPI00186947	CLN2	non-mem		2	ceroid-lipofuscinosis, neuronal 2, late infantile (Jansky-Bielschowsky disease)
IPI00180478	HMGCS1	non-mem		3	3-hydroxy-3-methylglutaryl-Coenzyme A synthase 1 (soluble)
IPI00023286	MTHFD1	non-mem		6	methylenetetrahydrofolate dehydrogenase (NADP+ dependent), methenyltetrahydrofolate cyclohydrolase, formyltetrahydrofolate synthetase
IPI00014177	MTM1	non-mem		3	myotubular myopathy 1
IPI00163799	EIF4G2	non-mem		4	eukaryotic translation initiation factor 4 gamma, 2
IPI00218830	GSPT1	non-mem		2	G1 to S phase transition 1
IPI00012069	ARMET	non-mem		2	arginine-rich, mutated in early stage tumors
IPI00019407	SUPV3L1	non-mem		2	suppressor of var1, 3-like 1 (S. cerevisiae)
IPI00031812	GAA	non-mem		16	glucosidase, alpha; acid (Pompe disease, glycogen

					storage disease type II)
IPI00142634	MYO5C	non-mem		15	myosin VC
IPI00075080	STK10	non-mem		3	serine/threonine kinase 10
IPI00183688	USP7	non-mem		5	ubiquitin specific protease 7 (herpes virus-associated)
IPI00186735	UTRN	non-mem		13	utrophin (homologous to dystrophin)
IPI00024989	ZW10	non-mem		4	ZW10 homolog, centromere/kinetochore protein (Drosophila)
IPI00020338	BLMH	non-mem		2	bleomycin hydrolase
IPI00219285	DNCLI2	non-mem		3	dynein, cytoplasmic, light intermediate polypeptide 2
IPI00029515	KIAA0692	non-mem		5	KIAA0692 protein
IPI00007248	PRP19	non-mem		4	PRP19/PSO4 homolog (S. cerevisiae)
IPI00004534	CTDSP1	non-mem		3	CTD (carboxy-terminal domain, RNA polymerase II, polypeptide A) small phosphatase 1
IPI00169383	GDAP1	non-mem		2	ganglioside-induced differentiation-associated protein 1
IPI00011200	MRPS27	non-mem		2	mitochondrial ribosomal protein S27
IPI00026952	TNPO3	non-mem		2	transportin 3
IPI00219563	ACTB	non-mem		127	actin, beta
IPI00014897	ARHGEF2	non-mem		2	rho/rac guanine nucleotide exchange factor (GEF) 2
IPI00164240	PIP5K2B	non-mem		5	phosphatidylinositol-4-phosphate 5-kinase, type II, beta
IPI00021794	SYT1	non-mem		3	synaptotagmin I
IPI00032473	TYK2	non-mem		5	tyrosine kinase 2
IPI00183002	NONO	non-mem		2	non-POU domain containing, octamer-binding
IPI00220145	SMAD3	non-mem		2	SMAD, mothers against DPP homolog 3 (Drosophila)
IPI00220616	WARS	non-mem		2	tryptophanyl-tRNA synthetase
IPI00183626	CAPZB	non-mem		9	capping protein (actin filament) muscle Z-line, beta
IPI00178551	C2orf18	non-mem		4	chromosome 2 open reading frame 18
IPI00006714	FAM38A	non-mem		6	family with sequence similarity 38, member A
IPI00004358	KPNB3	non-mem		4	karyopherin (importin) beta 3
IPI00016342	KRT3	non-mem		2	keratin 3
IPI00032395	NUP107	non-mem		2	nucleoporin 107kDa
IPI00220980	FKBP3	non-mem		3	FK506 binding protein 3, 25kDa
IPI00027434	BLVRA	non-mem		2	biliverdin reductase A
IPI00186221	EHD4	non-mem		7	EH-domain containing 4
IPI00022770	KRTHB4	non-mem		5	keratin, hair, basic, 4

IPI00164477	MRPL18	non-mem		2	mitochondrial ribosomal protein L18
IPI00219153	COPB	non-mem		3	coatomer protein complex, subunit beta
IPI00021266	CSNK1G2	non-mem		6	casein kinase 1, gamma 2
IPI00219155	EPLIN	non-mem		22	epithelial protein lost in neoplasm beta
IPI00022747	ROCK1	non-mem		2	Rho-associated, coiled-coil containing protein kinase 1
IPI00029731	TNC	non-mem		4	tenascin C (hexabrachion)
IPI00176627	DDX5	non-mem		2	DEAD (Asp-Glu-Ala-Asp) box polypeptide 5
IPI00003918	PFKL	non-mem		4	phosphofructokinase, liver
IPI00000494	PGM3	non-mem		2	phosphoglucomutase 3
IPI00027271	TSG101	non-mem		4	tumor susceptibility gene 101
IPI00042717	HIST1H2BO	non-mem		11	histone 1, H2bo
IPI00176854	PFN2	non-mem		2	profilin 2
IPI00221097	APXL	non-mem		3	apical protein-like (Xenopus laevis)
IPI00219163	IARS	non-mem		3	isoleucine-tRNA synthetase
IPI00221088	HIST1H1D	non-mem		2	histone 1, H1d
IPI00005549	TMEM30B	non-mem		2	transmembrane protein 30B
IPI00017256	CAPN7	non-mem		3	calpain 7
IPI00021986	EIF3S8	non-mem		3	eukaryotic translation initiation factor 3, subunit 8, 110kDa
IPI00218397	FRAP1	non-mem		9	FK506 binding protein 12-rapamycin associated protein 1
IPI00017375	KIAA0674	non-mem		3	KIAA0674
IPI00072377	MRPS22	non-mem		2	mitochondrial ribosomal protein S22
IPI00181020	TSTA3	non-mem		3	tissue specific transplantation antigen P35B
IPI00180553	ZNF262	non-mem		2	zinc finger protein 262
IPI00172421	IDH3A	non-mem		5	isocitrate dehydrogenase 3 (NAD+) alpha
IPI00105995	IMPDH2	non-mem		2	IMP (inosine monophosphate) dehydrogenase 2
IPI00167989	TTK	non-mem		2	TTK protein kinase
IPI00067049	ACOX3	non-mem		2	acyl-Coenzyme A oxidase 3, pristanoyl
IPI00178339	COPB2	non-mem		4	coatomer protein complex, subunit beta 2 (beta prime)
IPI00181144	SEMA3C	non-mem		5	sema domain, immunoglobulin domain (Ig), short basic domain, secreted, (semaphorin) 3C
IPI00018140	BCKDHA	non-mem		2	branched chain keto acid dehydrogenase E1, alpha polypeptide (maple syrup urine disease)

IPI00183783	FLJ10900	non-mem		4	hypothetical protein FLJ10900
IPI00181580	AZI1	non-mem		2	likely ortholog of mouse 5-azacytidine induced gene 1
IPI00056553	FARP2	non-mem		9	FERM, RhoGEF and pleckstrin domain protein 2
IPI00018401	PGAM1	non-mem		8	phosphoglycerate mutase 1 (brain)
IPI00100160	PRKAR1A	non-mem		3	protein kinase, cAMP-dependent, regulatory, type I, alpha (tissue specific extinguisher 1)
IPI00186039	RPS23	non-mem		11	ribosomal protein S23
IPI00030131	DNAJC3	non-mem		2	DnaJ (Hsp40) homolog, subfamily C, member 3
IPI00180240	ENO3	non-mem		4	enolase 3, (beta, muscle)
IPI00099607	MRPL1	non-mem		3	mitochondrial ribosomal protein L1
IPI00218754	FLJ10514	non-mem		2	hypothetical protein FLJ10514
IPI00176492	CASK	non-mem		25	calcium/calmodulin-dependent serine protein kinase (MAGUK family)
IPI00030275	CPA3	non-mem		2	carboxypeptidase A3 (mast cell)
IPI00168647	FKSG44	non-mem		2	FKSG44 gene
IPI00153007	FLNC	non-mem		9	filamin C, gamma (actin binding protein 280)
IPI00031195	GSN	non-mem		13	gelsolin (amyloidosis, Finnish type)
IPI00100673	EPS15L1	non-mem		4	epidermal growth factor receptor pathway substrate 15-like 1
IPI00011676	NOLC1	non-mem		3	nucleolar and coiled-body phosphoprotein 1
IPI00220922	OSBPL9	non-mem		3	oxysterol binding protein-like 9
IPI00018146	PREB	non-mem		10	prolactin regulatory element binding
IPI00021263	C20orf116	non-mem		10	chromosome 20 open reading frame 116
IPI00005043	INADL	non-mem		7	InaD-like protein
IPI00005695	ch-TOG	non-mem		4	KIAA0097 gene product
IPI00177877	FLJ21019	non-mem		4	hypothetical protein FLJ21019
IPI00186729	MACF1	non-mem		11	microtubule-actin crosslinking factor 1
IPI00013808	ETF1	non-mem		4	eukaryotic translation termination factor 1
IPI00163552	RPL26L1	non-mem		11	ribosomal protein L26-like 1
IPI00074231	LASS5	non-mem		2	LAG1 longevity assurance homolog 5 (S. cerevisiae)
IPI00216581	C14orf151	non-mem		2	chromosome 14 open reading frame 151
IPI00024976	KIF3B	non-mem		3	kinesin family member 3B

IPI00032426	RNF130	non-mem		2	ring finger protein 130
IPI00186104	WWP2	non-mem		3	Nedd-4-like ubiquitin-protein ligase
IPI00168383	EIF3S10	non-mem		6	eukaryotic translation initiation factor 3, subunit 10 theta, 150/170kDa
IPI00221392	PPID	non-mem		4	peptidylprolyl isomerase D (cyclophilin D)
IPI00180255	AHCYL1	non-mem		4	S-adenosylhomocysteine hydrolase-like 1
IPI00179187	HSPA1L	non-mem		17	heat shock 70kDa protein 1-like
IPI00162239	LIMS1	non-mem		2	LIM and senescent cell antigen-like domains 1
IPI00183572		non-mem		2	Full length insert cDNA YH77E09
IPI00171301	MAGED2	non-mem		6	melanoma antigen, family D, 2
IPI00019529	THRAP2	non-mem		4	thyroid hormone receptor associated protein 2
IPI00171002		non-mem		2	Data not found
IPI00186207	CUL1	non-mem		2	cullin 1
IPI00171626	PGM1	non-mem		4	phosphoglucomutase 1
IPI00176600	CUL2	non-mem		3	cullin 2
IPI00165682	ACSL4	non-mem		4	acyl-CoA synthetase long-chain family member 4
IPI00155536	USP16	non-mem		3	ubiquitin specific protease 16
IPI00165273	C20orf194	non-mem		2	chromosome 20 open reading frame 194
IPI00171444	TUBA6	non-mem		38	tubulin alpha 6
IPI00044667	USP20	non-mem		3	ubiquitin specific protease 20
IPI00177532	PDLIM7	non-mem		2	PDZ and LIM domain 7 (enigma)
IPI00175830	PSMD3	non-mem		2	proteasome (prosome, macropain) 26S subunit, non-ATPase, 3
IPI00168114	USP10	non-mem		2	ubiquitin specific protease 10
IPI00170436	C14orf173	non-mem		2	chromosome 14 open reading frame 173
IPI00171906	PABPC1	non-mem		7	poly(A) binding protein, cytoplasmic 1
IPI00060920	CDK5RAP2	non-mem		4	CDK5 regulatory subunit associated protein 2
IPI00018927	NT5C2	non-mem		2	5'-nucleotidase, cytosolic II
IPI00171477	ACADL	non-mem		3	acyl-Coenzyme A dehydrogenase, long chain
IPI00184177	ADP-GK	non-mem		7	ATP-dependent glucokinase
IPI00167917	CSNK1A1	non-mem		5	casein kinase 1, alpha 1
IPI00168255	IDH3B	non-mem		4	isocitrate dehydrogenase 3 (NAD+) beta
IPI00101927	PCTK1	non-mem		2	PCTAIRE protein kinase 1
IPI00219799	CDK5	non-mem		2	cyclin-dependent kinase 5
IPI00220507	HSPC065	non-mem		3	HSPC065 protein
IPI00013638	PRKACA	non-mem		12	protein kinase, cAMP-

					dependent, catalytic, alpha
IPI00217853	COBLL1	non-mem		5	COBL-like 1
IPI00001578	RPL3L	non-mem		3	ribosomal protein L3-like
IPI00184806	STK25	non-mem		4	serine/threonine kinase 25 (STE20 homolog, yeast)
IPI00032413	CUTL1	non-mem		3	cut-like 1, CCAAT displacement protein (Drosophila)
IPI00064666	FLJ23436	non-mem		3	hypothetical protein FLJ23436
IPI00220304	FUCA1	non-mem		3	fucosidase, alpha-L- 1, tissue
IPI00171217	JIK	non-mem		14	STE20-like kinase
IPI00030450	STRBP	non-mem		2	spermatid perinuclear RNA binding protein
IPI00107872	LTBP4	non-mem		3	latent transforming growth factor beta binding protein 4
IPI00182447	ASXL1	non-mem		2	additional sex combs like 1 (Drosophila)
IPI00062958	FLJ21439	non-mem		2	hypothetical protein FLJ21439
IPI00177774	RBM21	non-mem		2	RNA binding motif protein 21
IPI00027423	ALB	non-mem		5	albumin
IPI00003461	FLJ21168	non-mem		2	hypothetical protein FLJ21168
IPI00018001	RPL18A	non-mem		12	ribosomal protein L18a
IPI00003590	FLJ23471	non-mem		4	MICAL-like 2
IPI00180305	KIAA0431	non-mem		2	KIAA0431 protein
IPI00178857	RPL7	non-mem		17	ribosomal protein L7
IPI00143887	ADPRT	non-mem		3	ADP-ribosyltransferase (NAD+; poly (ADP-ribose) polymerase)
IPI00062120	BIRC6	non-mem		3	baculoviral IAP repeat-containing 6 (apollon)
IPI00008351	VIM	non-mem		2	vimentin
IPI00006615	RBM27	non-mem		3	RNA binding motif protein 27
IPI00166387	FVT1	non-mem		3	follicular lymphoma variant translocation 1
IPI00029629	PA2G4	non-mem		7	proliferation-associated 2G4, 38kDa
IPI00152228	APC2	non-mem		3	adenomatosis polyposis coli 2
IPI00032808	HELZ	non-mem		3	helicase with zinc finger domain
IPI00186527	OS-9	non-mem		16	amplified in osteosarcoma
IPI00062469	RNF20	non-mem		3	ring finger protein 20
IPI00184284	TNRC15	non-mem		2	trinucleotide repeat containing 15
IPI00183985	UGCGL1	non-mem		13	UDP-glucose ceramide glucosyltransferase-like 1
IPI00152709	LASP1	non-mem		21	LIM and SH3 protein 1
IPI00171822	OSBPL8	non-mem		21	oxysterol binding protein-like 8

IPI00167298	DDX18	non-mem		2	DEAD (Asp-Glu-Ala-Asp) box polypeptide 18
IPI00218608	EPRS	non-mem		5	glutamyl-prolyl-tRNA synthetase
IPI00016961	DHX30	non-mem		4	DEAH (Asp-Glu-Ala-His) box polypeptide 30
IPI00034277	DTX2	non-mem		3	deltex homolog 2 (Drosophila)
IPI00006484	EPS8	non-mem		13	epidermal growth factor receptor pathway substrate 8
IPI00024344	EXOC7	non-mem		8	exocyst complex component 7
IPI00020430	HSPA9B	non-mem		23	heat shock 70kDa protein 9B (mortalin-2)
IPI00000425	ZNF560	non-mem		2	zinc finger protein 560
IPI00178673	SEC3L1	non-mem		9	SEC3-like 1 (S. cerevisiae)
IPI00016665	TMOD2	non-mem		2	tropomodulin 2 (neuronal)
IPI00007730	LGP1	non-mem		2	D11lgp1e-like
IPI00183548	SFPQ	non-mem		3	splicing factor proline/glutamine rich (polypyrimidine tract binding protein associated)
IPI00029239	TAGLN	non-mem		2	transgelin
IPI00220772	ACTN3	non-mem		11	actinin, alpha 3
IPI00026942	SHH	non-mem		2	sonic hedgehog homolog (Drosophila)
IPI00152488	TXNRD2	non-mem		2	thioredoxin reductase 2
IPI00221393	DLST	non-mem		9	dihydrolipoamide S-succinyltransferase (E2 component of 2-oxo-glutarate complex)
IPI00101942	ABI1	non-mem		33	abl-interactor 1
IPI00011284	ABI2	non-mem		37	abl interactor 2
IPI00015480	ACAT2	non-mem		10	acetyl-Coenzyme A acetyltransferase 2 (acetoacetyl Coenzyme A thiolase)
IPI00032406	ACO2	non-mem		3	aconitase 2, mitochondrial
IPI00220146	ACPP	non-mem		5	acid phosphatase, prostate
IPI00026558	ACTC	non-mem		22	actin, alpha, cardiac muscle
IPI00001754	AIG1	non-mem		13	androgen-induced 1
IPI00012107	ALDH4A1	non-mem		10	aldehyde dehydrogenase 4 family, member A1
IPI00008299	ALDOA	non-mem		17	aldolase A, fructose-bisphosphate
IPI00027253	ANXA11	non-mem		32	annexin A11
IPI00217717	ARHGDIA	non-mem		5	Rho GDP dissociation inhibitor (GDI) alpha
IPI00216336	ARL6IP2	non-mem		34	ADP-ribosylation factor-like 6 interacting protein 2
IPI00100656	ARPC1A	non-mem		26	actin related protein 2/3 complex, subunit 1A, 41kDa
IPI00021327	ARSD	non-mem		20	arylsulfatase D
IPI00144014	ARVCF	non-mem		5	armadillo repeat gene deletes

					in velocardiofacial syndrome
IPI00027232	ASAH1	non-mem		29	N-acylsphingosine amidohydrolase (acid ceramidase) 1
IPI00152302	ATP5J2	non-mem		28	ATP synthase, H+ transporting, mitochondrial F0 complex, subunit f, isoform 2
IPI00166982	BNIP1	non-mem		25	BCL2/adenovirus E1B 19kDa interacting protein 1
IPI00220845	C9orf78	non-mem		7	chromosome 9 open reading frame 78
IPI00029741	CALM2	non-mem		5	calmodulin 2 (phosphorylase kinase, delta)
IPI00220592	CAPN5	non-mem		26	calpain 5
IPI00019690	CCT6A	non-mem		7	chaperonin containing TCP1, subunit 6A (zeta 1)
IPI00217559	CHD5	non-mem		25	chromodomain helicase DNA binding protein 5
IPI00006097	CNDP2	non-mem		25	CNDP dipeptidase 2 (metallopeptidase M20 family)
IPI00027542	CSE1L	non-mem		29	CSE1 chromosome segregation 1-like (yeast)
IPI00151987	CSNK1G1	non-mem		17	casein kinase 1, gamma 1
IPI00105068	CSNK2B	non-mem		24	casein kinase 2, beta polypeptide
IPI00106766	CTNNAL1	non-mem		5	catenin (cadherin-associated protein), alpha-like 1
IPI00183568	CTSB	non-mem		12	cathepsin B
IPI00009447	CTTN	non-mem		31	cortactin
IPI00004462	D1S155E	non-mem		21	NRAS-related gene
IPI00014958	DDX11	non-mem		9	DEAD/H (Asp-Glu-Ala-Asp/His) box polypeptide 11 (CHL1-like helicase homolog, S. cerevisiae)
IPI00031909	DIAPH1	non-mem		19	diaphanous homolog 1 (Drosophila)
IPI00010267	DKFZP564J 0863	non-mem		26	DKFZP564J0863 protein
IPI00015148	DNAJB1	non-mem		16	DnaJ (Hsp40) homolog, subfamily B, member 1
IPI00106884	DNAJB6	non-mem		3	DnaJ (Hsp40) homolog, subfamily B, member 6
IPI00024320	DNCI2	non-mem		28	dynein, cytoplasmic, intermediate polypeptide 2
IPI00024185	DNM2	non-mem		14	dynamin 2
IPI00019254	DTNA	non-mem		37	dystrobrevin, alpha
IPI00098365	EEF1A1	non-mem		33	eukaryotic translation elongation factor 1 alpha 1
IPI00184580	EEF2	non-mem		4	eukaryotic translation elongation factor 2
IPI00027493	EFG1	non-mem		13	mitochondrial elongation factor G1
IPI00219626	EHD3	non-mem		35	EH-domain containing 3

IPI00012486	EIF5B	non-mem		36	eukaryotic translation initiation factor 5B
IPI00020104	EPB41L4B	non-mem		32	erythrocyte membrane protein band 4.1 like 4B
IPI00220429	EPB41L5	non-mem		26	erythrocyte membrane protein band 4.1 like 5
IPI00093681	EPS8L1	non-mem		2	EPS8-like 1
IPI00103940	ETEA	non-mem		27	expressed in T-cells and eosinophils in atopic dermatitis
IPI00219214	FARSLA	non-mem		16	phenylalanine-tRNA synthetase-like, alpha subunit
IPI00101374	FARSLB	non-mem		8	phenylalanine-tRNA synthetase-like, beta subunit
IPI00007165	FAU	non-mem		3	Finkel-Biskis-Reilly murine sarcoma virus (FBR-MuSV) ubiquitously expressed (fox derived); ribosomal protein S30
IPI00062679	FBXO10	non-mem		33	F-box protein 10
IPI00056521	FGA	non-mem		14	fibrinogen, A alpha polypeptide
IPI00074334	FKBP4	non-mem		29	FK506 binding protein 4, 59kDa
IPI00028051	FLII	non-mem		10	flightless I homolog (Drosophila)
IPI00030847	FLJ10326	non-mem		36	mitochondrial isoleucine tRNA synthetase
IPI00182760	FLJ20254	non-mem		15	hypothetical protein FLJ20254
IPI00008463	FLJ23420	non-mem		8	hypothetical protein FLJ23420
IPI00219620	FXR1	non-mem		2	fragile X mental retardation, autosomal homolog 1
IPI00217704	G3BP2	non-mem		9	Ras-GTPase activating protein SH3 domain-binding protein 2
IPI00219794	G6PD	non-mem		32	glucose-6-phosphate dehydrogenase
IPI00219183	GAPD	non-mem		20	glyceraldehyde-3-phosphate dehydrogenase
IPI00215920	GARS	non-mem		23	glycyl-tRNA synthetase
IPI00021695	GLA	non-mem		26	galactosidase, alpha
IPI00028610	GNA11	non-mem		19	guanine nucleotide binding protein (G protein), alpha 11 (Gq class)
IPI00221246	GRSF1	non-mem		38	G-rich RNA sequence binding factor 1
IPI00009236	GTF2I	non-mem		13	general transcription factor II, i
IPI00164996	GYG	non-mem		26	glycogenin
IPI00216516	GYS1	non-mem		6	glycogen synthase 1 (muscle)
IPI00011302	H2AFY	non-mem		19	H2A histone family, member Y
IPI00025861	H3F3B	non-mem		5	H3 histone, family 3B

					(H3.3B)
IPI00184784	HADHSC	non-mem		27	L-3-hydroxyacyl-Coenzyme A dehydrogenase, short chain
IPI00014587	HCAP-G	non-mem		17	chromosome condensation protein G
IPI00030548	HCMOGT-1	non-mem		24	sperm antigen HCMOGT-1
IPI00021019	HIST1H1B	non-mem		18	histone 1, H1b
IPI00186905	HIST1H1C	non-mem		5	histone 1, H1c
IPI00221254	HIST1H2BG	non-mem		8	histone 1, H2bg
IPI00219996	HIST1H3H	non-mem		34	histone 1, H3h
IPI00023343	HIST1H4K	non-mem		32	histone 1, H4k
IPI00060445	HIST2H2AA	non-mem		32	histone 2, H2aa
IPI00178440	HNRPK	non-mem		6	heterogeneous nuclear ribonucleoprotein K
IPI00218697	HNRPM	non-mem		19	heterogeneous nuclear ribonucleoprotein M
IPI00219244	HSPA1A	non-mem		38	heat shock 70kDa protein 1A
IPI00027082	HSPA6	non-mem		30	heat shock 70kDa protein 6 (HSP70B')
IPI00185623	HSPA8	non-mem		38	heat shock 70kDa protein 8
IPI00185344	HSPB1	non-mem		12	heat shock 27kDa protein 1
IPI00002884	HSPCB	non-mem		24	heat shock 90kDa protein 1, beta
IPI00004343	HSPD1	non-mem		12	heat shock 60kDa protein 1 (chaperonin)
IPI00029625	HSPG2	non-mem		15	heparan sulfate proteoglycan 2 (perlecan)
IPI00216995	HSPH1	non-mem		8	heat shock 105kDa/110kDa protein 1
IPI00180415	IDH2	non-mem		23	isocitrate dehydrogenase 2 (NADP+), mitochondrial
IPI00004901	ILF3	non-mem		33	interleukin enhancer binding factor 3, 90kDa
IPI00179397	ILK	non-mem		39	integrin-linked kinase
IPI00182076	IPO7	non-mem		13	importin 7
IPI00000006	KEAP1	non-mem		17	kelch-like ECH-associated protein 1
IPI00170690	KIAA0522	non-mem		11	KIAA0522 protein
IPI00043215	KIAA1102	non-mem		6	KIAA1102 protein
IPI00215995	KIAA1449	non-mem		38	WD repeat endosomal protein
IPI00010697	KIDINS220	non-mem		11	likely homolog of rat kinase D-interacting substance of 220 kDa
IPI00107540	KRT10	non-mem		24	keratin 10 (epidermolytic hyperkeratosis; keratosis palmaris et plantaris)
IPI00221383	LCHN	non-mem		38	LCHN protein
IPI00020446	LGALS8	non-mem		6	lectin, galactoside-binding, soluble, 8 (galectin 8)
IPI00179252	LOC51337	non-mem		13	mesenchymal stem cell protein DSCD75

IPI00003635	LRCH4	non-mem		25	leucine-rich repeats and calponin homology (CH) domain containing 4
IPI00217922	M17S2	non-mem		11	membrane component, chromosome 17, surface marker 2 (ovarian carcinoma antigen CA125)
IPI00023461	MAN2B1	non-mem		38	mannosidase, alpha, class 2B, member 1
IPI00022558	MAP4	non-mem		17	microtubule-associated protein 4
IPI00000736	MAPK1	non-mem		5	mitogen-activated protein kinase 1
IPI00220312	MDS032	non-mem		20	uncharacterized hematopoietic stem/progenitor cells protein MDS032
IPI00016503	MGEA6	non-mem		4	meningioma expressed antigen 6 (coiled-coil proline-rich)
IPI00009123	M-RIP	non-mem		19	myosin phosphatase-Rho interacting protein
IPI00165621	MRPL17	non-mem		20	mitochondrial ribosomal protein L17
IPI00009790	MRPL37	non-mem		35	mitochondrial ribosomal protein L37
IPI00219613	MRPS6	non-mem		28	mitochondrial ribosomal protein S6
IPI00024727	MST4	non-mem		2	Mst3 and SOK1-related kinase
IPI00215942	MUC6	non-mem		5	mucin 6, gastric
IPI00183286	MYH9	non-mem		8	myosin, heavy polypeptide 9, non-muscle
IPI00179070	MYL6	non-mem		34	myosin, light polypeptide 6, alkali, smooth muscle and non-muscle
IPI00107831	MYO10	non-mem		6	myosin X
IPI00182086	MYO1B	non-mem		3	myosin IB
IPI00016339	MYO1D	non-mem		13	myosin ID
IPI00017367	MYO5A	non-mem		20	myosin VA (heavy polypeptide 12, myoxin)
IPI00177832	MYO5B	non-mem		8	myosin VB
IPI00168686	MYO6	non-mem		10	myosin VI
IPI00007824	MYO7A	non-mem		38	myosin VIIA (Usher syndrome 1B (autosomal recessive, severe))
IPI00165205	NCL	non-mem		35	nucleolin
IPI00015476	NEBL	non-mem		6	nebulette
IPI00022891	NEDD4L	non-mem		39	neural precursor cell expressed, developmentally down-regulated 4-like
IPI00184792	NEDD5	non-mem		17	neural precursor cell expressed, developmentally down-regulated 5
IPI00003843	NICE-4	non-mem		5	NICE-4 protein

IPI00028055	NMT1	non-mem		15	N-myristoyltransferase 1
IPI00015843	NQO1	non-mem		3	NAD(P)H dehydrogenase, quinone 1
IPI00170692	NSDHL	non-mem		31	NAD(P) dependent steroid dehydrogenase-like
IPI00219299	NSEP1	non-mem		25	nuclease sensitive element binding protein 1
IPI00012728	OK/SW-cl.56	non-mem		12	beta 5-tubulin
IPI00072923	OSBPL1A	non-mem		38	oxysterol binding protein-like 1A
IPI00217708	OSBPL5	non-mem		4	oxysterol binding protein-like 5
IPI00179338	PARVA	non-mem		25	parvin, alpha
IPI00220019	PCMT1	non-mem		2	protein-L-isoaspartate (D-aspartate) O-methyltransferase
IPI00221164	PCOLN3	non-mem		13	procollagen (type III) N-endopeptidase
IPI00187030	PDHA1	non-mem		18	pyruvate dehydrogenase (lipoamide) alpha 1
IPI00003854	PEPP2	non-mem		27	phosphoinositol 3-phosphate-binding protein-2
IPI00029133	PEPP3	non-mem		29	phosphoinositol 3-phosphate-binding protein-3
IPI00015880	PFAS	non-mem		26	phosphoribosylformylglycinamidine synthase (FGAR amidotransferase)
IPI00014230	PGK1	non-mem		21	phosphoglycerate kinase 1
IPI00026570	PHGDH	non-mem		28	phosphoglycerate dehydrogenase
IPI00185889	PKP3	non-mem		11	plakophilin 3
IPI00185317	PLCB1	non-mem		18	phospholipase C, beta 1 (phosphoinositide-specific)
IPI00166002	PLCB4	non-mem		36	phospholipase C, beta 4
IPI00107873	PPFIA1	non-mem		10	protein tyrosine phosphatase, receptor type, f polypeptide (PTPRF), interacting protein (liprin), alpha 1
IPI00103509	PPGB	non-mem		8	protective protein for beta-galactosidase (galactosialidosis)
IPI00011770	PPIL3	non-mem		22	peptidylprolyl isomerase (cyclophilin)-like 3
IPI00022442	PPP1R12A	non-mem		6	protein phosphatase 1, regulatory (inhibitor) subunit 12A
IPI00220060	PPP2R5C	non-mem		30	protein phosphatase 2, regulatory subunit B (B56), gamma isoform
IPI00025239	PPP3CA	non-mem		29	protein phosphatase 3 (formerly 2B), catalytic subunit, alpha isoform (calcineurin A alpha)
IPI00221298	PTBP1	non-mem		38	polypyrimidine tract binding

					protein 1
IPI00186214	PTD004	non-mem		12	hypothetical protein PTD004
IPI00015920	PTPN13	non-mem		19	protein tyrosine phosphatase, non-receptor type 13 (APO-1/CD95 (Fas)-associated phosphatase)
IPI00100754	PYGB	non-mem		7	phosphorylase, glycogen; brain
IPI00184377	RAB7	non-mem		17	RAB7, member RAS oncogene family
IPI00182020	RAFTLIN	non-mem		23	raft-linking protein
IPI00024145	RENT1	non-mem		16	regulator of nonsense transcripts 1
IPI00099529	RHOC	non-mem		16	ras homolog gene family, member C
IPI00184396	RHOG	non-mem		29	ras homolog gene family, member G (rho G)
IPI00005202	RPL15	non-mem		38	ribosomal protein L15
IPI00217835	RPL17	non-mem		21	ribosomal protein L17
IPI00178346	RPL22	non-mem		7	ribosomal protein L22
IPI00219824	RPL23A	non-mem		14	ribosomal protein L23a
IPI00217766	RPL27	non-mem		18	ribosomal protein L27
IPI00001985	RPL3	non-mem		33	ribosomal protein L3
IPI00032516	RPL35A	non-mem		38	ribosomal protein L35a
IPI00063186	RPL39	non-mem		28	ribosomal protein L39
IPI00021551	RPL4	non-mem		16	ribosomal protein L4
IPI00025163	RPL5	non-mem		7	ribosomal protein L5
IPI00218593	RPL6	non-mem		27	ribosomal protein L6
IPI00185332	RPS25	non-mem		30	ribosomal protein S25
IPI00023135	RPS26	non-mem		38	ribosomal protein S26
IPI00005990	RPS29	non-mem		31	ribosomal protein S29
IPI00219934	RPS3A	non-mem		37	ribosomal protein S3A
IPI00005719	RPS9	non-mem		38	ribosomal protein S9
IPI00186100	RRAGC	non-mem		9	Ras-related GTP binding C
IPI00183356	RSU1	non-mem		28	Ras suppressor protein 1
IPI00187143	RW1	non-mem		12	RW1 protein
IPI00217943	SBF1	non-mem		24	SET binding factor 1
IPI00005728	SEC23A	non-mem		30	Sec23 homolog A (S. cerevisiae)
IPI00029740	SET	non-mem		5	SET translocation (myeloid leukemia-associated)
IPI00023149	SF1	non-mem		37	splicing factor 1
IPI00012545	SIP	non-mem		5	Siah-interacting protein
IPI00219648	SKP1A	non-mem		24	S-phase kinase-associated protein 1A (p19A)
IPI00014219	SMG1	non-mem		10	PI-3-kinase-related kinase SMG-1
IPI00181370	SPATA13	non-mem		35	spermatogenesis associated 13
IPI00184864	SQSTM1	non-mem		28	sequestosome 1
IPI00218440	SRPK1	non-mem		21	SFRS protein kinase 1
IPI00045396	STAT3	non-mem		6	signal transducer and activator of transcription 3 (acute-phase response factor)

IPI00023639	SYNCRIP	non-mem		22	synaptotagmin binding, cytoplasmic RNA interacting protein
IPI00182933	TAGLN2	non-mem		2	transgelin 2
IPI00025822	TAX1BP1	non-mem		31	Tax1 (human T-cell leukemia virus type I) binding protein 1
IPI00020210	TBRG4	non-mem		25	transforming growth factor beta regulator 4
IPI00101617	TCP1	non-mem		28	t-complex 1
IPI00009904	TIP120A	non-mem		34	TBP-interacting protein
IPI00020944	TKT	non-mem		30	transketolase (Wernicke-Korsakoff syndrome)
IPI00008266	TMPO	non-mem		5	thymopoietin
IPI00221382	TMSB4X	non-mem		8	thymosin, beta 4, X-linked
IPI00032415	TNPO2	non-mem		12	transportin 2 (importin 3, karyopherin beta 2b)
IPI00015842	TOP2A	non-mem		16	topoisomerase (DNA) II alpha 170kDa
IPI00215743	TPM1	non-mem		13	tropomyosin 1 (alpha)
IPI00185423	TRAP1	non-mem		6	heat shock protein 75
IPI00006280	TTC17	non-mem		3	tetratricopeptide repeat domain 17
IPI00104128	UBE2V1	non-mem		23	ubiquitin-conjugating enzyme E2 variant 1
IPI00029190	VANGL1	non-mem		15	vang-like 1 (van gogh, Drosophila)
IPI00009235	VPS24	non-mem		30	vacuolar protein sorting 24 (yeast)
IPI00027194	WASL	non-mem		33	Wiskott-Aldrich syndrome-like
IPI00220924	WDR1	non-mem		8	WD repeat domain 1
IPI00217384	YWHAQ	non-mem		22	tyrosine 3-monooxygenase/tryptophan 5-monooxygenase activation protein, theta polypeptide
IPI00019018	YWHAZ	non-mem		11	tyrosine 3-monooxygenase/tryptophan 5-monooxygenase activation protein, zeta polypeptide
IPI00182665	ZDHHC13	non-mem		14	zinc finger, DHHC domain containing 13
IPI00074962	ZNF183	non-mem		28	zinc finger protein 183 (RING finger, C3HC4 type)
IPI00186889	ZNF185	non-mem		28	zinc finger protein 185 (LIM domain)

Table S3. Expression for 408 genes whose protein products were identified with MS/MS. Expression values were derived from the relative frequency of SAGE tags within tissue specific libraries. Both row-normalized (mean=0, standard deviation=1) and un-normalized data are shown. Positive numbers indicate increased expression relative to normal breast tissue. Left hand column (Cluster, *C*) indicates gene assignment to one of the SOM-derived clusters based on its expression profile across all 6 subsets of tissue

		Normalized						Un-normalized					
C	*Name*	*ER-*	*ER+*	*Node-*	*Node+*	*DCIS*	*IDC*	*ER-*	*ER+*	*Node-*	*Node+*	*DCIS*	*IDC*
0	ABI1	0.5	0.5	0.5	0.5	0.2	-2.0	0	0	0	0	-11	-100
0	ACSL4	0.6	0.6	0.6	0.6	-1.2	-1.4	0	0	0	0	-5.3	-5.9
0	ACTN1	0.6	0.6	0.6	0.6	-0.6	-1.8	0	0	0	0	-3	-5.9
0	ATP1B3	0.6	0.6	0.6	0.6	-1.5	-1.0	0	0	0	0	-2.9	-2.2
0	ATP5J	1.1	0.4	0.2	0.7	-1.2	-1.2	3.7	2.6	2.3	3	0	0
0	ATP5J2	0.6	0.6	0.9	0.3	-1.3	-1.3	2.6	2.6	3	2.1	0	0
0	ATP5L	1.6	-0.1	0.2	0.4	-1.1	-1.1	5.2	2	2.5	2.9	0	0
0	ATP5O	1.1	0.2	1.0	0.1	-1.2	-1.2	4.3	2.5	4.1	2.4	0	0
0	B3GAT3	0.8	0.3	0.8	0.5	-1.3	-1.3	4.2	3.2	4.2	3.5	0	0
0	BZRP	0.8	0.8	0.6	0.4	-1.3	-1.3	2.9	3	2.6	2.4	0	0
0	C20orf142	1.1	0.4	0.5	0.5	-1.2	-1.2	7.3	4.9	5.4	5.3	0	0
0	CCT3	0.9	0.3	1.2	-0.1	-1.2	-1.2	3.4	2.4	3.8	1.8	0	0
0	CHCHD1	0.9	0.6	0.9	0.1	-1.2	-1.2	8.8	7.6	8.7	5.6	0	0
0	CPNE3	0.3	1.1	0.5	0.6	-1.2	-1.2	3.8	5.7	4.3	4.4	0	0
0	CUL2	0.7	0.4	1.3	-0.1	-1.2	-1.2	6.6	5.4	8.5	3.7	0	0
0	DDB1	0.7	0.6	0.6	0.6	-1.3	-1.3	2.8	2.7	2.6	2.7	0	0
0	EIF4G2	0.6	0.6	0.6	0.6	-1.1	-1.4	0	0	0	0	-1.7	-2
0	EPHB3	1.6	0.2	0.3	-0.1	-1.0	-1.0	8.8	4.2	4.6	3.1	0	0
0	EPLIN	0.6	0.6	0.6	0.6	-0.8	-1.7	0	0	0	0	-7.1	-11
0	FLJ10587	0.6	0.6	0.6	0.6	-1.3	-1.3	0	0	0	0	-100	-100
0	FLJ20297	0.7	0.6	1.0	0.3	-1.3	-1.3	3.2	3	3.8	2.5	0	0
0	FLJ20625	0.8	0.5	0.7	0.6	-1.3	-1.3	5.3	4.5	4.9	4.7	0	0
0	FLOT1	0.7	0.7	0.3	0.9	-1.3	-1.3	2.7	2.6	2.1	2.9	0	0
0	GARS	0.6	0.6	0.6	0.6	-1.2	-1.3	0	0	0	0	-1.9	-2
0	GNG5	0.6	0.6	0.6	0.6	-1.3	-1.3	0	0	0	0	-1.9	-1.9
0	GRIM19	0.4	0.6	1.1	0.4	-1.2	-1.2	2.1	2.4	3	2.1	0	0
0	GSN	0.6	0.6	0.6	0.6	-1.6	-0.9	0	0	0	0	-2.4	-1.6
0	HIBADH	1.4	0.0	0.8	0.1	-1.1	-1.1	11	5	8.4	5.4	0	0
0	HSPD1	0.4	0.4	0.4	0.4	0.3	-2.0	0	0	0	0	-4.5	-100
0	HSPE1	0.6	0.6	0.6	0.6	-1.1	-1.5	0	0	0	0	-1.9	-2.3
0	JWA	0.8	0.6	1.0	0.1	-1.2	-1.2	3.4	3.1	3.7	2.2	0	0
0	KIAA0103	0.7	0.7	0.9	0.3	-1.3	-1.3	2.9	2.9	3.2	2.3	0	0
0	MDH1	1.4	-0.2	1.0	-0.2	-1.0	-1.0	6.3	2	5.2	2	0	0
0	MRPL37	0.8	0.4	0.9	0.4	-1.3	-1.3	4.3	3.4	4.4	3.4	0	0
0	MTX1	1.4	-0.1	0.7	0.2	-1.1	-1.1	11.6	4.5	8.2	6	0	0
0	NCL	0.6	0.6	0.6	0.6	-1.7	-0.7	0	0	0	0	-2.4	-1.4
0	NDUFV1	0.7	0.8	0.0	1.0	-1.2	-1.2	2.6	2.7	1.7	3	0	0
0	NOLC1	0.6	0.6	0.6	0.6	-1.1	-1.5	0	0	0	0	-1.7	-2.1
0	PHGDH	0.3	0.8	0.7	0.7	-1.3	-1.3	2.9	3.8	3.5	3.5	0	0
0	PPIF	0.6	0.6	0.6	0.6	-1.5	-1.0	0	0	0	0	-2.6	-2
0	PRDX5	1.1	-0.1	1.2	-0.1	-1.1	-1.1	5.7	2.7	6	2.6	0	0
0	PSMC5	0.5	0.6	0.7	0.8	-1.3	-1.3	2	2.1	2.2	2.3	0	0

0	RAB5C	1.2	0.4	0.2	0.7	-1.2	-1.2	2.7	1.8	1.6	2.2	0	0
0	RAB7	0.6	0.6	0.6	0.6	-1.7	-0.7	0	0	0	0	-5.3	-2.9
0	RPL15	0.5	0.5	0.5	0.5	0.2	-2.0	0	0	0	0	-13	-100
0	SELT	0.9	0.5	0.7	0.5	-1.3	-1.3	3	2.5	2.8	2.5	0	0
0	SLC1A4	1.0	0.6	0.2	0.8	-1.2	-1.2	35.4	29.2	23.3	32.4	0	0
0	SNX3	0.6	0.6	0.6	0.6	-1.2	-1.3	0	0	0	0	-2.3	-2.4
0	STUB1	0.8	0.4	0.6	0.7	-1.3	-1.3	4.3	3.4	3.9	4.1	0	0
0	TOMM70A	1.2	0.4	0.5	0.3	-1.2	-1.2	4	2.7	2.9	2.5	0	0
0	TOP2A	0.6	0.6	0.6	0.6	-1.3	-1.3	100	100	100	100	0	0
0	VIM	0.6	0.6	0.6	0.6	-1.8	-0.6	0	0	0	0	-3.1	-1.6
0	VPS45A	1.3	0.1	0.5	0.4	-1.2	-1.2	6.5	3.4	4.2	4.1	0	0
0	YWHAE	0.6	0.6	0.6	0.6	-1.6	-0.9	0	0	0	0	-2	-1.4
1	COPB2	-0.4	-0.4	2.0	-0.4	-0.4	-0.4	0	0	100	1.6	0	0
1	DBN1	-0.6	1.3	1.3	-0.6	-0.7	-0.7	5.6	100	100	2.9	0	0
1	GABARAP	0.2	0.2	1.1	0.9	-1.6	-0.7	0	0	2.6	1.9	-4.8	-2.3
1	KRT8	-0.8	0.9	1.6	-0.4	-0.4	-0.9	1.6	4.3	5.4	2.2	2.2	1.3
1	MRPS23	-0.1	-0.1	1.9	0.0	-0.9	-0.9	3.2	3.2	10.7	3.3	0	0
1	PGRMC2	0.1	0.7	1.2	-0.3	-1.7	0.1	3.1	3.4	3.7	2.9	2.2	3.1
1	RPS5	-0.4	0.2	0.9	0.9	-1.7	0.1	-2.9	-1.6	0	0	-5.6	-1.8
1	ZAP128	0.3	-0.4	1.7	-0.3	-1.3	0.0	10.1	9	12.3	9.1	7.7	9.6
2	ALDOA	-0.6	-0.6	0.3	1.9	-0.6	-0.6	0	0	1.7	5.1	0	0
2	ANXA5	-0.5	-0.5	1.2	1.2	-1.3	0.0	-2.9	-2.9	0	0	-4.2	-2
2	APLP2	-0.6	-0.6	1.5	1.1	-0.6	-0.6	0	0	2.2	1.8	0	0
2	ARPC1A	-0.6	-0.6	1.4	1.2	-0.6	-0.6	0	0	2.6	2.4	0	0
2	ATP1B1	-0.6	-0.6	1.9	0.4	-0.6	-0.6	0	0	7.5	2.9	0	0
2	ATP5C1	-0.6	-0.6	0.6	1.8	-0.6	-0.6	0	0	2.4	4.7	0	0
2	BDH	-0.6	-0.6	1.3	1.3	-0.6	-0.6	0	0	100	100	0	0
2	C11orf2	-0.6	-0.6	1.4	1.1	-0.6	-0.6	0	0	2	1.7	0	0
2	C20orf24	-0.6	-0.6	1.5	1.1	-0.6	-0.6	0	0	3	2.4	0	0
2	C6orf49	-0.6	-0.6	1.4	1.2	-0.6	-0.6	0	0	2.7	2.4	0	0
2	CYP51A1	-0.6	-0.6	1.0	1.6	-0.6	-0.6	0	0	2.4	3.3	0	0
2	DPP7	-0.6	-0.6	1.3	1.3	-0.6	-0.6	0	0	2	2	0	0
2	FBP1	-0.6	-0.6	1.4	1.2	-0.6	-0.6	0	0	7.8	7.1	0	0
2	GFRA1	-0.6	-0.6	1.3	1.3	-0.6	-0.6	0	0	100	100	0	0
2	GNB2	-0.6	-0.6	1.3	1.3	-0.6	-0.6	0	0	3.5	3.4	0	0
2	GPI	-0.6	-0.6	1.4	1.1	-0.6	-0.6	0	0	2.1	1.8	0	0
2	HLA-C	-0.5	-1.2	1.2	1.2	-0.4	-0.4	-2.2	-3.2	0	0	-2.1	-2.1
2	HSPA5BP1	-0.6	-0.6	1.2	1.4	-0.6	-0.6	0	0	5	5.7	0	0
2	KIAA0763	-0.6	-0.6	1.4	1.1	-0.6	-0.6	0	0	5.8	5	0	0
2	KIAA0776	-0.6	-0.6	1.3	1.3	-0.6	-0.6	0	0	15.5	15	0	0
2	LAMA5	-0.6	-0.6	1.0	1.5	-0.6	-0.6	0	0	5.3	6.9	0	0
2	MRPS24	-1.3	-0.7	1.1	1.1	0.0	-0.2	-5.3	-4	0	0	-2.5	-2.9
2	PDHA1	-0.6	-0.6	1.5	1.1	-0.6	-0.6	0	0	2.6	2.1	0	0
2	PRDX2	-0.6	-0.6	1.1	1.5	-0.6	-0.6	0	0	2	2.5	0	0
2	QSCN6	-0.6	-0.6	1.3	1.3	-0.6	-0.6	0	0	3.7	3.7	0	0
2	RNF130	-0.6	-0.6	1.4	1.2	-0.6	-0.6	0	0	2.6	2.4	0	0
2	RPL17	-1.0	-0.2	1.2	1.2	-1.1	-0.2	-2	-1.3	0	0	-2.1	-1.3
2	RPL18	-0.9	-0.9	1.3	1.3	-0.3	-0.4	-2	-2	0	0	-1.5	-1.6
2	SCARB2	-0.6	-0.6	1.6	1.0	-0.6	-0.6	0	0	3.9	2.8	0	0
2	SEMA3C	-0.6	-0.6	1.9	0.4	-0.6	-0.6	0	0	5.1	2	0	0
2	SLC7A2	-0.6	-0.6	1.7	0.8	-0.6	-0.6	0	0	5.5	3.4	0	0
2	SNX17	-0.5	-0.5	1.9	0.3	-0.5	-0.5	0	0	6.5	2.1	0	0
2	SOD1	-0.6	-0.6	1.6	0.9	-0.6	-0.6	0	0	2.8	2	0	0
2	UGDH	-0.6	-0.6	1.4	1.2	-0.6	-0.6	0	0	3.9	3.6	0	0
3	ARF1	-1.2	-1.2	1.2	0.3	0.4	0.5	0	0	2.9	1.8	2	2.1
3	ATP6AP1	-1.2	-1.2	0.5	0.4	1.1	0.5	0	0	2.5	2.4	3.5	2.6

3	BCMP11	-1.2	-1.2	0.4	1.3	0.6	0.1	0	0	4.9	7.6	5.4	4
3	CORO1B	-1.2	-1.2	1.1	0.4	0.4	0.6	0	0	5.3	3.7	3.8	4.2
3	CYB5	-1.3	-1.3	0.9	0.4	0.6	0.6	0	0	3.4	2.6	2.9	2.8
3	GPSN2	-1.2	-1.2	1.2	0.3	0.1	0.8	0	0	6.4	4.1	3.6	5.5
3	GSTM3	-1.2	-1.2	0.1	1.1	0.9	0.3	0	0	7	12.2	10.9	7.8
3	KIAA1324	-1.2	-1.2	1.2	0.3	0.1	0.7	0	0	6.3	3.8	3.3	5
3	KRT19	-1.0	-1.0	-0.1	0.7	1.6	-0.2	0	0	2.5	4.9	7.4	2.4
3	LOC400451	-1.2	-1.2	0.7	0.1	1.0	0.7	0	0	12.6	8.7	14.3	13
3	LTBP4	-1.7	-0.7	0.6	0.6	0.6	0.6	-4	-2.3	0	0	0	0
3	LZTS2	-1.3	-1.2	0.6	0.6	0.6	0.6	-3.6	-3.4	0	0	0	0
3	MAGED2	-1.1	-1.1	-0.1	1.3	1.0	-0.1	0	0	2.9	6.8	6	2.7
3	MAL2	-1.2	-1.2	0.4	1.1	0.7	0.4	0	0	2.6	3.7	3.1	2.6
3	MLP	-1.1	-1.1	1.3	-0.3	0.7	0.5	0	0	8.4	2.6	6.3	5.5
3	MR-1	-1.3	-1.3	0.8	0.7	0.6	0.5	0	0	3.9	3.7	3.6	3.3
3	MUC1	-1.2	-1.2	1.2	0.2	0.2	0.9	0	0	4.7	2.7	2.7	4.2
3	MYO5C	-1.3	-1.3	0.7	0.7	0.2	0.9	0	0	5.8	5.6	4.3	6.3
3	PLXND1	-1.3	-1.3	0.7	0.4	0.9	0.5	0	0	6.5	5.6	7	5.8
3	PPAP2C	-1.3	-1.3	1.0	0.4	0.7	0.5	0	0	12.6	9.4	11	10
3	RAB25	-1.3	-1.3	0.5	1.0	0.7	0.4	0	0	3.9	5	4.4	3.6
3	RPL27	-1.5	-1.1	0.6	0.6	0.6	0.6	-1.6	-1.3	0	0	0	0
3	RPS9	-1.7	-0.5	0.3	0.7	1.1	-0.1	-2.1	-1.8	-1.6	-1.5	-1.4	-1.7
3	SCD	-1.3	-1.3	0.6	0.6	0.6	0.6	0	0	100	100	100	100
3	TACSTD2	-1.4	-1.2	0.6	0.6	0.6	0.6	-4	-3.7	0	0	0	0
3	TMEM30A	-1.9	-0.5	0.6	0.6	0.6	0.6	-6.3	-2.7	0	0	0	0
3	TMP21	-1.3	-1.3	0.8	0.7	0.2	0.7	0	0	3.2	3.1	2.3	3.1
3	TUBA6	-1.1	-0.5	0.0	1.1	1.3	-0.8	-2.7	-2.5	-2.3	-1.9	-1.8	-2.6
4	C1QBP	0.0	0.0	0.0	0.0	-1.7	1.5	0	0	0	0	-2.2	1.9
4	CANX	-0.8	0.6	0.6	-0.1	-1.5	1.2	1.8	2	2	1.9	1.7	2.1
4	CAV1	0.3	0.4	0.7	-0.1	-2.0	0.7	-4.2	-3.7	-2.4	-5.9	-14	-2.3
4	COL1A1	0.3	0.5	0.6	0.0	-2.0	0.5	2.1	2.4	2.6	1.6	-1.5	2.4
4	DDX3X	0.0	0.0	0.0	0.0	-1.6	1.5	0	0	0	0	-1.5	1.4
4	EEF1G	-0.2	-0.2	-0.8	1.2	-1.1	1.2	0	0	-1.3	2.8	-1.9	2.8
4	EPHX1	-0.2	0.1	-0.2	0.5	-1.6	1.5	2.6	2.7	2.6	2.8	2.2	3.1
4	MFGE8	0.5	0.5	0.5	0.5	-2.0	0.0	0	0	0	0	-9.1	-1.8
4	MLPH	-0.9	0.6	-0.4	1.5	-1.2	0.4	4.9	7.7	5.9	9.2	4.4	7.2
4	PEX19	-0.1	0.7	0.7	-0.1	-1.9	0.6	5.1	6.1	6.1	5.1	2.8	5.9
4	PPIA	0.8	0.2	0.2	0.2	-2.0	0.5	2.1	1.9	1.9	1.9	1.2	2
4	PSAP	-0.8	1.2	-0.8	0.3	-1.0	1.1	-1.4	4.6	-1.3	2.1	-2	4.4
4	RPL36	0.9	0.8	-0.6	-0.6	-1.4	0.9	1.9	1.7	-1.2	-1.2	-2.6	1.8
4	RPL39	0.2	0.6	0.4	0.2	-2.0	0.6	-1.6	-1.4	-1.5	-1.6	-2.6	-1.4
4	RPL4	0.2	0.6	0.5	0.3	-2.0	0.4	-2	-1.4	-1.5	-1.8	-5.9	-1.7
4	RPL7	0.9	0.6	-0.6	-0.6	-1.4	1.1	2.9	2.5	0	0	-1.5	3.4
4	RPLP2	0.0	0.9	0.7	-0.4	-1.8	0.5	-1.6	-1.2	-1.3	-1.8	-2.4	-1.4
4	RPS14	0.8	0.9	-0.4	-0.4	-1.7	0.8	1.4	1.5	0	0	-1.6	1.4
4	RPS15A	1.0	0.1	0.2	0.2	-1.9	0.3	2.9	1.6	1.7	1.7	-1.4	1.8
4	RPS29	0.1	0.1	0.1	0.1	-1.8	1.3	0	0	0	0	-2.1	1.2
4	SF1	0.5	0.5	0.5	0.5	-2.0	0.2	0	0	0	0	-100	-13
4	TPI1	-0.1	1.9	-0.2	-0.3	-1.1	-0.2	2	9.1	1.8	1.3	-1.4	1.6
4	TRA1	0.5	0.4	0.3	0.4	-2.0	0.3	2.9	2.7	2.5	2.7	-1.5	2.5
4	TRIM25	0.4	0.4	0.4	0.4	-2.0	0.3	0	0	0	0	-100	-7.7
4	VPS41	0.5	1.1	-0.9	0.7	-1.5	0.1	7.1	8	5	7.5	4	6.5
5	APP	1.1	-1.1	0.9	-0.9	-0.7	0.8	2	-2.3	1.6	-1.9	-1.5	1.4
5	ATP2B4	0.1	1.0	0.8	-1.2	-1.2	0.6	4	4.5	4.4	3.2	3.2	4.3
5	CNDP2	-0.5	0.4	1.5	-1.1	-0.9	0.6	5.3	7.1	9.1	4.2	4.6	7.5
5	CNP	1.4	-0.8	0.9	-1.0	-0.8	0.3	5.1	3	4.6	2.8	3	4.1
5	DAF	0.9	-0.3	0.9	-0.8	-1.4	0.7	-4	-5.6	-4	-6.3	-7.1	-4.3

5	DNCI2	0.1	0.6	1.0	-0.8	-1.6	0.6	3.4	3.8	4.1	2.8	2.2	3.8
5	EEF1A1	0.1	-0.1	1.3	-1.1	-1.1	0.9	-1.7	-1.8	-1.2	-2.2	-2.2	-1.4
5	EFHD1	-0.1	-0.6	1.8	-0.8	-0.8	0.5	6.9	6.2	9.7	5.9	5.9	7.9
5	FARP1	0.8	0.9	0.7	-1.0	-1.4	0.0	10.5	11	10.3	4.8	3.6	8.1
5	FASN	0.8	-0.5	1.3	-0.8	-1.3	0.4	12.4	9.4	13.4	8.7	7.5	12
5	FLJ14803	0.5	0.4	1.1	-0.7	-1.6	0.3	12	11.6	14.1	7.5	4.3	11
5	FLNB	0.7	-0.3	1.3	-1.0	-1.2	0.6	6	4.1	7.2	2.6	2.3	5.8
5	GTF2I	0.5	-0.2	1.3	-0.7	-1.4	0.7	8.5	6.9	10.1	5.8	4.3	8.8
5	LAMR1	0.7	0.6	0.7	-1.1	-1.4	0.6	1.4	1.2	1.4	-1.3	-1.7	1.2
5	NDUFA5	-0.5	0.6	1.2	-0.5	-1.5	0.6	2.8	3.9	4.5	2.8	1.8	3.9
5	PAI-RBP1	0.7	0.0	1.0	-0.9	-1.5	0.8	-4.3	-6.3	-3.4	-9.1	-11	-4
5	RPL30	1.0	-0.6	0.9	-0.8	-1.3	0.8	1.4	-1.1	1.2	-1.4	-2.1	1.1
5	RPL37A	0.4	0.2	1.0	-0.7	-1.7	0.8	-2.3	-2.4	-1.9	-3	-3.7	-2
5	RPL6	0.9	-0.6	1.1	-0.7	-1.3	0.6	-1.5	-2.6	-1.4	-2.7	-3.1	-1.7
5	RPLP1	0.8	0.6	0.6	-1.6	-0.9	0.6	1.7	1.3	1.2	-4	-2.2	1.3
5	RPS4X	1.0	0.4	0.6	-1.0	-1.5	0.5	2.1	1.1	1.3	-1.4	-2.3	1.2
5	RPS8	0.2	0.2	1.0	-0.9	-1.5	0.9	0	0	1.5	-2.1	-3.3	1.3
5	SET	0.9	-0.3	0.8	-0.5	-1.6	0.7	-2.7	-8.3	-3.1	-9.1	-14	-3.6
5	ZDHHC13	-0.9	0.9	1.0	-0.9	-0.9	0.9	-100	-20	-12.5	-100	-100	-20
6	ASAH1	-0.9	-0.9	1.5	-0.2	-0.3	0.9	0	0	32.3	10	8	24
6	EIF4A1	1.2	-1.8	0.4	-0.2	0.2	0.2	-1.4	-2.9	-1.8	-2.1	-1.9	-1.9
6	GAPD	0.9	-1.7	0.8	-0.4	-0.2	0.7	2.1	-7.1	1.8	-2.4	-1.8	1.5
6	GOLGA2	-0.6	-0.6	1.5	-0.6	-0.6	1.0	-100	-100	-33.3	-100	-100	-50
6	PCBP1	0.4	-2.0	0.4	0.4	0.4	0.4	-2.3	-100	-2.4	-2.4	0	0
6	PCYOX1	-1.0	-1.0	1.0	0.7	-0.7	1.0	0	0	17.5	15	2.4	18
6	PKM2	-0.8	-0.8	1.4	-0.6	-0.4	1.2	0	0	15.5	1.5	2.3	14
6	RPL11	0.4	-2.0	0.4	0.4	0.4	0.5	-1.4	-5	-1.4	-1.4	-1.3	-1.2
6	RPL3	0.4	-2.0	0.6	0.4	0.2	0.6	-1.4	-5	-1.1	-1.4	-1.7	-1.1
7	ACADVL	-1.5	0.3	0.1	-0.1	1.6	-0.4	-4.2	-2.6	-2.8	-3	-1.4	-3.2
7	ANXA1	-1.9	0.7	0.5	-0.2	0.4	0.5	-33	-7.7	-9.1	-	-10	-9.1
7	CAT	-2.0	0.7	0.4	0.0	0.4	0.6	-100	-11	-20	-	-20	-14
7	CD151	-1.8	0.7	1.1	-0.1	-0.1	0.3	1.7	2.3	2.4	2.1	2.1	2.2
7	CD44	-1.9	0.4	0.4	1.0	-0.1	0.1	-5.3	-2.9	-2.9	-2.3	-3.4	-3.2
7	CD63	-1.9	-0.3	0.6	0.6	0.6	0.6	-7.1	-2.4	0	0	0	0
7	CRAT	-2.0	0.2	0.7	0.7	0.3	0.1	-14	-2.9	0	0	-2	-3.1
7	CRIP2	-1.7	0.0	-0.2	1.1	0.9	-0.2	-4.3	3.5	2.3	8.6	7.5	2.6
7	EEF1D	-1.8	1.3	0.1	0.1	0.1	0.1	-3	1.8	0	0	0	0
7	ELOVL5	-2.0	0.7	0.3	0.3	0.3	0.3	-17	2.9	0	0	0	0
7	FAU	-1.6	0.4	0.9	-0.1	-0.6	0.9	-2	-1.6	-1.5	-1.7	-1.8	-1.5
7	GNB2L1	-1.8	0.4	0.7	0.4	-0.6	0.9	-3.2	-1.9	-1.7	-1.9	-2.5	-1.6
7	HSPA1A	-1.7	0.7	-0.4	0.4	1.1	-0.1	-25	-9.1	-16.7	-	-6.3	-14
7	LDLR	-2.0	0.3	0.4	0.4	0.4	0.4	-100	-4.2	0	0	0	0
7	MYADM	-1.3	0.6	0.7	0.7	0.7	-1.3	-100	-3.8	0	0	2.1	-100
7	NT5C2	-1.8	0.0	0.0	0.3	1.2	0.2	-1.3	1.2	1.2	1.5	2.8	1.4
7	PKD1-like	-1.1	1.7	0.1	-0.3	-0.8	0.3	4.8	7.2	5.8	5.5	5.1	6
7	RPL36A	-1.7	0.3	-0.3	-0.2	0.9	0.9	-5.9	-1.4	-2.7	-2.5	0	0
7	RPLP0	-1.3	0.4	0.8	0.6	0.7	-1.3	-100	-17	1.4	-7.1	-1.4	-100
7	RPS15	-1.9	0.7	0.3	0.3	-0.2	0.8	-9.1	1.9	0	0	-2	2.1
7	RPS24	-1.3	0.7	0.7	-1.3	0.6	0.7	-100	1.4	1.4	-100	-1.8	1.5
7	SEC61B	-1.7	0.4	-0.6	0.1	0.9	0.9	-8.3	-1.6	-5	-2.5	0	0
7	SLC39A14	-2.0	0.2	0.4	0.6	0.6	0.2	-100	-20	-12.5	-4.5	-4.8	-20
7	TNC	-1.8	0.5	0.8	-0.3	0.0	0.8	-14	-4.3	-3.2	-7.7	-6.7	-3.3
7	UGCG	-2.0	0.3	0.5	0.5	0.6	0.2	-100	-9.1	0	0	5.7	-13
7	WDR1	-2.0	0.2	0.5	0.3	0.7	0.3	-100	-25	-14.3	-20	-9.1	-20
8	ARHGAP1	1.2	-0.2	-0.5	0.1	-1.6	0.9	7.1	5.3	4.9	5.7	3.5	6.8
8	C10orf58	1.3	-0.4	0.2	0.2	-1.7	0.4	35.4	22.7	27.2	27.4	12.4	29

8	C15orf22	1.5	-0.2	0.2	-0.4	-1.5	0.4	4.1	2.8	3.1	2.6	1.8	3.2
8	CALM2	1.7	-1.4	-0.1	-0.1	-0.1	-0.1	2	-1.5	0	0	0	0
8	CFL1	1.7	-0.7	-0.2	0.2	-1.2	0.2	3.9	1.9	2.3	2.6	1.5	2.6
8	DCXR	1.3	-0.4	-1.0	0.9	-1.1	0.2	9.7	4.4	2.4	8.3	2.2	6.2
8	DDT	1.5	-1.1	0.8	-0.4	-0.9	0.1	4.3	1.9	3.7	2.6	2.1	3
8	GLB1	1.6	-0.7	0.7	-0.7	-0.9	0.1	14.5	5.4	11.2	5.3	4.5	8.5
8	GNAS	1.6	-1.6	0.0	0.0	0.0	0.0	1.8	-1.7	0	0	0	0
8	H3F3B	1.7	-0.1	-0.9	0.6	-0.9	-0.4	5.1	3.2	2.3	3.9	2.3	2.8
8	IDH2	1.6	-0.9	0.6	-0.8	-0.7	0.1	9.1	4.9	7.4	5	5.1	6.5
8	LOC114971	1.7	-0.9	0.4	0.0	-1.2	0.0	6.2	3.1	4.6	4.2	2.7	4.1
8	NDUFA4	1.2	-0.2	-0.2	0.8	-1.6	0.0	3	2.3	2.3	2.8	1.6	2.4
8	NICE-4	2.0	-0.8	0.0	-0.2	-0.7	-0.3	6.5	2.9	3.9	3.7	3.1	3.6
8	NME1	1.5	-0.1	0.4	-0.1	-1.5	-0.1	3.5	2.9	3.1	2.9	2.4	2.9
8	PFKP	1.9	-0.7	0.1	-0.2	-1.0	0.1	6.6	-7.1	-2.9	-4.5	-8.3	-2.9
8	PTPRF	0.9	-0.7	0.9	0.2	-1.7	0.4	37.9	16.2	36.9	27.4	2.8	30
8	RPL23	1.2	-0.2	-0.5	0.7	-1.6	0.4	7.4	2.7	1.6	5.6	-2	4.5
8	RPL27A	1.2	0.1	-1.2	0.4	-1.2	0.7	3.8	1.5	-1.3	2.1	-1.3	2.7
8	RPS25	1.9	-0.1	-0.5	-0.1	-1.1	-0.1	1.9	-1.3	-1.9	-1.2	-2.8	-1.3
8	SIPA1L3	1.4	0.4	-0.6	0.0	-1.5	0.3	10.6	8.6	6.6	7.7	4.8	8.3
8	SLC29A1	2.0	-0.3	-0.4	-0.4	-0.4	-0.4	97.8	6.5	0	0	0	0
8	TCP1	1.7	-0.6	-0.6	0.7	-0.6	-0.6	-1.7	-2.6	-2.6	-2.1	-2.6	-2.6
8	VIL2	1.8	-0.8	-0.8	0.4	-0.6	0.0	4.5	2.4	2.4	3.4	2.5	3
8	ZNF183	1.3	-0.6	0.5	-0.3	-1.5	0.6	5.5	3	4.4	3.4	1.7	4.5
9	ATP5A1	0.1	0.1	1.5	-1.7	0.1	0.1	0	0	1.4	-1.7	0	0
9	B3GALT4	0.1	0.1	1.5	-1.7	0.1	0.1	0	0	1.2	-1.5	0	0
9	CNN1	0.2	0.5	0.5	-2.0	0.4	0.4	-13	-4.2	-3.3	-100	-6.7	-5
9	COX5B	0.6	-1.0	1.6	-1.0	-0.1	-0.1	3.3	2.8	3.6	2.8	3.1	3.1
9	DNAJB6	0.2	0.7	0.6	-2.0	0.0	0.6	-5	-1.9	-2.3	-20	-6.7	-2.6
9	DST	0.2	0.5	0.6	-2.0	0.1	0.6	-20	-11	-5.6	-100	-25	-8.3
9	ENAH	1.1	0.0	0.6	-1.8	0.0	0.0	4.6	3.7	4.2	2.2	3.7	3.7
9	FLNA	0.0	0.0	1.5	-1.6	0.0	0.0	0	0	2	-2.2	0	0
9	HMGCS1	-0.1	-0.1	1.8	-1.3	-0.1	-0.1	0	0	2.2	-1.4	0	0
9	HNRPA2B1	0.0	0.0	1.6	-1.6	0.0	0.0	0	0	1.9	-1.8	0	0
9	HSPH1	-0.1	0.3	1.1	-1.8	-0.1	0.6	-4.2	-3.7	-2.6	-6.7	-4.2	-3.3
9	KIAA1007	1.2	-0.6	0.5	-1.7	0.2	0.3	4	-14	-3.1	-25	-6.3	-4.8
9	MAP1LC3B	0.6	0.6	0.2	-2.0	0.2	0.3	0	0	-2.3	-	-2.3	-1.9
9	NOTCH2	0.3	0.6	0.7	-1.9	-0.2	0.6	-6.7	-4.3	-2.9	-25	-11	-4.3
9	OCIA	-0.5	-0.5	1.1	-1.5	0.7	0.7	0	0	2.7	-1.7	2	1.9
9	PDLIM1	0.1	0.3	0.4	-2.0	0.6	0.6	-5.6	-3.7	-2.4	-25	0	0
9	RPL31	-0.9	0.8	1.0	-1.3	-0.5	0.8	-2.6	-1.8	-1.7	-2.8	-2.4	-1.8
9	RPS20	1.2	-0.4	1.3	-1.0	-0.5	-0.7	1.5	-1.6	1.6	-2.9	-1.8	-2.2
9	RPS7	0.0	0.0	1.6	-1.6	0.0	0.0	0	0	1.8	-1.9	0	0
9	S100A10	-0.2	-0.1	1.1	-1.8	0.7	0.2	-2.3	-2.2	-1.4	-3.3	-1.7	-2
9	SQLE	1.3	-0.4	0.8	-1.6	-0.3	0.2	17.2	9.3	15.1	4	9.9	12
9	TAGLN	0.8	0.0	0.7	-1.8	-0.3	0.6	3	-2	2.5	-	-4.5	1.6
9	TFRC	0.1	0.1	1.4	-1.7	0.1	0.1	0	0	2.3	-3.2	0	0
9	UBA52	0.1	0.1	1.5	-1.7	0.1	0.1	0	0	1.6	-2	0	0
10	ERBB2	0.9	-0.9	-1.2	0.4	1.2	-0.5	109	32.4	21.3	88.5	121	51
10	FADS2	1.5	-1.3	0.3	-0.9	0.2	0.1	52.2	20.5	38.8	24.1	37.6	36
10	HSPCA	0.4	-0.4	-1.1	0.9	1.3	-1.1	-8.3	-14	-20	-4.8	-1.5	-20
10	HSPCB	1.8	-1.0	-0.2	-0.2	0.3	-0.7	5.7	-2.3	0	0	1.4	-1.6
10	NSEP1	1.1	-1.1	0.3	0.3	0.9	-1.3	-2.2	-3.3	-2.6	-2.6	-2.3	-3.4
10	PRKDC	0.5	-1.7	-0.2	-0.2	1.3	0.2	43	-100	0	0	100	26
10	PVRL2	0.1	0.1	0.1	0.1	1.4	-1.8	0	0	0	0	1.6	-2.3
10	RPL12	1.0	-0.7	-1.1	0.9	0.8	-0.9	-1.5	-6.7	-7.7	-1.8	-2	-7.1
10	RPS3A	1.1	-0.4	-0.5	0.9	0.5	-1.5	-1.3	-3.2	-3.3	-1.6	-2	-4.5

10	RPS6	0.9	-0.6	-0.6	-0.6	1.6	-0.6	-2.2	-2.6	-2.6	-2.6	-2	-2.6
10	SERPINE1	1.1	-1.1	0.3	-1.1	1.1	-0.3	-9.1	-14	-11.1	-	-9.1	-13
10	SPTAN1	0.0	0.0	0.0	0.0	1.6	-1.5	0	0	0	0	2.4	-2.2
10	TPM1	1.0	-1.6	0.4	0.6	0.5	-0.8	-2.2	-5.3	-2.9	-2.6	-2.8	-4.3
10	VDAC3	-0.1	-0.7	-0.2	-0.8	2.0	-0.3	4.8	2.7	4.5	2.5	11.5	4.2
11	AGR2	-0.6	-0.6	-0.6	-0.6	1.8	0.7	0	0	0	0	9.6	5.2
11	ANXA2	-0.9	-0.8	-0.6	-0.2	1.3	1.3	-2.8	-2.6	-2.4	-1.9	0	0
11	ARL6IP	-0.6	-0.6	-0.6	-0.6	1.3	1.3	0	0	0	0	3.2	3.1
11	CAPN1	-0.6	-0.6	-0.6	-0.6	1.1	1.5	0	0	0	0	3.5	4.4
11	COMT	-0.6	-0.6	-0.6	-0.6	1.6	1.0	0	0	0	0	5.2	3.8
11	DHRS2	-0.5	-0.5	-0.5	-0.5	2.0	0.0	0	0	0	0	19.1	3.8
11	DP1L1	-0.6	-0.6	-0.6	-0.6	1.2	1.4	0	0	0	0	5.4	5.8
11	DSTN	-0.2	-0.9	-0.2	-1.1	1.2	1.2	-2.3	-3.4	-2.2	-3.8	0	0
11	ERBB3	-0.6	-0.6	-0.6	-0.6	1.7	0.8	0	0	0	0	2.9	1.8
11	FKSG44	-0.6	-0.6	-0.6	-0.6	1.3	1.3	0	0	0	0	3	3.1
11	FLJ11029	-0.6	-0.6	-0.6	-0.6	1.8	0.6	0	0	0	0	3.5	1.8
11	FLJ21439	-0.6	-0.6	-0.6	-0.6	1.3	1.3	0	0	0	0	100	100
11	GPAA1	-0.6	-0.6	-0.6	-0.6	1.4	1.2	0	0	0	0	2.3	2
11	GSDML	-0.6	-0.6	-0.6	-0.6	1.6	0.9	0	0	0	0	3.6	2.4
11	Hs.20726	-0.6	-0.6	-0.6	-0.6	1.3	1.3	0	0	0	0	5.7	5.6
11	KRT18	-0.6	-0.6	-0.6	-0.6	1.5	1.0	0	0	0	0	2	1.5
11	LYPLA2	-0.6	-0.6	-0.6	-0.6	1.4	1.2	0	0	0	0	2	1.8
11	MARCKS	-0.9	0.0	-0.4	-0.5	1.9	-0.1	-9.1	-3.4	-5.9	-6.3	8.5	-4.3
11	PBP	-0.6	-0.6	-0.6	-0.6	1.3	1.3	0	0	0	0	1.4	1.4
11	PIGS	-0.6	-0.6	-0.6	-0.6	1.0	1.5	0	0	0	0	4.6	6
11	PLCB4	-0.5	-0.5	-0.5	-0.5	2.0	-0.1	0	0	0	0	100	14
11	QP-C	-0.6	-0.6	-0.6	-0.6	1.3	1.3	0	0	0	0	1.7	1.7
11	RHOC	-0.6	-0.6	-0.6	-0.6	1.1	1.5	0	0	0	0	1.7	2.1
11	RPL19	-0.6	-0.9	-0.4	-0.6	1.3	1.3	-1.6	-1.8	-1.4	-1.6	0	0
11	RPL22	-0.6	-0.9	-0.4	-0.7	1.3	1.3	-1.9	-2.2	-1.7	-2	0	0
11	SLC39A9	-0.6	-0.6	-0.6	-0.6	1.1	1.5	0	0	0	0	2.8	3.5
11	SLC7A5	-0.3	-1.3	-0.7	-0.1	1.2	1.2	-4.2	-7.1	-5.3	-3.6	0	0
11	TAPBP	-0.6	-0.6	-0.6	-0.6	1.4	1.2	0	0	0	0	2.7	2.5
11	TETRAN	-0.6	-0.6	-0.6	-0.6	1.3	1.3	0	0	0	0	4.3	4.4
12	C17orf28	1.5	1.0	-0.6	-0.6	-0.6	-0.6	10.1	7.6	0	0	0	0
12	C22orf5	1.9	0.4	-0.6	-0.6	-0.6	-0.6	6.7	2.5	0	0	0	0
12	CAD	1.7	0.7	-0.6	-0.6	-0.6	-0.6	5.9	3.4	0	0	0	0
12	CGI-51	1.6	1.0	-0.6	-0.6	-0.6	-0.6	4.3	3.1	0	0	0	0
12	ch-TOG	1.7	0.8	-0.6	-0.6	-0.6	-0.6	5.5	3.4	0	0	0	0
12	COX5A	1.6	0.9	-0.6	-0.6	-0.6	-0.6	2.8	2	0	0	0	0
12	CYC1	1.5	1.1	-0.6	-0.6	-0.6	-0.6	2.3	1.9	0	0	0	0
12	E2IG4	1.4	1.1	-0.6	-0.6	-0.6	-0.6	3.3	2.8	0	0	0	0
12	ECT2	1.6	0.9	-0.6	-0.6	-0.6	-0.6	22.7	16.2	0	0	0	0
12	EEF2	1.2	1.2	-0.5	-0.3	-1.4	-0.2	0	0	-1.3	-1.2	-2	-1.1
12	EPS8	1.9	0.3	-0.6	-0.6	-0.6	-0.6	6.4	2.2	0	0	0	0
12	FKBP3	0.7	1.7	-0.6	-0.6	-0.6	-0.6	2.5	4.5	0	0	0	0
12	FLJ21749	1.5	1.1	-0.6	-0.6	-0.6	-0.6	4.2	3.4	0	0	0	0
12	FLJ32421	1.2	1.4	-0.6	-0.6	-0.6	-0.6	3.8	4.3	0	0	0	0
12	FLOT2	1.8	0.7	-0.6	-0.6	-0.6	-0.6	3.3	1.8	0	0	0	0
12	GANAB	1.4	1.1	-0.6	-0.6	-0.6	-0.6	2.2	1.9	0	0	0	0
12	GBAS	1.2	1.4	-0.6	-0.6	-0.6	-0.6	2.7	3	0	0	0	0
12	GGH	1.8	0.5	-0.6	-0.6	-0.6	-0.6	7.6	3.4	0	0	0	0
12	HDLBP	1.7	0.8	-0.6	-0.6	-0.6	-0.6	2.2	1.4	0	0	0	0
12	HINT1	1.3	1.3	-0.6	-0.6	-0.6	-0.6	2.2	2.2	0	0	0	0
12	HM13	1.3	1.0	-0.8	0.2	-1.2	-0.5	2.5	2.4	1.9	2.2	1.8	2
12	KIAA0368	1.6	0.9	-0.6	-0.6	-0.6	-0.6	2.8	1.9	0	0	0	0

12	LGALS3	1.1	1.1	0.0	-0.2	-0.6	-1.4	0	0	-1.6	-1.9	-2.5	-3.6
12	LOC51337	1.1	1.5	-0.6	-0.6	-0.6	-0.6	3.7	4.6	0	0	0	0
12	LRRC8	1.2	1.2	-0.6	-0.9	0.0	-0.9	0	0	-3.4	-4	-2.2	-4
12	MAGED1	0.8	1.7	-0.6	-0.6	-0.6	-0.6	2.5	4	0	0	0	0
12	MTCH1	1.7	0.8	-0.6	-0.6	-0.6	-0.6	2.4	1.5	0	0	0	0
12	MYH9	1.4	1.2	-0.6	-0.6	-0.6	-0.6	3	2.7	0	0	0	0
12	NDUFS2	1.8	0.6	-0.6	-0.6	-0.6	-0.6	4.7	2.4	0	0	0	0
12	PGD	1.6	0.9	-0.6	-0.6	-0.6	-0.6	2.7	1.8	0	0	0	0
12	RHBDF1	1.4	1.2	-0.6	-0.6	-0.6	-0.6	2.9	2.7	0	0	0	0
12	RPL28	1.2	1.2	-0.6	-0.2	-1.2	-0.5	0	0	-1.5	-1.2	-2	-1.4
12	RPL32	1.2	1.2	-0.8	-0.2	-1.1	-0.3	0	0	-1.6	-1.1	-1.8	-1.2
12	RPS17	0.6	1.4	-1.0	0.6	-1.0	-0.7	-2	-1.4	-3.1	-2	-3.1	-2.9
12	SLC9A3R2	1.7	0.7	-0.6	-0.6	-0.6	-0.6	7.6	4.3	0	0	0	0
12	SORT1	1.4	1.2	-0.6	-0.6	-0.6	-0.6	4.1	3.8	0	0	0	0
12	STARD3	1.8	0.5	-0.6	-0.6	-0.6	-0.6	7.3	3.4	0	0	0	0
12	SYPL	1.5	1.1	-0.6	-0.6	-0.6	-0.6	2.2	1.8	0	0	0	0
12	TRIP6	2.0	0.0	-0.5	-0.5	-0.5	-0.5	7	1.4	0	0	0	0
12	UQCRH	1.5	1.1	-0.6	-0.6	-0.6	-0.6	1.7	1.4	0	0	0	0
12	WWP2	1.5	1.0	-0.6	-0.6	-0.6	-0.6	11.4	8.6	0	0	0	0
13	ALDH4A1	0.7	0.7	-1.3	-1.3	0.3	0.9	8.4	8.6	0	0	6.7	9.2
13	BCKDHA	0.4	1.0	-1.2	-1.2	0.9	0.1	3.9	5.4	0	0	5	3.1
13	BLVRA	1.1	0.6	-1.2	-1.2	0.1	0.7	4.8	3.8	0	0	2.7	3.9
13	C9orf78	0.9	0.8	-1.3	-1.3	0.3	0.5	2.1	2	0	0	1.5	1.7
13	CCT7	0.6	0.6	-1.6	-1.0	0.6	0.6	0	0	-2.3	-1.7	0	0
13	CD59	0.4	0.5	-1.7	-0.7	0.8	0.7	-2.3	-2.2	-4.2	-3.3	-1.9	-2
13	CLDN3	0.5	0.4	-1.2	-1.2	1.3	0.1	2	1.8	0	0	2.9	1.5
13	DKFZP564	1.3	0.5	-1.2	-1.2	0.3	0.3	3.5	2.3	0	0	2	2.1
13	ENTPD8	0.7	0.6	-1.3	-1.3	0.3	1.0	3.3	3.1	0	0	2.6	3.8
13	HSGP25L2	0.9	0.6	-1.3	-1.3	0.6	0.4	1.8	1.6	0	0	1.6	1.4
13	JUP	0.8	0.6	-1.3	-1.3	0.7	0.6	1.7	1.5	0	0	1.6	1.5
13	MGC10084	1.1	0.6	-1.2	-1.2	0.6	0.2	27.8	21.6	0	0	21	16
13	MGC5395	1.5	0.1	-1.1	-1.1	0.6	0.0	4.7	2.1	0	0	3	1.9
13	PABPC1	0.6	0.6	-0.7	-1.8	0.6	0.6	0	0	-1.4	-2.6	0	0
13	PHLDA1	0.6	0.6	-1.9	-0.5	0.6	0.6	0	0	-5.6	-2.4	0	0
13	PPP1CB	0.8	0.5	-1.2	-1.2	0.0	1.0	3.4	2.9	0	0	2	3.7
13	RAB1B	0.5	1.0	-1.3	-1.3	0.5	0.5	2	2.5	0	0	1.9	2
13	RAB6A	0.8	1.2	-1.2	-1.2	0.2	0.3	3.6	4.4	0	0	2.6	2.7
13	SLC11A2	1.2	0.4	-1.2	-1.2	0.6	0.3	12.6	8.6	0	0	9.6	8.1
13	TMSB4X	0.6	0.6	-1.7	-0.7	0.6	0.6	0	0	-2.1	-1.2	0	0
13	TXN	0.6	0.6	-1.4	-1.2	0.6	0.6	0	0	-1.8	-1.6	0	0
14	ACO2	0.4	0.7	-1.8	0.5	0.7	-0.5	-14	-3.7	-100	-9.1	-3.8	-50
14	CLCN3	1.0	1.0	-1.6	0.2	-0.3	-0.3	0	0	-11.1	-3.3	-5.6	-5.6
14	CLU	0.6	0.6	-1.6	1.2	-0.3	-0.4	0	0	-4.5	1.2	-1.9	-2.1
14	CTNNAL1	1.0	1.0	-1.6	0.2	-0.3	-0.3	0	0	-12.5	-3.8	-6.3	-6.3
14	DDX5	0.4	0.4	-2.0	0.4	0.4	0.5	1.6	2	-16.7	1.6	2	2.2
14	EPHA2	0.4	0.4	-2.0	0.3	0.4	0.4	0	0	-100	-6.3	0	0
14	F11R	0.0	0.0	-1.5	1.6	0.0	0.0	0	0	-1.4	1.6	0	0
14	GBF1	0.6	0.5	-1.9	0.3	0.7	-0.3	-6.7	-7.7	-33.3	-10	-5.9	-17
14	GEM	0.6	0.7	-1.3	0.4	0.8	-1.3	-14	-11	-100	-25	-4.5	-100
14	HLA-A	0.1	0.1	-1.8	1.4	0.1	0.1	0	0	-2.4	1.6	0	0
14	IGHG1	1.3	0.3	-1.4	0.8	-0.5	-0.5	6.8	2.9	-2.9	5	0	0
14	ITGB1	0.4	0.4	-2.0	0.4	0.4	0.4	0	0	-100	-2.1	-1.5	-1.7
14	LDHB	0.5	0.5	-2.0	0.5	0.4	0.1	-7.1	-6.7	-100	-8.3	-10	-20
14	LITAF	0.6	0.1	-1.8	0.6	0.9	-0.3	-4.3	-6.7	-16.7	-4.3	-2.8	-9.1
14	MGST1	1.2	-0.2	-1.7	0.5	0.5	-0.2	2.4	2.2	2	2.3	2.3	2.2
14	NAGLU	0.5	0.5	-2.0	0.5	0.0	0.5	-5.3	-8.3	-100	-7.1	-25	-7.1

14	NPM1	0.7	1.0	-1.4	0.7	-1.0	0.0	-1.4	-1.3	-2	-1.4	-1.9	-1.6
14	PPP2CB	0.1	0.9	-1.6	0.9	0.4	-0.8	-2.9	-2.3	-4.2	-2.3	-2.7	-3.6
14	RPL10A	0.6	0.6	-1.9	0.3	0.6	-0.2	1.2	1.3	-100	-	-1.5	-33
14	RPL26	0.4	0.4	-2.0	0.4	0.4	0.4	-2.1	-1.4	-100	-2.9	-2.1	-1.5
14	RPL35A	0.0	1.2	-1.8	0.5	0.5	-0.3	-1.7	-1.2	-2.4	-1.5	-1.5	-1.8
14	RPL38	1.3	-0.5	-1.1	1.2	-0.4	-0.6	1.8	-1.6	-2.7	1.5	-1.4	-1.9
14	RPL5	0.5	0.7	-1.9	0.0	0.0	0.7	-1.9	-1.5	-7.1	-2.9	-3	-1.4
14	RPL7A	0.6	0.0	-2.0	0.6	0.5	0.3	-2.9	-8.3	-25	-3.2	-4.5	-5.9
14	RPS16	0.8	0.6	-1.3	0.8	0.3	-1.3	-1.4	-1.5	-2.6	-1.4	-1.7	-2.6
14	RPS23	0.4	0.4	-2.0	0.4	0.4	0.4	-1.7	-1.6	-100	-2.2	-4	-1.3
14	RPS3	0.0	0.0	-1.6	1.6	0.0	0.0	0	0	-1.3	1.3	0	0
14	SLC9A3R1	0.3	-0.2	-1.6	1.3	0.6	-0.4	6.1	5.1	2.6	7.9	6.6	4.9
14	SOD2	0.7	0.2	-1.3	0.5	1.0	-1.3	-17	-25	-50	-20	-13	-50
14	TPT1	0.2	1.3	-1.8	0.2	0.0	0.1	-1.2	1.1	-5.9	-1.3	-1.7	-1.5
15	ARPC1B	-0.4	1.9	-0.2	-0.8	0.2	-0.8	3.6	5.5	3.8	3.3	4.1	3.3
15	BANF1	-0.9	0.8	-0.9	1.0	1.0	-0.9	-100	-10	-100	2.4	2.5	-100
15	BCAP31	0.0	0.7	-1.0	0.0	1.5	-1.2	2.7	3.1	2.2	2.7	3.5	2.1
15	COX6C	-0.7	1.0	-0.8	1.5	-0.7	-0.2	7.1	22.5	6.4	27.1	7.4	12
15	DNAJB1	-1.2	0.1	-0.1	0.5	1.5	-0.9	-5.9	-4.8	-5	-4.5	-3.7	-5.6
15	FXYD3	-1.0	0.9	-0.8	0.3	1.4	-0.7	2.3	4.5	2.5	3.8	5	2.6
15	GLO1	-0.8	1.9	-0.5	0.1	-0.2	-0.5	2.6	3.5	2.7	2.9	2.8	2.7
15	NACA	-0.8	0.0	-0.8	0.8	1.6	-0.8	-1.6	-1.5	-1.6	-1.4	-1.3	-1.6
15	RPL13	-0.6	1.3	-1.4	0.2	0.8	-0.3	-2.7	-1.5	-3.2	-2.2	-1.8	-2.5
15	RPL35	-0.7	1.5	-1.1	-0.6	0.5	0.5	-1.5	1.3	-2	-1.4	0	0
15	RPS11	-1.3	0.8	-1.3	0.8	0.3	0.8	-2.8	-2	-2.8	-2	-2.2	-2
15	RTN4	-0.9	0.6	-1.6	0.6	0.7	0.7	-5.6	-2.3	-7.1	-2.2	-2	-2.1
15	S100A14	-0.7	0.7	-0.9	1.4	0.5	-0.9	1.7	2.3	1.6	2.6	2.2	1.6
15	SPINT2	-0.9	-0.4	-0.6	1.2	1.4	-0.7	2.7	3.4	3.2	5.8	6.1	3
15	SQSTM1	0.1	0.1	-1.2	1.0	1.2	-1.1	0	0	-2.2	1.5	1.9	-2
15	VAMP5	-0.2	1.5	-1.2	0.0	0.8	-0.9	2.5	3.2	2.1	2.6	2.9	2.2

Appendix B

Table S1. IPI identifier for 2235 unmodified proteins identified with MS/MS in the HMEC cell line and the duplicate cancer mixture runs. The presence of 8 forms of PTMs (1's) in this subset of proteins was identified by iterative searches against MS/MS spectra using the spectra filter and threshold parameters as indicated. False positive rates were determined using a reverse database methodology and were standardized by picking appropriate values for the e-value thresholds. 234 "core" proteins (yellow) had their unmodified protein forms identified in all 3 runs and were used to determine differential PTMs. Although PTMs were detected among non-"core" proteins (red), they were not included in subsequent analysis due to the absence of the corresponding unmodified form in one of the runs.

	HMEC Unmodified	SCX1 Unmodified	SCX2 Unmodified	HMEC Acetylation	HMEC OGlcNac	HMEC Glucosylation	HMEC Hydroxylation	HMEC C-Mannosylation	HMEC Palmitoylation	HMEC Phosphorylation	HMEC S-Nitrosylation	CANCER1 Acetylation	CANCER1 OGlcNac	CANCER1 Glucosylation	CANCER1 Hydroxylation	CANCER1 C-Mannosylation	CANCER1 Palmitoylation	CANCER1 Phosphorylation	CANCER1 S-Nitrosylation	CANCER2 Acetylation	CANCER2 OGlcNac	CANCER2 Glucosylation	CANCER2 Hydroxylation	CANCER2 C-Mannosylation	CANCER2 Palmitoylation	CANCER2 Phosphorylation	CANCER2 S-Nitrosylation
log(e-value)<	-3.0	-3.0	-3.0	-1.9	-1.7	-1.8	-1.6	-1.9	-1.7	-1.6	-1.9	-1.6	-1.6	-1.6	-1.3	-1.8	-1.4	-1.4	-1.6	-1.9	-1.6	-1.6	-1.4	-2.2	-1.5	-1.4	-1.8
Contrast angle	40	40	40	73	73	73	73	73	73	73	73	80	80	80	80	80	80	80	80	80	80	80	80	80	80	80	80
False positive rate (%)	1	1	1	5	5	5	5	5	5	5	5	5	5	5	5	5	5	5	5	5	5	5	5	5	5	5	5
IPI00159899		1	1	0	1	0	0	0	1	0	0	0	1	0	0	0	0	0	1	1	0	1	0	1	1	0	0
IPI00256684		1	1	0	1	0	0	0	0	0	0	0	0	0	1	0	0	0	0	0	1	0	0	0	1	0	0
IPI00016621		1	1	0	1	0	0	0	0	0	0	0	0	0	0	0	0	0	0	0	0	0	0	0	1	1	0
IPI00220991		1	1	0	1	1	0	0	0	0	0	0	0	0	0	0	0	0	0	0	0	0	0	0	0	0	0
IPI00215914		1	1	0	1	0	0	0	0	0	0	0	0	0	1	0	0	0	0	0	0	0	0	0	0	0	0
IPI00471928		1	1	1	1	0	0	0	0	0	0	0	0	0	1	0	0	0	0	0	0	0	0	0	0	0	0
IPI00303476		1	1	0	1	0	1	0	0	1	0	0	0	0	0	0	0	0	0	0	0	0	0	0	0	0	0
IPI00024920		1	1	0	1	0	0	0	0	0	0	0	0	0	0	0	0	0	0	0	0	0	0	0	0	0	0
IPI00220487		1	1	0	1	0	0	0	0	0	0	0	0	0	0	0	0	0	0	0	0	0	0	0	0	0	0
IPI00007611		1	1	0	1	0	0	0	0	0	0	0	0	0	0	0	1	0	0	0	0	0	0	0	0	0	0
IPI00465178		1	1	0	1	0	0	0	0	0	0	0	0	0	0	0	1	0	0	0	0	0	1	0	0	0	0
IPI00007682		1	1	0	1	0	0	0	1	0	0	0	0	0	0	0	0	0	0	0	0	0	0	0	0	0	0
IPI00007812		1	1	0	1	0	0	0	0	0	0	0	0	0	0	0	0	0	0	0	0	0	0	0	0	0	0
IPI00299571		1	1	0	1	0	0	0	0	0	0	0	0	1	0	0	0	0	0	0	0	1	0	0	0	0	0
IPI00004488		1	1	0	1	0	0	0	0	0	0	0	0	0	0	0	0	0	0	0	0	0	0	0	0	0	0
IPI00019906		1	1	0	1	0	0	0	0	0	0	0	0	0	0	0	1	0	0	0	0	0	0	0	0	0	0
IPI00024726		1	1	0	1	0	0	0	0	0	0	0	0	0	0	0	0	0	1	0	0	0	0	0	1	0	0
IPI00009236		1	1	0	1	0	0	0	0	0	0	0	0	0	0	0	0	0	0	0	0	0	0	0	0	0	0
IPI00297160		1	1	0	1	1	0	0	0	0	0	0	0	0	0	0	0	0	0	0	1	0	0	0	0	0	0
IPI00010896		1	1	0		0	0	0	0	0	0	0	0	0	0	0	0	0	0	0	0	0	0	0	1	0	0
IPI00001960		1	1	0	1	0	0	0	0	0	0	0	0	0	0	0	0	0	0	0	0	0	0	0	0	0	0
IPI00455383		1	1	0	1	0	0	0	0	1	1	0	0	0	1	0	0	0	1	0	0	1	1	0	0	0	0
IPI00375513		1	1	0	1	0	0	0	0	0	0	0	0	0	0	0	0	0	0	1	0	0	0	0	0	0	0
IPI00016613		1	1	0	1	0	0	0	0	0	0	0	0	0	0	0	1	0	0	0	0	0	0	0	0	0	0
IPI00017292		1	1	0	1	1	0	1	0	0	0	0	0	1	1	0	0	0	0	0	0	0	0	0	1	0	0
IPI00029601		1	1	0	1	0	1	0	0	0	0	0	0	0	0	0	0	1	0	0	0	0	0	0	0	0	0
IPI00028931		1	1	0		0	0	0	1	0	0	0	0	0	0	0	0	0	0	1	1	0	0	0	1	0	0
IPI00289334		1	1	0	1	1	1	0	0	0	1	0	0	0	0	0	0	0	0	0	0	0	0	0	0	0	0
IPI00022793		1	1	0	1	0	0	0	1	0	0	0	0	1	0	0	0	0	0	0	0	0	0	0	0	1	0

IPI00171903		1	1	1	1	0	0	0	0	0	0	0	0	0	0	0	0	0	0	0	0	0	0	0	0	0	0	0
IPI00013744		1	1	0		0	0	0	0	0	0	1	0	0	0	0	1	1	0	0	0	0	0	0	0	0	0	0
IPI00215995		1	1	0	1	0	0	0	1	1	0	0	0	0	1	0	0	0	0	1	0	0	0	1	0	0	0	0
IPI00027505		1	1	0	1	0	0	0	0	0	0	0	1	0	0	0	0	0	0	0	0	0	0	0	0	0	0	0
IPI00220847		1	1	0	1	0	0	0	0	0	0	0	0	1	1	0	0	0	0	0	1	0	1	0	1	0	1	0	1
IPI00000070		1	1	0	1	0	0	0	0	0	0	0	0	0	0	0	1	0	0	0	0	0	0	0	0	0	0	0
IPI00217975		1	1	0	1	0	0	0	0	1	0	0	0	0	0	0	0	0	0	0	0	0	0	0	1	0	0	0
IPI00030910		1	1	0	1	0	0	0	0	0	0	0	0	1	0	0	0	0	0	0	0	0	0	0	0	0	0	0
IPI00023461		1	1	0	1	0	0	0	1	0	0	1	0	0	0	0	0	0	0	0	0	0	0	0	0	0	0	1
IPI00216184		1	1	0	1	0	0	0	0	0	0	0	1	0	0	0	0	0	0	0	1	1	0	0	0	0	0	0
IPI00026952		1	1	0		0	0	0	0	0	0	0	0	0	0	0	0	0	0	0	0	1	0	0	0	0	0	0
IPI00168184		1	1	0	1	1	0	0	0	0	0	0	0	0	0	0	0	0	0	0	0	0	0	0	0	0	0	0
IPI00017367		1	1	0	1	0	0	0	0	0	0	0	0	0	1	0	0	0	0	0	0	0	0	0	0	0	0	0
IPI00024705		1	1	0	1	0	0	0	0	0	0	0	0	0	0	0	0	0	0	0	0	0	0	1	0	0	0	0
IPI00019472		1	1	0	1	0	0	0	0	0	0	0	0	0	0	0	0	0	0	0	0	0	0	1	0	0	0	0
IPI00007188		1	1	0	1	0	0	0	0	0	0	0	0	0	0	0	0	0	0	0	0	0	0	1	0	0	0	0
IPI00220194		1	1	0	1	0	0	0	0	0	0	0	0	0	0	0	0	0	0	0	0	1	0	0	0	0	0	0
IPI00027493		1	1	1	1	0	0	0	0	0	0	0	0	0	0	0	0	0	0	1	0	0	0	0	0	0	0	0
IPI00333015		1	1	0	1	1	0	0	0	0	1	0	0	0	1	0	1	0	0	0	0	1	0	0	0	0	0	0
IPI00022462		1	1	0	1	0	0	0	0	0	0	1	0	0	0	0	0	0	0	0	0	0	0	0	0	0	0	0
IPI00298994		1	1	0	1	0	0	0	0	0	0	0	1	1	0	0	0	0	0	0	0	1	0	0	1	0	0	0
IPI00028055		1	1	0	1	0	0	0	0	0	0	0	0	0	1	0	0	0	0	0	0	0	0	0	0	0	0	0
IPI00027230		1	1	0	1	0	0	0	0	0	0	1	0	0	0	0	0	0	0	0	0	0	0	0	0	0	0	0
IPI00013847		1	1	0	1	0	0	0	0	0	0	0	0	0	0	0	0	0	0	0	0	0	0	1	0	0	0	0
IPI00026964		1	1	0	1	0	0	0	0	0	0	0	1	0	0	0	0	0	0	0	0	0	0	0	0	0	0	0
IPI00216308		1	1	0	1	0	0	0	0	0	0	0	0	0	0	0	0	0	0	0	0	0	0	0	0	0	0	0
IPI00419707		1	1	0	1	0	1	0	0	0	0	1	0	0	1	0	0	0	0	0	0	0	1	0	0	0	0	0
IPI00009895		1	1	0	1	0	0	0	0	0	0	0	0	0	0	0	0	0	0	0	0	0	0	0	0	0	0	0
IPI00441320		1	1	0	1	0	0	0	0	0	0	0	0	1	0	0	0	0	0	0	0	0	0	0	0	0	0	0
IPI00011522		1	1	0	1	0	0	1	0	0	0	0	0	0	0	0	0	0	0	0	0	0	0	0	0	0	0	0
IPI00021439		1	1	1	1	0	1	0	0	0	1	0	0	0	1	0	0	0	0	0	0	0	1	0	0	0	0	0
IPI00013508		1	1	0	1	0	1	0	1	0	0	0	0	0	0	0	1	0	0	0	0	0	0	0	0	0	0	0
IPI00013808		1	1	0	1	0	1	0	0	0	0	0	0	0	0	0	0	0	0	0	0	0	0	1	0	0	0	0
IPI00005159		1	1	0	1	0	0	0	0	0	0	0	0	0	0	0	0	0	0	0	0	0	0	0	0	0	0	0
IPI00021812		1	1	0	1	0	1	1	1	1	0	0	0	1	1	0	1	1	0	1	0	0	1	0	0	0	0	0
IPI00465439		1	1	0		0	1	0	0	0	0	1	0	0	0	0	0	0	0	0	0	0	0	0	0	0	0	0
IPI00218918		1	1	0	1	0	0	0	0	0	0	0	0	0	0	0	0	0	0	0	0	0	0	0	0	0	0	0
IPI00024095		1	1	0	1	0	0	0	0	0	0	0	1	0	0	0	0	0	0	0	0	0	0	0	0	0	0	0
IPI00221225		1	1	0	1	0	0	0	0	0	0	0	0	0	0	0	0	0	0	0	0	0	0	0	0	0	0	0
IPI00329801		1	1	0	1	0	0	0	0	0	0	0	0	0	0	0	0	0	0	0	0	0	0	0	0	0	0	0
IPI00002459		1	1	0	1	0	0	0	0	0	0	0	0	0	0	0	1	0	0	0	0	0	0	0	0	0	0	0
IPI00007426		1	1	0	1	0	0	0	0	0	0	0	0	0	0	0	1	1	0	0	0	0	0	1	0	0	0	0
IPI00000477		1	1	0	1	0	0	0	0	0	0	0	0	0	0	0	0	0	0	0	0	0	0	0	0	0	0	0
IPI00289499		1	1	0		0	1	0	0	0	0	0	0	0	0	0	1	0	0	0	0	1	0	0	0	0	0	0
IPI00220935		1	1	0	1	0	0	0	0	0	0	0	0	0	0	0	1	0	0	0	0	1	0	0	0	0	0	0
IPI00456750		1	1	0	1	0	0	0	0	0	0	0	0	0	0	0	1	0	0	0	0	0	0	0	0	0	0	0
IPI00395627		1	1	0		0	0	0	0	0	0	0	0	0	1	0	0	0	0	0	0	1	0	0	0	0	0	0
IPI00020599		1	1	1	1	0	0	0	0	0	0	1	0	0	0	0	0	0	0	0	0	0	0	0	0	0	0	0
IPI00025084		1	1	0	1	1	0	0	0	1	0	0	1	0	1	0	0	0	0	0	0	0	0	0	0	0	0	0
IPI00005969		1	1	0	1	0	0	0	0	0	0	0	0	0	0	0	0	0	0	0	0	0	0	0	0	0	0	0
IPI00297779		1	1	1	1	0	0	0	0	0	0	0	0	1	0	0	0	0	0	0	0	0	0	0	0	0	0	0
IPI00027626		1	1	0	1	0	0	0	0	0	0	1	0	0	0	0	0	0	0	0	0	0	0	0	0	0	0	0
IPI00013122		1	1	1	1	0	1	0	0	0	0	0	0	0	0	0	0	0	0	0	0	0	0	0	0	0	0	0
IPI00016786		1	1	0	1	1	0	0	0	0	0	0	0	0	0	0	0	0	0	0	0	0	0	0	0	0	0	0
IPI00012011		1	1	0	1	1	1	0	0	0	0	0	0	0	1	0	0	0	0	0	0	0	0	0	0	0	0	0
IPI00298237		1	1	0	1	0	0	0	0	0	0	0	0	0	0	0	0	0	0	0	0	0	0	0	1	0	0	0

IPI00007058		1	1	1	1	C	C	C	C	C	C	C	1	1	C	C	C	C	C	C	1	C	C	C	C	C	C
IPI00024403		1	1	C	1	C	C	C	C	C	C	C	C	C	C	C	C	C	C	C	C	C	C	C	C	1	1
IPI00383539		1	1	C	1	C	C	C	C	C	C	C	C	C	1	C	C	C	C	C	C	C	1	C	C	C	C
IPI00442073		1	1	C	1	C	C	C	C	C	C	C	C	C	C	C	C	C	C	C	C	C	C	C	C	C	C
IPI00215948		1	1	C	1	C	C	C	C	C	C	C	C	C	C	C	C	1	C	C	C	C	1	C	1	1	C
IPI00219742		1	1	C	1	C	C	C	C	C	C	C	C	C	1	C	C	1	C	C	C	C	1	C	C	C	C
IPI00295741		1	1	1	1	C	C	C	C	C	1	C	C	C	C	C	C	C	C	C	C	C	C	C	C	C	1
IPI00003406		1	1	C	1	C	C	C	C	C	C	C	C	C	C	C	C	C	C	C	C	C	C	C	C	C	C
IPI00015911		1	1	C	1	C	C	C	C	C	C	C	C	C	C	C	C	C	C	C	C	1	C	C	C	C	C
IPI00012535		1	1	C	1	C	C	C	C	C	C	C	C	C	C	C	C	C	C	C	C	C	C	C	C	C	1
IPI00456969		1	1	C	1	C	1	C	C	C	C	C	1	1	C	C	C	1	C	1	1	1	C	C	1	C	C
IPI00216348		1	1	C	1	C	C	C	C	C	C	C	C	C	C	C	C	C	C	C	C	C	C	C	C	C	C
IPI00011592		1	1	C	1	C	C	C	C	C	C	C	C	C	C	C	1	C	C	C	C	C	C	C	C	1	C
IPI00031045		1	1	C	1	C	C	C	C	C	C	C	C	C	C	C	C	C	C	C	C	C	C	C	C	C	C
IPI00011416		1	1	C	1	C	C	C	C	C	C	C	C	C	C	C	C	C	C	C	C	C	C	C	C	C	1
IPI00025447		1	1	1	1	C	1	C	1	C	1	1	C	1	C	1	C	C	C	1	C	1	C	1	C	C	C
IPI00186290		1	1	C	1	C	1	C	C	C	C	C	C	C	1	1	C	C	C	C	C	C	C	C	C	C	C
IPI00017184		1	1	C	1	C	C	C	C	C	C	C	C	C	C	C	C	C	1	C	C	C	C	C	C	C	C
IPI00005578		1	1	C	1	C	C	C	C	C	C	C	C	C	C	C	C	C	C	C	C	C	C	C	C	C	C
IPI00025491		1	1	C	1	C	1	C	C	C	C	C	C	C	1	C	C	C	C	C	C	C	C	C	C	C	C
IPI00006935		1	1	C	1	C	C	C	C	C	C	C	C	C	C	C	C	C	C	C	C	C	C	C	C	C	C
IPI00465248		1	1	C	1	C	1	C	C	C	C	C	C	C	1	C	C	C	C	C	C	1	C	C	1	C	C
IPI00218474		1	1	C	1	C	C	C	1	C	C	C	C	C	C	C	C	C	C	C	C	C	C	C	C	1	C	C
IPI00008918		1	1	C	1	C	C	1	C	C	C	C	C	C	1	C	C	1	C	C	C	C	C	C	C	C	C
IPI00013452		1	1	1	1	C	C	C	1	C	C	C	C	1	1	C	C	C	C	C	C	C	C	C	C	C	C
IPI00383313		1	1	C	1	C	C	C	C	C	C	C	C	C	1	C	C	C	C	C	C	C	C	C	C	C	C
IPI00009904		1	1	C	1	C	C	C	C	C	C	C	C	C	C	C	C	1	C	C	C	C	C	C	C	C	C
IPI00418433		1	1	C	1	1	1	C	1	C	C	C	C	C	1	C	C	C	C	C	1	1	C	C	C	C	C
IPI00219005		1	1	C	1	C	C	C	C	C	C	C	C	C	C	C	C	C	C	C	C	C	C	C	C	C	C
IPI00328161		1	1	C	1	C	C	C	C	C	C	1	C	C	C	C	C	C	C	C	C	C	C	C	C	C	C
IPI00031023		1	1	1	1	C	C	C	C	C	C	C	C	C	C	C	C	C	C	C	C	C	C	C	C	1	C
IPI00333541		1	1	C	1	C	1	C	1	1	C	C	C	C	1	C	1	1	C	C	C	C	C	C	C	C	C
IPI00022418		1	1	C	1	C	C	C	C	C	C	C	C	C	C	C	C	C	C	C	C	C	1	C	C	1	C
IPI00179890		1	1	C	1	1	C	C	C	C	C	C	C	C	C	C	C	C	C	C	C	C	C	C	C	C	C
IPI00219018		1	1	C	1	C	1	C	C	C	1	C	C	C	1	C	C	C	C	C	C	C	C	C	C	C	C
IPI00031461		1	1	C	1	C	C	C	C	C	C	C	C	C	C	C	C	C	C	C	C	C	C	C	C	1	C
IPI00220766		1	1	C	1	C	C	C	C	C	C	C	C	C	C	C	C	C	C	C	C	C	C	C	C	C	C
IPI00215685		1	1	C	1	C	C	C	C	C	C	C	C	C	C	C	C	C	C	C	C	C	C	C	C	C	C
IPI00016801		1	1	C	1	C	C	C	C	C	C	C	C	C	C	C	C	C	C	C	1	1	C	C	C	C	C
IPI00003348		1	1	C	1	C	C	C	C	C	C	C	1	C	C	1	C	C	C	C	C	C	C	C	C	C	C
IPI00013896		1	1	C	1	C	C	C	C	C	C	C	1	C	C	C	C	1	C	C	C	C	C	C	C	C	C
IPI00018206		1	1	C	1	C	C	C	C	1	C	C	C	C	C	C	C	C	C	C	C	C	C	C	C	C	C
IPI00027497		1	1	C	1	C	C	C	C	C	C	C	C	C	C	C	C	C	C	C	C	C	C	C	C	C	C
IPI00025252		1	1	1	1	C	1	C	C	C	C	C	C	1	C	C	C	C	C	C	C	C	C	C	C	C	C
IPI00157144		1	1	C		1	C	C	C	C	C	C	C	C	C	C	C	C	C	C	C	C	C	C	C	C	C	C
IPI00031522		1	1	C	1	C	C	C	C	C	C	C	C	C	C	C	C	1	1	C	C	C	C	C	C	C	C
IPI00453473		1	1	C	1	C	C	C	C	C	C	C	C	C	C	C	C	C	C	C	C	C	C	C	C	C	C
IPI00008475		1	1	C	1	C	C	C	C	C	C	C	C	C	C	C	C	C	C	C	C	C	C	C	C	C	C
IPI00304925		1	1	C		1	C	C	C	C	C	C	C	C	1	C	1	C	C	1	C	C	C	C	C	C	C
IPI00003362		1	1	C	1	1	C	C	C	C	C	C	C	C	1	C	C	C	C	C	C	C	C	C	C	C	C
IPI00007765		1	1	C	1	C	C	C	C	C	C	C	C	C	C	C	C	C	1	C	C	C	C	1	C	C
IPI00025512		1	1	C	1	C	1	C	C	1	C	C	C	C	C	C	C	C	C	C	C	C	C	C	1	C
IPI00414676		1	1	C	1	C	1	C	C	C	C	1	C	1	C	C	1	C	C	1	C	C	C	C	C	C
IPI00472102		1	1	C	1	C	C	C	C	C	C	C	C	C	C	C	C	C	C	C	C	C	C	C	C	C	1
IPI00000877		1	1	C	1	C	C	C	C	C	C	C	C	C	C	C	C	C	C	1	C	C	C	1	C	C
IPI00009342		1	1	1	1	1	C	C	C	C	C	C	C	1	1	C	C	C	C	1	C	C	C	C	C	C	C

IPI00010105		1	1	C	I	C	C	C	C	C	C	C	C	C	1	C	C	C	C	C	C	C	C	C	C	C	C
IPI00011633		1	1	C	I	C	C	C	C	C	C	C	C	C	C	C	C	C	C	C	C	C	C	C	C	C	C
IPI00420079		1	1	1	I	C	C	C	C	C	C	C	1	C	C	C	C	1	C	C	C	1	C	C	C	C	C
IPI00328163		1	1	C	I	C	1	C	C	C	C	C	C	C	C	C	C	C	C	C	C	C	C	C	C	C	C
IPI00412243		1	1	C	I	C	C	C	C	C	C	C	C	C	C	1	C	C	C	C	C	C	C	C	C	C	C
IPI00220985		1	1	C	I	C	C	C	C	C	C	C	C	C	1	C	C	C	C	C	1	C	C	C	C	C	C
IPI00418411		1	1	C	I	C	C	C	C	1	C	C	C	C	C	1	C	C	C	C	C	C	C	C	C	C	C
IPI00001718		1	1	C	I	C	C	C	C	C	C	C	C	C	C	C	C	C	C	C	C	C	C	1	C	1	C
IPI00027032		1	1	C	I	C	C	C	C	C	C	C	C	C	C	C	1	C	C	C	C	C	C	C	C	C	1
IPI00183169		1	1	C		C	C	C	1	1	C	C	C	C	C	C	C	C	C	C	C	C	C	C	C	1	C
IPI00030919		1	1	C	I	C	C	C	C	C	C	C	C	C	1	C	C	C	1	C	C	C	C	C	C	C	C
IPI00022143		1	1	C	I	C	C	C	C	1	C	C	C	C	C	C	C	C	C	1	C	C	C	C	C	C	C
IPI00291006		1	1	C	I	1	C	C	C	C	1	C	C	C	C	C	C	C	1	1	C	C	C	C	C	C	C
IPI00002236		1	1	C	I	C	C	C	C	C	C	C	C	C	C	C	C	C	C	C	C	C	C	C	C	C	C
IPI00031605		1	1	C	I	C	C	C	C	C	C	C	C	C	C	C	C	C	C	C	C	C	C	C	C	C	C
IPI00033494		1	1	C		C	C	C	C	C	C	C	C	C	C	C	C	C	C	C	C	C	C	C	C	C	C
IPI00397526		1	1	C	I	C	1	C	1	C	C	C	C	C	1	C	C	1	C	C	C	C	C	C	C	C	1
IPI00019502		1	1	1		1	1	C	1	C	C	C	C	C	1	C	C	C	C	C	C	C	C	C	C	C	1
IPI00066374		1	1	C	I	C	1	C	C	1	C	C	C	C	C	C	C	C	C	C	C	C	C	C	C	C	C
IPI00414980		1	1	C	I	C	C	C	C	C	C	C	C	C	C	C	C	C	C	C	C	C	C	C	C	C	C
IPI00008455		1	1	1	I	C	C	C	C	C	C	C	C	1	1	C	C	C	C	C	1	C	C	C	1	C	C
IPI00012048		1	1	C	I	C	C	C	C	C	C	C	C	C	C	C	C	C	C	C	C	C	C	C	C	C	C
IPI00026260		1	1	C	I	C	C	C	C	C	C	C	C	C	C	C	C	C	C	C	C	C	C	C	C	C	C
IPI00027499		1	1	C	I	C	C	C	C	C	C	C	C	C	C	C	C	C	C	C	C	C	C	C	C	C	C
IPI00031812		1	1	C	I	1	C	C	C	C	C	C	C	C	C	C	C	C	C	1	1	C	C	C	C	1	C
IPI00022334		1	1	C	I	C	C	C	C	C	C	C	C	C	C	C	C	C	C	C	C	C	C	C	C	C	C
IPI00098902		1	1	C		1	C	C	C	C	C	C	C	1	C	C	C	C	C	C	C	C	C	C	C	C	C
IPI00299000		1	1	C	I	C	C	C	1	C	C	C	C	C	C	C	C	C	C	C	C	C	C	C	C	C	C
IPI00012066		1	1	C	I	C	C	C	C	C	C	C	C	C	C	C	C	C	C	C	C	1	1	C	C	C	C
IPI00246058		1	1	C	I	C	1	C	1	C	C	C	C	C	C	C	C	C	C	C	C	C	C	C	C	C	C
IPI00010414		1	1	C	I	C	C	C	C	C	C	C	C	C	C	C	C	C	C	C	C	C	C	C	C	C	C
IPI00169383		1	1	C	I	C	1	C	C	C	C	C	C	C	C	C	C	C	1	C	C	C	C	C	C	C	C
IPI00217872		1	1	C	I	C	C	C	C	C	C	C	C	C	C	1	C	C	C	C	C	C	C	C	C	C	C
IPI00011200		1	1	C		C	1	C	C	C	C	C	C	C	C	C	C	C	C	C	C	C	C	C	C	C	C
IPI00419262		1	1	C	I	1	C	C	C	C	C	1	C	C	C	C	C	C	C	C	C	C	C	C	C	C	C
IPI00298057		1	1	C	I	C	C	C	C	C	C	C	C	C	C	C	C	C	C	C	C	C	C	C	C	C	C
IPI00218236		1	1	C		C	C	C	C	C	C	C	C	C	C	C	C	C	C	C	C	C	C	C	C	C	1
IPI00005705		1	1	C	I	C	C	C	C	C	C	C	C	C	C	C	C	C	C	C	C	C	1	C	C	C	C
IPI00011937		1	1	C	I	C	C	C	C	C	C	C	C	C	C	C	C	C	C	C	C	C	C	C	C	C	C
IPI00011126		1	1	C	I	C	C	C	C	C	C	C	C	C	C	C	1	C	C	C	C	C	C	C	C	C	C
IPI00384051		1	1	C	I	C	C	C	C	C	C	C	C	C	C	C	C	C	C	C	C	C	C	C	C	C	C
IPI00297261		1	1	C	I	C	C	C	C	C	C	C	C	C	C	C	C	C	C	C	C	C	C	C	C	C	C
IPI00016513		1	1	C	I	C	C	C	C	C	C	C	C	C	1	C	C	C	C	C	C	1	C	C	C	C	C
IPI00291928		1	1	C	I	C	C	C	C	C	C	C	C	C	C	C	C	C	C	C	C	C	C	C	C	C	C
IPI00005719		1	1	C	I	C	C	C	C	C	C	C	1	C	C	C	C	C	C	1	C	C	C	C	C	C	C
IPI00008964		1	1	C	I	C	C	C	C	C	C	C	1	C	C	C	C	C	C	C	C	C	1	C	C	C	C
IPI00015148		1	1	C	I	C	C	C	C	C	C	1	C	C	C	C	C	C	C	C	C	C	C	C	C	C	C
IPI00027252		1	1	C	I	C	C	C	C	1	C	C	C	C	C	C	C	C	C	C	C	C	C	C	C	C	C
IPI00024933		1	1	C	I	C	C	C	C	C	C	C	C	C	C	C	C	C	C	C	C	C	C	C	C	C	C
IPI00025329		1	1	C	I	C	C	C	C	C	C	C	C	C	C	C	C	C	C	C	C	C	C	C	C	C	C
IPI00247583		1	1	C	I	C	C	C	C	C	C	C	C	C	C	C	C	C	C	C	C	C	C	C	C	C	C
IPI00464972		1	1	C	I	C	C	C	C	C	C	C	C	C	C	C	C	C	C	C	C	C	C	C	C	C	1
IPI00219156		1	1	C	I	C	C	C	C	C	C	C	C	C	C	C	C	C	C	C	C	C	C	C	C	C	C
IPI00215790		1	1	C	I	C	C	C	C	C	C	C	C	C	C	C	C	C	C	C	C	C	C	C	C	C	C
IPI00329389		1	1	C	I	C	C	C	C	C	C	C	C	C	C	C	C	C	C	C	C	1	C	C	C	C	C
IPI00031691		1	1	C	I	C	C	C	C	C	1	C	C	C	C	C	C	1	1	C	C	C	C	C	C	C	C

IPI00008530		1	1	C	I	C	C	C	C	C	C	C	C	C	C	C	C	C	C	C	C	1	C	C	C	C	C
IPI00008529		1	1	C	I	C	C	C	C	C	C	C	C	C	C	C	C	1	C	C	C	C	1	C	C	1	C
IPI00008438		1	1	C	I	C	C	C	C	1	C	C	C	C	C	C	C	C	C	C	C	C	C	C	C	C	C
IPI00026271		1	1	C	I	C	C	C	C	C	C	C	C	C	C	C	C	C	C	C	C	C	C	C	C	C	C
IPI00216153		1	1	C	I	C	1	C	C	C	C	C	C	C	C	C	C	C	C	C	C	C	C	C	C	C	C
IPI00221091		1	1	C	I	C	C	C	C	C	C	C	C	C	C	C	C	C	C	C	C	C	C	C	C	C	C
IPI00221092		1	1	C	I	C	C	C	C	C	C	C	C	C	C	C	C	C	C	C	C	1	C	C	C	C	C
IPI00218606		1	1	C	I	C	C	C	C	C	C	C	C	C	C	C	C	C	C	C	C	C	C	C	C	C	C
IPI00011253		1	1	C	I	1	C	C	C	C	C	C	C	C	C	C	C	C	C	C	C	C	C	C	C	C	C
IPI00217030		1	1	C		C	C	C	1	C	C	C	C	C	C	C	C	C	C	C	C	C	C	C	C	C	C	C
IPI00013415		1	1	C	I	C	C	C	C	C	C	C	C	C	C	C	C	C	1	1	C	C	C	C	C	C	C
IPI00183695		1	1	C	I	C	C	C	C	C	C	C	C	C	C	C	C	C	C	C	C	C	C	C	C	C	C
IPI00013895		1	1	C	I	C	C	C	1	C	C	1	C	C	C	C	C	C	C	1	C	C	C	C	C	C	C
IPI00010214		1	1	C	I	C	C	C	C	C	C	C	C	C	C	C	C	C	C	C	C	C	C	C	C	C	C
IPI00062120		1	1	C	I	C	C	C	C	C	C	C	C	C	C	C	C	C	C	C	C	C	C	C	C	C	C
IPI00217143		1	1	C	I	C	C	C	C	C	C	C	1	1	C	C	C	C	C	C	C	C	C	C	C	C	1
IPI00032140		1	1	C	I	C	C	C	C	C	C	C	C	C	C	C	C	C	C	1	C	C	C	C	C	C	C
IPI00002520		1	1	C	I	C	C	C	C	C	C	C	C	C	C	C	C	C	C	C	C	C	C	C	C	C	C
IPI00072534		1	1	1	I	1	C	C	1	C	C	C	C	C	C	C	C	C	C	C	C	C	C	C	C	C	C
IPI00140420		1	1	C	I	C	C	C	C	1	C	1	C	C	C	1	C	C	C	C	C	C	C	C	C	C	C
IPI00328097		1	1	C	I	C	1	C	C	C	C	C	C	C	C	C	C	C	C	C	C	C	C	C	C	C	C
IPI00009634		1	1	C	I	C	C	C	C	C	C	C	C	C	C	C	C	C	C	C	C	C	C	C	C	C	C
IPI00019971		1	1	C	I	C	C	C	C	C	C	C	C	C	C	C	C	C	C	C	C	C	C	C	C	C	C
IPI00024057		1	1	C	I	C	C	C	C	C	C	C	C	C	C	C	C	C	C	C	C	C	C	C	C	C	C
IPI00100160		1	1	1	I	C	C	C	C	1	C	C	C	C	C	C	1	C	C	C	C	C	C	C	C	1	C
IPI00007752		1	1	C	I	C	1	C	C	C	1	C	C	C	C	C	C	C	C	C	C	C	C	C	C	C	C
IPI00013683		1	1	C	I	1	1	C	C	C	1	C	C	C	1	C	C	C	C	C	C	C	C	C	C	C	C
IPI00027107		1	1	C	I	C	C	C	C	C	C	C	C	C	C	C	C	C	C	C	C	C	C	C	C	C	C
IPI00301058		1	1	C	I	C	C	C	C	C	C	C	C	1	C	C	C	C	C	1	C	C	C	C	C	C	C
IPI00022774		1	1	C	I	C	1	C	C	C	C	C	C	C	1	C	C	C	C	C	C	C	C	C	C	C	C
IPI00182856		1	1	C	I	C	C	C	C	C	C	1	C	C	C	C	C	C	C	C	C	C	C	C	C	C	C
IPI00220834		1	1	C	I	C	1	C	C	C	C	C	C	C	1	C	C	C	C	C	C	C	1	C	C	C	C
IPI00216318		1	1	1		C	C	C	C	C	C	C	C	C	1	C	C	C	C	C	C	C	C	C	C	C	C
IPI00000816		1	1	C	I	C	1	C	C	C	C	C	C	C	1	C	C	C	C	C	C	C	C	C	C	C	C
IPI00220642		1	1	C	I	C	1	C	C	C	C	C	C	C	1	C	C	C	C	C	C	C	C	C	C	C	C
IPI00018146		1	1	C	I	C	1	C	C	C	C	C	C	C	C	C	C	C	C	C	C	C	C	C	C	C	C
IPI00220906		1	1	C	I	C	C	C	C	C	C	C	C	C	C	C	C	C	C	C	C	C	C	C	C	C	C
IPI00013302	0	1	1	C	I	C	C	C	C	C	C	C	C	C	C	C	C	1	C	1	C	C	C	C	C	C	1
IPI00001091	0	1	1	C	I	C	C	C	C	C	C	C	C	C	1	C	1	C	C	1	C	1	C	C	1	C	C
IPI00006482	0	1	1	C	I	C	C	C	C	C	C	C	C	C	1	C	C	C	C	C	C	C	1	C	C	C	C
IPI00024368	0	1	1	C	I	C	C	C	C	C	1	C	1	1	C	C	C	C	C	C	1	1	C	C	C	C	C
IPI00027235	0	1	0	C	I	C	C	C	C	C	C	C	C	C	C	C	C	1	C	C	C	1	C	C	C	1	C
IPI00015346	0	1	1	C	I	C	C	C	C	C	C	C	C	C	1	C	1	C	C	C	1	C	1	1	C	C	C
IPI00016703	0	1	1	C	I	C	C	C	C	C	C	C	C	C	1	C	C	C	1	C	C	C	1	C	C	C	C
IPI00032406	0	0	1	C	I	C	C	C	C	C	C	C	C	C	1	C	C	C	C	C	C	C	1	C	C	C	1
IPI00023780	0	0	1	C	I	C	C	C	C	C	C	C	C	C	1	C	C	C	1	C	C	C	C	C	C	C	1
IPI00013933	1	1	0	1		C	C	C	1	C	C	1	C	C	C	C	C	C	C	1	1	C	C	1	C	1	C
IPI00100362	0	1	0	C	I	C	C	C	C	C	C	C	1	C	C	C	1	1	1	C	C	C	C	C	C	1	C	C
IPI00021267	0	1	1	C	I	C	C	C	C	C	C	1	C	C	C	C	1	C	C	1	C	C	C	C	C	C	C
IPI00300384	0	1	1	C	I	C	C	C	C	C	C	C	C	1	1	C	C	1	1	C	C	C	1	C	C	1	C
IPI00024773	0	1	1	C	I	C	C	C	C	C	C	C	1	C	C	1	1	C	1	C	C	1	C	1	C	C	C
IPI00414717	0	1	1	C	I	C	C	C	C	C	C	1	C	C	1	C	C	C	C	C	C	C	1	C	C	C	C
IPI00004671	0	1	1	C	I	C	C	C	C	C	C	C	1	C	1	C	1	1	C	C	C	C	C	C	C	1	C
IPI00289819	0	1	1	C	I	C	C	C	C	C	C	C	1	1	C	C	C	1	C	C	1	1	1	C	C	C	C
IPI00025803	0	0	1	C	I	C	C	C	C	C	C	C	1	1	C	C	C	C	C	C	1	C	C	C	C	C	1
IPI00029741	0	1	1	C	I	C	C	C	C	1	C	C	C	C	C	C	C	C	1	C	C	1	C	1	1	C	1

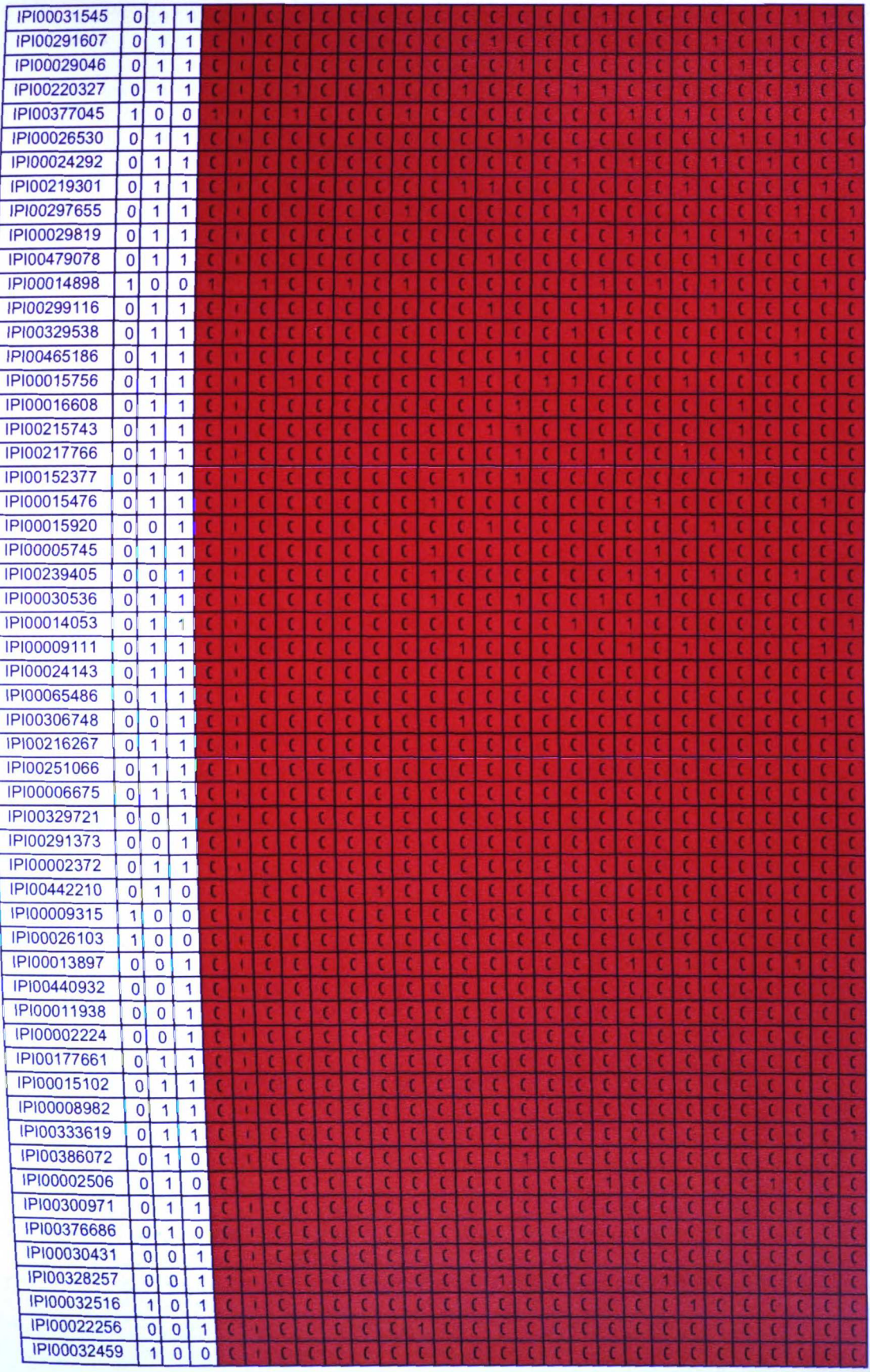

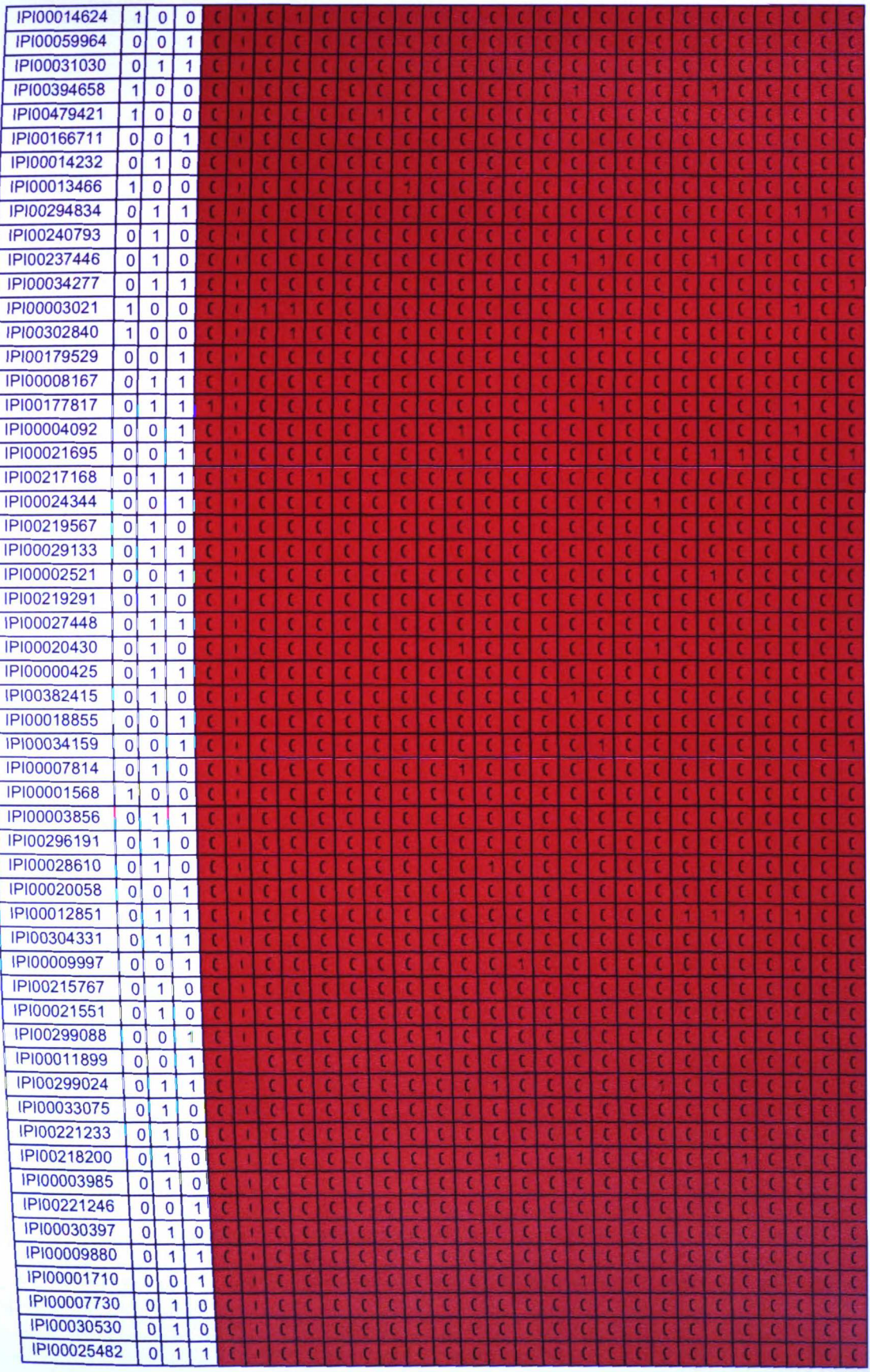

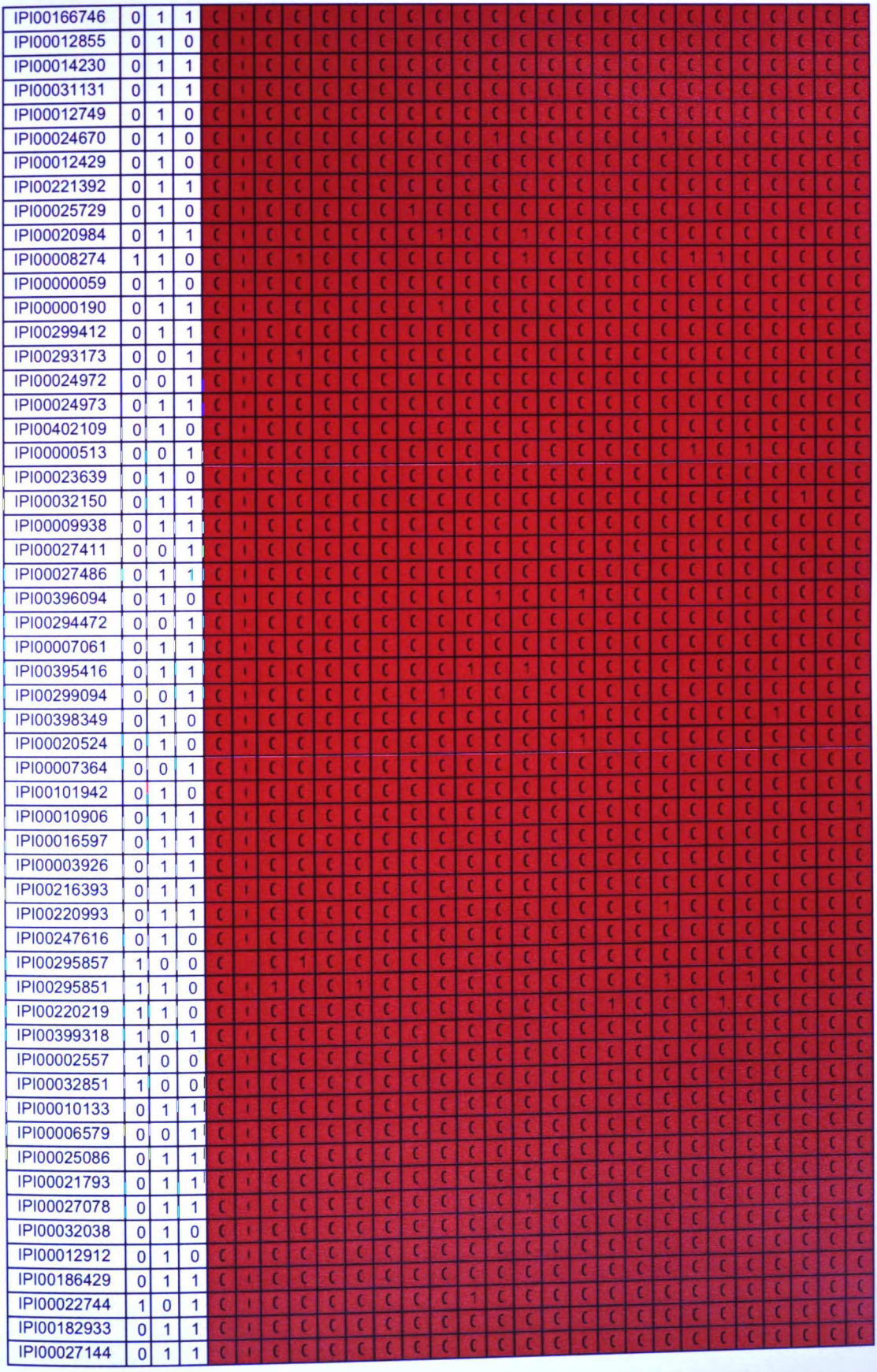

IPI00166746	0	1	1
IPI00012855	0	1	0
IPI00014230	0	1	1
IPI00031131	0	1	1
IPI00012749	0	1	0
IPI00024670	0	1	0
IPI00012429	0	1	0
IPI00221392	0	1	1
IPI00025729	0	1	0
IPI00020984	0	1	1
IPI00008274	1	1	0
IPI00000059	0	1	0
IPI00000190	0	1	1
IPI00299412	0	1	1
IPI00293173	0	0	1
IPI00024972	0	0	1
IPI00024973	0	1	1
IPI00402109	0	1	0
IPI00000513	0	0	1
IPI00023639	0	1	0
IPI00032150	0	1	1
IPI00009938	0	1	1
IPI00027411	0	0	1
IPI00027486	0	1	1
IPI00396094	0	1	0
IPI00294472	0	0	1
IPI00007061	0	1	1
IPI00395416	0	1	1
IPI00299094	0	0	1
IPI00398349	0	1	0
IPI00020524	0	1	0
IPI00007364	0	0	1
IPI00101942	0	1	0
IPI00010906	0	1	1
IPI00016597	0	1	1
IPI00003926	0	1	1
IPI00216393	0	1	1
IPI00220993	0	1	1
IPI00247616	0	1	0
IPI00295857	1	0	0
IPI00295851	1	1	0
IPI00220219	1	1	0
IPI00399318	1	0	1
IPI00002557	1	0	0
IPI00032851	1	0	0
IPI00010133	0	1	1
IPI00006579	0	0	1
IPI00025086	0	1	1
IPI00021793	0	1	1
IPI00027078	0	1	1
IPI00032038	0	1	0
IPI00012912	0	1	0
IPI00186429	0	1	1
IPI00022744	1	0	1
IPI00182933	0	1	1
IPI00027144	0	1	1

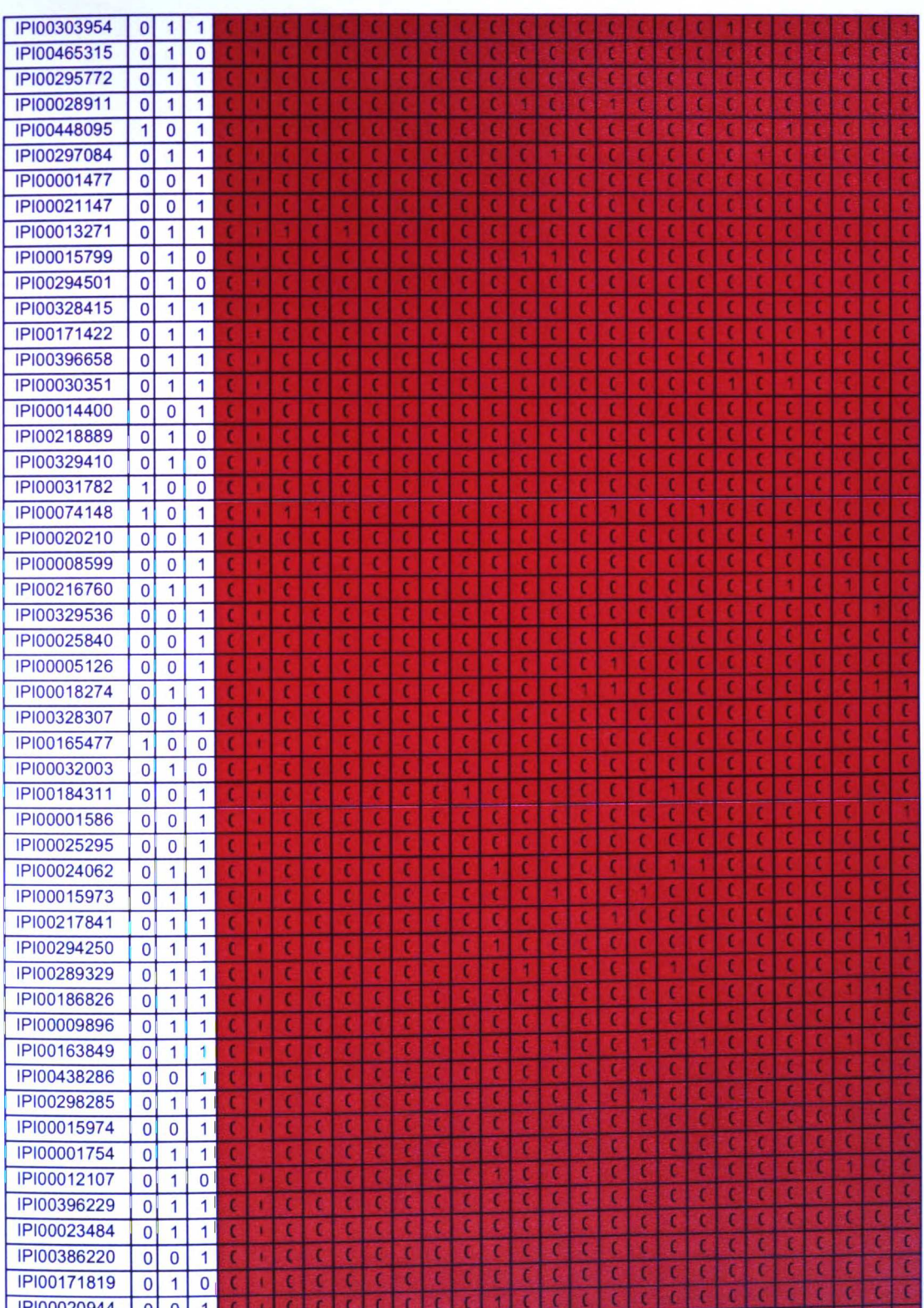

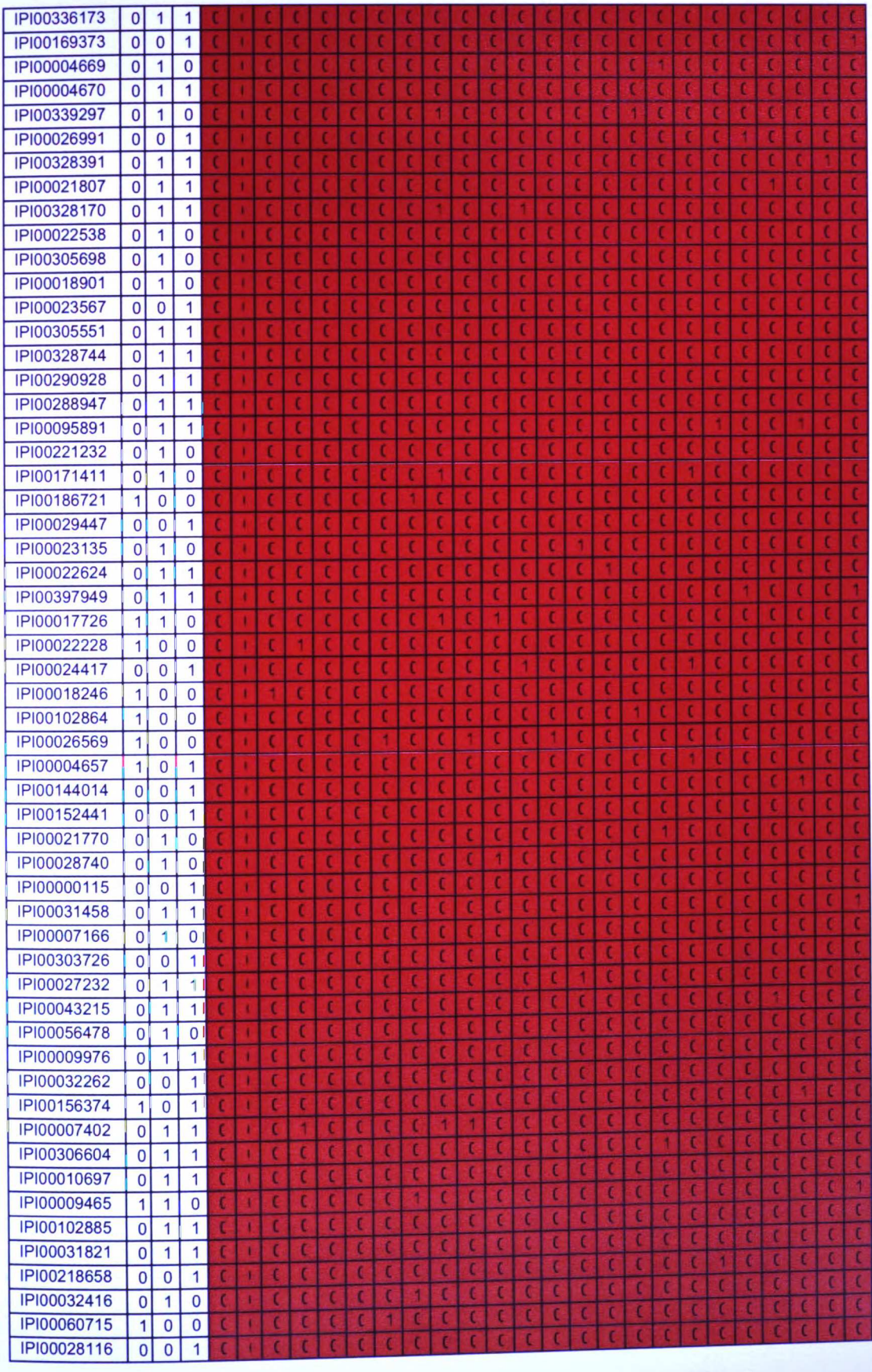

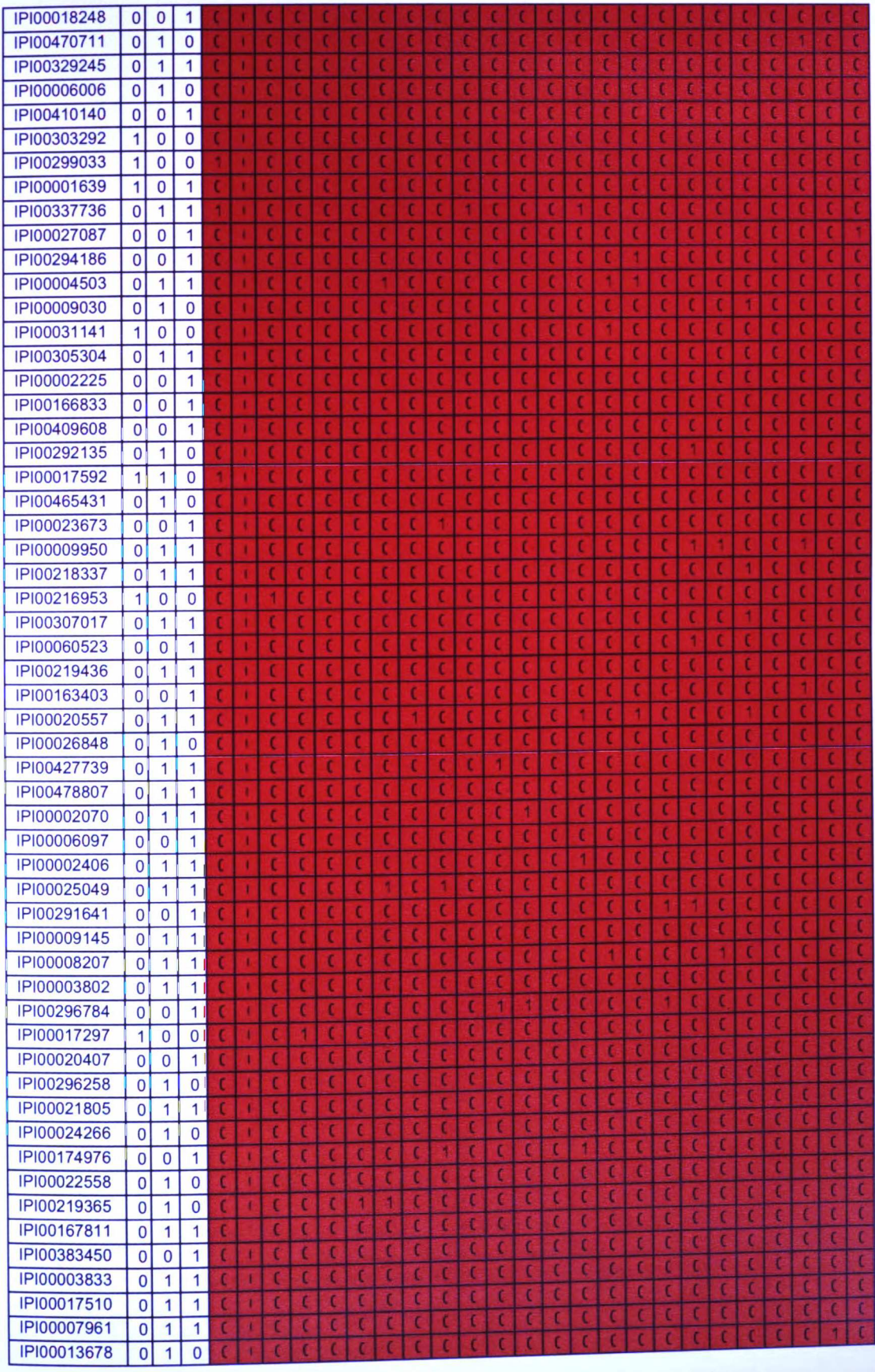

IPI00018248	0	0	1
IPI00470711	0	1	0
IPI00329245	0	1	1
IPI00006006	0	1	0
IPI00410140	0	0	1
IPI00303292	1	0	0
IPI00299033	1	0	0
IPI00001639	1	0	1
IPI00337736	0	1	1
IPI00027087	0	0	1
IPI00294186	0	0	1
IPI00004503	0	1	1
IPI00009030	0	1	0
IPI00031141	1	0	0
IPI00305304	0	1	1
IPI00002225	0	0	1
IPI00166833	0	0	1
IPI00409608	0	0	1
IPI00292135	0	1	0
IPI00017592	1	1	0
IPI00465431	0	1	0
IPI00023673	0	0	1
IPI00009950	0	1	1
IPI00218337	0	1	1
IPI00216953	1	0	0
IPI00307017	0	1	1
IPI00060523	0	0	1
IPI00219436	0	1	1
IPI00163403	0	0	1
IPI00020557	0	1	1
IPI00026848	0	1	0
IPI00427739	0	1	1
IPI00478807	0	1	1
IPI00002070	0	1	1
IPI00006097	0	0	1
IPI00002406	0	1	1
IPI00025049	0	1	1
IPI00291641	0	0	1
IPI00009145	0	1	1
IPI00008207	0	1	1
IPI00003802	0	1	1
IPI00296784	0	0	1
IPI00017297	1	0	0
IPI00020407	0	0	1
IPI00296258	0	1	0
IPI00021805	0	1	1
IPI00024266	0	1	0
IPI00174976	0	0	1
IPI00022558	0	1	0
IPI00219365	0	1	0
IPI00167811	0	1	1
IPI00383450	0	0	1
IPI00003833	0	1	1
IPI00017510	0	1	1
IPI00007961	0	1	1
IPI00013678	0	1	0

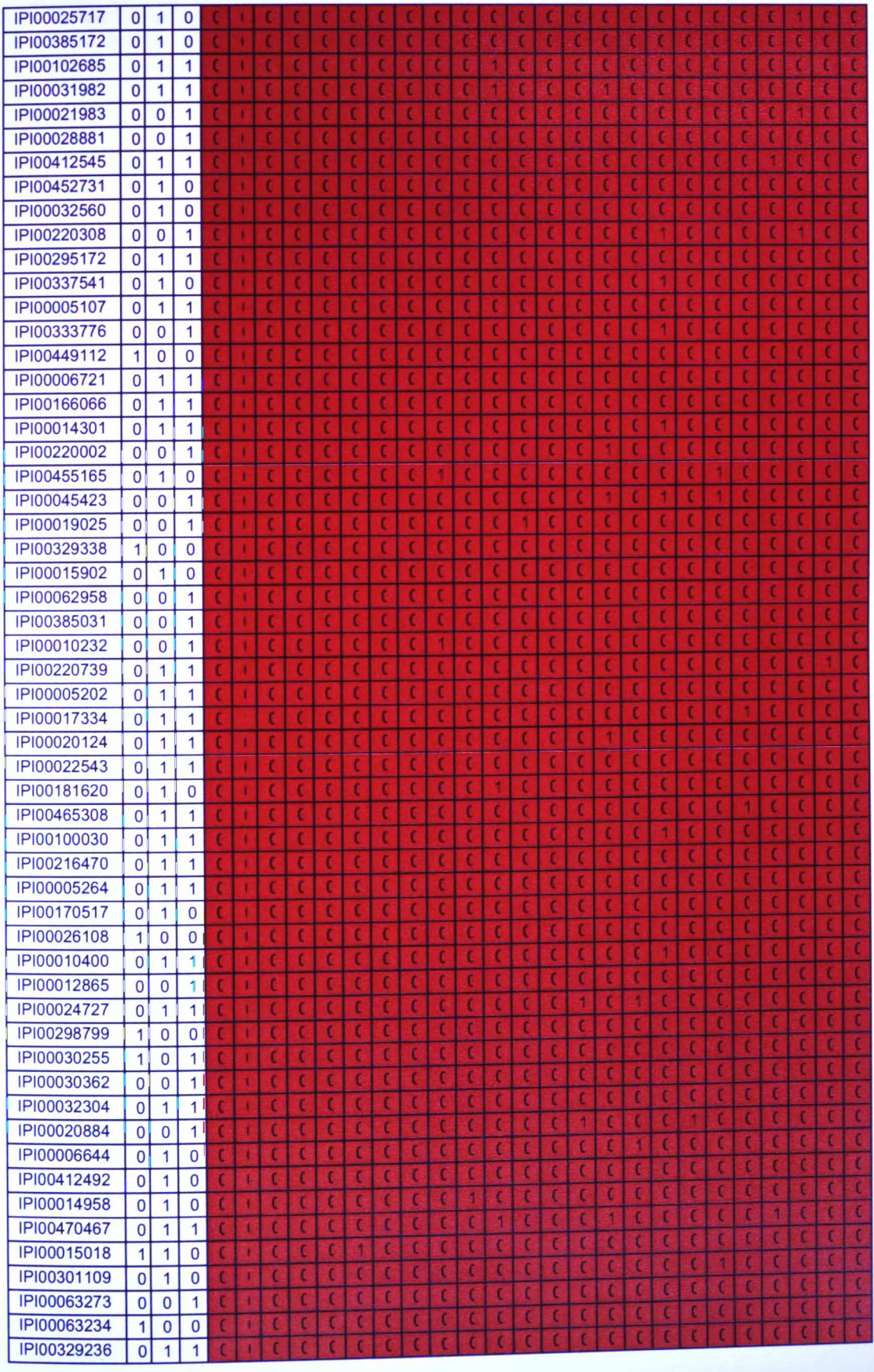

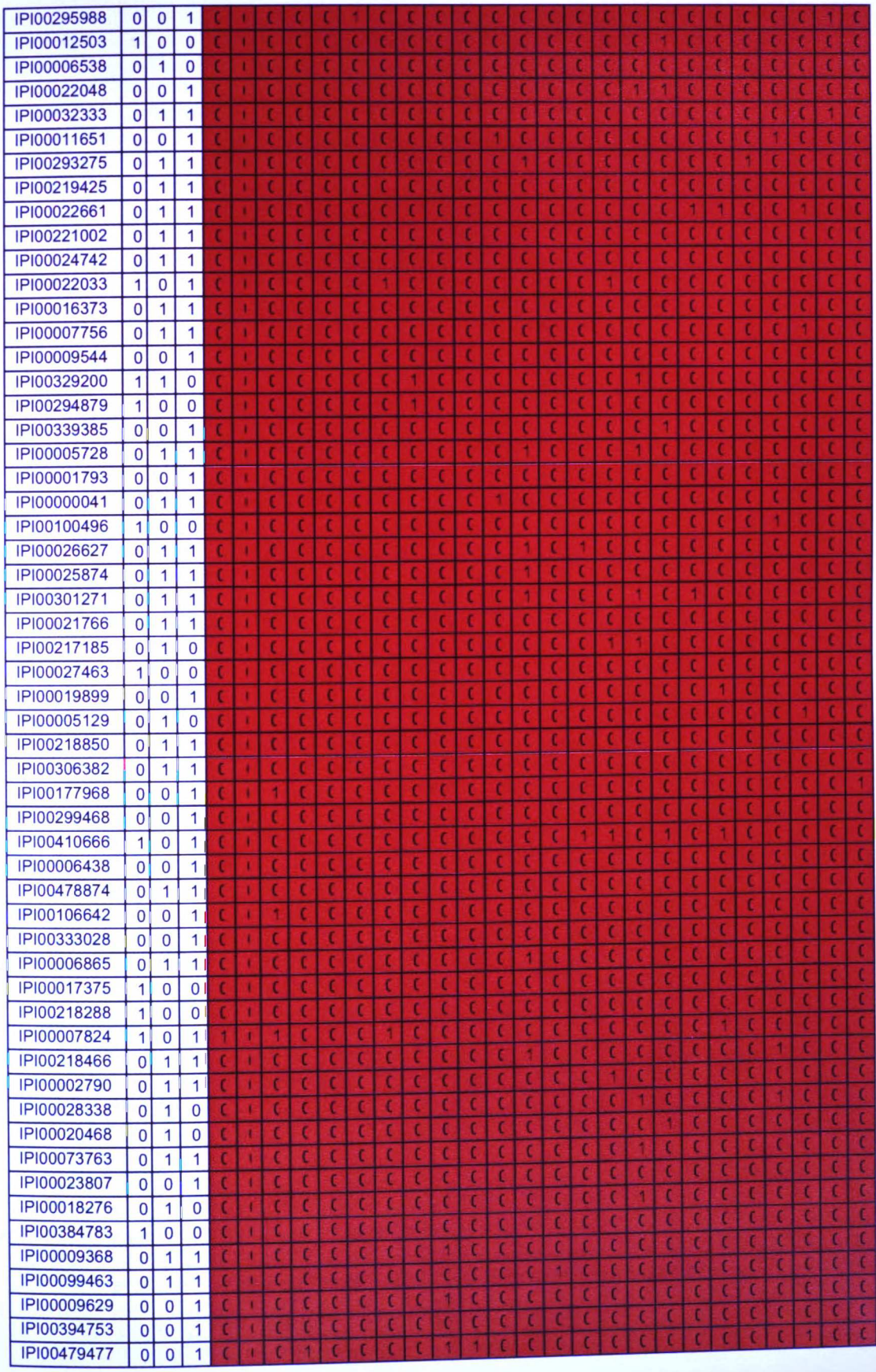

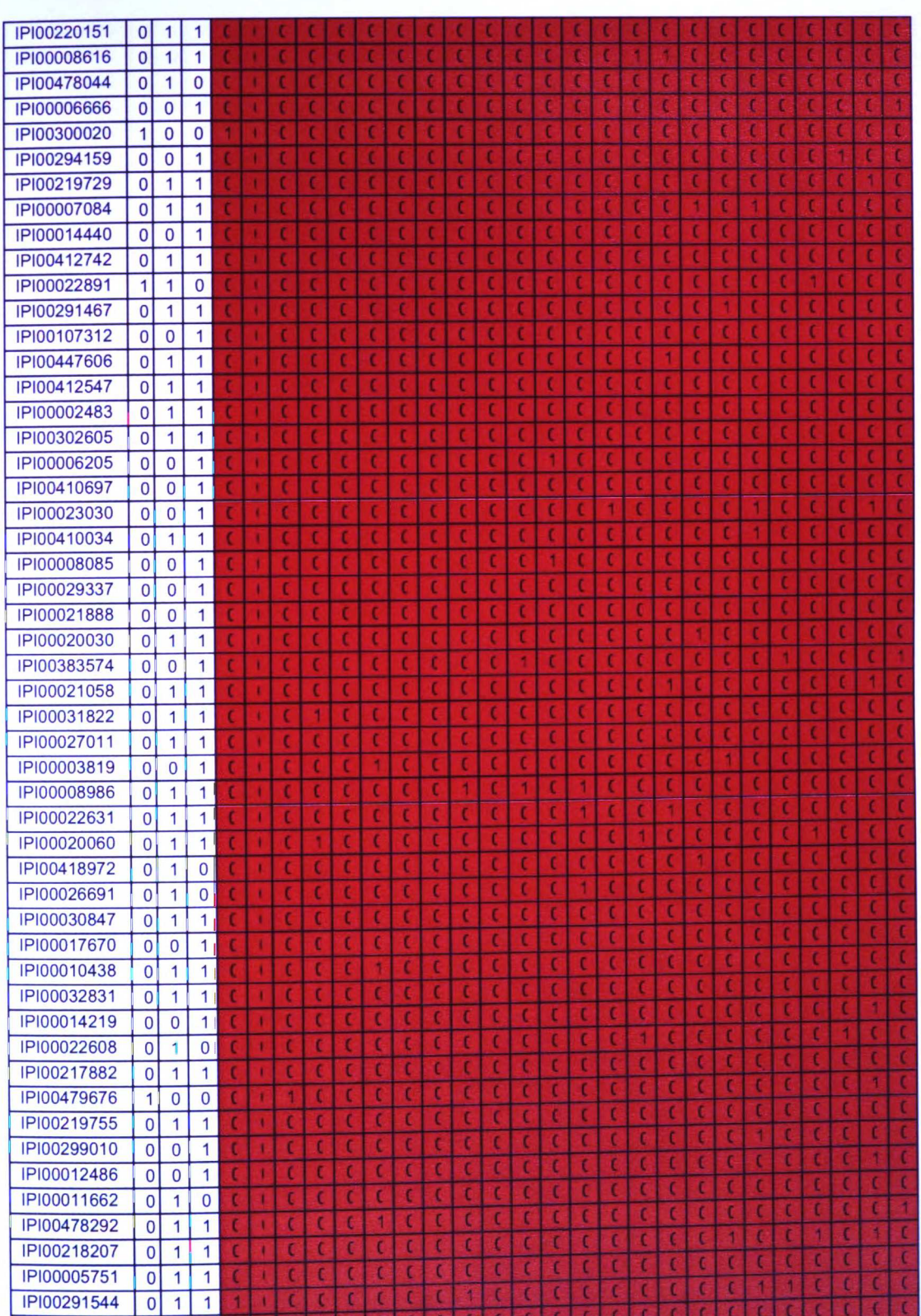

IPI00220151	0	1	1
IPI00008616	0	1	1
IPI00478044	0	1	0
IPI00006666	0	0	1
IPI00300020	1	0	0
IPI00294159	0	0	1
IPI00219729	0	1	1
IPI00007084	0	1	1
IPI00014440	0	0	1
IPI00412742	0	1	1
IPI00022891	1	1	0
IPI00291467	0	1	1
IPI00107312	0	0	1
IPI00447606	0	1	1
IPI00412547	0	1	1
IPI00002483	0	1	1
IPI00302605	0	1	1
IPI00006205	0	0	1
IPI00410697	0	0	1
IPI00023030	0	0	1
IPI00410034	0	1	1
IPI00008085	0	0	1
IPI00029337	0	0	1
IPI00021888	0	0	1
IPI00020030	0	1	1
IPI00383574	0	0	1
IPI00021058	0	1	1
IPI00031822	0	1	1
IPI00027011	0	1	1
IPI00003819	0	0	1
IPI00008986	0	1	1
IPI00022631	0	1	1
IPI00020060	0	1	1
IPI00418972	0	1	0
IPI00026691	0	1	0
IPI00030847	0	1	1
IPI00017670	0	0	1
IPI00010438	0	1	1
IPI00032831	0	1	1
IPI00014219	0	0	1
IPI00022608	0	1	0
IPI00217882	0	1	1
IPI00479676	1	0	0
IPI00219755	0	1	1
IPI00299010	0	0	1
IPI00012486	0	0	1
IPI00011662	0	1	0
IPI00478292	0	1	1
IPI00218207	0	1	1
IPI00005751	0	1	1
IPI00291544	0	1	1
IPI00385267	0	1	1
IPI00295098	0	1	1
IPI00301021	0	0	1
IPI00425902	0	0	1
IPI00001922	0	1	1

IPI00000865	0	1	1
IPI00166512	0	0	1
IPI00219682	0	1	1
IPI00477195	0	1	1
IPI00477418	0	1	0
IPI00329332	0	1	1
IPI00395514	0	1	1
IPI00012028	0	1	1
IPI00027194	0	1	1
IPI00018067	1	0	0
IPI00029730	0	1	1
IPI00012005	0	1	1
IPI00013930	0	1	0
IPI00289876	0	1	1
IPI00009225	0	1	0
IPI00020887	0	0	1
IPI00009507	0	1	1
IPI00009439	0	0	1
IPI00012902	0	1	1
IPI00154565	0	1	1
IPI00060201	0	1	0
IPI00296215	0	1	1
IPI00297910	0	1	1
IPI00101026	0	0	1
IPI00001382	0	0	1
IPI00011167	0	1	0
IPI00299719	0	1	1
IPI00005733	0	0	1
IPI00218252	1	0	0
IPI00012545	0	1	1
IPI00007309	0	1	1
IPI00216219	1	0	1
IPI00003843	1	0	1
IPI00293451	0	1	1
IPI00165394	0	1	1
IPI00019018	0	0	1
IPI00101374	0	0	1
IPI00018415	0	1	1
IPI00021985	0	1	1
IPI00007165	0	1	1
IPI00062679	0	1	1
IPI00166785	0	1	1
IPI00056521	0	1	1
IPI00030131	0	1	0
IPI00021975	0	1	0
IPI00296379	0	1	0
IPI00004413	0	1	0
IPI00024364	1	0	0
IPI00023191	1	0	0
IPI00023186	0	1	0
IPI00024976	0	1	0
IPI00015602	0	0	1
IPI00307572	0	1	1
IPI00219111	0	1	1
IPI00294933	0	0	1
IPI00030936	1	0	0

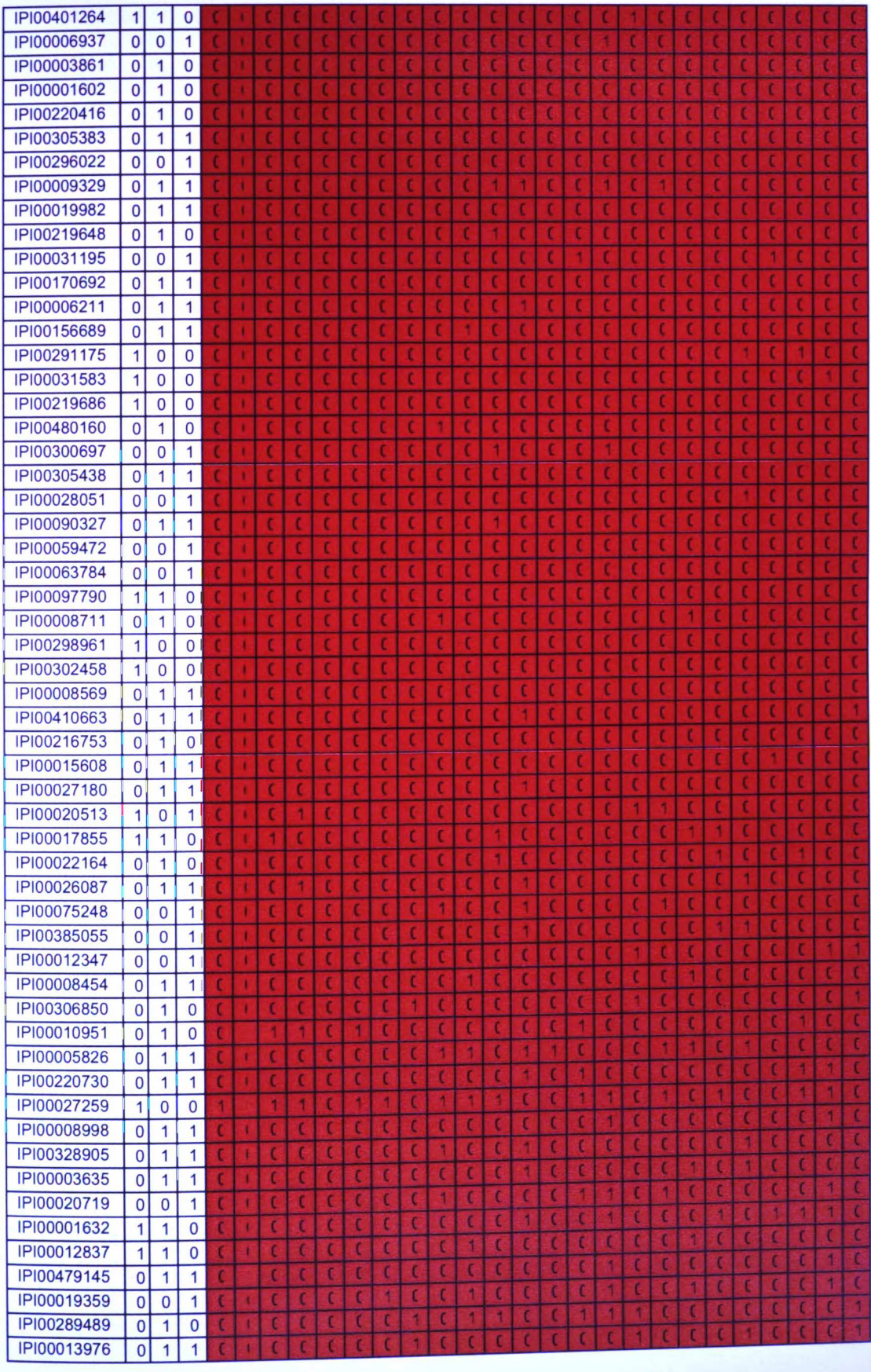

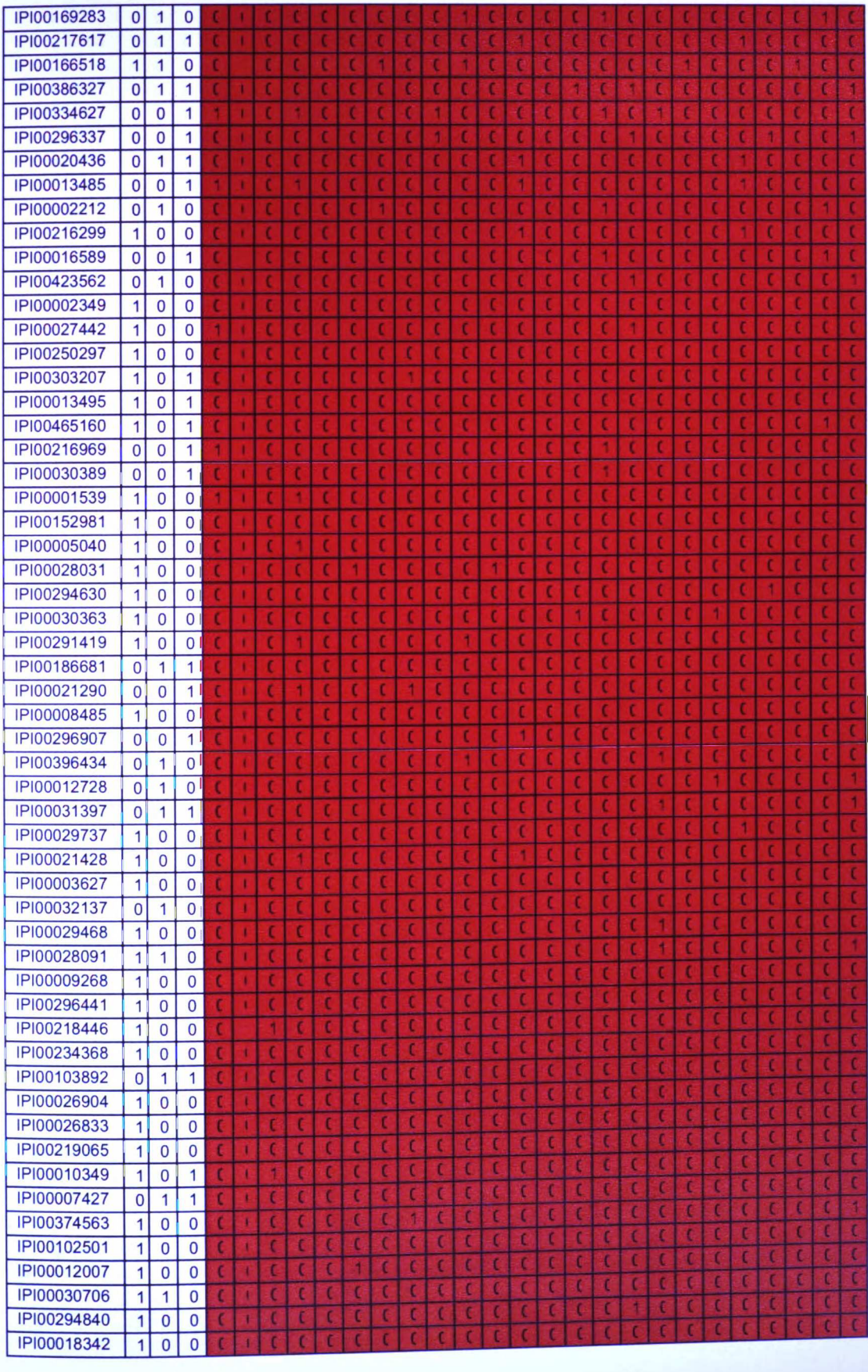

IPI00215901	0	0	1
IPI00016568	1	0	0
IPI00220271	1	0	0
IPI00413641	1	0	0
IPI00105407	1	0	0
IPI00029733	1	0	0
IPI00291483	1	0	0
IPI00022434	1	0	0
IPI00026663	1	0	0
IPI00217871	1	1	0
IPI00221234	1	0	0
IPI00479877	1	0	0
IPI00418262	1	0	0
IPI00005781	0	0	1
IPI00044683	0	0	1
IPI00186093	0	0	1
IPI00153060	1	0	0
IPI00333558	0	1	1
IPI00339320	1	0	0
IPI00449263	1	0	0
IPI00007423	1	0	0
IPI00165393	1	0	0
IPI00002460	1	0	0
IPI00218835	1	0	0
IPI00411677	1	0	0
IPI00337741	1	0	0
IPI00215911	1	0	0
IPI00295485	1	0	0
IPI00439694	0	0	1
IPI00168479	1	0	0
IPI00218693	1	0	0
IPI00013184	1	0	0
IPI00215918	1	0	0
IPI00175169	1	0	0
IPI00002186	0	0	1
IPI00021257	0	1	0
IPI00020728	0	0	1
IPI00020567	1	0	1
IPI00217418	0	0	1
IPI00386947	0	1	0
IPI00003815	1	0	0
IPI00413517	1	0	0
IPI00328544	0	1	1
IPI00152007	0	0	1
IPI00472160	1	0	0
IPI00418545	0	1	0
IPI00449907	0	1	1
IPI00060031	0	1	1
IPI00018871	0	1	1
IPI00007183	0	0	1
IPI00332835	0	0	1
IPI00333068	0	1	1
IPI00005160	1	1	0
IPI00005162	0	1	0
IPI00007263	0	0	1
IPI00007280	0	1	0

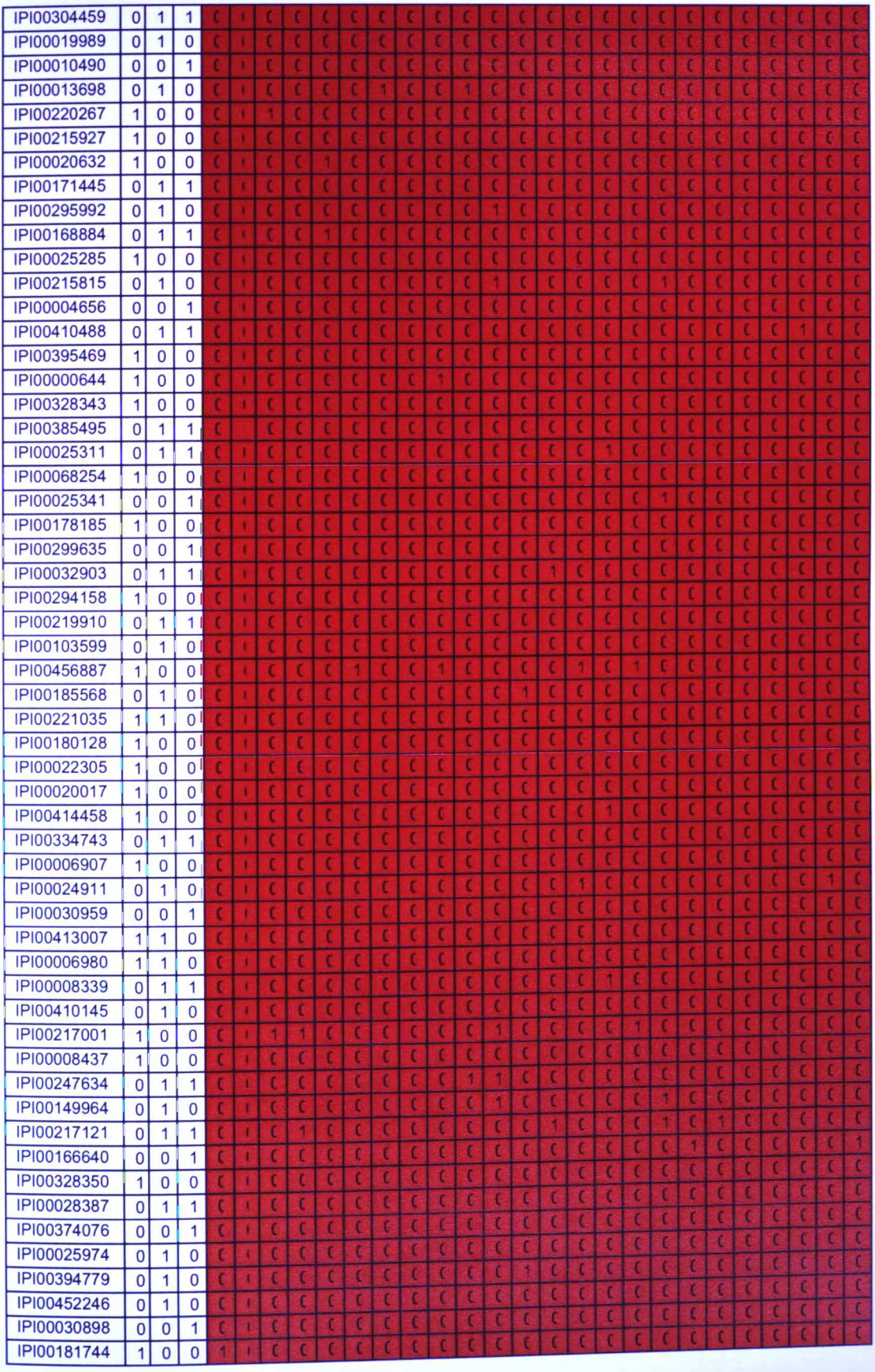

IPI00304459	0	1	1
IPI00019989	0	1	0
IPI00010490	0	0	1
IPI00013698	0	1	0
IPI00220267	1	0	0
IPI00215927	1	0	0
IPI00020632	1	0	0
IPI00171445	0	1	1
IPI00295992	0	1	0
IPI00168884	0	1	1
IPI00025285	1	0	0
IPI00215815	0	1	0
IPI00004656	0	0	1
IPI00410488	0	1	1
IPI00395469	1	0	0
IPI00000644	1	0	0
IPI00328343	1	0	0
IPI00385495	0	1	1
IPI00025311	0	1	1
IPI00068254	1	0	0
IPI00025341	0	0	1
IPI00178185	1	0	0
IPI00299635	0	0	1
IPI00032903	0	1	1
IPI00294158	1	0	0
IPI00219910	0	1	1
IPI00103599	0	1	0
IPI00456887	1	0	0
IPI00185568	0	1	0
IPI00221035	1	1	0
IPI00180128	1	0	0
IPI00022305	1	0	0
IPI00020017	1	0	0
IPI00414458	1	0	0
IPI00334743	0	1	1
IPI00006907	1	0	0
IPI00024911	0	1	0
IPI00030959	0	0	1
IPI00413007	1	1	0
IPI00006980	1	1	0
IPI00008339	0	1	1
IPI00410145	0	1	0
IPI00217001	1	0	0
IPI00008437	1	0	0
IPI00247634	0	1	1
IPI00149964	0	1	0
IPI00217121	0	1	1
IPI00166640	0	0	1
IPI00328350	1	0	0
IPI00028387	0	1	1
IPI00374076	0	0	1
IPI00025974	0	1	0
IPI00394779	0	1	0
IPI00452246	0	1	0
IPI00030898	0	0	1
IPI00181744	1	0	0

IPI00009659	1	0	0
IPI00374082	0	0	1
IPI00334916	0	1	1
IPI00253323	1	0	0
IPI00024627	0	0	1
IPI00032426	1	0	1
IPI00004310	0	0	1
IPI00304527	0	0	1
IPI00020007	0	1	1
IPI00465226	0	1	0
IPI00034205	0	1	0
IPI00168383	0	1	0
IPI00006566	0	0	1
IPI00018237	0	1	1
IPI00031107	1	0	0
IPI00218414	1	0	0
IPI00032561	0	0	1
IPI00106646	1	0	0
IPI00301263	1	0	1
IPI00014516	1	0	0
IPI00014537	1	1	0
IPI00098624	1	0	0
IPI00183066	1	0	0
IPI00172636	1	0	0
IPI00103175	0	1	1
IPI00011285	1	0	0
IPI00289758	1	0	0
IPI00003765	0	0	1
IPI00026185	1	0	1
IPI00005914	1	0	0
IPI00158625	1	0	0
IPI00103516	0	0	1
IPI00219307	1	0	0
IPI00016723	1	1	0
IPI00295386	1	0	0
IPI00290526	1	0	0
IPI00465425	0	0	1
IPI00290770	1	0	1
IPI00302927	1	0	0
IPI00010720	1	1	0
IPI00018465	1	0	0
IPI00302925	1	0	0
IPI00152488	0	0	1
IPI00027983	1	0	0
IPI00006547	0	1	0
IPI00033025	1	0	0
IPI00026689	0	1	1
IPI00005689	0	1	0
IPI00411511	0	1	0
IPI00374694	0	1	0
IPI00014264	1	0	1
IPI00419920	1	0	0
IPI00101049	0	1	0
IPI00329600	0	1	1
IPI00218924	0	1	1
IPI00028275	0	0	1

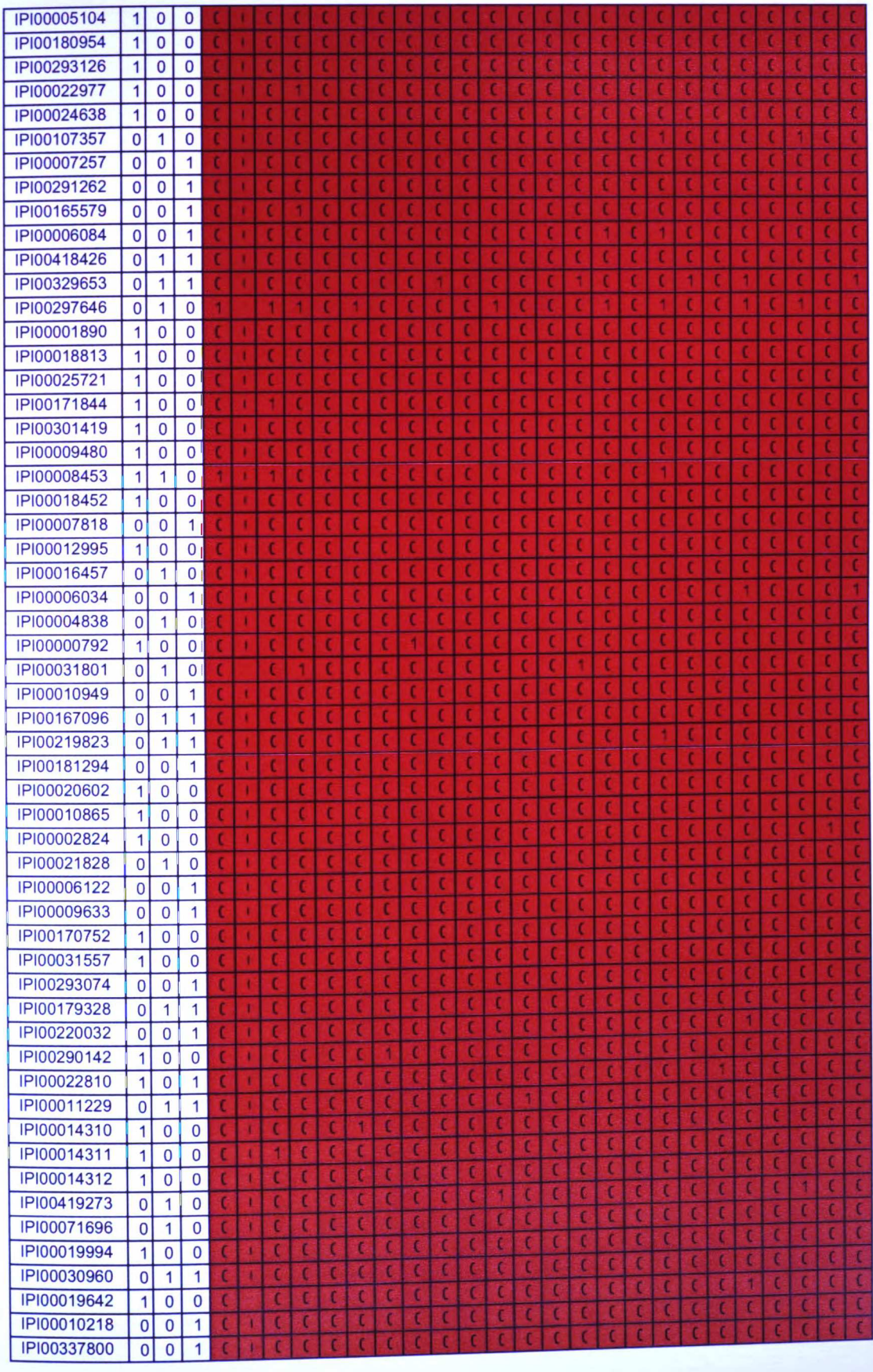

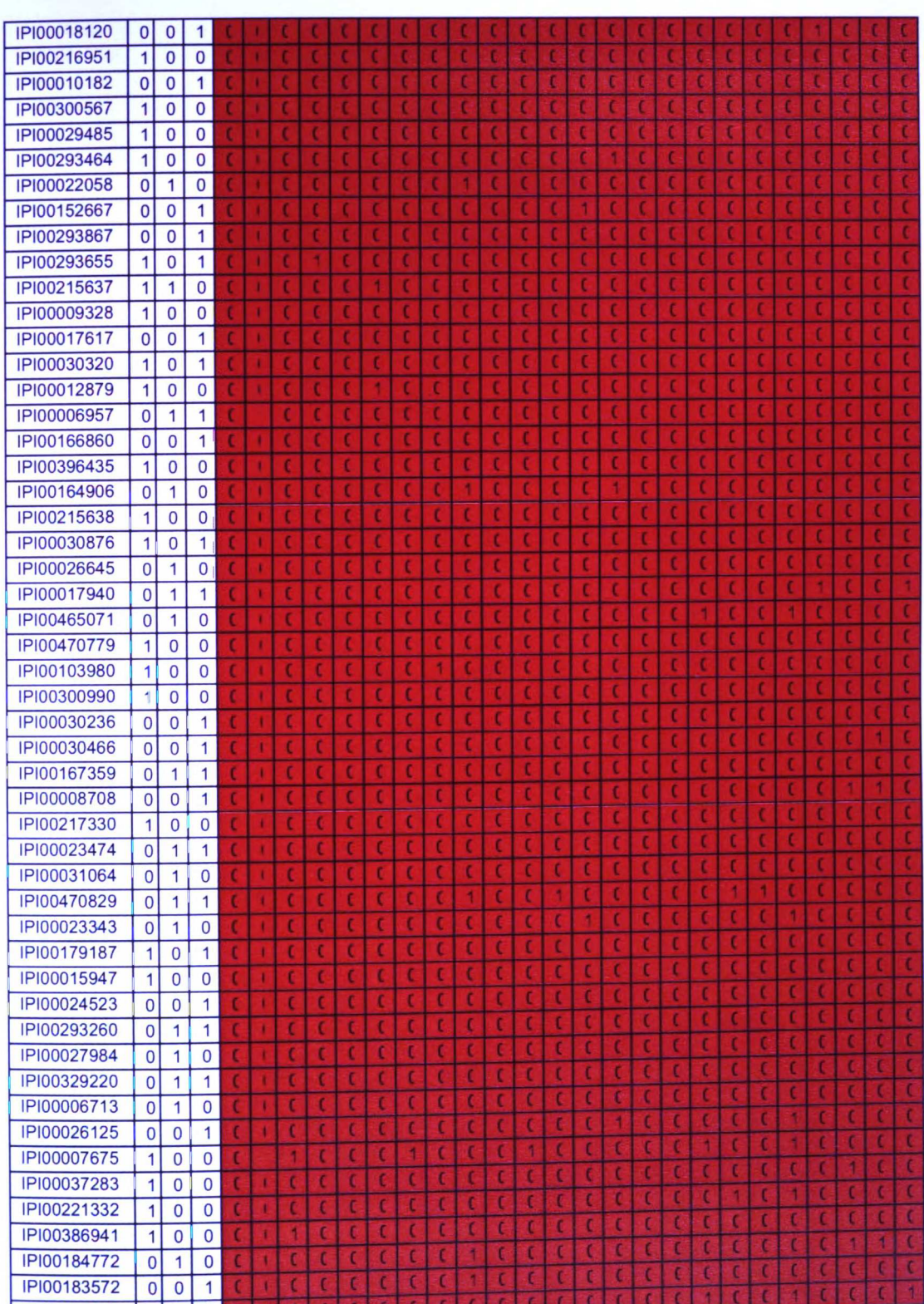

IPI00008991	1	0	0
IPI00031836	1	0	0
IPI00413293	0	1	0
IPI00024993	0	1	0
IPI00216448	0	0	1
IPI00014424	0	1	1
IPI00178440	1	1	0
IPI00064086	1	0	1
IPI00003588	1	0	0
IPI00000875	1	0	0
IPI00293026	1	0	0
IPI00100980	1	0	0
IPI00021458	0	0	1
IPI00012462	1	0	0
IPI00028083	1	0	0
IPI00005979	1	0	0
IPI00219678	1	1	0
IPI00021728	0	0	1
IPI00297982	1	0	0
IPI00029012	1	0	1
IPI00012795	1	0	0
IPI00006182	1	1	0
IPI00290460	1	0	0
IPI00011257	1	0	0
IPI00013068	1	0	0
IPI00465233	1	0	1
IPI00006181	1	0	0
IPI00334191	1	0	0
IPI00030296	1	1	0
IPI00027485	1	0	0
IPI00220365	1	0	0
IPI00015952	1	0	0
IPI00411704	1	0	0
IPI00299254	1	0	1
IPI00034071	0	0	1
IPI00217918	0	1	0
IPI00015944	1	0	0
IPI00001466	0	0	1
IPI00374054	0	0	1
IPI00013769	1	0	0
IPI00216171	1	0	0
IPI00007249	0	1	0
IPI00397519	0	1	0
IPI00397379	0	0	1
IPI00300584	0	1	1
IPI00290337	0	1	1
IPI00157535	1	1	0
IPI00026512	0	0	1
IPI00411706	1	0	0
IPI00027820	0	0	1
IPI00172656	0	1	1
IPI00429191	1	0	0
IPI00010810	0	0	1
IPI00004902	1	0	0
IPI00003766	1	0	0
IPI00103064	0	1	1

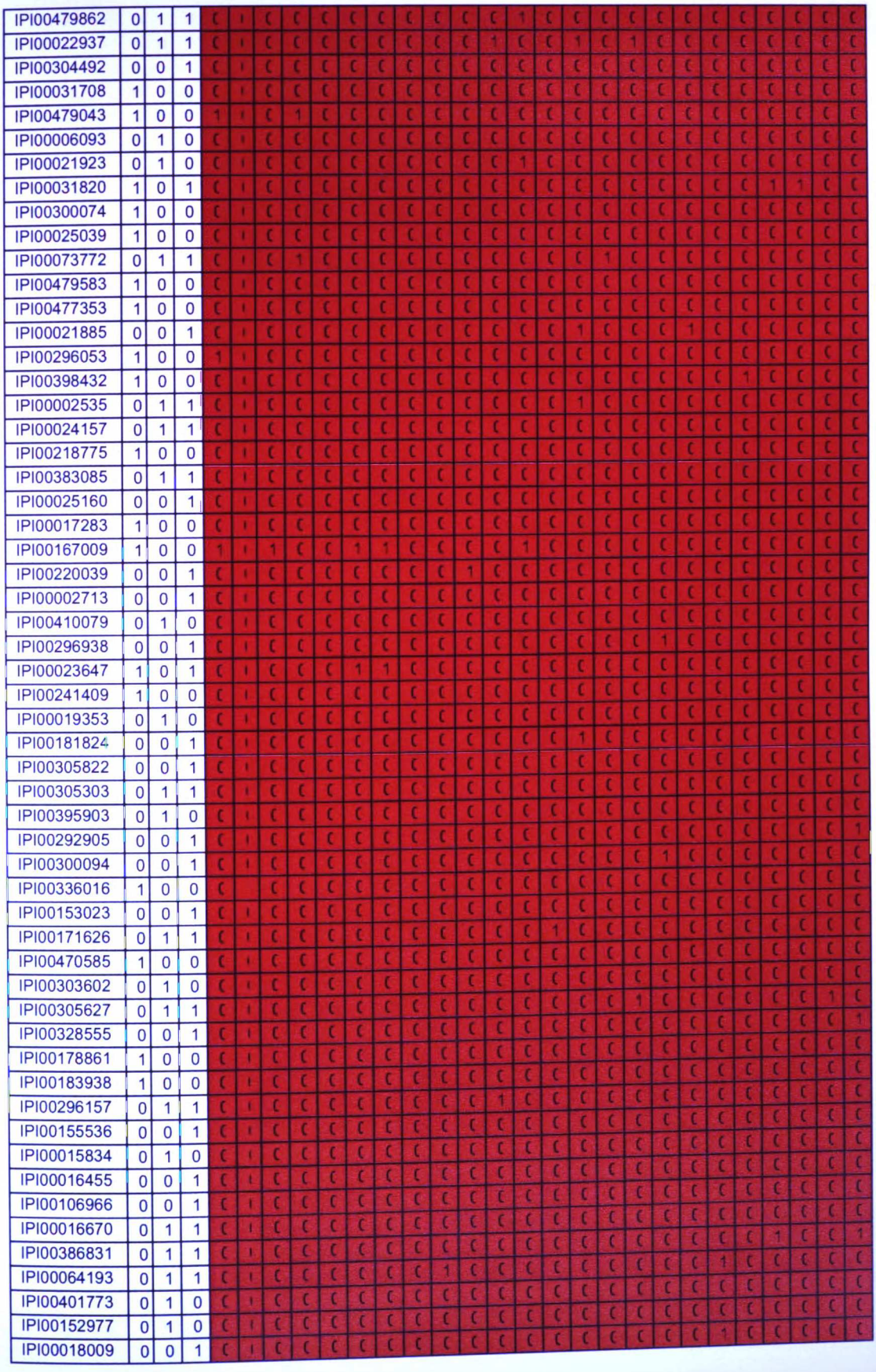

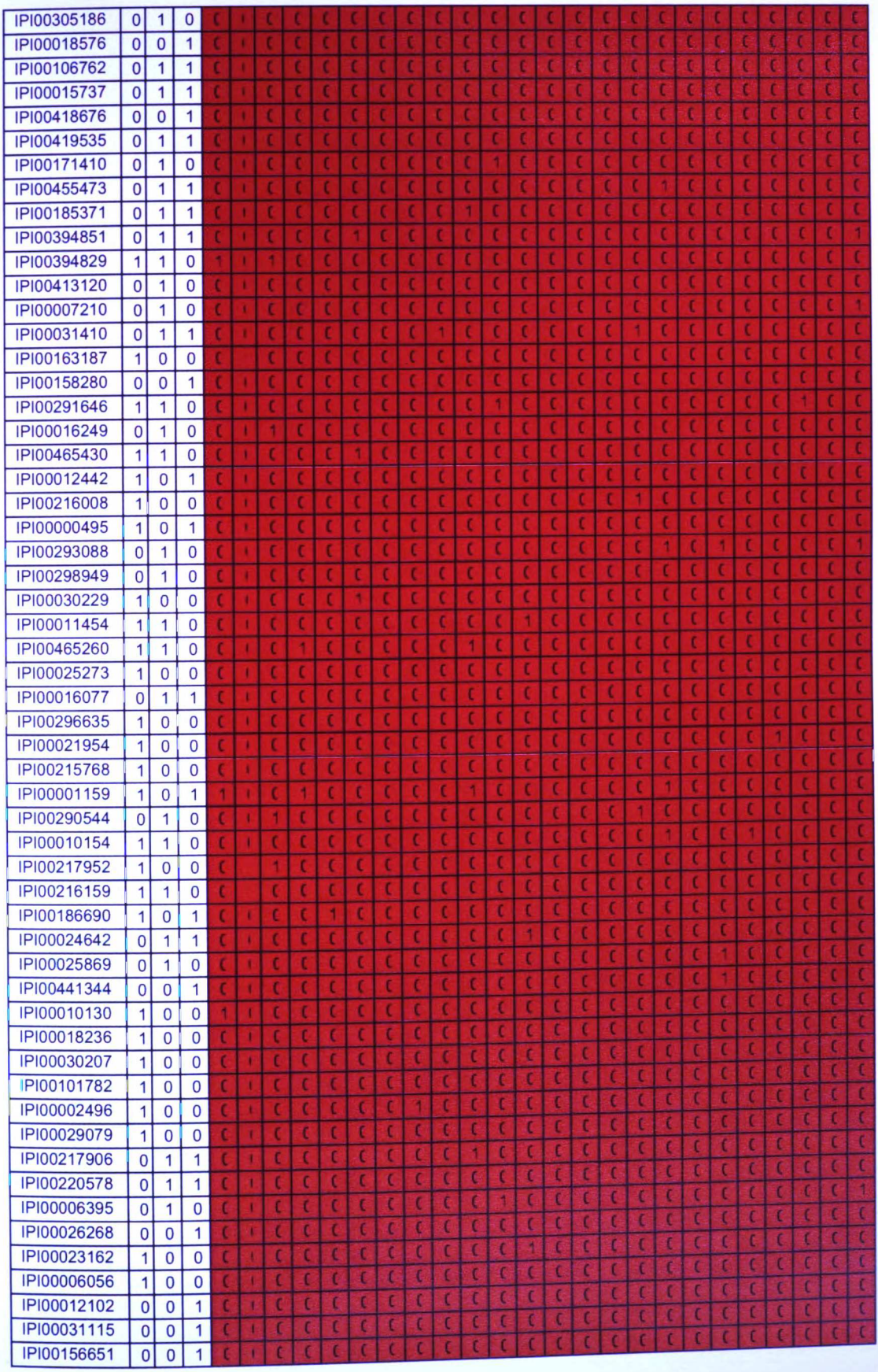

IPI00305186	0	1	0
IPI00018576	0	0	1
IPI00106762	0	1	1
IPI00015737	0	1	1
IPI00418676	0	0	1
IPI00419535	0	1	1
IPI00171410	0	1	0
IPI00455473	0	1	1
IPI00185371	0	1	1
IPI00394851	0	1	1
IPI00394829	1	1	0
IPI00413120	0	1	0
IPI00007210	0	1	0
IPI00031410	0	1	1
IPI00163187	1	0	0
IPI00158280	0	0	1
IPI00291646	1	1	0
IPI00016249	0	1	0
IPI00465430	1	1	0
IPI00012442	1	0	1
IPI00216008	1	0	0
IPI00000495	1	0	1
IPI00293088	0	1	0
IPI00298949	0	1	0
IPI00030229	1	0	0
IPI00011454	1	1	0
IPI00465260	1	1	0
IPI00025273	1	0	0
IPI00016077	0	1	1
IPI00296635	1	0	0
IPI00021954	1	0	0
IPI00215768	1	0	0
IPI00001159	1	0	1
IPI00290544	0	1	0
IPI00010154	1	1	0
IPI00217952	1	0	0
IPI00216159	1	1	0
IPI00186690	1	0	1
IPI00024642	0	1	1
IPI00025869	0	1	0
IPI00441344	0	0	1
IPI00010130	1	0	0
IPI00018236	1	0	0
IPI00030207	1	0	0
IPI00101782	1	0	0
IPI00002496	1	0	0
IPI00029079	1	0	0
IPI00217906	0	1	1
IPI00220578	0	1	1
IPI00006395	0	1	0
IPI00026268	0	0	1
IPI00023162	1	0	0
IPI00006056	1	0	0
IPI00012102	0	0	1
IPI00031115	0	0	1
IPI00156651	0	0	1

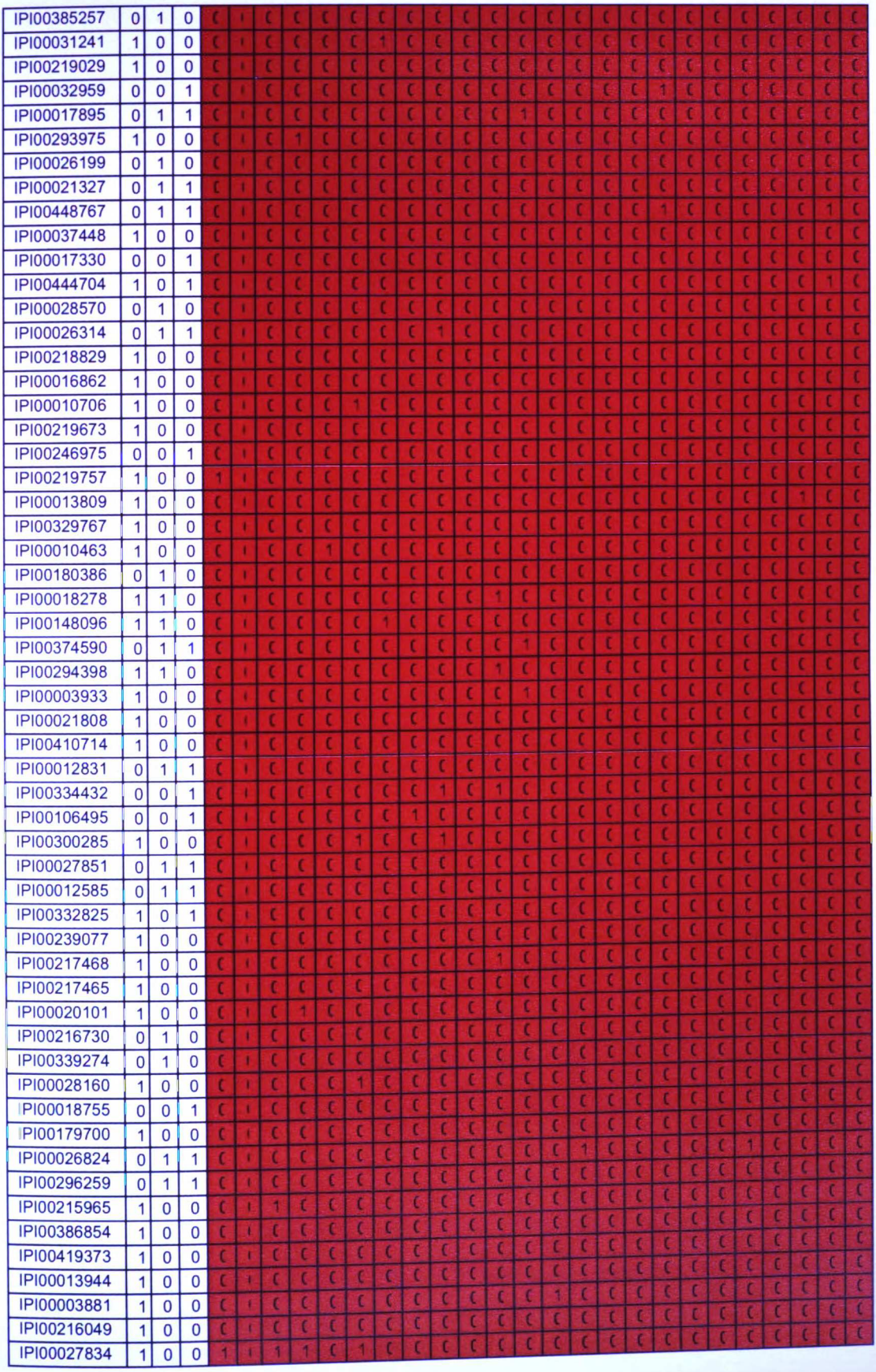

IPI00385257	0	1	0
IPI00031241	1	0	0
IPI00219029	1	0	0
IPI00032959	0	0	1
IPI00017895	0	1	1
IPI00293975	1	0	0
IPI00026199	0	1	0
IPI00021327	0	1	1
IPI00448767	0	1	1
IPI00037448	1	0	0
IPI00017330	0	0	1
IPI00444704	1	0	1
IPI00028570	0	1	0
IPI00026314	0	1	1
IPI00218829	1	0	0
IPI00016862	1	0	0
IPI00010706	1	0	0
IPI00219673	1	0	0
IPI00246975	0	0	1
IPI00219757	1	0	0
IPI00013809	1	0	0
IPI00329767	1	0	0
IPI00010463	1	0	0
IPI00180386	0	1	0
IPI00018278	1	1	0
IPI00148096	1	1	0
IPI00374590	0	1	1
IPI00294398	1	1	0
IPI00003933	1	0	0
IPI00021808	1	0	0
IPI00410714	1	0	0
IPI00012831	0	1	1
IPI00334432	0	0	1
IPI00106495	0	0	1
IPI00300285	1	0	0
IPI00027851	0	1	1
IPI00012585	0	1	1
IPI00332825	1	0	1
IPI00239077	1	0	0
IPI00217468	1	0	0
IPI00217465	1	0	0
IPI00020101	1	0	0
IPI00216730	0	1	0
IPI00339274	0	1	0
IPI00028160	1	0	0
IPI00018755	0	0	1
IPI00179700	1	0	0
IPI00026824	0	1	1
IPI00296259	0	1	1
IPI00215965	1	0	0
IPI00386854	1	0	0
IPI00419373	1	0	0
IPI00013944	1	0	0
IPI00003881	1	0	0
IPI00216049	1	0	0
IPI00027834	1	0	0

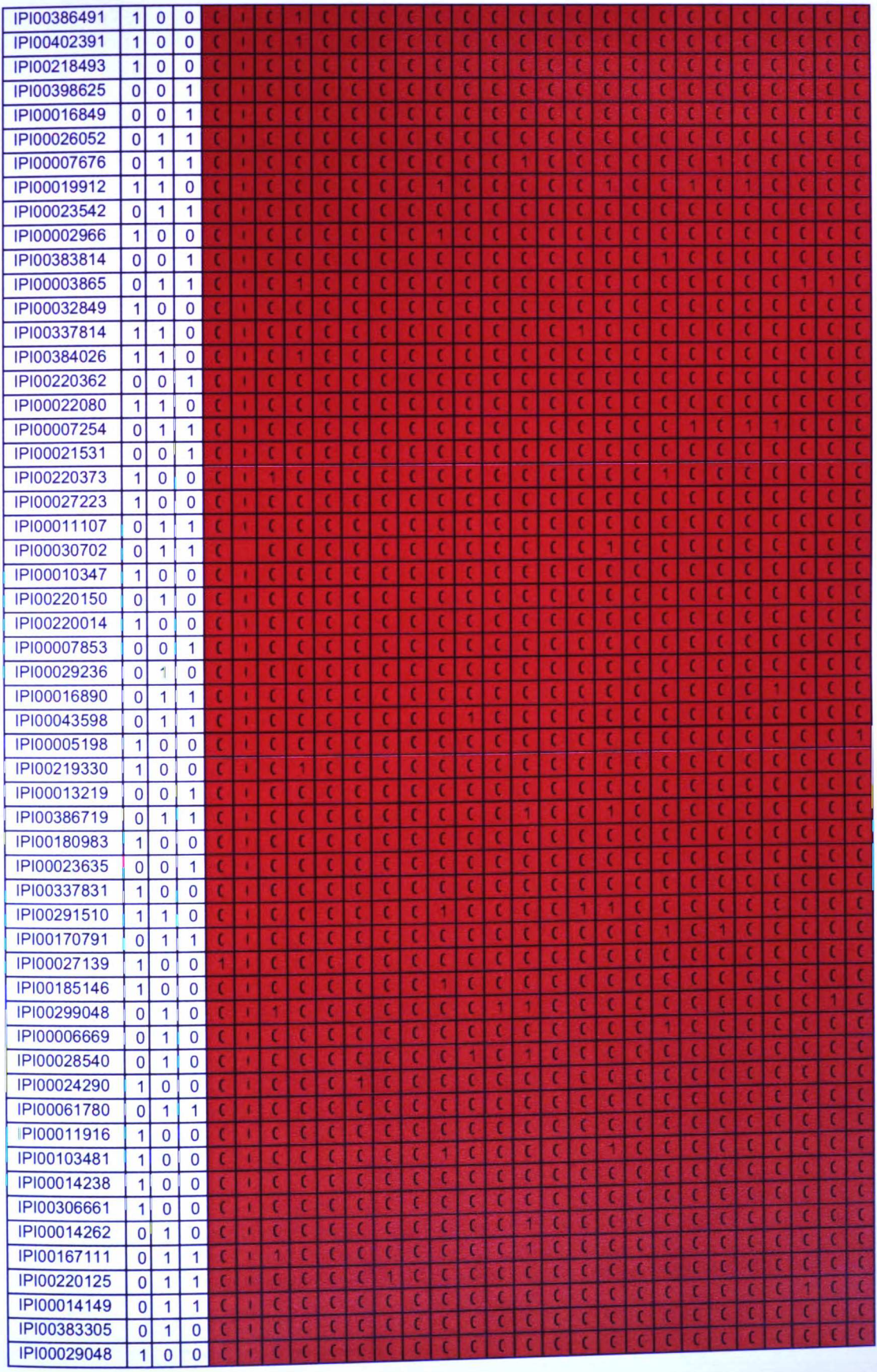

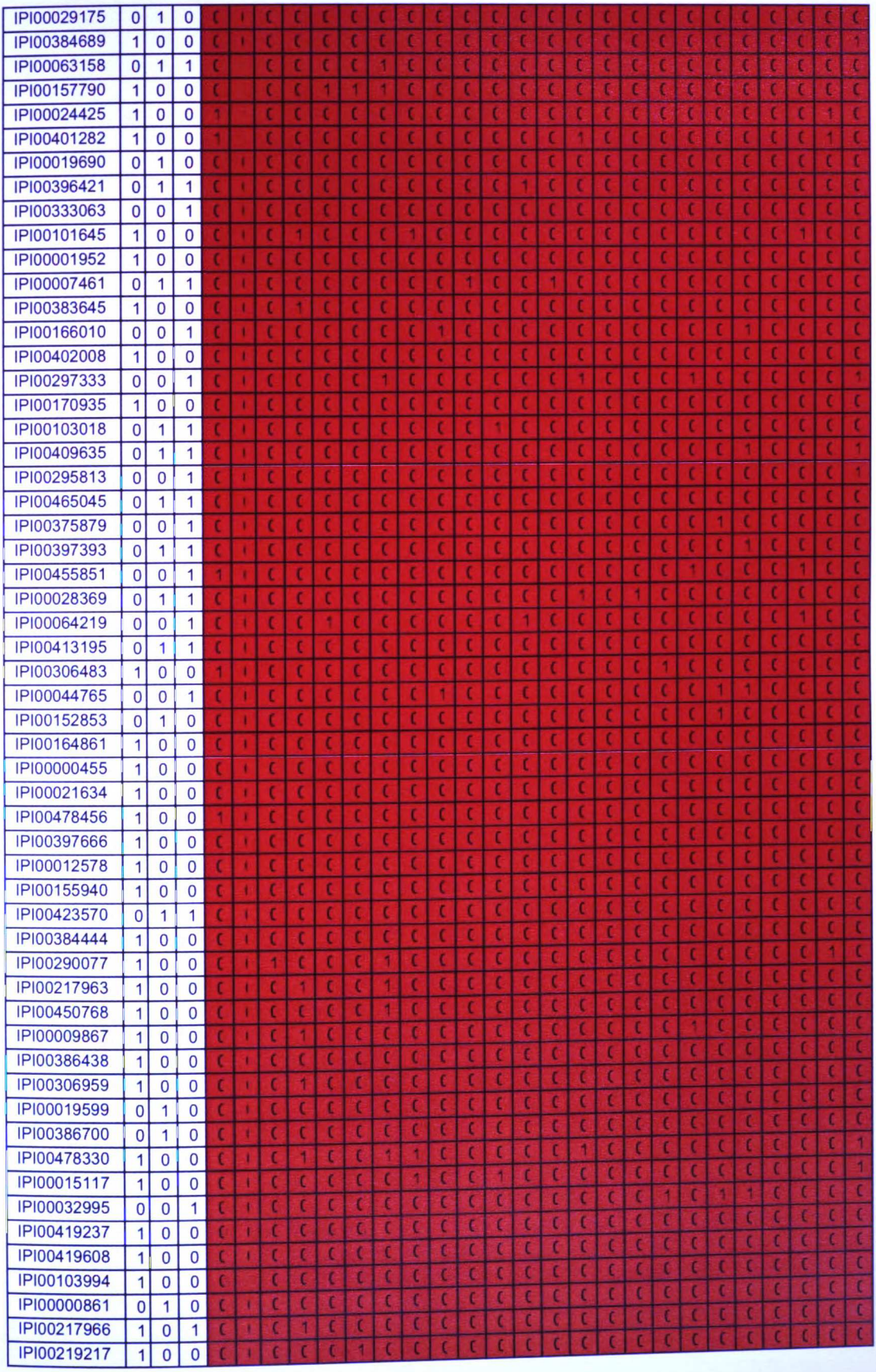

IPI00029175	0	1	0
IPI00384689	1	0	0
IPI00063158	0	1	1
IPI00157790	1	0	0
IPI00024425	1	0	0
IPI00401282	1	0	0
IPI00019690	0	1	0
IPI00396421	0	1	1
IPI00333063	0	0	1
IPI00101645	1	0	0
IPI00001952	1	0	0
IPI00007461	0	1	1
IPI00383645	1	0	0
IPI00166010	0	0	1
IPI00402008	1	0	0
IPI00297333	0	0	1
IPI00170935	1	0	0
IPI00103018	0	1	1
IPI00409635	0	1	1
IPI00295813	0	0	1
IPI00465045	0	1	1
IPI00375879	0	0	1
IPI00397393	0	1	1
IPI00455851	0	0	1
IPI00028369	0	1	1
IPI00064219	0	0	1
IPI00413195	0	1	1
IPI00306483	1	0	0
IPI00044765	0	0	1
IPI00152853	0	1	0
IPI00164861	1	0	0
IPI00000455	1	0	0
IPI00021634	1	0	0
IPI00478456	1	0	0
IPI00397666	1	0	0
IPI00012578	1	0	0
IPI00155940	1	0	0
IPI00423570	0	1	1
IPI00384444	1	0	0
IPI00290077	1	0	0
IPI00217963	1	0	0
IPI00450768	1	0	0
IPI00009867	1	0	0
IPI00386438	1	0	0
IPI00306959	1	0	0
IPI00019599	0	1	0
IPI00386700	0	1	0
IPI00478330	1	0	0
IPI00015117	1	0	0
IPI00032995	0	0	1
IPI00419237	1	0	0
IPI00419608	1	0	0
IPI00103994	1	0	0
IPI00000861	0	1	0
IPI00217966	1	0	1
IPI00219217	1	0	0

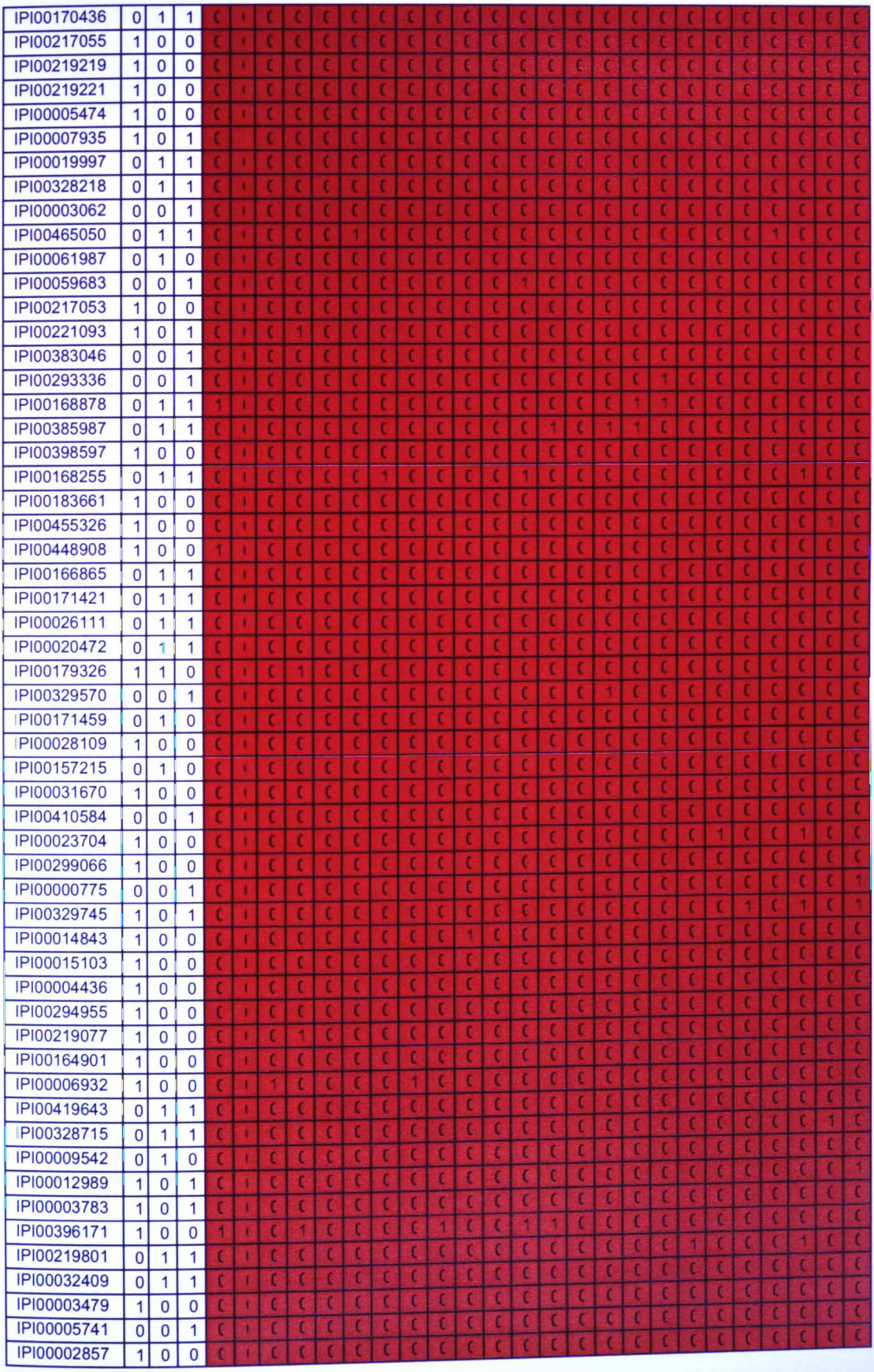

IPI00170436	0	1	1
IPI00217055	1	0	0
IPI00219219	1	0	0
IPI00219221	1	0	0
IPI00005474	1	0	0
IPI00007935	1	0	1
IPI00019997	0	1	1
IPI00328218	0	1	1
IPI00003062	0	0	1
IPI00465050	0	1	1
IPI00061987	0	1	0
IPI00059683	0	0	1
IPI00217053	1	0	0
IPI00221093	1	0	1
IPI00383046	0	0	1
IPI00293336	0	0	1
IPI00168878	0	1	1
IPI00385987	0	1	1
IPI00398597	1	0	0
IPI00168255	0	1	1
IPI00183661	1	0	0
IPI00455326	1	0	0
IPI00448908	1	0	0
IPI00166865	0	1	1
IPI00171421	0	1	1
IPI00026111	0	1	1
IPI00020472	0	1	1
IPI00179326	1	1	0
IPI00329570	0	0	1
IPI00171459	0	1	0
IPI00028109	1	0	0
IPI00157215	0	1	0
IPI00031670	1	0	0
IPI00410584	0	0	1
IPI00023704	1	0	0
IPI00299066	1	0	0
IPI00000775	0	0	1
IPI00329745	1	0	1
IPI00014843	1	0	0
IPI00015103	1	0	0
IPI00004436	1	0	0
IPI00294955	1	0	0
IPI00219077	1	0	0
IPI00164901	1	0	0
IPI00006932	1	0	0
IPI00419643	0	1	1
IPI00328715	0	1	1
IPI00009542	0	1	0
IPI00012989	1	0	1
IPI00003783	1	0	1
IPI00396171	1	0	0
IPI00219801	0	1	1
IPI00032409	0	1	1
IPI00003479	1	0	0
IPI00005741	0	0	1
IPI00002857	1	0	0

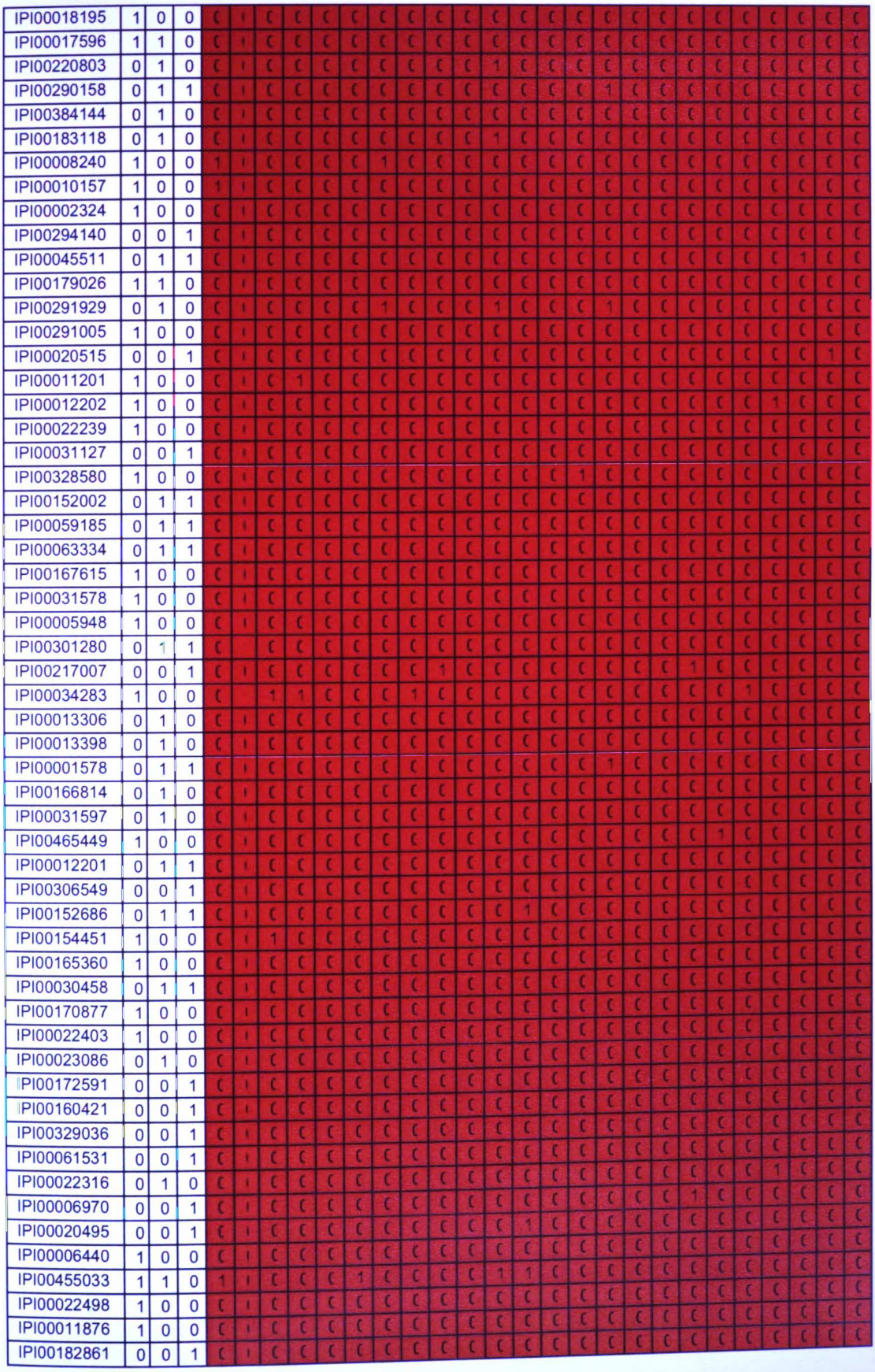

IPI00018195	1	0	0
IPI00017596	1	1	0
IPI00220803	0	1	0
IPI00290158	0	1	1
IPI00384144	0	1	0
IPI00183118	0	1	0
IPI00008240	1	0	0
IPI00010157	1	0	0
IPI00002324	1	0	0
IPI00294140	0	0	1
IPI00045511	0	1	1
IPI00179026	1	1	0
IPI00291929	0	1	0
IPI00291005	1	0	0
IPI00020515	0	0	1
IPI00011201	1	0	0
IPI00012202	1	0	0
IPI00022239	1	0	0
IPI00031127	0	0	1
IPI00328580	1	0	0
IPI00152002	0	1	1
IPI00059185	0	1	1
IPI00063334	0	1	1
IPI00167615	1	0	0
IPI00031578	1	0	0
IPI00005948	1	0	0
IPI00301280	0	1	1
IPI00217007	0	0	1
IPI00034283	1	0	0
IPI00013306	0	1	0
IPI00013398	0	1	0
IPI00001578	0	1	1
IPI00166814	0	1	0
IPI00031597	0	1	0
IPI00465449	1	0	0
IPI00012201	0	1	1
IPI00306549	0	0	1
IPI00152686	0	1	1
IPI00154451	1	0	0
IPI00165360	1	0	0
IPI00030458	0	1	1
IPI00170877	1	0	0
IPI00022403	1	0	0
IPI00023086	0	1	0
IPI00172591	0	0	1
IPI00160421	0	0	1
IPI00329036	0	0	1
IPI00061531	0	0	1
IPI00022316	0	1	0
IPI00006970	0	0	1
IPI00020495	0	0	1
IPI00006440	1	0	0
IPI00455033	1	1	0
IPI00022498	1	0	0
IPI00011876	1	0	0
IPI00182861	0	0	1

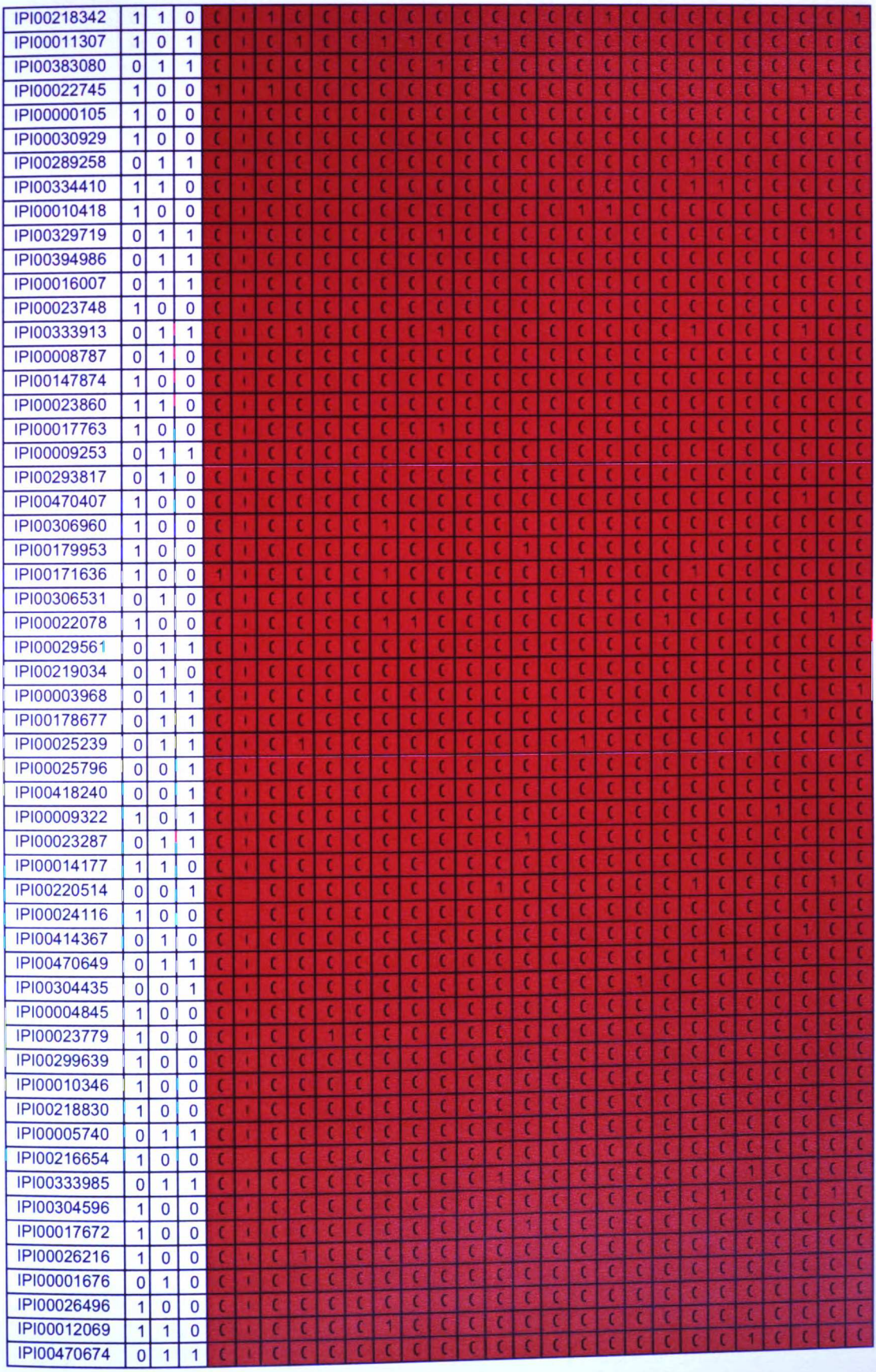

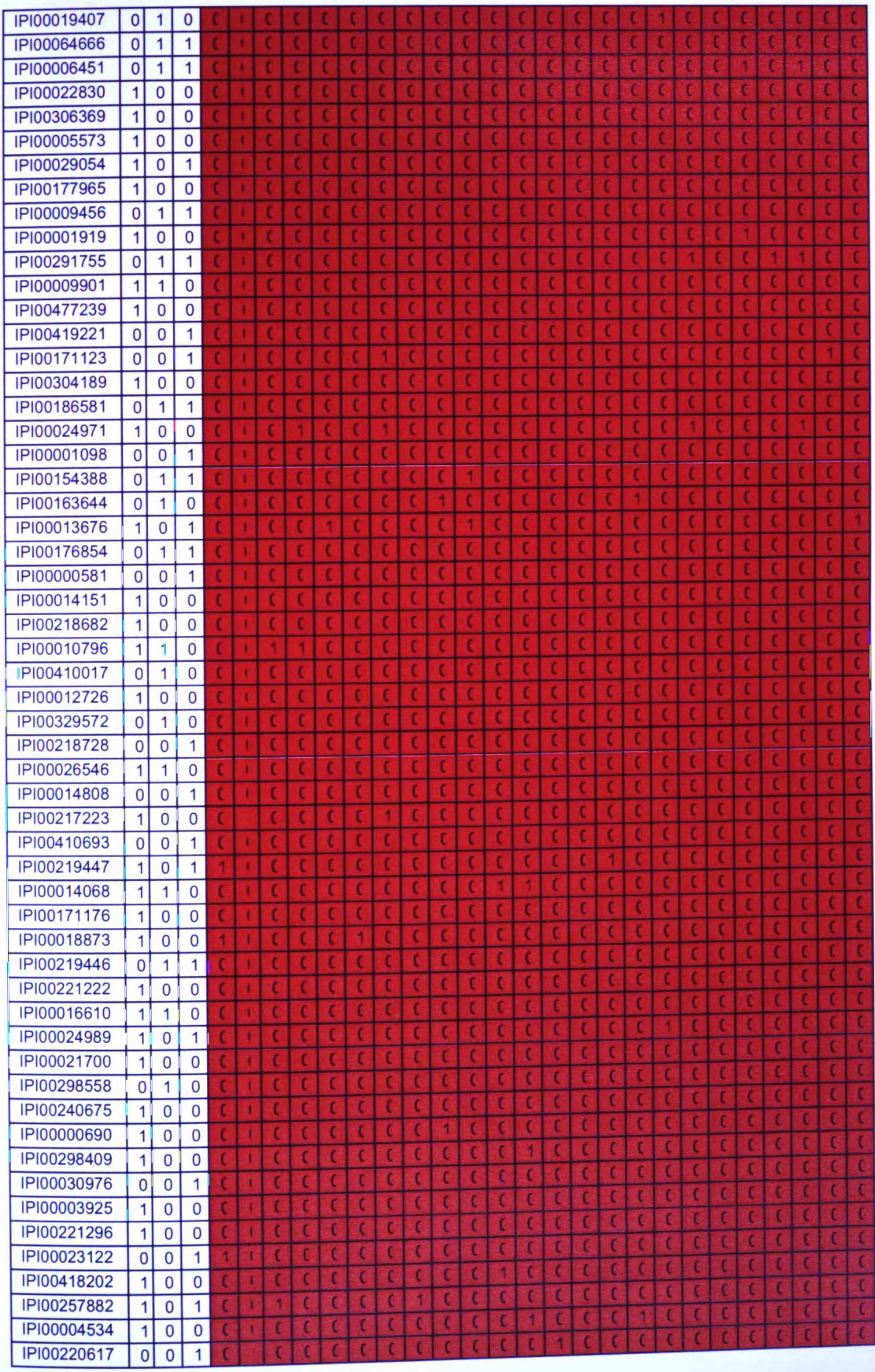

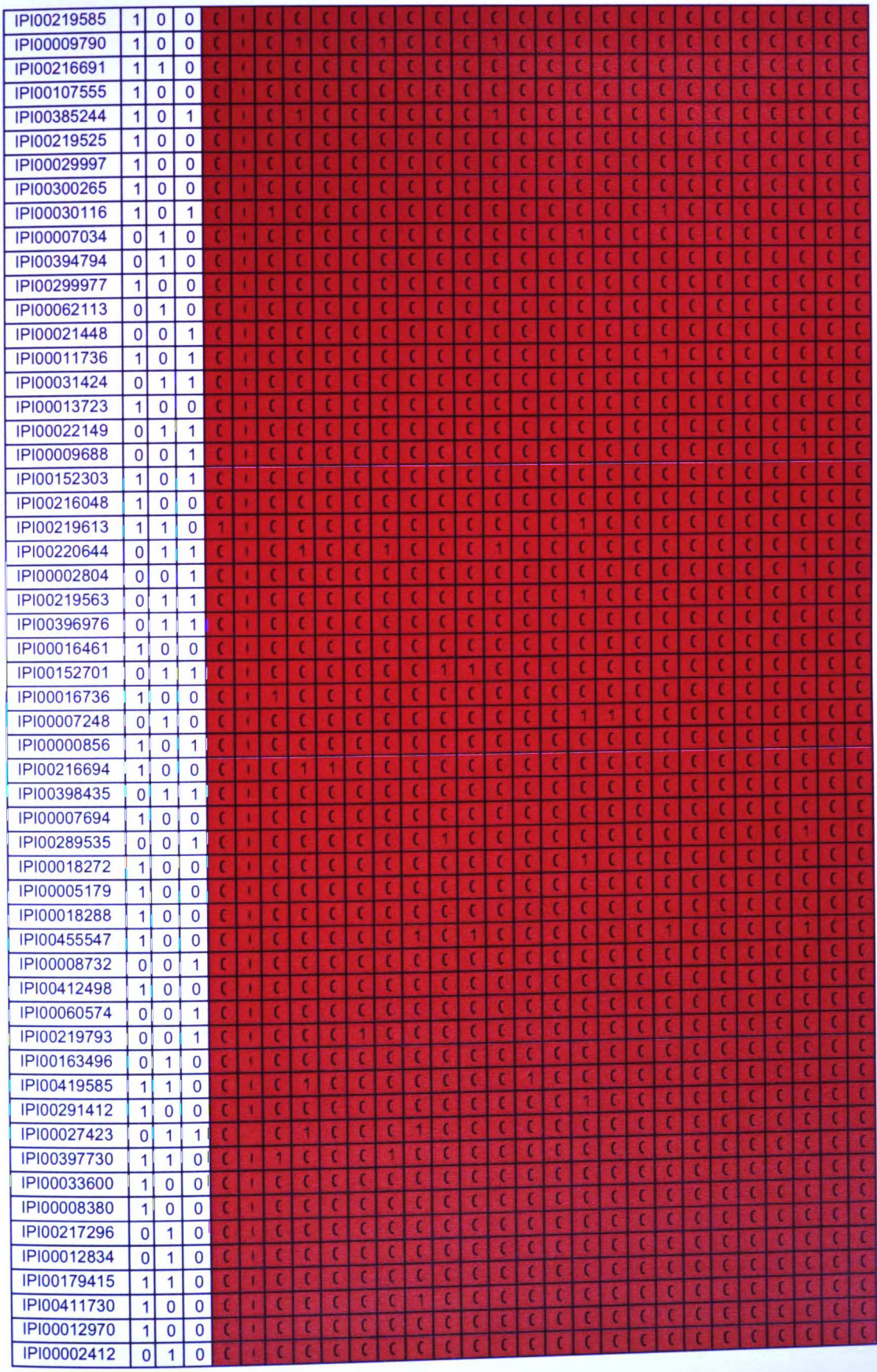

IPI00219585	1	0	0
IPI00009790	1	0	0
IPI00216691	1	1	0
IPI00107555	1	0	0
IPI00385244	1	0	1
IPI00219525	1	0	0
IPI00029997	1	0	0
IPI00300265	1	0	0
IPI00030116	1	0	1
IPI00007034	0	1	0
IPI00394794	0	1	0
IPI00299977	1	0	0
IPI00062113	0	1	0
IPI00021448	0	0	1
IPI00011736	1	0	1
IPI00031424	0	1	1
IPI00013723	1	0	0
IPI00022149	0	1	1
IPI00009688	0	0	1
IPI00152303	1	0	1
IPI00216048	1	0	0
IPI00219613	1	1	0
IPI00220644	0	1	1
IPI00002804	0	0	1
IPI00219563	0	1	1
IPI00396976	0	1	1
IPI00016461	1	0	0
IPI00152701	0	1	1
IPI00016736	1	0	0
IPI00007248	0	1	0
IPI00000856	1	0	1
IPI00216694	1	0	0
IPI00398435	0	1	1
IPI00007694	1	0	0
IPI00289535	0	0	1
IPI00018272	1	0	0
IPI00005179	1	0	0
IPI00018288	1	0	0
IPI00455547	1	0	0
IPI00008732	0	0	1
IPI00412498	1	0	0
IPI00060574	0	0	1
IPI00219793	0	0	1
IPI00163496	0	1	0
IPI00419585	1	1	0
IPI00291412	1	0	0
IPI00027423	0	1	1
IPI00397730	1	1	0
IPI00033600	1	0	0
IPI00008380	1	0	0
IPI00217296	0	1	0
IPI00012834	0	1	0
IPI00179415	1	1	0
IPI00411730	1	0	0
IPI00012970	1	0	0
IPI00002412	0	1	0

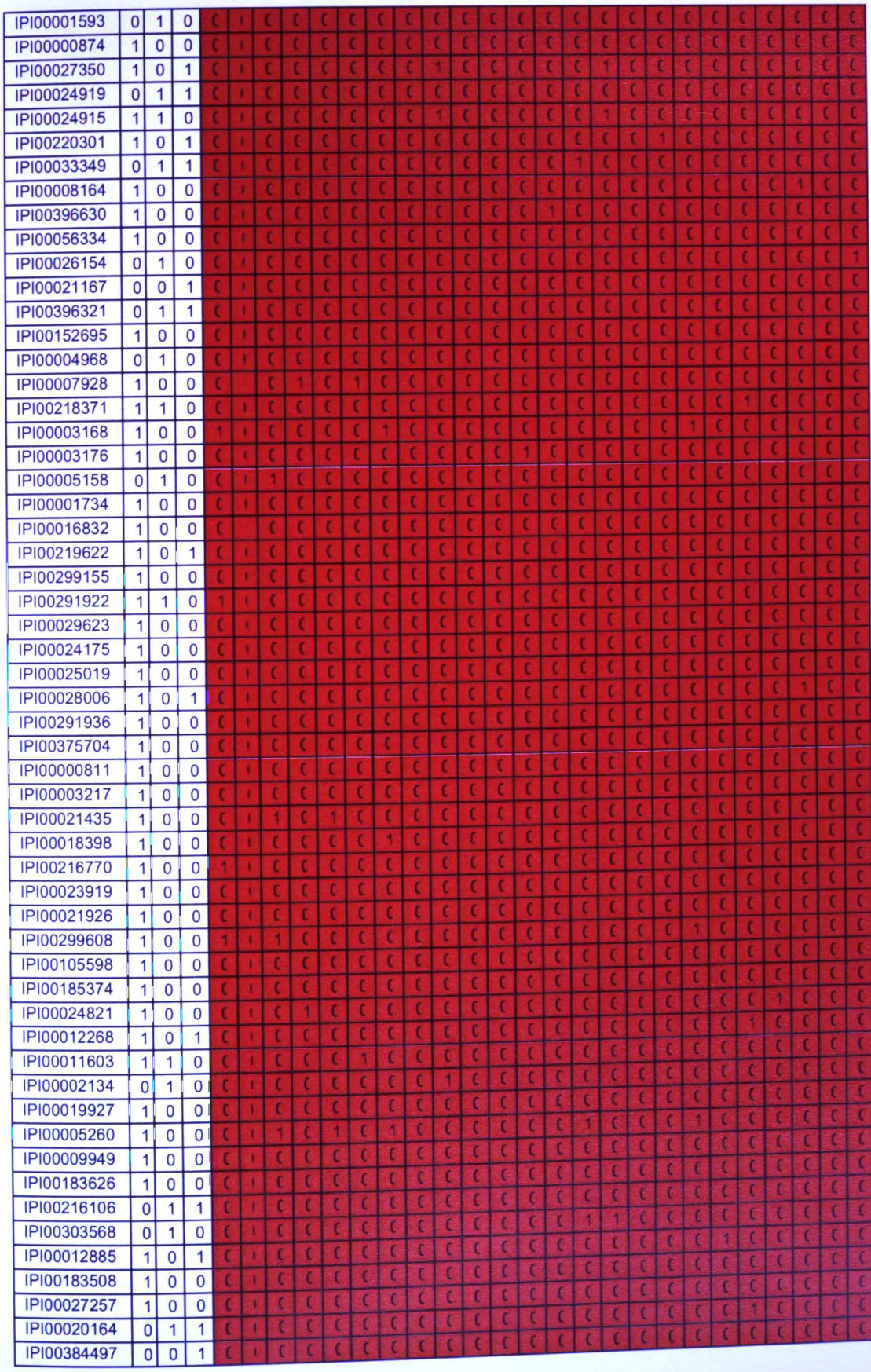

IPI00001593	0	1	0
IPI00000874	1	0	0
IPI00027350	1	0	1
IPI00024919	0	1	1
IPI00024915	1	1	0
IPI00220301	1	0	1
IPI00033349	0	1	1
IPI00008164	1	0	0
IPI00396630	1	0	0
IPI00056334	1	0	0
IPI00026154	0	1	0
IPI00021167	0	0	1
IPI00396321	0	1	1
IPI00152695	1	0	0
IPI00004968	0	1	0
IPI00007928	1	0	0
IPI00218371	1	1	0
IPI00003168	1	0	0
IPI00003176	1	0	0
IPI00005158	0	1	0
IPI00001734	1	0	0
IPI00016832	1	0	0
IPI00219622	1	0	1
IPI00299155	1	0	0
IPI00291922	1	1	0
IPI00029623	1	0	0
IPI00024175	1	0	0
IPI00025019	1	0	0
IPI00028006	1	0	1
IPI00291936	1	0	0
IPI00375704	1	0	0
IPI00000811	1	0	0
IPI00003217	1	0	0
IPI00021435	1	0	0
IPI00018398	1	0	0
IPI00216770	1	0	0
IPI00023919	1	0	0
IPI00021926	1	0	0
IPI00299608	1	0	0
IPI00105598	1	0	0
IPI00185374	1	0	0
IPI00024821	1	0	0
IPI00012268	1	0	1
IPI00011603	1	1	0
IPI00002134	0	1	0
IPI00019927	1	0	0
IPI00005260	1	0	0
IPI00009949	1	0	0
IPI00183626	1	0	0
IPI00216106	0	1	1
IPI00303568	0	1	0
IPI00012885	1	0	1
IPI00183508	1	0	0
IPI00027257	1	0	0
IPI00020164	0	1	1
IPI00384497	0	0	1

IPI00289082	1	0	0
IPI00006714	0	0	1
IPI00106928	0	1	0
IPI00176903	1	0	0
IPI00165651	0	0	1
IPI00023591	1	0	0
IPI00220030	1	0	0
IPI00296864	0	1	1
IPI00004358	1	0	0
IPI00470525	1	0	0
IPI00305092	1	0	0
IPI00026665	1	0	0
IPI00014439	1	0	0
IPI00014877	0	1	1
IPI00376394	0	1	1
IPI00021328	0	0	1
IPI00335140	0	1	1
IPI00007866	0	1	1
IPI00014577	0	1	1
IPI00031169	0	1	1
IPI00007755	0	1	1
IPI00010491	0	1	1
IPI00014376	0	0	1
IPI00014377	0	1	0
IPI00300096	0	1	1
IPI00032808	0	1	1
IPI00014235	1	0	0
IPI00290518	1	0	0
IPI00023510	0	1	0
IPI00017344	0	1	0
IPI00016339	0	1	0
IPI00217943	0	1	0
IPI00030304	0	0	1
IPI00016342	0	1	1
IPI00028481	0	1	0
IPI00016372	0	1	1
IPI00022664	1	0	0
IPI00295849	1	0	0
IPI00102897	0	0	1
IPI00219675	0	1	1
IPI00010270	1	0	0
IPI00008223	0	1	0
IPI00032395	0	0	1
IPI00181006	1	0	0
IPI00217519	0	1	1
IPI00004397	0	1	1
IPI00216044	1	0	0
IPI00012507	1	0	1
IPI00221083	1	0	0
IPI00009607	0	1	1
IPI00004860	1	0	0
IPI00180305	1	0	0
IPI00395865	1	0	1
IPI00024320	0	1	0
IPI00033611	1	0	0
IPI00003706	1	0	0

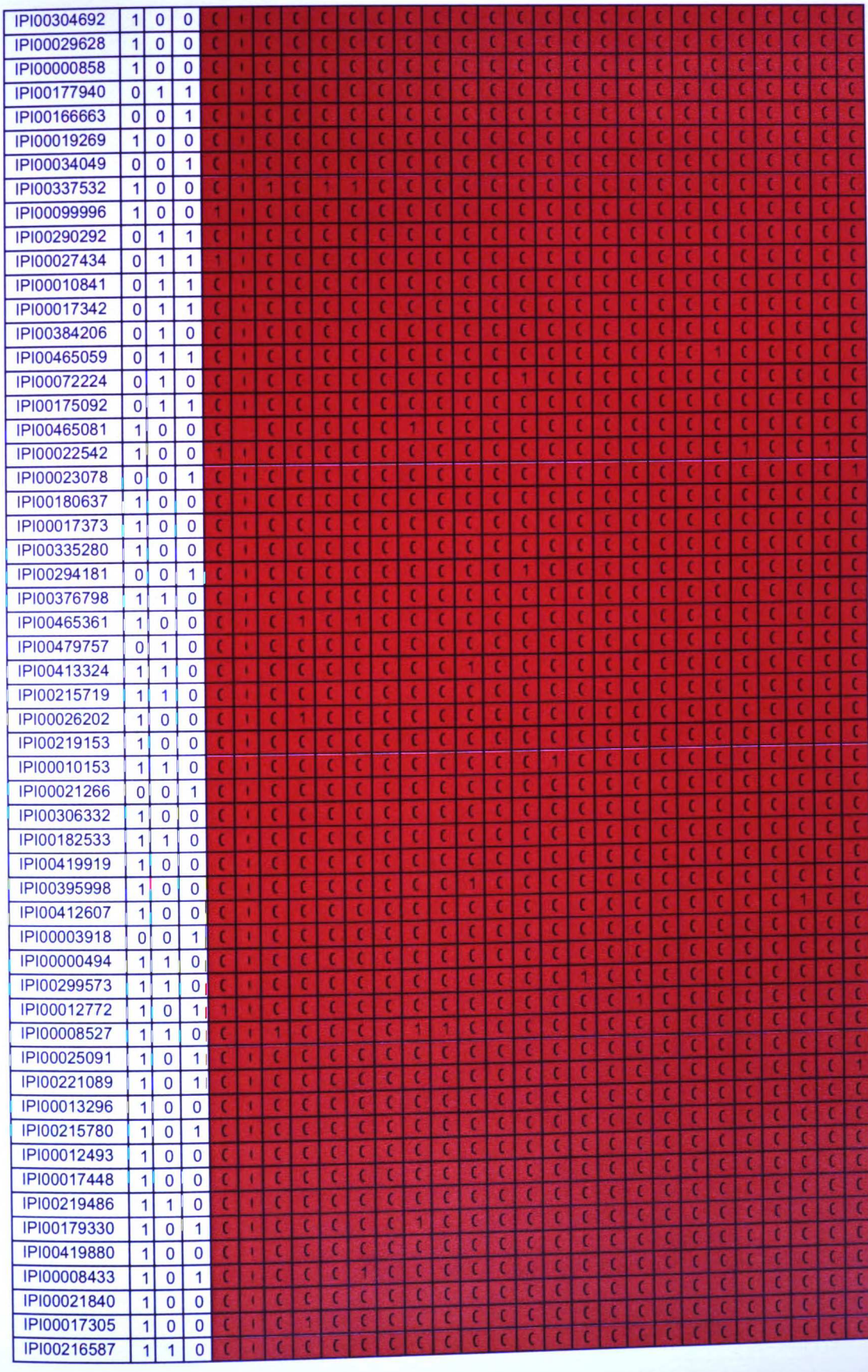

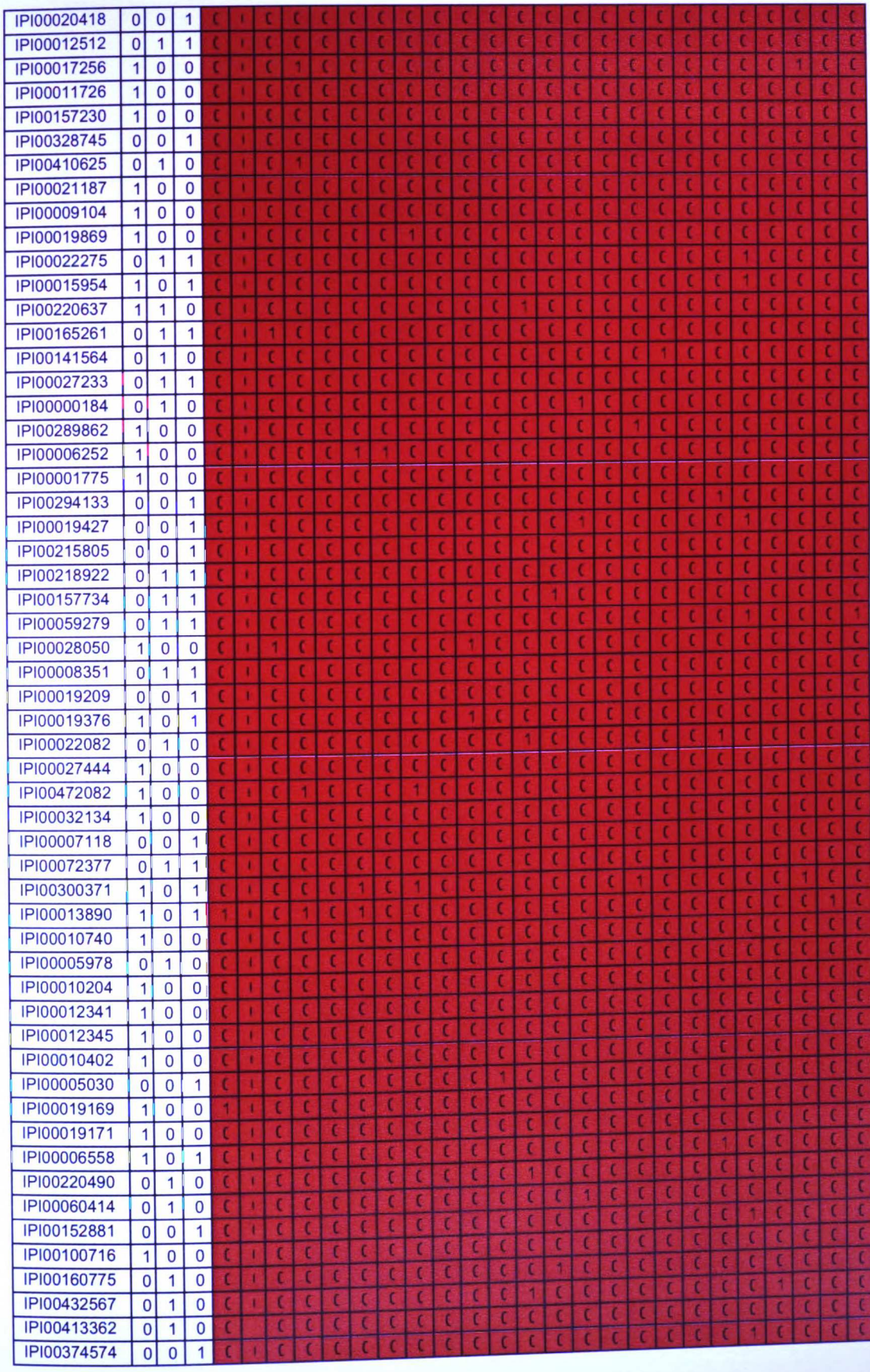

IPI00020418	0	0	1
IPI00012512	0	1	1
IPI00017256	1	0	0
IPI00011726	1	0	0
IPI00157230	1	0	0
IPI00328745	0	0	1
IPI00410625	0	1	0
IPI00021187	1	0	0
IPI00009104	1	0	0
IPI00019869	1	0	0
IPI00022275	0	1	1
IPI00015954	1	0	1
IPI00220637	1	1	0
IPI00165261	0	1	1
IPI00141564	0	1	0
IPI00027233	0	1	1
IPI00000184	0	1	0
IPI00289862	1	0	0
IPI00006252	1	0	0
IPI00001775	1	0	0
IPI00294133	0	0	1
IPI00019427	0	0	1
IPI00215805	0	0	1
IPI00218922	0	1	1
IPI00157734	0	1	1
IPI00059279	0	1	1
IPI00028050	1	0	0
IPI00008351	0	1	1
IPI00019209	0	0	1
IPI00019376	1	0	1
IPI00022082	0	1	0
IPI00027444	1	0	0
IPI00472082	1	0	0
IPI00032134	1	0	0
IPI00007118	0	0	1
IPI00072377	0	1	1
IPI00300371	1	0	1
IPI00013890	1	0	1
IPI00010740	1	0	0
IPI00005978	0	1	0
IPI00010204	1	0	0
IPI00012341	1	0	0
IPI00012345	1	0	0
IPI00010402	1	0	0
IPI00005030	0	0	1
IPI00019169	1	0	0
IPI00019171	1	0	0
IPI00006558	1	0	1
IPI00220490	0	1	0
IPI00060414	0	1	0
IPI00152881	0	0	1
IPI00100716	1	0	0
IPI00160775	0	1	0
IPI00432567	0	1	0
IPI00413362	0	1	0
IPI00374574	0	0	1

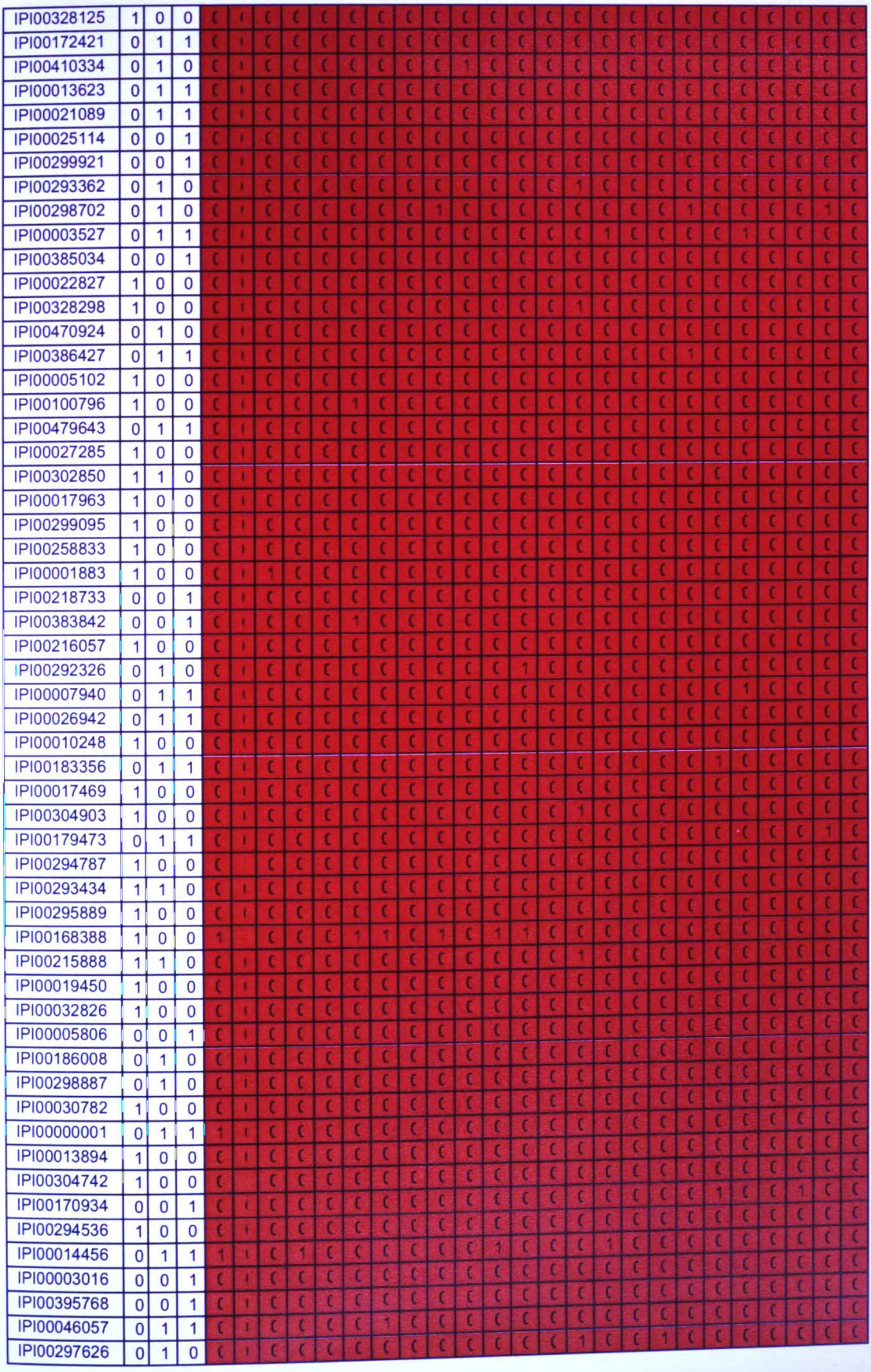

IPI00328125	1	0	0
IPI00172421	0	1	1
IPI00410334	0	1	0
IPI00013623	0	1	1
IPI00021089	0	1	1
IPI00025114	0	0	1
IPI00299921	0	0	1
IPI00293362	0	1	0
IPI00298702	0	1	0
IPI00003527	0	1	1
IPI00385034	0	0	1
IPI00022827	1	0	0
IPI00328298	1	0	0
IPI00470924	0	1	0
IPI00386427	0	1	1
IPI00005102	1	0	0
IPI00100796	1	0	0
IPI00479643	0	1	1
IPI00027285	1	0	0
IPI00302850	1	1	0
IPI00017963	1	0	0
IPI00299095	1	0	0
IPI00258833	1	0	0
IPI00001883	1	0	0
IPI00218733	0	0	1
IPI00383842	0	0	1
IPI00216057	1	0	0
IPI00292326	0	1	0
IPI00007940	0	1	1
IPI00026942	0	1	1
IPI00010248	1	0	0
IPI00183356	0	1	1
IPI00017469	1	0	0
IPI00304903	1	0	0
IPI00179473	0	1	1
IPI00294787	1	0	0
IPI00293434	1	1	0
IPI00295889	1	0	0
IPI00168388	1	0	0
IPI00215888	1	1	0
IPI00019450	1	0	0
IPI00032826	1	0	0
IPI00005806	0	0	1
IPI00186008	0	1	0
IPI00298887	0	1	0
IPI00030782	1	0	0
IPI00000001	0	1	1
IPI00013894	1	0	0
IPI00304742	1	0	0
IPI00170934	0	0	1
IPI00294536	1	0	0
IPI00014456	0	1	1
IPI00003016	0	0	1
IPI00395768	0	0	1
IPI00046057	0	1	1
IPI00297626	0	1	0

IPI00096066	1	0	0
IPI00026970	1	0	0
IPI00021302	0	0	1
IPI00059242	1	0	0
IPI00328319	1	0	0
IPI00018140	0	1	1
IPI00166996	0	1	1
IPI00024102	1	0	0
IPI00166036	0	1	1
IPI00002232	0	1	1
IPI00006283	0	1	1
IPI00410485	0	0	1
IPI00329633	1	0	0
IPI00106559	0	1	0
IPI00005585	0	1	0
IPI00022450	1	0	0
IPI00030774	1	0	1
IPI00018402	1	0	0
IPI00386189	1	0	0
IPI00000948	0	1	1
IPI00290566	1	1	0
IPI00479875	1	0	0
IPI00024097	1	0	0
IPI00006372	0	1	0
IPI00020928	0	1	0
IPI00099999	1	0	0
IPI00328840	1	0	0
IPI00418497	0	1	1
IPI00299214	0	1	1
IPI00021716	1	1	0
IPI00384668	0	1	0
IPI00151710	0	1	1
IPI00092641	0	0	1
IPI00005087	1	0	0
IPI00304589	1	1	0
IPI00386422	0	0	1
IPI00023137	0	0	1
IPI00017842	0	1	1
IPI00465028	1	0	1
IPI00014581	1	0	0
IPI00218820	1	0	0
IPI00218320	1	0	0
IPI00010779	1	0	0
IPI00020416	1	0	0
IPI00009943	1	0	0
IPI00030275	1	0	0
IPI00029629	1	0	0
IPI00438229	1	0	0
IPI00073096	1	0	0
IPI00152001	0	1	1
IPI00307165	1	0	0
IPI00479523	0	0	1
IPI00018804	1	0	0
IPI00301561	0	0	1
IPI00021016	1	0	0
IPI00018434	0	1	0

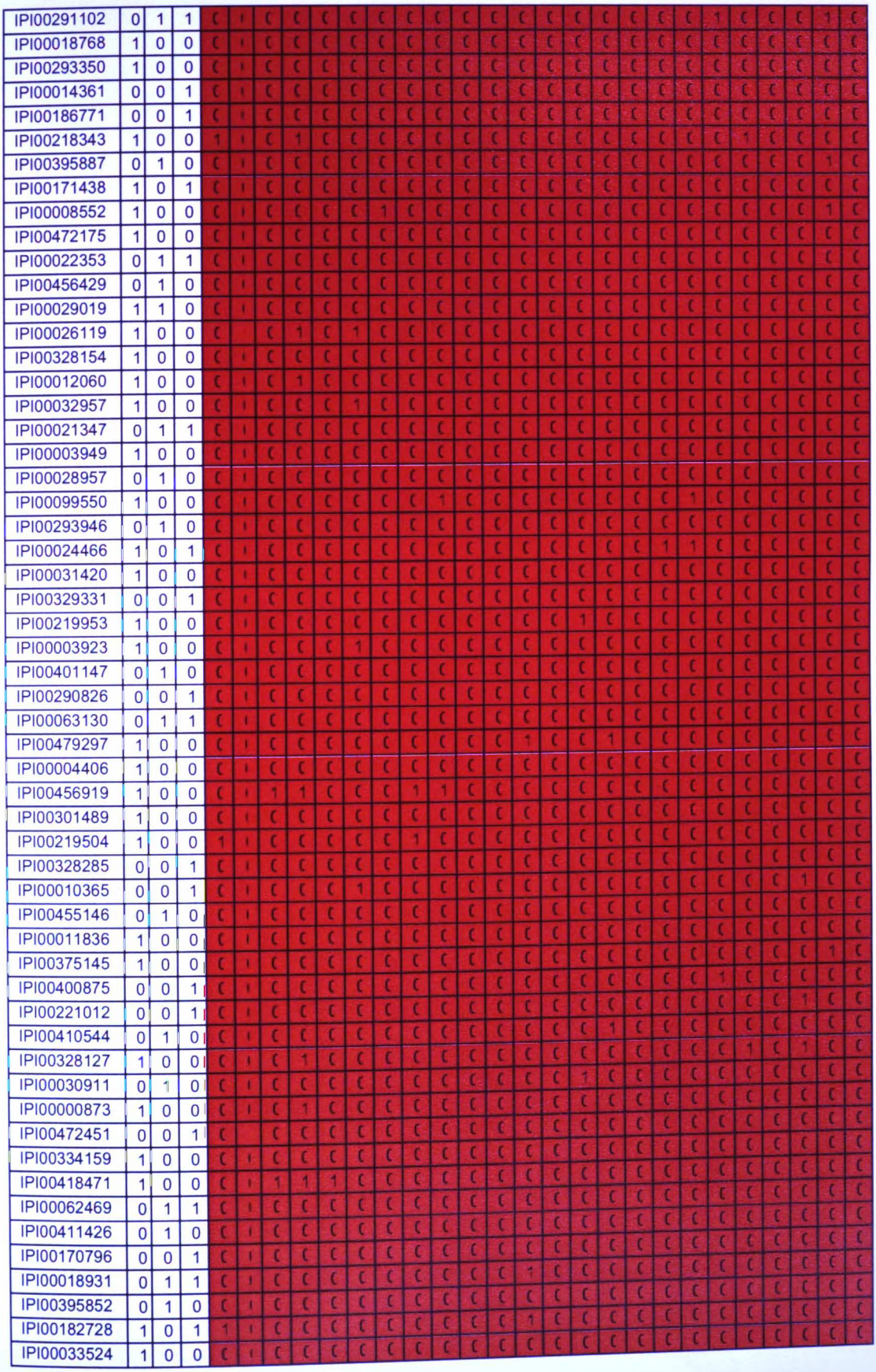

IPI00291102	0	1	1
IPI00018768	1	0	0
IPI00293350	1	0	0
IPI00014361	0	0	1
IPI00186771	0	0	1
IPI00218343	1	0	0
IPI00395887	0	1	0
IPI00171438	1	0	1
IPI00008552	1	0	0
IPI00472175	1	0	0
IPI00022353	0	1	1
IPI00456429	0	1	0
IPI00029019	1	1	0
IPI00026119	1	0	0
IPI00328154	1	0	0
IPI00012060	1	0	0
IPI00032957	1	0	0
IPI00021347	0	1	1
IPI00003949	1	0	0
IPI00028957	0	1	0
IPI00099550	1	0	0
IPI00293946	0	1	0
IPI00024466	1	0	1
IPI00031420	1	0	0
IPI00329331	0	0	1
IPI00219953	1	0	0
IPI00003923	1	0	0
IPI00401147	0	1	0
IPI00290826	0	0	1
IPI00063130	0	1	1
IPI00479297	1	0	0
IPI00004406	1	0	0
IPI00456919	1	0	0
IPI00301489	1	0	0
IPI00219504	1	0	0
IPI00328285	0	0	1
IPI00010365	0	0	1
IPI00455146	0	1	0
IPI00011836	1	0	0
IPI00375145	1	0	0
IPI00400875	0	0	1
IPI00221012	0	0	1
IPI00410544	0	1	0
IPI00328127	1	0	0
IPI00030911	0	1	0
IPI00000873	1	0	0
IPI00472451	0	0	1
IPI00334159	1	0	0
IPI00418471	1	0	0
IPI00062469	0	1	1
IPI00411426	0	1	0
IPI00170796	0	0	1
IPI00018931	0	1	1
IPI00395852	0	1	0
IPI00182728	1	0	1
IPI00033524	1	0	0

IPI00019640	0	1	0	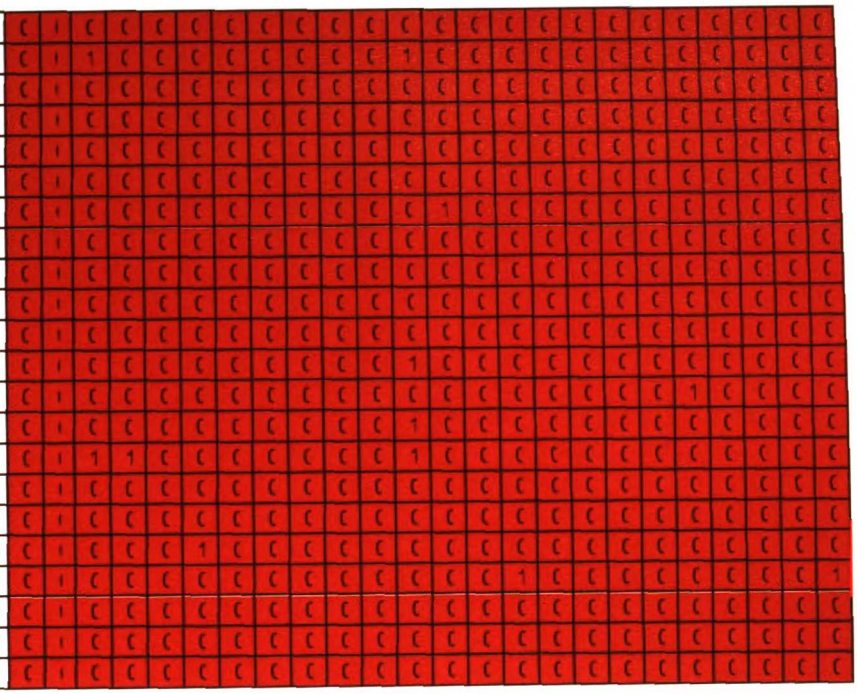
IPI00295400	1	1	0	
IPI00022007	0	1	0	
IPI00014263	1	0	0	
IPI00167072	0	1	0	
IPI00470587	1	0	0	
IPI00013010	0	1	0	
IPI00166584	1	0	0	
IPI00306290	1	0	0	
IPI00009326	1	0	0	
IPI00007074	1	0	0	
IPI00013981	0	1	1	
IPI00007607	0	1	1	
IPI00216319	1	1	0	
IPI00021263	1	1	0	
IPI00332936	1	0	0	
IPI00183979	0	0	1	
IPI00000893	1	0	0	
IPI00103874	1	0	0	
IPI00005688	1	0	0	
IPI00032955	1	0	0	
IPI00011631	0	0	1	

Appendix C

Table S1. 1,468 [*in-silico*] tryptic peptides that occurred in more than one protein in our PMT database. 96% of these peptides occur in alternative splice forms/isomers of the same gene product.

Peptide	SwissProt Accession	SwissProt ID
AAEVFFETFNVPALFISMQAVLSLYATG R	ACTZ_HUMAN	P61163
	ACTY_HUMAN	P42025
AAFLTGR	ARSD_HUMAN	P51689
	ARSE_HUMAN	P51690
AANILVGENLVCK	YES_HUMAN	P07947
	SRC_HUMAN	P12931
AAPGYHMAK	PHS1_HUMAN	P06737
	PHS3_HUMAN	P11216
	PHS2_HUMAN	P11217
AASGEAKPK	H14_HUMAN	P10412
	H15_HUMAN	P16401
	H12_HUMAN	P16403
AAVPDAVGK	AT1A3_HUMAN	P13637
	AT1A2_HUMAN	P50993
AAVPSGASTGIYEALELR	ENOA_HUMAN	P06733
	ENOG_HUMAN	P09104
	ENOB_HUMAN	P13929
AAYFGVYDTAK	ADT1_HUMAN	P12235
	ADT3_HUMAN	P12236
AAYLQSLNSADLLK	MYH8_HUMAN	P13535
	MYH2_HUMAN	Q9UKX2
ACGVLETIR	MYO5C_HUMAN	Q9NQX4
	MYO5B_HUMAN	Q9ULV0
ACNCLLLK	ENOG_HUMAN	P09104
	ENOB_HUMAN	P13929
ACSPSYSGG	ALU1_HUMAN	P39188
	ALU5_HUMAN	P39192
ACYLSINPQK	ACTZ_HUMAN	P61163
	ACTY_HUMAN	P42025
ADALQAGASQFETSAAK	VAM2_HUMAN	P63027
	VAM3_HUMAN	Q15836
ADEWLMK	MYH9_HUMAN	P35579
	MYH10_HUMAN	P35580
ADFCIIHYAGK	MYH9_HUMAN	P35579
	MYH10_HUMAN	P35580
ADIAESQVNK	MYH3_HUMAN	P11055
	MYH1_HUMAN	P12882
	MYH7_HUMAN	P12883
	MYH6_HUMAN	P13533
	MYH8_HUMAN	P13535
	MYH2_HUMAN	Q9UKX2
	MYH13_HUMAN	Q9UKX3
	MYH4_HUMAN	Q9Y623
ADIGIAMGISGSDVSK	AT1A2_HUMAN	P50993
	AT1A4_HUMAN	Q13733

	HS90A_HUMAN	P07900
ADLINNLGTIAK	HS90B_HUMAN	P08238
	EHD1_HUMAN	Q9H4M9
ADQIETQQLMR	EHD3_HUMAN	Q9NZN3
	K2C6A_HUMAN	P02538
	K2C6B_HUMAN	P04259
	K2C6C_HUMAN	P48666
ADTLTDEINFLR	K2C6E_HUMAN	P48668
	K2C3_HUMAN	P12035
AEAEALYQTK	K2C4_HUMAN	P19013
	K2C6A_HUMAN	P02538
	K2C6B_HUMAN	P04259
	K2C6C_HUMAN	P48666
AEAESWYQTK	K2C6E_HUMAN	P48668
	MYH3_HUMAN	P11055
	MYH1_HUMAN	P12882
	MYH2_HUMAN	Q9UKX2
AEDEEEINAELTAK	MYH4_HUMAN	Q9Y623
	HSP71_HUMAN	P08107
AEDEVQR	HS70L_HUMAN	P34931
AEHLCQQLPIPGPVEEMLAEVNATITDII SALVTSTFIIEK	STA5A_HUMAN	P42229
	STA5B_HUMAN	P51692
	STA5A_HUMAN	P42229
AEHQVGEDGFLLK	STA5B_HUMAN	P51692
	ALU2_HUMAN	P39189
AEIAPLHSSLGDR	ALU8_HUMAN	P39195
	UDB17_HUMAN	O75795
AEMWLIR	UDB15_HUMAN	P54855
	MYO1F_HUMAN	O00160
AEQEEYVQEGIR	MYO1E_HUMAN	Q12965
	STA5A_HUMAN	P42229
AEVQSNR	STA5B_HUMAN	P51692
	PCBP1_HUMAN	Q15365
AFAMIIDK	PCBP2_HUMAN	Q15366
AFITHAGSHGVYESICNGVPMVMMPLF GDQMDNAK	UD16_HUMAN	P19224
	UD11_HUMAN	P22309
AFITHGGTNGIYEAIYHGIPMVGIPLFAD QHDNIAHMK	UDB17_HUMAN	O75795
	UDB15_HUMAN	P54855
AFMEALQAGADISMIGQFGVGFYSAYLV AEK	HS90A_HUMAN	P07900
	HS90B_HUMAN	P08238
	TBA1_MERUN	P68360
	TBA1_MACFA	P68367
	TBA6_HUMAN	Q9BQE3
AFVHWYVGEGMEEGEFSEAR	TBA8_HUMAN	Q9NY65
	HSP71_HUMAN	P08107
AFYPEEISSMVLTK	HS70L_HUMAN	P34931
	BGAL_HUMAN	P16278
AGATLDLLVENMGR	BGAM_HUMAN	P16279
AGFAGDDAPR	ACTS_MOUSE	P68134

	ACTB_BOVIN	P60712
	ACTA_RABIT	P62740
	ACTC_HUMAN	P68032
	ACTH_HUMAN	P63267
AGFAGDQIPK	ACTZ_HUMAN	P61163
	ACTY_HUMAN	P42025
AGGFGGGR	K2C3_HUMAN	P12035
	K22O_HUMAN	Q01546
AGGSYGFGGAGSGFGFGGGAGIGFGL	K2C6B_HUMAN	P04259
GGGAGLAGGFGGPGFPVCPPGGIQEV TVNQSLLTPLNLQIDPAIQR	K2C6E_HUMAN	P48668
AGLLGLLEEMR	MYH1_HUMAN	P12882
	MYH7_HUMAN	P12883
	MYH6_HUMAN	P13533
	MYH8_HUMAN	P13535
	MYH2_HUMAN	Q9UKX2
	MYH13_HUMAN	Q9UKX3
AGLLGTLEEMR	MYH3_HUMAN	P11055
	MYH4_HUMAN	Q9Y623
AGLQFPVGR	H2AC_HUMAN	P02261
	H2AX_HUMAN	P16104
	H2AZ_HUMAN	P17317
	H2AO_HUMAN	P20670
	H2AG_HUMAN	P20671
	H2AA_HUMAN	P28001
	H2AL_HUMAN	Q93077
	H2AE_HUMAN	Q99878
AGPHCEK	LTB1S_HUMAN	P22064
	LTB1L_HUMAN	Q14766
AGQLTSEEDTLSLVTADHSHVFSFGGY PLR	PPB1_HUMAN	P05187
	PPBN_HUMAN	P10696
AGQVAYLEK	MYO5C_HUMAN	Q9NQX4
	MYO5B_HUMAN	Q9ULV0
AGTQIENIEEDFR	ACTN2_HUMAN	P35609
	ACTN3_HUMAN	Q08043
AGVLAGHDNR	GBB1_BOVIN	P62871
	GBB2_HUMAN	P62879
	GBB4_HUMAN	Q9HAV0
AGVLAHLEEER	MYH9_HUMAN	P35579
	MYH10_HUMAN	P35580
AHEGARPMR	COR1B_HUMAN	Q9BR76
	COR1C_HUMAN	Q9ULV4
AHLQTHSDVK	SLUG_HUMAN	O43623
	SNAI_HUMAN	O95863
AHQVVEDGYEFFAK	PP1A_HUMAN	P62136
	PP1B_HUMAN	P62140
AIDGLNR	AK1C2_HUMAN	P52895
	AK1C1_HUMAN	Q04828
AIEEGYR	EPHA4_HUMAN	P54764
	EPHA7_HUMAN	Q15375

AIGGGLSSVGGGSSTIK	K2C6A_HUMAN	P02538
	K2C6C_HUMAN	P48666
	K2C6E_HUMAN	P48668
AIGVLTSGGDAQGMNAAVR	K6PL_HUMAN	P17858
	K6PP_HUMAN	Q01813
AILVDLEPGTMDSVR	TBB5_MOUSE	P99024
	TBB3_HUMAN	Q13509
AIMTYVSCFYHAFAGAEQAETAANR	ACTN2_HUMAN	P35609
	ACTN3_HUMAN	Q08043
AITDAAMMAEELK	MYH3_HUMAN	P11055
	MYH1_HUMAN	P12882
	MYH7_HUMAN	P12883
	MYH6_HUMAN	P13533
	MYH8_HUMAN	P13535
	MYH2_HUMAN	Q9UKX2
	MYH13_HUMAN	Q9UKX3
	MYH4_HUMAN	Q9Y623
AITSAYYR	RB11A_MOUSE	P62492
	RAB25_HUMAN	P57735
	RB11B_HUMAN	Q15907
ALAAAGYDVEK	H14_HUMAN	P10412
	H13_HUMAN	P16402
	H12_HUMAN	P16403
ALCTGEK	PPIF_HUMAN	P30405
	RBP2_HUMAN	P49792
	PPID_HUMAN	Q08752
ALDFIASK	ACTN4_HUMAN	O43707
	ACTN3_HUMAN	Q08043
ALDTMNFDVIK	PABP1_HUMAN	P11940
	PABP4_HUMAN	Q13310
ALEEALEAK	MYH10_HUMAN	P35580
	MYH11_HUMAN	P35749
ALEEANADLEVK	K1C14_HUMAN	P02533
	K1C16_HUMAN	P08779
	K1C13_HUMAN	P13646
	K1C15_HUMAN	P19012
ALELDPNLYR	MYH10_HUMAN	P35580
	MYH11_HUMAN	P35749
ALENDPDCR	PLSL_HUMAN	P13796
	PLST_HUMAN	P13797
ALESALK	KIF5C_HUMAN	O60282
	KINH_HUMAN	P33176
ALETNTHVK	TMOD3_HUMAN	Q9NYL9
	TMOD2_HUMAN	Q9NZR1
ALFPGDSEIDQLFR	CDK2_HUMAN	P24941
	CDK3_HUMAN	Q00526
ALGQNPTNAEVLK	MLEY_HUMAN	P14649
	MYL6_BOVIN	P60661
	MYL6_HUMAN	P60660

ALGTNPTNAEVR	MLE1_HUMAN	P05976
	MLE3_HUMAN	P06741
ALLQLLR	MFNG_HUMAN	O00587
	DHI2_HUMAN	P80365
ALLQMVQQFAVDFEK	DYN1_HUMAN	Q05193
	DYN3_HUMAN	Q9UQ16
ALLSAVTR	CTN2_HUMAN	P26232
	CTN1_HUMAN	P35221
ALPGLSK	LTB1S_HUMAN	P22064
	LTB1L_HUMAN	Q14766
ALQEAHQQALDDLQAEEDK	MYH3_HUMAN	P11055
	MYH7_HUMAN	P12883
ALQEAHQQTLDDLQAEEDK	MYH1_HUMAN	P12882
	MYH2_HUMAN	Q9UKX2
ALTETIMFDDAIER	PPB1_HUMAN	P05187
	PPBN_HUMAN	P10696
ALTVPELTQQMFDAK	TBBX_MOUSE	P68372
	TBB3_HUMAN	Q13509
ALYDAELSQMQTHISDTSVVLSMDNNR	K2C6A_HUMAN	P02538
	K2C6B_HUMAN	P04259
	K2C6C_HUMAN	P48666
	K2C6E_HUMAN	P48668
ALYDTFSAFGNILSCK	PABP1_HUMAN	P11940
	PABP4_HUMAN	Q13310
AMAIADALGK	UD16_HUMAN	P19224
	UD11_HUMAN	P22309
AMDTLGIEYGDK	GNAO1_HUMAN	P09471
	GNAO2_HUMAN	P29777
AMGIMNSFVNDIFER	H2B_BOVIN	P62808
	H2BR_HUMAN	P06899
	H2BF_HUMAN	P33778
	H2BS_HUMAN	P57053
	H2BB_HUMAN	P58876
	H2BQ_HUMAN	Q16778
	H2BJ_HUMAN	Q93079
	H2BD_HUMAN	Q99877
	H2BE_HUMAN	Q99879
	H2BC_HUMAN	Q99880
ANGQENGHVK	MACS_HUMAN	P29966
	MRP_HUMAN	P49006
ANGTTVHVGIHPSK	RL26_MOUSE	P61255
	RL26L_HUMAN	Q9UNX3
ANLLQAEIEELR	MYH1_HUMAN	P12882
	MYH2_HUMAN	Q9UKX2
ANSEVAQWR	MYH3_HUMAN	P11055
	MYH1_HUMAN	P12882
	MYH7_HUMAN	P12883
	MYH6_HUMAN	P13533
	MYH8_HUMAN	P13535

	MYH4_HUMAN	Q9Y623
APDFVFYAPR	EZRI_HUMAN	P15311
	MOES_HUMAN	P26038
	RADI_HUMAN	P35241
APEIMLNSK	MK03_HUMAN	P27361
	MK01_HUMAN	P28482
APILIATDVASR	DDX5_HUMAN	P17844
	DDX17_HUMAN	Q92841
APPRPANFCIFSR	ALU5_HUMAN	P39192
	ALU8_HUMAN	P39195
APVIPATR	ALU7_HUMAN	P39194
	ALU8_HUMAN	P39195
APVVPATR	ALU1_HUMAN	P39188
	ALU2_HUMAN	P39189
	ALU5_HUMAN	P39192
APWIEQEGPEYWDQETR	1A03_HUMAN	P04439
	1A01_HUMAN	P30443
APWIEQEGPEYWDR	1B07_HUMAN	P01889
	1B08_HUMAN	P30460
AQIWDTAGQER	RB11A_MOUSE	P62492
	RB11B_HUMAN	Q15907
AQLEFNQIK	MYH7_HUMAN	P12883
	MYH6_HUMAN	P13533
AQYEEIAQR	K2C6A_HUMAN	P02538
	K2C6B_HUMAN	P04259
	K2C4_HUMAN	P19013
	K22E_HUMAN	P35908
	K2C6C_HUMAN	P48666
	K2C6E_HUMAN	P48668
ASFNHFDR	ACTN2_HUMAN	P35609
	ACTN3_HUMAN	Q08043
ASGLGDHCEDINECLEDK	LTB1S_HUMAN	P22064
	LTB1L_HUMAN	Q14766
ASGPPVSELITK	H14_HUMAN	P10412
	H13_HUMAN	P16402
	H12_HUMAN	P16403
ASLENSLEETK	K1C14_HUMAN	P02533
	K1C16_HUMAN	P08779
ASTSTTIR	K2C6A_HUMAN	P02538
	K2C6B_HUMAN	P04259
	K2C6C_HUMAN	P48666
	K2C6E_HUMAN	P48668
ASYVASTK	CTN2_HUMAN	P26232
	CTN1_HUMAN	P35221
ATAGDTHLGGEDFDNR	HSP71_HUMAN	P08107
	HSP76_HUMAN	P17066
	HS70L_HUMAN	P34931
ATALQPGR	ALU1_HUMAN	P39188
	ALU2_HUMAN	P39189

	ALU8_HUMAN	P39195
ATDGGGR	FATH_HUMAN	Q14517
	FAT2_HUMAN	Q9NYQ8
ATDMTFK	MYH7_HUMAN	P12883
	MYH6_HUMAN	P13533
ATDTSFK	MYH3_HUMAN	P11055
	MYH1_HUMAN	P12882
	MYH8_HUMAN	P13535
	MYH2_HUMAN	Q9UKX2
	MYH13_HUMAN	Q9UKX3
	MYH4_HUMAN	Q9Y623
ATENDIYNFFSPLNPVR	HNRH1_HUMAN	P31943
	HNRPF_HUMAN	P52597
ATIISEQQAK	STA5A_HUMAN	P42229
	STA5B_HUMAN	P51692
ATLEQTER	MYH3_HUMAN	P11055
	MYH1_HUMAN	P12882
	MYH2_HUMAN	Q9UKX2
ATTASQAK	HSP47_HUMAN	P29043
	SPH2_HUMAN	P50454
ATYDGNHDTFR	ERD21_HUMAN	P24390
	ERD22_HUMAN	P33947
AVAAGNSCR	TLN1_HUMAN	Q9Y490
	TLN2_HUMAN	Q9Y4G6
AVAISLPK	HSP47_HUMAN	P29043
	SPH2_HUMAN	P50454
AVCMLSNTTAIAEAWAR	TBA1_MERUN	P68360
	TBA1_MACFA	P68367
	TBA8_HUMAN	Q9NY65
AVDEMNGK	PABP1_HUMAN	P11940
	PABP3_HUMAN	Q9H361
AVDGYVKPQIK	STA5A_HUMAN	P42229
	STA5B_HUMAN	P51692
AVFPSIVGRPR	ACTS_MOUSE	P68134
	ACTB_BOVIN	P60712
	ACTG_ANSAN	P63256
	ACTA_RABIT	P62740
	ACTC_HUMAN	P68032
	ACTH_HUMAN	P63267
AVFVDLEPTVIDEVR	TBA1_MERUN	P68360
	TBA6_HUMAN	Q9BQE3
AVFWIEFVMR	UDB17_HUMAN	O75795
	UDB15_HUMAN	P54855
AVLCPPPVK	RAC3_HUMAN	P60763
	RAC4_HUMAN	O95916
AVLNPLCQVDYR	SC23A_HUMAN	Q15436
	SC23B_HUMAN	Q15437
AVLSAEQLR	HSP47_HUMAN	P29043
	SPH2_HUMAN	P50454

	TBBX_MOUSE	P68372
AVLVDLEPGTMDSVR	TBB4Q_HUMAN	Q99867
	PABP1_HUMAN	P11940
AVNSATGVPTV	PABP3_HUMAN	Q9H361
	RB11A_MOUSE	P62492
AVPTDEAR	RB11B_HUMAN	Q15907
	PABP1_HUMAN	P11940
	PABP4_HUMAN	Q13310
AVTEMNGR	PABP3_HUMAN	Q9H361
	MYH7_HUMAN	P12883
AVVEQTER	MYH6_HUMAN	P13533
	MA1A2_HUMAN	O60476
AWLMSDK	MA1A1_HUMAN	P33908
	PIPNB_HUMAN	P48739
AWNAYPYCR	PIPNA_HUMAN	Q00169
	PLST_HUMAN	P13797
AYFHLLNQIAPK	PLSI_HUMAN	Q14651
	IF1AY_HUMAN	O14602
AYGELPEHAK	IF1AX_HUMAN	P47813
	TBA1_MERUN	P68360
AYHEQLSVAEITNACFEPANQMVK	TBA1_MACFA	P68367
	1B08_HUMAN	P30460
AYLEGTCVEWLR	1C04_HUMAN	P30504
	PPB1_HUMAN	P05187
AYTVLLYGNGPGYVLK	PPBN_HUMAN	P10696
	BGAL_HUMAN	P16278
AYVAVDGIPQGVLER	BGAM_HUMAN	P16279
	MT2_HUMAN	P02795
	MT1G_HUMAN	P13640
	MT1I_HUMAN	P80295
	MT1K_HUMAN	P80296
CAQGCICK	MT1L_HUMAN	P80297
	UD16_HUMAN	P19224
CCAYGYR	UD11_HUMAN	P22309
	MYL6_BOVIN	P60661
CDFTEDQTAEFK	MYL6_HUMAN	P60660
	RAB3D_HUMAN	O95716
	RAP1B_BOVIN	P61223
CDLEDER	RAP1A_BOVIN	P62833
	RAB3A_HUMAN	P20336
CDMEDER	RAB3C_HUMAN	Q96E17
CEDIDECLNPSTCPDEQCVNSPGSYQC VPCTEGFR	LTB1S_HUMAN	P22064
	LTB1L_HUMAN	Q14766
	MYH1_HUMAN	P12882
CEETHAELEASQK	MYH2_HUMAN	Q9UKX2
	K1C14_HUMAN	P02533
CEMEQQNQEYK	K1C17_HUMAN	Q04695
CENTEGSFLCICPAGFMASEEGTNCIDV DECLRPDVCGEGHCVNTVGAFR	LTB1S_HUMAN	P22064
	LTB1L_HUMAN	Q14766

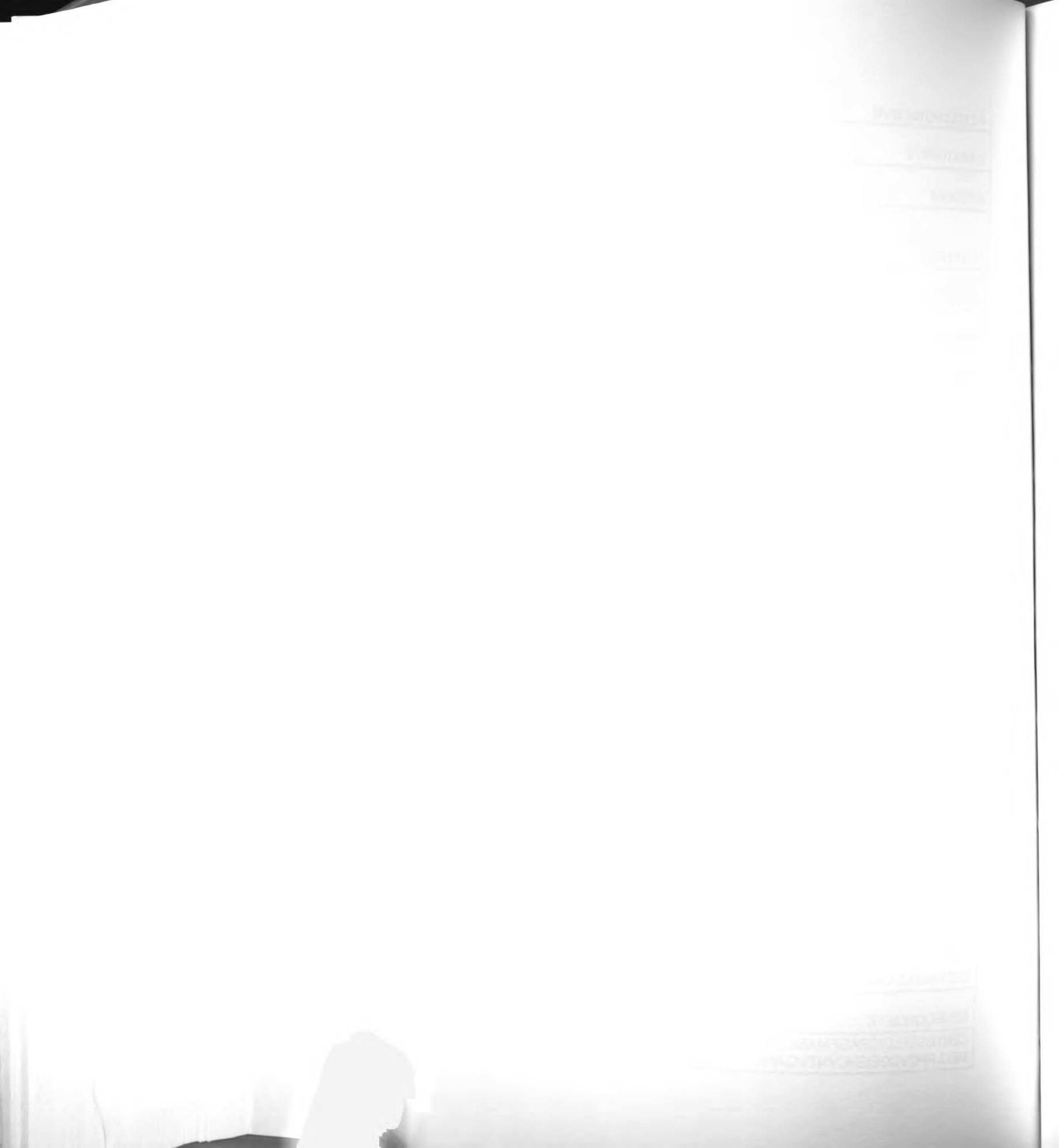

CEYCDSGYR	LTB1S_HUMAN	P22064
	LTB1L_HUMAN	Q14766
CFQETIGSQCGK	LTB1S_HUMAN	P22064
	LTB1L_HUMAN	Q14766
CIAQMVNSQAANIR	BIG2_HUMAN	Q9Y6D5
	BIG1_HUMAN	Q9Y6D6
CIIPNETK	MYH3_HUMAN	P11055
	MYH1_HUMAN	P12882
	MYH7_HUMAN	P12883
	MYH8_HUMAN	P13535
	MYH2_HUMAN	Q9UKX2
	MYH4_HUMAN	Q9Y623
CIIPNHEK	MYH9_HUMAN	P35579
	MYH10_HUMAN	P35580
	MYH11_HUMAN	P35749
CIKPNDEK	MYO5C_HUMAN	Q9NQX4
	MYO5B_HUMAN	Q9ULV0
CIKPNDK	MYO1B_HUMAN	O43795
	MYO1D_HUMAN	O94832
CIKPNETK	MYO1F_HUMAN	O00160
	MYO1E_HUMAN	Q12965
CINTDGSYK	LTB1S_HUMAN	P22064
	LTB1L_HUMAN	Q14766
CIRPAESNEQIEETDVYQDLCWEHLSDE YVCSRPLVGK	LTB1S_HUMAN	P22064
	LTB1L_HUMAN	Q14766
CLCLPGYVPSDKPNYCTPLNTALNLEK	LTB1S_HUMAN	P22064
	LTB1L_HUMAN	Q14766
CLCYQGFQAPQDGQGCVDVNECELLS GVCGEAFCENVEGSFLCVCADENQEYS PMTGQCR	LTB1S_HUMAN	P22064
	LTB1L_HUMAN	Q14766
CLSEFACNAAFPDTSMEAIR	BIG2_HUMAN	Q9Y6D5
	BIG1_HUMAN	Q9Y6D6
CLVEELR	CP2CI_HUMAN	P33260
	CP2CJ_HUMAN	P33261
CMVEWSK	BIG2_HUMAN	Q9Y6D5
	BIG1_HUMAN	Q9Y6D6
CNGVLEGIR	MYH3_HUMAN	P11055
	MYH1_HUMAN	P12882
	MYH7_HUMAN	P12883
	MYH6_HUMAN	P13533
	MYH8_HUMAN	P13535
	MYH9_HUMAN	P35579
	MYH10_HUMAN	P35580
	MYH11_HUMAN	P35749
	MYH2_HUMAN	Q9UKX2
	MYH13_HUMAN	Q9UKX3
	MYH4_HUMAN	Q9Y623
CPEALFQPSFLGMESCGIHETTFNSIMK	ACTB_BOVIN	P60712
	ACTG_ANSAN	P63256
CPETLFQPSFIGMESAGIHETTYNSIMK	ACTS_MOUSE	P68134

	ACTA_RABIT	P62740
	ACTC_HUMAN	P68032
	ACTH_HUMAN	P63267
CPLPGTAAFK	LTB1S_HUMAN	P22064
	LTB1L_HUMAN	Q14766
CQLEINFNTLQTK	ACTN4_HUMAN	O43707
	ACTN2_HUMAN	P35609
	ACTN3_HUMAN	Q08043
CQYVTEK	ALDOA_HUMAN	P04075
	ALDOC_HUMAN	P09972
CSETYETK	UN84A_HUMAN	O94901
	UN84B_HUMAN	Q9UH99
CTCGQGYQLSAAK	LTB1S_HUMAN	P22064
	LTB1L_HUMAN	Q14766
CTPHYIR	MYO1F_HUMAN	O00160
	MYO1E_HUMAN	Q12965
CVDIDECTQVQHLCSQGR	LTB1S_HUMAN	P22064
	LTB1L_HUMAN	Q14766
CVVVGDGAVGK	RAC3_HUMAN	P60763
	RAC2_HUMAN	P15153
	CDC42_CANFA	P60952
	CDC42_MOUSE	P60766
	RHOG_CRICR	P84097
CWALGFYPAEITLTWQR	1B07_HUMAN	P01889
	HLAH_HUMAN	P01893
	1A03_HUMAN	P04439
	1A01_HUMAN	P30443
	1B08_HUMAN	P30460
DADECLLFGQEICK	LTB1S_HUMAN	P22064
	LTB1L_HUMAN	Q14766
DAFLVFR	BIG2_HUMAN	Q9Y6D5
	BIG1_HUMAN	Q9Y6D6
DAGVIAGLNVLR	HSP71_HUMAN	P08107
	HS70L_HUMAN	P34931
DALLNWLK	PK3CD_HUMAN	O00329
	PK3CB_HUMAN	P42338
DALVDFSEQYTPEADPYFIQDR	LTB1S_HUMAN	P22064
	LTB1L_HUMAN	Q14766
DAVLLVFANK	ARF3_RAT	P61206
	ARF5_HUMAN	P84085
	ARF1_RAT	P84079
DAWEIPR	YES_HUMAN	P07947
	SRC_HUMAN	P12931
DAYSSFGSR	DDX3X_HUMAN	O00571
	DDX3Y_HUMAN	O15523
DAYVQALAR	BIG2_HUMAN	Q9Y6D5
	BIG1_HUMAN	Q9Y6D6
DCEAEVR	2AAA_HUMAN	P30153
	2AAB_HUMAN	P30154

DDEVQVVR	RL26_MOUSE	P61255
	RL26L_HUMAN	Q9UNX3
DDEYDYLFK	RB11A_MOUSE	P62492
	RB11B_HUMAN	Q15907
DDPSTIEK	CDC42_CANFA	P60952
	CDC42_MOUSE	P60766
DDQVFPMNPPK	MYH1_HUMAN	P12882
	MYH2_HUMAN	Q9UKX2
DEEIDQLK	MYH8_HUMAN	P13535
	MYH2_HUMAN	Q9UKX2
DEEIEQLK	MYH3_HUMAN	P11055
	MYH13_HUMAN	Q9UKX3
DEEMEQAK	MYH7_HUMAN	P12883
	MYH6_HUMAN	P13533
DEEVHAGLGELLR	HSP47_HUMAN	P29043
	SPH2_HUMAN	P50454
DEQNEEK	MYH10_HUMAN	P35580
	MYH11_HUMAN	P35749
DFANTIPGHGGIMDR	CDS2_HUMAN	O95674
	CDS1_HUMAN	Q92903
DFIDCFLIK	CP2CI_HUMAN	P33260
	CP2CJ_HUMAN	P33261
DFLDEYIFLAVGR	DDX3X_HUMAN	O00571
	DDX3Y_HUMAN	O15523
DFLESIR	SC15A_HUMAN	Q8TAG9
	SC15B_HUMAN	Q9Y2D4
DFLRPFEHIMK	BIG2_HUMAN	Q9Y6D5
	BIG1_HUMAN	Q9Y6D6
DFLSEASIMGQFDHPNIIR	EPHA8_HUMAN	P29322
	EPHB3_HUMAN	P54753
DFVVGVLDLCR	TRPC3_HUMAN	Q13507
	TRPC7_HUMAN	Q9HCX4
DGADFAK	ALDOA_HUMAN	P04075
	ALDOC_HUMAN	P09972
DGARPDVTESESGSPEYR	PPB1_HUMAN	P05187
	PPBN_HUMAN	P10696
DGEDQTQDTELVETRPAGDGTFQK	HLAH_HUMAN	P01893
	1A03_HUMAN	P04439
	1A01_HUMAN	P30443
DGEDQTQDTELVETRPAGDR	1B07_HUMAN	P01889
	1B08_HUMAN	P30460
DGPNALTPPPTTPEWVK	AT1A3_HUMAN	P13637
	AT1A2_HUMAN	P50993
DGVSLCRPGWSAVAR	ALU2_HUMAN	P39189
	ALU8_HUMAN	P39195
DGVSPCWPGWSR	ALU5_HUMAN	P39192
	ALU7_HUMAN	P39194
	ALU8_HUMAN	P39195
DHADSNIVIMLVGNK	RB11A_MOUSE	P62492

	RB11B_HUMAN	Q15907
DHPAVAATLNNLAVLYGK	KLC1_HUMAN	Q07866
	KLC2_HUMAN	Q9H0B6
DIDDLELTLAK	MYH3_HUMAN	P11055
	MYH1_HUMAN	P12882
	MYH7_HUMAN	P12883
	MYH6_HUMAN	P13533
	MYH8_HUMAN	P13535
	MYH2_HUMAN	Q9UKX2
	MYH4_HUMAN	Q9Y623
DIDECQQGNLCVNGQCK	LTB1S_HUMAN	P22064
	LTB1L_HUMAN	Q14766
DIDTAAK	AT5G1_HUMAN	P05496
	AT5G3_HUMAN	P48201
	AT5G2_HUMAN	Q06055
DIILQSNPLLEAFGNAK	MYO1F_HUMAN	O00160
	MYO1E_HUMAN	Q12965
DIQSLPR	EHD1_HUMAN	Q9H4M9
	EHD3_HUMAN	Q9NZN3
DITDHMDR	NOTC1_HUMAN	P46531
	NOTC2_HUMAN	Q04721
DIVLVAYSALGSHR	AK1C2_HUMAN	P52895
	AK1C1_HUMAN	Q04828
DIVNMLMHHDR	PHS3_HUMAN	P11216
	PHS2_HUMAN	P11217
DIVQFVPFR	CPNE3_HUMAN	O75131
	CPNE2_HUMAN	Q96FN4
DLEEATLQHEATAAALR	MYH7_HUMAN	P12883
	MYH6_HUMAN	P13533
DLEEATLQHEATAATLR	MYH1_HUMAN	P12882
	MYH2_HUMAN	Q9UKX2
	MYH13_HUMAN	Q9UKX3
DLGEELEALK	MYH9_HUMAN	P35579
	MYH11_HUMAN	P35749
DLGEGHFGK	JAK1_HUMAN	P23458
	TYK2_HUMAN	P29597
DLGSLQAPPPGFTPFSCLSLPSSWDYR	ALU2_HUMAN	P39189
	ALU3_HUMAN	P39190
DLGSLQPPPPGFK	ALU5_HUMAN	P39192
	ALU7_HUMAN	P39194
	ALU8_HUMAN	P39195
DLKPENILLDEEGHIK	KS6A2_HUMAN	Q15349
	KS6A1_HUMAN	Q15418
DLLDLLVEAK	DDX3X_HUMAN	O00571
	DDX3Y_HUMAN	O15523
DLLDVSK	KIF5C_HUMAN	O60282
	KINH_HUMAN	P33176
DLLLDPAWEK	ACTN4_HUMAN	O43707
	ACTN2_HUMAN	P35609

	ACTN3_HUMAN	Q08043
DLLNALK	UDB17_HUMAN	O75795
	UDB15_HUMAN	P54855
DLMACAQTGSGK	DDX3X_HUMAN	O00571
	DDX4_HUMAN	Q9NQI0
DLNYCFSGMSDHR	HNRH1_HUMAN	P31943
	HNRH2_HUMAN	P55795
DLSTIEPLK	AN32C_HUMAN	O43423
	AN32D_HUMAN	O95626
	AN32A_HUMAN	P39687
DLTDYLMK	ACTS_MOUSE	P68134
	ACTB_BOVIN	P60712
	ACTG_ANSAN	P63256
	ACTA_RABIT	P62740
	ACTC_HUMAN	P68032
	ACTH_HUMAN	P63267
DLYANNVLSGGTTMYPGIADR	ACTA_RABIT	P62740
	ACTC_HUMAN	P68032
	ACTH_HUMAN	P63267
DLYANTVLSGGTTMYPGIADR	ACTB_BOVIN	P60712
	ACTG_ANSAN	P63256
DLYLASVFHATAFELDTDGNPFDQDIYGR	HSP47_HUMAN	P29043
	SPH2_HUMAN	P50454
DNNLLGR	HSP71_HUMAN	P08107
	HSP76_HUMAN	P17066
	HS70L_HUMAN	P34931
DPLNETVVGLYQK	MYH3_HUMAN	P11055
	MYH1_HUMAN	P12882
	MYH7_HUMAN	P12883
	MYH2_HUMAN	Q9UKX2
	MYH13_HUMAN	Q9UKX3
	MYH4_HUMAN	Q9Y623
DPPASASQSAGITGVSHR	ALU2_HUMAN	P39189
	ALU3_HUMAN	P39190
	ALU5_HUMAN	P39192
DPSEEIEILLR	KS6A2_HUMAN	Q15349
	KS6A1_HUMAN	Q15418
DPVQLNLLYVQAR	TLN1_HUMAN	Q9Y490
	TLN2_HUMAN	Q9Y4G6
DQATYEDFVEGLR	MLE1_HUMAN	P05976
	MLE3_HUMAN	P06741
DQAVENILVSPVVVASSLGLVSLGGK	HSP47_HUMAN	P29043
	SPH2_HUMAN	P50454
DQCEDIDECQHR	LTB1S_HUMAN	P22064
	LTB1L_HUMAN	Q14766
DQGTYEDYVEGLR	MYL6_BOVIN	P60661
	MYL6_HUMAN	P60660
DQPGQHGETPSLLK	ALU7_HUMAN	P39194
	ALU8_HUMAN	P39195

	NDK8_HUMAN	O60361
DRPFFPGLVK	NDKB_HUMAN	P22392
	UD16_HUMAN	P19224
DRPVEPLDLAVFWVEFVMR	UD11_HUMAN	P22309
	RASN_HUMAN	P01111
DSDDVPMVLVGNK	RASH_HUMAN	P01112
	LTB1S_HUMAN	P22064
DSDDYAQLCNIPVTGR	LTB1L_HUMAN	Q14766
DSGHHDEAWAHNSSNYTLPAFYMGNF	BGAL_HUMAN	P16278
SIPSGIPDLPQDTFIQFPGWTK	BGAM_HUMAN	P16279
	PK3CD_HUMAN	O00329
DSLALGK	PK3CB_HUMAN	P42338
	SH3G1_HUMAN	Q99961
DSLDIEVK	SH3G2_HUMAN	Q99962
	1433T_HUMAN	P27348
	1433Z_HUMAN	P63104
	1433B_HUMAN	P31946
	1433S_HUMAN	P31947
	1433G_MOUSE	P61982
	1433E_MOUSE	P62259
DSTLIMQLLR	1433F_HUMAN	Q04917
	BGAL_HUMAN	P16278
DSWLDHV	BGAM_HUMAN	P16279
	ACTS_MOUSE	P68134
	ACTB_BOVIN	P60712
	ACTG_ANSAN	P63256
	ACTA_RABIT	P62740
	ACTC_HUMAN	P68032
DSYVGDEAQSK	ACTH_HUMAN	P63267
	GNA11_HUMAN	P29992
DTILQLNLK	GNAQ_HUMAN	P50148
	MYH7_HUMAN	P12883
DTQIQLDDAVR	MYH6_HUMAN	P13533
	MYH3_HUMAN	P11055
DTQLHLDDALR	MYH1_HUMAN	P12882
	HSP47_HUMAN	P29043
DTQSGSLLFIGR	SPH2_HUMAN	P50454
	K2C6A_HUMAN	P02538
	K2C6B_HUMAN	P04259
	K2C5_HUMAN	P13647
	K2C6C_HUMAN	P48666
DVDAAYMNK	K2C6E_HUMAN	P48668
	MP2K2_HUMAN	P36507
DVKPSNILVNSR	MP2K1_HUMAN	Q02750
	KIF5C_HUMAN	O60282
DVLEGYNGTIFAYGQTSSGK	KINH_HUMAN	P33176
	PDIA4_HUMAN	P13667
DVLIEFYAPWCGHCK	PDIA3_HUMAN	P30101
DVNAAIATIK	TBA1_MERUN	P68360

	TBA6_HUMAN	Q9BQE3
DVQGWGENDR	PP1A_HUMAN	P62136
	PP1B_HUMAN	P62140
DVYDDGK	KS6A2_HUMAN	Q15349
	KS6A1_HUMAN	Q15418
DVYIVQDLMETDLYK	MK03_HUMAN	P27361
	MK01_HUMAN	P28482
DWISFGHK	MTMR7_HUMAN	Q9Y216
	MTMR6_HUMAN	Q9Y217
DWNDMER	ACTZ_HUMAN	P61163
	ACTY_HUMAN	P42025
DWNVDLIPK	GDIA_HUMAN	P31150
	GDIB_HUMAN	P50395
DYIALNEDLR	1B07_HUMAN	P01889
	HLAH_HUMAN	P01893
	1A03_HUMAN	P04439
	1A01_HUMAN	P30443
	1B08_HUMAN	P30460
	1C04_HUMAN	P30504
DYQELMNVK	K2C3_HUMAN	P12035
	K22E_HUMAN	P35908
	K22O_HUMAN	Q01546
DYSPYFK	K1C14_HUMAN	P02533
	K1C16_HUMAN	P08779
DYYFALAHTVR	PHS1_HUMAN	P06737
	PHS2_HUMAN	P11217
EAAEGLR	TLN1_HUMAN	Q9Y490
	TLN2_HUMAN	Q9Y4G6
EAAEMGK	EF1A1_HUMAN	P68104
	EF1A2_HUMAN	Q05639
EAEAGESLEPGR	ALU5_HUMAN	P39192
	ALU7_HUMAN	P39194
	ALU8_HUMAN	P39195
EAELAVSR	ALU2_HUMAN	P39189
	ALU3_HUMAN	P39190
EAELGAR	PABP1_HUMAN	P11940
	PABP3_HUMAN	Q9H361
EAEPLCK	KLC1_HUMAN	Q07866
	KLC2_HUMAN	Q9H0B6
EAESCDCLQGFQLTHSLGGGTGSGMG TLLISK	TBBX_MOUSE	P68372
	TBB5_MOUSE	P99024
EAEVAVSR	ALU5_HUMAN	P39192
	ALU7_HUMAN	P39194
	ALU8_HUMAN	P39195
EAFLLFDR	MLE1_HUMAN	P05976
	MLE3_HUMAN	P06741
EAFQLFDR	MYL6_BOVIN	P60661
	MYL6_HUMAN	P60660
EAFQNAYLELGGLGER	AT1A3_HUMAN	P13637

	AT1A4_HUMAN	Q13733
EALISQLTR	MYH7_HUMAN	P12883
	MYH6_HUMAN	P13533
EAQPGQSQVSYQGLPVQK	LTB1S_HUMAN	P22064
	LTB1L_HUMAN	Q14766
EAQTLQQYR	STA5A_HUMAN	P42229
	STA5B_HUMAN	P51692
ECDNALR	TLN1_HUMAN	Q9Y490
	TLN2_HUMAN	Q9Y4G6
ECISIHVGQAGVQIGNACWELYCLEHGI QPDGQMPSDK	TBA1_MERUN	P68360
	TBA6_HUMAN	Q9BQE3
ECYYNLNDASLCDNVLAPNVTK	LTB1S_HUMAN	P22064
	LTB1L_HUMAN	Q14766
EDAANNYAR	TBA1_MERUN	P68360
	TBA1_MACFA	P68367
	TBA6_HUMAN	Q9BQE3
	TBA8_HUMAN	Q9NY65
EDGISAAK	GNAO1_HUMAN	P09471
	GNAO2_HUMAN	P29777
EDGQEYAQVIK	IF1AY_HUMAN	O14602
	IF1AH_HUMAN	O75642
	IF1AX_HUMAN	P47813
EDIFYTSK	AK1C4_HUMAN	P17516
	AK1C3_HUMAN	P42330
	AK1C2_HUMAN	P52895
	AK1C1_HUMAN	Q04828
EDLVFIFWAPESAPLK	COF1_HUMAN	P23528
	COF2_HUMAN	Q9Y281
EDMAALEK	TBA1_MERUN	P68360
	TBA1_MACFA	P68367
	TBA6_HUMAN	Q9BQE3
EDQSILCTGESGAGK	MYH9_HUMAN	P35579
	MYH10_HUMAN	P35580
	MYH11_HUMAN	P35749
EDQTEYLEER	HS90A_HUMAN	P07900
	HS90B_HUMAN	P08238
EEALHQFR	DDX3X_HUMAN	O00571
	DDX3Y_HUMAN	O15523
EEELQAALAR	MYH9_HUMAN	P35579
	MYH11_HUMAN	P35749
EEEVEALMAGQEDSNGCINYEAFVK	MLE1_HUMAN	P05976
	MLE3_HUMAN	P06741
EEGEAFAR	RAB2A_HUMAN	P61019
	RAB2B_HUMAN	Q8WUD1
EELAYLK	K1C14_HUMAN	P02533
	K1C17_HUMAN	Q04695
EELVAAVEDVR	CTN2_HUMAN	P26232
	CTN1_HUMAN	P35221
EEPVEALTFSR	LTB1S_HUMAN	P22064

	LTB1L_HUMAN	Q14766
EEPWVDPNSPVLLEDPVLCALAK	AK1C2_HUMAN	P52895
	AK1C1_HUMAN	Q04828
EEQAEPDGTEVADK	MYH3_HUMAN	P11055
	MYH1_HUMAN	P12882
	MYH8_HUMAN	P13535
	MYH2_HUMAN	Q9UKX2
	MYH13_HUMAN	Q9UKX3
	MYH4_HUMAN	Q9Y623
EESEESDDDMGFGLFD	RLA1_HUMAN	P05386
	RLA2_HUMAN	P05387
EETPLFLAAR	NOTC1_HUMAN	P46531
	NOTC2_HUMAN	Q04721
	NOTC3_HUMAN	Q9UM47
EFIIALSVTSR	NCALD_HUMAN	P61601
	HPCA_RAT	P84076
	HPCL1_HUMAN	P37235
EFIYYADVK	RAB9A_HUMAN	P51151
	RAB9B_HUMAN	Q9NP90
EFTDYLFNK	SOS1_HUMAN	Q07889
	SOS2_HUMAN	Q07890
EFTNVYIK	PABP1_HUMAN	P11940
	PABP4_HUMAN	Q13310
EGIEWEFIDFGMDLAACIELIEKPMGIFSILEEECMFPK	MYH13_HUMAN	Q9UKX3
	MYH4_HUMAN	Q9Y623
EGIEWTFIDFGMDLAACIELIEKPMGIFSILEEECMFPK	MYH3_HUMAN	P11055
	MYH1_HUMAN	P12882
	MYH2_HUMAN	Q9UKX2
EGIEWTFIDFGMDLQACIDLIEKPMGIMSILEEECMFPK	MYH7_HUMAN	P12883
	MYH6_HUMAN	P13533
EGLELPEDEEEK	HS90A_HUMAN	P07900
	HS90B_HUMAN	P08238
EGLLLWCQR	ACTN4_HUMAN	O43707
	ACTN2_HUMAN	P35609
	ACTN3_HUMAN	Q08043
EGLVDTAVK	RPC1_HUMAN	O14802
	RPA1_HUMAN	O95602
EGNGTVMGAEIR	MYL6_BOVIN	P60661
	MYL6_HUMAN	P60660
EGNGTVMGAELR	MLE1_HUMAN	P05976
	MLE3_HUMAN	P06741
	MYL3_HUMAN	P08590
EGSYEAAK	NOTC2_HUMAN	Q04721
	NOTC3_HUMAN	Q9UM47
EHALLAYTLGVK	EF1A1_HUMAN	P68104
	EF1A2_HUMAN	Q05639
EHGLIFMETSAK	RAB2A_HUMAN	P61019
	RAB2B_HUMAN	Q8WUD1
EIAQDFK	H33_HUMAN	P84243

	H31_HUMAN	P68431
	H3T_HUMAN	Q16695
EICPGGMGYTVSGVHR	LTB1S_HUMAN	P22064
	LTB1L_HUMAN	Q14766
EIEVDSSPSVLEILDTAGTEQFASMR	RAP2A_HUMAN	P10114
	RAP2B_MOUSE	P61226
EIFLSQPILLELEAPLK	PP1A_HUMAN	P62136
	PP1B_HUMAN	P62140
EIIDLVLDR	TBA1_MERUN	P68360
	TBA6_HUMAN	Q9BQE3
EIISFGSGYGGNSLLGK	PPCKC_HUMAN	P35558
	PPCKM_HUMAN	Q16822
EINSPNLLK	SOS1_HUMAN	Q07889
	SOS2_HUMAN	Q07890
EIPSLDQEK	LTB1S_HUMAN	P22064
	LTB1L_HUMAN	Q14766
EIQHHLK	SH3G1_HUMAN	Q99961
	SH3G2_HUMAN	Q99962
EIQMLAR	DDX3X_HUMAN	O00571
	DDX3Y_HUMAN	O15523
EIQTAVR	H2B_BOVIN	P62808
	H2BR_HUMAN	P06899
	H2BF_HUMAN	P33778
	H2BS_HUMAN	P57053
	H2BB_HUMAN	P58876
	H2BQ_HUMAN	Q16778
	H2BJ_HUMAN	Q93079
	H2BD_HUMAN	Q99877
	H2BE_HUMAN	Q99879
	H2BC_HUMAN	Q99880
EISYAIK	DYN1_HUMAN	Q05193
	DYN3_HUMAN	Q9UQ16
EITALAPSTMK	ACTS_MOUSE	P68134
	ACTB_BOVIN	P60712
	ACTG_ANSAN	P63256
	ACTA_RABIT	P62740
	ACTC_HUMAN	P68032
	ACTH_HUMAN	P63267
EITYMHSEGILAGELK	GFPT2_HUMAN	O94808
	GFPT1_HUMAN	Q06210
EIVESGR	HIP1_HUMAN	O00291
	HIP1R_HUMAN	O75146
EIVHIQAGQCGNQIGAK	TBB5_MOUSE	P99024
	TBB3_HUMAN	Q13509
EIYSHMTCATDTQNVK	GNAT1_HUMAN	P11488
	GNAT2_HUMAN	P19087
EIYTHFTCATDTK	GNAI1_HUMAN	P63096
	GNAI2_HUMAN	P04899
	GNAI3_HUMAN	P08754

	IF41_HUMAN	P60842
ELAQQIQK	IF42_HUMAN	Q14240
	DDX3X_HUMAN	O00571
ELAVQIYEEAR	DDX3Y_HUMAN	O15523
	MYH1_HUMAN	P12882
	MYH7_HUMAN	P12883
	MYH6_HUMAN	P13533
	MYH8_HUMAN	P13535
	MYH2_HUMAN	Q9UKX2
	MYH13_HUMAN	Q9UKX3
ELEEISER	MYH4_HUMAN	Q9Y623
	MYH1_HUMAN	P12882
ELEGEVESEQK	MYH2_HUMAN	Q9UKX2
	TLN1_HUMAN	Q9Y490
ELIECAR	TLN2_HUMAN	Q9Y4G6
	HS90B_HUMAN	P08238
ELISNASDALDK	ENPL_HUMAN	P14625
	GPC4_HUMAN	O75487
ELLENAEK	GPC6_HUMAN	Q9Y625
	PAK3_HUMAN	O75914
ELLQHPFLK	PAK2_HUMAN	Q13177
	GBB2_HUMAN	P62879
ELPGHTGYLSCCR	GBB4_HUMAN	Q9HAV0
	GOGB1_HUMAN	Q14789
ELQELLK	MPP6_HUMAN	Q9NZW5
	KIF5C_HUMAN	O60282
	KINH_HUMAN	P33176
ELQTLHNLR	KINN_HUMAN	Q12840
ELQVLHECNSPYIVGFYGAFYSDGEISIC MEHMDGGSLDQVLK	MP2K2_HUMAN	P36507
	MP2K1_HUMAN	Q02750
	MYH1_HUMAN	P12882
	MYH7_HUMAN	P12883
	MYH8_HUMAN	P13535
	MYH2_HUMAN	Q9UKX2
ELTYQTEEDR	MYH4_HUMAN	Q9Y623
	TLN1_HUMAN	Q9Y490
ELVAQGK	TLN2_HUMAN	Q9Y4G6
EMEEFVQSSGENGIVVFSLGSMISNMS EESANMIASALAQIPQK	UDB17_HUMAN	O75795
	UDB15_HUMAN	P54855
	HS90A_HUMAN	P07900
EMLQQSK	HS90B_HUMAN	P08238
	EHD4_HUMAN	Q9H223
EMPSVFGK	EHD3_HUMAN	Q9NZN3
	1433T_HUMAN	P27348
	1433Z_HUMAN	P63104
EMQPTHPIR	1433B_HUMAN	P31946
	TRPC3_HUMAN	Q13507
ENDEVNEGELK	TRPC7_HUMAN	Q9HCX4
ENIAIVER	MYH7_HUMAN	P12883

	MYH6_HUMAN	P13533
ENLVFLAQK	STA5A_HUMAN	P42229
	STA5B_HUMAN	P51692
ENNTGYINASHIK	PTN14_HUMAN	Q15678
	PTN21_HUMAN	Q16825
ENPLQFK	EZRI_HUMAN	P15311
	RADI_HUMAN	P35241
ENQSILITGESGAGK	MYH3_HUMAN	P11055
	MYH1_HUMAN	P12882
	MYH7_HUMAN	P12883
	MYH6_HUMAN	P13533
	MYH8_HUMAN	P13535
	MYH2_HUMAN	Q9UKX2
	MYH4_HUMAN	Q9Y623
EQADFAVEALAK	MYH10_HUMAN	P35580
	MYH11_HUMAN	P35749
EQDTSAHLER	MYH3_HUMAN	P11055
	MYH1_HUMAN	P12882
	MYH7_HUMAN	P12883
	MYH6_HUMAN	P13533
	MYH8_HUMAN	P13535
	MYH2_HUMAN	Q9UKX2
	MYH13_HUMAN	Q9UKX3
	MYH4_HUMAN	Q9Y623
EQGQNLAR	RAP1B_BOVIN	P61223
	RAP1A_BOVIN	P62833
EQGVLSFWR	ADT2_HUMAN	P05141
	ADT3_HUMAN	P12236
EQLAIVER	MYH3_HUMAN	P11055
	MYH8_HUMAN	P13535
	MYH13_HUMAN	Q9UKX3
EQLAMVER	MYH1_HUMAN	P12882
	MYH2_HUMAN	Q9UKX2
	MYH4_HUMAN	Q9Y623
EQLLQSNPVLEAFGNAK	MYO1B_HUMAN	O43795
	MYO1A_HUMAN	Q9UBC5
EQLQGLNDR	NFM_HUMAN	P07197
	AINX_HUMAN	Q16352
EQLVEMTGLSPR	ISL1_MOUSE	P61372
	ISL2_HUMAN	Q96A47
EQYEEEQEAK	MYH1_HUMAN	P12882
	MYH13_HUMAN	Q9UKX3
	MYH4_HUMAN	Q9Y623
EQYEEEQEGK	MYH3_HUMAN	P11055
	MYH8_HUMAN	P13535
EQYEEETEAK	MYH7_HUMAN	P12883
	MYH6_HUMAN	P13533
ESIFCIQYNIR	MYH3_HUMAN	P11055
	MYH4_HUMAN	Q9Y623

	NRX3B_HUMAN	Q9HDB5
ESSSTTGMVVGIVAAAALCILILLYAMYK	NRX1A_HUMAN	Q9ULB1
	PCBP1_HUMAN	Q15365
ESTGAQVQVAGDMLPNSTER	PCBP2_HUMAN	Q15366
	H2BR_HUMAN	P06899
	H2BF_HUMAN	P33778
ESYSIYVYK	H2BQ_HUMAN	Q16778
	H2B_BOVIN	P62808
	H2BS_HUMAN	P57053
	H2BB_HUMAN	P58876
	H2BJ_HUMAN	Q93079
	H2BD_HUMAN	Q99877
	H2BE_HUMAN	Q99879
ESYSVYVYK	H2BC_HUMAN	Q99880
	STA5A_HUMAN	P42229
ETALQQK	STA5B_HUMAN	P51692
	GFPT2_HUMAN	O94808
ETDCGVHINAGPEIGVASTK	GFPT1_HUMAN	Q06210
	BMR1B_HUMAN	O00238
ETEIYQTVLMR	BMR1A_HUMAN	P36894
	TYB4_HUMAN	P62328
ETIEQEK	TYB10_HORSE	P63314
	NIPS2_HUMAN	O75323
ETSNLYK	NIPS1_HUMAN	Q9BPW8
	TLN1_HUMAN	Q9Y490
EVANSTANLVK	TLN2_HUMAN	Q9Y4G6
	K1C14_HUMAN	P02533
EVATNSELVQSGK	K1C17_HUMAN	Q04695
	TBBX_MOUSE	P68372
EVDEQMLNVQNK	TBB5_MOUSE	P99024
	RHOA_BOVIN	P61585
EVFEMATR	RHOC_HUMAN	P08134
	PCBP1_HUMAN	Q15365
EVGSIIGK	PCBP2_HUMAN	Q15366
	KIF5C_HUMAN	O60282
	KINH_HUMAN	P33176
EVLQALEELAVNYDQK	KINN_HUMAN	Q12840
EVLSAAAAAGVSVAFGAPIGGVLFSLEE VSYYFPLK	CLCN4_HUMAN	P51793
	CLCN5_HUMAN	P51795
	KS6A2_HUMAN	Q15349
EVMFTEEDVK	KS6A1_HUMAN	Q15418
	RAB4A_HUMAN	P20338
EVTFLEASR	RAB4B_HUMAN	P61018
	CTN2_HUMAN	P26232
EYAQVFR	CTN1_HUMAN	P35221
EYQDLLNVK	NFM_HUMAN	P07197
	VIME_HUMAN	P08670
	NFH_HUMAN	P12036
	DESM_HUMAN	P17661

	AINX_HUMAN	Q16352
EYQELMNVK	K2C6A_HUMAN	P02538
	K2C6B_HUMAN	P04259
	K2C8_HUMAN	P05787
	K2C6C_HUMAN	P48666
	K2C6E_HUMAN	P48668
EYQELMSVK	K2C7_HUMAN	P08729
	K2C4_HUMAN	P19013
EYQLNDSAK	GNAO1_HUMAN	P09471
	GNAO2_HUMAN	P29777
EYQLSDSAK	GNA14_HUMAN	O95837
	GNA11_HUMAN	P29992
EYTDVYPEIIER	MAGD2_HUMAN	Q9UNF1
	MAGD1_HUMAN	Q9Y5V3
FACNGTVIEHPEYGEVIQLQGDQR	SUI13_HUMAN	O60739
	SUI1_HUMAN	P41567
FAEHVFR	NCALD_HUMAN	P61601
	HPCA_RAT	P84076
	HPCL1_HUMAN	P37235
FAIQDISVEETSAK	ACTN4_HUMAN	O43707
	ACTN2_HUMAN	P35609
	ACTN3_HUMAN	Q08043
FASFIDK	K2C6A_HUMAN	P02538
	K2C6B_HUMAN	P04259
	K2C8_HUMAN	P05787
	K2C7_HUMAN	P08729
	K2C3_HUMAN	P12035
	K2C5_HUMAN	P13647
	K2C4_HUMAN	P19013
	K22E_HUMAN	P35908
	K2C6C_HUMAN	P48666
	K2C6E_HUMAN	P48668
	K22O_HUMAN	Q01546
FCLGLLSNVNR	SMAD3_HUMAN	P84022
	SMAD5_HUMAN	Q99717
FDDTNPEK	SYEP_HUMAN	P07814
	SYQ_HUMAN	P47897
FDGALNVDLTEFQTNLVPYPR	TBA1_MERUN	P68360
	TBA1_MACFA	P68367
	TBA6_HUMAN	Q9BQE3
	TBA8_HUMAN	Q9NY65
FDLGQDVIDFTGHALALYR	GDIA_HUMAN	P31150
	GDIB_HUMAN	P50395
FDLMYAK	TBA1_MERUN	P68360
	TBA1_MACFA	P68367
	TBA6_HUMAN	Q9BQE3
	TBA8_HUMAN	Q9NY65
FDLTGIPPAPR	HS70L_HUMAN	P34931
	HSP72_HUMAN	P54652

FDQLLAEEK	MYH9_HUMAN	P35579
	MYH10_HUMAN	P35580
	MYH11_HUMAN	P35749
FDSDAASPR	1B07_HUMAN	P01889
	1B08_HUMAN	P30460
	1C04_HUMAN	P30504
FEELCSDLFR	HSP71_HUMAN	P08107
	HSP76_HUMAN	P17066
FEIWDTAGQER	RAB5A_HUMAN	P20339
	RAB5B_HUMAN	P61020
	RAB5C_HUMAN	P51148
FELSGIPPAPR	HSP71_HUMAN	P08107
	HSP76_HUMAN	P17066
FFETESR	ALU2_HUMAN	P39189
	ALU3_HUMAN	P39190
	ALU5_HUMAN	P39192
	ALU8_HUMAN	P39195
FFETSAK	RAB10_HUMAN	P61026
	RAB13_HUMAN	P51153
FFYSDQNVDSR	TLN1_HUMAN	Q9Y490
	TLN2_HUMAN	Q9Y4G6
FGANAILGVSLAVCK	ENOA_HUMAN	P06733
	ENOG_HUMAN	P09104
	ENOB_HUMAN	P13929
FGPALSVK	PABP1_HUMAN	P11940
	PABP3_HUMAN	Q9H361
FGSCVPHTTRPK	DLG4_HUMAN	P78352
	DLG2_HUMAN	Q15700
FHEFHSPALEDADFDNKPMVLLVGQYSTGK	EHD1_HUMAN	Q9H4M9
	EHD3_HUMAN	Q9NZN3
FHTSRPESFAIYK	LAMC1_HUMAN	P11047
	LAMC3_HUMAN	Q9Y6N6
FIAVGYVDDTQFVR	1A03_HUMAN	P04439
	1A01_HUMAN	P30443
	1C04_HUMAN	P30504
FIDTTSK	RL3_HUMAN	P39023
	RL3L_HUMAN	Q92901
FIGAGAATVGVAGSGAGIGTVFGSLIIGYAR	AT5G1_HUMAN	P05496
	AT5G3_HUMAN	P48201
	AT5G2_HUMAN	Q06055
FISVGYVDDTQFVR	1B07_HUMAN	P01889
	HLAH_HUMAN	P01893
	1B08_HUMAN	P30460
FLEQQNK	K2C6A_HUMAN	P02538
	K2C6B_HUMAN	P04259
	K2C8_HUMAN	P05787
	VIME_HUMAN	P08670
	K2C7_HUMAN	P08729
	K2C3_HUMAN	P12035

	K2C5_HUMAN	P13647
	K2C6C_HUMAN	P48666
	K2C6E_HUMAN	P48668
	K22O_HUMAN	Q01546
FLEQQNQVLQTK	K2C1_HUMAN	P04264
	K22E_HUMAN	P35908
FLIWDTAGQER	RAB31_HUMAN	Q13636
	RB22A_HUMAN	Q9UL26
FLMANGQLVK	GDIA_HUMAN	P31150
	GDIB_HUMAN	P50395
FLNSFEELQAEECGILNGCENGR	LTB1S_HUMAN	P22064
	LTB1L_HUMAN	Q14766
FNPFVTSDR	RL26_MOUSE	P61255
	RL26L_HUMAN	Q9UNX3
FNQCNTTR	PPB1_HUMAN	P05187
	PPBN_HUMAN	P10696
FPGQLNADLR	TBBX_MOUSE	P68372
	TBB5_MOUSE	P99024
	TBB3_HUMAN	Q13509
	TBB4Q_HUMAN	Q99867
FPPNIVNIHVK	LTB1S_HUMAN	P22064
	LTB1L_HUMAN	Q14766
FPSEYVPTVFDNYAVTVMIGGEPYTLGL FDTAGQEDYDR	CDC42_CANFA	P60952
	CDC42_MOUSE	P60766
FPYVALSK	PPB1_HUMAN	P05187
	PPBN_HUMAN	P10696
FQPVHDLTIGVEFGAR	RAB2A_HUMAN	P61019
	RAB2B_HUMAN	Q8WUD1
FRPSLEER	CTN2_HUMAN	P26232
	CTN1_HUMAN	P35221
FSCLSLPSSWDYR	ALU5_HUMAN	P39192
	ALU7_HUMAN	P39194
	ALU8_HUMAN	P39195
FSDSEIGGITIAWK	STA5A_HUMAN	P42229
	STA5B_HUMAN	P51692
FSGGFGAR	DDX3X_HUMAN	O00571
	DDX3Y_HUMAN	O15523
FSPAGPILSIR	PABP1_HUMAN	P11940
	PABP3_HUMAN	Q9H361
FSWNVWPSSR	SC23A_HUMAN	Q15436
	SC23B_HUMAN	Q15437
FTGSEIR	MPPB_HUMAN	O75439
	UQCR1_HUMAN	P31930
FTSASDVWSYGIVMWEVMSYGERPYW DMSNQDVIK	EPHA4_HUMAN	P54764
	EPHA7_HUMAN	Q15375
FVFAAVK	GNA14_HUMAN	O95837
	GNA11_HUMAN	P29992
	GNAQ_HUMAN	P50148
FVFDAVTDIIIK	GNAT1_HUMAN	P11488

	GNAT2_HUMAN	P19087
FVIKPIDK	EZRI_HUMAN	P15311
	MOES_HUMAN	P26038
	RADI_HUMAN	P35241
FYEEVHDLER	NP1L1_HUMAN	P55209
	NP1L4_HUMAN	Q99733
GAAGALLVYDITR	RAB2A_HUMAN	P61019
	RAB2B_HUMAN	Q8WUD1
GAAGALLVYDITSR	RAB4A_HUMAN	P20338
	RAB4B_HUMAN	P61018
GAALSVDIR	UDB17_HUMAN	O75795
	UDB15_HUMAN	P54855
GADIMYTGTVDCWR	ADT1_HUMAN	P12235
	ADT3_HUMAN	P12236
GADSLEDFLYHEGYACTSIHGDR	DDX3X_HUMAN	O00571
	DDX3Y_HUMAN	O15523
GAESVTEEK	STA5A_HUMAN	P42229
	STA5B_HUMAN	P51692
GAGVTLNVLEMTSEDLENALK	UD16_HUMAN	P19224
	UD11_HUMAN	P22309
GAMGFILMYDITNEESFNAVQDWSTQIK	RAB3A_HUMAN	P20336
	RAB3C_HUMAN	Q96E17
GAMGIMLVYDITNEK	RAB8A_CANFA	P61007
	RAB8B_HUMAN	Q92930
GAPHLRPAAHDLTWYQYHSLDVIGFLLA VVLTVAFITFK	UD16_HUMAN	P19224
	UD11_HUMAN	P22309
GASVNLYMFIGGTNFAYWNGANSPYAA QPTSYDYDAPLSEAGDLTEK	BGAL_HUMAN	P16278
	BGAM_HUMAN	P16279
GAVGALLVYDIAK	RB11A_MOUSE	P62492
	RB11B_HUMAN	Q15907
GAWSNVLR	ADT2_HUMAN	P05141
	ADT1_HUMAN	P12235
	ADT3_HUMAN	P12236
GCALQCAILSPAFK	HS74L_HUMAN	O95757
	HSP74_HUMAN	P34932
GCHLLVATPGR	DDX3X_HUMAN	O00571
	DDX3Y_HUMAN	O15523
GCTLSAEDK	GNAI1_HUMAN	P63096
	GNAI3_HUMAN	P08754
GCTLSAEER	GNAO1_HUMAN	P09471
	GNAO2_HUMAN	P29777
GDCINTAGSYDCTCPDGFQLDDNK	LTB1S_HUMAN	P22064
	LTB1L_HUMAN	Q14766
GDDLLPAGTEDYIHIR	SUI13_HUMAN	O60739
	SUI1_HUMAN	P41567
GDFCIQVGR	NDK8_HUMAN	O60361
	NDKA_HUMAN	P15531
	NDKB_HUMAN	P22392
GDGPICLVLAPTR	DDX5_HUMAN	P17844

	DDX17_HUMAN	Q92841
GEHPGLSIGDVAK	HMG1_HUMAN	P09429
	HMG1X_HUMAN	Q9UGV6
GELANFR	BIG2_HUMAN	Q9Y6D5
	BIG1_HUMAN	Q9Y6D6
GEVNAADAFDIGSFDEEDTK	ARBK1_HUMAN	P25098
	ARBK2_HUMAN	P35626
GFEFTLMVVGESGLGK	SEPT2_HUMAN	Q15019
	SEPT7_HUMAN	Q16181
GFFLFVEGGR	PPB1_HUMAN	P05187
	PPBN_HUMAN	P10696
GFGFVCFSSPEEATK	PABP1_HUMAN	P11940
	PABP4_HUMAN	Q13310
	PABP3_HUMAN	Q9H361
GFGFVSFER	PABP1_HUMAN	P11940
	PABP3_HUMAN	Q9H361
GFGGGGYGGFYNSDGYGGNYNSQGV DWWGN	DDX3X_HUMAN	O00571
	DDX3Y_HUMAN	O15523
GFMVLIEK	MTMR7_HUMAN	Q9Y216
	MTMR6_HUMAN	Q9Y217
GFPGYMYTDLATIYER	VATB1_HUMAN	P15313
	VATB2_HUMAN	P21281
GFSANSAR	K2C6A_HUMAN	P02538
	K2C6C_HUMAN	P48666
	K2C6E_HUMAN	P48668
GFTMLAR	ALU5_HUMAN	P39192
	ALU7_HUMAN	P39194
	ALU8_HUMAN	P39195
GFVPAGESSSEAGGENYK	LTB1S_HUMAN	P22064
	LTB1L_HUMAN	Q14766
GGDLFTR	KS6A2_HUMAN	Q15349
	KS6A1_HUMAN	Q15418
GGFGEVYGCR	ARBK1_HUMAN	P25098
	ARBK2_HUMAN	P35626
GGGQIIPTAR	EF2_HUMAN	P13639
	U5S1_HUMAN	Q15029
GGSYSQAACSDSAQGSDVSLTA	1B07_HUMAN	P01889
	1B08_HUMAN	P30460
GGSYTQAASSDSAQGSDVSLTACK	1A03_HUMAN	P04439
	1A01_HUMAN	P30443
GGTPSAFDR	K6PL_HUMAN	P17858
	K6PP_HUMAN	Q01813
GHYTEGAELVDSVLDVVR	TBBX_MOUSE	P68372
	TBB5_MOUSE	P99024
	TBB3_HUMAN	Q13509
GHYTIGK	TBA1_MERUN	P68360
	TBA1_MACFA	P68367
	TBA6_HUMAN	Q9BQE3
GIAAGMK	EPHA2_HUMAN	P29317

	EPHB3_HUMAN	P54753
GIDVQQVSLVINYDLPTNR	IF41_HUMAN	P60842
	IF42_HUMAN	Q14240
GIIDCVVR	ADT2_HUMAN	P05141
	ADT1_HUMAN	P12235
GITIDISLWK	EF1A1_HUMAN	P68104
	EF1A2_HUMAN	Q05639
GITMATAK	TLN1_HUMAN	Q9Y490
	TLN2_HUMAN	Q9Y4G6
GIYAYGFEKPSAIQQR	IF41_HUMAN	P60842
	DDX48_HUMAN	P38919
	IF42_HUMAN	Q14240
GKPDAAK	HMG1_HUMAN	P09429
	HMG1X_HUMAN	Q9UGV6
GLATFCLDK	PGRC1_HUMAN	O00264
	PGRC2_HUMAN	O15173
GLDFEAK	CADH1_HUMAN	P12830
	CADH3_HUMAN	P22223
GLDVEDVK	DDX5_HUMAN	P17844
	DDX17_HUMAN	Q92841
GLFIIDDK	PRDX1_HUMAN	Q06830
	PRDX4_HUMAN	Q13162
GLGDCLVK	ADT2_HUMAN	P05141
	ADT3_HUMAN	P12236
GLGFSIAGGVGNQHIPGDNSIYVTK	DLG4_HUMAN	P78352
	DLG2_HUMAN	Q15700
GLPFGCSK	HNRH1_HUMAN	P31943
	HNRH2_HUMAN	P55795
GLPHVIYCR	SMAD3_HUMAN	P84022
	SMAD5_HUMAN	Q99717
GLTVMFEIMK	BIG2_HUMAN	Q9Y6D5
	BIG1_HUMAN	Q9Y6D6
GLVGEIIK	NDKA_HUMAN	P15531
	NDKB_HUMAN	P22392
GLVSNLTLSSNILTDWTIFPLDTEDAVR	BGAL_HUMAN	P16278
	BGAM_HUMAN	P16279
GLYQGFNVSVQGIIIYR	ADT2_HUMAN	P05141
	ADT1_HUMAN	P12235
GMGGAFVLVLYDEIK	ADT2_HUMAN	P05141
	ADT1_HUMAN	P12235
GMGGWEGGIR	ARSD_HUMAN	P51689
	ARSE_HUMAN	P51690
GMGYMPK	COR1A_HUMAN	P31146
	COR1C_HUMAN	Q9ULV4
GMLPDPK	ADT2_HUMAN	P05141
	ADT1_HUMAN	P12235
	ADT3_HUMAN	P12236
GMQDLVEDFK	K2C6A_HUMAN	P02538
	K2C6C_HUMAN	P48666

GNFQTIGLSAAAR	PPB1_HUMAN	P05187
	PPBN_HUMAN	P10696
GNHECASINR	PP1A_HUMAN	P62136
	PP1B_HUMAN	P62140
GNLANVIR	ADT2_HUMAN	P05141
	ADT1_HUMAN	P12235
	ADT3_HUMAN	P12236
GPELLVDYQMYDYSLDMWSLGCMLAS MIFR	CSK21_HUMAN	P68400
	CSK22_HUMAN	P19784
GPLGPNWK	PIPNB_HUMAN	P48739
	PIPNA_HUMAN	Q00169
GPLINSEFYTGWLDHWGQPHSTIK	BGAL_HUMAN	P16278
	BGAM_HUMAN	P16279
GPPGPPGK	CO1A1_HUMAN	P02452
	CO5A1_HUMAN	P20908
GPQLTLFVPQHILMTSAPNTITVLELEWA PCSSDDPELCAVTFVDRPVIGSSVTYDH PSKPVEK	BGAL_HUMAN	P16278
	BGAM_HUMAN	P16279
GPSYGLSAEVK	CLP3_HUMAN	Q15417
	CLP2_HUMAN	Q99439
GPVFVKPK	LTB1S_HUMAN	P22064
	LTB1L_HUMAN	Q14766
GQEFETSLANMVKPR	ALU7_HUMAN	P39194
	ALU8_HUMAN	P39195
GQTVQQVYNAVGALAK	MYH1_HUMAN	P12882
	MYH8_HUMAN	P13535
	MYH4_HUMAN	Q9Y623
GQVWINGFNLGR	BGAL_HUMAN	P16278
	BGAM_HUMAN	P16279
GSCGIGGGIGGGSSR	K1C14_HUMAN	P02533
	K1C16_HUMAN	P08779
GSGGLGGACGGAGFGSR	K2C6A_HUMAN	P02538
	K2C6B_HUMAN	P04259
	K2C6C_HUMAN	P48666
	K2C6E_HUMAN	P48668
GSGIVTR	MX2_HUMAN	P20592
	DYN1_HUMAN	Q05193
	DYN3_HUMAN	Q9UQ16
GSLLDFLK	YES_HUMAN	P07947
	SRC_HUMAN	P12931
GSPLLIGVR	GFPT2_HUMAN	O94808
	GFPT1_HUMAN	Q06210
GSSFQTVSALFR	MYH3_HUMAN	P11055
	MYH1_HUMAN	P12882
	MYH8_HUMAN	P13535
	MYH2_HUMAN	Q9UKX2
	MYH4_HUMAN	Q9Y623
GSSFQTVSALHR	MYH7_HUMAN	P12883
	MYH6_HUMAN	P13533
GSSIFGLAPGK	PPB1_HUMAN	P05187

	PPBN_HUMAN	P10696
GSTAGGCR	CAN1_HUMAN	P07384
	CAN2_HUMAN	P17655
GTGASGSFK	H14_HUMAN	P10412
	H15_HUMAN	P16401
	H13_HUMAN	P16402
	H12_HUMAN	P16403
GTLEDQIIQANPALEAFGNAK	MYH7_HUMAN	P12883
	MYH6_HUMAN	P13533
GTLEPVEK	HS70L_HUMAN	P34931
	HSP72_HUMAN	P54652
GTLVQTK	H14_HUMAN	P10412
	H15_HUMAN	P16401
	H13_HUMAN	P16402
	H12_HUMAN	P16403
GVEICIATPGR	DDX5_HUMAN	P17844
	DDX17_HUMAN	Q92841
GVGIISEGNETVEDIAAR	AT1A3_HUMAN	P13637
	AT1A2_HUMAN	P50993
GVPQIEVTFDIDANGILNVTATDK	HSP71_HUMAN	P08107
	HS70L_HUMAN	P34931
GVVDSEDLPLNISR	HS90A_HUMAN	P07900
	HS90B_HUMAN	P08238
GVVEVTHDLQK	HSP47_HUMAN	P29043
	SPH2_HUMAN	P50454
GVVVLAK	AK1C4_HUMAN	P17516
	AK1C3_HUMAN	P42330
	AK1C2_HUMAN	P52895
	AK1C1_HUMAN	Q04828
GWFPILFELSCIINR	BIG2_HUMAN	Q9Y6D5
	BIG1_HUMAN	Q9Y6D6
GWNGQCLDVDECLEPNVCANGDCSNL EGSYMCSCHK	LTB1S_HUMAN	P22064
	LTB1L_HUMAN	Q14766
GYDFAAVLEWFAER	EHD1_HUMAN	Q9H4M9
	EHD3_HUMAN	Q9NZN3
GYDVDFPR	GFPT2_HUMAN	O94808
	GFPT1_HUMAN	Q06210
GYDVIAQAQSGTGK	IF41_HUMAN	P60842
	IF42_HUMAN	Q14240
GYEEWLLNEIR	ACTN4_HUMAN	O43707
	ACTN2_HUMAN	P35609
GYNSIGR	HNRH1_HUMAN	P31943
	HNRH2_HUMAN	P55795
GYSFTTTAER	ACTB_BOVIN	P60712
	ACTG_ANSAN	P63256
GYSFVTTAER	ACTS_MOUSE	P68134
	ACTA_RABIT	P62740
	ACTC_HUMAN	P68032
	ACTH_HUMAN	P63267

	1B07_HUMAN	P01889
GYYNQSEAGSHTLQSMYGCDVGPDGR	1B08_HUMAN	P30460
	MYH3_HUMAN	P11055
	MYH1_HUMAN	P12882
	MYH7_HUMAN	P12883
	MYH6_HUMAN	P13533
HADSVAELGEQIDNLQR	MYH2_HUMAN	Q9UKX2
	DDX3X_HUMAN	O00571
HAIPIIK	DDX3Y_HUMAN	O15523
	H2B_BOVIN	P62808
	H2BR_HUMAN	P06899
	H2BF_HUMAN	P33778
	H2BS_HUMAN	P57053
	H2BB_HUMAN	P58876
	H2BQ_HUMAN	Q16778
	H2BJ_HUMAN	Q93079
	H2BD_HUMAN	Q99877
	H2BE_HUMAN	Q99879
HAVSEGTK	H2BC_HUMAN	Q99880
	DLG2_HUMAN	Q15700
HCILDVSGNAIK	DLG3_HUMAN	Q92796
	ALU1_HUMAN	P39188
	ALU2_HUMAN	P39189
	ALU3_HUMAN	P39190
HCTPAWATER	ALU8_HUMAN	P39195
	MYH3_HUMAN	P11055
	MYH1_HUMAN	P12882
	MYH7_HUMAN	P12883
	MYH6_HUMAN	P13533
	MYH8_HUMAN	P13535
	MYH2_HUMAN	Q9UKX2
	MYH13_HUMAN	Q9UKX3
HDCDLLR	MYH4_HUMAN	Q9Y623
	PP1A_HUMAN	P62136
HDLDLICR	PP1B_HUMAN	P62140
	ACTN4_HUMAN	O43707
	ACTN2_HUMAN	P35609
HEAFESDLAAHQDR	ACTN3_HUMAN	Q08043
	BMR1B_HUMAN	O00238
HENILGFIAADIK	BMR1A_HUMAN	P36894
	RHOA_BOVIN	P61585
HFCPNVPIILVGNK	RHOC_HUMAN	P08134
	HS90A_HUMAN	P07900
HFSVEGQLEFR	HS90B_HUMAN	P08238
	AK1C3_HUMAN	P42330
HIDSAHLYNNEEQVGLAIR	AK1C1_HUMAN	Q04828
	DYN1_HUMAN	Q05193
HIFALFNTEQR	DYN3_HUMAN	Q9UQ16
HILYNEQR	STA5A_HUMAN	P42229

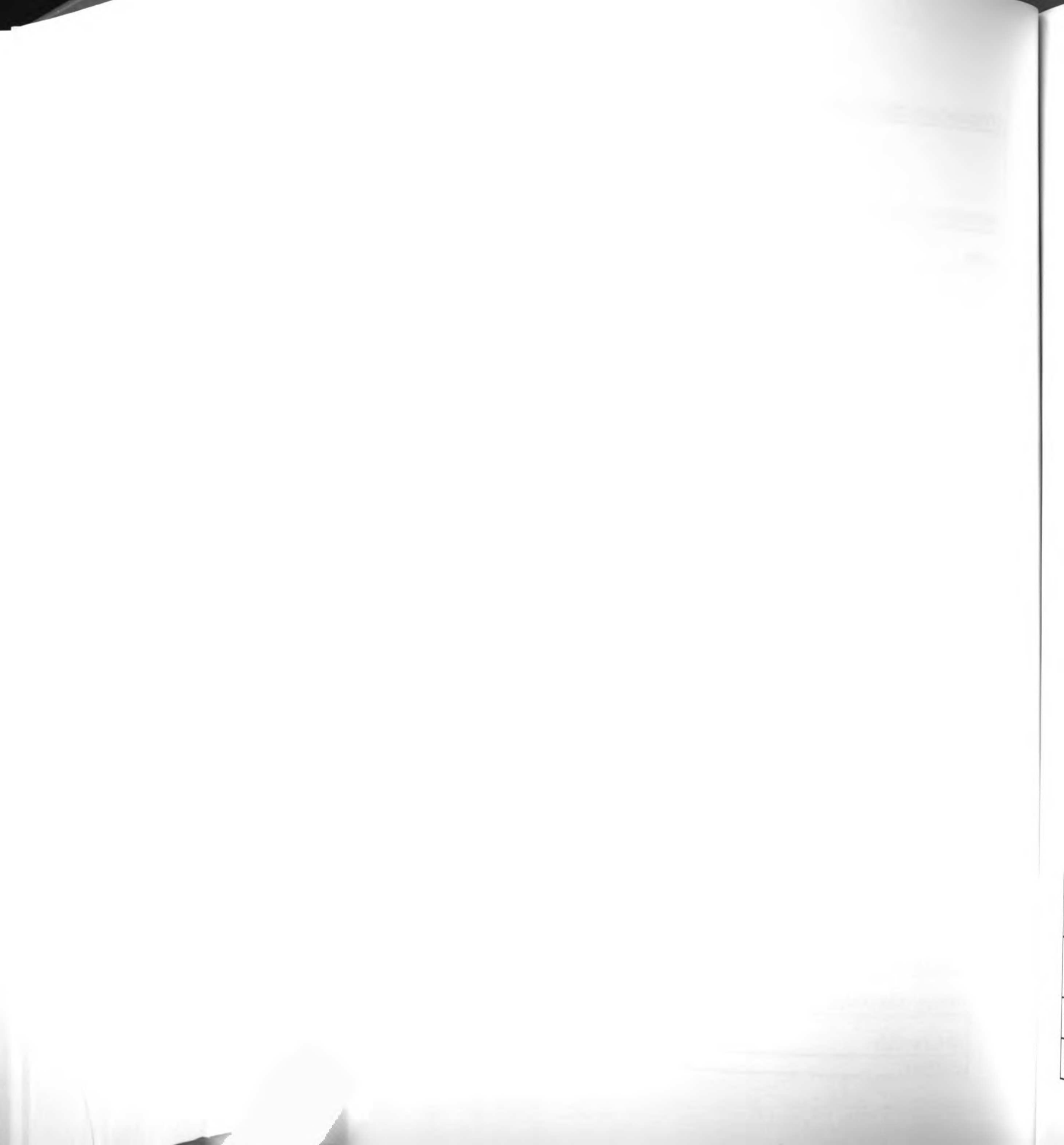

	STA5B_HUMAN	P51692
HLAGLGLTEAIDK	HSP47_HUMAN	P29043
	SPH2_HUMAN	P50454
HLCAHGQCR	LTB1S_HUMAN	P22064
	LTB1L_HUMAN	Q14766
HLHFTLVK	PHS1_HUMAN	P06737
	PHS3_HUMAN	P11216
	PHS2_HUMAN	P11217
HLQINQTFEELR	STA5A_HUMAN	P42229
	STA5B_HUMAN	P51692
HLQLAIR	H2AC_HUMAN	P02261
	H2AX_HUMAN	P16104
	H2AZ_HUMAN	P17317
	H2AO_HUMAN	P20670
	H2AG_HUMAN	P20671
	H2AA_HUMAN	P28001
	H2AL_HUMAN	Q93077
	H2AE_HUMAN	Q99878
HLTYENVER	RB11A_MOUSE	P62492
	RB11B_HUMAN	Q15907
HNDDEQYAWESSAGGSFTVR	HS90A_HUMAN	P07900
	HS90B_HUMAN	P08238
HPMDLSTVK	BRD2_HUMAN	P25440
	BRD3_HUMAN	Q15059
HPPEASVQIHQVSR	LTB1S_HUMAN	P22064
	LTB1L_HUMAN	Q14766
HQGVMVGMGQK	ACTS_MOUSE	P68134
	ACTB_BOVIN	P60712
	ACTG_ANSAN	P63256
	ACTA_RABIT	P62740
	ACTC_HUMAN	P68032
	ACTH_HUMAN	P63267
HQVEYLGLK	MYO1F_HUMAN	O00160
	MYO1E_HUMAN	Q12965
HTGPNSPDTANDGFVR	HNRH1_HUMAN	P31943
	HNRH2_HUMAN	P55795
HTMMFSATFPK	DDX3X_HUMAN	O00571
	DDX3Y_HUMAN	O15523
HTNYTMEHIR	ACTN4_HUMAN	O43707
	ACTN2_HUMAN	P35609
HTTNLTLWFEK	SOS1_HUMAN	Q07889
	SOS2_HUMAN	Q07890
HVAVTNMNEHSSR	KIF5C_HUMAN	O60282
	KINH_HUMAN	P33176
	KINN_HUMAN	Q12840
HVINFDLPSDIEEYVHR	DDX3X_HUMAN	O00571
	DDX3Y_HUMAN	O15523
HVLATLGEK	MLE1_HUMAN	P05976
	MLE3_HUMAN	P06741

	VATB1_HUMAN	P15313
HVLVILTDMSSYAEALR	VATB2_HUMAN	P21281
	MYL6_BOVIN	P60661
HVLVTLGEK	MYL6_HUMAN	P60660
	PPB1_HUMAN	P05187
HVPDSGATATAYLCGVK	PPBN_HUMAN	P10696
	BIG2_HUMAN	Q9Y6D5
HWWQDLFR	BIG1_HUMAN	Q9Y6D6
	ARF3_RAT	P61206
	ARF4_HUMAN	P18085
	ARF5_HUMAN	P84085
HYFQNTQGLIFVVDSNDR	ARF1_RAT	P84079
	YES_HUMAN	P07947
IADFGLAR	FGFR4_HUMAN	P22455
	KPCA_HUMAN	P17252
IADFGMCK	KPCD_HUMAN	Q05655
	AK1C4_HUMAN	P17516
	AK1C3_HUMAN	P42330
	AK1C2_HUMAN	P52895
IADGSVK	AK1C1_HUMAN	Q04828
	CTN2_HUMAN	P26232
IAEAGSR	CTN1_HUMAN	P35221
	RBP2_HUMAN	P49792
IAELLCK	RN5A_HUMAN	Q05823
	MYH1_HUMAN	P12882
	MYH8_HUMAN	P13535
IAEQELLDASER	MYH2_HUMAN	Q9UKX2
	H2B_BOVIN	P62808
	H2BR_HUMAN	P06899
	H2BF_HUMAN	P33778
	H2BS_HUMAN	P57053
	H2BB_HUMAN	P58876
	H2BQ_HUMAN	Q16778
	H2BJ_HUMAN	Q93079
	H2BD_HUMAN	Q99877
IAGEASR	H2BE_HUMAN	Q99879
	AT1A2_HUMAN	P50993
IAGLCNR	AT1A4_HUMAN	Q13733
	CTN2_HUMAN	P26232
IALYCHQLNICSK	CTN1_HUMAN	P35221
	TRPC3_HUMAN	Q13507
IAYILPANESFGPLQISLGR	TRPC7_HUMAN	Q9HCX4
	PGFRB_HUMAN	P09619
	KIT_HUMAN	P10721
	PGFRA_HUMAN	P16234
	MK03_HUMAN	P27361
ICDFGLAR	MK01_HUMAN	P28482
	LTB1S_HUMAN	P22064
IDGPTGQK	LTB1L_HUMAN	Q14766

	PPB1_HUMAN	P05187
IDHGHHESR	PPBN_HUMAN	P10696
	SC23A_HUMAN	Q15436
IDMNLTDLLGELQR	SC23B_HUMAN	Q15437
	MYH1_HUMAN	P12882
	MYH8_HUMAN	P13535
IEAQNKPFDAK	MYH4_HUMAN	Q9Y623
	MYH1_HUMAN	P12882
	MYH2_HUMAN	Q9UKX2
	MYH13_HUMAN	Q9UKX3
IEDMAMMTHLHEPAVLYNLK	MYH4_HUMAN	Q9Y623
	MYH3_HUMAN	P11055
	MYH1_HUMAN	P12882
	MYH2_HUMAN	Q9UKX2
IEELEEEIEAER	MYH4_HUMAN	Q9Y623
	EPHB3_HUMAN	P54753
IEEVIGAGEFGEVCR	EPHB4_HUMAN	P54760
	MLE1_HUMAN	P05976
IEFEQFLPMMQAISNNK	MLE3_HUMAN	P06741
	GSH2_HUMAN	Q9BZM3
IEIATYLNLSEK	GSHI_HUMAN	Q9H4S2
	K2C1_HUMAN	P04264
IEISELNR	K22E_HUMAN	P35908
	TRPC3_HUMAN	Q13507
IERPHDYFCK	TRPC7_HUMAN	Q9HCX4
	PP1A_HUMAN	P62136
IFCCHGGLSPDLQSMEQIR	PP1B_HUMAN	P62140
	PPCKC_HUMAN	P35558
IFHVNWFR	PPCKM_HUMAN	Q16822
	BIG2_HUMAN	Q9Y6D5
IFTGSTR	BIG1_HUMAN	Q9Y6D6
	GNAO1_HUMAN	P09471
IGAADYQPTEQDILR	GNAO2_HUMAN	P29777
	IGF1R_HUMAN	P08069
IGDFGMTR	INSRR_HUMAN	P14616
	CDC2_HUMAN	P06493
	CDK2_HUMAN	P24941
IGEGTYGVVYK	CDK3_HUMAN	Q00526
	SC15A_HUMAN	Q8TAG9
IGETAMK	SC15B_HUMAN	Q9Y2D4
	LTB1S_HUMAN	P22064
IGFGPDPTFSSCVPDPPVISEEK	LTB1L_HUMAN	Q14766
	EZRI_HUMAN	P15311
	MOES_HUMAN	P26038
IGFPWSEIR	RADI_HUMAN	P35241
	EF1A1_HUMAN	P68104
IGGIGTVPVGR	EF1A2_HUMAN	Q05639
	DDX3X_HUMAN	O00571
IGLDFCK	DDX3Y_HUMAN	O15523

	PLSL_HUMAN	P13796
IGLFADIELSR	PLST_HUMAN	P13797
	EPHB3_HUMAN	P54753
IGVTLAGHQK	EPHB4_HUMAN	P54760
	MYH7_HUMAN	P12883
	MYH6_HUMAN	P13533
	MYH13_HUMAN	Q9UKX3
IHFGATGK	MYH4_HUMAN	Q9Y623
	MYH3_HUMAN	P11055
	MYH1_HUMAN	P12882
	MYH8_HUMAN	P13535
IHFGTTGK	MYH2_HUMAN	Q9UKX2
	TBA1_MERUN	P68360
	TBA1_MACFA	P68367
IHFPLATYAPVISAEK	TBA6_HUMAN	Q9BQE3
	ZN208_HUMAN	O43345
IHTGEKPYK	ZN319_HUMAN	Q9P2F9
	ACTS_MOUSE	P68134
	ACTB_BOVIN	P60712
	ACTG_ANSAN	P63256
	ACTA_RABIT	P62740
	ACTC_HUMAN	P68032
IIAPPER	ACTH_HUMAN	P63267
	IKKB_HUMAN	O14920
IIDLGYAK	IKKA_HUMAN	O15111
	GNAO1_HUMAN	P09471
IIHEDGFSGEDVK	GNAO2_HUMAN	P29777
	EHD4_HUMAN	Q9H223
	EHD1_HUMAN	Q9H4M9
IILLFDAHK	EHD3_HUMAN	Q9NZN3
	GRP78_HUMAN	P11021
	HS70L_HUMAN	P34931
IINEPTAAAIAYGLDK	HSP72_HUMAN	P54652
	HSP71_HUMAN	P08107
IINEPTAAAIAYGLDR	HSP76_HUMAN	P17066
	GNA11_HUMAN	P29992
IIYSHFTCATDTENIR	GNAQ_HUMAN	P50148
	MOES_HUMAN	P26038
ILALCMGNHELYMR	RADI_HUMAN	P35241
	MGR7_HUMAN	Q14831
ILDTCSR	MGR4_HUMAN	Q14833
	BGAL_HUMAN	P16278
ILLLLLVLLLLGPTR	BGAM_HUMAN	P16279
	ARF3_RAT	P61206
	ARF4_HUMAN	P18085
	ARF5_HUMAN	P84085
ILMVGLDAAGK	ARF1_RAT	P84079
ILQDSLGGNCR	KIF5C_HUMAN	O60282
	KINH_HUMAN	P33176

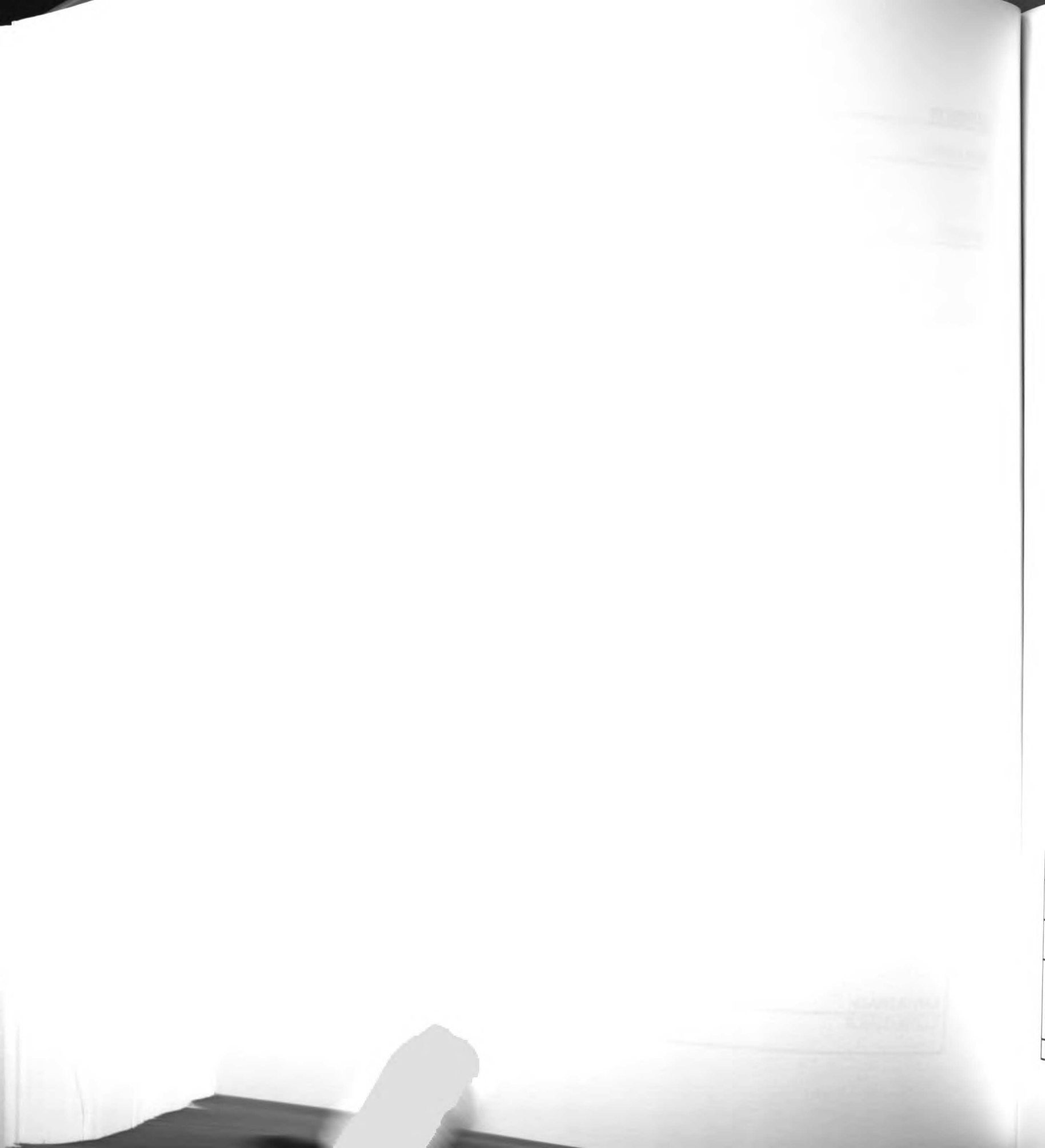

	KINN_HUMAN	Q12840
ILYADFK	MYH1_HUMAN	P12882
	MYH2_HUMAN	Q9UKX2
	MYH13_HUMAN	Q9UKX3
	MYH4_HUMAN	Q9Y623
ILYGDFK	MYH3_HUMAN	P11055
	MYH8_HUMAN	P13535
ILYGDFR	MYH7_HUMAN	P12883
	MYH6_HUMAN	P13533
ILYSQCGDVMR	MLEY_HUMAN	P14649
	MYL6_BOVIN	P60661
	MYL6_HUMAN	P60660
IMNTFSVVPSPK	TBBX_MOUSE	P68372
	TBB5_MOUSE	P99024
	TBB3_HUMAN	Q13509
IMSSPLSK	RL26_MOUSE	P61255
	RL26L_HUMAN	Q9UNX3
INATLETK	MYH7_HUMAN	P12883
	MYH6_HUMAN	P13533
INETDTFGPGDDDEIQFDDIGDDDEDIDDI	IF1AY_HUMAN	O14602
	IF1AH_HUMAN	O75642
	IF1AX_HUMAN	P47813
INFDVTGYIVGANIETYLLEK	MYH10_HUMAN	P35580
	MYH11_HUMAN	P35749
INHEGEVNR	RBBP4_HUMAN	Q09028
	RBBP7_HUMAN	Q16576
INISEGNCPER	PCBP1_HUMAN	Q15365
	PCBP2_HUMAN	Q15366
INQQLDTK	MYH3_HUMAN	P11055
	MYH1_HUMAN	P12882
	MYH8_HUMAN	P13535
	MYH2_HUMAN	Q9UKX2
	MYH13_HUMAN	Q9UKX3
	MYH4_HUMAN	Q9Y623
INVNEIFYDLVR	RAP1B_BOVIN	P61223
	RAP1A_BOVIN	P62833
IPDEELR	SH3G1_HUMAN	Q99961
	SH3G2_HUMAN	Q99962
IPIFSAAGLPHNEIAAQICR	VATB1_HUMAN	P15313
	VATB2_HUMAN	P21281
IPQTVLWR	UD16_HUMAN	P19224
	UD11_HUMAN	P22309
IPSGLFIPSMAVGAIAGR	CLCN4_HUMAN	P51793
	CLCN5_HUMAN	P51795
IQLELNQVK	MYH1_HUMAN	P12882
	MYH8_HUMAN	P13535
	MYH2_HUMAN	Q9UKX2
	MYH4_HUMAN	Q9Y623
IQVHYYEDGNVQLVSHK	CAZA2_HUMAN	P47755

	CAZA1_HUMAN	P52907
ISAPQER	ACTZ_HUMAN	P61163
	ACTY_HUMAN	P42025
ISDLGLACDFSK	ARBK1_HUMAN	P25098
	ARBK2_HUMAN	P35626
ISEQFTAMFR	TBBX_MOUSE	P68372
	TBB5_MOUSE	P99024
	TBB3_HUMAN	Q13509
ISFLENNLEQLTK	KIF5C_HUMAN	O60282
	KINH_HUMAN	P33176
	KINN_HUMAN	Q12840
ISIGGGSCAISGGYGSR	K2C6A_HUMAN	P02538
	K2C6B_HUMAN	P04259
	K2C6C_HUMAN	P48666
	K2C6E_HUMAN	P48668
ISNFLLEK	MYO1F_HUMAN	O00160
	MYO1E_HUMAN	Q12965
ISPFEHQTYCQR	MK03_HUMAN	P27361
	MK01_HUMAN	P28482
ISSVLAGGSCR	K1C14_HUMAN	P02533
	K1C16_HUMAN	P08779
ITGANAK	EHD1_HUMAN	Q9H4M9
	EHD3_HUMAN	Q9NZN3
ITGMLLEIDNSELLHMLESPESLR	PABP1_HUMAN	P11940
	PABP4_HUMAN	Q13310
ITITNDK	HSP71_HUMAN	P08107
	HSP76_HUMAN	P17066
	HS70L_HUMAN	P34931
	HSP72_HUMAN	P54652
ITLSQVGDVLR	MLE1_HUMAN	P05976
	MLE3_HUMAN	P06741
ITMQNLNDR	K1C13_HUMAN	P13646
	K1C15_HUMAN	P19012
IVAECNAVR	CTN2_HUMAN	P26232
	CTN1_HUMAN	P35221
IVAPPGGR	DPYL3_HUMAN	Q14195
	DPYL2_HUMAN	Q16555
IVATKPLYVALAQR	PABP1_HUMAN	P11940
	PABP3_HUMAN	Q9H361
IVDQIRPDR	DDX5_HUMAN	P17844
	DDX17_HUMAN	Q92841
IVEQDTMPPK	DDX3X_HUMAN	O00571
	DDX3Y_HUMAN	O15523
IVESMQSTLDAEIR	MYH1_HUMAN	P12882
	MYH2_HUMAN	Q9UKX2
IVFQEFR	MYH10_HUMAN	P35580
	MYH11_HUMAN	P35749
IVNDDQSFYADIYMEDGLIK	DPYL3_HUMAN	Q14195
	DPYL2_HUMAN	Q16555

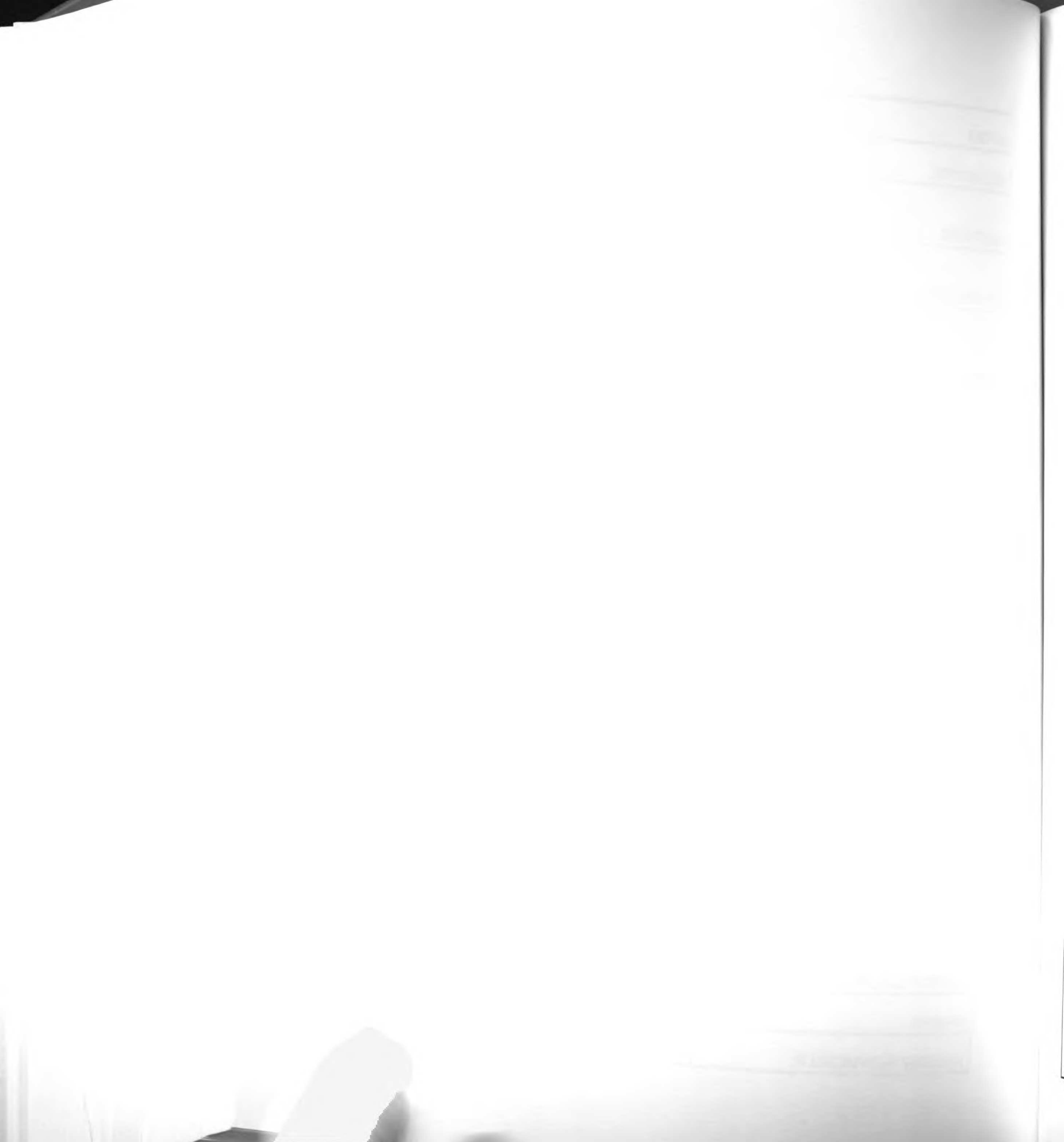

	ACTA_RABIT	P62740
IWHHSFYNELR	ACTH_HUMAN	P63267
	ACTS_MOUSE	P68134
	ACTB_BOVIN	P60712
	ACTG_ANSAN	P63256
IWHHTFYNELR	ACTC_HUMAN	P68032
	ACTZ_HUMAN	P61163
IWQYVYSK	ACTY_HUMAN	P42025
	GBB1_BOVIN	P62871
IYAMHWGTDSR	GBB2_HUMAN	P62879
	HPCA_RAT	P84076
IYANFFPYGDASK	HPCL1_HUMAN	P37235
	PP1A_HUMAN	P62136
IYGFYDECK	PP1B_HUMAN	P62140
	PHS3_HUMAN	P11216
IYYLSLEFYMGR	PHS2_HUMAN	P11217
	ARBK1_HUMAN	P25098
KKPHASVGTHGYMAPEVLQK	ARBK2_HUMAN	P35626
	H14_HUMAN	P10412
KPAGAAK	H13_HUMAN	P16402
	EF1B_HUMAN	P24534
KPALVAK	EF1D_HUMAN	P29692
	EZRI_HUMAN	P15311
	MOES_HUMAN	P26038
KPDTIEVQQMK	RADI_HUMAN	P35241
	UDB17_HUMAN	O75795
KPNTLGSNTR	UDB15_HUMAN	P54855
	LTB1S_HUMAN	P22064
KPSYHGYNQMMECLPGYK	LTB1L_HUMAN	Q14766
	OSR8_HUMAN	Q9BZF1
KPYNPILGETFR	OSR5_HUMAN	Q9H0X9
	PHS1_HUMAN	P06737
	PHS3_HUMAN	P11216
LAACFLDSMATLGLAAYGYGIR	PHS2_HUMAN	P11217
	K1C14_HUMAN	P02533
	K1C18_HUMAN	P05783
	K1C16_HUMAN	P08779
	K1C15_HUMAN	P19012
LAADDFR	K1C17_HUMAN	Q04695
	ADT2_HUMAN	P05141
	ADT1_HUMAN	P12235
LAADVGK	ADT3_HUMAN	P12236
	CDC2_HUMAN	P06493
	CDK2_HUMAN	P24941
	CDK9_HUMAN	P50750
	CDK3_HUMAN	Q00526
	CDK6_HUMAN	Q00534
	CDK5_HUMAN	Q00535
LADFGLAR	PCTK1_HUMAN	Q00536

	CADH1_HUMAN	P12830
LADMYGGGEDD	CADH3_HUMAN	P22223
LADQCTGLQGFLVFHSFGGGTGSGFTS	TBA1_MERUN	P68360
LLMER	TBA6_HUMAN	Q9BQE3
	STA5A_HUMAN	P42229
LAEIIWQNR	STA5B_HUMAN	P51692
	BRD4_HUMAN	O60885
LAELQEQLK	BRD3_HUMAN	Q15059
	1433T_HUMAN	P27348
	1433Z_HUMAN	P63104
	1433B_HUMAN	P31946
	1433S_HUMAN	P31947
	1433G_MOUSE	P61982
	1433E_MOUSE	P62259
LAEQAER	1433F_HUMAN	Q04917
	MYH7_HUMAN	P12883
LAEQELIETSER	MYH6_HUMAN	P13533
	AK1C4_HUMAN	P17516
	AK1C3_HUMAN	P42330
LAIEAGFR	AK1C1_HUMAN	Q04828
	2AAA_HUMAN	P30153
LAIIEYMPLLAGQLGVEFFDEK	2AAB_HUMAN	P30154
	K2C8_HUMAN	P05787
	K2C7_HUMAN	P08729
LALDIEIATYR	K2C4_HUMAN	P19013
	K2C6A_HUMAN	P02538
	K2C6B_HUMAN	P04259
	K2C3_HUMAN	P12035
	K2C5_HUMAN	P13647
	K22E_HUMAN	P35908
	K2C6C_HUMAN	P48666
	K2C6E_HUMAN	P48668
LALDVEIATYR	K22O_HUMAN	Q01546
	VATB1_HUMAN	P15313
LALTTAEFLAYQCEK	VATB2_HUMAN	P21281
	MYH1_HUMAN	P12882
	MYH2_HUMAN	Q9UKX2
LAQLITR	MYH4_HUMAN	Q9Y623
	MYH3_HUMAN	P11055
	MYH1_HUMAN	P12882
	MYH7_HUMAN	P12883
	MYH6_HUMAN	P13533
	MYH8_HUMAN	P13535
	MYH2_HUMAN	Q9UKX2
	MYH13_HUMAN	Q9UKX3
LASADIETYLLEK	MYH4_HUMAN	Q9Y623
	ACTN2_HUMAN	P35609
LASELLEWIR	ACTN3_HUMAN	Q08043
LASYLDK	K1C14_HUMAN	P02533

	K1C16_HUMAN	P08779
	K1C15_HUMAN	P19012
	K1C9_HUMAN	P35527
	K1C17_HUMAN	Q04695
	TBBX_MOUSE	P68372
	TBB5_MOUSE	P99024
	TBB3_HUMAN	Q13509
LAVNMVPFPR	TBB4Q_HUMAN	Q99867
	MP2K2_HUMAN	P36507
LCDFGVSGQLIDSMANSFVGTR	MP2K1_HUMAN	Q02750
	ACTS_MOUSE	P68134
	ACTA_RABIT	P62740
	ACTC_HUMAN	P68032
LCYVALDFENEMATAASSSSLEK	ACTH_HUMAN	P63267
	ACTB_BOVIN	P60712
LCYVALDFEQEMATAASSSSLEK	ACTG_ANSAN	P63256
	MYH7_HUMAN	P12883
LDEAEQIALK	MYH6_HUMAN	P13533
	MYH3_HUMAN	P11055
	MYH1_HUMAN	P12882
	MYH8_HUMAN	P13535
	MYH2_HUMAN	Q9UKX2
LDEAEQLALK	MYH13_HUMAN	Q9UKX3
	BIG2_HUMAN	Q9Y6D5
LDGNAIVDFVR	BIG1_HUMAN	Q9Y6D6
	RRAS_HUMAN	P10301
LDILDTAGQEEFGAMR	RRAS2_MOUSE	P62071
	EHD1_HUMAN	Q9H4M9
LDISDEFSEVIK	EHD3_HUMAN	Q9NZN3
	DYN1_HUMAN	Q05193
LDLMDEGTDAR	DYN3_HUMAN	Q9UQ16
	MYH9_HUMAN	P35579
LDPHLVLDQLR	MYH10_HUMAN	P35580
	STMN1_HUMAN	P16949
LEAAEER	STMN3_HUMAN	Q9NZ72
	MP2K2_HUMAN	P36507
LEAFLTQK	MP2K1_HUMAN	Q02750
	IF1AH_HUMAN	O75642
LEAMCFDGVK	IF1AX_HUMAN	P47813
	ALU5_HUMAN	P39192
	ALU7_HUMAN	P39194
LECSGAISAHCNLR	ALU8_HUMAN	P39195
	MYH3_HUMAN	P11055
	MYH1_HUMAN	P12882
	MYH7_HUMAN	P12883
	MYH6_HUMAN	P13533
	MYH8_HUMAN	P13535
	MYH2_HUMAN	Q9UKX2
LEDECSELK	MYH4_HUMAN	Q9Y623

LEDEEEMNAELTAK	MYH7_HUMAN	P12883
	MYH6_HUMAN	P13533
LEEAGGATSAQIEMNK	MYH1_HUMAN	P12882
	MYH2_HUMAN	Q9UKX2
LEEAGGATSVQIEMNK	MYH7_HUMAN	P12883
	MYH6_HUMAN	P13533
LEFSIYPAPQVSTAVVEPYNSILTTHTTL EHSDCAFMVDNEAIYDICR	TBA1_MERUN	P68360
	TBA1_MACFA	P68367
	TBA6_HUMAN	Q9BQE3
LEGLEDALQK	K2C6A_HUMAN	P02538
	K2C6B_HUMAN	P04259
	K2C6C_HUMAN	P48666
	K2C6E_HUMAN	P48668
LEGPFNIESVMDPIDVK	GPC4_HUMAN	O75487
	GPC6_HUMAN	Q9Y625
LEGVVTK	EPHB6_HUMAN	O15197
	EPHB3_HUMAN	P54753
LEIEAETDR	DYN1_HUMAN	Q05193
	DYN3_HUMAN	Q9UQ16
LELDDVTSNMEQIIK	MYH7_HUMAN	P12883
	MYH6_HUMAN	P13533
LENCNYAVELGK	PLSL_HUMAN	P13796
	PLST_HUMAN	P13797
LEPGQPQLSPGISAIHLHPQFPVVIEK	LTB1S_HUMAN	P22064
	LTB1L_HUMAN	Q14766
LEQCLQLR	MCF2L_HUMAN	O15068
	HAPIP_HUMAN	O60229
LEQEEYMK	MYO5C_HUMAN	Q9NQX4
	MYO5B_HUMAN	Q9ULV0
LEQEIATYR	K1C14_HUMAN	P02533
	K1C16_HUMAN	P08779
	K1C13_HUMAN	P13646
	K1C15_HUMAN	P19012
	K1C17_HUMAN	Q04695
LEQELFSGGNTGINFEK	DDX3X_HUMAN	O00571
	DDX3Y_HUMAN	O15523
LEQLKPR	TLN1_HUMAN	Q9Y490
	TLN2_HUMAN	Q9Y4G6
LEQQVDDLEGSLEQEK	MYH1_HUMAN	P12882
	MYH7_HUMAN	P12883
	MYH6_HUMAN	P13533
	MYH8_HUMAN	P13535
	MYH2_HUMAN	Q9UKX2
	MYH4_HUMAN	Q9Y623
LESIISGAALMADSSCTR	CTN2_HUMAN	P26232
	CTN1_HUMAN	P35221
LEVGTETIIDK	HMCS2_HUMAN	P54868
	HMCS1_HUMAN	Q01581
LEVYPTSLTK	UDB17_HUMAN	O75795

	UDB15_HUMAN	P54855
LFDDDETGK	CETN2_HUMAN	P41208
	CETN1_HUMAN	Q12798
LFDSICNNK	GNAI1_HUMAN	P63096
	GNAI2_HUMAN	P04899
	GNAI3_HUMAN	P08754
	GNAO2_HUMAN	P29777
LFDVGGQR	GNAO1_HUMAN	P09471
	GNAO2_HUMAN	P29777
LFFLQVK	EZRI_HUMAN	P15311
	MOES_HUMAN	P26038
	RADI_HUMAN	P35241
LFMILWLK	CLIC6_HUMAN	Q96NY7
	CLIC4_HUMAN	Q9Y696
LFNNSSSHLEDYSGLSVSWSQFNR	STA5A_HUMAN	P42229
	STA5B_HUMAN	P51692
LFPLIQAMHPTLAGK	PABP1_HUMAN	P11940
	PABP3_HUMAN	Q9H361
LFYADHPFIFLVR	HSP47_HUMAN	P29043
	SPH2_HUMAN	P50454
LGEGEGSMTK	SNX6_HUMAN	Q9UNH7
	SNX5_HUMAN	Q9Y5X3
LGEHNIEVLEGNEQFINAAK	TRY1_HUMAN	P07477
	TRY2_HUMAN	P07478
LGEIVTTIPTIGFNVETVEYK	ARF3_RAT	P61206
	ARF4_HUMAN	P18085
	ARF5_HUMAN	P84085
	ARF1_RAT	P84079
LGELQTTAGR	K2C3_HUMAN	P12035
	K22O_HUMAN	Q01546
LGEMWNNTAADDK	HMG1_HUMAN	P09429
	HMG1X_HUMAN	Q9UGV6
LGLALNFSVFYYEILNSPEK	1433Z_HUMAN	P63104
	1433B_HUMAN	P31946
LGLHSLR	ARF3_RAT	P61206
	ARF1_RAT	P84079
LGLQAPATTPG	ALU2_HUMAN	P39189
	ALU3_HUMAN	P39190
	ALU7_HUMAN	P39194
LGPDDPNVAK	KLC1_HUMAN	Q07866
	KLC2_HUMAN	Q9H0B6
LHDPQLMGIIPR	KIF5C_HUMAN	O60282
	KINN_HUMAN	Q12840
LHFFMPGFAPLTSR	TBBX_MOUSE	P68372
	TBB5_MOUSE	P99024
LHSCLPADTLQGHR	HIP1_HUMAN	O00291
	HIP1R_HUMAN	O75146
LHWVEFQNK	VPP1_HUMAN	Q93050
	VPP2_HUMAN	Q9Y487

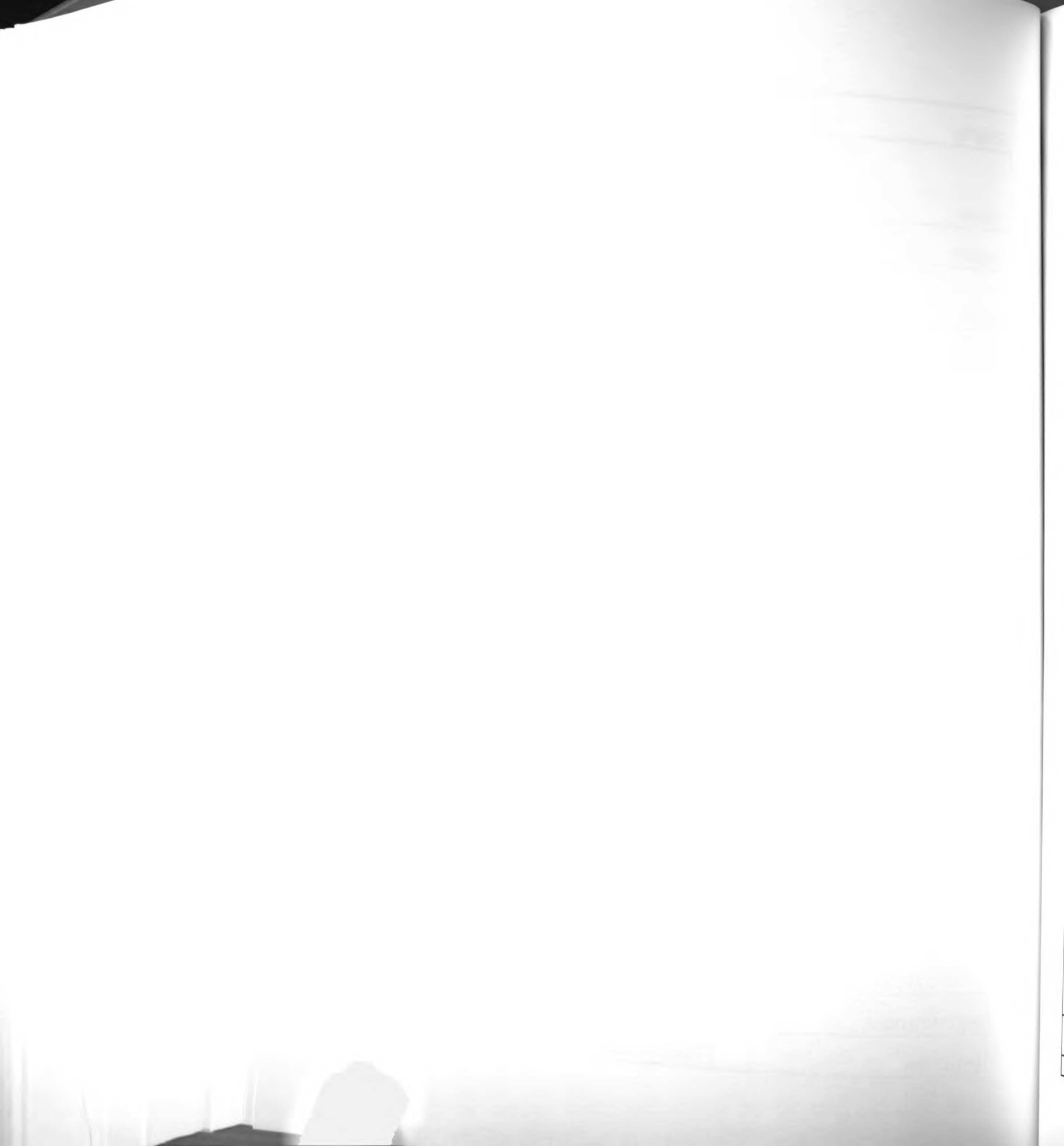

	KS6A2_HUMAN	Q15349
LHYAFQTEGK	KS6A1_HUMAN	Q15418
	YES_HUMAN	P07947
LIEDNEYTAR	SRC_HUMAN	P12931
	NCAM2_HUMAN	O15394
LIEENEK	STK31_HUMAN	Q9BXU1
	AT1A3_HUMAN	P13637
	ATP4A_HUMAN	P20648
	AT1A2_HUMAN	P50993
	AT12A_HUMAN	P54707
LIFDNLK	AT1A4_HUMAN	Q13733
	IQGA1_HUMAN	P46940
LIFQMPQNK	IQGA2_HUMAN	Q13576
	ALU2_HUMAN	P39189
LIFVFLVETGFHR	ALU3_HUMAN	P39190
	HSP71_HUMAN	P08107
	GRP78_HUMAN	P11021
	HS70L_HUMAN	P34931
LIGDAAK	HSP72_HUMAN	P54652
	MP2K2_HUMAN	P36507
LIHLEIKPAIR	MP2K1_HUMAN	Q02750
	AT1A3_HUMAN	P13637
	AT1A2_HUMAN	P50993
	AT12A_HUMAN	P54707
LIIVEGCQR	AT1A4_HUMAN	Q13733
	GBB1_BOVIN	P62871
	GBB2_HUMAN	P62879
LIIWDSYTTNK	GBB4_HUMAN	Q9HAV0
	MYH1_HUMAN	P12882
	MYH8_HUMAN	P13535
LINDLTAQR	MYH2_HUMAN	Q9UKX2
	TBA1_MERUN	P68360
	TBA1_MACFA	P68367
	TBA6_HUMAN	Q9BQE3
LISQIVSSITASLR	TBA8_HUMAN	Q9NY65
	MYH3_HUMAN	P11055
	MYH8_HUMAN	P13535
LLASIDIDHTQYK	MYH2_HUMAN	Q9UKX2
	K2C6A_HUMAN	P02538
	K2C6B_HUMAN	P04259
	NFH_HUMAN	P12036
	K2C5_HUMAN	P13647
	K22E_HUMAN	P35908
	K2C6C_HUMAN	P48666
	K2C6E_HUMAN	P48668
LLEGEECR	K22O_HUMAN	Q01546
	LAM1_HUMAN	P20700
LLEGEEER	LAM2_HUMAN	Q03252
LLEGEESR	K2C8_HUMAN	P05787

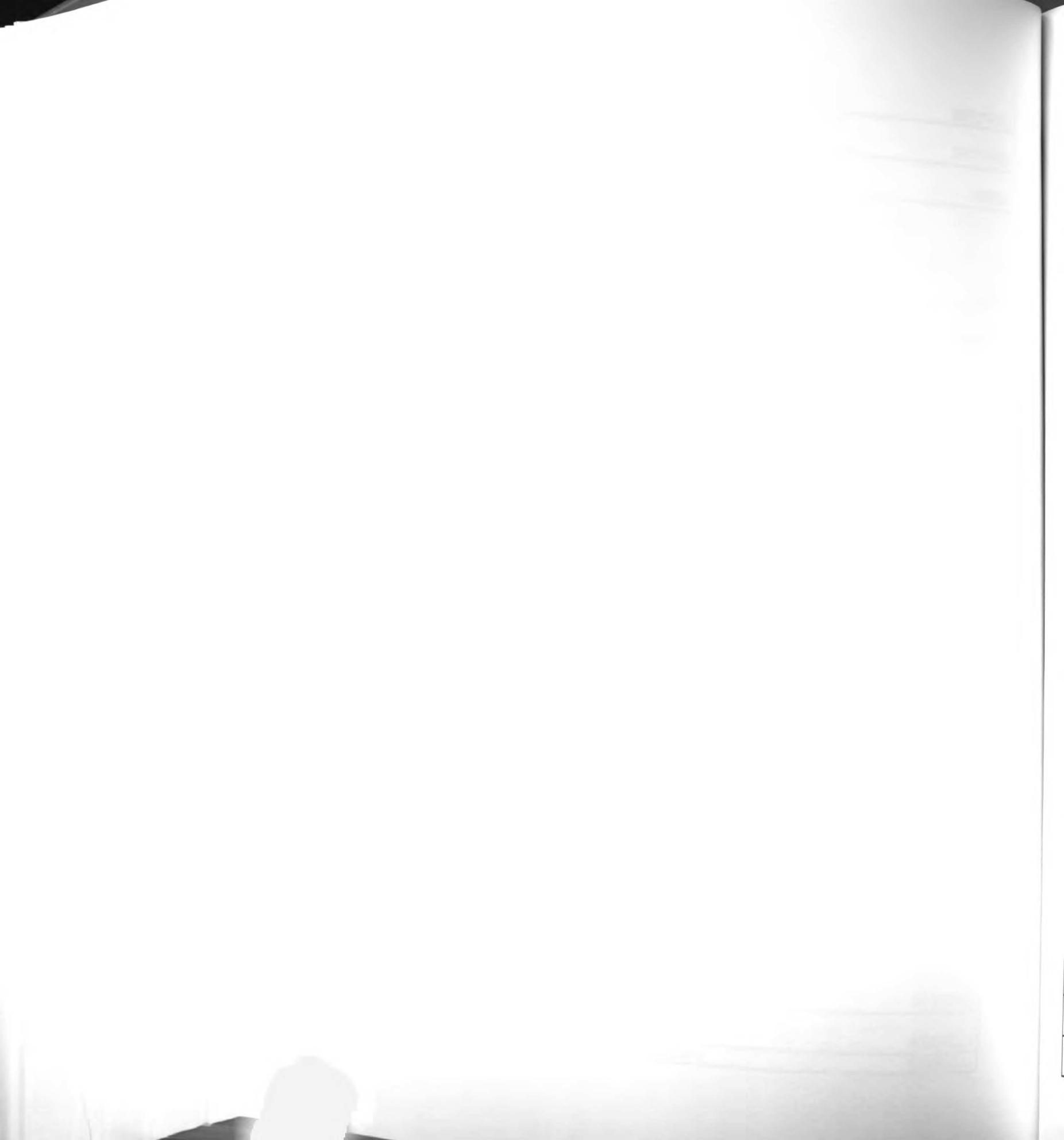

	VIME_HUMAN	P08670
	K2C7_HUMAN	P08729
	DESM_HUMAN	P17661
	PERI_HUMAN	P41219
	NFM_HUMAN	P07197
LLEGEETR	AINX_HUMAN	Q16352
	CLCN3_HUMAN	P51790
	CLCN4_HUMAN	P51793
LLGIITK	CLCN5_HUMAN	P51795
	IGF1R_HUMAN	P08069
LLGVVSQGQPTLVIMELMTR	INSRR_HUMAN	P14616
	RAB10_HUMAN	P61026
	RAB8A_CANFA	P61007
	RAB13_HUMAN	P51153
	RAB15_HUMAN	P59190
	RAB8B_HUMAN	Q92930
LLLIGDSGVGK	RAB1B_HUMAN	Q9H0U4
	GNAI1_HUMAN	P63096
	GNAI2_HUMAN	P04899
	GNAI3_HUMAN	P08754
	GNAO1_HUMAN	P09471
	GNAT1_HUMAN	P11488
	GNAT2_HUMAN	P19087
	GNAO2_HUMAN	P29777
LLLLGAGESGK	GNAL_HUMAN	P38405
	GNA14_HUMAN	O95837
	GNA11_HUMAN	P29992
LLLLGTGESGK	GNAQ_HUMAN	P50148
	CAZA2_HUMAN	P47755
LLLNNDNLLR	CAZA1_HUMAN	P52907
	H2B_BOVIN	P62808
	H2BR_HUMAN	P06899
	H2BF_HUMAN	P33778
	H2BS_HUMAN	P57053
	H2BB_HUMAN	P58876
	H2BQ_HUMAN	Q16778
	H2BJ_HUMAN	Q93079
	H2BD_HUMAN	Q99877
	H2BE_HUMAN	Q99879
LLLPGELAK	H2BC_HUMAN	Q99880
	ADT2_HUMAN	P05141
	ADT1_HUMAN	P12235
LLLQVQHASK	ADT3_HUMAN	P12236
	EHD1_HUMAN	Q9H4M9
LLPLEEHYR	EHD3_HUMAN	Q9NZN3
	AN32A_HUMAN	P39687
LLPQLTYLDGYDR	AN32B_HUMAN	Q92688
	HPCA_RAT	P84076
LLQCDPSSASQF	HPCL1_HUMAN	P37235

	HSP76_HUMAN	P17066
LLQDFFNGK	HSP72_HUMAN	P54652
	PAK3_HUMAN	O75914
LLQTSNITK	PAK2_HUMAN	Q13177
	MYH7_HUMAN	P12883
LLSSLDIDHNQYK	MYH6_HUMAN	P13533
	GBB1_BOVIN	P62871
	GBB2_HUMAN	P62879
	GBB3_HUMAN	P16520
LLVSASQDGK	GBB4_HUMAN	Q9HAV0
	BIG2_HUMAN	Q9Y6D5
LLYNLEMEQMAK	BIG1_HUMAN	Q9Y6D6
	P85B_HUMAN	O00459
LLYPVSK	P85A_HUMAN	P27986
	HNRH1_HUMAN	P31943
LMAMQRPGPYDRPGAGR	HNRH2_HUMAN	P55795
	BRD4_HUMAN	O60885
	BRD2_HUMAN	P25440
LMFSNCYK	BRD3_HUMAN	Q15059
	RBBP4_HUMAN	Q09028
LMIWDTR	RBBP7_HUMAN	Q16576
	ACTN4_HUMAN	O43707
	ACTN2_HUMAN	P35609
LMLLLEVISGER	ACTN3_HUMAN	Q08043
	HS74L_HUMAN	O95757
LMNETTAVALAYGIYK	HSP74_HUMAN	P34932
	BGAL_HUMAN	P16278
LMPPPPQK	BGAM_HUMAN	P16279
	EHD1_HUMAN	Q9H4M9
LNAFGNAFLNR	EHD3_HUMAN	Q9NZN3
	MTMR7_HUMAN	Q9Y216
LNAMANR	MTMR6_HUMAN	Q9Y217
	AK1C2_HUMAN	P52895
LNDGHFMPVLGFGTYAPAEVPK	AK1C1_HUMAN	Q04828
	EPHB3_HUMAN	P54753
LNDGQFTVIQLVGMLR	EPHB4_HUMAN	P54760
LNGEGVGQVNISVVQSTVSSGYGGASG VGSGLGLGGGSSYSYGSGLGVGGGFS SSSGR	K2C6A_HUMAN	P02538
	K2C6B_HUMAN	P04259
	K2C6C_HUMAN	P48666
	2AAA_HUMAN	P30153
LNIISNLDCVNEVIGIR	2AAB_HUMAN	P30154
	ALU5_HUMAN	P39192
	ALU7_HUMAN	P39194
LNPGGGGCSEPR	ALU8_HUMAN	P39195
	2AAA_HUMAN	P30153
LNSLCMAWLVDHVYAIR	2AAB_HUMAN	P30154
	STA5A_HUMAN	P42229
LNVHMNPPQVK	STA5B_HUMAN	P51692
LNVWDLSK	RBBP4_HUMAN	Q09028

	RBBP7_HUMAN	Q16576
LPEEHAR	KPCI_HUMAN	P41743
	KPCZ_HUMAN	Q05513
LPGEAQK	BIG2_HUMAN	Q9Y6D5
	BIG1_HUMAN	Q9Y6D6
LPGSSDSPASASR	ALU5_HUMAN	P39192
	ALU7_HUMAN	P39194
	ALU8_HUMAN	P39195
LPLQDVYK	EF1A1_HUMAN	P68104
	EF1A2_HUMAN	Q05639
LPNSVLGK	EHD4_HUMAN	Q9H223
	EHD3_HUMAN	Q9NZN3
LQAAGNAVK	TLN1_HUMAN	Q9Y490
	TLN2_HUMAN	Q9Y4G6
LQCFDMDECQDPSSCIDGQCVNTEGSY NCFCTHPMVLDASEK	LTB1S_HUMAN	P22064
	LTB1L_HUMAN	Q14766
LQDLVDK	MYH3_HUMAN	P11055
	MYH1_HUMAN	P12882
	MYH7_HUMAN	P12883
	MYH6_HUMAN	P13533
	MYH8_HUMAN	P13535
	MYH2_HUMAN	Q9UKX2
	MYH13_HUMAN	Q9UKX3
	MYH4_HUMAN	Q9Y623
LQDVFEMR	BRD4_HUMAN	O60885
	BRD3_HUMAN	Q15059
LQHELEEAEER	MYH8_HUMAN	P13535
	MYH2_HUMAN	Q9UKX2
	MYH4_HUMAN	Q9Y623
LQIQCVVEDDK	EF1B_HUMAN	P24534
	EF1D_HUMAN	P29692
LQIWDTAGQER	RAB10_HUMAN	P61026
	RAB3D_HUMAN	O95716
	RAB3A_HUMAN	P20336
	RAB4A_HUMAN	P20338
	RAB4B_HUMAN	P61018
	RAB8A_CANFA	P61007
	RAB14_RAT	P61107
	RAB35_HUMAN	Q15286
	RAB8B_HUMAN	Q92930
	RAB37_HUMAN	Q96AX2
	RB39B_HUMAN	Q96DA2
	RAB3C_HUMAN	Q96E17
	RAB1B_HUMAN	Q9H0U4
LQIWDTAGQESFR	RAB2A_HUMAN	P61019
	RAB2B_HUMAN	Q8WUD1
LQLSLGIIPVEEENPDFWNR	PPB1_HUMAN	P05187
	PPBN_HUMAN	P10696
LQLWDIAGQER	RAB7L_HUMAN	O14966

	RAB32_HUMAN	Q13637
LQNEIEDLMVDVER	MYH7_HUMAN	P12883
	MYH6_HUMAN	P13533
LQNEVEDLMIDVER	MYH1_HUMAN	P12882
	MYH4_HUMAN	Q9Y623
LQNEVEDLMLDVER	MYH8_HUMAN	P13535
	MYH2_HUMAN	Q9UKX2
LQPAQTAAK	PPB1_HUMAN	P05187
	PPBN_HUMAN	P10696
LQPGSVK	CLP1_HUMAN	P51911
	CLP3_HUMAN	Q15417
LQQFFNHHMFVLEQEEYK	MYH3_HUMAN	P11055
	MYH1_HUMAN	P12882
	MYH7_HUMAN	P12883
	MYH6_HUMAN	P13533
	MYH8_HUMAN	P13535
	MYH2_HUMAN	Q9UKX2
	MYH13_HUMAN	Q9UKX3
	MYH4_HUMAN	Q9Y623
LQQIFIELTLK	MYO1F_HUMAN	O00160
	MYO1B_HUMAN	O43795
	MYO1E_HUMAN	Q12965
LQQLFNHTMFILEQEEYQR	MYH9_HUMAN	P35579
	MYH10_HUMAN	P35580
	MYH11_HUMAN	P35749
LQQTQEYFIIQYQESLR	STA5A_HUMAN	P42229
	STA5B_HUMAN	P51692
LQVQEQR	CK015_HUMAN	Q9NQ34
	TMEM9_HUMAN	Q9P0T7
LRPLSYPDTDVILMCFSIDSPDSLENIPEK	RHOA_BOVIN	P61585
	RHOC_HUMAN	P08134
LRPLSYPQTDVFLVCFSVVSPSSFENVK	CDC42_CANFA	P60952
	CDC42_MOUSE	P60766
LSELDDR	VAM2_HUMAN	P63027
	VAM3_HUMAN	Q15836
LSLEEFIR	NCALD_HUMAN	P61601
	HPCA_RAT	P84076
	HPCL1_HUMAN	P37235
LSMYGVDLHHAK	E41L2_HUMAN	O43491
	E41L1_HUMAN	Q9H4G0
LSPEELLLR	PLSL_HUMAN	P13796
	PLST_HUMAN	P13797
	PLSI_HUMAN	Q14651
LSPSPSSR	LAM1_HUMAN	P20700
	LAM2_HUMAN	Q03252
LSSLIILMPHHVEPLER	HSP47_HUMAN	P29043
	SPH2_HUMAN	P50454
LSTIALALGVER	2AAA_HUMAN	P30153
	2AAB_HUMAN	P30154

	TBA1_MERUN	P68360
	TBA1_MACFA	P68367
LSVDYGK	TBA6_HUMAN	Q9BQE3
	ALU2_HUMAN	P39189
LTASSASR	ALU3_HUMAN	P39190
	ALU5_HUMAN	P39192
	ALU7_HUMAN	P39194
LTATSASR	ALU8_HUMAN	P39195
	PAK3_HUMAN	O75914
LTDFGFCAQITPEQSK	PAK2_HUMAN	Q13177
	KPCI_HUMAN	P41743
LTDYGMCK	KPCZ_HUMAN	Q05513
	VPP1_HUMAN	Q93050
LTFLNSFK	VPP2_HUMAN	Q9Y487
	MYH3_HUMAN	P11055
	MYH1_HUMAN	P12882
	MYH8_HUMAN	P13535
	MYH13_HUMAN	Q9UKX3
LTGAVMHYGNMK	MYH4_HUMAN	Q9Y623
	CEAM5_HUMAN	P06731
LTIESTPFNVAEGK	CEAM6_HUMAN	P40199
	MYH7_HUMAN	P12883
LTQESIMDLENDK	MYH6_HUMAN	P13533
	TBBX_MOUSE	P68372
LTTPTYGDLNHLVSATMSGVTTCLR	TBB5_MOUSE	P99024
	SOS1_HUMAN	Q07889
LTYHMYADPNFVR	SOS2_HUMAN	Q07890
	DDX3X_HUMAN	O00571
LVDMMER	DDX3Y_HUMAN	O15523
	RAB3D_HUMAN	O95716
LVDVICEK	RAB3A_HUMAN	P20336
	RHOA_BOVIN	P61585
LVIVGDGACGK	RHOC_HUMAN	P08134
	RAB5A_HUMAN	P20339
	RAB5B_HUMAN	P61020
LVLLGESAVGK	RAB5C_HUMAN	P51148
	ILEU_HUMAN	P30740
LVLVNAIYFK	SPB8_HUMAN	P50452
	MYO1B_HUMAN	O43795
LVMSYVAAVCGK	MYO1A_HUMAN	Q9UBC5
	BIG2_HUMAN	Q9Y6D5
LVNDLSK	BIG1_HUMAN	Q9Y6D6
	STA5A_HUMAN	P42229
LVTQDTENELK	STA5B_HUMAN	P51692
	RAP1B_BOVIN	P61223
LVVLGSGGVGK	RAP1A_BOVIN	P62833
	RASN_HUMAN	P01111
	RASH_HUMAN	P01112
LVVVGAGGVGK	RASK_HUMAN	P01116

LVVVGGGGVGK	RRAS_HUMAN	P10301
	RRAS2_MOUSE	P62071
LVYQNIFTAMQAMIR	GNA14_HUMAN	O95837
	GNA11_HUMAN	P29992
	GNAQ_HUMAN	P50148
LWCVLKPGVLLIYK	OSR8_HUMAN	Q9BZF1
	OSR5_HUMAN	Q9H0X9
LWGDSGIQECFNR	GNAO1_HUMAN	P09471
	GNAO2_HUMAN	P29777
LYDQHLGK	MYH3_HUMAN	P11055
	MYH8_HUMAN	P13535
	MYH2_HUMAN	Q9UKX2
	MYH13_HUMAN	Q9UKX3
LYEQHLGK	MYH1_HUMAN	P12882
	MYH4_HUMAN	Q9Y623
LYGPSSVSFADDFVR	HSP47_HUMAN	P29043
	SPH2_HUMAN	P50454
LYLILDFLR	KS6A2_HUMAN	Q15349
	KS6A1_HUMAN	Q15418
LYLVDLAGSEK	KIF5C_HUMAN	O60282
	KINH_HUMAN	P33176
	KINN_HUMAN	Q12840
LYSESLAR	GDIA_HUMAN	P31150
	GDIB_HUMAN	P50395
LYSTWIGGSILASLDTFK	ACTZ_HUMAN	P61163
	ACTY_HUMAN	P42025
MAAEALR	MYH1_HUMAN	P12882
	MYH2_HUMAN	Q9UKX2
MAAEAQK	MYH7_HUMAN	P12883
	MYH6_HUMAN	P13533
MADLEAVLADVSYLMAMEK	ARBK1_HUMAN	P25098
	ARBK2_HUMAN	P35626
MALDIEIAAYR	NFM_HUMAN	P07197
	NFH_HUMAN	P12036
	AINX_HUMAN	Q16352
MALDIEIATYR	VIME_HUMAN	P08670
	PERI_HUMAN	P41219
MAVMAPR	HLAH_HUMAN	P01893
	1A03_HUMAN	P04439
	1A01_HUMAN	P30443
MCYLTIK	COPG2_HUMAN	Q9UBF2
	COPG_HUMAN	Q9Y678
MDENQFVAVTSTNAAK	DPYL3_HUMAN	Q14195
	DPYL2_HUMAN	Q16555
MEDTEPFSAELLSAMMR	GNAO1_HUMAN	P09471
	GNAO2_HUMAN	P29777
MEGDLNEMEIQLNHANR	MYH1_HUMAN	P12882
	MYH8_HUMAN	P13535
	MYH2_HUMAN	Q9UKX2

	MYH4_HUMAN	Q9Y623
MEGDLNEMEIQLSHANR	MYH7_HUMAN	P12883
	MYH6_HUMAN	P13533
MFDVGGQR	GNAI1_HUMAN	P63096
	GNAI2_HUMAN	P04899
	GNAI3_HUMAN	P08754
	GNAT1_HUMAN	P11488
	GNAT2_HUMAN	P19087
MFEIDYSR	BGAL_HUMAN	P16278
	BGAM_HUMAN	P16279
MFLWMVTR	MYH1_HUMAN	P12882
	MYH8_HUMAN	P13535
	MYH13_HUMAN	Q9UKX3
	MYH4_HUMAN	Q9Y623
MFNWMVTR	MYH7_HUMAN	P12883
	MYH6_HUMAN	P13533
MFVDLNPDSDK	GNA11_HUMAN	P29992
	GNAQ_HUMAN	P50148
MFVLDEADEMLSR	IF41_HUMAN	P60842
	IF42_HUMAN	Q14240
MGIYVGAK	K6PL_HUMAN	P17858
	K6PP_HUMAN	Q01813
MHGLNDALDNLR	NDF6_HUMAN	Q96NK8
	NDF4_HUMAN	Q9HD90
MHHDIVR	NOTC1_HUMAN	P46531
	NOTC2_HUMAN	Q04721
MINLSVPDTIDER	PLSL_HUMAN	P13796
	PLST_HUMAN	P13797
MIYASSK	DEST_HUMAN	P60981
	COF1_HUMAN	P23528
	COF2_HUMAN	Q9Y281
MLAEDELR	ARF3_RAT	P61206
	ARF1_RAT	P84079
MLDMGFEPQIR	DDX3X_HUMAN	O00571
	DDX3Y_HUMAN	O15523
	DDX5_HUMAN	P17844
	DDX17_HUMAN	Q92841
MLEYALK	STRN_HUMAN	O43815
	STRN4_HUMAN	Q9NRL3
MLHVDPHQR	KS6A2_HUMAN	Q15349
	KS6A1_HUMAN	Q15418
MLLYTEVTR	GDIA_HUMAN	P31150
	GDIB_HUMAN	P50395
MLQDTEDK	WASF1_HUMAN	Q92558
	WASF3_HUMAN	Q9UPY6
MLVMAPR	1B07_HUMAN	P01889
	1B08_HUMAN	P30460
MMMQSGR	ADT2_HUMAN	P05141
	ADT1_HUMAN	P12235

	ADT3_HUMAN	P12236
MNGMLLNDR	PABP1_HUMAN	P11940
	PABP4_HUMAN	Q13310
MPEDESTPEK	NCALD_HUMAN	P61601
	HPCA_RAT	P84076
	HPCL1_HUMAN	P37235
MPGFLVR	BGAL_HUMAN	P16278
	BGAM_HUMAN	P16279
MQGTLEDQIISANPLLEAFGNAK	MYH1_HUMAN	P12882
	MYH8_HUMAN	P13535
	MYH4_HUMAN	Q9Y623
MQIEVFFK	BIG2_HUMAN	Q9Y6D5
	BIG1_HUMAN	Q9Y6D6
MSAGGDFGNPLR	RAB6C_HUMAN	Q9H0N0
	RAB6B_HUMAN	Q9NRW1
MSELEQLR	GBB2_HUMAN	P62879
	GBB4_HUMAN	Q9HAV0
MSSDSEMAIFGEAAPFLR	MYH1_HUMAN	P12882
	MYH4_HUMAN	Q9Y623
MSSYAFFVQTCR	HMG1_HUMAN	P09429
	HMG2_HUMAN	P26583
MSVAGLK	SH3G1_HUMAN	Q99961
	SH3G2_HUMAN	Q99962
MSVIWDK	DPYL3_HUMAN	Q14195
	DPYL2_HUMAN	Q16555
MTCFDVNECDELNNR	LTB1S_HUMAN	P22064
	LTB1L_HUMAN	Q14766
MTEEEVEMLVAGHEDSNGCINYEAFVR	MYL6_BOVIN	P60661
	MYL6_HUMAN	P60660
MTLGMIWTIILR	ACTN4_HUMAN	O43707
	ACTN2_HUMAN	P35609
	ACTN3_HUMAN	Q08043
MTQIMFETFNTPAMYVAIQAVLSLYASGR	ACTB_BOVIN	P60712
	ACTG_ANSAN	P63256
MTQIMFETFNVPAMYVAIQAVLSLYASGR	ACTS_MOUSE	P68134
	ACTA_RABIT	P62740
	ACTC_HUMAN	P68032
	ACTH_HUMAN	P63267
MVALSLK	TLN1_HUMAN	Q9Y490
	TLN2_HUMAN	Q9Y4G6
MVCDVVSR	GNAO1_HUMAN	P09471
	GNAO2_HUMAN	P29777
MVDVGGQR	GNA14_HUMAN	O95837
	GNAZ_HUMAN	P19086
	GNA11_HUMAN	P29992
	GNAQ_HUMAN	P50148
	GNA12_HUMAN	Q03113
MVMTVFACLMGK	PLSL_HUMAN	P13796
	PLSI_HUMAN	Q14651

MVSLLQEK	MYH7_HUMAN	P12883
	MYH6_HUMAN	P13533
	MYH13_HUMAN	Q9UKX3
MVSSVMK	NCALD_HUMAN	P61601
	HPCA_RAT	P84076
	HPCL1_HUMAN	P37235
MVTLMQEK	MYH1_HUMAN	P12882
	MYH4_HUMAN	Q9Y623
MVVSFNR	IQGA1_HUMAN	P46940
	IQGA2_HUMAN	Q13576
NALAHALQSAR	MYH7_HUMAN	P12883
	MYH6_HUMAN	P13533
NALAHALQSSR	MYH3_HUMAN	P11055
	MYH8_HUMAN	P13535
	MYH2_HUMAN	Q9UKX2
NALESYAFNMK	HSP71_HUMAN	P08107
	HS70L_HUMAN	P34931
NAYEESLDQLETLK	MYH1_HUMAN	P12882
	MYH2_HUMAN	Q9UKX2
NAYEESLEHLETFK	MYH7_HUMAN	P12883
	MYH6_HUMAN	P13533
NCAAYLK	MYH9_HUMAN	P35579
	MYH10_HUMAN	P35580
	MYH11_HUMAN	P35749
NDEELNK	H2AC_HUMAN	P02261
	H2AX_HUMAN	P16104
	H2AO_HUMAN	P20670
	H2AG_HUMAN	P20671
	H2AA_HUMAN	P28001
	H2AL_HUMAN	Q93077
	H2AE_HUMAN	Q99878
NEDVQLR	2AAA_HUMAN	P30153
	2AAB_HUMAN	P30154
NEFNLESK	RB11A_MOUSE	P62492
	RB11B_HUMAN	Q15907
NENESEK	IF1AY_HUMAN	O14602
	IF1AH_HUMAN	O75642
	IF1AX_HUMAN	P47813
NFGEDMDDER	PABP1_HUMAN	P11940
	PABP3_HUMAN	Q9H361
NGFCLNTRPGYECYCK	LTB1S_HUMAN	P22064
	LTB1L_HUMAN	Q14766
NGFEQFCINFVNEK	MYO1F_HUMAN	O00160
	MYO1E_HUMAN	Q12965
NGGGFLFPPSYVPVVMSELSDQMIFME R	UDB17_HUMAN	O75795
	UDB15_HUMAN	P54855
NGQGFALVYSITAQSTFNDLQDLR	RAP1B_BOVIN	P61223
	RAP1A_BOVIN	P62833
NGQGFILVYSLVNQQSFQDIKPMR	RAP2A_HUMAN	P10114

	RAP2B_MOUSE	P61226
NGVYLAK	IQGA1_HUMAN	P46940
	IQGA2_HUMAN	Q13576
NHEEEMK	K1C13_HUMAN	P13646
	K1C15_HUMAN	P19012
NHEEEMNALR	K1C14_HUMAN	P02533
	K1C17_HUMAN	Q04695
NICFFSTNCVEGTAR	AT1A2_HUMAN	P50993
	AT1A4_HUMAN	Q13733
NIDGWEGK	SOS1_HUMAN	Q07889
	SOS2_HUMAN	Q07890
NIIHGSDSVK	NDK8_HUMAN	O60361
	NDKB_HUMAN	P22392
NILGGTVFR	IDHC_HUMAN	O75874
	IDHP_HUMAN	P48735
NILVNSNLVCK	EPHA2_HUMAN	P29317
	EPHB3_HUMAN	P54753
	EPHB4_HUMAN	P54760
	EPHA4_HUMAN	P54764
	EPHA7_HUMAN	Q15375
NISFNDK	EZRI_HUMAN	P15311
	MOES_HUMAN	P26038
	RADI_HUMAN	P35241
NISFTVWDVGGQDK	ARF3_RAT	P61206
	ARF1_RAT	P84079
NLAENISR	PHS1_HUMAN	P06737
	PHS3_HUMAN	P11216
	PHS2_HUMAN	P11217
NLDDGIDDER	PABP1_HUMAN	P11940
	PABP3_HUMAN	Q9H361
NLDIERPTYTNLNR	TBA1_MERUN	P68360
	TBA1_MACFA	P68367
	TBA6_HUMAN	Q9BQE3
	TBA8_HUMAN	Q9NY65
NLDLDSIIAEVK	K2C6A_HUMAN	P02538
	K2C6B_HUMAN	P04259
	K2C5_HUMAN	P13647
	K22E_HUMAN	P35908
	K2C6C_HUMAN	P48666
	K2C6E_HUMAN	P48668
NLEAVETLGSTSTICSDK	AT1A3_HUMAN	P13637
	AT1A2_HUMAN	P50993
	AT1A4_HUMAN	Q13733
NLEQTVK	MYH3_HUMAN	P11055
	MYH1_HUMAN	P12882
	MYH8_HUMAN	P13535
	MYH13_HUMAN	Q9UKX3
NLFEQFR	AT11A_HUMAN	P98196
	AT11B_HUMAN	Q9Y2G3

NLIIFLGDGMGVSTVTAAR	PPB1_HUMAN	P05187
	PPBN_HUMAN	P10696
NLINQTTAK	BIG2_HUMAN	Q9Y6D5
	BIG1_HUMAN	Q9Y6D6
NLLSVAYK	1433T_HUMAN	P27348
	1433Z_HUMAN	P63104
	1433B_HUMAN	P31946
	1433S_HUMAN	P31947
	1433G_MOUSE	P61982
	1433E_MOUSE	P62259
	1433F_HUMAN	Q04917
NLQEAEEWYK	VIME_HUMAN	P08670
	PERI_HUMAN	P41219
NLQLDYVDLYLIHFPVSVKPGEEVIPK	AK1C2_HUMAN	P52895
	AK1C1_HUMAN	Q04828
NLQQEISDLTEQIAEGGK	MYH1_HUMAN	P12882
	MYH8_HUMAN	P13535
	MYH2_HUMAN	Q9UKX2
	MYH4_HUMAN	Q9Y623
NLTEEMAGLDEIIAK	MYH7_HUMAN	P12883
	MYH6_HUMAN	P13533
NLTEEMAGLDETIAK	MYH1_HUMAN	P12882
	MYH8_HUMAN	P13535
	MYH2_HUMAN	Q9UKX2
	MYH4_HUMAN	Q9Y623
NLVQEWLAK	PPB1_HUMAN	P05187
	PPBN_HUMAN	P10696
NMEQTIK	MYH7_HUMAN	P12883
	MYH6_HUMAN	P13533
NMEQTVK	MYH2_HUMAN	Q9UKX2
	MYH4_HUMAN	Q9Y623
NMITGTSQADCAVLIVAAGVGEFEAGIS K	EF1A1_HUMAN	P68104
	EF1A2_HUMAN	Q05639
NMMAACDPR	TBBX_MOUSE	P68372
	TBB5_MOUSE	P99024
	TBB3_HUMAN	Q13509
NMQDLVEDLK	K2C6B_HUMAN	P04259
	K2C6E_HUMAN	P48668
NMVPQQALVIR	AT1A3_HUMAN	P13637
	AT1A2_HUMAN	P50993
	AT1A4_HUMAN	Q13733
NNDLLFR	MYO1C_HUMAN	O00159
	MYO1A_HUMAN	Q9UBC5
NNLASCYLK	KLC1_HUMAN	Q07866
	KLC2_HUMAN	Q9H0B6
NNLLQAELEELR	MYH7_HUMAN	P12883
	MYH6_HUMAN	P13533
NNVITLNITGK	BGAL_HUMAN	P16278
	BGAM_HUMAN	P16279

NPQAVLDVLK	PAK3_HUMAN	O75914
	PAK2_HUMAN	Q13177
NQSIIVSGESGAGK	MYO5C_HUMAN	Q9NQX4
	MYO5B_HUMAN	Q9ULV0
NSSYFVEWIPNNVK	TBBX_MOUSE	P68372
	TBB5_MOUSE	P99024
	TBB3_HUMAN	Q13509
NSTIPTK	HSP71_HUMAN	P08107
	HS70L_HUMAN	P34931
NSVFQQGMK	AT1A3_HUMAN	P13637
	AT1A2_HUMAN	P50993
NTDQASMPDNTAAQK	MYH9_HUMAN	P35579
	MYH11_HUMAN	P35749
NTEGSFQCVCDQGYR	LTB1S_HUMAN	P22064
	LTB1L_HUMAN	Q14766
NTEGSFR	LTB1S_HUMAN	P22064
	LTB1L_HUMAN	Q14766
NTNDANSCQIIIPQNQVNR	GDIA_HUMAN	P31150
	GDIB_HUMAN	P50395
NTNPNFVR	MYH9_HUMAN	P35579
	MYH10_HUMAN	P35580
NTQGILK	MYH8_HUMAN	P13535
	MYH2_HUMAN	Q9UKX2
	MYH4_HUMAN	Q9Y623
NTQPVAK	LTB1S_HUMAN	P22064
	LTB1L_HUMAN	Q14766
NTTIPTK	GRP75_HUMAN	P38646
	HSP72_HUMAN	P54652
NVFDEAILAALEPPETQPK	CDC42_CANFA	P60952
	CDC42_MOUSE	P60766
NVHELEK	MYH6_HUMAN	P13533
	MYH10_HUMAN	P35580
	MYH11_HUMAN	P35749
NVQFVFDAVTDVIIK	GNAI1_HUMAN	P63096
	GNAI2_HUMAN	P04899
	GNAI3_HUMAN	P08754
NWYSDADVPASAR	PPB1_HUMAN	P05187
	PPBN_HUMAN	P10696
PGAVAHACNPSTLGGR	ALU1_HUMAN	P39188
	ALU2_HUMAN	P39189
	ALU3_HUMAN	P39190
	ALU5_HUMAN	P39192
	ALU7_HUMAN	P39194
QAADMILLDDNFASIVTGVEEGR	AT1A3_HUMAN	P13637
	AT1A2_HUMAN	P50993
	AT1A4_HUMAN	Q13733
QAEEAEEQANTNLSK	MYH7_HUMAN	P12883
	MYH6_HUMAN	P13533
QAFTQQIEELK	MYH1_HUMAN	P12882

	MYH2_HUMAN	Q9UKX2
	MYH4_HUMAN	Q9Y623
QALEDLEK	KLC1_HUMAN	Q07866
	KLC2_HUMAN	Q9H0B6
QALMSELK	PGFRB_HUMAN	P09619
	PGFRA_HUMAN	P16234
QAQDLAR	RASH_HUMAN	P01112
	RASK_HUMAN	P01116
QCANLQAAIADAEQR	K2C6A_HUMAN	P02538
	K2C6B_HUMAN	P04259
	K2C6C_HUMAN	P48666
QCLVTHNGR	CLCN3_HUMAN	P51790
	CLCN5_HUMAN	P51795
QCMYPLSVHLTK	LTB1S_HUMAN	P22064
	LTB1L_HUMAN	Q14766
QDAYDGK	1A03_HUMAN	P04439
	1A01_HUMAN	P30443
QDISSLR	TRPC3_HUMAN	Q13507
	TRPC7_HUMAN	Q9HCX4
QDLLAYLQR	CTN2_HUMAN	P26232
	CTN1_HUMAN	P35221
QDLPNAMNAAEITDK	ARF3_RAT	P61206
	ARF1_RAT	P84079
QEAEQLK	GBB1_BOVIN	P62871
	GBB3_HUMAN	P16520
QEAEQLR	GBB2_HUMAN	P62879
	GBB4_HUMAN	Q9HAV0
QEAPPHIFSISDNAYQFMLTDR	MYH3_HUMAN	P11055
	MYH1_HUMAN	P12882
	MYH8_HUMAN	P13535
	MYH2_HUMAN	Q9UKX2
	MYH13_HUMAN	Q9UKX3
	MYH4_HUMAN	Q9Y623
QECCCTSGAGWGDNCEIFPCPVLGTAE FTEMCPK	LTB1S_HUMAN	P22064
	LTB1L_HUMAN	Q14766
QEDCCGTVGTSWGFNK	LTB1S_HUMAN	P22064
	LTB1L_HUMAN	Q14766
QEDVIATANLSR	TLN1_HUMAN	Q9Y490
	TLN2_HUMAN	Q9Y4G6
QEGCQDIATQLISNMDIDVILGGGR	PPB1_HUMAN	P05187
	PPBN_HUMAN	P10696
QEIAEINR	K2C6A_HUMAN	P02538
	K2C6B_HUMAN	P04259
	K2C6C_HUMAN	P48666
	K2C6E_HUMAN	P48668
QENGVNPGGGACSEPR	ALU2_HUMAN	P39189
	ALU3_HUMAN	P39190
QEVPSWLENMAYEHHYK	DDX3X_HUMAN	O00571
	DDX3Y_HUMAN	O15523

	ACTS_MOUSE	P68134
	ACTA_RABIT	P62740
QEYDEAGPSIVHR	ACTC_HUMAN	P68032
	ACTB_BOVIN	P60712
QEYDESGPSIVHR	ACTG_ANSAN	P63256
	PHS1_HUMAN	P06737
	PHS3_HUMAN	P11216
QEYFVVAATLQDIIR	PHS2_HUMAN	P11217
	K1C14_HUMAN	P02533
QFTSSSSMK	K1C16_HUMAN	P08779
	PLST_HUMAN	P13797
QFVTPADVVSGNPK	PLSI_HUMAN	Q14651
	IF41_HUMAN	P60842
QFYINVER	IF42_HUMAN	Q14240
	AT1A3_HUMAN	P13637
QGAIVAVTGDGVNDSPALK	AT1A2_HUMAN	P50993
	ARBK1_HUMAN	P25098
QGETLALNER	ARBK2_HUMAN	P35626
	LTB1S_HUMAN	P22064
QGTYYDPVK	LTB1L_HUMAN	Q14766
	RASN_HUMAN	P01111
QGVEDAFYTLVR	RASH_HUMAN	P01112
	AT11A_HUMAN	P98196
QGYEDWLR	AT11B_HUMAN	Q9Y2G3
	BGAL_HUMAN	P16278
QHYGFVLYR	BGAM_HUMAN	P16279
	NDK8_HUMAN	O60361
QHYIDLK	NDKB_HUMAN	P22392
	HSP47_HUMAN	P29043
QHYNCEHSK	SPH2_HUMAN	P50454
	ADT2_HUMAN	P05141
QIFLGGVDK	ADT3_HUMAN	P12236
	PRDX2_HUMAN	P32119
QITVNDLPVGR	PRDX1_HUMAN	Q06830
	VATB1_HUMAN	P15313
QIYPPINVLPSLSR	VATB2_HUMAN	P21281
	CDC42_CANFA	P60952
QKPITPETAEK	CDC42_MOUSE	P60766
	LTB1S_HUMAN	P22064
QLCCCSVGK	LTB1L_HUMAN	Q14766
	K2C6A_HUMAN	P02538
	K2C6B_HUMAN	P04259
	K2C5_HUMAN	P13647
	K2C6C_HUMAN	P48666
QLDSIVGER	K2C6E_HUMAN	P48668
	MYH1_HUMAN	P12882
QLEEEIK	MYH2_HUMAN	Q9UKX2
	MYH3_HUMAN	P11055
QLEEENK	DPOE2_HUMAN	P56282

QLEMILNKPGLK	AK1C4_HUMAN	P17516
	AK1C3_HUMAN	P42330
	AK1C1_HUMAN	Q04828
QLFDQVVK	EZRI_HUMAN	P15311
	MOES_HUMAN	P26038
	RADI_HUMAN	P35241
QLFHPEQLITGK	TBA1_MERUN	P68360
	TBA1_MACFA	P68367
	TBA6_HUMAN	Q9BQE3
	TBA8_HUMAN	Q9NY65
QLGHEEDYALGK	ARBK1_HUMAN	P25098
	ARBK2_HUMAN	P35626
QLIVGVNK	EF1A1_HUMAN	P68104
	EF1A2_HUMAN	Q05639
QLLQANPILEAFGNAK	MYH9_HUMAN	P35579
	MYH11_HUMAN	P35749
QLSLDINK	BRD4_HUMAN	O60885
	BRD2_HUMAN	P25440
QLSQSLLPAIVELAEDAK	2AAA_HUMAN	P30153
	2AAB_HUMAN	P30154
QLSSLSK	WASF1_HUMAN	Q92558
	WASF3_HUMAN	Q9UPY6
QLTLLESDLYR	SOS1_HUMAN	Q07889
	SOS2_HUMAN	Q07890
QMCMIMMEMTDFTR	CTN2_HUMAN	P26232
	CTN1_HUMAN	P35221
QMDTNNDGK	HPCA_RAT	P84076
	HPCL1_HUMAN	P37235
QMSGAQIK	PCBP1_HUMAN	Q15365
	PCBP2_HUMAN	Q15366
QNLEPLFEQYINNLR	K2C6A_HUMAN	P02538
	K2C6B_HUMAN	P04259
	K2C5_HUMAN	P13647
	K2C6C_HUMAN	P48666
	K2C6E_HUMAN	P48668
QNVASEK	BIG2_HUMAN	Q9Y6D5
	BIG1_HUMAN	Q9Y6D6
QNVQVFEFQLTSEEMK	AK1C2_HUMAN	P52895
	AK1C1_HUMAN	Q04828
QPALRPHVHK	ISL1_MOUSE	P61372
	ISL2_HUMAN	Q96A47
QPPQVLK	STAT6_HUMAN	P42226
	STA5A_HUMAN	P42229
	STA5B_HUMAN	P51692
QQAHDLLINKPDGTFLLR	STA5A_HUMAN	P42229
	STA5B_HUMAN	P51692
QQEGESR	LDHA_HUMAN	P00338
	LDHB_HUMAN	P07195
QQLAGNGGPPEGSLDVLQSWCEK	STA5A_HUMAN	P42229

	STA5B_HUMAN	P51692
QQLFSYAILGFALSEAMGLFCLMVAFLIL FAM	AT5G1_HUMAN	P05496
	AT5G3_HUMAN	P48201
	AT5G2_HUMAN	Q06055
QQQLTAMK	MYH9_HUMAN	P35579
	MYH11_HUMAN	P35749
QQTIILDDELIQWK	STA5A_HUMAN	P42229
	STA5B_HUMAN	P51692
QSASGTK	K6PL_HUMAN	P17858
	K6PP_HUMAN	Q01813
QSETPSQK	ALU2_HUMAN	P39189
	ALU3_HUMAN	P39190
	ALU5_HUMAN	P39192
	ALU8_HUMAN	P39195
QSLETICLLLAYK	PP1A_HUMAN	P62136
	PP1B_HUMAN	P62140
QTLMWSATWPK	DDX5_HUMAN	P17844
	DDX17_HUMAN	Q92841
QTQIFTTYSDNQPGVLIQVYEGER	HSP71_HUMAN	P08107
	HS70L_HUMAN	P34931
QTTYTECCCLYGEAWGMQCALCPLK	LTB1S_HUMAN	P22064
	LTB1L_HUMAN	Q14766
QTVAVGVIK	EF1A1_HUMAN	P68104
	EF1A2_HUMAN	Q05639
QVAASTAQLLVACK	TLN1_HUMAN	Q9Y490
	TLN2_HUMAN	Q9Y4G6
QVELALWDTAGQEDYDR	RHOB_RAT	P62747
	RHOA_BOVIN	P61585
	RHOC_HUMAN	P08134
QVHPDTGISSK	H2B_BOVIN	P62808
	H2BR_HUMAN	P06899
	H2BF_HUMAN	P33778
	H2BS_HUMAN	P57053
	H2BB_HUMAN	P58876
	H2BQ_HUMAN	Q16778
	H2BJ_HUMAN	Q93079
	H2BD_HUMAN	Q99877
	H2BE_HUMAN	Q99879
	H2BC_HUMAN	Q99880
QVLEELTELPVMVELASDFLDR	GFPT2_HUMAN	O94808
	GFPT1_HUMAN	Q06210
QVSLEAWLQR	STA5A_HUMAN	P42229
	STA5B_HUMAN	P51692
QVVIDGETCLLDILDTAGQEEYSAMR	RASN_HUMAN	P01111
	RASH_HUMAN	P01112
	RASK_HUMAN	P01116
QYFIGVLDIAGFEIFDFNSFEQLCINFTNE K	MYH7_HUMAN	P12883
	MYH6_HUMAN	P13533
QYFIGVLDIAGFEIFDFNSLEQLCINFTNE	MYH1_HUMAN	P12882

K	MYH8_HUMAN	P13535
	MYH2_HUMAN	Q9UKX2
	MYH13_HUMAN	Q9UKX3
	MYH4_HUMAN	Q9Y623
QYKPVVYSNTIQSLAAIVR	GNAO1_HUMAN	P09471
	GNAO2_HUMAN	P29777
QYLCVALSK	BIG2_HUMAN	Q9Y6D5
	BIG1_HUMAN	Q9Y6D6
QYPISLVLAPTR	DDX3X_HUMAN	O00571
	DDX3Y_HUMAN	O15523
RPPPRPANFCIFSR	ALU2_HUMAN	P39189
	ALU7_HUMAN	P39194
RRPIHHHVGK	LTB1S_HUMAN	P22064
	LTB1L_HUMAN	Q14766
SAEPEVATAPPEK	LTB1S_HUMAN	P22064
	LTB1L_HUMAN	Q14766
SAIGEGMTR	VATB1_HUMAN	P15313
	VATB2_HUMAN	P21281
SALQSINEWAAQTTDGK	HSP47_HUMAN	P29043
	SPH2_HUMAN	P50454
SALTIQLIQNHFVDEYDPTIEDSYR	RASN_HUMAN	P01111
	RASH_HUMAN	P01112
	RASK_HUMAN	P01116
SALTLQFMYDEFVEDYEPTK	RALA_HUMAN	P11233
	RALB_HUMAN	P11234
SALTVQFVQGIFVEK	RAP1B_BOVIN	P61223
	RAP1A_BOVIN	P62833
SANFQKPK	MYH8_HUMAN	P13535
	MYH2_HUMAN	Q9UKX2
SAPATGGVK	H31_HUMAN	P68431
	H3T_HUMAN	Q16695
SAVLQEAR	COPG2_HUMAN	Q9UBF2
	COPG_HUMAN	Q9Y678
SAVVSGSSR	K2C3_HUMAN	P12035
	K22O_HUMAN	Q01546
SAYLMGLNSADLLK	MYH7_HUMAN	P12883
	MYH6_HUMAN	P13533
SCAGISGK	ERD21_HUMAN	P24390
	ERD22_HUMAN	P33947
SCAHDWVYE	NDK8_HUMAN	O60361
	NDKB_HUMAN	P22392
SCCSCCPVGCAK	MT2_HUMAN	P02795
	MT1E_HUMAN	P04732
	MT1G_HUMAN	P13640
	MT1I_HUMAN	P80295
	MT1K_HUMAN	P80296
	MT1L_HUMAN	P80297
SCLLLQFTDK	RAB2A_HUMAN	P61019
	RAB2B_HUMAN	Q8WUD1

SDEMNVK	MYL6_BOVIN	P60661
	MYL6_HUMAN	P60660
SDPSIVR	NCALD_HUMAN	P61601
	HPCA_RAT	P84076
	HPCL1_HUMAN	P37235
SEAPPHIFSISDNAYQYMLTDR	MYH7_HUMAN	P12883
	MYH6_HUMAN	P13533
SEIDHVK	K2C6A_HUMAN	P02538
	K2C6B_HUMAN	P04259
	K2C6C_HUMAN	P48666
	K2C6E_HUMAN	P48668
SEISELR	K1C14_HUMAN	P02533
	K1C17_HUMAN	Q04695
SFFAALVAAFTLR	CLCN4_HUMAN	P51793
	CLCN5_HUMAN	P51795
SGETEDTFIADLVVGLCTGQIK	ENOA_HUMAN	P06733
	ENOG_HUMAN	P09104
	ENOB_HUMAN	P13929
SGFSSISVSR	K2C6B_HUMAN	P04259
	K2C6C_HUMAN	P48666
	K2C6E_HUMAN	P48668
SGPFGQIFRPDNFVFGQSGAGNNWAK	TBBX_MOUSE	P68372
	TBB5_MOUSE	P99024
SGVSLAALK	H14_HUMAN	P10412
	H13_HUMAN	P16402
	H12_HUMAN	P16403
SHLGGWGHR	BGAL_HUMAN	P16278
	BGAM_HUMAN	P16279
SHSIFLINIK	KIF5C_HUMAN	O60282
	KINN_HUMAN	Q12840
SIAAATSALVK	TLN1_HUMAN	Q9Y490
	TLN2_HUMAN	Q9Y4G6
SIATLAITTLLK	COPG2_HUMAN	Q9UBF2
	COPG_HUMAN	Q9Y678
SIDIWSVGCILAEMLSNRPIFPGK	MK03_HUMAN	P27361
	MK01_HUMAN	P28482
SIGVSNFNR	AK1C3_HUMAN	P42330
	AK1C1_HUMAN	Q04828
SINPDEAVAYGAAVQAAILMGDK	HSP71_HUMAN	P08107
	HS70L_HUMAN	P34931
SINPFGNSR	CLCN3_HUMAN	P51790
	CLCN4_HUMAN	P51793
	CLCN5_HUMAN	P51795
SINPPCVPFFGIYLTNILK	SOS1_HUMAN	Q07889
	SOS2_HUMAN	Q07890
SIQFVDWCPTGFK	TBA1_MERUN	P68360
	TBA1_MACFA	P68367
SIQVDGK	RB11A_MOUSE	P62492
	RB11B_HUMAN	Q15907

	BIG2_HUMAN	Q9Y6D5
SKPNLLK	BIG1_HUMAN	Q9Y6D6
	ALU2_HUMAN	P39189
	ALU3_HUMAN	P39190
SLALSPR	ALU8_HUMAN	P39195
	AN32A_HUMAN	P39687
SLDLFNCEVTNLNDYR	AN32B_HUMAN	Q92688
	ATS10_HUMAN	Q9H324
SLDSFCK	ATS6_HUMAN	Q9UKP5
	SOS1_HUMAN	Q07889
SLEIEPR	SOS2_HUMAN	Q07890
	PABP1_HUMAN	P11940
SLGYAYVNFQQPADAER	PABP4_HUMAN	Q13310
	K1C13_HUMAN	P13646
SLLEGQDAK	K1C15_HUMAN	P19012
	MYH7_HUMAN	P12883
SLQSLLK	MYH6_HUMAN	P13533
	KIF5C_HUMAN	O60282
SLSALGNVISALAEGTK	KINN_HUMAN	Q12840
	HSP47_HUMAN	P29043
SLSNSTAR	SPH2_HUMAN	P50454
	MYH3_HUMAN	P11055
	MYH1_HUMAN	P12882
	MYH7_HUMAN	P12883
	MYH6_HUMAN	P13533
	MYH8_HUMAN	P13535
	MYH13_HUMAN	Q9UKX3
SLSTELFK	MYH4_HUMAN	Q9Y623
	HS90A_HUMAN	P07900
SLTNDWEDHLAVK	HS90B_HUMAN	P08238
	K2C6A_HUMAN	P02538
	K2C6B_HUMAN	P04259
	K2C6C_HUMAN	P48666
SLYGLGGSK	K2C6E_HUMAN	P48668
	BGAL_HUMAN	P16278
SLYPLTFIQVK	BGAM_HUMAN	P16279
	MYH7_HUMAN	P12883
SNAAAAALDK	MYH6_HUMAN	P13533
	MYH1_HUMAN	P12882
	MYH13_HUMAN	Q9UKX3
SNNFQKPKPAK	MYH4_HUMAN	Q9Y623
	CP2CI_HUMAN	P33260
SPCMQDR	CP2CJ_HUMAN	P33261
	ALU2_HUMAN	P39189
SPDLVIRPPRPPK	ALU3_HUMAN	P39190
	DDX3X_HUMAN	O00571
SPILVATAVAAR	DDX3Y_HUMAN	O15523
	IDHC_HUMAN	O75874
SPNGTIR	IDHP_HUMAN	P48735

SPYLYPLYGLGELPQGFAR	GDIA_HUMAN	P31150
	GDIB_HUMAN	P50395
SQEVEDK	KIF5C_HUMAN	O60282
	KINH_HUMAN	P33176
SQHFGRPR	ALU1_HUMAN	P39188
	ALU2_HUMAN	P39189
	ALU3_HUMAN	P39190
	ALU5_HUMAN	P39192
	ALU7_HUMAN	P39194
SSRPAWPTW	ALU7_HUMAN	P39194
	ALU8_HUMAN	P39195
SSVLENFVGR	DYN1_HUMAN	Q05193
	DYN3_HUMAN	Q9UQ16
SSWVMTCAYAPSGNYVACGGLDNICSIYNLK	GBB1_BOVIN	P62871
	GBB4_HUMAN	Q9HAV0
STCIYGGAPK	DDX5_HUMAN	P17844
	DDX17_HUMAN	Q92841
STELLIR	H33_HUMAN	P84243
	H31_HUMAN	P68431
	H3T_HUMAN	Q16695
STGEAFVQFASQEIAEK	HNRH1_HUMAN	P31943
	HNRH2_HUMAN	P55795
STHPHFVR	MYH1_HUMAN	P12882
	MYH7_HUMAN	P12883
	MYH8_HUMAN	P13535
	MYH2_HUMAN	Q9UKX2
	MYH13_HUMAN	Q9UKX3
	MYH4_HUMAN	Q9Y623
STHPPPLPAK	LTB1S_HUMAN	P22064
	LTB1L_HUMAN	Q14766
STIGVEFATR	RB11A_MOUSE	P62492
	RB11B_HUMAN	Q15907
STLEPVEK	HSP71_HUMAN	P08107
	HSP76_HUMAN	P17066
STLMFGQR	KIF5C_HUMAN	O60282
	KINN_HUMAN	Q12840
STMVGTPYWMAPEVVTR	PAK3_HUMAN	O75914
	PAK2_HUMAN	Q13177
STNLLLTR	SC15A_HUMAN	Q8TAG9
	SC15B_HUMAN	Q9Y2D4
STTTGHLIYK	EF1A1_HUMAN	P68104
	EF1A2_HUMAN	Q05639
SVAQAGVQWR	ALU1_HUMAN	P39188
	ALU2_HUMAN	P39189
	ALU3_HUMAN	P39190
	ALU8_HUMAN	P39195
SVDETLR	PRDX1_HUMAN	Q06830
	PRDX4_HUMAN	Q13162
SVEMHHEALSEALPGDNVGFNVK	EF1A1_HUMAN	P68104

	EF1A2_HUMAN	Q05639
SVGVVTTTR	PPB1_HUMAN	P05187
	PPBN_HUMAN	P10696
SWTAADMAAQITK	HLAH_HUMAN	P01893
	1A03_HUMAN	P04439
	1A01_HUMAN	P30443
SWTAADTAAQITQR	1B07_HUMAN	P01889
	1B08_HUMAN	P30460
	1C04_HUMAN	P30504
SYELPDGQVITIGNER	ACTS_MOUSE	P68134
	ACTB_BOVIN	P60712
	ACTG_ANSAN	P63256
	ACTA_RABIT	P62740
	ACTC_HUMAN	P68032
	ACTH_HUMAN	P63267
SYGIPFIETSAK	RASN_HUMAN	P01111
	RASK_HUMAN	P01116
SYHIFYQILSNK	MYH3_HUMAN	P11055
	MYH4_HUMAN	Q9Y623
SYHIFYQIMSNK	MYH1_HUMAN	P12882
	MYH13_HUMAN	Q9UKX3
SYHIFYQITSNK	MYH8_HUMAN	P13535
	MYH2_HUMAN	Q9UKX2
TAAENEFVTLK	K2C6A_HUMAN	P02538
	K2C6B_HUMAN	P04259
	K2C6C_HUMAN	P48666
	K2C6E_HUMAN	P48668
TAFTSTQLLELER	GSH2_HUMAN	Q9BZM3
	GSHI_HUMAN	Q9H4S2
TAIEAFNETIK	P85B_HUMAN	O00459
	P85A_HUMAN	P27986
TAVAPIER	ADT2_HUMAN	P05141
	ADT1_HUMAN	P12235
	ADT3_HUMAN	P12236
TAVCDIPPR	TBBX_MOUSE	P68372
	TBB5_MOUSE	P99024
TCAYTNHTVLPEALER	PHS3_HUMAN	P11216
	PHS2_HUMAN	P11217
TCEDIDECVNNTVCDSHGFCDNTAGSFR	LTB1S_HUMAN	P22064
	LTB1L_HUMAN	Q14766
TCLLISYTTNK	CDC42_CANFA	P60952
	CDC42_MOUSE	P60766
TCLLIVFSK	RHOB_RAT	P62747
	RHOA_BOVIN	P61585
	RHOC_HUMAN	P08134
TCQDINECEHPGLCGPQGECLNTEGSFHCVCQQGFSISADGR	LTB1S_HUMAN	P22064
	LTB1L_HUMAN	Q14766
TCYAANPRPDALMK	ISL1_MOUSE	P61372
	ISL2_HUMAN	Q96A47

TCYNIYLASK	BIG2_HUMAN	Q9Y6D5
	BIG1_HUMAN	Q9Y6D6
TDGALLVNAMFFKPHWDEK	HSP47_HUMAN	P29043
	SPH2_HUMAN	P50454
TEAGATVTVK	MYH1_HUMAN	P12882
	MYH4_HUMAN	Q9Y623
TEAVASSLYDILAR	BGAL_HUMAN	P16278
	BGAM_HUMAN	P16279
TEELEEAK	MYH3_HUMAN	P11055
	MYH1_HUMAN	P12882
	MYH7_HUMAN	P12883
	MYH6_HUMAN	P13533
	MYH8_HUMAN	P13535
	MYH2_HUMAN	Q9UKX2
	MYH13_HUMAN	Q9UKX3
	MYH4_HUMAN	Q9Y623
TELLVDR	EKI1_HUMAN	Q9HBU6
	EKI2_HUMAN	Q9NVF9
TFIAIKPDGVQR	NDKA_HUMAN	P15531
	NDKB_HUMAN	P22392
TFLTTYR	SOS1_HUMAN	Q07889
	SOS2_HUMAN	Q07890
TFTAWCNSHLR	ACTN4_HUMAN	O43707
	ACTN2_HUMAN	P35609
	ACTN3_HUMAN	Q08043
TFTDCFNCLPIAAIVDEK	PP1A_HUMAN	P62136
	PP1B_HUMAN	P62140
TFVLEVMGR	K6PL_HUMAN	P17858
	K6PP_HUMAN	Q01813
TGAEGAVLDEAK	KIF5C_HUMAN	O60282
	KINH_HUMAN	P33176
	KINN_HUMAN	Q12840
TGEGFLCVFAINNTK	RASH_HUMAN	P01112
	RASK_HUMAN	P01116
TGETALHLAAR	NOTC1_HUMAN	P46531
	NOTC3_HUMAN	Q9UM47
TGLYNYYDDEK	HSP47_HUMAN	P29043
	SPH2_HUMAN	P50454
TGTLTQNR	AT1A3_HUMAN	P13637
	ATP4A_HUMAN	P20648
	AT1A2_HUMAN	P50993
	AT12A_HUMAN	P54707
	AT1A4_HUMAN	Q13733
TGTQYLLR	SPB6_HUMAN	P35237
	SPB8_HUMAN	P50452
THINIVVIGHVDSGK	EF1A1_HUMAN	P68104
	EF1A2_HUMAN	Q05639
THMTHHPISDHEATLR	HLAH_HUMAN	P01893
	1A03_HUMAN	P04439

	1A01_HUMAN	P30443
THTMEGK	KIF5C_HUMAN	O60282
	KINH_HUMAN	P33176
	KINN_HUMAN	Q12840
THVTHHPISDHEATLR	1B07_HUMAN	P01889
	1B08_HUMAN	P30460
THYDPPR	HNRH1_HUMAN	P31943
	HNRH2_HUMAN	P55795
TIELDGK	RAB8A_CANFA	P61007
	RAB8B_HUMAN	Q92930
	RAB1B_HUMAN	Q9H0U4
TIEYLQPNPASR	SH3G1_HUMAN	Q99961
	SH3G2_HUMAN	Q99962
TIGGGDDSFNTFFSETGAGK	TBA1_MERUN	P68360
	TBA6_HUMAN	Q9BQE3
TIGVITK	DYN1_HUMAN	Q05193
	DYN3_HUMAN	Q9UQ16
TIHELEK	MYH3_HUMAN	P11055
	MYH7_HUMAN	P12883
TIITYPWFQNSSVILFLNK	GNA11_HUMAN	P29992
	GNAQ_HUMAN	P50148
TILEELVQR	UDB17_HUMAN	O75795
	UDB15_HUMAN	P54855
TILSGFIIR	CLCN3_HUMAN	P51790
	CLCN4_HUMAN	P51793
	CLCN5_HUMAN	P51795
TIQFVDWCPTGFK	TBA6_HUMAN	Q9BQE3
	TBA8_HUMAN	Q9NY65
TITTAYYR	RAB3D_HUMAN	O95716
	RAB3A_HUMAN	P20336
	RAB8A_CANFA	P61007
	RAB13_HUMAN	P51153
	RAB8B_HUMAN	Q92930
	RAB3C_HUMAN	Q96E17
TKPIWTR	HS90A_HUMAN	P07900
	HS90B_HUMAN	P08238
TLHNLVIQYASQGR	KLC1_HUMAN	Q07866
	KLC2_HUMAN	Q9H0B6
TLITVAHTDGNYLGNSWHEILK	BIG2_HUMAN	Q9Y6D5
	BIG1_HUMAN	Q9Y6D6
TLLLLLSGALALTQTWAGSHSMR	1A03_HUMAN	P04439
	1A01_HUMAN	P30443
TLTTVQGIADDYDK	SUI13_HUMAN	O60739
	SUI1_HUMAN	P41567
TNAACAALDK	MYH1_HUMAN	P12882
	MYH2_HUMAN	Q9UKX2
TNGITPR	PHS1_HUMAN	P06737
	PHS3_HUMAN	P11216
	PHS2_HUMAN	P11217

TNLSVHEDK	KINH_HUMAN	P33176
	KINN_HUMAN	Q12840
TPALIALR	AK1C4_HUMAN	P17516
	AK1C3_HUMAN	P42330
	AK1C2_HUMAN	P52895
	AK1C1_HUMAN	Q04828
TPFLLVGTQIDLR	CDC42_CANFA	P60952
	CDC42_MOUSE	P60766
TPGAMEHELVLHQLR	MYH1_HUMAN	P12882
	MYH8_HUMAN	P13535
	MYH2_HUMAN	Q9UKX2
	MYH4_HUMAN	Q9Y623
TPSSDVLVFDYTK	RBBP4_HUMAN	Q09028
	RBBP7_HUMAN	Q16576
TPVSEDMLGR	VATB1_HUMAN	P15313
	VATB2_HUMAN	P21281
TQLEELEDELQATEDAK	MYH9_HUMAN	P35579
	MYH10_HUMAN	P35580
	MYH11_HUMAN	P35749
TQTIHSTYSHQQVIPHVYPVAAK	LTB1S_HUMAN	P22064
	LTB1L_HUMAN	Q14766
TSACGLFSVCYPR	2AAA_HUMAN	P30153
	2AAB_HUMAN	P30154
TSGHDHPDVATMLNILALVYR	KLC1_HUMAN	Q07866
	KLC2_HUMAN	Q9H0B6
TSPPVPVEVAPEASTSSASQVIAPTQVT EINECTVNPDICGAGHCINLPVR	LTB1S_HUMAN	P22064
	LTB1L_HUMAN	Q14766
TSTDLDVDVDQPK	LTB1S_HUMAN	P22064
	LTB1L_HUMAN	Q14766
TSVFVAEPK	MYH8_HUMAN	P13535
	MYH2_HUMAN	Q9UKX2
TSVFVVDPK	MYH1_HUMAN	P12882
	MYH4_HUMAN	Q9Y623
TTGIVETHFTFK	GNAI1_HUMAN	P63096
	GNAI2_HUMAN	P04899
	GNAI3_HUMAN	P08754
	GNAO1_HUMAN	P09471
	GNAO2_HUMAN	P29777
TTGIVLDSGDGVTHNVPIYEGYALPHAIM R	ACTS_MOUSE	P68134
	ACTA_RABIT	P62740
	ACTC_HUMAN	P68032
	ACTH_HUMAN	P63267
TTGIVMDSGDGVTHTVPIYEGYALPHAIL R	ACTB_BOVIN	P60712
	ACTG_ANSAN	P63256
TTGVVLDSGDGVTHAVPIYEGFAMPHSI MR	ACTZ_HUMAN	P61163
	ACTY_HUMAN	P42025
TTHPHFVR	MYH3_HUMAN	P11055
	MYH6_HUMAN	P13533
TTLPQDCSNPAPLSSPLNGVHDR	BGAL_HUMAN	P16278

	BGAM_HUMAN	P16279
TTPSYVAFTDTER	HSP71_HUMAN	P08107
	HSP76_HUMAN	P17066
	HS70L_HUMAN	P34931
	HSP72_HUMAN	P54652
TVALWDLR	RBBP4_HUMAN	Q09028
	RBBP7_HUMAN	Q16576
TVFDEAIR	RAC3_HUMAN	P60763
	RAC4_HUMAN	O95916
	RAC2_HUMAN	P15153
TVGAALDILCPSGPIK	BGAL_HUMAN	P16278
	BGAM_HUMAN	P16279
TVGQLYK	MYH9_HUMAN	P35579
	MYH10_HUMAN	P35580
	MYH11_HUMAN	P35749
TVLLLLSAALALTETWAGSHSMR	1B07_HUMAN	P01889
	1B08_HUMAN	P30460
TVLVIAHR	TAP2_HUMAN	Q03519
	ABCBA_HUMAN	Q9NRK6
TVMIGGK	PHS3_HUMAN	P11216
	PHS2_HUMAN	P11217
TYDYLFK	RAB8A_CANFA	P61007
	RAB8B_HUMAN	Q92930
TYGVSFFLVK	TLN1_HUMAN	Q9Y490
	TLN2_HUMAN	Q9Y4G6
TYSWDNAQVILVGNK	RAB3D_HUMAN	O95716
	RAB3C_HUMAN	Q96E17
TYTHEVVTLWYR	CDK2_HUMAN	P24941
	CDK3_HUMAN	Q00526
TYWDFEFPRPFLPNVDFVGGLHCKPAK PLPK	UDB17_HUMAN	O75795
	UDB15_HUMAN	P54855
VACIGAWHPAR	RL3_HUMAN	P39023
	RL3L_HUMAN	Q92901
VADFGLAR	SRC_HUMAN	P12931
	FRK_HUMAN	P42685
VAEIPFNSTNK	AT1A3_HUMAN	P13637
	AT1A2_HUMAN	P50993
	AT12A_HUMAN	P54707
	AT1A4_HUMAN	Q13733
VAEITGEIQQYQNQPYCLR	SOS1_HUMAN	Q07889
	SOS2_HUMAN	Q07890
VAGITGAR	ALU7_HUMAN	P39194
	ALU8_HUMAN	P39195
VAGTTGAR	ALU1_HUMAN	P39188
	ALU2_HUMAN	P39189
	ALU5_HUMAN	P39192
VAPEEHPTLLTEAPLNPK	ACTS_MOUSE	P68134
	ACTA_RABIT	P62740
	ACTC_HUMAN	P68032

	ACTH_HUMAN	P63267
VAPEEHPVLLTEAPLNPK	ACTB_BOVIN	P60712
	ACTG_ANSAN	P63256
VCLLGDTGVGK	RAB31_HUMAN	Q13636
	RB22A_HUMAN	Q9UL26
VDEAVAVLQAHQAK	PABP1_HUMAN	P11940
	PABP3_HUMAN	Q9H361
VDIWSLGIMAIEMVEGEPPYLNENPLR	PAK3_HUMAN	O75914
	PAK2_HUMAN	Q13177
VDNSSLTGESEPQTR	AT1A3_HUMAN	P13637
	ATP4A_HUMAN	P20648
	AT1A2_HUMAN	P50993
VDWLTEK	IF41_HUMAN	P60842
	DDX48_HUMAN	P38919
	IF42_HUMAN	Q14240
VEAQLALK	SNPH_HUMAN	O15079
	K1472_HUMAN	Q9NX95
VEDMAELTCLNEASVLHNLK	MYH9_HUMAN	P35579
	MYH10_HUMAN	P35580
VEEEEER	MYH9_HUMAN	P35579
	MYH10_HUMAN	P35580
VEIIANDQGNR	HSP71_HUMAN	P08107
	GRP78_HUMAN	P11021
	HS70L_HUMAN	P34931
	HSP72_HUMAN	P54652
VELQELNDR	VIME_HUMAN	P08670
	DESM_HUMAN	P17661
VFAPYACGSGIPEIK	CLCN3_HUMAN	P51790
	CLCN4_HUMAN	P51793
	CLCN5_HUMAN	P51795
VFDMLNR	IF41_HUMAN	P60842
	IF42_HUMAN	Q14240
VFFDLMR	RALA_HUMAN	P11233
	RALB_HUMAN	P11234
VFFTTEEASWFR	BMR1B_HUMAN	O00238
	BMR1A_HUMAN	P36894
VGAGAPVYLAAVLEYLTAEILELAGNAA R	H2AC_HUMAN	P02261
	H2AX_HUMAN	P16104
	H2AG_HUMAN	P20671
	H2AA_HUMAN	P28001
	H2AL_HUMAN	Q93077
	H2AE_HUMAN	Q99878
VGCNPNEDVAIFAVDSLR	BIG2_HUMAN	Q9Y6D5
	BIG1_HUMAN	Q9Y6D6
VGGAEGTK	SH3G1_HUMAN	Q99961
	SH3G2_HUMAN	Q99962
VGINYQPPTVVPGGDLAK	TBA1_MERUN	P68360
	TBA1_MACFA	P68367
	TBA6_HUMAN	Q9BQE3

	TBA8_HUMAN	Q9NY65
VGNEYVTK	MYH3_HUMAN	P11055
	MYH1_HUMAN	P12882
	MYH7_HUMAN	P12883
	MYH6_HUMAN	P13533
	MYH8_HUMAN	P13535
	MYH2_HUMAN	Q9UKX2
	MYH13_HUMAN	Q9UKX3
VGSTSENITQK	DDX3X_HUMAN	O00571
	DDX3Y_HUMAN	O15523
VHAIPLR	GBB1_BOVIN	P62871
	GBB2_HUMAN	P62879
	GBB3_HUMAN	P16520
VHAYIISSLK	EHD1_HUMAN	Q9H4M9
	EHD3_HUMAN	Q9NZN3
VHIEIGPDGR	HNRH1_HUMAN	P31943
	HNRPF_HUMAN	P52597
	HNRH2_HUMAN	P55795
VHTGEKPYK	ZNF24_HUMAN	P17028
	ZN319_HUMAN	Q9P2F9
VIFLENYR	PHS1_HUMAN	P06737
	PHS3_HUMAN	P11216
	PHS2_HUMAN	P11217
VIGSGCNLDSAR	LDHA_HUMAN	P00338
	LDHB_HUMAN	P07195
VILEIDNAR	K1C13_HUMAN	P13646
	K1C15_HUMAN	P19012
VILLGDGGVGK	RAB9A_HUMAN	P51151
	RAB9B_HUMAN	Q9NP90
VIMATNR	PRS8_PIG	P62197
	PRS4_HUMAN	P62191
VIMVGSGGVGK	RALA_HUMAN	P11233
	RALB_HUMAN	P11234
VIMVTGDHPITAK	AT1A3_HUMAN	P13637
	ATP4A_HUMAN	P20648
	AT1A2_HUMAN	P50993
	AT12A_HUMAN	P54707
	AT1A4_HUMAN	Q13733
VINEEYK	RBBP4_HUMAN	Q09028
	RBBP7_HUMAN	Q16576
VIQQLEGAFALVFK	GFPT2_HUMAN	O94808
	GFPT1_HUMAN	Q06210
VIQYFATIAVTGEK	MYH1_HUMAN	P12882
	MYH8_HUMAN	P13535
	MYH2_HUMAN	Q9UKX2
	MYH4_HUMAN	Q9Y623
VISSIEQK	1433T_HUMAN	P27348
	1433B_HUMAN	P31946
	1433G_MOUSE	P61982

	1433F_HUMAN	Q04917
VKPLLQVTR	MYH10_HUMAN	P35580
	MYH11_HUMAN	P35749
VLAAVYK	ALDOA_HUMAN	P04075
	ALDOC_HUMAN	P09972
VLDELTLAR	K1C14_HUMAN	P02533
	K1C16_HUMAN	P08779
	K1C15_HUMAN	P19012
	K1C17_HUMAN	Q04695
VLDFEHFLPMLQTVAK	MYL6_BOVIN	P60661
	MYL6_HUMAN	P60660
VLGNPSNEELNAK	MLE1_HUMAN	P05976
	MLE3_HUMAN	P06741
VLITTDLLAR	IF41_HUMAN	P60842
	IF42_HUMAN	Q14240
VLNASAIPEGQFIDSK	MYH1_HUMAN	P12882
	MYH8_HUMAN	P13535
	MYH2_HUMAN	Q9UKX2
	MYH4_HUMAN	Q9Y623
VLNQQLTNHIR	DYN1_HUMAN	Q05193
	DYN3_HUMAN	Q9UQ16
VLVWPTEYSHWINMK	UDB17_HUMAN	O75795
	UDB15_HUMAN	P54855
VLWPQLCEALNMK	STA5A_HUMAN	P42229
	STA5B_HUMAN	P51692
VLYPNDNFFEGK	PHS1_HUMAN	P06737
	PHS3_HUMAN	P11216
	PHS2_HUMAN	P11217
VMLGETNPADSKPGTIR	NDK8_HUMAN	O60361
	NDKA_HUMAN	P15531
	NDKB_HUMAN	P22392
VMMEGGR	PABP1_HUMAN	P11940
	PABP3_HUMAN	Q9H361
VMTDESGK	PABP1_HUMAN	P11940
	PABP3_HUMAN	Q9H361
VMVTNVTSLLK	TLN1_HUMAN	Q9Y490
	TLN2_HUMAN	Q9Y4G6
VNKPPYPK	PLSL_HUMAN	P13796
	PLST_HUMAN	P13797
VNNTFCQDINECQLQGVCPNGECLNTM GSYR	LTB1S_HUMAN	P22064
	LTB1L_HUMAN	Q14766
VNYGAYINDFK	BGAL_HUMAN	P16278
	BGAM_HUMAN	P16279
VPEGPIPPSTPK	BGAL_HUMAN	P16278
	BGAM_HUMAN	P16279
VPFAVPDK	STA5A_HUMAN	P42229
	STA5B_HUMAN	P51692
VPTTGIIEYPFDLENIIFR	GNA14_HUMAN	O95837
	GNA11_HUMAN	P29992

VPYPGMVNR	YES_HUMAN	P07947
	SRC_HUMAN	P12931
VQAILLPQPPE	ALU5_HUMAN	P39192
	ALU7_HUMAN	P39194
	ALU8_HUMAN	P39195
VQEGYTCDCLDGYHLDTAK	LTB1S_HUMAN	P22064
	LTB1L_HUMAN	Q14766
VQHASPAGTYAHTVNR	PPB1_HUMAN	P05187
	PPBN_HUMAN	P10696
VQHELDEAEER	MYH7_HUMAN	P12883
	MYH6_HUMAN	P13533
VQLLHSQNTSLINQK	MYH7_HUMAN	P12883
	MYH6_HUMAN	P13533
VQLLHTQNTSLINTK	MYH1_HUMAN	P12882
	MYH8_HUMAN	P13535
	MYH2_HUMAN	Q9UKX2
	MYH4_HUMAN	Q9Y623
VRPCVVYGGADIGQQIR	DDX3X_HUMAN	O00571
	DDX3Y_HUMAN	O15523
VSCLGVTDDGMAVATGSWDSFLK	GBB1_BOVIN	P62871
	GBB2_HUMAN	P62879
VSDFGLSR	EPHA2_HUMAN	P29317
	EPHA8_HUMAN	P29322
	EPHB3_HUMAN	P54753
	EPHB4_HUMAN	P54760
	EPHA7_HUMAN	Q15375
VSDTVVEPYNATLSVHQLVENTDETYCI DNEALYDICFR	TBBX_MOUSE	P68372
	TBB5_MOUSE	P99024
VSGGLEVLAEK	AN32C_HUMAN	O43423
	AN32A_HUMAN	P39687
VSLEEIYSGCTK	DNJB1_HUMAN	P25685
	DNJB4_HUMAN	Q9UDY4
VSPDLEWHAACLK	ISL1_MOUSE	P61372
	ISL2_HUMAN	Q96A47
VSYFEIYLDK	KIF5C_HUMAN	O60282
	KINH_HUMAN	P33176
	KINN_HUMAN	Q12840
VTIAQGGVLPNIQAVLLPK	H2AC_HUMAN	P02261
	H2AO_HUMAN	P20670
	H2AG_HUMAN	P20671
	H2AA_HUMAN	P28001
	H2AL_HUMAN	Q93077
	H2AE_HUMAN	Q99878
VTLELGGK	ALDH2_HUMAN	P05091
	AL1A3_HUMAN	P47895
VTMQNLNDR	K1C14_HUMAN	P02533
	K1C16_HUMAN	P08779
VTTMDAELEFAIQPNTTGK	EZRI_HUMAN	P15311
	MOES_HUMAN	P26038

	RADI_HUMAN	P35241
VVCDENGSK	PABP1_HUMAN	P11940
	PABP4_HUMAN	Q13310
VVDSLQTSLDAETR	MYH7_HUMAN	P12883
	MYH6_HUMAN	P13533
VVGVIGASGSSVSIMVANILR	MGR7_HUMAN	Q14831
	MGR4_HUMAN	Q14833
VVHIIQSR	BRD4_HUMAN	O60885
	BRD3_HUMAN	Q15059
VVLDGEEVQIDILDTAGQEDYAAIR	RALA_HUMAN	P11233
	RALB_HUMAN	P11234
VVLIGDSGVGK	RB11A_MOUSE	P62492
	RB11B_HUMAN	Q15907
VVSEGGKPK	HSP76_HUMAN	P17066
	HSP72_HUMAN	P54652
VVVLGSGGVGK	RAP2A_HUMAN	P10114
	RAP2B_MOUSE	P61226
VVVVQAISALCQK	COPG2_HUMAN	Q9UBF2
	COPG_HUMAN	Q9Y678
VWINTSDIILVGLR	IF1AY_HUMAN	O14602
	IF1AH_HUMAN	O75642
	IF1AX_HUMAN	P47813
VWVLTGDK	AT11A_HUMAN	P98196
	AT11B_HUMAN	Q9Y2G3
VYGALMWSLGK	EHD4_HUMAN	Q9H223
	EHD1_HUMAN	Q9H4M9
	EHD3_HUMAN	Q9NZN3
VYIDPFTYEDPNEAVR	EPHB3_HUMAN	P54753
	EPHB4_HUMAN	P54760
VYIGSFWSHPLLIPDNR	EHD1_HUMAN	Q9H4M9
	EHD3_HUMAN	Q9NZN3
WAAVVVPSGEEQR	1B07_HUMAN	P01889
	HLAH_HUMAN	P01893
	1A03_HUMAN	P04439
	1A01_HUMAN	P30443
	1B08_HUMAN	P30460
	1C04_HUMAN	P30504
WAIADAQSAIEK	SOS1_HUMAN	Q07889
	SOS2_HUMAN	Q07890
WDDSGNDIIVLAK	CTN2_HUMAN	P26232
	CTN1_HUMAN	P35221
WDQFYSEVLGRPTTLFETMGK	UDB17_HUMAN	O75795
	UDB15_HUMAN	P54855
WELSSQPTIPIVGIIAGLVLLGAVITGAVV AAVMWR	1A03_HUMAN	P04439
	1A01_HUMAN	P30443
WEPSSQSTVPIVGIVAGLAVLAVVVIGAV VAAVMCR	1B07_HUMAN	P01889
	1B08_HUMAN	P30460
WFTDTSIILFLNK	GNAI1_HUMAN	P63096
	GNAI2_HUMAN	P04899

	GNAO2_HUMAN	P29777
WIHCFEDVTAIIFCVALSGYDQVLHEDET TNR	GNAO1_HUMAN	P09471
	GNAO2_HUMAN	P29777
WIHCFEGVTAIIFCVALSDYDLVLAEDEE MNR	GNAI1_HUMAN	P63096
	GNAI3_HUMAN	P08754
WIHCFENVTSIMFLVALSEYDQVLVESD NENR	GNA11_HUMAN	P29992
	GNAQ_HUMAN	P50148
WLPQNDLLGHPK	UDB17_HUMAN	O75795
	UDB15_HUMAN	P54855
WLPQNDLLGHPMTR	UD16_HUMAN	P19224
	UD11_HUMAN	P22309
WLPVYKPEVVAAYR	MYH8_HUMAN	P13535
	MYH13_HUMAN	Q9UKX3
WLTPVIPALWEAEAGGSR	ALU2_HUMAN	P39189
	ALU3_HUMAN	P39190
	ALU5_HUMAN	P39192
WMVIQTLTR	BIG2_HUMAN	Q9Y6D5
	BIG1_HUMAN	Q9Y6D6
WTAPEAALYGR	YES_HUMAN	P07947
	SRC_HUMAN	P12931
WTAPEAIAFR	EPHA8_HUMAN	P29322
	EPHB4_HUMAN	P54760
WTAPEAIAYR	EPHB3_HUMAN	P54753
	EPHA4_HUMAN	P54764
WTEGLISASK	HIP1_HUMAN	O00291
	HIP1R_HUMAN	O75146
WTLLQEQGTK	K2C6A_HUMAN	P02538
	K2C6B_HUMAN	P04259
	K2C5_HUMAN	P13647
	K2C6C_HUMAN	P48666
	K2C6E_HUMAN	P48668
WVPEITHHCPK	CDC42_CANFA	P60952
	CDC42_MOUSE	P60766
WYLSGFYK	OSR8_HUMAN	Q9BZF1
	OSR5_HUMAN	Q9H0X9
YAAWMIYTYSGLFCVTVNPYK	MYH1_HUMAN	P12882
	MYH6_HUMAN	P13533
	MYH8_HUMAN	P13535
	MYH2_HUMAN	Q9UKX2
	MYH13_HUMAN	Q9UKX3
	MYH4_HUMAN	Q9Y623
YADDSFTPAFVSTVGIDFK	RAB3D_HUMAN	O95716
	RAB3A_HUMAN	P20336
YAFVNWINK	PLSL_HUMAN	P13796
	PLST_HUMAN	P13797
YALYDATYETK	COF1_HUMAN	P23528
	COF2_HUMAN	Q9Y281
YASICQQNGIVPIVEPEILPDGDHDLK	ALDOA_HUMAN	P04075
	ALDOC_HUMAN	P09972

YAWVLDK	EF1A1_HUMAN	P68104
	EF1A2_HUMAN	Q05639
YCFPNYVGRPK	ACTZ_HUMAN	P61163
	ACTY_HUMAN	P42025
YDDMAAAMK	1433B_HUMAN	P31946
	1433G_MOUSE	P61982
YDPTIEDFYR	RAP2A_HUMAN	P10114
	RAP2B_MOUSE	P61226
YDPTIEDSYR	RAP1B_BOVIN	P61223
	RAP1A_BOVIN	P62833
YEDEINK	K2C6A_HUMAN	P02538
	K2C6B_HUMAN	P04259
	K2C1_HUMAN	P04264
	K2C8_HUMAN	P05787
	K2C3_HUMAN	P12035
	K2C5_HUMAN	P13647
	K22E_HUMAN	P35908
	K2C6C_HUMAN	P48666
	K2C6E_HUMAN	P48668
	K22O_HUMAN	Q01546
YEELQVTAGR	K2C6A_HUMAN	P02538
	K2C6B_HUMAN	P04259
	K2C6C_HUMAN	P48666
	K2C6E_HUMAN	P48668
YEESQSELESSQK	MYH7_HUMAN	P12883
	MYH6_HUMAN	P13533
YEETQAELEASQK	MYH8_HUMAN	P13535
	MYH4_HUMAN	Q9Y623
YEFGIFNQK	PHS3_HUMAN	P11216
	PHS2_HUMAN	P11217
YENELALR	K1C13_HUMAN	P13646
	K1C15_HUMAN	P19012
YETDAIQR	MYH3_HUMAN	P11055
	MYH1_HUMAN	P12882
	MYH7_HUMAN	P12883
	MYH6_HUMAN	P13533
	MYH8_HUMAN	P13535
	MYH2_HUMAN	Q9UKX2
	MYH13_HUMAN	Q9UKX3
	MYH4_HUMAN	Q9Y623
YEVAVPLCK	KLC1_HUMAN	Q07866
	KLC2_HUMAN	Q9H0B6
YFAGNLASGGAAGATSLCFVYPLDFAR	ADT2_HUMAN	P05141
	ADT1_HUMAN	P12235
	ADT3_HUMAN	P12236
YFFTSVSRPGR	1A03_HUMAN	P04439
	1A01_HUMAN	P30443
YFLPFELACQSK	BIG2_HUMAN	Q9Y6D5
	BIG1_HUMAN	Q9Y6D6

YFPTQALNFAFK	ADT2_HUMAN	P05141
	ADT1_HUMAN	P12235
	ADT3_HUMAN	P12236
YFVDINIQNK	SNPH_HUMAN	O15079
	K1472_HUMAN	Q9NX95
YFYLFPNR	ARBK1_HUMAN	P25098
	ARBK2_HUMAN	P35626
YGEVWMGK	BMR1B_HUMAN	O00238
	BMR1A_HUMAN	P36894
YGNIIAYDHSR	PTPRM_HUMAN	P28827
	PTPRK_HUMAN	Q15262
YGNPWEK	PHS1_HUMAN	P06737
	PHS3_HUMAN	P11216
	PHS2_HUMAN	P11217
YGQHPNIITLK	KS6A2_HUMAN	Q15349
	KS6A1_HUMAN	Q15418
YHEDFEK	NEBL_HUMAN	O76041
	NEBU_HUMAN	P20929
YHSLAPMYYR	RAB5A_HUMAN	P20339
	RAB5B_HUMAN	P61020
	RAB5C_HUMAN	P51148
YIDQEELNK	HS90A_HUMAN	P07900
	HS90B_HUMAN	P08238
YIHSANVLHR	MK03_HUMAN	P27361
	MK01_HUMAN	P28482
YIIIGDTGVGK	RAB2A_HUMAN	P61019
	RAB2B_HUMAN	Q8WUD1
YIPPHLR	DDX3X_HUMAN	O00571
	DDX3Y_HUMAN	O15523
YISGSIHYSR	BGAL_HUMAN	P16278
	BGAM_HUMAN	P16279
YKPVCNQVECHPYFNQR	AK1C2_HUMAN	P52895
	AK1C1_HUMAN	Q04828
YLECSALTQR	RAC3_HUMAN	P60763
	RAC2_HUMAN	P15153
YLGLLENVR	MYO1B_HUMAN	O43795
	MYO1A_HUMAN	Q9UBC5
YLLEQDFPGMR	EHD4_HUMAN	Q9H223
	EHD3_HUMAN	Q9NZN3
YLTLDIFAGPPNYPFSDEY	AK1C2_HUMAN	P52895
	AK1C1_HUMAN	Q04828
YLTVAAVFR	TBBX_MOUSE	P68372
	TBB5_MOUSE	P99024
YLVLDEADR	DDX3X_HUMAN	O00571
	DDX3Y_HUMAN	O15523
	DDX4_HUMAN	Q9NQI0
YMACCLLYR	TBA1_MERUN	P68360
	TBA1_MACFA	P68367
	TBA6_HUMAN	Q9BQE3

YMDIEFDFK	MYO1B_HUMAN	O43795
	MYO1A_HUMAN	Q9UBC5
YMNSGPVVAMVWEGLNVVK	NDK8_HUMAN	O60361
	NDKB_HUMAN	P22392
YNADEAR	IF1AY_HUMAN	O14602
	IF1AH_HUMAN	O75642
	IF1AX_HUMAN	P47813
YNPPDHEVVAMAR	BRD4_HUMAN	O60885
	BRD3_HUMAN	Q15059
YPENFFLLR	PP1A_HUMAN	P62136
	PP1B_HUMAN	P62140
YPIEHGIITNWDDMEK	ACTS_MOUSE	P68134
	ACTA_RABIT	P62740
	ACTC_HUMAN	P68032
	ACTH_HUMAN	P63267
YPIEHGIVTNWDDMEK	ACTB_BOVIN	P60712
	ACTG_ANSAN	P63256
YPIPPPDAK	MP2K2_HUMAN	P36507
	MP2K1_HUMAN	Q02750
YPPPLIPPR	ARBK1_HUMAN	P25098
	ARBK2_HUMAN	P35626
YQQEVDR	KIF5C_HUMAN	O60282
	KINH_HUMAN	P33176
	KINN_HUMAN	Q12840
YRPGTVALR	H33_HUMAN	P84243
	H31_HUMAN	P68431
	H3T_HUMAN	Q16695
YSVWIGGSILASLSTFQQMWISK	ACTB_BOVIN	P60712
	ACTG_ANSAN	P63256
	ACTA_RABIT	P62740
	ACTC_HUMAN	P68032
YTCHVQHEGLPEPLTLR	HLAH_HUMAN	P01893
	1C04_HUMAN	P30504
YTCHVQHEGLPKPLTLR	1B07_HUMAN	P01889
	1A03_HUMAN	P04439
	1A01_HUMAN	P30443
	1B08_HUMAN	P30460
YTCICYEGYR	LTB1S_HUMAN	P22064
	LTB1L_HUMAN	Q14766
YTGTRPSNLANNTILVK	UD16_HUMAN	P19224
	UD11_HUMAN	P22309
YTRPTPVQK	DDX3X_HUMAN	O00571
	DDX3Y_HUMAN	O15523
YTTTSSSSR	K2C6A_HUMAN	P02538
	K2C6B_HUMAN	P04259
	K2C6C_HUMAN	P48666
	K2C6E_HUMAN	P48668
YVECSALTQR	CDC42_CANFA	P60952
	CDC42_MOUSE	P60766

YVIYIER	RL26_MOUSE	P61255
	RL26L_HUMAN	Q9UNX3
YYLDSLDR	GNAO1_HUMAN	P09471
	GNAO2_HUMAN	P29777
YYSGLIYTYSGLFCVVINPYK	MYH9_HUMAN	P35579
	MYH10_HUMAN	P35580

Appendix D

Table S1. Abundance ratios for 514 proteins quantified across 5 cells (with replicates)

SPN	HMEC(A)	HMEC(B)	BT474(A)	BT474(B)	SKBR3(A)	SKBR3(B)	MCF7c18(A)	MCF7c18(B)	MDA231(A)	MDA231(B)
P01112		1.789			0.384	0.366	3.218		2.032	1.676
P01118	2.285				0.728	0.205				
P01121								1.095		
Q14764						1.685				
P26572						0.510				
P46777	0.444		0.857	1.157	0.861		1.398	0.998		
P42655	0.299		1.123	1.278					0.430	
Q14847			0.841	0.632						
P26639	0.552		0.864	22.557						
P18621	0.601		1.117	1.051						
P26640	1.016		3.607	2.778						
Q06830	2.004	0.888	1.325	1.692						
P26641	0.760		0.949	2.122						
Q9Y4L1		0.729								
Q9Y4P3		0.484		0.804	1.052	0.699		1.603	1.297	14.664
P42704		0.488		0.406						
Q9Y5K8		0.960			1.036	1.197	3.253			1.045
Q9Y5M8	0.649		0.748	1.119						
Q14974	0.868		1.324	2.309						
Q9Y624				0.604						
Q9Y696					1.712	1.810				
P28288		1.415				4.988	22.768	18.391		1.744
P50895				0.608						
Q9Y672			0.841							
P18859						2.091				
Q16513				0.957						
P50914				1.161						
Q16555	0.291							0.436		
P34931	1.012		0.533	0.530						1.007
P34932	1.054		2.420	3.013		1.854				2.874
P50990	0.860		0.839	1.444		2.096				
P50993	0.351	0.816	1.668	1.748	0.957	0.754			0.857	
P50995						1.273			2.031	
P11016	1.282	1.334	1.245	1.086					1.796	2.215
P11021	0.798		1.041	1.051	0.786		2.421			0.497
P11047	1.259	0.467	0.831	0.765				1.188		
Q16643				0.460						
P11117								1.514		
P36543	0.507	1.441								0.874
P36578	1.023		0.935	0.853		0.449		1.062		
P11177	2.025	0.271	0.631	0.673						
Q16781			3.254							

P11216		0.382	0.600	0.599			1.716			
Q16851	0.514			0.978						
Q14789		0.866				0.754			0.549	0.341
P54136	0.539		1.051	0.811						
P38117										0.453
P38159									0.439	
O15142	0.469		1.052	1.054		2.632				
O15143						0.348			0.481	0.488
O15144	0.512	0.835			1.263	0.981	0.467			
P01922	0.494									
O15173					0.430					
P52907	0.529			1.193						
Q01130			0.882	0.771						
Q9UI12	0.685		0.745	0.714						
P52943				0.700						
O15371	0.489		0.960			0.943				
Q9Y6I9				0.774	0.811					0.417
P46459	1.021		0.666	0.670	2.539		1.614		1.373	1.168
P13073	0.783	1.493	1.624	1.420					0.832	0.785
O15400						2.480	1.427	1.241		
P05091			0.218	0.401						
P05092	1.227		0.772	0.690					1.977	
Q9BR76				1.071						
P05141		1.272						0.904	1.352	
P21181				1.231						
O15551	0.914									
P48047			0.602	0.610						
P38606	0.779		0.589	3.315						
P05215	0.879		1.079	2.222	0.487					
P05217	0.772		1.038	1.004	0.734	0.791	1.234	1.490	0.861	0.840
Q9UL26			1.672							
P38646		1.547		0.991	0.730	0.742	0.977	1.058		
P21281	0.770		1.403	1.373						
P54709					1.055	0.782				
Q9UKM7					0.576	0.576				
Q01518	0.732		0.632	0.763			0.993	2.344	0.996	0.986
P21333	0.426	0.685	1.172	1.449	0.683	2.691	10.185	3.176	1.069	1.390
P46778		0.567		0.671		1.014			0.644	1.164
P46782				2.642						
P46783					0.391					0.807
Q9UM54		0.826				1.505				
Q01581	0.820		0.729	0.771						
P05386		0.591	3.576							
P05387	0.593		1.149	1.045						
P05388	0.868		0.685	1.443					0.688	0.729
Q15125										
Q9H0U4	1.650	0.887	1.131						0.704	
P13489		0.622								
Q9Y230				2.614						
Q9UNL2				1.647					0.722	0.853
P46939										

P46940	0.469	1.714	1.033	1.107	0.537	1.530	2.718	1.751		7.469
Q9GZU7									23.869	14.897
Q9Y6N5			0.530	0.331						
Q01813	0.597	0.530	2.057	2.261	1.013					
P13637	0.508	0.816	3.882	2.965	0.879	0.759		1.639		3.450
P13639	0.722	0.686	1.655	1.538	1.983	2.653	0.762	2.356	0.756	0.997
P13646	0.757	1.122		0.991	0.475	0.546	2.741	1.903	0.918	0.613
P13647	0.151			0.393						
P13662				1.506						
P13693	0.483			3.670	0.649	0.775	0.444	0.143		
Q12907				1.023						
Q16891		0.363				0.613				
P56537	1.101		0.760	0.723						
P31146		1.323	1.096	1.219	0.566					0.908
P23131	0.993		1.919	1.212						
P31150				1.037						
Q9HCY8	1.246			2.859						
Q9UPN3				0.735						
P15153	1.049									
Q01970	0.508	0.585		2.227		2.376			0.806	0.537
O00159	0.939	0.561	0.966	1.193		1.926				
Q9UQ80				1.638						
P48643	0.826	0.617	1.172	1.255						
P48669	0.229	5.217	0.726	0.802	5.842	30.876	16.915		2.556	7.419
P07237	0.781	0.845	0.640	1.196	0.550	0.927				1.639
O00299	0.719		0.917	1.166	0.973					
P58107				0.766						
P15309		1.792								
P48735			0.335	0.366						
Q03527	0.768	0.941		1.018						
P21912			0.942	0.682						
P07339	0.662		0.800	1.672		2.928				
P23396	0.683		1.328	1.268						
P21964				0.566						
O43242					0.532		1.468			2.042
P23458					1.979	2.036	4.133			1.387
Q13155		0.880		0.974						
P23526	0.478	0.684	1.743	1.710		0.319				0.713
P23528	1.001		0.797	1.623	0.438					
P15531					0.563	0.670	2.266			
P15559					3.788	0.662				1.424
O00506				0.887						
Q13200	0.717			1.151						
Q13263			0.606							
Q13283				0.786					1.942	
Q9HAV0	0.675									
P17066	1.157	0.407	0.764	0.759		0.608	1.436	2.452	0.735	0.848
P17075		7.281		3.790						
P33121				0.741						
P25120	0.564	0.564			0.415		0.736			

Q13347				1.079						
P33176	0.454		0.845	1.217						
O43520	0.412				1.502	1.599				
Q64252			0.995	1.281						
Q16543	0.780	1.076		0.645						
Q13418		0.451								
P41250	0.447		0.825	1.366		0.644				
Q13423						1.763	9.393		0.419	0.305
P23821					3.742					
P07814			0.663	0.589	3.735					
O43674						1.358			0.517	
P07858								7.471	0.900	0.957
O43707	0.456	0.928	1.095	1.289	0.498	0.560	0.849	1.021	2.018	1.936
P31930			1.614	1.551		1.769				
P31943	0.762	1.053	1.080	1.120	0.738	0.670	1.234	1.240	1.411	1.268
P31947	1.162		1.497	2.467						
P31949				0.793						
P25388		0.761		0.903						
O14672	0.467			0.871				1.072		
O43795		1.100		1.168						
Q15019	0.750			0.898		0.953			0.604	0.582
Q13616					0.814				1.091	
Q13636	0.434		0.747							
Q05639	0.828		1.642	2.304	0.453	0.742			0.893	0.839
Q05655				0.773						
Q9NP72			0.488		0.880	0.994	2.258	1.641	1.598	1.380
Q15155				0.808						
Q13740				2.276						
P09526			1.088	1.140						
P19012	0.119	0.927								
Q15262										0.956
Q13813	1.512			5.407	1.427	1.463		1.446	0.931	0.880
Q9NX57					0.314	0.522				0.771
P09622			0.396	0.375						
Q9NQX4						0.775				
P51114	0.620			0.531						
P51148			2.201	2.174						
P51149	0.969		1.110	0.959						
P51153		0.485		0.830	1.244			2.152		2.988
O88386	0.434	1.053	0.578	0.933	1.244				2.817	2.965
Q15365				1.444						
P25705	1.256		0.378	0.440						
Q15392									0.931	0.601
P25763				1.231						
P00367			0.391	0.452	0.977	1.961				1.076
Q9H4M9	0.721	0.720	1.417		0.353	0.382				
P35232			0.841	0.987						
P35239				1.942						
P35241	0.622	0.881	0.741	0.665				2.164	0.716	0.558
Q15436				0.556						
P35287				0.732		0.560	1.299			
P00403				0.548						

Q99714			0.467	0.357						
Q99798				0.525						
P27348	0.467		0.788	0.804		1.138	0.961			
P27361				0.313						
P00505		0.980		1.114	1.023	1.353	1.381		1.990	1.941
P17987	0.919		1.215	1.294						
Q99832	1.113			2.755						
Q9UGV6					0.613	1.269	4.247	3.276	0.830	0.713
Q15642		5.136			19.310				2.456	3.067
Q15654	0.476	0.468								
P43490	1.235		0.731	0.685						
P10113			1.088	1.351						
P10114									1.496	
P35527	0.469					2.059				
P51571		0.474								
Q15758				0.742	3.775					
P35579	0.378	0.503	1.162	1.424	1.362	1.602	1.653	1.729	1.337	1.473
P35580	0.382		0.976	3.577	0.637					1.353
P29034	0.049	0.656			0.460	0.668				
P29043	1.375	0.587	1.522	1.315	0.373	0.331				
P35613	1.225									
Q15833	0.547	0.675	0.787	1.338	0.606	0.971	0.956	0.848	1.153	0.906
Q15836		0.847								0.515
P02248		0.666			2.161	2.041	2.207	3.428		3.250
P19634					2.900	1.847	2.051	2.414	0.906	0.891
P37108							3.555			
P29144				0.869						
P35749	0.493		1.259	1.222	0.528		1.300			
P27797	0.472	0.990		0.429	0.967	0.866	2.786	3.762	1.601	1.379
P00938	0.760		2.330	1.894						
P27824		1.636	1.247	1.284	1.147	1.548		1.272		
Q9Y265	0.918		1.484	2.298						
P29312	0.390		1.043	0.828						
P29316		0.608	0.633	0.734	0.509					
P29322				0.046						
P53396	0.446	1.286	1.203	0.910	1.069	1.231	3.066			2.741
P35908	0.552									
P02538	0.224	6.827	0.726	0.802	4.771	30.876	11.665	4.833	2.430	6.419
P10586	0.991		0.980	1.002						
P02568	0.801	0.519	1.460	1.310	1.810	1.505	1.661		0.846	0.662
P35998	1.627		1.544							
P02570	0.613	0.383	1.544	1.591	1.230		1.668	1.248		0.617
P02593		0.596	0.468	0.430	1.854	0.327	0.540	0.612		2.500
Q92485				0.640						
P29401	0.396		1.630	1.275	0.713	2.033				1.045
P10606				0.924						
P12081				3.277						
Q09666	0.502	0.765	1.327	1.282	1.129	1.073	1.800	3.881	1.577	1.786
P04075	0.424		0.961	1.061	0.876					
P10660	0.857			1.178	0.398	0.534	1.123			

P10696		1.161								
Q13443						2.455				
Q92544		0.508		11.723						
Q9P2B2		0.646	0.583	0.525	0.750	0.638			0.367	0.373
Q92597		1.024			2.405	2.164				
Q00341						2.123			1.851	2.011
P20172					1.169		0.855			
P29597					1.407	1.434	2.876	2.892		1.387
P02786	1.267		1.188	1.520	1.288	0.430			0.845	0.849
P39023				0.740	1.023					
P55072	1.841	1.371	0.659	0.692						
P55084			0.419	0.325						
P12268				2.128						
P04259	0.229	5.217	0.726	0.802	4.771	30.876	9.039	3.578	2.345	5.752
P29692	1.141		1.386	1.478						
Q92796						1.059				
P55209	1.441	1.068	2.510	2.082						
P47210										0.543
P53801					1.132	1.068				
Q9H4G0	0.442	0.743		0.880	1.217	3.709	2.296	1.941	4.645	2.243
Q00610	0.793	0.610	0.713	0.754	2.265	1.362	2.458	2.580	0.814	3.501
P12429	0.378		0.762	0.981	4.032	0.627				
O75131		3.550			0.461					
P53990						6.604				
Q00765		1.293					0.855			8.347
O14908	0.707		0.928	2.108						
O14936		1.190		2.598	1.433	1.265	1.723		0.756	0.748
P30044				0.974						
Q02224					0.305	0.344		1.308		
P20618	0.690		1.100							
P20645				0.962						
P04626	0.682	0.655	1.039	1.183	3.068	1.628	1.880		1.258	1.037
P20674			0.926							
P04643		0.857			0.508					
P30101	0.667	0.990	0.913	0.883	0.590	0.561				
O75363				0.818					0.801	
P04720	0.778	0.476	1.469	2.852	1.071	0.742	0.783	1.373	0.893	1.749
P04765	0.604		0.966	1.190	6.800	0.744				1.237
P04792	0.760	0.733	0.705	0.682		0.350			0.683	
P39656	1.283	0.897	1.200	0.572	0.262	0.403				
P04843		0.521	1.065	0.926		0.734				
P04899				0.726					0.645	
Q9H444	0.514	0.636		0.930						
O75531	13.137		0.850							
P22314	0.777	0.467	0.658	0.623	0.375	0.480		0.996		
P47755						1.519				
Q02543						1.092		1.228		
P55786	0.532									
P22392	1.004		0.735	0.691	0.563					

P14373			0.399	0.974		0.744				
P04901				0.932	0.657			2.387	1.655	0.677
P06396	0.554	0.376	0.642	0.847						
P06493					0.851	0.803			0.871	0.922
P30519				0.704						
P49368	0.650	1.138	1.135	1.254			1.873			
Q9Y446							1.235			
O75976		0.943		0.781						
P49411			0.644	1.180						
O75844				0.819						
O75874				0.611						
P14625	0.520		1.678	1.546	0.908	0.814			1.800	
P08069				1.244						
Q02878	0.553		0.727	1.371	0.501			3.790		
P22695				0.352	2.200	2.698	5.801	6.455	1.101	1.085
P32119			0.914							
P16106	5.119		0.384	0.417	0.354	1.100				
P08134	2.523			1.703						
O75955		0.762								
P49588	0.630		0.453							
P30740			1.185							
P08195	0.731	0.607	3.139	1.069	0.683	1.302	1.445	1.844	1.021	1.199
P06744	0.451	0.896	0.547	0.481	0.682	0.604	0.973	1.075		1.084
P06749	0.726	0.601		0.974		0.624				
P06756				1.159						
P40227	0.838		1.423	1.748		2.394			0.650	0.955
P08238	0.895	0.571	0.901	1.079	1.872	1.133		1.017	3.403	
P08240				0.487						
P49748	1.752			0.482						
P49755		0.359	0.737	0.650						
P32391	0.350		1.031	0.622						
P40429			0.383							
P24410				0.887	1.932	2.663				
O60282	0.411		0.845	1.136						
Q14152		0.617		0.737					0.736	0.751
Q14157				0.767						
O60361	1.004		0.689	0.578	0.563					
P24534	1.106		2.971	2.646						
P24572	0.398		1.353	1.505						
Q14204	0.316			1.164						
Q14240	0.606			1.511	0.544	0.744				0.322
Q14247				0.570						0.785
Q14254				0.803						
Q12846						0.554				
Q9UM47				1.033						
O95336	0.759			1.042						1.172
P18124	0.750	1.016	0.389	0.519	1.478					
Q9H0N0			0.576	0.976					1.345	
P24752										
P08758	0.287	0.624	0.828	0.758						
Q14451						1.626				

P18282	0.944	0.738	0.585	1.831			23.935			
Q9HDC9			0.800	0.577						
P08865	0.683	0.543	1.305	1.356	0.675	0.811				
P08886		0.620	0.584	0.645						
O95573		0.494		1.957						
P50395	1.469	1.059		1.143						
P40926	2.802		0.738	1.121						
P40939	1.156		0.463	0.624						
O60763				0.212						
Q9Y2A7				1.860						
P50402				0.669						
P50416				1.362				1.775	0.660	0.884
Q08043	0.525			4.258						
P50454	1.328	0.587	1.549	1.216	0.373	0.331				
Q14651	0.663			1.037						
O60841				0.812						
Q13733		0.955		1.213		0.813				
Q9Y376				0.834						
Q9Y3F4		0.606		1.402	2.549	2.764			0.785	0.790
Q16181				1.534	1.901	0.421		2.651		
Q96S52				0.592			1.983			
Q96DT5	0.614	0.690	1.123	1.204	1.430	1.658	1.285	3.316	0.621	1.012
Q96FQ6			0.656	0.472						
Q9BZF1				0.723		0.732				
P09467			0.246							
Q9H0E2						0.548				
P05218	0.718	0.670	0.923	0.948	0.808		1.234	1.490	1.772	1.532
P58876	4.631	2.250	1.223	1.066						
Q9C0C2			0.634							0.295
Q08379								0.619		
Q96TA1		0.755		0.647	0.942	0.893				0.566
Q96KP4				0.756						
Q9P0L0	0.783		0.797	0.878						
Q8N3R9		0.388								
Q9NZW5		0.478		0.588						1.009
Q9Y490		1.678			1.461	1.103	6.069	5.648		0.731
P20338					0.507	0.566			1.003	0.905
P48960		2.082								
P14923	0.403	0.910		0.608	0.715					
O00515		0.576		1.152						
P41091				0.863						
P06733	0.633	0.912	2.832	2.607						
P12956	1.518		0.884	1.136	3.070					
P39019					0.752		0.514			
Q96KP1		0.638								
P26438					1.178					
P06576	1.742	1.403	0.514	0.413						
P35221	0.635	0.604	0.526	0.547	0.557				0.910	0.713
P78371	0.965	0.787	1.293	1.328	0.820	0.996				
P16152	0.618									
P10159	0.776			1.274						

P09104	0.649									
P36952	0.360	0.674								
P07355	0.368	0.576	3.281	2.920	0.435	0.469	1.385			2.164
P21796			0.628	0.966		0.844				0.623
Q13724				0.870	0.832				0.837	1.014
P15311	0.554	0.348	0.852	1.183	1.796	1.897	3.295		2.454	2.149
P08670	1.577	0.676	1.590	0.955	0.506	0.336	1.221	1.197		0.251
P31946	0.805		0.603	0.679	0.413	3.176		0.969		
Q04917	0.279									
P02304	3.397		0.245	0.472						
Q93077	1.856		0.695	0.665					2.321	1.654
P18031				1.774						
P09058	1.065	1.691	0.940	0.884	0.653	0.437	0.781	1.163	1.277	1.486
P07737	0.786		2.380	2.772						
P13797	0.603	0.643		1.341						
O00186						1.908	1.013			
P14868				0.937				2.989		
P09972				1.299						
P12750				1.504						0.438
P22234	0.655				1.535	1.161	3.898	3.445		
Q16881	0.558			0.853						
P07900	1.180	1.119	0.876	1.531		0.537	1.541	1.138	1.525	1.859
P11233			0.559	0.523			1.623			
P53621	0.604	0.945	0.736	0.568					1.187	
P12931		1.093								
Q06210						2.052	10.201			
P08729	0.588	1.195	0.722	0.994	1.693	1.391				0.551
P08779	0.273	1.073	0.847	0.685						
P00338	0.268	0.876	7.563	3.260	0.511			1.398	0.838	0.914
P51572				0.899	1.673	3.253	0.932	0.725	1.238	2.193
P40925	1.265		1.243	1.218						1.450
Q9BQE3	0.820		1.212	1.029		1.722				
P17317									0.843	0.709
P38378									0.767	0.794
P39028	1.457			1.180						
P00387				0.582						
Q15286			0.887		0.430					
Q04695	0.841	1.002		0.724	1.693	1.808	4.796	2.346	1.733	2.115
P02533	0.595	0.964	0.809	1.234	0.990	0.945	2.312	0.959	1.172	1.866
P13928		0.509								
Q99747					1.792	0.746				
P04083	0.514		1.105	2.781						
P20648		0.526	1.661	1.754						
Q99653	1.071				0.818	0.785				
P31939	0.887		1.232	1.334						
Q02790	0.492		0.604	0.355						
P04406	0.573		1.154	1.167	1.582	0.671				
P17174		0.706		0.857						
P51970				0.571						
P09960	0.581				2.633			0.473	0.998	
P16435		0.951			2.205	0.836			1.751	

P11518	0.721			1.164	2.200					
P39026		0.637	0.665	0.623						
P35268	0.974		1.887	1.217		0.333		1.960		
P08526						0.399				
P04645				1.140						
P46776			0.960	0.775	0.987					
P02433	0.777		1.830		0.623					
P49241	0.828	0.808	0.897	1.198	1.668	0.695	2.571	2.026		0.724
P26373					0.572	0.744		1.114	0.813	1.022
P05787	4.720	0.401	0.631	0.692	0.776		1.477			1.016
P07195	0.795		28.886	13.139				0.433		
P17931				0.629						
O15027						0.357				
P26038	0.636		1.101	0.859	0.965	0.239	1.384		0.865	0.940
Q9UKS6					1.170	4.409		0.690		
P30086									0.599	
P18669	0.529		1.696	1.122						
P07205	0.675		1.477	1.447						
P28074				0.747						
P21291									2.624	4.304
P05198							2.380		1.328	1.255
Q13308								1.817		
P04439					0.577	0.787				
Q02978				0.708						
P13861	0.814	0.749			0.494	0.702				
P53025	0.577			1.360						
Q9Y281	1.173		0.645	2.182	0.438					
P04844					1.400	1.445				1.216
O96000				1.850						
Q15005										0.842
P11166							1.399			
P35606							3.054	2.001		2.767
Q15084	0.781		1.223	1.077						
P27635	0.604	0.442				0.912				
P04264	6.178		2.105	1.350						
P09896				0.298						
P50991	1.263		2.200	2.932						
P38663				1.287						
Q14318				0.740						
P14927			0.662	1.473						
Q9UBC5	0.594			0.497						
O43776	0.590		0.708	0.608		1.589				
P80723			0.455	0.551						1.158
P82932	0.951		2.117	2.094					1.746	
Q08209			0.996	1.180						
P35214	0.358		0.731	0.664	1.000	1.449		0.986		1.262
P14786	0.531	0.871	1.334	1.432	0.527	0.647	1.852	2.462	6.875	10.663
P13641		0.943	0.636							
P10809	2.030		0.986	2.234						
O00559					0.885					

P49006		0.496							0.860	0.765
P13010	1.489		0.665							
P10768	0.346									
P11717				1.670						
P05783	4.630		0.592	0.586						0.958
P21851	0.996	1.520			1.636	1.795	0.616			
P07954				0.643						
P46781		0.578			1.648	1.872	2.524		1.352	1.444
P39027	0.507			0.934	0.459					
P17008	0.746			1.062	1.884			9.073		
P08708	0.748	0.743								
P30054						0.588				
Q99460						3.068			0.766	0.768
P09525				0.745						
P08133	0.761	0.593	1.044	0.958	0.496	0.619			0.951	1.416
Q9UQ16		2.436								
O94832	1.479	0.916	0.662	0.679	3.388	4.052	3.989		1.810	1.528

Table S2. List of 86 proteins with at least a 3-fold difference in protein abundance between cancer cell lines (BT474, MDA231, SKBR3, MCF7c18) and the HMEC cell line. Average (AVG) protein abundances are calculated relative to the Reference mixture. Values highlighted in green indicate >3.0-fold decrease in expression and those highlighted in red indicate >3.0-fold increase in expression relative to HMEC. The numbers of peptides used to calculate average abundance ratios for each protein are also shown (c). Gray shading (c) indicates the percent deviation among constituent peptides. Proteins are listed according to subcellular location as determined by GO annotations.

<20% dev	<30% dev		<40% dev				>40% dev			
	HMEC		BT-474		SKBR-3		MCF7c18		MDA231	
DESCRIPTION	avg	c	avg	c	avg	c	avg	c	avg	c
copine III	0.28	3			2.17	2				
lactate dehydrogenase A	1.14	2	0.13	6	1.96	2	0.72	4	1.19	2
lactate dehydrogenase B	1.26	7	0.03	3			2.31	2		
heat shock 90kDa protein 1,B	1.75	2	1.11	16	0.53	2	0.98	4	0.29	2
leukotriene A4 hydrolase	1.72	2			0.38	2	2.11	2	1	2
tumor protein, translationally-controlled 1	2.07	2	0.27	3	1.29	2	7.02	2		
pyruvate kinase	1.15	3	0.75	17	1.9	3	0.41	2	0.15	3
villin 2	2.88	3	1.17	7	0.56	2	0.3	2	0.47	4
phosphoglycerate mutase 1	1.89	6	0.59	2						
S-adenosylhomocysteine hydrolase	2.09	6	0.57	3	3.13	2			1.4	2
tyrosine 3-monooxygenase activation protein, gamma	2.79	4	1.37	4	1	4	1.01	2	0.79	3
tyrosine 3-monooxygenase activation protein, epsilon	3.35	5	0.89	4					2.32	2
chaperonin containing TCP1,8	1.16	4	1.19	5	0.48	2			0.35	2
ATP citrate lyase	2.24	4	0.83	5	0.94	3	0.33	2	0.36	2
6-phosphofructokinase, type C	1.89	4	0.49	3	0.99	2				
Cdc42-interacting protein 4	0.19	1			0.05	2			0.36	1
myosin IC	1.78	4	1.04	2	0.52	2				
myosin, light peptide 6	2.52	5	0.74	3						
ARP2 actin-related protein 2	2.13	2	0.95	2	0.38	2				
keratin 6A	4.47	9	1.38	5	0.21	4	0.21	2	0.41	5
actin, beta	2.61	2	0.65	19	0.81	3	0.8	2	1.62	3
keratin 6B	4.37	8	1.38	5	0.21	4	0.28	3	0.43	6
keratin 18	0.22	2	1.69	3					1.04	2
keratin 8	2.49	2	1.58	11	1.29	2	0.68	2	0.98	2
profilin 1	1.27	3	0.42	2						
keratin 16	3.66	5	1.18	3						
destrin	1.06	3	1.71	3			0.04	2		
filamin A, alpha	2.35	20	0.85	14	1.46	4	0.31	3	0.94	6
radixin	1.61	7	1.35	5			0.46	2	1.79	5
keratin 9	2.13	2			0.49	2				
myosin, heavy polypeptide 9	2.65	30	0.86	30	0.73	20	0.61	11	0.75	1
myosin, heavy polypeptide 10	2.62	2	1.02	4	1.57	2			0.74	3
Ras GTPase-activating-like protein IQGAP1	2.13	7	0.97	4	1.86	4	0.37	3	0.13	4
										3

keratin 6B	4.37	8	1.38	5	0.17	3	0.06	2	0.39	4		
actinin, alpha 3	1.9	2	0.23	2								
spectrin, alpha 1	0.66	4	0.18	7	0.7	4	0.69	4	1.14	5		
dynein	3.16	3	0.86	2								
band 4.1-like 1 protein	2.26	2	1.14	7	0.82	2	0.52	4	0.45	9		
talin 1	0.6	3			0.91	3	0.18	3	1.37	3		
78 kDa glucose-regulated protein	1.25	13	0.96	11	1.27	2	0.41	2	0.56	3		
tumor rejection antigen 1	1.92	7	0.6	4	1.23	3			0.56	2		
calreticulin	2.12	3	2.33	4	1.16	2	0.36	2	0.62	2		
dolichyl-diphosphooligosaccharide-protein glycosyltransferase	1.11	4	0.83	2	3.82	2						
cathepsin D	1.51	3	1.25	3	0.34	2						
acyl-CoA synthetase LC 3	2.02	3	0.51	2								
ATP synthase, beta polypeptide	0.57	8	1.94	10								
ATP synthase, alpha subunit,1	0.8	4	2.65	6								
malate dehydrogenase 2, NAD	0.36	4	1.35	6								
Acyl Coenzyme A dehydrogenase	0.57	2	2.08	2								
actinin, alpha 4	2.19	12	0.91	7	2.01	7	1.18	3	0.5	6		
barrier to autointegration factor 1	0.08	3	1.18	2								
histone H4	0.29	4	4.08	3								
Alpha enolase	1.58	13	0.35	9								
heat shock 70kDa protein 1B	2.45	4	1.31	17	1.64	4	0.7	2	1.36	4		
histone 1	0.2	2	2.6	2	2.83	2						
valyl-tRNA synthetase 2	0.98	5	0.28	2						1		
AHNAK nucleoprotein	1.99	56	0.75	30	0.93	16	0.56	11	0.63	1		
ATP-binding cassette, sub-family D (ALD), member 3	0.71	5			0.2	2	0.05	2	0.57	2		
ATPase, Class I, type 8B, 1	2.43	2			0.67	2						
Transforming protein p21/H-Ras-1; v-Ha-ras Harvey rat sarcoma viral oncogene homolog	0.56	3			2.73	4	0.31	1	0.54	1		
Transforming protein p21; v-Ki-ras2 Kirsten rat sarcoma viral oncogene homolog	0.44	2			4.89	2						
calmodulin 1	1.68	4	2.14	4	3.05	1	1.74	1	0.4	1		
annexin A2	1.74	4	0.3	11	2.3	2	0.72	2	0.46	4		
ATPase, Na/K transporting, A3	1.97	2	0.26	4	1.32	4	0.61	2	0.29	2		
ATPase, H/K exchanging, alpha	1.9	2	0.6	2								
ATPase, Na/K transporting, A2	2.85	2	0.6	4	1.33	3						
RAB13, member RAS oncogene	2.06	2	1.2	2	0.8	2	0.46	2	0.33	2		
RAB10, member RAS oncogene	2.3	2	1.73	2	0.8	2			0.36	2		

clathrin, heavy polypeptide	1.64	5	1.4	14	0.73	5	0.41	4	1.23	2
ribosomal protein, large, P1	1.69	2	0.28	2						
ribosomal protein L7a	1.39	2	0.86	2	0.45	3				
ribosomal protein S16	1.34	3	0.94	2	0.53	3	0.11	4		
ribosomal protein S9	1.73	2			0.61	3	0.4	2	0.74	2
ribosomal protein L6	1.81	4	1.38	3	2	4	0.26	2		
ribosomal protein L5	2.25	3	1.17	4	1.16	2	0.72	2		
triosephosphate isomerase 1	1.32	7	0.43	8						
phosphorylase, glycogen	2.62	2	1.67	2			0.58	2		
phosphoribosylaminoimidazole carboxylase	1.53	2			0.86	2	0.26	2		
S100 calcium binding protein A2	20.3	2			2.18	2				
transketolase	2.52	7	0.61	7	1.4	4			0.96	2
Polyposis locus protein 1	0.77	2					1.17	2	0.12	2
phospholipase C, beta 3	1.97	3	0.45	2	0.42	2			1.24	2
transmembrane 9 superfamily 4	1.97	3	0.09	3						
serine/threonine kinase receptor associated protein	1.65	3	0.71	3	0.36	2			1.27	4
transducin (beta)-like 2	2.07	2	1.24	2	1.43	3	0.62	2	0.77	4
ATPase, H+ transporting,V1,D	1.04	2			0.84	2	0.31	2		